

The Upper Cretaceous to Palaeogene
Sedimentary History and Tectonic Evolution
of the Bala Basin Central Anatolia, Turkey.

A thesis submitted for the Degree of Doctor
of Philosophy in the University of London.

by

Mehmet Fahrettin Emre

Bedford College London

1985

ProQuest Number: 10098512

All rights reserved

INFORMATION TO ALL USERS

The quality of this reproduction is dependent upon the quality of the copy submitted.

In the unlikely event that the author did not send a complete manuscript and there are missing pages, these will be noted. Also, if material had to be removed, a note will indicate the deletion.



ProQuest 10098512

Published by ProQuest LLC(2016). Copyright of the Dissertation is held by the Author.

All rights reserved.

This work is protected against unauthorized copying under Title 17, United States Code.
Microform Edition © ProQuest LLC.

ProQuest LLC
789 East Eisenhower Parkway
P.O. Box 1346
Ann Arbor, MI 48106-1346

To the memory of my father Mr ISMET EMRE

RHBNC

1579423 4



a30214 015794234b

ABSTRACT

The study area is situated on the northern extension of the Tuzgolu basin, (Central Anatolia) and contains Upper Cretaceous - Tertiary volcanic, clastic, and carbonate rocks with evaporites deposited on an ophiolitic melange basement, the Ankara Melange. The present structure of the area is the result of tectonism during late Alpine movements. The movements controlled the timing and conditions of sediment accumulation.

The Bala basin evolved on the northern continental margin of the Kirsehir block. A brief period of south dipping subduction, which originated a continental island arc, was followed by oblique subduction, transform fault and continent to continent collision stages. These determined the shape and depositional characteristics of the basin. This is supported by independent magnetic evidence which suggests a 90° anti-clockwise rotation of the Kirsehir block during the Upper Cretaceous - Eocene period.

Deposition of sediments occurred in two phases. The Upper Cretaceous - Middle Eocene phase contains seven formations. Four are believed to have been deposited in a deep marine environment by mass movements and turbidity currents sometimes forming submarine fans, and two are shallow marine to continental deposits. The seventh is composed mainly of Andean type calc-alkaline volcanic rocks and their pyroclastics and was formed by subaerial lava flows. The formations reflect conditions of deposition in different parts of the basin and therefore some are the time equivalent of others. The Middle Eocene to probably Oligocene phase consists of two interfingering formations deposited in continental and marine environments of deposition.

Palaeocurrent and petrographic data suggest that during the first phase, the source area was to the southeast and formed by volcanic rocks of Sarikaya formation and Ankara Melange, while in the second phase sediments were derived

from multiple marginal sources, including the sedimentary rocks of the first phase.

ACKNOWLEDGEMENT

The author is indebted to the Mineral Research and Exploration Institute for providing the grant as well as for the use of the Institute's facilities during the field work.

The author gratefully acknowledges the unfailing support, encouragement and guidance of his supervisor Professor A.J. Smith, in every stage of the present research. This thesis would not have been completed without his constant interest and critical reading.

Special thanks are extended to the academic and technical staff of the Geology Department of the Bedford College. Amongst the academic staff Dr. A. Saunders for stimulating discussions and suggestions on orogenic volcanic rock and their plate tectonic interpretation, Dr. G. Mariner for her help during the mineralogical and chemical analyses of rocks, Dr. D. Powell and Dr. P. Banham for fruitful discussion on structural geology and magmatic rocks, Dr. T. Rose for his help and suggestions for the identification of fossils will be remembered. Miss R. Fricher and Mrs S. Bishop for their kind help and assistance. Mr. S Houlding, Mr. N. Sinclair, Mr. J. Mock and Mr. J. Keith for their technical assistance and help deserve special thanks.

The author also wishes to thank Dr. A.G. Adams of the Natural History Museum and S. Tekler of M.T.A. for identification of microfossils, professor D.J. Shearman for useful discussion in aspects of limestone diagenesis, Dr. O. Varol of Robertson Research Institute for identification of Nannofossils and Professor T.N. Norman of Middle East Technical University and Dr. F.Y. Oktay of Istanbul Technical University for useful discussions on the geology of the Central Anatolia.

Additionally the author extends his thanks to Mrs. J. Lowers for undertaking the difficult task of typing the final manuscript.

Last but by no means least the author is perpetually indebted to his wife, Tulin for her moral and financial support, without which this thesis would never have been completed.

C O N T E N T S

	Page
TITLE PAGE	1
ABSTRACT	2
ACKNOWLEDGEMENTS	4
CONTENTS	6
LIST OF TABLES PLATES AND FIGURES	13
CHAPTER 1 - INTRODUCTION	21
1.1 - General	21
1.1.1 - Location	21
1.1.2 - Topography	21
1.1.3 - Climate and Vegetation	25
1.1.4 - Transport conditions and settlement	28
1.2 - Aim of study	28
1.3 - Method of study	28
1.4 - Nomenclature	31
1.5 - Previous works	35
1.6 - Regional geological setting of the Bala area	38
1.6.1 - Kirsehir Massif	38
1.6.2 - Ankara Melange	39
1.6.3 - Upper Cretaceous - Early Tertiary Sediments	44
1.6.4 - Neogene deposits	44
1.6.5 - Quaternary deposits	47
1.6.6 - Igneous rocks	47
1.6.7 - General stratigraphy of the Bala area	47
CHAPTER 2 - SARIDERE VOLCANIC FORMATION	49
2.1 - General Introduction	49
2.2 - Andesite	51
2.2.1 - General description	51
2.3 - Dacitic tuff and ignimbrites	55
2.3.1 - General description	55
2.4 - Agglomerates	58
2.4.1 - General description	58
2.5 - Conglomerates	58
2.5.1 - General description	60
2.6 - Age of the Saridere volcanic formation	60
2.7 - Source and mode of deposition	60

	PAGE
CHAPTER 3 - KAMISLI FORMATION	64
3.1 - General Introduction	64
3.2 - Distribution, thickness and field relations	65
3.3 - Conglomerates	67
3.3.1 - General description	67
3.4 - Sandstones	70
3.4.1 - General description	70
3.4.2 - Texture	73
3.4.3 - Framework grains	73
3.4.4 - Matrix and cement	77
3.5 - Reworked-tuffs	77
3.5.1 - General description	77
3.6 - Shales and marls	78
3.6.1 - General description	82
3.7 - Sedimentary structures and current directions	82
3.8 - Weathering and alteration	86
3.9 - Fossils and age of the Kamisli formation	86
3.10 - Source area and environment of deposition	89
CHAPTER 4 - DAVDANLI FORMATION	
4.1 - General Introduction	94
4.2 - Distribution, thickness and field relation	96
4.3 - Conglomerates	98
4.3.1 - General description	98
4.3.2 - Lithology of the conglomerate clasts	100
4.4 - Sandstones	102
4.4.1 - General description	102
4.4.2 - Texture	103
4.4.3 - Framework grains	107
4.4.4 - Matrix and cement	109
4.5 - Shales and marls	109
4.5.1 - General description	109
4.6 - Sedimentary structures and current directions	110
4.7 - Weathering and alteration	113
4.8 - Fossils and age of the Davdanli formation	115
4.9 - Source area and environment of deposition of the Davdanli formation	115
CHAPTER 5 - DEGIRMENDERE FORMATION	121
5.1 - General Introduction	121
5.2 - Distribution, thickness and field relations	125
5.3 - Conglomerates	128
5.3.1 - General description	128

	PAGE
5.3.2 - Texture	133
5.3.3 - Lithology of the conglomerate clasts	133
5.3.4 - Matrix of the conglomerate	136
5.4 - Sandstones	136
5.4.1 - General description	136
5.4.2 - Texture	143
5.4.3 - Framework grains	143
5.4.4 - Matrix and cement	148
5.5 - Shales	148
5.5.1 - General description	148
5.6 - Sedimentary structures and current directions	150
5.7 - Weathering and alteration	157
5.8 - Fossils and age of the Degirmendere formation	157
5.9 - Source area and environment of deposition	157
CHAPTER 6 - UCEM FORMATION	163
6.1 - General Introduction	163
6.2 - SARIKAYA MEMBER	163
6.2.1 - General Introduction	163
6.2.2 - Distribution, thickness and field relations	167
6.2.3 - Conglomerates	171
6.2.3.1- General description	171
6.2.3.2- Lithology of the conglomerate clasts	175
6.2.4 - Sandstones	178
6.2.4.1- General description	178
6.2.4.2- Texture	178
6.2.4.3- Framework grains	181
6.2.4.4- Matrix and cement	182
6.2.5 - Compositional variation in the clastic rocks	182
6.2.6 - Mudstones	182
6.2.6.1- General description	182
6.2.7 - Sedimentary structures	184
6.2.8 - Weathering and alteration	184
6.2.9 - Age of the Sarikaya member	185
6.2.10- Source area and environment of deposition	185
6.3 - SEHRIBAN MEMBER	188
6.3.1 - General Introduction	188
6.3.2 - Distribution, thickness and field relations	190
6.3.3 - Conglomerates	190
6.3.3.1- General description	190
6.3.4 - Sandstones	192
6.3.4.1- General description	193
6.3.4.2- Texture	193
6.3.4.3- Framework grains	198
6.3.4.4- Matrix and cement	199
6.3.5 - Mudstones and marls	199
6.3.5.1- General description	199
6.3.6 - Age of the Sehriban member	200
6.3.7 - Source area and environment of deposition	200

	PAGE
CHAPTER 7 - KOCANINDAMBASI FORMATION	205
7.1 - General Introduction	205
7.2 - Distribution, thickness and field relations	209
7.3 - Subfacies I	210
7.3.1 - Texture	210
7.3.2 - Framework grains	210
7.3.3 - Binding agents	213
7.3.4 - Variation in the composition and texture	213
7.4 - Subfacies II	214
7.5 - Subfacies III	221
7.5.1 - Texture	224
7.5.2 - Framework grains	224
7.5.3 - Binding agents	225
7.6 - Subfacies IV	225
7.6.1 - Texture	229
7.6.2 - Framework grains	229
7.6.3 - Binding agents	231
7.7 - Fossils and age of the Kocanindambasi formation	231
7.8 - Environment of deposition	234
7.9 - Diagenesis and post-diagenetic changes	240
CHAPTER 8 - BAYAT FORMATION	254
8.1 - Introduction	254
8.2 - KUREBOGAZI MEMBER	254
8.2.1 - Description	254
8.2.1.1- Upper slope facies association	255
8.2.1.2- Lower slope facies association	274
8.2.2 - Interpretation	281
8.3 - ARDICLIPINAR MEMBER	282
8.3.1 - Description	282
8.3.2 - Interpretation	288
8.4 - BUYUKDERE MEMBER	289
8.4.1 - Description	289
8.4.1.1- Middle fan facies association	289
8.4.1.2- Outer fan facies association	296
8.4.2 - Interpretation	305
8.5 - Petrography	308
8.5.1 - Definition	308
8.5.2 - Limestone distoliths	308
8.5.3 - Rudaceous rocks	308
8.5.4 - Arenaceous rocks	310
8.5.5 - Mudstones	316
8.5.6 - Source area of the Bayat formation	317
8.6 - Distribution, thickness and field relations	317
8.7 - Fossils and age of the Bayat formation	319

CHAPTER 9 - KIZILDAG FORMATION	321
9.1 - General Introduction	
9.2 - Distribution, thickness and field relations	323
9.3 - Conglomerates	329
9.3.1 - General description	329
9.4 - Sandstones	333
9.4.1 - General description	333
9.4.2 - Texture	336
9.4.3 - Framework grains	336
9.4.4 - Matrix and cement	340
9.5 - Mudstones	341
9.5.1 - General description	341
9.6 - Evaporites	341
9.6.1 - General description	341
9.7 - Red colouration	343
9.8 - Sedimentary structures and current directions	347
9.9 - Age of the Kizildag formation	347
9.10 - Source area and environment of deposition	347
CHAPTER 10 - KEKLIKPINARI FORMATION	352
10.1 - General Introduction	352
10.2 - Distribution, thickness and field relations	354
10.3 - Sandstones	357
10.3.1- Sandstone and conglomeratic sandstone beds with upward thinning	357
10.3.2- Sheet-like sandstones	363
10.3.3- Gently dipping parallel laminated sandstones	363
10.3.4- Turbidite sandstones	367
10.4 - Shales and siltstones	367
10.5 - Limestones	367
10.5.1- Foraminiferal packstones	367
10.5.2- Micritic limestones	368
10.6 - Evaporites	372
10.7 - Conglomerates	372
10.8 - Deltaic deposits	378
10.8.1- General Introduction	378
10.8.2- Lithologies of the deltaic deposit	384
10.8.2.1- Conglomerates	384
10.8.2.2- Sandstones	384
10.8.2.3- Siltstones and shales	385
10.8.3- Interpretation	386
10.9 - Age of the Keklikpinari formation	389
10.10 - Source area and environment of deposition	389

	PAGE
CHAPTER 11 - STRUCTURAL GEOLOGY	394
11.1 Introduction	394
11.2 Syn-sedimentary	394
11.3 Tectonic structures	397
11.3.1 Folds	397
11.3.2 Faults	398
CHAPTER 12 - PALAEOGEOGRAPHY AND SEDIMENTARY HISTORY OF THE BALA BASIN.	403
CHAPTER 13 - GEOTECTONIC EVOLUTION OF BALA BASIN WITHIN THE FRAMEWORK OF ANATOLIAN MOBILE BELT.	432
13.1 Geotectonic evolution of Anatolian Mobile Belt	432
13.1.1 General Introduction	432
13.1.2 Historical background	432
13.2 A review of the geotectonic evolution of Anatolia within the concept of Plate Tectonic Theory	439
13.3 Geotectonic evolution of Bala area.	446
CHAPTER 14 - SUMMARY AND CONCLUSIONS.	462
REFERENCES	466
APPENDIX	478
I - Method used in petrographic studies.	478
II - Staining techniques for carbonate minerals	480
III - X-ray diffraction	482
IV - X-ray fluorescence spectrometry	484
V - Sample preparation for scanning electron microscopy for Nanno-fossils.	487
VI - Grain contact types and packing proximity	488
VII - Type section of Kamisli formation	489
VIII - Type section of Davdanli formation at Yan- iksirti.	490
IX - Type section of Degirmendere formation	491
X - Sketch map and section at Salideresi (Kurebogazi member)	492
XI - Type section of Ardiclipinar member	493
XII - Type section of Buyukdere member	494
XIII - Section of Buyukdere member measured at Geyikardici	495

ENCLOSURES

1. (MAP I): Geological Map of the Bala area
2. (MAP II): Structural Map of the Bala area
3. Geological cross sections of the Bala area
4. 1/10.000 scale map of the deltaic deposits.

TABLES, PLATES AND FIGURES

PAGE

TABLES

3.1	Modal composition of Kamisli formation's sandstones	74
4.1	Modal composition of Davdanli formation's sandstones	104
5.1	Modal composition of Degirmendere formation's sandstones	146
6.1	Modal composition of Ucem formation's sandstones	183
7.1	Comparison of the deep-water and shallow-water stromatolites with the Kocanindambasi formation's stromatolites.	237
8.1	Summary of facies characteristics showing distribution and relative prominence of diagnostic features.	283
8.2		
8.2	Modal composition of Bayat formation's arenaceous rocks.	313
9.1	Modal composition of Kizildag formation's sandstones	338
10.1	RI and RSI values of asymmetrical wave ripples.	360
10.2	Modal composition of Keklikpinari formation's sandstones	362
12.1	Chemical composition of the Bala Basin Volcanic Rock (BBVR)	405
12.2	Comparison of major element abundances of volcanic rocks of island arcs with BBVR.	408
12.3	Comparison of trace element abundances of volcanic rocks of island arcs with BBVR	410
12.4	Comparison of thoeleitic and calc-alkaline island arc magmas with BBVR	413
12.5	Generalised comparison of calc-alkaline volcanic rocks of island arcs, those of continental margins and BBVR.	413

	PAGE
PLATES	
1.1 Panaromic view of Kuredag	23
1.2 Escarpment formed by the Kocanindambasi formation	24
1.3 Badland topography on Kuzpınar	26
1.4 Serpentinite and limestone blocks in the Ankara Melange	43
1.5 Angular unconformity between the Kizıldag formation and Neogene deposits	45
1.6 Cross-stratification in the Neogene deposits	46
2.1 Angular unconformity between the Sarıdere Volcanic formation and Sarıkaya member.	52
2.2 Photomicrograph of andesite	54
2.3 Bedding in the dacitic tuff layers	56
2.4 Photomicrographs of dacitic tuff and ignimbrite.	57
2.5 Photomicrograph of agglomerate	59
2.6 Disorganized red conglomerates	61
3.1 Panaromic view of the Kamisli formation.	66
3.2 Conglomerates in the Kamisli formation.	68
3.3 <u>Tbce</u> and <u>Tde</u> type sandstone-shale alternation.	71
3.4 Massive sandstone beds	72
3.5 Photomicrographs of sandstones	75
3.6 Occurrence of reworked-tuff layers	79
3.7 Sedimentary structures and bedding in fine grained reworked-tuff layers.	80
3.8 Photomicrographs of reworked tuffs.	81
3.9 Slump folds in between undisturbed beds	84
3.10 Large scale slump folds	85
3.11 Photomicrograph of nanno-fossils	87-88
4.1 Upward fining and thinning sequences in the lower part of the Davdanlı formation	97
4.2 Upward coarsening and thickening sequences	99
4.3 Occurrences of conglomerates	101
4.4 Photomicrograph of sandstone Type I	105
4.5 Photomicrograph of sandstone Type II	106
4.6 Trace fossils.	111-12

	PAGE
4.7 Slump sheets and slump balls.	114
5.1 Inner fan channel.	126
5.2 Upward fining and thinning sequences.	127
5.3 Matrix-supported conglomerates.	129-30
5.4 Disorganized conglomerates.	131
5.5 Graded conglomerates.	132
5.6 Roundness and shape of conglomerates.	134-35
5.7 Photomicrographs of andesitic, dacitic and rhyolitic conglomerate clasts.	137-38
5.6 Massive sandstone.	139
5.7 Pebbly sandstone.	141
5.8 Regularly bedded <u>Tabe</u> , <u>Tbce</u> and <u>Tde</u> type sandstones and shales.	142
5.9 Photomicrographs of sandstones.	144-45
5.10 Injection structures.	149
5.11 Occurrence of plant fragments.	151-52
5.12 Ball and pillow structures.	153
5.13 Sole structures.	154-55
5.14 Slump fold.	156
6.1 Angular disconformity between the Ucem and Kizildag formations.	172
6.2 Angular disconformity between the Ucem and Kizildag formations.	173
6.3 Conglomerates of the Kizildag formation.	174
6.4 Interbedded conglomerate and sandstone.	176
6.5 Sheet-like sandstones.	179
6.6 Photomicrograph of sandstone.	180
6.7 Conglomerates in Sehiban member.	191
6.8 Photomicrograph of sandstone of the lower unit of Sehiban member.	194
6.9 Photomicrograph of sandstone of the upper unit of Sehiban member.	195
6.10 Burrow in sandstone.	196
6.11 Interbedded sandstone and mudstones	197
6.12 Bioturbation in marl	201

	PAGE
7.1	Panaromic view of Kocanindambasi formation. 207
7.2	Boundary relationships of Kocanindambasi formation with Ucem formation. 208
7.3	Photomicrograph of bioclastic packstone. 211
7.4	Photomicrograph showing parallel fibrous wall structure of a brachiopod shell. 212
7.5	Photomicrograph showing radial fibrous pattern in a rotaliid wall. 212
7.6	Photomicrographs of stromatolites and oncolites. 215-16
7.7	Photomicrograph of coral-algal boundstone. 218
7.8	Coral head.
7.9	Coral head in the lower part of the Kocanindambasi section. 220
7.10	Photomicrograph of bioclastic grainstone. 222
7.11	Photomicrograph of large benthonic foraminiferal packstone. 223
7.12	Photomicrographs of echinoid fragments. 226-27
7.13	Photomicrographs of small benthonic foraminiferal packstone. 228
7.14	Photomicrographs of agglutinating <u>Textularia</u> . 230
7.15	Photomicrographs of bryozoans. 232-33
7.16	Photomicrograph showing micritization of bioclastic fragments. 241
7.17	Photomicrograph showing compaction features. 243
7.18	Photomicrographs of fibrous and bladed cements. 244-45
7.19	Photomicrographs of solution cavity fills.. 247
7.20	Photomicrographs showing inversion of aragonite to calcite. 248-49
7.21	Photomicrograph showing replacement of walls of Foraminifers by sparry calcite. 251-52
7.22	Photomicrographs of algal boring. 251-52
7.23	Photomicrograph of blocky and bladed cement. 251-52
8.1	<u>Tab</u> e type sandstone with reduced <u>a</u> division. 258
8.2	Couplet sandstone. 260
8.3	Upward fining and thinning sequence in the Buyukdere section. 261
8.4	Conglomerate-sandstone and conglomerate sequences. 263

	PAGE
8.5	Folded channel-fill deposits. 264
8.6	Clast supported conglomerates. 265
8.7	Matrix-supported conglomerates 266
8.8	V-shaped channel. 269
8.9	Channel-fill conglomerates 269
8.10	Slump sequences 270
8.11	Slump folds and sheets 271-72
8.12	Occurrences of limestone olistoliths. 275-76
8.13	Graded and graded-stratified conglomerates in lower slope sequences 277-78
8.14	Conglomeratic and massive sandstone beds. 279
8.15	Slump sequences in the lower slope. 280
8.16	Inner fan conglomerate and sandstones with a large limestone olistolith. 285
8.17	Appearances of inner fan deposits along Uzunkolun valley 286
8.18	Two successive upward fining and thinning sequences. 290
8.19	<u>Tabce</u> and graded-stratified conglomerate bed. 294
8.20	Outer fan lobe sequence. 297
8.21	Upward thickening of outer fan lobe. 298
8.22	Typical occurrence of fan fringe-basinal deposits. 300
8.23	<u>Tbce</u> and <u>Tbcde</u> type sandstone beds. 301
8.24	Trace fossils. 302-03
8.25	Photomicrographs of sandstones 311
8.26	Photomicrographs of calcarenites. 313
9.1	Disconformity between the Bayat and Kizildag formations. 326
9.2	Boundary relationship of the Kizildag and Keklikpinari formation 328
9.3	Channels within a mudstone sequence 330
9.4	Occurrence of conglomerates 331
9.5	Large and small scale trough cross-strati- fication 334
9.6	Sandstone-mudstone intercalation 335
9.7	Photomicrograph of sandstones 337
9.8	Laminated evaporites

	PAGE
9.9	Haematite haloes 345
9.10	Haematite free contact 346
10.1	Matrix-supported disorganized conglomerate. 356
10.2	Sandstone with hummocky cross stratification. 358
10.3	Wave ripples. 359
10.4	Photomicrograph of sandstones. 361
10.5	Sheet-like sandstones. 364
10.6	Gently dipping parallel laminated sandstones around Goktepe. 365
10.7	Gently dipping parallel laminated sandstones at NE of Ergin. 366
10.8	Foraminiferal packstone. 369
10.9	Micritic limestone lens. 370
10.10	Photomicrograph of micritic limestone with dolomite rhombs. 371
10.11	Photomicrograph showing faecal pellets. 373
10.12	Limestone with organic matter rich laminae 374
10.13	Evaporite lens 375
10.14	Subaqueous shrinkage cracks 376
10.15	Thick conglomerate beds 377
10.16	Sandstone and shale interrelation with lens shaped conglomerate bed in deltaic deposit. 380
10.17	Upward coarsening sequence in deltaic deposit. 381
10.18	Laminated and wave-ripple cross laminated siltstone and shale 381
10.19	Distributory channel fill deposits 382
10.20	Two trough-cross bedded distributory channel-fill deposits. 383
10.21	Panaromic view of the deltaic deposits. 387
10.22	Slump folds in the deltaic deposits 388
11.1	High angle reverse fault 399
11.2	Bench fold and reverse fault 400
11.3	Normal fault 402

	PAGE
FIGURES	
1.1 Location map.	22
1.2 Topography and drainage map	27
1.3 Geological location map.	29
1.4 Classification used for sedimentary rocks.	32
1.5 Classification used for pyroclastic rocks.	33
1.6 Stratigraphic correlation table.	36
1.7 Stratigraphic column for the Bala area.	48
2.1 Section measured at Saridere.	50
4.1 Section measured at Ortakisla.	95
5.1 Section measured at K. Bayat	122
5.2 Section measured at Cataltepe.	123
6.1 Section measured at Halaclikisla.	165
6.2 Section measured at Saridere (Saridere II).	166
6.3 Section measured at Cesmederesi.	168
6.4 Correlation of stratigraphic columns of Ucem formation.	169
6.5 Section measured at Sehriban.	189
7.1 Section measured at Kocanindambasi.	206
8.1 Section measured at Kurebogazi.	256
8.2 Section measured at Sarlalikdere.	257
8.3 Simplified section of Buyukdere.	291
8.4 Simplified section of Geyikardici.	292
9.1 Section measured at Kizildag.	322
9.2 Correlation of stratigraphic columns of Kizildag and Keklikpinari formations in the SE.	324
9.3 Correlation of stratigraphic columns of Kizildag and Keklikpinari formation in the W, NE and N.	325
10.1 Section measured at Keklikpinari.	353
10.2 Section measured at Asartepe.	355
10.3 Section measured at Korattepe.	379
12.1 Chemical classification of Bala Basin Volcanic Rocks (BBVR).	406
12.2 AMF diagram of BBVR.	406
12.3 Oxides vs SiO ₂ diagram of BBVR.	409
12.4 Trace element vs SiO ₂ diagram of BBVR.	411

PAGE

12.5	Sample/Chondorite diagram.	414
12.6	Palaeogeographical map of Lower Maastrichtian	416
12.7	Palaeogeographical map of Middle-Upper Maastrichtian.	418
12.8	Palaeogeographical map of Early Palaeocene.	420
12.9	Palaeogeographical map of Middle-Late Palaeocene.	424
12.10	Palaeogeographical map of Early-Middle Eocene.	
12.11	Palaeogeographical map of Middle Eocene-probable Oligocene	430
13.1	Tectonic units of Anatolia (2 maps).	435
13.2	Plate tectonic evolution of eastern Mediterranean.	440
13.3	Plate tectonic evolution of Anatolia	442
13.4	Palaeogeographic maps of the Ankara-Tuzgolu region (<u>6</u> maps).	448-50
13.5	Stratigraphic correlation table of Ankara-Tuzgolu region.	451-52
13.6	A-C-Palaeotectonic map of the Ankara-Tuzgolu region (3 maps).	455

C H A P T E R 1

INTRODUCTION

1.1 General

1.1.1 Location:

The area studied, known as the Bala basin, is situated on the southern foothills of the Elmadag, between the Ankara highs to the north and the Konya ovasi (plain) to the south. It lies between $33^{\circ} 08' 00''$ and $39^{\circ} 52' 44''$ N and is bounded to the N and NE by the Elmadag, to the W by Bala town, to the S by the Tuz Golu basin, to the E, by the Kirsehir massif. It is situated 60 km. SE of Ankara and covers approximately 500 km². (Fig 1.1).

1.1.2 Topography:

The main topographical feature in the area is Kuredag which is formed by series of NE-SW lying hills standing 400-600 m. above the surrounding flat land (Plate 1.1) The alignment of these continuous hills parallel the general NE-SW structural trend; the morphological features in different areas indicate that structural trend and the different physical characteristics of the formations were the main reasons for the present day topography of the area. At the southeastern-most part of the area lies a flat-land which is bisected by small valleys and situated between Konya plain in the southwest and, in the northeast, slopes of the Kuredag. The Kocanindambasi limestone (see Chp. 7) outcrops in the tops of the first chain of hills forming an impressive escarpment on their SW side (Plate 1.2) This hills are usually conical and continuous in the NE and become isolated in the SW. The second and third chain of hills are formed by the NE-SW aligned plunging anticlines, where the Degirmendere and Bayat formations crop out. These chains of usually flat topped hills are separated by relatively deep-cut valleys.

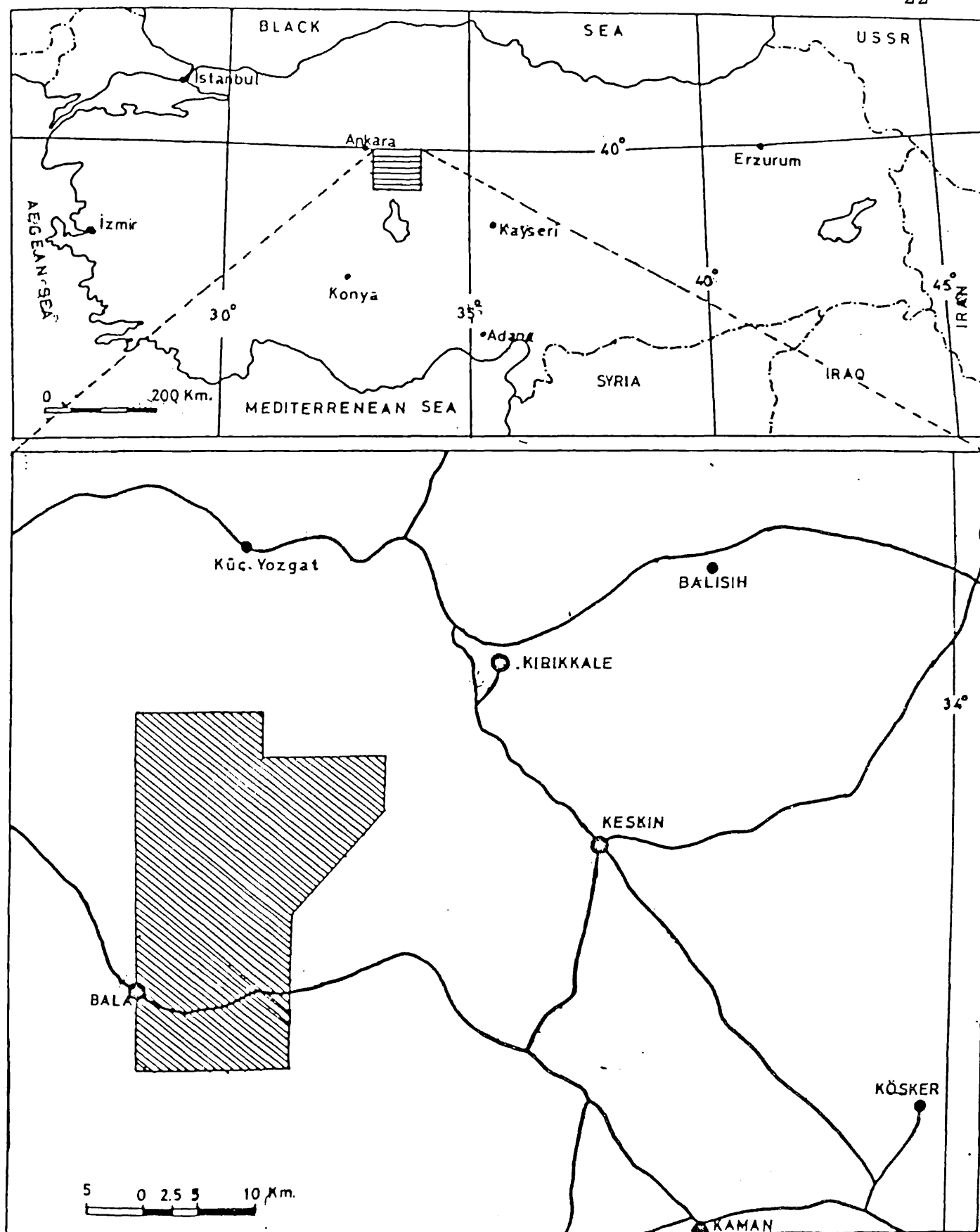


Fig. 1.1. Location Map.



Plate 1.1 - Panoramic view of the northern flank of Kuredag taken from the
Cukurcakozu valley (F8) looking SSE.



Plate 1.2 - Escarpment formed by the Kocanindambasi formation at Saridere valley (Q12)

Gullies are abundant in the shale-dominated areas forming a badland topography. (Plate 1.3) The last chain of hills with flat tops was formed by the Kamisli and Davdanli formations. The next topographical future is a small plain situated between the northeastern foothills of the Kuredag and southwestern foothills of the Elmadag and filled by alluvial deposits of the Cukurcakozu dere.

The drainage system of the area studied is dominated by small streams which flow only during the rainy seasons. Five major drainage systems were differentiated (see Fig 1.2). The first is separated by Geyikardici-Komusalani water-divide to the SW. The streams in this drainage system generally flow orthogonally or oblique to the general trend and from NW to SE. In the second system streams flow from SE to NW and join to the Cukurcakozu dere before it flows in to the Kizilirmak river. In the third system the general trend of the streams is north to south; it occurs in the southwestern part of the area and is bounded by Kussivrisi-Geyikardici-Fatma Tepe-Bahcekarada water-divided. The fourth and fifth drainage systems are relatively small and occur in the western-most part of the area and separated by Kartaltepe water-divide. Streams run from north to south in the former and from SE to NE in the latter.

1.1.3 Climate and Vegetation:

The area is characterized by a typical continental climate: in general summers are hot and dry and winters are cold. Most of the rainfall is confined to the winter and spring months with a small amount of snow.

The only type of natural vegetation occurs as patchy forest which is usually confined to the higher grounds of the area. Nearly all lowland areas are cultivated.



Plate 1.3 - Showing gullies and badland topography
formed on the shale dominated lithologies
of the Bayat formation. Location (N10)

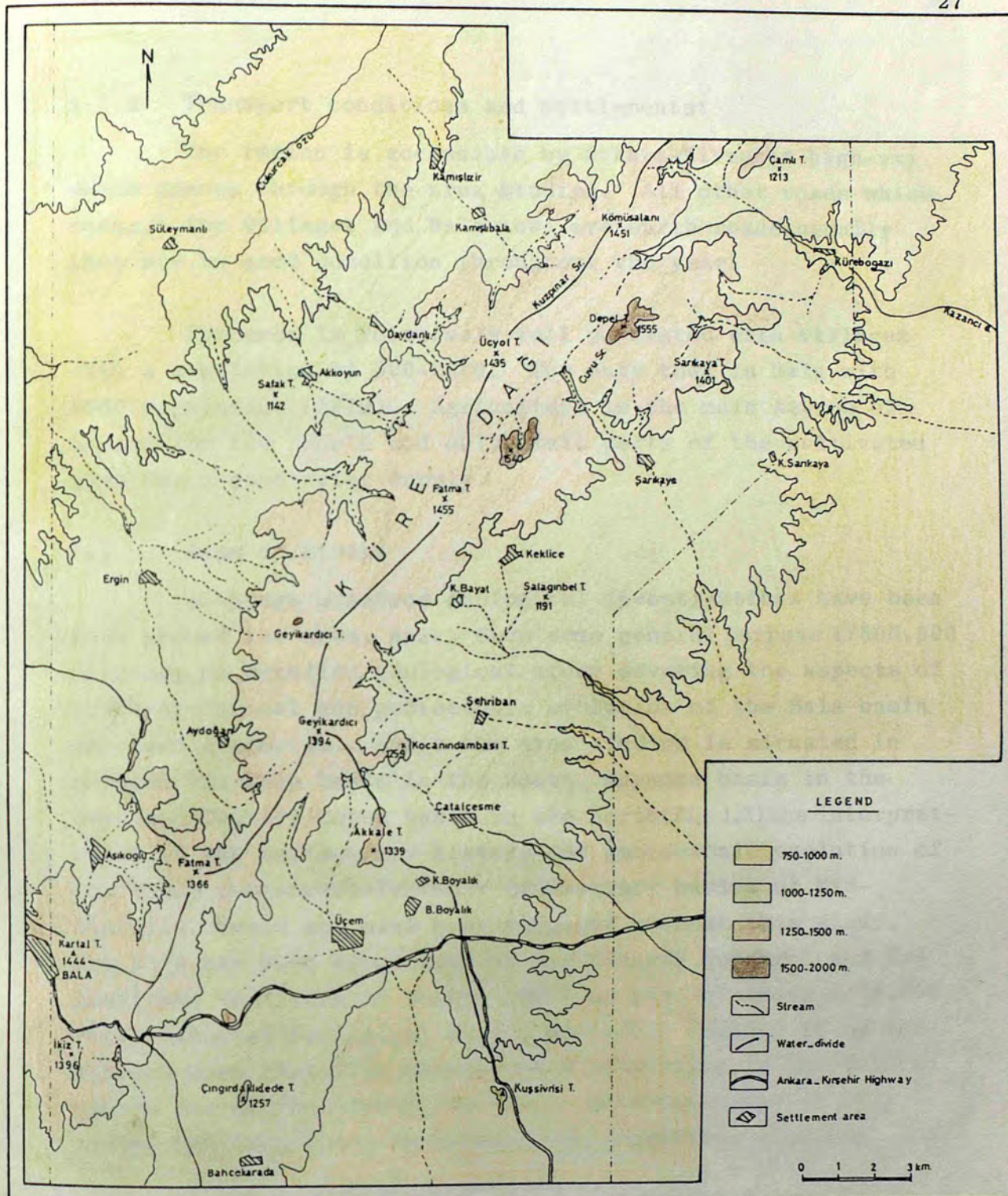


Fig 1.2. Topographical map showing stream catchment areas.
(The area studied falls within the dot-dashed lines).

1.1.4 Transport conditions and settlements:

The region is accessible by Ankara-Kirsehir high-way which passes through the area studied. All other roads which connect the villages and Bala town are earth roads, usually they are in good condition throughout the year.

The area is relatively well populated with villages with a population of 500-2000. The only town in Bala with 6660 population (1979). Agriculture is the main source of income for the people and only small parts of the cultivated land has a good water supply.

1.2 Aims of study:

Although numerous geological investigations have been made around the area, apart from some general purpose 1/500.000 mapping, no detailed geological study covering the aspects of sedimentological and geotectonic evolution of the Bala basin had been attempted. Since the area studied is situated in between Tuz Golu basin in the south, Haymana basin in the west and Cankiri-Corum basin in the north (Fig 1.3) the interpretation of the sedimentary history and geotectonic evolution of the Upper Cretaceous-Tertiary sedimentary basins of Mid-Anatolia would not have been complete without this study. The work has been encouraged by the Mineral Research and Exploration Institute of Turkey (MTA) as part of their 1/25.000 scale National Geological Survey Project. Further it is the author's hope that this thesis would be of value in the future search for hydro-carbons, since a growing number of oil fields have been found in successions of deep-sea clastics.

1.3 Methods of Study

Research on the Bala basin was carried out in two stages. The first stage involved geological mapping and the measurement of detailed stratigraphical sections where the formations are well exposed and complete; this occupied a total

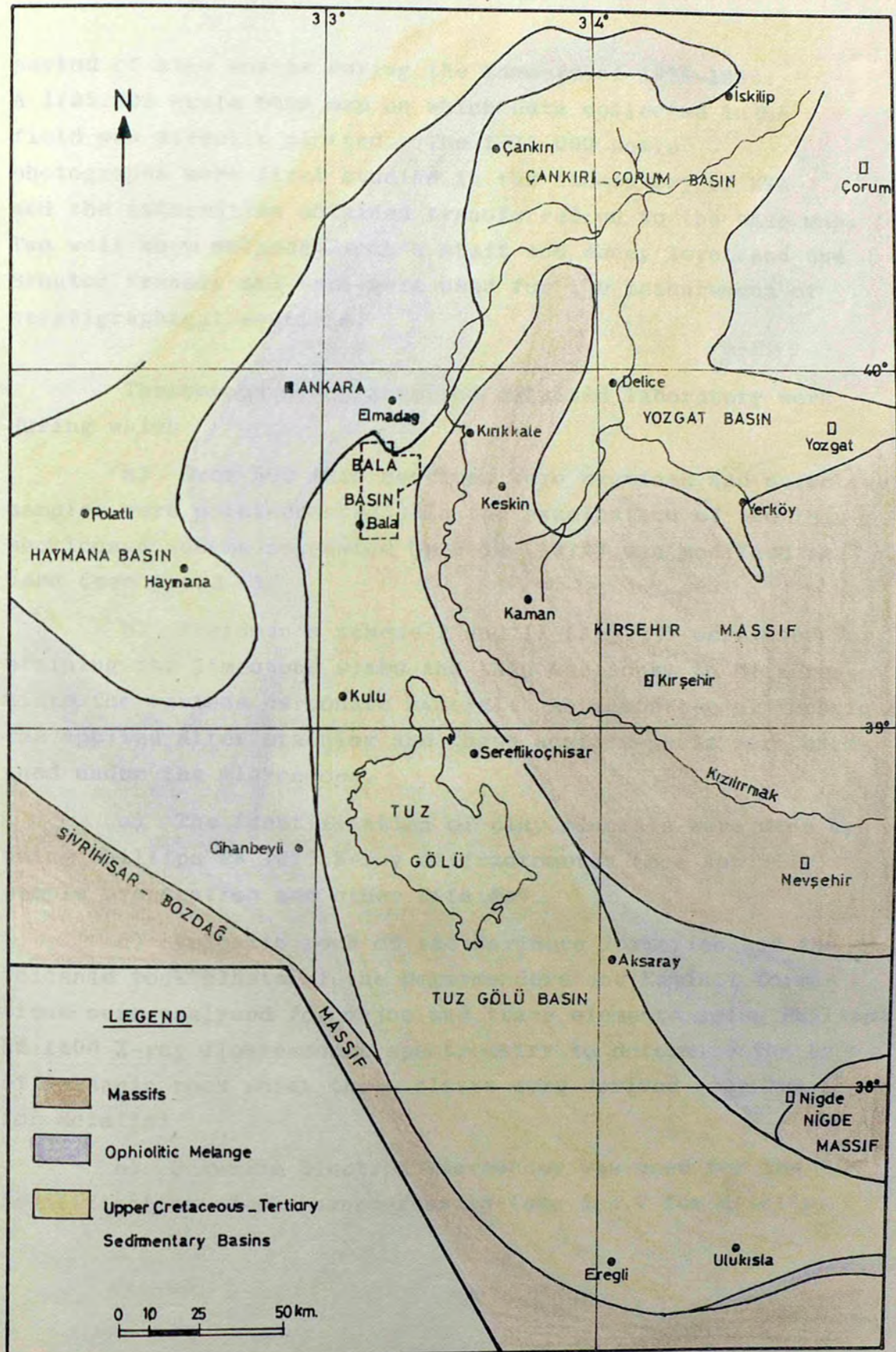


Fig 1.3. Geological location map. Area studied for this thesis is also shown.

period of nine months during the summers of 1978-1980. A 1/25.000 scale base map on which data collected in the field was directly plotted. The 1/35.000 scale photographs were first studied in the laboratory of MTA and the information obtained transferred on to the base map. Two well know methods-Jacob's staff and Abney level and the Brunton transit and tape-were used for the measurement of stratigraphical sections.

The second stage involved detailed laboratory work during which

a) Over 500 thin sections were examined and selective samples were point-counted. In the examination of the thin sections a scheme suggested by Folk (1974) was modified and used (see App. I)

b) Freidman's scheme I and II (App. II) were used for staining the limestone slabs and thin sections, to differentiate the various carbonate mineral. An acetate-peel technique was applied after staining and these acetate-peels were examined under the microscope.

c) The identification of clay minerals were made by using Phillips PW 1010 X-ray diffractometer (see App. III) sample preparation and other details).

d) Volcanic rock of the Saridere formation and the volcanic rock clasts of the Degirmendere and Kamisli formations were analysed for major and trace elements using Phillips PW 1400 X-ray flourescence spectrometry to determine the type of volcanic rock which these clasts were derived (see App. IV for details)

e) Scanning Electron Microscopy was used for the identification of the nanno-fossils (see App. V for details)

1.4 Nomenclature:

4a Rock colour: determined by comparison with the Rock-Colour Chart published by the Geological Society of America.

4b Grain size and shape: Wentworth's (1922) grain size scale was used. In the field, the UCL grain size comparator which was prepared according to Wentworth (1922) was used. The shape of the clasts of conglomerate was determined by using the method described by Zingg (1935)

4c Roundness, fabric and textural maturity: Roundness of the clasts of conglomerate and grains of sandstone were described by comparing them to the visual chart proposed by Powers (1953). The term fabric is reserved for "the manner of mutual arrangement in space of the components of a rock body and of the boundaries between these components" (International Tectonic Dictionary). Therefore fabric has included grain orientation, packing proximity and grain contact types. (For details see App II) Textural maturity of clastic rocks was determined using the scheme proposed by Folk (1974) (see App. I)

4d Quartz types of the detrital grains were established by using criteria suggested by Folk (1974).

4e Classifications of sedimentary rocks: For the classification of conglomerate the terminology proposed by Pettijohn (1975) was used (Fig 1.4B) Folk's (1974) classification was adopted for sandstones (Fig 1.4C). Carbonate rocks were named by using Dunham's (1962) terminology (Fig 1.4A)

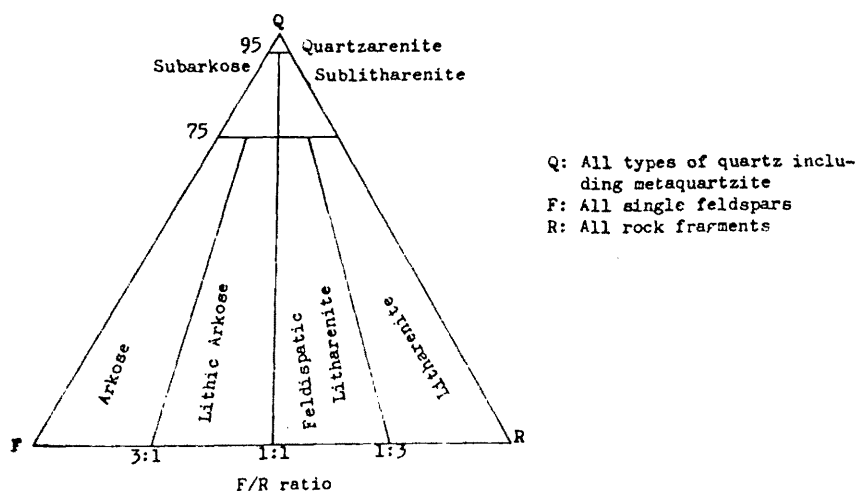
4f Classification of pyroclastic rocks: Fisher's (1961) grade size definition was adopted (Fig 1.5A) The term tuff which was further classified according to the terminology proposed by Pettijohn (1975) (Fig 1.5C) was determined using Fisher's (1966) classification for size mixtures of pyroclastic fragments (Fig 1.5B).

DEPOSITIONAL TEXTURE RECOGNIZABLE					DEPOSITIONAL TEXTURE NOT RECOGNIZABLE
Original components not bound together during deposition			Original components were bound together during deposition		
Contains mud		Lacks mud and grain-supported			
Mud-supported	Grain-supported				
Less than 10 % grains	More than 10 % grains				
<u>Mudstone</u>	<u>Wackestone</u>	<u>Packstone</u>	<u>Grainstone</u>	<u>Boundstone</u>	Crystalline carbonate

A- Dunham's classification of carbonate rocks (1962)

EPICLASTIC	Extraformational	Orthoconglomerates (matrix < 15%)	Metastable < 10%	Orthoquartzitic(oligomict) cong.
			Metastable > 10%	Petromict conglomerate(limestone cong., granite cong., and so on
		Paraconglomerates (matrix > 15%)- diamictites	Laminated matrix	Laminated conglomeratic mudstone or argillite
			Nonlaminated matrix	Tillite (glacial)
				Tilloid or Gerollton(nonglacial)
		Intraformational Intraformational conglomerates and breccias		
PYROCLASTIC	Volcanic breccias and agglomerates			
CATACLASTIC	Landslide and slump breccias			
	Fault and fold (Reibungs) breccias;"tectonic moraines"			
	Collapse and solution breccias			
METEORIC	Impact breccias			

B- Pettijohn's (1975) classification of conglomerates and breccias.

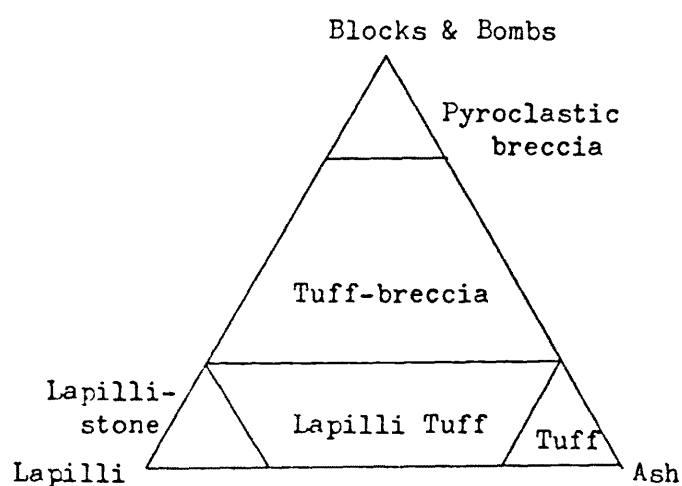


C- Folk's classification of sandstones (1974)

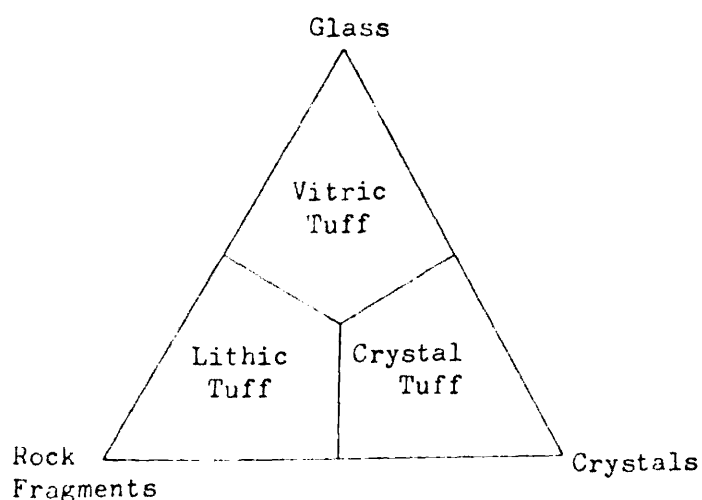
Fig. 1.4. Classifications used for sedimentary rocks.

Grade size (mm)		Pyroclastic fragments	
256	64	Coarse	Blocks and Bombs
		Fine	
		Lapilli	
2			
1/16		Coarse	Ash
		Fine	

A- Grade size limits for pyroclastic fragments.(Fisher 1961)



B-Rock terms for size mixtures of pyroclastic fragments.(Fisher 1966)



C- Compositional classification of tuffs.(Pettijohn 1975)

Fig. 1.5. Classifications used for pyroclastic rocks.

4g Definitions of terms olistolith, slump deposits and melange: The term olistolith was used for the blocks which are bigger than four metres in diameter and found in submarine slump deposits (Abbate et al 1970). The use of the term olistostrome was avoided due to considerable confusion in the use of this term in geologic literature. Instead sediments deposited by submarine sliding and slumping were called submarine slump deposits. Melange, as in the case of Ankara melange, is defined in this thesis as: "a body of chaotically mixed rocks, containing diverse rock types" and processes involved during its formation are not clearly distinguished (see I for detail discussion)

4h Definition of diagenetic terms: Terms which were used to describe diagenetic features in limestone were adopted from Folk (1965) and Bathurst (1976)

Replacement: One mineral replaces another of different composition e.g. feldspar - calcite.

Inversion: A mineral is replaced by its polymorph without going through void stage e.g. aragonite - calcite

. Recrystallization: An undeformed mineral changes its form grain size or orientation e.g. calcite mud or fibres - calcite mosaic etc.

Neomorphism: Describes the process in which an older mineral is replaced by new crystals of the same mineral or a polymorph.

Aggrading neomorphism: A mosaic of finely crystalline carbonate is replaced by a coarser mosaic.

Solution Cavity Fill: A mineral dissolves leaving a cavity which was filled later by another mineral

Micrite: Carbonate mud formed by crystals of 1-4 micron in diameter

Microspar: 4-40 micron-sized calcite crystals forming a mosaic.

Sparry calcite: Calcite crystals coarsely crystalline then microspar and appear transparent in thin sections.

1.5 Previous Work: Many geological studies were carried out in the general region but as mentioned earlier no particular work on the Bala basin has been done. Therefore studies summarized in the following pages were done around the area studied. (Fig 1.6)

F. Baykal (1943) who was amongst the first to visit the area, noted that sedimentary rocks of Bala basin unconformably overlies the Ankara melange and considered these sediments Eocene in age.

The first comprehensive study in the region was published by Rigo de Rigi and Cortesini in 1959, in the Haymana-Polatli area. They described six different formations in the sedimentary rocks and mentioned the reefal character of the lower Cretaceous limestone. In 1960 C.G. Schmidt, working in the same area, noted three disconformities between the Eocene sedimentary rocks of the area and described two additional formations in the Palaeozoic and mid-Mesozoic. He also dated the Upper Cretaceous sedimentary rocks as being Campanian-Maastrichtian in age, in contrast to Rigo de Rigi & Cortesini's earlier conclusion of Cenomanian-Maastrichtian.

Stratigraphic Unit	System	Series	Stage	RIGO and CONTESINI 1959	SCHMIDT 1960	NORMAN 1972	ALTINER 1974	ARIHAN 1975	GÖKÇEN 1976	UNALAN et al 1976	BATMAN 1977	EMRE 198
PALAEZOIC	QUATERNARY	NEOGENE	Bar.	Alluvium				Alluvium	Alluvium	Alluvium	Alluvium	Alluvium
				Ağasiyirici Fm				Clastics	Sogulca Fm	Terri- genous	Deveci	Fluvial depos
					Horhor Fm	Bahsili Fm	Kolosmantepo Fm	Bula Fm.				Keklikpinari Fm
					Çayraz Fm	Kecilli Fm			Yamak Fm		Kartalteppe Fm	Kizil dag Fm
MESOZOIC	QUATERNARY	PALAEOGENE	Lut.									
MESOZOIC	QUATERNARY	Eocene	Ypr.									
MESOZOIC	QUATERNARY	Oligocene	Tha.									
MESOZOIC	QUATERNARY	Miocene	Mon.									
MESOZOIC	QUATERNARY	Pliocene	Dan.									
MESOZOIC	QUATERNARY	Upper Cretaceous	Maa.									
MESOZOIC	QUATERNARY	Lower Cretaceous	Cam.									
MESOZOIC	QUATERNARY	Triassic	San.									
MESOZOIC	QUATERNARY	Jurassic	Con.									
MESOZOIC	QUATERNARY	Triassic	Tur.									
MESOZOIC	QUATERNARY	Jurassic	Cen.									

In Altiner (1974) K:Kamışlı Fm, Y:Yanıkşir Fm, A:Ardıcılpinar Fm
 In EMRE (1984) KF:Kamışlı Fm, SVF: Sarıkaya Volcanic Fm, DF: Davdanlı Fm
 (Shaded areas represents non-deposition or erosion)

Fig 1.6 - Comparison of lithostratigraphic units presented here with previous regional studies

In 1972-1973, T.N. Norman published the findings from his studies on the Upper Cretaceous-Lower Tertiary sedimentary rocks of the Kirikkale-Yahsihan area. In this detail sedimentological work he proposed two different stratigraphical columns in the west and east and differentiated seven formations in the west and six formations in the east, by giving detailed description of the sedimentary rocks and their facies interpretation. He also concluded that these sediments were deposited on the ophiolitic part of Ankara melange (Irmak formation) without an apparent disconformity.

Altiner (1974) working in the area between Kamislibala and Keklice, attempted a palaeontological zonation of the sedimentary rocks and gave a list of fossil assemblages.

Following these works, a regional study covering the Tuz gölü, Haymana and Bala basins was made by Arikan (1975). He measured several sections from the sedimentary rocks of the above mentioned basins with particular attention given to the Tuz gölü basin and came to the conclusion that the Tuz gölü basin was evolved within a NW-SE aligned, elongate, intra-continental structural trough and contains over 10.000 metres of sediment which represents a complete sedimentary cycle. He also noted that the uplift of the Haymana basin after the deposition of the Middle Eocene nummulitic limestone resulted in the separation of the basin from Tuz gölü basin which were parts of a single depositional site during the Upper Senonian-Middle-Eocene time interval. The Tuz gölü basin's relation with the Bala and Cankiri-Corum basins was first established in the Palaeocene and continued to the end of the Upper Eocene and possibly into the Oligocene.

In 1976 S.L. Gökçen and Unalan et al separately published their findings on the stratigraphy and sedimentology of the Haymana basin, paying particular attention to the sedimentology and reported that the Upper Cretaceous-Lower Tertiary

sediments of this area consist mostly of flysch sequences which include re-sedimented conglomerate, limestone and sandstone turbidites. Unalan et al (1976) working in the northern part of basin, concentrated on the general stratigraphy and structural geology and concluded that the sedimentary rocks were deposited on the Ankara melange with a marked discontinuity in a NW-SE aligned basin which on both flanks showed down-to-basin step faulting.

The most recent studies in the region have been made by Norman et al (1979 and 1980). In these studies an attempt was made to correlate the Upper Cretaceous-Lower Tertiary sedimentary rocks of the Haymana, Sungurlu and Kirikkale areas. They suggested that these sediments were deposited mostly on the Ankara melange formation within a series of interconnected basins.

1.6 Regional geological setting of the Bala area.

1.6.1. Kirsehir Massif:

The Kirsehir massif is exposed in the E and SE of the Bala area and composed of gneiss and amphibolite in the lower part and marble/calcschist, quartzite/quartziteschist and micaschist in the upper part. (Erkan 1981, Seymen 1981). These rocks are thought to be the product of a medium pressure/high temperature regional metamorphism of a sedimentary succession of orthoquartzite, siltstone, sandy marl and shale. (Seymen 1981). The age of the metamorphism of these rocks is still hotly debated and ages ranging from Ordovician (Brinkmann 1976) to immediately pre-Cretaceous (Erkan 1981) and just pre-Palaeocene* (Goncuglu 1981) have been proposed. The Massif was cut by a number of mainly granitic plutons, one of which is Karaca ali pluton (see below), during the Upper Cretaceous and Early Palaeocene interval.

* This age is given to Nigde Massif (see Fig 1.3) which is generally considered to be the southern-most extension of the Kirsehir Massif.

1.6.2 Ankara Melange

The Ankara Melange has a limited exposure in the northern and southeastern corners of the area studied (see Map I) and while only general purpose mapping and some random sampling with no detailed work was carried out by the author, its importance as a source area and its role in the geotectonic evolution of the region make it necessary to give a short account of its distribution, field relations, rock types and tectonic style here.

The term Ankara Melange was first used by Bailey & McCallien (1950, 1953) for a stratigraphical succession containing blocks of limestone, serpentinite, radiolarite, pillow lavas, ultramafic and sedimentary rock within a sandstone, shale and/or tuff matrix. It is probably the most complex lithological unit in Turkey not only because of the complexity of its geology but also due to the confusion caused by mis-interpretations and lack of stratigraphical unity in the geological literature. As it can be seen in Fig 13.5 the Ankara Melange is not a single Melange but is comprised of at the least two melanges separated in time and space. Any attempt to explain this unit as the product of a single event must be wrong. (see below). Here the Ankara Melange is divided into three lithological units

a. the Triassic lower part, called Karakaya formation, following Bingol's (1976) nomenclature

b. the middle part composed of Jurassic carbonates, and

c. the Cretaceous upper part which will be discussed under the heading of Ankara Melange.

a. the Karakaya formation which has been given different local names (Dikmen greywackes (Erol 1956), Melange with metamorphic blocks and Melange with limestone blocks (Norman 1975), Hisarlikaya formation (Batman 1978 a,b), Ankara Flysch (Erk 1980) and Kosrelik formation (Akyurek 1981)), consists

of sericite schist, chlorite schist, calcschist and partly well preserved meta-sandstone, meta-conglomerate and meta-volcanic (spilite and diabase) intercalations in the lower part and conglomerate sandstone, siltstone, mudstone, chert, volcanics and limestone alternations together with abundant clastic and limestone blocks in the upper part of the formation (Akyurek 1981, Norman 1975). Meta-periolodite and diabase dykes cutting the metamorphics in the lower part of the formation have also been reported. (Akyurek 1981, Akyurek et al 1979). The clastic and limestone blocks are Permian and Carbonifereous in age and reported to be found in large wash-out channels (Akyurek 1981). These lithologies are believed to be deposited mainly as distal and proximal turbidites within a small marginal sea which was opened due to the Early Triassic rifting (see sections 13.2 & 13.3) Sengor & Yilmaz 1981 and Bingol 1976.

b. Jurassic carbonates overlie the Karakaya formation with an angular unconformity and consist of basal conglomerates (clasts of which were mainly derived from the Karakaya formation) at the base and red to grey limestone and marl intercalations towards the top. This unit is believed to be deposited in quiet platform conditions (Sengor & Yilmaz 1981, Akyurek 1981, Unalan 1981, Batman 1978 a, Arikan 1975)

c. The Ankara Melange which also has a number of local names (e.g. serpentinite - radiolarite series (Erol 1956), Coloured melange (Gannser 1959), Melange with ophiolitic blocks (Norman 1975), Derekoy formation (Unalan et al 1976, Batman 1978 a, b) and Eldivan ophiolitic complex (Akyurek 1981),) shows significant changes in thickness, stratigraphical arrangement of particular rock types and in tectonic style in different parts of the region. Here it is divided into two units in order to simplify the description. The first Unit (Unit I) is exposed in the area between Kalecik and Elmadag (ENE of Ankara) (see Fig 13.4 & 5) and was described by Akyurek et al (1979) and Akyurek (1981). It consists of periodite dunite, harzburgite and pyroxenite at the base gabbro and diabase

dykes in the middle and spilitic pillow lavas and pelagic sediments towards the top, indicating a complete oceanic crust setting. The lower boundary of Unit I with the underlying Jurassic carbonates or with the Karakaya formation, where the former is absent, is always tectonic, while its upper boundary with a Senonian - Maastrichtian flysch succession which contains levels of ophiolitic olistostromedeposits, is a disconformity. This unit is thought to be emplaced from the N (present geographical position) as a nappe during the Albian-Aptian interval. The second Unit (Unit II) of the Ankara Melange covers vast areas in the region and is exposed SSE of the Unit I. (Fig 13.4) It is made up of chaotically mixed blocks of agglomerates, pillow lavas, radiolarites, limestones, serpentinites, spilites, cherts, hornblendites, gabbros, diorites and diabase within an ophiolitic tuff, agglomerate and shale matrix. (Batman 1978 b, Arikian 1975, Norman 1972, 1975). However Unalan (1981) has separated the Unit II into i) a unit with limestone blocks which contains abundant Upper Jurassic-Lower Cretaceous limestone blocks within a turbiditic sandstone and shale succession, at the base and ii) ophiolitic melange which consists of serpentinite, limestone, radiolarite and various volcanic rock blocks within turbiditic sandstone and shale matrix and which is seen to the SE of Ankara. The former overlies the Jurassic carbonates or Karakaya formation with a distinct disconformity and passes up to the latter with a transitional boundary. According to Unalan the ophiolitic upper part has a transitional boundary with a Senonian flysch sequence. However he did not mention whether this flysch sequence is part of the Upper Cretaceous-Tertiary sediments.

Thicknesses ranging from less than 500 m (Norman 1972) to over 2000 m. (Unalan 1981, Ketin 1963) have been measured or estimated for Unit II and its lower boundary relation with the underlying lithologies varies from tectonic to a disconformity in different parts of the region (see Fig 13.5). The nature of its upper boundary is again controversial, for according to Norman (1972, 1980) it has a transitional boundary with

the turbidites of the Upper Cretaceous - Tertiary sediments, while Erol (1956), Ketin (1963), Arikan (1975) and Batman (1978) favour disconformity between these two.

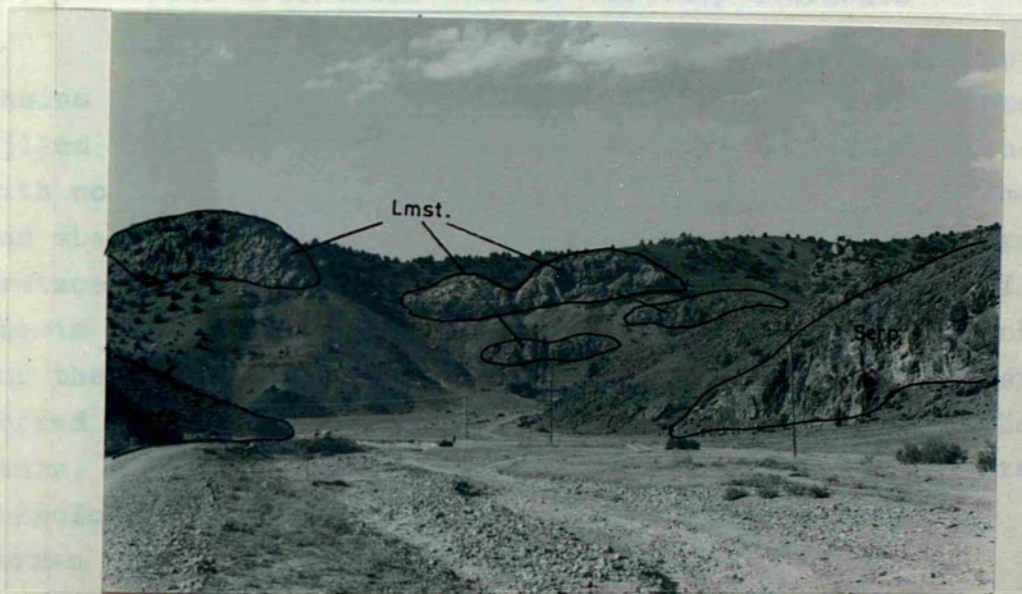
The age of Unit II could only be established on the basis of the ages obtained from the limestone blocks, since no age diagnostic fossil has been found in the matrix, (except in the unit with limestone blocks of Unalan (1981) where various species of Globotruncanas have been found and a Senonian age is given) and ages ranging from Lower Cretaceous to Campanian have been proposed.

Two models have been suggested for the formation of the Ankara Melange. The first one, proposed by Gansser (1959) and later supported by Norman (1975) and Unalan (1981), suggests a sedimentary melange origin involving large scale submarine slumping. The second argues a tectonic shearing during obduction (Hsu 1971). This view has recently been taken up by Gorur et al (1983) and the Ankara Melange has been interpreted as an accretionary prism against the Sakarya Continent.

In the area studied, the Unit II of the Ankara Melange has a faulted boundary with the overlying Upper Cretaceous - Palaeogene sediments and has two principal exposures. In the N it is made up of up to 1 km long serpentinite, radiolarite and basaltic pillow lava blocks (Plate 1.4) within a tuffaceous sandstone and shale intercalation with occasional conglomerates. The original bedding properties of the radiolarite (0.5-10 cm thickly bedded, structureless radiolarites, sometimes intercalated with 1-5 cm. thick reddish brown micritic limestone layers) and limestone (5-20 cm. thickly bedded recrystallized limestones) can be seen in larger blocks. The conglomerates are made up of well to subrounded serpentinite, radiolarite, limestone basalt and sandstone clasts and form up to 2 m. thick structureless beds. Sandstones are 10 cm. to 2.5 m. thick and are structureless to graded. In the ESE of the area studied a lithological unit containing bedded dolerite lavas, spilitic

pillow lavas, red silty sandstone and turbidite conglomerates and tuffaceous sandstones, can be observed. (Norman 1972). (Due to extremely poor exposure no work by the author has been done on this unit). On the basis of lithological and age similarities it is thought to be equivalent to the Ankara Melange (Norman 1980, 1973). An Upper Cretaceous (post-Campanian) age is proposed for the upper part of both units. (Norman 1973)

Upper Cretaceous - Early Tertiary Sediments



Neogene Deposits

The Neogene deposits of the Ankara Melange Formation of Gura.

Plate 1.4 - This shows blocks of serpentinites and limestones within the volcanoclastic sandstone and conglomerate matrix of the Ankara Melange at Kamislidere (J4)

In the 5 where a lacustrine-sandstone sequence of deposition is suggested for these units (Norman 1973). In the area studied, the Neogene deposits are described and similar to the 5 where a lacustrine-sandstone sequence of deposition is suggested for these units (Norman 1973). The Neogene deposits are described and similar to the 5 where a lacustrine-sandstone sequence of deposition is suggested for these units (Norman 1973). The Neogene deposits are described and similar to the 5 where a lacustrine-sandstone sequence of deposition is suggested for these units (Norman 1973).

pillow lavas, red siliceous shales and turbiditic conglomerates and tuffaceous sandstones, can be observed. (Norman 1972).

(Due to extremely poor exposure no work by the author has been done on this unit). On the basis of lithological and age similarities it is thought to be equivalent to the Ankara Melange (Norman 1980, 1972). An Upper Cretaceous (post-Campanian) age is proposed for the upper part of both units. (Norman 1972)

1.6.3 Upper Cretaceous - Early Tertiary Sediments

During the Maastrichtian to Palaeogene a number of small basins (Tuzgolu, Haymana, Bala, Cankiri-Corum) were formed and filled mainly by turbiditic conglomerates, sandstones and shales with continental red beds, sometimes with evaporites, limestones and shallow marine clastics in the basin margins. The Upper Cretaceous-Palaeogene sedimentary rocks are the subject of this thesis and will be discussed in detail in the following chapters. For the sediment succession of the other basins, the reader is referred to Unalan et al (1976) and Gokcen (1977) for the Haymana basin, Arikan (1975), Uygun (1981) and Gorur (1981) for the Tuzgolu basin, Senalp (1974) for the Cankiri-Corum basin and Norman et al (1980) for a general review.

1.6.4 Neogene deposits

The Neogene deposits (Cihanbeyli formation of Gorur 1981) overlie the older rocks of the region with an angular unconformity (Plate 1.5) and consist of sandstones, siltstone, claystone and tuff and basalt intercalation in the N and sandstone-siltstone, marl, tuff and evaporite intercalation in the S where a lacustrine-alluvial environment of deposition is suggested for these sediments (Uygun 1981). In the area studied, the Neogene sediments are brownish red, massive to crudely bedded and sometimes cross-stratified (Plate 1.6) semi-consolidated to consolidated, sandy conglomerates, muddy sandstones and sandy mudstones which are thought to be alluvial in origin.

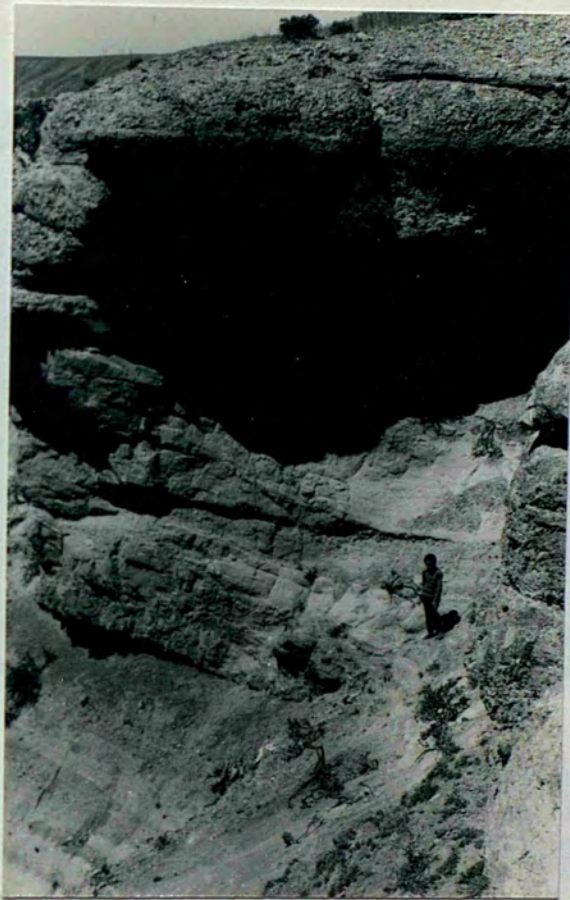


Plate 1.5 - Shows an angular unconformity between the Kizildag formation and the Neogene deposits. (E19)

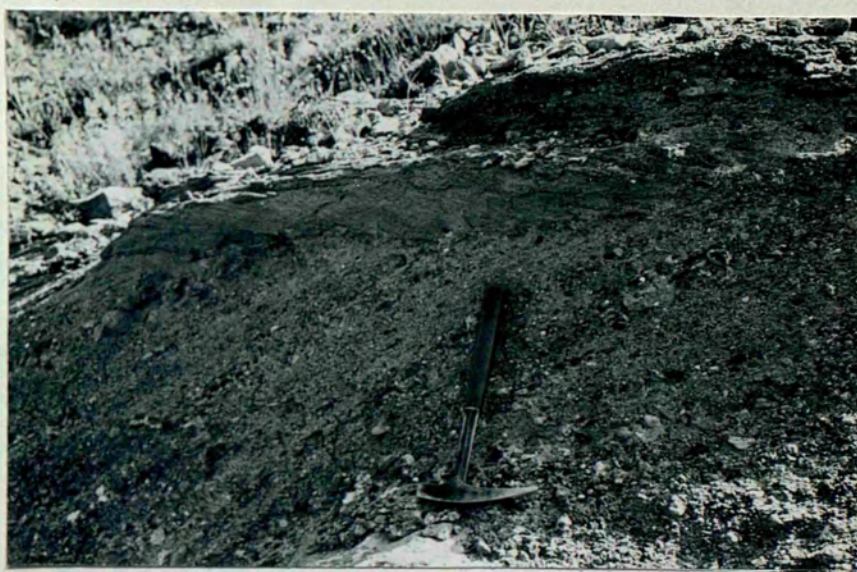


Plate 1.6 - Well developed cross-stratification
in the sandstones of the Neogene deposits
(D15)

1.6.5 Quaternary deposits

These sediments consist of modern alluvium in the valley of the area studied and are comprised of yellowish brown unconsolidated to semi-consolidated, poorly sorted and crudely bedded gravels, sands and silts. Clasts show compositional variations depending on the predominance of particular rock types in the local source area. Sands and silts predominate in downstream areas with occasional gravels.

1.6.6 Igneous Rocks

i Karacaali pluton

The Karacaali pluton is exposed in ESE of the Bala area and is part of the Upper Cretaceous - Lower Palaeocene igneous ring surrounding the Kirsehir massif from S to NE. It consists of acid-intermediate granitic rocks with rhyolite and felsite dykes and sills and was intruded through the Kirsehir Massif and Ankara Melange, metamorphising and metasomatising the contacts. The age of the emplacement is thought to be earliest Lower Palaeocene (Norman 1972)

ii Neogene - Quaternary volcanics

These volcanics cover large areas in the region and are the products of four main volcanic episodes in the Oligocene, Miocene (Aksaray volcanics), Pliocene-Pleistocene (Karacadag volcanics) and Pleistocene-Holocene (Hasandag volcanics). They are mainly basaltic and andesitic in composition and are thought to be related to post-collision volcanism (Tibetan type volcanism) (Sengor & Yilmaz 1981).

1.7 General stratigraphy of the Bala area.

A figure (Fig 1.7) illustrates in a simplified manner the relationships between the principal formations of the Bala area and links them to the stratigraphic column.

C H A P T E R 2

SARIDERE VOLCANIC FORMATION

2.1 General Introduction

With its generally white colour, this is one of the most distinctive formations in the area studied. It consists of andesites, dacitic tuff, ignimbrites and agglomerates with red to reddish brown conglomerates. The formation is best observed along the Saridere (R13) valley, the site of the type section.

The base of the formation could not be seen due to faulting (see Map I) and it is seen to start with crudely stratified ignimbrites and tuffs for the first 21 m of the section (Fig. 2.1). The following 19 m is dominated by relatively well bedded, sometimes indistinctively graded, 10-50 cm thick tuff beds which in some cases contain scattered pebble and cobble size ignimbrite clasts. The next 13 is made up of poorly bedded, up to 2 m thick, red to reddish brown conglomerates with some sandstones. Apart from a few parallel laminations in sandstones, no sedimentary structures are observed within these rocks. The next 22 m is dominated by massive ignimbrites and matrix supported agglomerates which occur in varying thicknesses and in random order. Ignimbrite blocks and boulders, sometimes with high sphericity and up to 6 m diameter also occur in this part. The remaining 41 m of the section consists of poor to well bedded (the latter is usually confined to the upper part) 20-70 cm thick, generally graded tuff beds and occasional well indurated, thin and poorly stratified ignimbrite layers and agglomerates.

The Saridere volcanics have an elongate exposure on the S-SE margin of the Bala basin, parallel to the general NE-SW trend and it forms a good stratigraphical marker. Andesites are observed between Keklice^{" "}k (M16) and Kucuksekid-^{" "}eresi (N16) without any stratification. Tuffs and ignimbrites

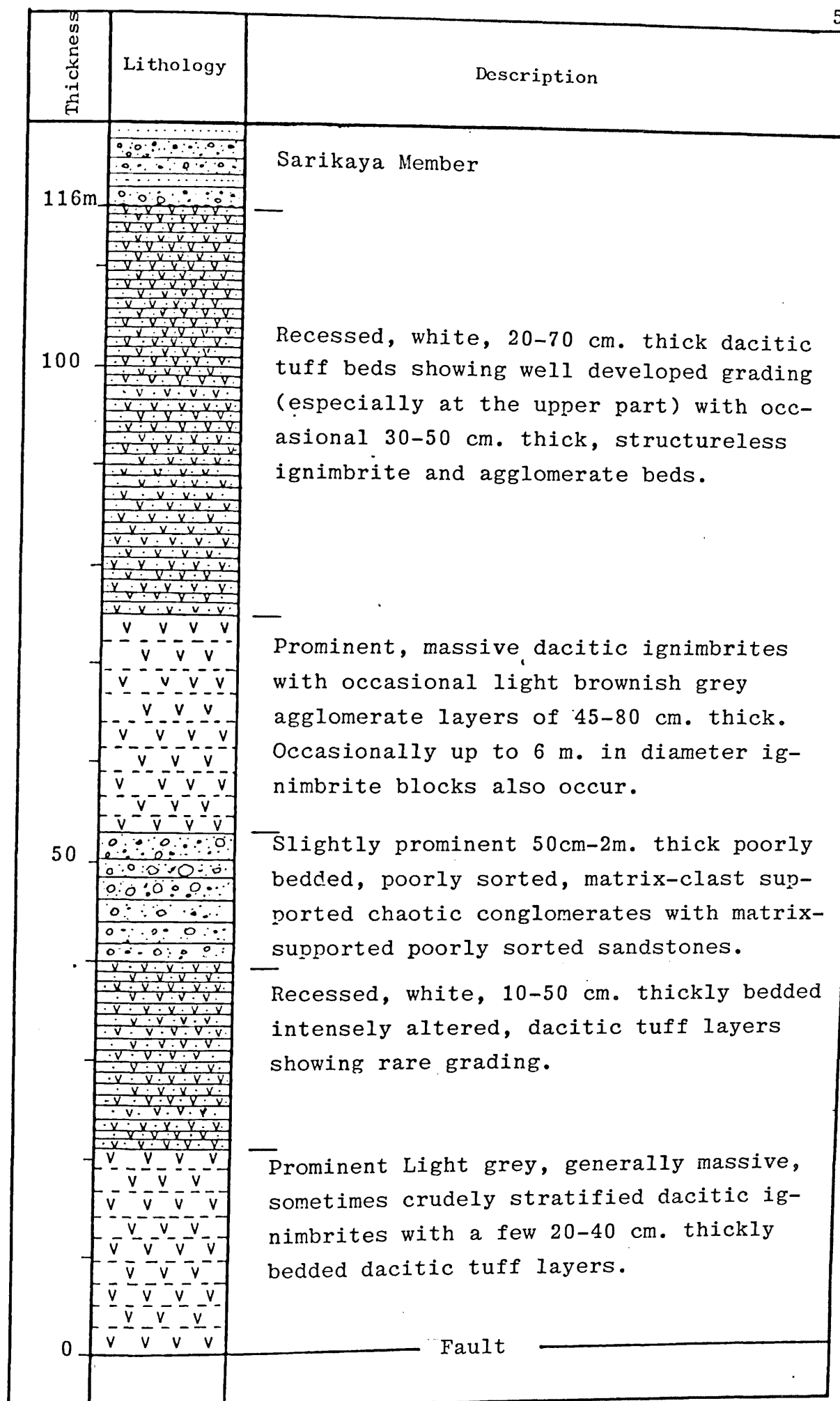


Fig 2.1 - Type section of the Saridere volcanic formation at Saridere valley (R13). Lithology is not to scale.

which overlies the andesites with an indistinctive erosional surface, are uniform in composition and appearance in the area between Kurebogazi (V8) and Sarikaya (Q14). Tuffs also occur in the area between Salaginbeltepe Hill (N17) and Fetik tepe Hill (L22), where tuffs are 20-30 cm thick and are randomly intercalated with red sandstones, and around Cingirdaklidedetepe Hill (F31). Conglomerates are found as two wedge shape bodies; the first occurs SE of Kurebogazi where it is thickest and thins towards the SW along the strike, the second is exposed around Camlibel Hill (Q14) and thins towards the NE. Although the thickness of this formation along the strike is not determinable due to faulting, tuffs appear to be thicker in the NE and die out towards SW and basinward i.e. to the NW. A 116 m sequence has been recorded in the Saridere section: the lower boundary of the formation is always faulted, therefore the stratigraphic relationship between the basement rocks and this formation is not known. The boundary of this formation with the overlying Sarikaya member (Chp.6), in most cases, is rather difficult to determine due to poor exposure caused by intense alteration and staining of tuffs by iron-oxide percolating from the overlying red beds. However in areas where these two formations are well exposed, an angular disconformity between these two formations is observed. (Plate 2.1)

2.2 Andesite

2.2.1 General description

Andesites are a moderate yellowish brown (10 YR 5/4) and occur as a massive unit at the base of the formation. Macroscopically they show porphyritic texture in which medium to large, white plagioclase and dark brown mafic mineral phenocrysts stand out within a light brown groundmass. Their compositional and textural properties are rather constant along the exposed outcrop and they are less affected by alteration than the tuffs.



Plate 2.1 - Shows the angular disconformity between the dacitic tuff of the Saridere volcanic formation, dipping with 45° - 50° to the left and red conglomerates and sandstones of the Sarikaya member dipping 18° - 25° to the left, at Kurebogazi (U8).

Microscopically, the andesites contain plagioclase, clinopyroxene and mica-phenocrysts set in a fine grained, sometimes cryptocrystalline, groundmass which is made up of randomly distributed plagioclase microliths, opaque minerals and microcrystalline quartz (most probably due to devitrification). (Plate 2.2)

Plagioclases are usually large to medium euhedral phenocrysts and although they show carlsbad, combined carlsbad and albite, pericline, albite twinning and normal zoning, the last two appear to be dominant types. Plagioclases are andesine - labradorite in composition (determined by extinction angles of 24° - 30° on plagioclase crystals with albite twinning) and usually show varying degrees of alteration.

Clinopyroxenes consist of generally medium to fine crystals and in most cases have been strongly altered. It is almost, therefore, impossible to determine the clinopyroxene precisely by optical means. However, in some relatively well preserved examples, irregular patches which show clinopyroxene can be observed and, on the basis of extinction angles which are symmetric and 38° - 42° , augite or diopside can be suggested.

Micas are biotite showing strong pleochroism and parallel extinction and occur as large flakes. Biotites, too, are intensely altered to chlorite and in some cases to limonite and haematite.

Quartz, together with magnetite and other unidentified heavy minerals, occurs as an accessory mineral.

Chemical composition of these rocks (Ch. 12, Table 12.1) shows that they contain 57-61% SiO_2 and are notably rich in Al (17-19%).



Plate 2.2 - Photomicrograph of a porphyritic andesite. Euhedral plagioclase (labradorite-andesine) and clinopyroxene (slightly darker coloured than plagioclase) phenocrysts within cryptocrystalline matrix which contains plagioclase microliths. The black patches are clinopyroxenes which are completely altered to iron-oxide. Sample 767-II, 15x XN.

On the basis of their mineral composition and texture, together with their chemical composition, these rocks may be called andesites, belonging to the calc-alkaline orogenic suite (Hatch et al. 1972, Gill 1981).

2.3 Dacitic tuff and ignimbrites

2.3.1 General description

Tuffs and ignimbrites are white (N9) to medium light grey (N6) and together make up the substantial proportion of this formation. In outcrops and under the microscope both rock types can, in most of the cases, be easily identified. The ignimbrites are generally darker in colour, unstratified to poorly stratified and are relatively better preserved than the tuffs which are almost completely altered and show bedding and grading. In outcrop, ignimbrites occur as bold massive units within the soft earth-like masses of tuff. Bedding properties in tuffs are only observable in the outcrops which show lesser degrees of alteration and where 10-70 cm thickly bedded and graded beds are observed. (Plate 2.3)

Microscopically, ignimbrites and tuffs are differentiated by their degrees of preservation and abundance of phenocrysts. The latter are relatively well preserved, unbroken and abundant in the ignimbrites. Both rocks are made up of partially to completely altered feldspars and mica phenocrysts with a small amount of quartz, set in a chert-like groundmass which most probably resulted from the devitrification of original volcanic glass, shard structures of which, in some cases, are visible as dark curved, spiculelike shadows. (Plate 2.4)

Feldspars are generally medium to large phenocrysts, euhedral in the ignimbrites and usually broken in the tuffs. Their identification is rather difficult due to kaolinization, vacuolization and, in lesser amounts, sericitization (or



Plate 2.3 - Shows parallel, laterally continuous bedding of dacitic tuffs, underlying the red conglomerates of Sarikaya member. Locality (R13)

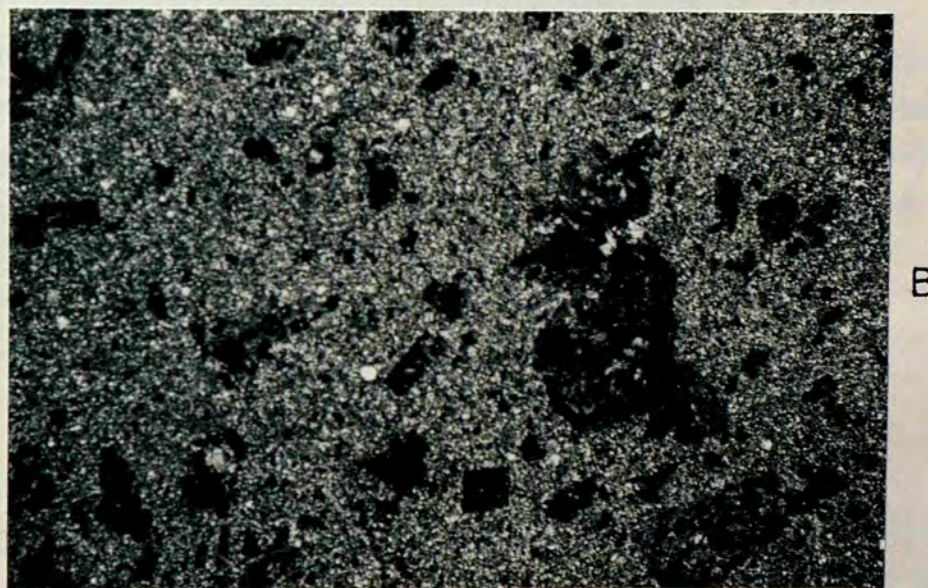


Plate 2.4 - Photomicrographs of dacitic ignimbrite and tuff.

- A. Ignimbrite with porphyritic texture is mainly composed of K-feldspars some of which (black ones in the photograph) shows vacuolization, quartz and mica within a fine grained chert-like groundmass. Sample 1271, 15x.
- B. Tuff contains intensely altered K-feldspar phenocrysts within chert-like groundmass. Sample 744, 15x, XN.

illitization) and replacement of feldspar by calcite. Kaolinite which gives the white colour to these rocks, forms tiny flakes on the feldspar crystals and is identified by its very low grey birefringence. Vacuolization is the second most common type of alteration and appears cloudy and brownish in thin sections. Sericites or illites appear as bright white to yellowish red flakes under the crosspolarized light and have moderate indices and high birefringences. When unaltered, feldspars are generally orthoclase with subordinate amounts of microcline and plagioclase. Orthoclases usually occur as subhedral and anhedral forms and show carlsbad twinning.

Micas also, are strongly altered to dark isotropic brownish masses which are most probably limonite or chlorite, and show strong pleochroism and parallel extinction.

Although an optically based compositional classification of these rocks is not possible due to alteration, on the basis of their chemical composition (Table 12.1) which shows 65-68% SiO_2 , and their textural characteristic, they may be called dacitic crystal tuffs and ignimbrites (Hatch et al. 1972, Pettijohn 1975, and Gill 1981)

2.4 . Agglomerates

2.4.1 General description

Agglomerates are found closely associated with ignimbrites and are almost entirely composed of dacitic ignimbrite and tuff clasts. They are matrix supported and do not show any sedimentary structures. Clasts of the agglomerates are 3 mm to 5 cm in diameter and generally rounded to well rounded. The matrix is tuff which consists of a few fine feldspar crystals and microcrystalline quartz. Plate (2.5)

2.5 Conglomerates

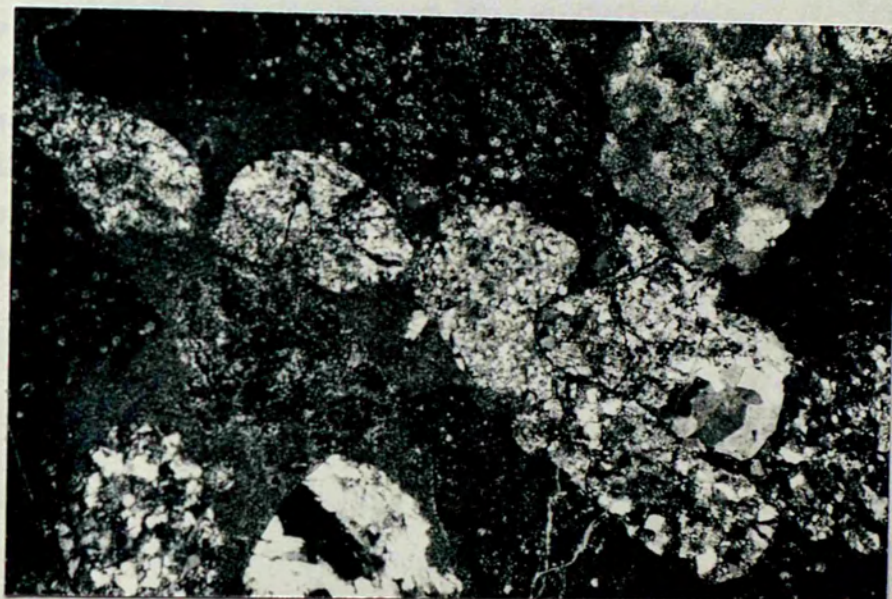


Plate 2.5 - Photomicrograph of agglomerate. It contains subrounded-angular dacitic ignimbrite clasts of various sizes within a tuffaceous matrix. Sample 3.6, 15x, XN.

2.5.1 General description

Conglomerates of this formation are red to reddish brown, 0.5 to 2.5 m thickly bedded, poorly sorted and occasionally alternate with tuffaceous red sandstone beds. Although structureless, flat based and laterally extensive conglomerate beds predominate in some localities, lens shaped, graded conglomerate layers cutting these massive conglomerates, are observed. Sandstones are massive but may show locally developed parallel lamination and indistinct grading. Variations in depositional texture, ranging from matrix supported conglomerates to pebbly sandstone, depend on the amount of matrix present. Clasts of the conglomerates are usually angular although a few well rounded ones occur and range from granule to 35 cm diameter boulders. Compositionally, clasts are entirely composed of dacitic tuff and ignimbrites and some andesites. The matrix is tuffaceous sandstone and shows similar composition to the tuffs.

2.6 Age of the Saridere Volcanic Formation

Because of the absence of fossils, the true age of this formation is not known, however a relative age can be suggested on the basis of its stratigraphical relationships with other formations. The presence of dacitic tuff clasts and andesitic rock clasts within the Degirmendere formation, (Ch. 6) which is believed to be Lower Palaeocene in age, and the absence of any tuff deposition in the Degirmendere formation which would have been suggestive of a contemporaneous igneous activity indicate that the Saridere formation was extruded before the Palaeocene. Additionally the presence of tuff beds and abundant fresh feldspar grains which are compositionally similar to the feldspars of the Saridere formation in the Lower Maastrichtian Kamisli formation, further suggest that the volcanic activity may have started as early as Lower Maastrichtian.

2.7 Source and mode of deposition

The volcanic and volcanoclastic rocks of the Saridere



Plate 2.6 - Occurrence of conglomerates. Note the matrix supported nature and tuffaceous matrix of the conglomerates. Locality (V8).

formation resulted from calc-alkaline volcanic activity, as indicated by their chemical composition (see Ch. 12). The stratigraphic setting of andesites and dacitic tuff and ignimbrites (see 2.1), their calc-alkaline affinity and the presence of a granite batholith at the N-NE of the formation suggest that the volcanic rocks came from the same magmatic province as the granite. Such calc-alkaline provinces (e.g. present day Andes) typically evolve through several successive magma-differentiation processes and clearly preclude the necessity of deriving the different rock types from tectonically distinct provinces (A.D. Saunders 1983 pers. comm.)

Although the limited exposure and strong weathering and alteration of the andesites makes their mode of occurrence rather difficult to determine, the presence of continental red beds associated with these rocks, the absence of pillow-lava structure which is characteristic of submarine eruption (Hatch et al. 1972), together with the absence of any marine sediments associated with andesites suggest that they were resulted from a subaerial lava flow or flows. As may be expected from a siliceous magma of dacitic composition which was incapable of producing lava-flows due to its high viscosity, extensive pyroclastics were deposited in the form of tuffs and ignimbrites. The presence of parallel bedding and grading without current produced sedimentary structures indicate that the tuffs were deposited from ash-falls and were not reworked. The ignimbrites are deposited from ash flows. The presence of tuff layers which under and overlie the ignimbrites and which are unstratified and more intensely altered than the ignimbrites, may be explained by the differential cooling between upper, middle and lower parts of the ash flow (Hatch et al. 1972, Pettijohn 1975). Agglomerates most probably resulted from the accumulation of lapilli. The absence of fossils and the presence of red colouration in the conglomerates of this formation suggest an alluvial origin for these

rocks. The structureless, poorly sorted and matrix supported conglomerates and pebbly sandstones most probably resulted from debris flows and mud flows respectively (Bull 1972). The graded conglomerate lenses associated with the debris flow deposits were generally accepted to be deposited in stream channels at the upper part of an alluvial fan (Bull 1972, Reineck and Singh 1978, Collinson 1980). The conclusion that the conglomerates and sandstones of this formation were deposited as an alluvial fan, is further implied by the presence of a local source area, the angularity of the clasts of conglomerate which indicate short transport, little or no abrasion and the wedge shape geometry of these rocks. The occurrence of two wedge shape bodies along the strike further suggests that there were at least two separate alluvial fan developments.

C H A P T E R 3

KAMISLI FORMATION

3.1 General Introduction

Of Lower Maastrichtian age, this is the oldest sedimentary formation of the Bala basin succession and consists of monotonously interbedded dark green to greenish grey volcanically muddy sandstones and shales with occasional dusky yellow to dark green reworked tuff layers in the lower part and sandy conglomerates in the upper part of the formation. The formation is best observed along Kamislidere valley (K 6,7) between Kamislizir (K6) and Kamislibala (L7) and this valley contains the type section.

In the type section, beds are entirely overturned and the formation has two parts. The stratigraphically lower part continues to 579 m from the base of the section and consists of generally 10-40 cm thickly bedded medium to fine grained sandstones and/or siltstones intercalating with thickly bedded and well developed shales and thin marl beds with sandstone/shale ratio of less than one. The sandstone beds are generally Tbce* and Tde type and lack well developed sole structures. This sequence is frequently interrupted by mostly upward fining and thinning sequences which are made up of coarse to fine grained reworked tuff beds alternating with glassy fine grained ones. The reworked tuff layers are generally Tabe or Tabce type beds and sometimes occur as conglomeratic reworked tuffs which are always confined to the base of sequences. They show compositional differences in the stratigraphic column: while dark green plagioclase - rich beds occur in the lower portion of the lower part, dusk yellow to white, K-feldspar dominated reworked-tuff beds are present in the upper portion. The upper part of the formation is again formed by alternations of thin sandstone, siltstone, marl and

* The notation refers to Bouma's (1962) definition of turbidites

thick shale beds. But here this sequence is interrupted by large to small scale submarine slump folds, frequently succeeded by thick (up to 5.5 m) massive, coarse to fine grained sandstone beds. (Plate 3.1) These sandstone beds are, commonly, overlain by coarse to fine grained Tab or Tae type sandstone beds alternating with shale. The thicknesses of the submarine slump folds ranges from 1.5 m to 40 m and their sense of facing direction is towards the N and NE. The massive sandstone beds do not show any sedimentary structures apart from occasional indistinct grading and dish structures and sometimes contain large well rounded intraformational pebbles "floating" in the sandstone matrix. The long axes of these pebbles are orientated parallel to the bedding plane. (see App.VII for details)

3.2 Distribution, thickness and field relations

The Kamisli formation outcrops in and around Kamislizir, Kamislibala and Davdanli (I 10) in the N and NE of the area studied. It is aligned parallel to the general NE-SW trend of the Bala basin and is tectonically much disturbed. A number of small and large scale submarine slump folds are observed throughout the formation. The conglomerates of the formation occur as isolated beds and are especially predominant towards the top of the formation. They are unevenly distributed and most of the beds wedge out in short distances or occur as lenses which are at the least 120 m. long. Although intensive faulting prevents accurate correlation, bed thickness, grain size of sandstones and sandstone/shale ratio of the formation appear to be constant throughout the formation.

Faulting and folding prevent accurate measurements of thickness, but in the Kamisli section 1186 m have been recorded. The lateral extension of the formation to the SW could not be observed due to faulting and cover of younger sediments, but in the NE it continues for several kilometres (Ilıcapınar Formation of Norman 1972). The lower boundary of the formation with the Ankara Melange is a thrust fault, thus



Plate 3.1 - Panoramic view of the Kamisli formation around Kamislizir. Beds are overturned. (Note a thick, massive sandstone bed overlying a slump fold towards the left of the photograph).

the nature of the boundary relation in the area studied, is not known. Unfortunately the boundary relationship of the Ankara Melange and the counterparts of Kamisli formation in the Haymana, Polatli, Tuzgolu and Kirikkale districts remains a controversy, a full account of which is given in section 1.5 and is discussed in detail in section 1.6. The upper boundary of the formation is best observed near Kamislibala where green-grey shales of the Kamisli formation gradually pass up to the yellowish brown shales of the succeeding Davdanli formation (Chp. 4)

3.3 Conglomerates

3.3.1 General description

Conglomerates are purplish brown to mixed red, greyish white and green in colour and predominate in the upper part of the formation. They are generally disorganized types, although some poorly graded layers also occur. Beds of the conglomerates, 70 cm to up to 12 m thick, show wedge and lens shape geometry and have sharp contacts with the under - and overlying beds without any erosional bases. (Plate 3.2) The conglomerates show marked compositional changes in different localities e.g. a 12 m thick conglomerate bed around Yesiltepe (L6) thins towards the NE and SW along the strike and is made up of a chaotic mixture of irregularly orientated serpentinite, radiolarite and limestone gravel and boulders set in a volcanoclastic sandstone matrix. In the area around Davdanli the conglomerates consist predominantly of volcanic rock clasts with subordinate amount of radiolarite, serpentinite, limestone and intraformational pebbles.

The size of the clasts ranges from granule^s to boulders but they are generally pebble to cobbles in size. The clasts are generally angular to subrounded and are oblate to spheroidal in shape (Zing 1935). The conglomerates show considerable variation in texture (even in the same bed) and both clast and matrix supported textures can be found in close proximity to each other. Sorting of the conglomerates ranges



A



B

Plate 3.2 - Occurrences of conglomerates in the Kamisli formation. A) matrix supported conglomerate composed of limestone (White), volcanic rock, serpentinite, radiolarite clasts and intraformational pebbles. (Hammer is 30 cm. in length) Locality (K6). B) Clast supported conglomerate made up of volcanic rock clasts with subordinate amount of radiolarite serpentinite and intraformational pebbles. Locality (J9)

from poor to extremely poor: they are texturally immature and may be classified as diamictites (Pettijohn 1975)

Lithologies present as clasts are serpentinite, radiolarite, limestone, volcanic rock and intraformational pebbles. Each of these types may become proportionally important in different localities. Serpentinite clasts are easily distinguished by their bright green colour and in thin sections they are composed of serpentine mineral antigorite cutting and surrounding the partly altered olivine and clinopyroxene phenocrysts. Radiolarites are recognized, in the field by their red colour and in the large boulders of them, 2-10 cm thick parallel bedding is observed. Radiolaria have lost their internal structure through recrystallization. Limestone clasts are greyish white and are entirely made up of micrite. Large boulders of limestone show either massive or thin bedding. Volcanic rock clasts (VRC) are andesitic and basaltic. Andesitic clasts defined by their mineralogical and chemical composition (chemical composition of a VRC which is believed to be the representative of this group given in Chapter 12 and in Table 12.1), are dark brown to brownish-grey in colour and in thin section they are composed of plagioclase (labrodorite and andesine) with scattered hornblende and clinopyroxene phenocrysts within a cryptocrystalline groundmass which contains randomly orientated, small plagioclase crystals of acicular habit. Various degrees of alteration are observed in the phenocrysts. Basaltic clasts are made up of intensely altered mafic minerals (probably clinopyroxene) and small plagioclase crystals (labrodorite-bytownite) which form a trachytic (flow) texture.

Matrix of the conglomerates ranges from sand to silt and clay size material and is compositionally similar to the sandstones and shales of the formation. The matrix is poorly sorted and is sometimes replaced by neomorphic sparry calcite.

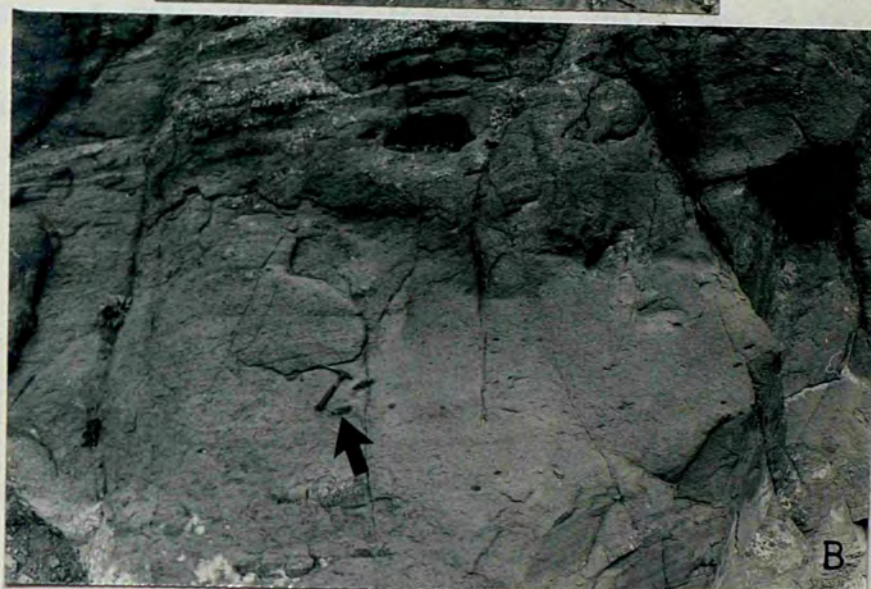
3.4 Sandstones

3.4.1 General description

Sandstones of the Kamisli formation are light olive-grey (5Y 5/2) to greyish-yellow (5Y 8/4) and occur in two different groups. Those which can appropriately be described by Bouma sequences are usually well cemented, coarse to fine grained and their bed thickness ranges from 5 cm to 150 cm. They sometimes occur as conglomeratic sandstones in which well developed grading, at the base of the bed, from granule size clasts to sand and eventually to parallel laminated silt size material, at the top, is observed. Bouma's complete combination of Tabcde is not found and beds with the divisions Tabce, Tabe (generally observed in coarse to medium grained and thick sandstone bed), Tbcde and Tde (usually in fine grained and thin sandstone beds) are observed. The beds appear to be laterally continuous although in some cases wedging-out of beds is seen. The most commonly observed sedimentary structures are graded bedding, parallel and convolute laminations and sole marks (flute casts are rare). These sandstones are relatively better sorted than the second group sandstones. The second group sandstones are generally structureless, coarse to fine grained, poor to well cemented, poorly sorted and sometimes contain large amounts of plant fragments in the upper parts of the beds. Some beds of this group sandstones occur as indistinctly graded thick (up to 4.5 m) beds in which dish structures and fluid escape pipes in the middle of the bed and parallel or convolute laminations at the top with scattered intraformational pebbles and shale and/or marl pebble and cobbles can be observed (plate 3.4). These sandstone beds generally have flat tops and bases and lack well developed sole marks. They are commonly found succeeding submarine slump folds and in some cases slump folds over - and underlying a thick sandstone of this type is also observed. Sandstones of this formation show compositional variation: some sandstones are predominated by



Plate 3.3 - Shows the typical occurrence of regularly bedded, Tbce and Tde type sandstone and shale alternations. Beds are overturned. The section shown is 21 m. from the top to bottom of the photograph. Kamisli section 9919



- Plate 3.4 - A. A massive sandstone bed overlying a small scale slump fold. Note the presence of various fluid escape pipes (dark branching figures) and dish structures, (dark lateral sinuous layers) (Hammer is 30 cm. in length) Kamisli section 9928)
- B. A massive sandstone bed with abundant intraformational sandstone marl and shale clasts. Note the random distribution of clasts and indistinctive grading of the bed. Bed is overturned. Kamisli section 9930.

feldspars others may be rich in volcanic rock fragments or skeletal grains. (Table 3.1). Thus the sandstones may be called lithic arkose with Feldspar/Rock fragment (F/R) ratios of one or more and feldspathic volcanic arenites with F/R ratio of less than one. (Plate 3.5)

3.4.2 Texture

The grain size of the sandstone ranges from coarse to fine but it is generally medium grained and there is no relationship between the composition and grain size. Generally the sand grains of the Kamisli formations sandstones are angular to subrounded. The roundness varies with composition in the case of volcanic rock fragments which are, relatively, more rounded than other grains. Grain contact types observed in the sandstones of this formation are highly variable, ranging from tangential to long, sutured and concave-convex, and they are randomly distributed. Packing proximity is between 30-60%. Sorting of sandstones is poor and they are texturally immature.

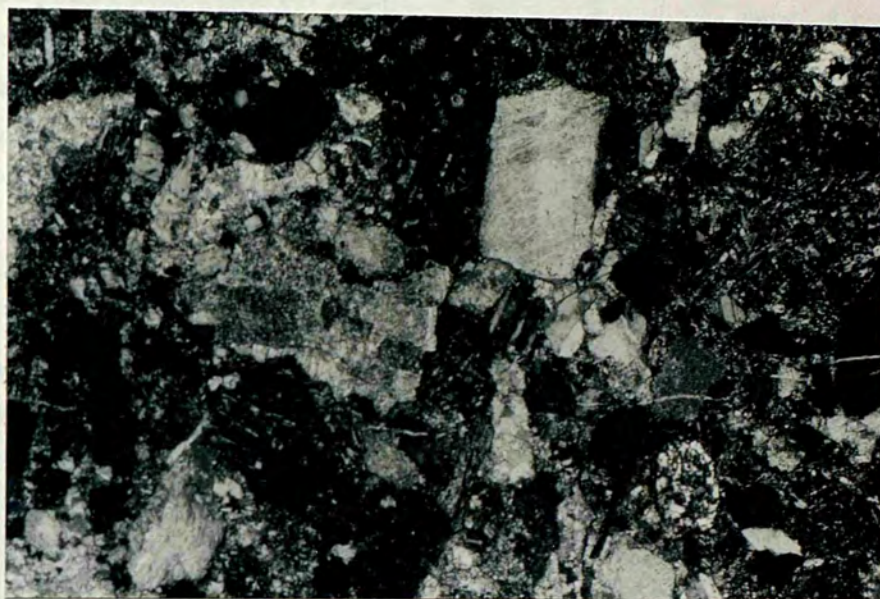
3.4.3 Framework grains

Volcanic Rock Fragments (VRF) occur in three different types. VRF which are composed of randomly orientated plagioclase microliths with or without plagioclase (labradorite - andesine) and/or strongly altered thus unidentifiable mafic mineral phenocrysts, which are believed to be andesitic in origin due to their compositional and textural similarities to the andesitic clasts of the conglomerates. The second type of VRF has a chert-like groundmass which sometimes shows "ghost" shard structures, and in some cases contains idiomorphic to subhedral feldspar and/or biotite phenocrysts. This type of VRF is thought to be of dacitic tuff or ignimbrite origin based on composition and the vitric groundmass. The third type of VRF is proportionally less than the previous two and shows either a trachytic (flow) texture, which is formed by the subparallel arrangement of microcrystalline lath-shaped feldspars, or a variolitic texture in which microcrys-

Parameters Sample No	Quartz	Feldspar	VRF	SRF	Cement	Matrix	Accessory Components	Others	Total %	Total Count
KZ-4	6.9	20.0	32.1	9.0	10.2	20.7	1.0	- -	99.9	508
KZ-26	8.4	17.7	34.5	4.8	11.1	18.9	1.2	3.4a	100.0	502
KB-84	5.8	25.8	26.0	11.7	5.8	20.2	4.7	- -	100.0	519
482	3.3	19.8	44.4	7.2	7.4	14.9	3.1	- -	100.0	516
576	3.3	28.5	28.3	0.9	3.6	12.5	3.6	19.2b	100.0	520
585	9.2	27.7	35.7	5.0	3.3	17.2	1.9	- -	100.0	514
592	3.1	33.8	13.8	3.8	0.2	38.0	7.3	- -	100.0	574
840	2.9	6.9	41.6	11.5	12.4	20.1	4.6	- -	100.0	522
478 (Tuff)	1.6	57.9	3.6	- -	- -	36.6	- -	0.3	100.0	503
480 (Tuff)	1.6	25.1	0.5	- -	- -	73.2	- -	- -	100.0	505

Table 3.1 - Modal composition of the Kamisli formation's sandstones.

a: Intraformational mud fragments, b: Clinopyroxene fragments.



A



B

Plate 3.5 - Photomicrograph of sandstones.

- A. Feldspar/volcanic arenite consists of volcanic rock fragments, feldspars and matrix. Sample 576, 35x, XN.
- B. Lithic arkose is mainly composed of feldspar, volcanic rock fragments and matrix. Sample KB-84, 35x, XN.

talline plagioclase fibres form a diverging or branching fan-like arrangement. Amygdaloidal cavities which are filled by calcite or chlorite are also observed in these VRF. These fragments generally do not contain any phenocrysts apart from very rarely observed, strongly altered mafic minerals, and thus are extremely difficult to assign to any volcanic rock clan by using their composition since, due to their fine size, the type of plagioclases could not be ascertained. However due to the existence of a variolitic texture, characteristic of crusts of basaltic pillow lavas (Hatch et al 1972), and the absence of K-feldspars, biotite and quartz, this type of VRF is thought to be of basaltic origin.

Though plagioclases are the most common type of feldspar, K-feldspars (orthoclase and sanidine) may become important in some thin sections. Plagioclase grains are often idiomorphic and subhedral and labradorite, andesine and bytownite occur in decreasing order of abundance. While albite twinning is the most observed twinning type, normal zoning and carlsbad twinning also occur. In some thin sections, the inner one or two zones of normal zonal plagioclase are replaced either by fine crystalline quartz or calcite microspars. Feldspars show varying degrees of alteration ranging from the unaltered to the completely altered. The alteration usually occurs in the form of vacuolization and kaolinization. The occurrence of completely altered feldspar grains in close proximity to the unaltered ones may indicate source, area alteration of the former.

Skeletal grains which are mollusc, brachiopod and echinoid fragments with some benthonic foraminifers either broken or as whole tests, are angular and may become proportionally important in some sandstone beds. (Table 3.1). The mollusc shell fragments retain their original shell shape but internal structure has been lost through recrystallization

Quartz show straight extinction with few inclusions and is generally a single quartz type. The quartz is of volcanic origin, angular and is quite rare. (Table 3.1)

Biotite, hematite, intensely altered mafic mineral (probably clinopyroxenes), which in one thin section constitutes 19.2% of the composition, chlorite and plant fragments occur as accessory components. The latter occur in the top of the sandstone beds.

3.4.4 Matrix and cement

The matrix of the sandstones which usually appears to be moderately to poorly sorted and cloudy under the microscope is composed of limonite, chlorite, micrite and microspar, sericite and/or illite and a few very fine grained quartz and feldspar grains.

Although no oxide and silica cement occurs, neomorphic sparry calcite which most probably resulted from the aggrading neomorphism of micrite, is frequently observed. It replaces the matrix, filling interparticle spaces: one neomorphic sparry calcite crystal as large as 500 micron with a poikilotopic texture was observed. In some cases partial replacement of feldspar and volcanic rock fragments by sparry calcite occurs.

3.5 Reworked-tuffs

3.5.1 General description

In the lower part of the formation some beds which are interbedded with glassy silt to clay grade layers, contain up to 98% feldspar crystals, together with some biotite, clinopyroxene and quartz of volcanic origin as detrital grains. The deposition of these rocks, because of their texture (see below) and composition, is believed to be closely related to volcanic eruptions in the source area (see 3.10). Thus to

differentiate these rocks from the sandstones of the formation, they are called reworked-tuff. The word reworked is used to express the secondary nature of these rocks in contrast to the primary pyroclastics which are deposited as a direct result of volcanic eruptions.

Beds of the reworked-tuffs occur in both upward fining and coarsening sequences thus their bed thickness ranges from 80-280 cm at the base, to 5-10 cm in the top part of the sequences. (Plate 3.6) They generally show grading, parallel and convolute laminations and also, some of the fine grained reworked tuff beds display flame structures (plate 3.7). On the basis of their feldspars, these rocks can be divided into two types. The first is dusky-yellow (5Y 6/4) (due to the alteration of feldspar to kaolinite) and consists of abundant, large to medium, idiomorphic K-feldspars together with plagioclase, volcanic quartz and biotite flakes within a very fine grained matrix which is glassy in parts and altered elsewhere. (Plate 3.8A) The matrix is always in high proportion and sometimes contains fine grained feldspar and quartz grains. Vacuolization is another alteration type of the K-feldspar which appears cloudy and brownish under the microscope. The second type of reworked-tuffs is light greenish-grey (5GY 8/1) grain supported and composed of abundant plagioclase (labrodorite and andesine) with a few percent of scattered clinopyroxene and volcanic quartz. (Plate 3.8B) The matrix of this type is fine grained and rich in chlorite.

Grain size of the reworked-tuffs varies from silt to coarse sand and granule size with grains always angular except for a few VRF which are subangular to subrounded. Descriptively, the reworked-tuffs of the Kamisli formations may be called crystal tuffs.

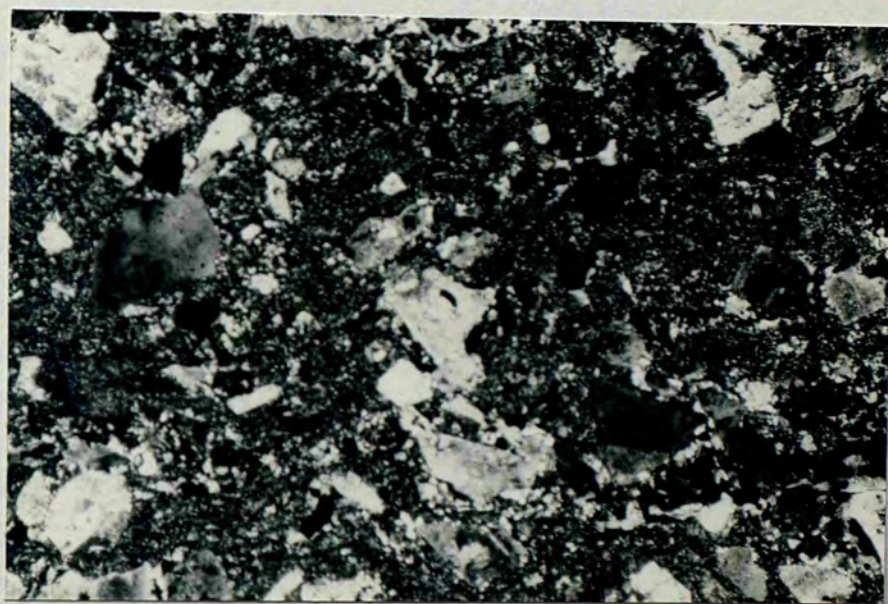
3.6 Shales and Marls



Plate 3.6 - The occurrence of thick and thinly bedded reworked-tuff layers. Beds are overturned (Hammer is 30 cm. in length). Kamisli section 9810



A



B

Plate 3.8 - Photomicrograph of re-worked tuffs.

- A. Crystal tuff: contains abundant K-feldspars with a few plagioclase in fine grained tuffaceous matrix. Sample 478, 35x, XN.
- B. Crystal tuff mainly consists of plagioclase with some K-feldspar within a tuffaceous matrix. Sample 480, 15x, XN

3.6.1 General description

Shales are light olive-grey (5Y 5/2), are found interbedded with conglomerate and sandstones and are tuffaceous. The thickness of a shale bed ranges from a few millimetres to 200 cm. Thick shale beds are usually structureless, though parallel thin beds are present locally. Thin shale beds generally occur on top of the graded beds as the "e" division of Boumas sequence and often show parallel laminations. They are very compact, although poorly cemented, medium thick shale beds occasionally occur. These contain abundant plant fragments in their upper parts. Shales are fine grained and contain a few detrital sand grains. Quartz appear to be the dominant sand size grain. In XRD analyses kaolinite, chlorite and illite are found.

Marls are light grey and are always found interbedded with Tde type sandstone beds. The thickness of the marl beds varies from 1 cm to 10 cm and they are generally structureless.

3.7 Sedimentary structures and current directions

The most frequent sedimentary structure is graded bedding. Convolute and parallel laminations are often observed in the upper part of graded beds. Sole structures are not always found but when present they are usually groove casts, prod marks and grazing tails. Flute casts are rare and generally confined to thick, coarse grained sandstone and conglomerate beds. Flame structures, low angle small cross-stratifications occur rarely. Submarine slump folds are widespread throughout the formation and occur on large and small scales. (Plate 3.9 & 10) The folds range from isoclinal to open and generally occur in successions which are predominated by shales. They can easily be distinguished from tectonic folds by the presence of undisturbed beds under - and overlying the folds. Their general sense of facing direction is towards the N and NE and when orientated to their original





A



B

Plate 3.10 - Large scale slump folds in A) the Kamisli type section and B) around Davdanli (J9)

position, they indicate slumping from S and SW. (see Fig 12.6)

Current directions are obtained by measurements of flute casts and when they are not present by groove casts, which generally indicate that flows were from the NE to SW, parallel to the basinal axis (Fig 12.6) Although some current reversals occur, they can be due to returning of turbidity current, free flow of which might have been obstructed by basin floor irregularities, probably a submarine slump fold, since there is no indication of a large scale ponding.

3.8 Weathering and alteration

Shales of this formation are weathered out due to their weak resistance against erosion. The sandstones and conglomerates, especially the well cemented ones, are more durable.

The light colour of the K-feldspar rich reworked-tuffs is the result of alteration of feldspars to kaolinite. Two other alteration products are limonite and hematite from the breakdown of iron-bearing minerals in the sandstones and conglomerates.

3.9 Fossils and age of the Kamisli formation.

Although shales of the formation do not appear to contain any Foraminifera, apart from some rare Globotruncana which could not be fully identified due to poor preservation, some marl beds contain nanno-fossils. (Plate 3.11) These are identified by O. Varol (pers comm) as being:

Prediscasphuera cretacea (Arkangelsky 1912) (Golina 1968)

Biscutum sp.

Woutsevaria sp.

Discorhabonus ignotus (Gorka 1957, Mawitivity 1971)

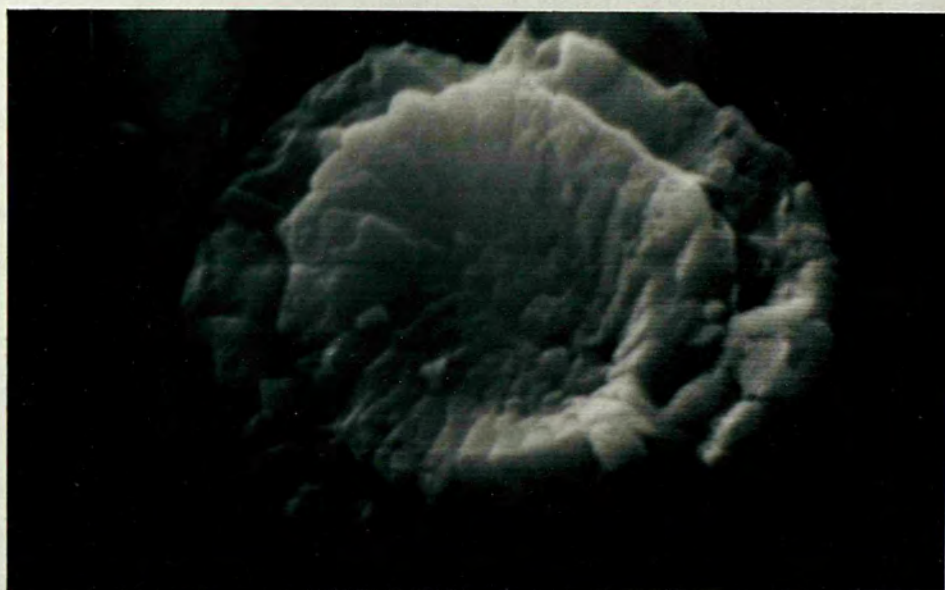
Cribresphacra ehrenbergi

and an Upper Cretaceous age is given.

Also in this formation Globotruncana lapparenti lapparenti Bolli has been found by Altiner (1974).



A



B



C

On the basis of this assemblage and its relationship with the underlying Senonian Ankara Melange and the overlying Middle-Upper Maastrichtian Davdanli formation, the Kamisli formation is given a Lower Maastrichtian age.

3.10 Source area and environment of deposition of the Kamisli formation

The mineral composition of sandstones of this formation suggests that the source area was mainly a volcanic terrain. The occurrence of reworked-tuff layers of different compositions (see 3.6) at different levels in the stratigraphical column indicates that, during the deposition of the lower part of the formation, there were time separated volcanic eruptions of different composition in the source area. The conclusion that these tuff beds were reworked is indicated by their poor sorting, matrix supported nature and sometimes poorly developed grading, since a tuff bed deposited by settling of volcanic ash in the water column is expected to produce well sorting and grading (Fiske and Matsuda 1964). The occurrence of fine grained reworked-tuff beds which are entirely made up of partly altered volcanic glass, overlying the coarse grained beds which contain orientated biotite flakes (long axes parallel to the bedding plane) as well as a glassy matrix and the presence of wavy lamination in the fine grained tuff beds further suggest that these tuff beds were deposited by current activity. The absence of palagonites, though it is difficult to identify the original glass due to alteration, the absence of even a ghost oolitic texture which is often observed in palagonites (Kerr 1959) sideromelans, and oscillatory zoning in plagioclase grains which are believed to be the indications of subaqueous eruptions (Bonatti 1968, Pettijohn 1975), together with the knowledge that the most of the subaqueous eruptions of a pyroclastic nature produces hyaloclastites rather than crystal tuff (Fairbridge & Bourgeois 1978), suggest that the volcanic eruptions were subaerial.

The presence of abundant angular and fresh feldspar and biotite fragments indicates that the volcanic eruptions were close to the basin, since the duration of transport was short. The occurrence of similar feldspar types, the similar composition and texture of volcanic rock fragments of the Kamisli formation and andesites and dacitic tuff and ignimbrites of the Saridere formation, together with the conclusion that volcanic eruptions were subaerial and close to the basin, suggest that the Seridere volcanic formation (Chp. 2) was infact the source area. Additionally although in lesser amount, the presence of basaltic rock fragments which are abundantly found in the Ankara Melange (see 1.6) as pillow lavas suggest that Ankara Melange was also eroded and supplied some material to the basin. The existence of angular skeletal fragments suggest another and local source.

The presence of serpentinite, radiolarite and limestone clasts together with VRC in the conglomerates of this formation and the marked compositional differences of these conglomerates in different localities suggest.

- a. the Ankara Melange was the main source area
- b. they are locally developed

The latter conclusion is also supported by the limited occurrence and length of the conglomerate beds which are wedge or lens shape perpendicular to the main current direction. Thus from all above conclusions together with the presence of andesitic clasts within the conglomerates but their complete absence in the Ankara Melange rocks in the north and northeastern margin of the basin, it can be concluded that the conglomerates were deposited by debris flows (see below) originating from the southeastern margin of the basin.

The environment of deposition of this formation can be considered on the basis of the sedimentary structures and the associated fossil assemblage. The absence of ripple-marks and

the poor sorting of rocks throughout the formation are proof of deposition below wave base. The following features in the sandstone-shale succession suggest deposition by mass-gravity processes in a deep sea environment (for estimates of depth, see below)

- a. Sandstones are moderate to poorly sorted and contain notable proportions of clay-grade material.
- b. Sandstone and conglomerate beds sometimes show erosional bases and in most of the cases, can be described by the Bouma sequence.
- c. Unimodal sedimentary directional structures are found.
- d. Submarine slumping features exist.
- e. Fossils are rare.

During deposition, although turbidity currents of differing densities were the main process in the transportation and deposition of these sediments, other mass-gravity transport mechanisms were also involved. The massive sandstone beds were, on the existence of dish structures and various fluid escape pipes, deposited from a flow in which the final grain support mechanism before deposition was the upward flow of the pore fluid (Walker 1978). The presence of matrix supported texture, chaotic distribution of clasts which are sometimes upward projecting and irregular top and base of beds together with the absence of channeling suggest that the conglomerates of the formation were deposited by debris flows. (Middleton & Hampton 1976)

The elongated occurrence of the Kamisli formation, possibly on the basin floor, can be explained by two different mechanisms. The first involves developments of a number of parallel submarine channels within the prograding middle fan area of a submarine fan, so that sediments transported by several pencontemporaneous turbidity currents fed by these channels form

coalescing suprafan lobes (Nomark 1970) which cover most of the basin floor, with oblique and transverse current directions to the basinal axis. The second explanation is that these turbidite beds were formed by turbidity currents flowing in the feeder channels and then turning to flow along the axis of the basin with a current directions parallel to the basinal axis. The presence of current direction parallel to the basinal axis, low sandstone/shale ratio, generally medium to fine grain size of sandstones and hemipelagic layers suggest that the Kamisli formation was deposited as basin plain turbidites by a mechanism similar to the second explanation. The evidence of current reversal indicates that deposition was taking place either on a flat or very gently inclined surface.

As was mentioned earlier, due to poor exposure and intense faulting and folding, the bedding continuity is of very little use for detailed facies interpretation. However vertical sequence variations can be satisfactorily used. The presence of reworked-tuff beds of Tabe, Tabce type within an upward fining and thinning sequence indicates that intermittent volcanic activity which supplied large amounts of clastic material as well as initiating high density turbidity currents through seismic shocks, were responsible for the deposition of these sequences. The occurrence of thick massive sandstone beds and sandstone beds of Tabe and Ta type, in the upper part of the formation, most probably resulted from large scale slumping as indicated by their association with submarine slump folds. Although there are a number of reasons which could have caused slumping and initiated high density turbidity currents, the most likely reason was earthquakes shocks, since there was no volcanic activity during the deposition of these later beds as indicated by the absence of reworked-tuff layers. Additionally the large size of some slump folds together with the fact that slump folds are generally found in shale dominated sequences

which suggest that slumping was not due to rapid deposition also supports the above conclusion. The occurrence of thick turbidite beds within a basin plain association, related to slump folds, have been reported in the flysch sequence of southwestern Pyrenees (Rupke 1976).

The presence of penecontemporaneous volcanic activity, rapid deposition (see Chp 12) and slump folds suggest strong tectonic activity throughout the deposition of this formation.

Certain conclusions concerning the depth of the basin during the deposition of this formation may be drawn from the presence of original carbonate clasts, planktonic foraminifers and the inferred environment of deposition of these rocks. The absence of carbonate dissolution in broken shell fragments and the presence of marl beds suggest that the depth of the basin was not greater than the Carbonate Compensation Depth (CCD). However Globotruncana are reported to have lived at least at 200 m in Cretaceous seas (Seheibnerova 1974). Thus the depth of the basin was somewhere in the bathyal zone (200-2000 m)

C H A P T E R 4

DAVDANLI FORMATION

4.1 General Introduction

The Davdanli formation is Middle to Upper Maastrichtian in age and consists of three facies. Facies A is made up of yellowish-brown to grey muddy-sandy-conglomerates, yellowish-brown to greenish-grey muddy-sandstones and light-brown to dark greenish grey shales and well exposed along the Ortakisla valley (G.19). Facies B is composed of greenish-grey shale and dark-grey muddy-sandstones. Facies C consists of alternations of light greenish-grey, well indurated muddy sandstones which sometimes develop into conglomeratic muddy sandstones, yellowish-brown to dark-green, poorly indurated muddy sandstones and yellowish-brown to dark-grey shales. Marly layers occasionally occur as thin beds intercalating with the well indurated sandstones.

The type section of the Facies A along the Ortakisla valley (see Fig 4.1) starts with a 15 m thick zone which contains thin bedded shales alternating occasionally with thin bedded siltstones or fine grained sandstones. In the next 100 m the lithology becomes dominated by coarse to medium grained sandstone beds which are randomly intercalated with shale and lens shaped conglomerate beds. Sandstone and conglomerate beds show graded bedding and parallel lamination although some massive beds occur. The next 60 m of the section is represented by alternating generally coarse grained, graded and parallel laminated sandstone beds and shales. In the next 140 m of the section, conglomerates are predominant, showing all types of texture (see 4.3.1) from pebbly sandstone to graded conglomerates associated with massive and graded sandstone beds with very thin or absent shaly layers. This part also contains Cenomanian limestone olistoliths at 290 m

THICKNESS(m)	LITHOLOGY	SAMPLE NUMBER	BED THICKNESS and SHAPE			TEXTURE			SEDIMENTARY STRUCTURES					SOLE MARKS & CURRENT DIRECTIONS	COLOUR	REMARKS	FORMATIONS		
			CONGLOMERATE	SANDSTONE	SHALE	BOULDERS GRAVEL	SAND			MUD	GRADING	LAMINATION	BALL & PILLOW					X-STRATIFICATION	MUD PELLETS
							Coarse	Medium	Fine										
		I-60,61																	
		I-59		40-50 SL	40-50 SL										db	Ball and pillow structure occurs occasionally.	Deg		
		I-58																	
		I-57																	
		I-56		30-40	10-20										db				
		I-55	850																
		I-54																	
		I-52,53		20-30	20-30										db	Poorly sorted disorganized conglomerate			
		I-51	75	10-20	10-20										db	Channellized conglomerate			
100		I-50	1240												db	Limestone olistoliths are 8-10 m. in diameter.			
		I-49	W,L												db				
		I-48	175	30-50	10-30										db	Lens shape conglomerate bed			
		I-47																	
		I-45		20-40	20-40										lby				
		I-44													db				
		I-43																	
		I-41	840												mdb	Poorly sorted disorgan. cong.			
		I-40																	
		I-39																	
250		I-38																	
		I-37																	
		I-35,36																	
		I-33,34	50-100 W,L	60-100 W,L	3-5 W,L									FC,GC 17	dgrg db	Conglomerates are poorly sorted, contain intraformational pebbles and sometimes occur as pebbly sandstones.			
		I-32												352		Wavy and parallel lamination observed in Tabco type sandstone beds.			
		I-31																	
200		I-30																	
		I-29	40-200 W,L	20-30 W,L											db dgb	Conglomerates contain scattered blocks.			
		I-27	50-100	30-50	5-10										db				
		I-26																	
		I-25																	
		I-24																	
		I-23		40-60	40-60									FC,GC 338	db dgr				
150		I-22																	
		I-21																	
		I-20		40-60	40-60									FC,GC 43	db dgr	Sandstones are generally poorly sorted.			
		I-19	140																
		I-18		20	5-15										db	Skeletal grains are relatively abundant in sandstones.			
		I-17		40-150															
100		I-16																	
		I-15																	
		I-14	80-110	20-40											db	Cong. as pebbly sandstone			
		I-13																	
UNEXPOSED																			
40		I-11	60-120	40-60	3-3										d-lb	Disorganized conglomerates			
		I-9		40-80 W,L	30-35 W,L										d-lb	Disorganized conglomerates are poorly sorted and show obvious erosional bases.			
		I-8																	
20		I-5,6		50	1-5										g&r	Siltstone-shale alternation			
		I-3																	
		I-2			10-20 SL										g&r	Shales are intensely fractured and contains high CaCO ₃			
		I-1																	

Fig 4.1 - Type section of the Davdanli formation's Facies C. (Lithology is not to scale). In bed thickness and shape column; SL: Sheet like, L: Lenticular, W: Wedge shaped. In colour column; d: dark, m: medium, l: light, b: brown, y: yellow, gr: green, g: grey.

above the base of the section. The topmost 30 m. of the section is made up of alternations of medium to thick bedded sandstone and shale beds and this typifies the passage zone between this facies and the Degirmendere formation.

Facies B consists of thin bedded (2-15 cm) shales and siltstone with subordinate medium to fine grained sandstone beds which are generally graded and/or parallel laminated and show abundant organic trails on the bottom of the beds. Because of its thin occurrence and poor exposure, a measured section from this facies could not be taken.

Facies C in the Yaniksirti section starts with a five metre thick passage zone between the Kamisli formation and this facies of the Davdanli formation. This zone consists of medium thick yellowish brown to grey shale beds with occasional appearances of thinly bedded (0-5 cm) siltstones. The remaining 635 m of the section is comprised of several cycles which are predominantly thinning and fining upward sequences (Plate 4.1) although some thickening and coarsening upward ones occur. These sequences consist of well indurated, generally graded sandstones, poorly indurated massive sandstone and shale intercalations. With varying sandstone/shale ratios, bed types and thickness of beds (see App VIII for details). Also up to 3 m. thick slump sheets, which are especially predominant in between 335 m. and 545 m. from the base of the section are observed. These slump sheets sometimes contain slump balls (Dzulynski & Walton 1965) and are under and overlaid by relatively undisturbed sandstone beds.

4.2 Distribution, thickness and field relations

Facies A is exposed as an tectonic inlier, which is elliptical in shape with a long axis of 800 m. and short axis of 400 m., of a SW plunging anticline along the Ortakisla valley. The actual thickness of the succession is not known because its lower boundary is not exposed. However a 345 m.

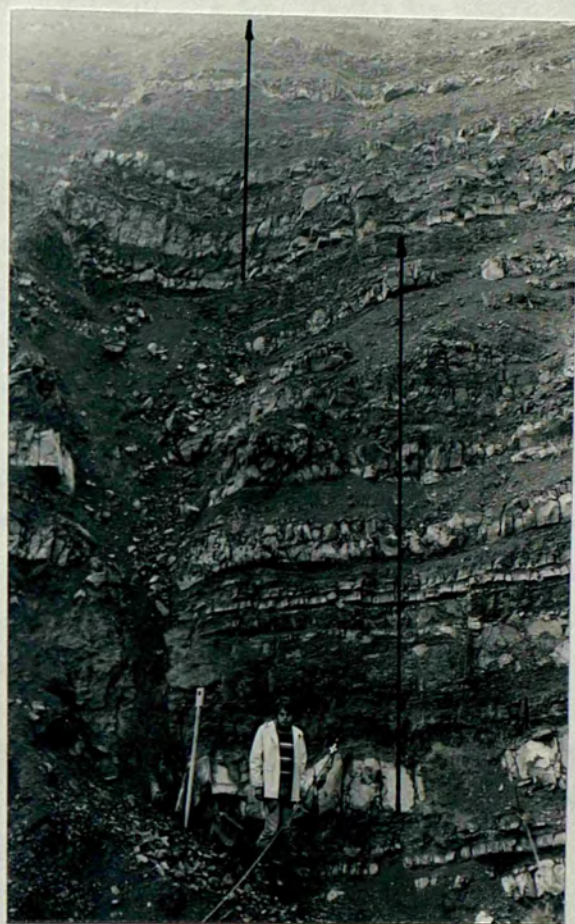


Plate 4.1 - Shows the upward fining and thinning sequences
in the lower part of the Yaniksirti section
9816 (App. VIII)

section was measured and it gradually passes up to the Degirmendere formation.

Facies B is also exposed as a tectonic inlier at the N of Kucukcorakli dere (P 13). Here the beds are laterally extensive and the facies is overlaid by Degirmendere formation.

Facies C outcrops in the N and NE of the area studied and lies parallel to the Kamisli formation. It is exposed for nearly 10 km. between Kamislibala (L7) and Akkoyun (H 12) and is intensely tectonized (see map I and Chp 11). The lateral extension of the facies towards the SW could not be seen due to faulting but in the NE it continues for many kilometres (Norman 1972). A marked gradual change in sandstone/shale ratio and thickness of sandstone beds from the NE to SW is observed. While the sandstone beds are thicker, more abundant and associated with slump deposits within upward fining sequences throughout the stratigraphic column in the NE part, in the SW the sandstone beds are thinner, less frequent, appear to be laterally extensive and slump deposits, missing in the lower part of the stratigraphical column, become dominant and thicker within upward coarsening and thickening sequences towards the top (Plate 4.2)

The true thickness of Facies C could not be measured due to faulting at its upper boundary but in the Yaniksirti sections 690 m. is recorded. Its lower boundary with the Kamisli formation is transitional. The upper boundary with the Buyukdere member of the Bayat formation is a reverse fault.

4.3 Conglomerates

4.3.1 General description

Conglomerates occur exclusively in Facies A as lenticular and wedge shape beds which are 70-850 cm. thick. Four



Plate 4.2 - The upper boundary of the Davdanli formation's Facies C at locality (J10). Beds are overturned and thrust fault runs along the valley between the Buyukdere formation at the left of the photograph and Davdanli formation. Note the upward coarsening and thickening sequences in the centre of the photograph.

types of conglomerates are present: inverse-to-normally graded, graded, graded stratified; and disorganized (Walker 1978) (Plate 4.3). While disorganized and graded conglomerate beds are common, graded-stratified and inverse-to-normal graded types rarely occur. The conglomerates generally show erosional bases. Pebble imbrications in which long axes of pebbles are orientated parallel to bedding, are occasionally observed. The graded-stratified and graded conglomerates show better sorting than the other two and they usually grade from pebble size clasts to sand and silt size grains with parallel lamination occurring in the graded-stratified types. In contrast the disorganized conglomerates do not show any sedimentary structures and contain relatively larger clasts than other conglomerates. They contain a proportionally high amount of matrix and sometimes a pebbly sandstone texture occurs

The size of the clasts of the conglomerates ranges from granule to 40 cm diameter boulders, the shape of the clasts is generally oblate (Zingg 1935) and roundness varies from subangular to rounded but they are generally subrounded. The sorting of the conglomerates is poor to extremely poor and they are texturally immature. The conglomerates are diamictites. (Pettijohn 1975)

The limestone olistoliths are found in Facies A and are 8-10 m. diameter. They are of two different types:
a) White, semi-recrystallized limestone which contains algae and broken shell fragments and b) bluish-grey, completely recrystallized micrite.

4.3.2 Lithology of the conglomerate clasts

Volcanic Rock Clasts (VRC) are mainly dacitic or rhyolitic, andesitic and basaltic in decreasing order of abundance. Dacitic or rhyolitic clasts are made up of a chert-like ground-mass with a few K-feldspar phenocrysts and biotite flakes.



A



B

Plate 4.3 - Occurrences of conglomerates; (A) Disorganized, sample I.40 at Ortakisla section (Fig. 4.1)
(B) Graded sample I.26 at Ortakisla section.

Andesitic VRC consists of plagioclase and clinopyroxene phenocrysts set in a cryptocrystalline groundmass which also contains randomly orientated, small plagioclase crystals of acicular habit. Basaltic clasts are medium dark-grey and are easy to recognize in the field by the presence of abundant cavities which are in some cases filled by calcite (amygdaloidal texture). Microscopically they contain abundant plagioclase (bytownite and labradorite) and olivine phenocrysts within a dark cryptocrystalline groundmass. All VRC show degrees of alteration. Limestone clasts are generally angular and either micrite or packstone which contains foraminifers and shell fragments.

The matrix of the conglomerates is made up of sand and silt size material, poorly sorted and is compositionally similar to sandstones.

4.4 Sandstones

4.4.1 General description

The sandstones of the Facies A are moderate yellowish-brown (10 YR 5/4) to greenish-grey (5 GY 6/1) and show graded bedding, occasional parallel lamination at the upper parts of the beds and small scale slumps or they can be massive without any sedimentary structures. The sandstones generally form 40-60 cm thick beds which alternate with shales and conglomerates. The medium to fine grained sandstone beds with small scale cross-stratification and parallel lamination at the lateral extension of thick conglomerate beds are also observed in this facies. Facies B sandstones are thinly bedded and generally subordinate to shales. They usually show grading or parallel lamination and are Tabe and Tde types. The sandstones in Facies C occur as two different types. The first, Type I (TI), is light greenish-grey (5 GY 8/1) and can be described as Tabe, Tabce, Tde, Tbce type beds in decreasing order of abundance. They are well indurated and always have

sharp contacts with the underlying beds. Very occasionally intraformational pebbles are present in the lower part of the beds. Thickness of the beds ranges from 5cm to 70cm. but they are usually 30-50 cm. thick. The composition of these sandstones differs from the Type II sandstones (see below) with regard to the amount of skeletal fragments which are more abundant in TI. (Table 4.1) They sometimes occur as conglomeratic sandstones which grade from gravel to sand and silt size grains. The TI sandstones frequently show wedging-outs, although some beds appear to be laterally continuous. These sandstone beds usually have well preserved sole marks and sometimes interbedded with 1-5 cm thick marl beds. The second type of sandstones (Type II: TII) is dark greenish grey (5 GY 4/1) to moderate yellowish-brown (10 YR 5/4) and occur as massive beds which very occasionally show parallel lamination at the top of the beds. They are usually thickly bedded (up to 120 cm) and generally show irregular contacts with the underlying beds. The massive sandstone beds sometimes contain abundant intraformational pebbles either scattered within the sandstone matrix in various sizes or showing sort of grading.

Well rounded mud pellets and in one occasion a cobble size basaltic rock clast which consists of large olivine and small plagioclase (bytownite-labradorite) phenocrysts within a dark cryptocrystalline groundmass are also observed. In one case a sedimentary structural division, in which the lower part is made up of structureless coarse to medium sandstone, the middle part contains intraformational pebbles and upper part is graded and parallel laminated, is observed within a one m. thick bed. The sandstones can be classified as volcanic arenites. (Folk 1974)

4.4.2 Texture

Grain size of the sandstones ranges from very coarse to fine but their median diameter falls within the coarse to medium sand range. In the case of the conglomeratic sandstones which contain 15-25% gravel size clasts, grain size varies from pebble to silt size material. There is no apparent comparison between the grain size and composition. Roundness of

Parameters Sample No	Quartz	Feldspar	VRF	SRF	Cement	Matrix	Accessory Components	Others	Total %	Total Count
KB-3(TI)	2.6	8.2	26.4	34.6	11.1	14.9	2.2	- -	100.0	508
KB-12(TII)	5.0	13.0	20.8	3.7	1.2	32.8	2.4	21.1a	100.0	504
I-4	5.9	11.7	57.7	2.3	6.8	13.6	2.3	- -	100.0	503
I-38	5.2	12.8	50.6	3.4	7.6	15.3	5.1	- -	100.0	500
I-56	9.8	10.0	50.4	6.8	8.2	10.4	4.4	- -	100.0	500
239(TI)	7.7	15.3	22.0	6.3	21.1	17.7	3.9	5.9b	99.9	508
486A(TI)	3.2	21.9	30.5	4.2	19.8	10.1	4.6	5.6b	99.9	524
613(TII)	7.8	18.1	29.4	5.8	9.2	16.9	0.6	12.2a	99.9	513
1030(TI)	6.7	7.1	31.4	24.7	12.2	10.9	6.9	- -	99.9	506

Table 4.1 - Modal composition of the Davdanli formation's sandstones Sedimentary Rock Fragments (SRF) includes skeletal and limestone fragments. Chert is included to Volcanic Rock Fragments (VRF). TI: Type I sandstones, TII: Type II sandstones, a: porosity b: chlorite.

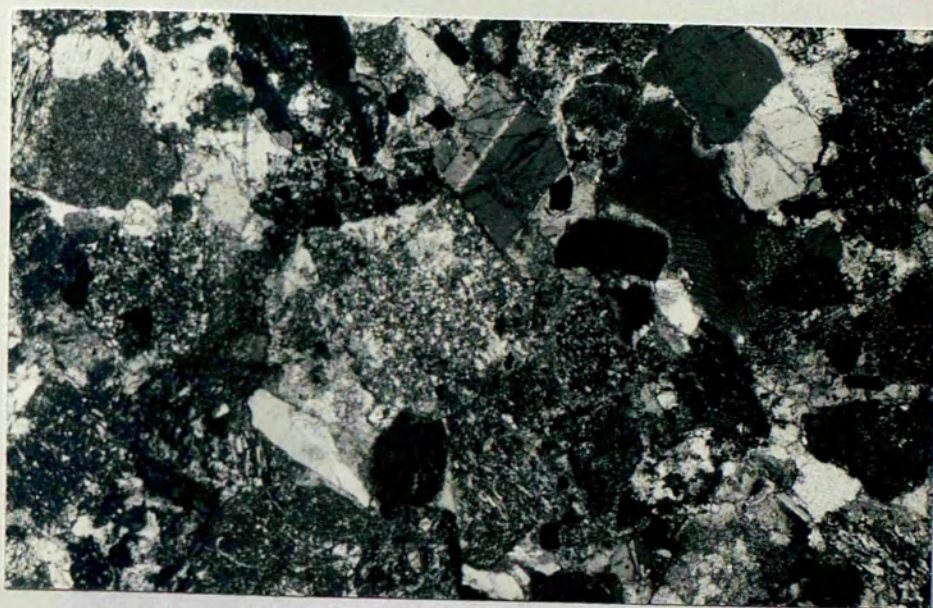


Plate 4.4 - Photomicrograph of Type I sandstone.

Volcanic arenite: It consists of volcanic rock fragments, feldspar, cement, matrix sedimentary rock fragments (Skeletal grains and limestone fragments) and quartz in decreasing order of abundance. Sample 486A, 35x, XN.

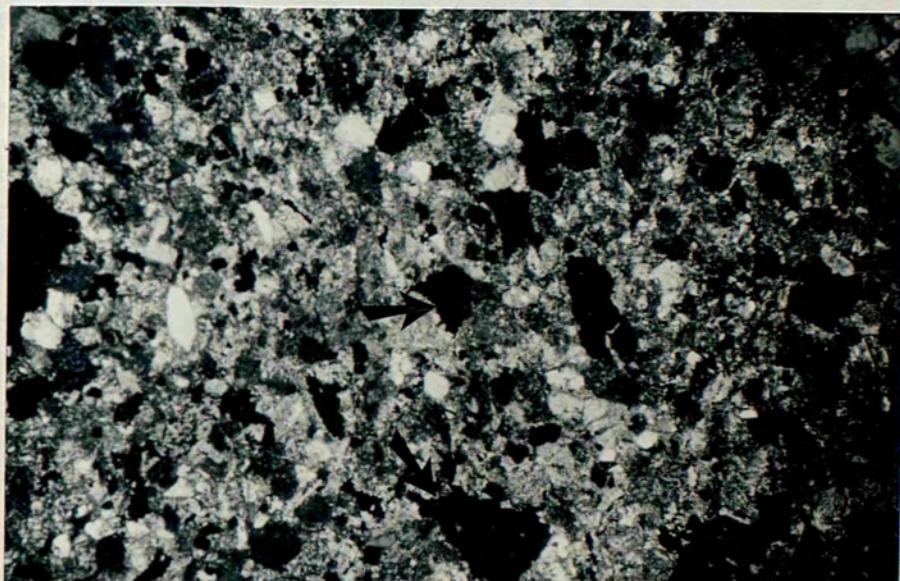


Plate 4.5 - Photomicrograph of Type II sandstone. Lithic arenite: consist mainly of volcanic rock fragments, feldspars, skeletal fragments and matrix. Note the high porosity of the rock (black irregular areas in the photograph). Sample KB-12, 15x, XN.

the sandstone grains varies with composition: skeletal fragments, quartz and some feldspar grains are comparatively more angular than volcanic rock fragments (Plate 4.4). Overall grains are usually subangular to subrounded. Sorting differs in TI and TII: the former is generally more poorly sorted than the latter. Packing proximity is higher in the TI (75%-50%) than TII for which 50%-30% packing proximity is calculated. Another significant textural difference between these sandstones is that TII contains up to 30% secondary porosity which is created by what appears to be the dissolution of matrix. (Plate 4.5) The sandstones of the Davdanli formation are texturally immature.

4.4.3 Framework grains

Volcanic Rock Fragments (VRF) are andesitic, dacitic or rhyolitic and basaltic rock fragments. Andesitic VRF consist of plagioclase (labrodorite-andesine) and altered mafic mineral phenocrysts within a cryptocrystalline groundmass which also contains small, randomly orientated, plagioclase crystals which are, on the basis of their textural and compositional similarities, identical to the andesitic VRF of the Kamisli formation. Dacitic or rhyolitic VRF have a fine to medium crystalline chert-like groundmass, which sometimes shows spherulitic texture, and frequently contains K-feldspar and/or altered biotites. Basaltic fragments show two different textures: the first displays trachytic (flow) texture which is formed by the subparallel arrangements of small lath-shaped plagioclase (bytownite-labrodorite) crystals within a dark groundmass. The second type consists of olivine and plagioclase (bytownite) phenocrysts set in a dark groundmass and this type resembles the basaltic rock clast found in the sandstones of this formation (see above).

Skeletal material consists of broken fragments of gastropods, bivalves, brachiopods, echinoids, bryozoans and algae (in decreasing order of abundance). Gastropods, although

retaining their initial shell shape, have lost their original internal structure through recrystallization and appear as a mosaic of cavity-filling sparry calcite. Bivalves show a crossed lamellar structure in contrast to the fibrous texture (in which fine fibres of calcite are elongated perpendicularly, or at low oblique angles, to the shell surface) of brachiopod shells. Echinoid fragments are distinguished by their dusty appearance and uniform extinction.

Feldspars are represented by plagioclase, K-feldspars and a few microcline. They are generally angular to subangular and show degrees of alterations. Plagioclases usually show albite twinning although some carlsbad and combined carlsbad-albite twinning and normal zoning occur. Sometimes a straight line or half of the idiomorphic crystals of plagioclase are observed and their extinction angle varies from 23° to 45° (andesine-labradorite-bytownite). K-feldspars are generally orthoclase which are identified by their high 2V values. There are also a few microclines with characteristic polysynthetic twinning.

Limestone fragments occur either as micrite or packstones in which some benthonic foraminifers and skeletal fragments are observed.

Benthonic foraminifers, generally as whole tests but sometimes broken, are also observed.

Quartz shows straight extinction, is almost free of inclusions and is usually of volcanic origin. Chalcedony with its characteristic radial texture occurs occasionally.

Accessory components are biotite, plant fragments chlorite and unidentifiable fragments of mafic minerals. Biotite occurs as flakes and in most cases is partly or completely altered to iron-oxides.

4.4.4 Matrix and Cement

The matrix of the sandstones is fine grained and composed of microspar, micrite, chlorite with some quartz grains. Also some very fine crystals which appear as bright to yellowish-red flakes under cross polarized light and have a high index, are observed: they may be sericite or illite. The matrix is poorly sorted and has been extensively replaced by neomorphic sparry calcite in TI sandstones, which appear to contain relatively more micrite than TII.

Original cement is almost absent in the sandstones of the Davdanli formation; when present it is always confined to TI sandstones and is exclusively calcite.

The difference in induration of TI and TII sandstones is caused by the extensive occurrence of neomorphic sparry calcite in the former as opposed to its limited occurrence in the latter. The most probable cause for this is the relatively high micrite content of the matrix, the higher proportion of skeletal fragments and the relatively better sorting of TI sandstones. All these factors seem to contribute to the aggrading neomorphism of micrite to microspar and sparry calcite leading to the better binding of grains of TI sandstones, making them more indurated. On the other hand the TII sandstones, bound by clay during early lithification were able to produce only a small amount of neomorphic sparry calcite due to the small proportion of original micrite in the matrix. During weathering the simple clay bonds are partly removed leaving a number of secondary pore spaces thus causing the poorly indurated nature of TII sandstones.

4.5 Shales and Marls

4.5.1 General description

The colour of the Davdanli formations shales varies from greyish-orange (10 YR 7/4) to greenish-grey (5 GY 6/1) and dark

greenish-grey (5 GY 4/1) depending upon the composition i.e. green rocks contain more chlorite than the brown which have a high illite and calcite content. Individual shale beds occur either as thick massive or parallel laminated thin beds. They are also observed as an e division of the graded sandstone beds showing parallel and/or convolute lamination. In Facies B, black shales, which are structureless and thinly bedded, are observed. Shales are fine grained (silt to clay grade) and sometimes contain a few small benthonic foraminifers, detrital quartz and feldspar grains and plant fragments which can be quite abundant in some shale beds. Marls are often confined to the upper part of the TI sandstone beds and sometimes occur as 5-10 cm. thick individual beds. They are light grey, frequently show parallel lamination, are free from plant fragments and detrital grains and contain abundant planktonic foraminifers: they could be termed hemipelagic layers. Occasional occurrences of bioturbation are also observed. In XRD analyses, kaolinite, illite and chlorite are found as clay minerals.

4.6 Sedimentary structures and current directions

Graded bedding with various sole structures, i.e. flute casts, groove casts, bounce casts, prod marks and organic trails (trace fossils) are the most common sedimentary structures found in all three facies of the formation. Flute casts tend to become larger in the coarse grained and thick sandstone beds. The lateral, shallow, freely winding or straight feeding trails of organisms (Nereites facies of Seilacher 1967) (Plate 4.6) are the commonly observed organic trails at the bottom of the sandstone beds. However, they differ in different facies of the formation for while Facies B contains only Granularia sp., Facies C shows Scolicia sp, Granularia sp and Taphrhelminthopsis sp. trace fossils (the depth significance of this is discussed later in this chapter). Convolute wavy and parallel laminations are often limited to the upper parts of the graded sandstone beds and are also found in thin bedded sandstones and shales. In the massive sandstones a few

Plate 4.6. Trace fossils found in the Davdanli formation.

- A. 1. Taphrhelminthopsis sp. (freely winding trails on the right of the photograph) and
2. Scolicia sp. (on the left of the photograph from Facie C. Coin is 1.5 cm. in diameter. Location (L9)
- B. Granularia sp. (straight tails) from Facies C. Location (L9)
- C. Granularia sp. from Facies B. Location (P12)



poorly developed parallel laminae may be present in the upper part of the beds. Slump balls which also occur in the facies are observed in between relatively undisturbed sandstone beds in the Facies C (Plate 4.7). Within these slump sheets, slump balls which are believed to result from tight infolding of semiconsolidated sandstone beds (Dzulynski & Walton 1965). Partly preserved and distorted bedding properties of sandstones can be observed within these slump balls. The slump balls are distinguished from concentric weathering by their variable size and by the occurrence of sandstone beds of similar composition and induration under and overlying the slump sheets and from ball and pillow structures by the absence of internal lamination and shale in between the balls. Small scale slump folds are also observed in this formation and their axis and sense of facing direction show considerable variation in different localities (see Fig 12.7).

Current directions are mostly determined by measurements of flute casts and groove casts, the latter used in places where the former are either absent or barely visible. They indicate that flows were mainly from SW and SE in Facies A, B and in the NE part of Facies C. But in the SW part of the last, they are generally from NE in the lower part and SE in the upper part.

4.7 Weathering and alteration

The poorly indurated sandstones of the formation are, as expected, more easily eroded than the well indurated ones. Shales are again intensely eroded.

Iron-oxide staining (mainly hematite and limonite) observed on the weathered surface of the sandstones and shales are the end product of the alteration of iron-bearing minerals (biotite and some mafic minerals) of these lithologies.

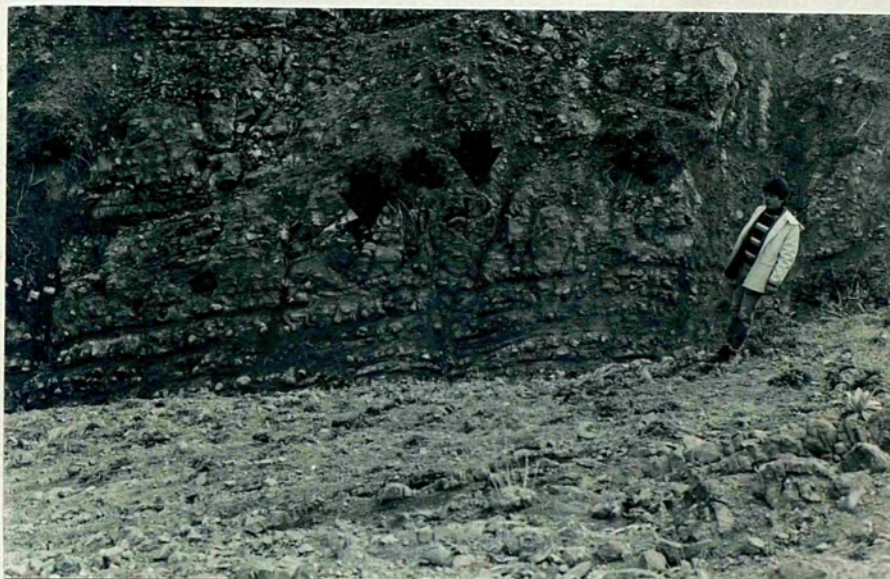


Plate 4.7 - Showing a zone dominated by slump balls structures. In the Yaniksirti section (see App.XIII) Photograph no. 9819.

4.8 Fossils and age of the Davdanli formation

Marly and shaly layers of this formation contain abundant amounts of planktonic foraminifers. Although a large number of Globotruncana sp. and Globigerina sp. are obtained from the marls and shales, unfortunately only a few of them are determinable as age indicators. These were identified by Dr. C.G. Adams (pers comm. 1982) as being

Globotruncana sp. (single keeled form)

Globotruncana sp. (double keeled form)

and a Late Cretaceous age is given. However Altiner (1974) in his detail palaeontological study, was able to identify numbers of Globotruncana sp. together with other planktonic foraminifers and designated a Middle-Upper Maastrichtian age for the Facies B and C. Also in the shales of the Facies A some planktonic foraminifers were identified as being Maastrichtian fauna by C.G Adams and S. Tekler (pers comm.) Accordingly a Middle-Upper Maastrichtian age, as proposed by Altiner (1974), is adopted for this formation.

4.9 Source area and environment of deposition of the Davdanli formation

The presence of volcanic rock clasts and angular feldspar grains in the sandstones and conglomerates of this formation suggest a nearby volcanic rock-dominated source area which was most probably the same volcanic terrain which provided material for the Kamisli formation (3.10) (indicated by similarities of feldspar and volcanic rock fragment types) Another source area which was contributing sediment to the basin was an intrabasinal source from which limestone fragments and clasts and skeletal fragments were derived. The intermittent predominance of these fragments in the stratigraphic column of Facies A and C may be interpreted as due to terrigenous sediment supply to the basin being low and they were transported from their original depositional area, most probably a shallow water carbonate environment, by longshore currents to the head of a submarine canyon or they were removed by storms

and then carried into the submarine canyon. Though the fractured nature of shells may suggest violent transport, it could well have been the result of either wave action or biological activity in the original environment of deposition of these fragments. It remains rather difficult to favour one of these conclusions at the expense of the other. The subrounded to rounded nature of conglomerate clasts with their oblate to spheroidal shape suggest a fluvial origin, in which they have had short transport but prolonged abrasion. The most likely explanation for the occurrence of large, angular Cenomanian limestone olistoliths, which differ markedly in composition and texture from the other limestone clasts and fragments of the formation, is that these rocks were exposed along the walls of a submarine canyon, collapsed due to earthquake shocks and subsequently transported down to the deeper part of the basin by traction.

The stratigraphical and sedimentological properties of the Davdanli formation, together with abundant planktonic foraminifers suggests a marine origin for these sediments. The conclusion that this formation was deposited in a deep marine environment, mainly by turbidity currents, is suggested by the absence of any wave produced sedimentary structures, the alternations of coarse and fine grained sediments, the presence of channelized conglomerates, olistoliths, various unimodal directional structures and the slumping features.

The sandstones and conglomeratic sandstones of this formation, which can be described in terms of the Bouma sequence as inverse-to-normally graded, graded and graded stratified conglomerates, were deposited by turbidity currents of differing densities. The massive sandstone beds which do not show fluid escape features are believed to result from very rapid deposition from suspension within a high density turbidity current (Middleton and Hampton 1976), with or without fluidization. (In the case of fluidization, if it took place, escape of pore fluid was less forceful, thus no fluid escape

features were developed).

The facies interpretation of this formation can be made on the basis of the relative abundance of particular rock types, vertical sequence changes, current directions, bedding properties of rocks and sedimentary structures. The occurrence of abundant, thick, wedge and lens shape conglomerate beds, olistoliths and current directions generally oblique and transverse to basinal axis in the Facies A, suggest that it was deposited on the inner area of a submarine fan. This conclusion is also supported by the following features.

a) The fining and thinning upward sequences, in which the thick conglomerate beds at the base are overlain by massive sandstone and/or graded and graded-stratified conglomerate beds and eventually by coarse to medium grained turbidite beds, are believed to be deposited in channels

b) The general absence of interchannel deposits in between these sequences which suggests that channels rarely shifted position

c) Although not always present, the occurrence of levee deposits as thin bedded, parallel laminated and small cross stratified, fine to medium grained sandstones.

The Facies B is rather difficult to assign to any specific facies due to its very limited, thin and poor exposure which prevents the observation of conclusive criteria. However the presence of a very low sandstone/shale ratio, medium to fine grained turbidite beds, abundant planktonic foraminifers (mainly Globotruncana sp) and its geographic position (see Map I) relative to the basinal axis and Facies A may suggest that this facies is deposited on a depositional slope.

The Facies C, in the NE part, with its generally upward fining and thinning sequences, together with the presence of shallow and wide channels which are filled by massive sandstones and turbidite beds of Tabe, Tabce and thin, well developed shale interbeds indicate that this facies is deposited on the upper part

(channeled part) of a midfan area. The occurrence of some submarine slump folds which are commonly observed in modern middle fan areas (Nomark 1974) and current directions transverse and oblique to the basinal axis also support the above conclusion. Additionally the presence of some upward coarsening and thickening sequences suggest that from time to time, this facies was deposited as suprafan depositional lobes (Walker & Mutti 1973).

The presence of very low sandstone/shale ration (<1) and thin, laterally extensive sandstone beds of mainly Tde and Tbce types suggest that this part of the Facies C was deposited on outer fan and/or basinal areas. The occurrence of upward coarsening sequences towards the top of the facies together with an increase in the thickness of sandstone beds and sandstone/shale ratio indicate that later in the deposition of this part, prograding middle fan depositional lobes were developing. These conclusions are also supported by the change from NE to SW current directions in the lower part to SE and SW to NE and NW current direction in the upper part of the facies in the SW part of the Facies C.

Strong tectonic activity in and around the basin during the deposition of this formation is indicated by rapid deposition; the presence of angular feldspar grains which suggests that the rate of erosion far outweighed the rate of weathering in the source area, requires rapid uplift (Folk 1974). The presence of slump balls and folds together with the evident vertical movement of a basinal block fault (see Chp. 12) further suggest contemporary tectonic activity.

The Davdanli formation resembles a number of ancient (Stanley & Unrug 1972, Mutti 1974, Walker 1978, Winn Jr & Dott Jr 1979 and Nemec et al 1980) and recent (Nomark 1974, Nelson & Nilsen 1974) submarine fan deposits with regard to sedimentation processes, current direction arrangements, bedding properties and sedimentary structures. It is generally agreed that the inner fan deposits are characterized by the presence of thick, coarse conglomerates which are deposited

in rarely shifting deep and narrow channels, sometimes with levee deposits and turbidite beds in the interchannel areas. The middle fan deposits are recognized by upward fining and thinning sequences and the presence of abundant rapidly migrating, shallow and wide channels which are usually filled by turbidite beds generally starting with division a of Bouma's sequence or massive to pebbly sandstone beds in the upper part (channeled part), by the presence of upward coarsening and thickening and the absence of obvious channeling in the lower part or prograding depositional lobes of outer fan (Mutti 1974) .

The presence of marl beds as hemipelagic layers and abundant planktonic foraminifers which do not show any apparent carbonate dissolution, in the e division of turbidite beds, suggest that the depth of the basin during the deposition of this formation was not greater than the Carbonate Compensation Depth (CCD) which has been estimated to be between 3500 m-5000 m. during the Cretaceous in Western Alpine basins (Besse & Butt 1976). For the upper palaeo-depth limit a conclusion can be made on the basis of trace fossils (ichnofauna) and planktonic foraminifers. The most common ichnogeneras found in the Facies C of the formation are Taphrhelminthopsis sp. (identified by comparison to plate 6a of Crimes (1977) and Ksiazkiewicz (1970) plate 2 and is believed to be characteristic of deep marine environments), Granularia sp. (identified by comparison to plate 3e of Crimes (1977) and is considered as a facies crossing ichnogenera) and Scolicia sp. (identified by comparison to Fig 1 of Seilacher 1962 and 4d of Ksiazkiewicz 1970). The similar association of these trace fossils has been recorded in the sandstones of depositional fan lobes of outer fan area in the Eocene submarine fans of Northern Spain (Crimes 1977) and in the distal turbidites of the Polish Carpathians and deposition in bathyal zone suggested (Ksiazkiewicz 1970). Additionally the abundance of trace fossils in the TI sandstones of Facies C may indicate a depth around 2000 m. As pointed out by Ksiazkiewicz (1975), the relative abundance of lateral shallow feeding trails increases towards 2000 m. and

decrease below this figure. Thus from all above criteria, together with the fact that Facies B contains only Granularia sp. which suggests relatively shallower depth for this facies, it is suggested that Facies C was deposited in between 2000 m-3500 m. and Facies B in relatively shallower depths. The palaeogeographic position and the inferred environment of deposition of Facies A suggest that this facies was deposited in a shallower part of the basin than Facies C, probably on the lower slope. This conclusion is also consistent with the Altiner's (1974) palaeodepth estimation of lower bathyal zone made on the basis of planktonic foraminifers of this formation.

C H A P T E R 5

DEGIRMENDERE FORMATION

5.1 General Introduction

This formation is Lower Palaeocene in age and can be easily recognized by its purplish-dark brown colour. It consists of muddy sandy-conglomerates to pebble-conglomerates, reddish purple to light brown muddy sandstones and yellowish brown to grey shales. The Degirmendere formation shows, in the predominant rock type, bedding properties and sedimentary structures, differences between its marginal and basinal exposures. Three stratigraphic sections, in addition to one which described in 4.1, in the marginal (K. Bayat and Cataltepe I) and in the basinward (Degirmendere) outcrops are measured and short accounts are given below.

In the K. Bayat (L8) section the formation is dominated by disorganized conglomerates and pebbly sandstones together with massive sandstones which sometimes show indistinct grading and contain slump balls. All these lithological types are randomly distributed throughout the section and particularly between 1-5 m and 65-73 m. These coarse beds are interrupted by sequences in which thin (10-20 cm thick) sandstone beds of Tabe, Tbce and Tde types intercalate with thin shale layers. Conglomerates are made up of volcanic rock clasts which range in size from granule to 70 cm diameter boulders (see Fig 5.1 for details)

In the Cataltepe (E29) section (Fig 5.2) the formation is represented in the first 68 m of the section from the base by 70-300 cm thick disorganized conglomerate beds alternating with occasional massive sandstone or pebbly sandstone beds. The conglomerates are dark brown to purple, poor to extremely poorly sorted and contain up to 1 m in

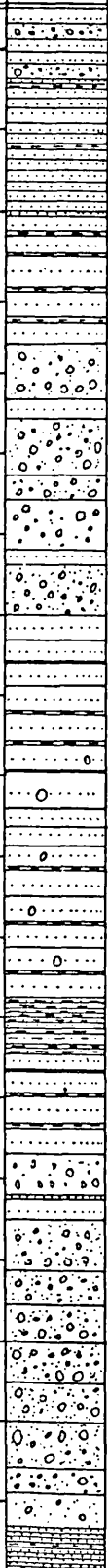
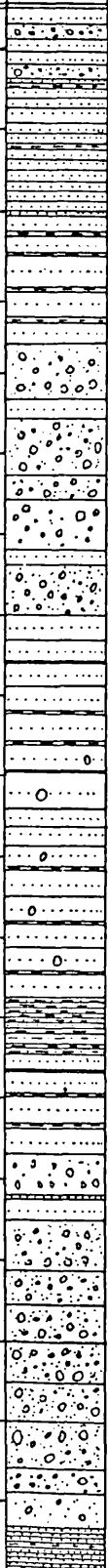
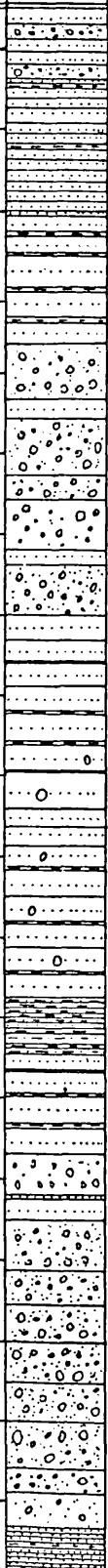
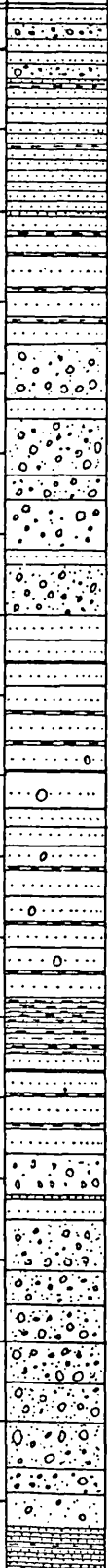
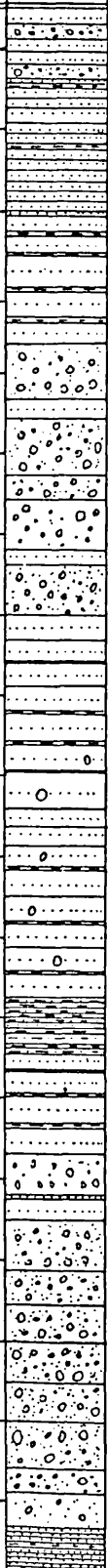
THICKNESS(m)	LITHOLOGY	SAMPLE NUMBER	BED THICKNESS and SHAPE			TEXTURE				SEDIMENTARY STRUCTURES				SOLE MARKS and CURRENT DIRECTIONS	COLOUR	REMARKS	FORMATION		
			CONGLOMERATE	SANDSTONE	SHALE	BOULDERS COBBLES GRAVEL	SAND			LIMESTONE	GRADING	LAMINATION	BALL & PILLOW					MUD PELLETS	PLANT FRAGMENTS
							Coarse	Medium	Fine										
195			50-80	40-110							•	•			db-lb	Grading is very indistinctive			
				30-75	5-15								•	•	•		db	Sandstones are sometimes amalgamated.	
150			80-250	30-50										•			db	Conglomerates are chaotic and their clasts are up to 35 cm. in diameter	
100				50-70	3-10						•	•		•	•		db	Sandstones contain up to 50 cm. in diameter intraformational pebbles and are sometimes amalgamated. Grading is occasional and parallel lamination occur in shales.	
					1-15						•						dbdg		
				50-70	3-10						•	•					db	Sandstones are amalgamated.	
50			50-300	20-80							•		•				db	Conglomerates are disorganized - matrix supported, contain up to 40 cm. in diameter intraformational pebbles and show rare indistinctive grading.	
				10-15	10						•	•					db, g db		
120																			

Fig 5.1 - K. Bayat section (Lithology is not to scale). In colour column d: dark, l: light b: brown, g: grey.

THICKNESS(m)	LITHOLOGY	SAMPLE NUMBER	BED THICKNESS and SHAPE			TEXTURE					SEDIMENTARY STRUCTURES					SOLE MARKS and CURRENT DIRECTIONS	COLOUR	REMARKS	FORMATION
			CONGLOMERATE	SANDSTONE	SHALE	BOULDERS GRAVEL	SAND			LIMESTONE	GRADING	LAMINATION	BALL & PILLOW	MUD PELLETS	PLANT FRAGMENTS				
							Coarse	Medium	Fine										
20		III-17 III-15,16 III-13,14 III-11,12 III-10 III-8,9 III-6,7 III-1,2 3,4,5	50		30-50 1-7 50 1-7 30-50											lg- db	Abundant worm borings and extensive bioturbation in marls Plant fragments occur frequently	Kurebogazi member	
150		II-1 II-2 II-3		20-30	20-30											dgbl	Shales are interbedded with occasional fine sst		
		II-4		5-10	5-10											dg	Thin bedded siltstone layers intercalate		
		II-5		3-15	3-15											dgbl			
		II-6		15-20	15-20										191	dgr g,bl			
		II-7																	
		II-8,9																	
100		II-10	30-200	10-15	10-15										283 301	dg	Conglomerates occur as channel-fill deposits		
		II-11																	
		II-12		10-30	10-170											dg	Shales are very fragile		
		II-13																	
		II-14	20-60	20-60	20-60											dgr b			
		II-15																	
50		II-16 II-17 II-18	70-100	30-90	10-60											y b db	Some conglomerate beds show a very vague grading Sorting is poor	Deginendere	
		II-19																	
		II-20	100-300	20-30												y b db	Disorganized conglomerates contain intraformational clasts		
		II-21,22															Extremely poorly sorted		

Fig 5.2 - Cataltepe section. (Lithology is not to scale)
In colour column; d: dark, l: light, g: grey
b: brown, bl: blue, y: yellow.

diameter boulders. The next 30 m of the section is made up of 20-60 cm thick graded conglomerate, Tae type sandstone and parallel laminated shale beds in the lower part, becoming alternations of Tabe type sandstone and parallel laminated shale beds towards the top with sandstone/shale ratio of 1:5. The remaining 88 m of the section is formed by the Kurebogazi member of the Bayat formation (8.2). Here this member overlies the Degirmendere formation with a gradual boundary (see 8.2.1 for the description of the upper part of this section).

The Degirmendere section (App IX) is measured along Degirmendere Valley (0-P13) and typifies the basinal exposures of the formation. Here the formation again show upward fining and thinning sequences which are sometimes interrupted by sequences in which medium to fine grained and medium bedded sandstone layers regularly alternate with shales. In between 0-160 and 240-300 m. of the section, the upward fining sequences start with 50 cm to 4 m. thick massive "amalgamated" sandstone or pebbly sandstone beds which contain spheroidal, well to very-well rounded (up to 3.5 m in diameter) volcanic rock pebble and boulders. These beds always have a sharp and irregular contact with the underlying beds and are overlain by sometimes indistinctly graded sandstone beds alternating with thin shale layers. The upward fining cycles are dominated by graded and disorganized conglomerate beds in between the 200-240 m and 300-330 m. of the section. All of the beds within these upward fining cycles form lens or wedge-shaped beds and, in some cases in the lateral extension of these beds, medium to fine grained thin bedded, sometimes parallel laminated sandstone and shale layers are observed. The last 40 m. of the section is represented by shale and fine sandstone alternations with some well rounded volcanic rock clasts scattered within these sediments.

5.2 Distribution, thickness and field relations

The Degirmendere formation is extensively exposed in the central and S and SW part of the area studied, usually in the core of the NE-SW trending anticlines, and has an irregular geometry. As was mentioned earlier the formation shows differences in its basinal and basin margin exposures: while matrix-supported conglomerates, associated with clast-supported conglomerate and massive sandstones are predominant in the latter, turbiditic sandstones with the clast-supported conglomerates and massive sandstones occur in the former outcrops. Due to intense faulting and thrusting in addition to poor exposures, except at a few localities e.g. NW of Keklicek (M16), SSW of K. Bayat (L18) and NNW of Kocanindambasi hill (J21), it is impossible to decide whether these conglomerates, in the basin margin deposits, are deposits of a single channel or part of a complex channel association. However in the above mentioned localities, especially NW of Keklicek, a single channel 70 m. thick, filled by conglomerates and massive sandstones, is observed. This channel has 200 m of observable length and is enclosed within a shale dominated sequence. A slumping of sandstones towards the channel axis is also observed (Plate 5.1) In the basinal exposures distinct upward fining and thinning sequences ranging, in thickness, from a few metres (Plate 5.2) to tens of metres (Degirmendere section) can be observed.

The total thickness of the formation is not known because the base is either not exposed or faulted in the areas where measured sections are taken. However the formation appears to show significant changes in thickness along strike (see cross sections) and thicknesses of 450 m, 180 m and 98 m are recorded in the Degirmendere, K. Bayat and Cataltepe sections respectively. In the Ortakisla deresi valley (F20) and NW of Kucuksekideresi, the lower boundary of the formation is seen to be transitional from the underlying Davdanli formation. (Chp 4) The Degirmendere formation shows a gradational



Plate 5.1 - A 51 m. thick conglomerate and massive sandstone within a single channel, enclosed by shale dominant turbiditic sequences. NW of Keklice (M16).

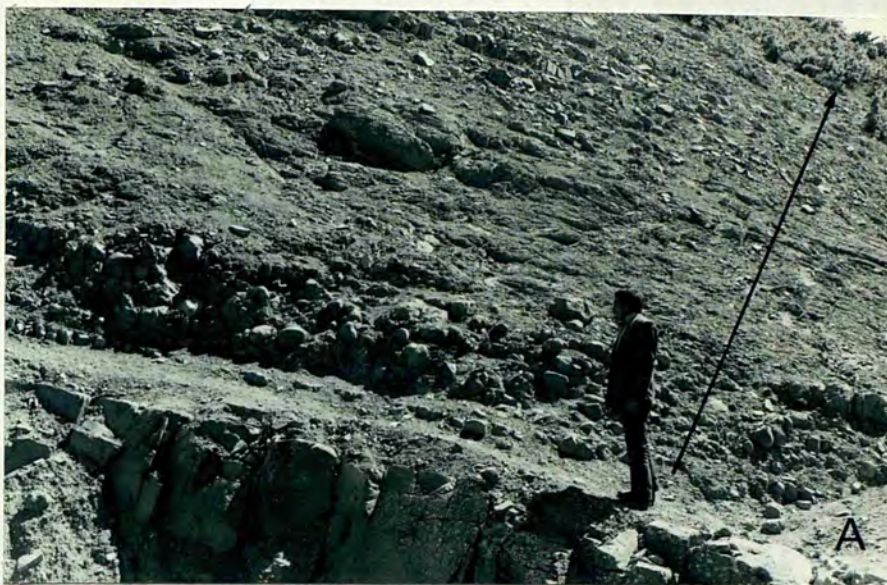


Plate 5.2 - Upward fining and thinning sequences. Note the occurrence of disorganized conglomerate beds which wedges out toward the left of the photograph A. Locality (K15). In photograph B three distinct cycles of varying sizes. Locality (I21).

boundary into the overlying Bayat formation (Chp 8)

5.3 Conglomerates

5.3.1 General description

Conglomerates are greyish-red-purple (5 RP 4/2) to dusky-red (5 R 3/4) and make up a large portion of this formation. They form beds a few decimetres to 10 m thick which frequently show erosional bases. Beds of the conglomerates are usually wedge shaped or lenticular and can be traced more than 200 m. in rare good exposures. The clasts may be as large as boulders, but generally the largest are cobbles and pebbles. Although the composition of the conglomerates are constant throughout the formation and composed of volcanic rock clasts, the roundness and sphericity of clasts show marked changes between localities and a general decrease in the sphericity and roundness of clasts towards the top of the formation is also observed.

The conglomerates may be divided into clast-supported and matrix-supported types, the latter differs from the pebbly sandstones (see below) as they contain more than 30% gravel size material. However a vertical and lateral gradation from pebbly sandstone to matrix supported conglomerates within some beds can be observed. (Plate 5.3A and 3B). The clast-supported conglomerates can be further subdivided as disorganized conglomerates without any sedimentary structures (Plate 5.4) and graded conglomerates which show grading, sometimes very indistinct, without parallel lamination at the upper parts of the beds. (Plate 5.5) The disorganized conglomerates, in some instances, evolve up into graded and parallel laminated sandstone beds. (Plate 5.4) Clasts in graded conglomerates are generally orientated with the long axes of clasts parallel to the bedding (Plate 5.3A) while no obvious clast orientation, apart from rare upward-projecting clasts, is observed in the matrix supported conglomerates.

Plate 5.3 - Matrix supported conglomerates in the basin margin deposits. Note the vertical (in A,B) and lateral (A) gradation of these conglomerates to pebbly sandstones and disorganized conglomerates and upward projecting clasts in the upper part of the bed (A). Hammer is 30 cm. in length. Localities A (M15) B (G26).





Plate 5.4 - Disorganized conglomerate overlain by parallel laminated sandstone towards the top of the bed without any apparent break. Note the slightly erosional base of the bed. Hammer is 30cm. in length. Locality (J15)

5.3.2 Texture

The matrix of the clasts varies from coarse to boulder, sometimes up to 10 cm in diameter and generally the matrix is fine to medium grained. The clasts are generally rounded to subrounded and are composed of various types of rocks, including igneous, metamorphic and sedimentary. The matrix is generally poor in cementation and is composed of fine to medium grained material. The clasts are generally rounded and are composed of various types of rocks, including igneous, metamorphic and sedimentary. The matrix is generally poor in cementation and is composed of fine to medium grained material.



5.3.3 Lithology

The lithology of the clasts varies from coarse to boulder, sometimes up to 10 cm in diameter and generally the matrix is fine to medium grained. The clasts are generally rounded to subrounded and are composed of various types of rocks, including igneous, metamorphic and sedimentary. The matrix is generally poor in cementation and is composed of fine to medium grained material. The clasts are generally rounded and are composed of various types of rocks, including igneous, metamorphic and sedimentary. The matrix is generally poor in cementation and is composed of fine to medium grained material.

Plate 5.5 - Graded conglomerate bed. Note the high degree of rounding and sphericity of clasts. Hammer is 30 cm. in length. Locality (I20).

5.3.2 Texture

The size of the clasts varies from granule to boulder, sometimes up to 75 cm. in diameter and, generally, the sizes increase in direct relation to bed thickness. There is no apparent comparison between composition and size, and clasts may range from angular to well rounded. The shape of the conglomerate clast varies from oblate to spheroidal (Zingg 1935) (Plate 5.6). The clast supported and matrix supported conglomerates show differences in sorting, the latter being more poorly sorted than the former, though overall they are generally poorly sorted: the conglomerates are texturally immature and can be classified as diamictites (Pettijohn 1975).

5.3.3 Lithology of conglomerate clasts

Volcanic Rock Clasts (VRC): These show a wide variation in composition and while dacite, dacitic-ignimbrite, andesitic tuff and rhyolite are present in decreasing order of abundance, andesite is the most common type. (Due to intense alteration of phenocrysts, chemical composition of rock is used in classification (Table 12.1)).

Andesites show a porphyritic texture in which euhedral to subhedral plagioclase (andesine-labrodorite) crystals with some mafic minerals and anhedral, small K-feldspar crystals are embedded into the cryptocrystalline groundmass. Plagioclase commonly shows albite twinning while occasional carlsbad twinning and normal zoning also occur. Mafic minerals are altered, except for a few anhedral clinopyroxenes which show high refractive indices, strong surface relief and dominant arcuate fractures along which brown ferruginous pseudomorphs develop. All stages of incipient alteration to complete pseudomorphs are present (Plate 5.7A).

Dacitic rock clasts are white to greyish white and are composed of euhedral to subhedral K-feldspar phenocrysts with limited amounts of plagioclase and strongly altered,

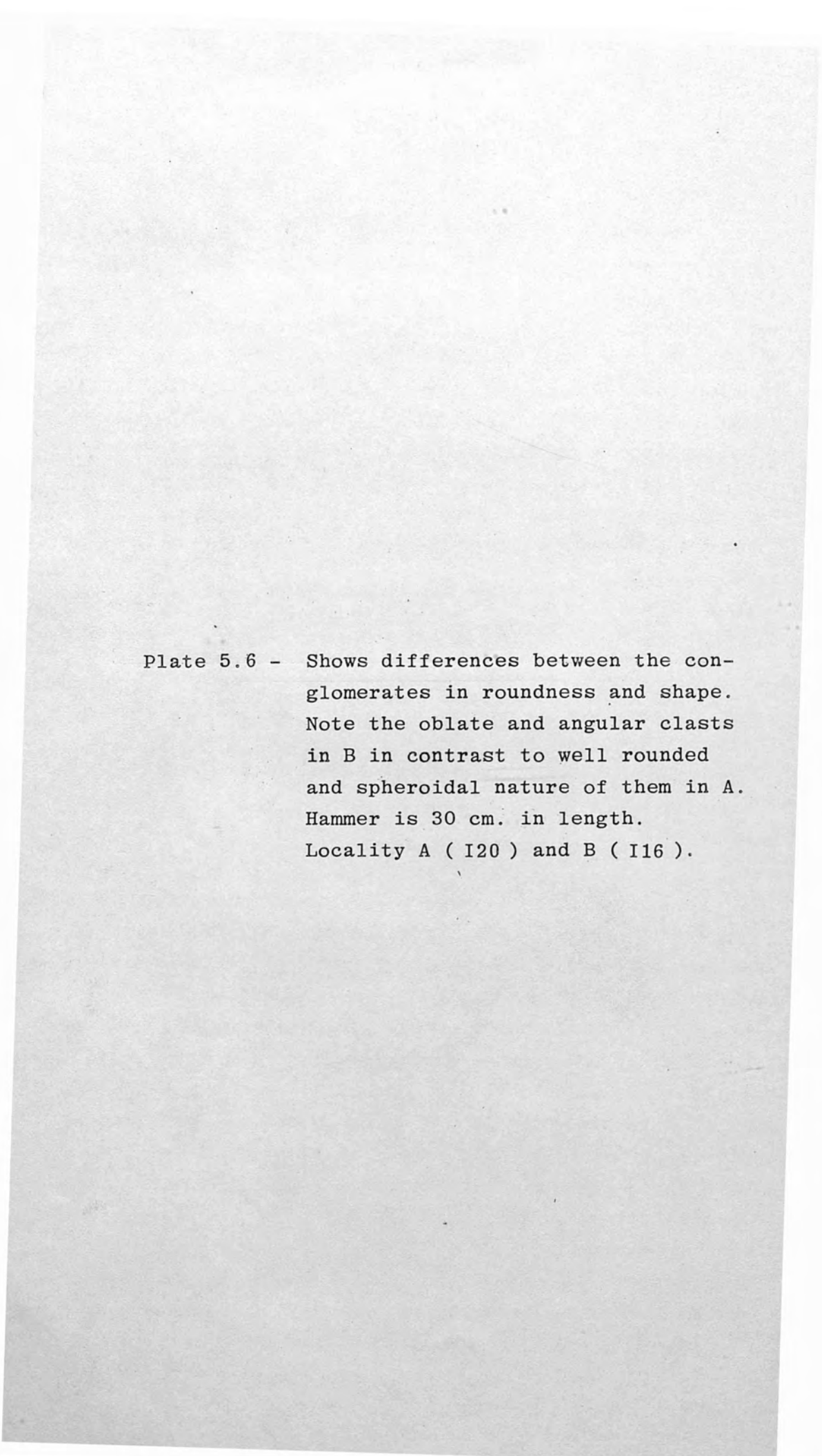
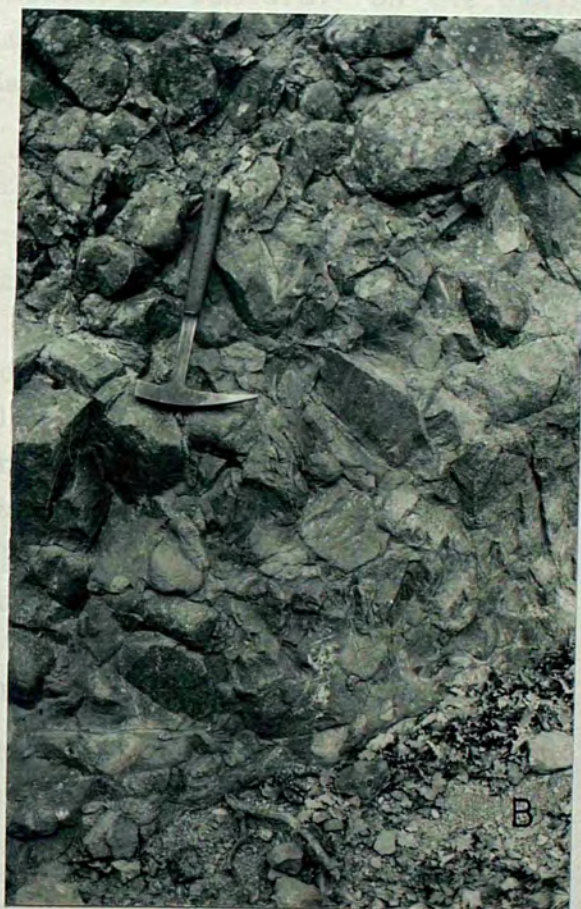


Plate 5.6 - Shows differences between the conglomerates in roundness and shape. Note the oblate and angular clasts in B in contrast to well rounded and spheroidal nature of them in A. Hammer is 30 cm. in length. Locality A (I20) and B (I16).



therefore unidentifiable, mafic minerals within a cryptocrystalline groundmass which in some cases is recrystallized to microcrystalline quartz (Plate 5.7B).

Andesitic tuffs have broken plagioclase crystals which show some degree of erosion and some epiclastic grains. They generally occur as welded tuffs which are quite difficult to differentiate from andesites.

Rhyolites (Plate 5.7C) are pinkish and contain euhedral and subhedral K-feldspar phenocrysts (with carlsbad and baveno twinning), medium to large anhedral quartz crystals and large biotite phenocrysts, which despite intense alteration, show parallel extinction. All of these constituents are in a cryptocrystalline to glassy groundmass which sometimes has spherulitic texture. On the basis of their chemical composition (see Table 12.1) they are sodi-potassic rhyolites (Hatch et al 1972).

5.3.4 Matrix of conglomerates

Composed of sand, silt and clay grade material the matrix is compositionally similar to that of sandstones. Although it is, overall, poorly sorted, the matrix is more poorly sorted in the matrix-supported and disorganized conglomerates than in the graded types. The matrix sometimes contains abundant plant fragments and is occasionally replaced by sparry calcite.

5.4 Sandstones (Volcanic arenites)

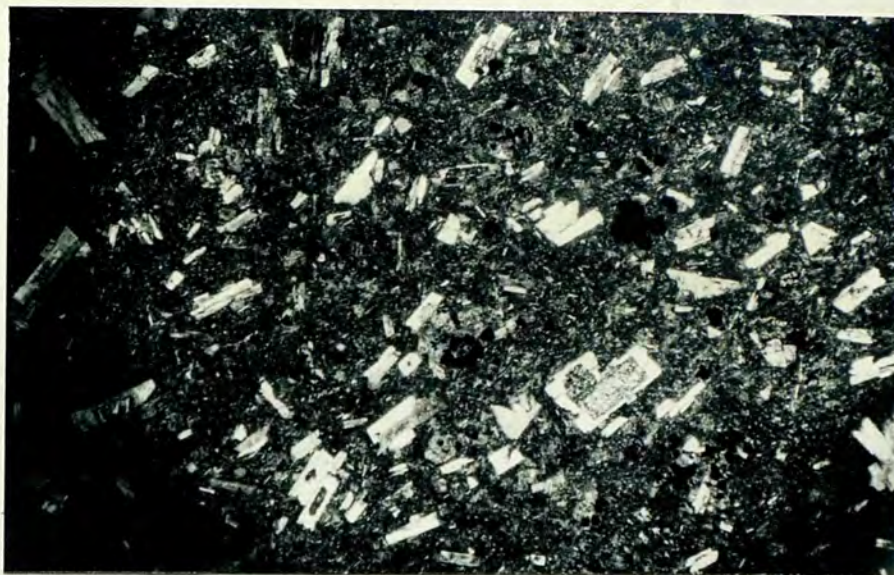
5.4.1 General description

Sandstones of the Degirmendere formation are pale reddish brown (10 R 5/4) to yellowish grey (5 Y 7/2) and occur in three distinct types:

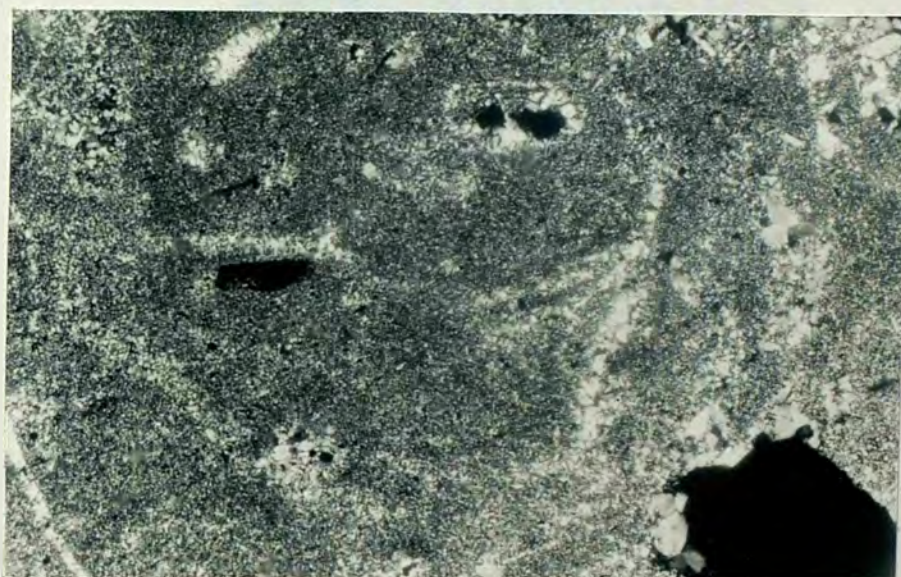
a) Massive sandstones (Plate 5.8): are coarse grained and sometimes contain granule to pebble size clasts in the

Plate 5.8 - Photomicrographs of volcanic rock clasts:

- A. Andesite shows porphyritic texture and consists of plagioclase and mafic mineral phenocrystal within a dark microcrystalline groundmass which contain feldspar micro-liths. Mafic minerals are extensively altered and cannot be determined.
Sample DD28, 15x, XN.
- B. Dacitic ignimbrite contain small completely altered (volumization) feldspar crystals within a chert like groundmass. Ghost shard structures are also visible.
Sample DD.17, 35xx, XN.
- C. Rhyolite: shows porphyritic texture in which K-feldspar, plagioclase and mica phenocrystals are embedded into a cryptocrystalline groundmass.
Sample 269E, 15x, XN.



A



B



C

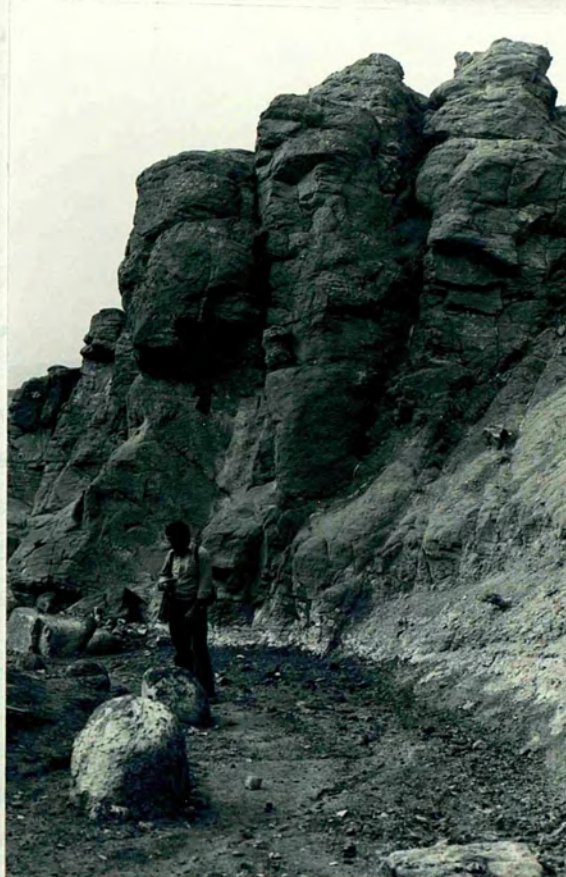


Plate 5.8 - Amalgamated massive sandstone beds. Note the locally developed laminations in different parts of the beds.

Locality (K19).

lower part of the beds. Bed thickness ranges from 50 cm. to 2 m. and beds are wedge shaped or lenticular. They are generally structureless although, in some cases, indistinct crude parallel stratification can be observed. Amalgamations of sandstone beds are common and shaly interbeds are either absent or thinly developed.

b) Pebbly sandstones: are similar to massive sandstone beds except for the occurrence of pebble and boulders and, occasionally, mud pellets and intraformational pebbles (Plate 5.9). All these clasts are randomly distributed and their proportion varies significantly from bed to bed. These clasts are sometimes up to 3 m. in diameter and exclusively of volcanic rock. Pebbly sandstones form beds 1 m. to 5 m. thick, wedge and lens shaped beds which show irregular bases and a sharp upper contact with the overlying beds.

c) This type of sandstone can be described by Bouma sequences and Tabce, The and Tde-type beds are commonly observed. This type of sandstone shows differences between the basin margin and basinal exposures. When they are interstratified with/or found in the lateral extension of the conglomerates and massive sandstone beds in the marginal areas, these beds are 5-25cm thick, parallel laminated and generally fine grained. This type of sandstone is interbedded with shales of similar thickness with sandstone/shale ratio of 1 or less (Plate 5.10). In the basinal exposures the sandstone beds are 20-50 cm. thick, coarse-medium grained and interbedded with shales of varying thickness. The sandstone beds frequently include plant fragments in their upper part, commonly show parallel laminations with occasional convolute or wavy laminations and although the beds can be traced further than is the case for the massive and pebbly sandstone beds, they, too, show lensing and wedging-out. Small scale submarine slump folds are found locally within these sandstones.



Plate 5.9 - Pebbly sandstone. Note the random distribution of clasts. Coin is 2.5 cm. in diameter. Locality (N15).



Plate 5.10 - Regularly bedded 5-20 cm. thick Tabe,
Tbce and Tde-type sandstone and shales
of similar thickness. Hammer is 30 cm.
in length.

Locality (I21)

5.4.2 Texture

The grain size of the sandstones varies from granules to silt size and there appears to be a positive relation between grain size and bed thickness as thicker the bed, coarser become the grain size. No obvious relationship is found between the grain size and composition, other than that rock fragments occur in the coarser grain sizes.

Although all degrees of rounding can be found, angular to subrounded grains predominate. Rock fragments are relatively well rounded in contrast to quartz and feldspar grains which are generally angular and fresh. No obvious grain orientation has been found and grain contacts vary from suture to tangential though the latter and long contacts dominate. Packing proximity is between 40%-80% and sorting varies between the sandstone types. Though overall they are poorly sorted, the massive and pebbly sandstones are relatively more poorly sorted than the sandstones with Bouma divisions. These sandstones are texturally immature.

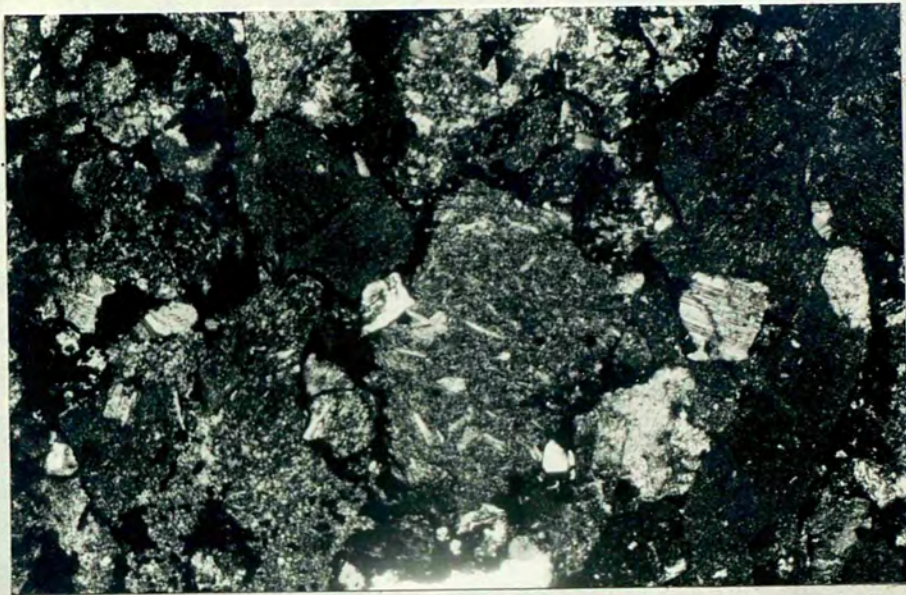
5.4.3 Framework grains

The sandstones of this formation are composed of volcanic rock fragments, chert, quartz and feldspar (Plate 5.11) and each of these fragments may become volumetrically important laterally as well as vertically in the stratigraphic column (Table 5.1).

Volcanic Rock Fragments (VRF) are andesitic and dacitic and/or rhyolitic (due to textural and compositional similarities of these VRF to the VRC of conglomerates) and intense alteration and replacement of phenocrysts and groundmass by calcite is commonly observed. Andesitic VRF have a cryptocrystalline groundmass in which partly to completely altered plagioclase and a few K-feldspar phenocrysts, sometimes with unidentifiable mafic mineral phenocrysts, are observed. The groundmass sometimes contains small plagioclase crystals of acicular habit forming a trachytic (flow)

Plate 5.11 - Photomicrograph of sandstones:

- A. Volcanic arenite, consists mainly of volcanic rock fragment, feldspar and quartz with tuffaceous matrix which is generally stained by hematite most probably leaching from the iron-bearing mineral of the volcanic rock fragments. Sample 435, 35x, XN.
- B. Volcanic arenite is composed of volcanic rock fragments, feldspar, quartz and clay mineral matrix. Sample DD.19, 35x, XN.



A



B

Parameters Sample No	Quartz	Feldspar	VRF	SRF	Cement	Matrix	Accessory Components	Others	Total %	Total Count
DD-3	9.8	10.2	59.8	0.4	0.6	18.4	0.8	-	100.0	500
DD-10	10.5	14.2	49.3	0.4	1.2	20.7	3.7	-	100.0	515
DD-19	5.3	5.3	42.2	1.8	1.6	41.0	2.8	-	100.0	505
DD-23	9.8	21.6	35.6	2.9	4.2	25.7	0.2	-	100.0	650
52	14.6	8.8	37.4	2.8	9.6	21.2	5.6	-	100.0	500
289	3.1	2.5	49.2	1.0	27.1	11.6	3.5	-	100.0	484
295	4.6	9.2	52.4	2.0	6.6	20.9	4.4	-	100.0	502
402	11.3	14.9	46.6	1.0	2.6	19.1	4.4	-	99.9	496
412	6.8	5.9	51.3	5.3	4.1	21.9	4.7	-	100.0	511
435	2.4	5.0	55.9	0.9	2.8	31.8	1.1	-	99.9	535
437	5.2	5.6	49.6	4.0	7.8	25.6	2.2	-	100.0	500
450A	5.0	1.4	34.6	32.8	9.4	14.2	2.6	-	100.0	500
464	10.0	5.0	43.0	5.9	19.4	14.1	2.5	-	99.9	558
658	8.7	4.3	56.8	1.5	3.0	23.5	2.0	-	100.0	538
669	8.1	5.1	57.3	0.6	6.1	18.6	4.2	-	100.00	506

Table 5.1 - Modal composition of the Degirmendere formation's sandstones. Sedimentary Rock Fragments (SRF) includes limestone and skeletal fragments, cherts are included to Volcanic Rock Fragments (VRF).

texture. The dacitic and/or rhyolitic rock fragments show K-feldspar phenocrysts and a few biotites within a glassy matrix which in most cases is devitrified to a microcrystalline quartz aggregate.

Feldspars: are either fresh or completely altered and are generally angular. Plagioclases are more common than K-feldspars and generally andesine-labrodarite in composition. They generally show albite twinning with occasional occurrences of normal zoning and carlsbad twinning.

Cherts are usually subangular to subrounded and occur as microcrystalline quartz aggregate. These fragments, in many respects, resemble the groundmass of the dacitic and rhyolitic rock fragments and are believed to have a volcanic origin, although a relict texture (e.g. ghost shard structures or spherulitic texture) which would have been indicative of volcanic origin is generally absent.

Quartz is usually single quartz type, although some composite quartz grains are also observed. The single quartz shows straight extinction with few inclusions and negative crystals which are needle shaped. They generally have large rounded corrosion embayments and are of volcanic origin. The composite quartz grains have slight to strong undulose extinction and are common quartz (Folk 1974)

Broken shell fragments and foraminifers, although rare, are also observed.

Biotite is the most common accessory mineral and easily distinguishable by its parallel extinction, cleavage and flake-like shape. Hematite usually occurs as an alteration product of biotites. Plant fragments and unidentified heavy minerals are also present as accessory components.

5.4.4 Matrix and Cement

The matrix of the sandstones is composed of tuffaceous material, clays minerals, most probably sericite and/or illite and micrite which is sometimes recrystallized to neomorphic sparry calcite. The matrix material is generally coated by hematite supplied from the breaking-down iron-bearing minerals of the VRF. This hematite coating was in the later stages of the diagenesis as indicated by the hematite infilling of the hairline fractures of detrital grains, caused during the compaction. The original cement is very rare and when present it is of calcite.

5.5 Shales

5.5.1 General description

The shales of the Degirmendere formation show differences, depending on the type of coarse clastics between which they are interbedded. When interbedded with conglomerates and massive or pebbly sandstones they are generally very thin (from few cm. to 25 cm. thick) and lens and wedge-shaped due to erosion caused by turbidity currents. They have sharp bases and tops and frequently show load cast injection structures (Plate 5.12). In the case of intercalation with Tabe, Tbc and Tde type sandstone beds, the shales are 10-50 cm. thick (thicker beds are usually observed in the upper part of the stratigraphical column of the basinal exposures, see Degirmendere section App. IX), parallel laminated and have sharp top but gradational bases. The shales are usually poorly sorted and composed of quartz, feldspar, micrite and clay minerals which on XRD analysis are found to be illite, kaolinite, chlorite and sericite. The grain size ranges from silt to clay grade material with a few scattered sand size grains. They are generally moderate to poorly cemented and indurated and are often stained by iron-oxide (limonite and hematite). The shales sometimes contain abundant plant fragments which, in one case, develop



Plate 5.12 - Injection structures. Note extremely poorly sorted nature of conglomerate in A. and wedging out of shale in B. Hammer is 30 cm. in length.
Localities A (O13) and B (T6).

a 2-3 cm. thick laminae (Plate 5.13).

5.6 Sedimentary structures and current directions

Slump balls (see section 4. for definition of slump balls) and load structures are the most common sedimentary structures observed in this formation. The latter exist mainly as ball and pillow structures (Potter and Pettijohn 1963) and mudstone tongues occur in between balls and pillows. Ball and pillow here covers a structure consisting of a sand layer which is broken-up into several ball or pillow-shaped, more or less ellipsoidal masses. In this formation they occur in shale dominated sequences in which sandstone balls and pillows are found sinking into shale (Plate 5.14). Their size ranges from 10 cm. to 2 m. across and they are persistent laterally. Their shapes also vary from completely flattened pillows to whorl-like balls. It is commonly agreed that this structure was formed due to liquifaction of mud-beneath a recently deposited sandstone layer or liquifaction of a sandstone layer itself (Blatt et al 1972, Reineck and Singh 1975, Dzulynski and Walton 1965 and Allen 1982). The cause of liquifaction can be due to either rapid deposition or sudden shock - most probably earthquakes (Middleton & Hampton 1976, Keunen 1958). The presence of laminae in some pillows indicates that complete liquifaction of sand did not take place. Other sedimentary structures include an indistinct grading in some sandstone and conglomerate beds, parallel laminations in sandstones and shales and occasional sole structures, such as groove casts and large flute cast (Plate 5.15). Slump folds which are generally confined to shale dominated sequences are seldom observed. They range from isoclinal to open folds in shape (Plate 5.16) and their axes and sense of facing direction differs in different localities (see Fig 12.) However as a rule no slump fold with a S to SE sense of facing direction is observed.

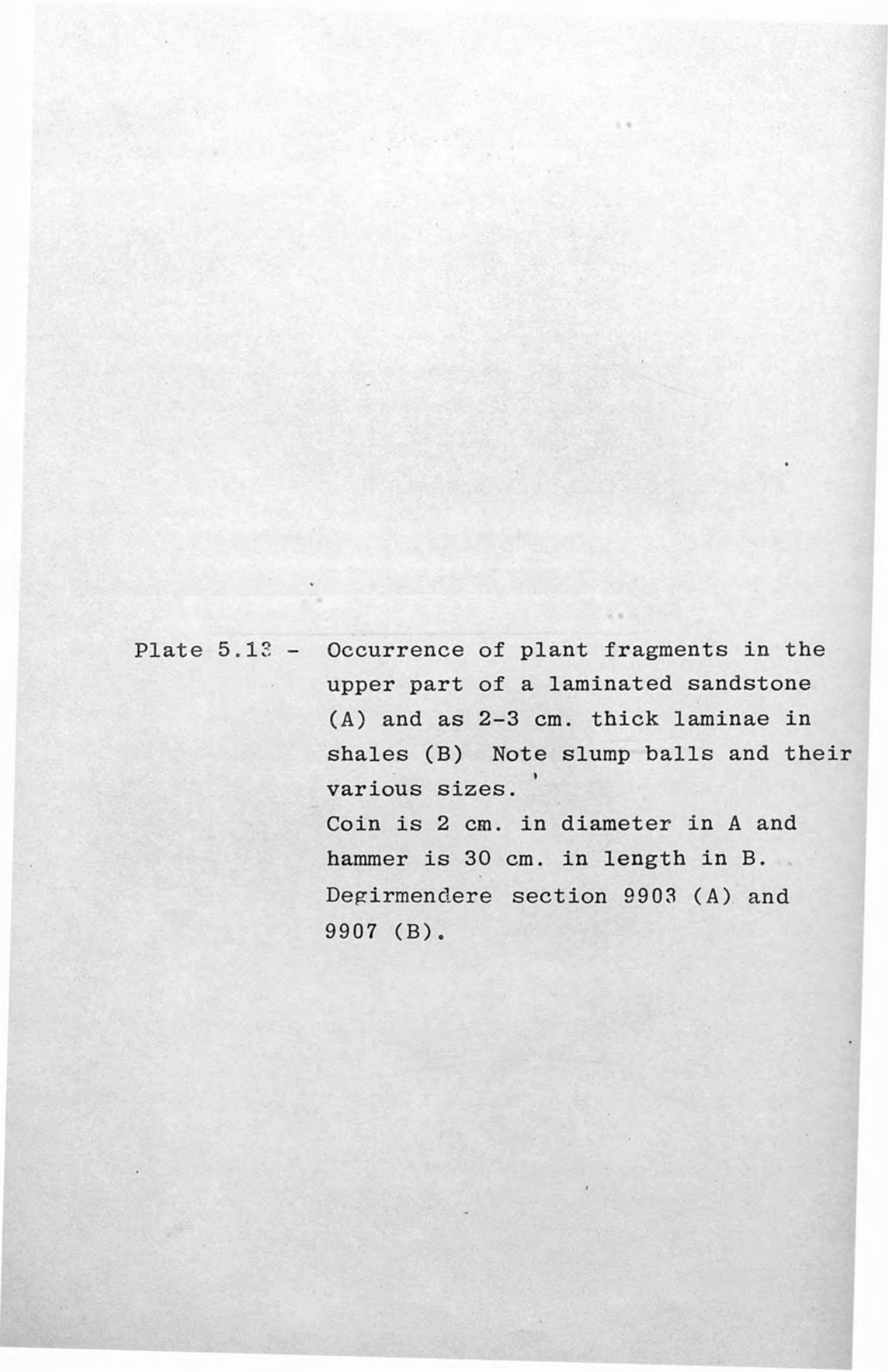


Plate 5.13 - Occurrence of plant fragments in the upper part of a laminated sandstone (A) and as 2-3 cm. thick laminae in shales (B) Note slump balls and their various sizes.

Coin is 2 cm. in diameter in A and hammer is 30 cm. in length in B. Degirmendere section 9903 (A) and 9907 (B).



A



B



Plate 5.14 - Ball and pillow structure. Note the laminated outer layer of the balls and pillows. Hammer is 30 cm. in length. Locality (T6).

Plate 5.15 - Flute casts on the base of the graded (A) and massive sandstone beds (B). Current is from lower left corner of A (pen is 15 cm. in length) and from bottom to top of B (penknife is 10 cm. in length).
Localities A (H18) and B (N14).

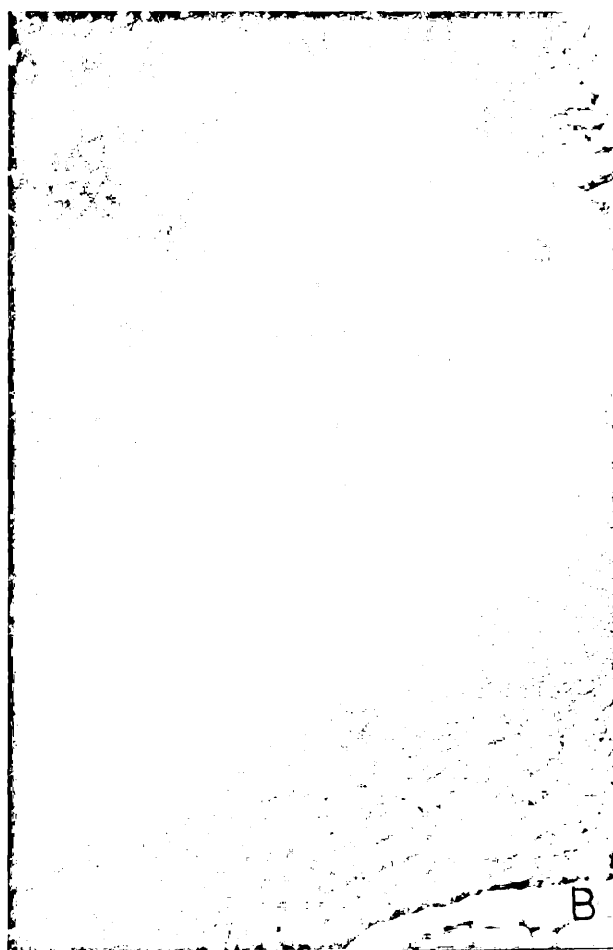
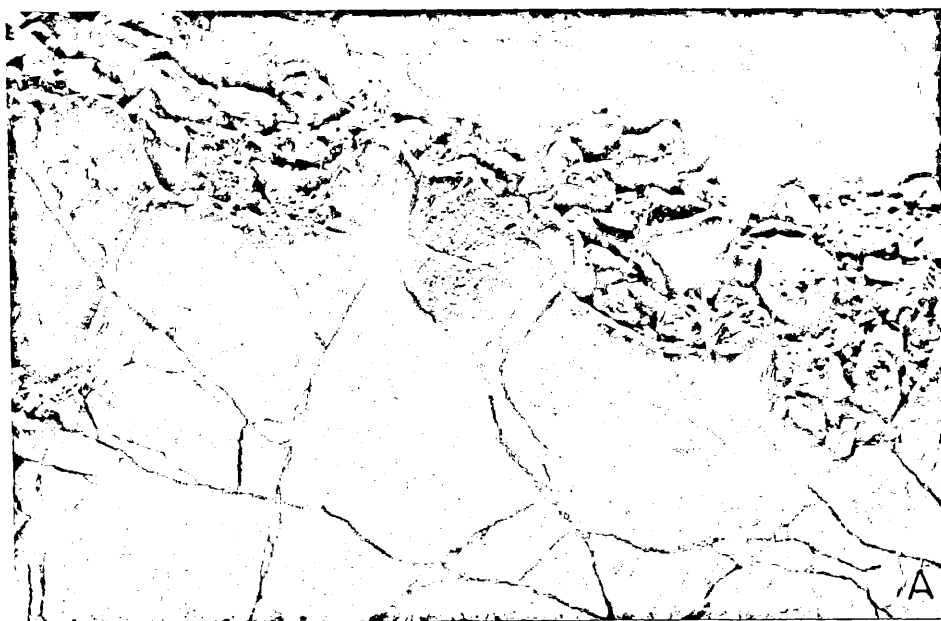




Plate 5.16 - An open slump fold in a shale dominated sequence in the basal exposures of the formation.

Locality (O12)

Current directions are obtained by the measurement of flute casts and, although they are generally from S, SE and SW, different localities give different directions (see Fig 12.8.) Directional values of the slump folds as an indication of palaeoslope direction and inclination, in spite of their diversity in directions of slumping which are from N, SE, SW and, S, but not from NE, can also be used. On this basis together with the member's stratigraphic position and the current directions, it can be concluded that palaeoslope strikes NE - SW and was inclined to the NW.

5.7 Weathering and alteration

The conglomerates of this formation show varying degrees of weathering depending on the amount of matrix present in them. Shales are less durable when compared with the sandstones and conglomerates.

The most obvious alteration product is the iron-oxide in the form of limonite and haematite which most probably resulted from the break-down of iron-bearing minerals of volcanic rock clasts and fragments, and they are more apparent in the sandstones and some shales.

5.8 Fossils and age of the Degirmendere formation

Apart from broken and/or whole benthonic foraminifers which are not identifiable, no fossils have been found in this formation. A lower Palaeocene age is designated for this member on the basis of its relation with the underlying Davdanli formation, which is Middle-Upper Maastrichtian in age, and the overlying Middle Palaeocene-Middle Eocene Bayat formation.

5.9 Source area and environment of deposition

The source area for the sediments of this formation, as indicated by their exclusively volcanic rock composition, was a volcanic terrain situated on the southeastern margin

of the basin. Textural and compositional similarities of andesitic and dacitic rock clasts of this formation with volcanic rocks of the Saridere volcanic formation (Chp 2), and their chemical composition similarities (see Table 12.1), suggest that the latter formation was the main source area.

The generally oblate to spheroidal shape of the conglomerate clasts suggests that they were carried down to their temporary, intermediate, deposition site by rivers, since it is generally accepted that fluvial pebbles show high sphericity in contrast with the flat shape of beach gravels (Blatt et al 1976). The high degree of rounding and sphericity of these clasts can be explained by the following factors:

- a) reworking of these clasts from older conglomerates
- b) these clasts have been subjected to considerable abrasion (Folk 1974, Pettijohn 1975)
- c) effect of the nature of source rock e.g. original jointing and vulnerability to chemical weathering.

Since there is no sedimentary formation exposed on the southeastern margin of the basin containing conglomerates of similar composition to those of the Degirmendere, it is extremely unlikely that the first factor was involved. The lower unit of the Sarikaya member, which was the time equivalent of the Degirmendere formation in the continental areas, indicates an alluvial fan depositional environment in which the main process of deposition was by debris flow with some small streams of sporadic occurrence which could not have provided the necessary prolonged abrasion. However, this member has a limited exposure (see 6.2.2) and its base is not observed in the area studied, therefore it is possible that for lower parts of this member and along strike in the NE part, the nature of deposition might have been different. This seems likely since the differences in rounding and sphericity of conglomerate clasts in different localities with the constant sphericity and roundness

of clasts at each locality (see Plate 5.), together with the predominance of small gravels in other localities (perhaps suggesting a longer transportation time than localities with large pebbles), may indicate that the basin was fed by separate rivers and/or streams with different flow regimes, maturity and catchment areas. Although no marked original jointing is observed in the present exposures of the Sari-dere volcanic rocks, it is possible to have jointing in volcanic rocks due to cooling. Additionally, volcanic rocks are known to be prone to chemical weathering. Thus the effect of a third factor could, in part, be responsible for the high degree of rounding and sphericity of clasts. The occurrence of fresh and altered feldspars in close proximity to each other and their angularity together with the presence of quartz of same degrees of rounding suggest

a) alteration of some feldspar grains in the source area

b) a tectonically active source area with a rugged topography and humid and warm to temperate climate (Folk 1974)

c) short duration of transport for these fragments. The predominance of plagioclase, which is thought to be unstable under surface conditions (Folk 1974), over K-feldspars indicates that most of the source area was covered by plagioclase - rich volcanic rocks and that plagioclases were removed immediately after weathering before soil-forming processes developed. From all the evidence it can be concluded that the volcanic rock dominated source area had a humid and warm to temperate climate, was tectonically active and crossed by a number of streams and rivers with high discharge rates and sediment loads. Intrabasinal sources provided the small amount of broken shell fragments and benthonic foraminifers together with intraformational pebbles and mud pellets.

A model for the environment of deposition of this

formation can be developed from the sedimentary structures, the geometry of sediments, fossil assemblages and this formation's position relative to underlying and overlying formations. The absence of criteria suggestive of shallow marine and continental environments (see 3.10 and 4.9) indicates that the sediments of the Degirmendere formation were deposited in a deep marine environment.

The matrix supported conglomerates with their sedimentary characteristics (the presence of upward projecting clasts, high matrix content, irregular base of the beds and the absence of scour marks) resemble subaqueous debris flows described by Middleton & Hampton 1976, Walker 1978. The other lithological types of the formation are believed to be deposited by high density currents (which deposited disorganized and graded conglomerates with grain interaction as the final grain support mechanism and massive and pebbly sandstones with liquefaction of sand as final depositional mechanism) to low-density turbidity currents (Tabe, Tbe and Tde-type sandstone beds) (Walker 1978). The occurrence of medium-fine grained thin bedded Tbce and Tde-type sandstone and shale intercalations, irregularly alternating or laterally passing to the channel-fill conglomerates, can be explained by the overflow of turbidity currents from the channels and depositing their load on the levees (Kulm & Nelson 1973, Nelson, Mutti, Lucci 1977, Walker 1978).

The presence of channelled conglomerates with levee deposits together with current directions generally transverse and oblique to the basinal axis suggest that the Degirmendere formation was deposited as submarine fans. This conclusion is further supported by the occurrence of matrix-supported conglomerates, which are believed to be deposited in the mouth of feederchannels, associated with clast-supported conglomerates and massive sandstones in the basin margin exposures of the formation. These contrast with the predominantly sandy nature of sediments with a

decrease in the number and frequency of conglomerate beds (only clast-supported types are observed) in the basinal areas, indicating a gradually increasing distance away from the source. The presence of thick poorly bedded, extremely poorly to poorly sorted channelled conglomerates, which contain up to boulder size clasts, massive sandstone and pebbly sandstone beds, the occurrence of levee deposits, either absent or thinly developed shale layers in between the conglomerates and the absence of evidence suggestive of rapid channel migration, such as well developed inter-channel deposits between the channel deposits, in the sediments of this formation exposed towards the margin of the basin, suggest that they were most probably deposited on the inner fan areas of submarine fans. In this part of the formation conglomerate and massive sandstone dominated pockets enclosed within a sequence of alternating Tabe and Tde-type sandstone and shale with sandstone/shale ratio of less than 1/10, are observed (Plate 5.1). Although these conglomerate pockets can be interpreted as feeder channel-fill deposits on a slope, on the absence of slump folds and deposits particularly within a tectonically active area, (Walker & Mutti 1973, Stanley et al 1975 and also see Kurebogazi member of the Bayat formation 8.2), they are believed to have resulted from the abandonment of a large inner-fan channels.

In the basinal exposures of the formation the presence of upward fining and thinning sequences (Plate 5.2 and see App.IX Degirmendere section), channeled conglomerate and sandstone beds with relatively longer lateral continuity than the inner fan channels, together with the occurrence of turbidite beds alternating with conglomerates and massive sandstones, indicate that these sediments were deposited on the upper (channeled) part of the middle fan areas.

All these interpretations are consistent with the character of ancient and modern submarine fans (ibid p118). Namely, the inner fan contains the thickest, most poorly

bedded, coarsest, least structured and most poorly sorted sand and gravels with biota which are mainly large shell fragments, plant debris displaced from the shallower depth, while middle fan is predominated by sand, shows rapid channel migration and upward fining and thinning cycles.

It can additionally be concluded that, due to the presence of differences in roundness and sphericity of conglomerate clasts and composition of sandstones in different localities, a number of small submarine fans were developed in the different parts of the basin during the deposition of this formation.

The palaeodepth of the basin during the deposition of this formation can only be estimated on the basis of its inferred environment of deposition as being somewhere on the base of the slope.

C H A P T E R 6

UCEM FORMATION

6.1 General Introduction

The Ucem formation (Early Palaeocene to Middle Eocene) is time transgressive and consists of conglomerates, sandstones and mudstones. The formation is divided into two members in terms of sedimentary structures and fossil assemblages. The first is named after Sarikaya (Q14) and consists of red to yellowish brown unfossiliferous conglomerates, sandstones and mudstones. The second is called after Sehriban (L21) and made up of fossiliferous sandstones, marls, mudstones and conglomerates. Due to the time-transgressive nature of the formation, the members are also divided into lower (Palaeocene) and upper (Eocene) units in which considerable changes in thickness, composition and fauna are observed. Although inferred, the environment of deposition remained essentially the same (see 6.2.10 and 6.3.6). The upper and lower units of the members of the Ucem formation show different boundary relations with other formations of the Bala basin. These variations are a reflection of the changing palaeogeography (see below).

6.2 SARIKAYA MEMBER

6.2.1 General Introduction

This member with its red colour, is one of the most distinctive lithological units in the Bala area and consists of red conglomerates, sandstones and mudstones. It is best observed around Halaclikisla hill (S12), along the valleys of Saridere (R13, Q12) and Cesmedesi (I26).

In the Halaclikisla section (Fig 6.1) the upper unit of the member is exposed, interfingering with the Sehriban member in between 213 and 248 m. from the base of the section. The section starts with 80 cm. to 4 m. thick, yellowish brown to red, poorly sorted conglomerate beds randomly alternating with muddy sandstones in the first 75 m. Conglomerate beds are structureless, matrix supported and have irregular bases. They are laterally extensive and in some occasions they are cut by graded to non-graded, cross-stratified, relatively better sorted, 30-80 cm. thick, lens shaped conglomerate beds. Sandstones occur either structureless or with poor to well defined parallel lamination and occasionally with cross-stratification. The latter type is less frequent and medium to fine grained. In between 75 and 213m. the section is dominated by thick muddy sandstones with occasional matrix supported conglomerates which are cut by graded conglomerates of varying thickness. Occasional parallel laminated, medium to fine grained thin (10-30 cm) sandstone beds are also observed in this part. The next 35 m. of the section is composed of light brown conglomerate, sandstones and, in lesser amounts, mudstones of the Sehriban member. Conglomerates are poorly sorted and contain varying amounts of broken or whole mega - and microfossil fragments in the upper part of the beds. Sandstones are better sorted parallel laminated or structureless and form 20 cm.-1 m thick beds. The remaining 47 m. of the section consists predominantly of muddy sandstones and lens shaped conglomerates of the Sarikaya member.

In the Saridere II section (Fig 6.2) the upper unit is observed and the member overlies the Saridere volcanic formation (Chp 2) with an unconformable boundary. The first 105 m of this section is made up of red to reddish brown up to 4 m thick, matrix supported conglomerates and structureless, coarse to fine grained, muddy-sandstone to sandy-mudstone layers. Conglomerates are poorly sorted and do not show erosional bases or sedimentary structures. The next 132 m. consists of red

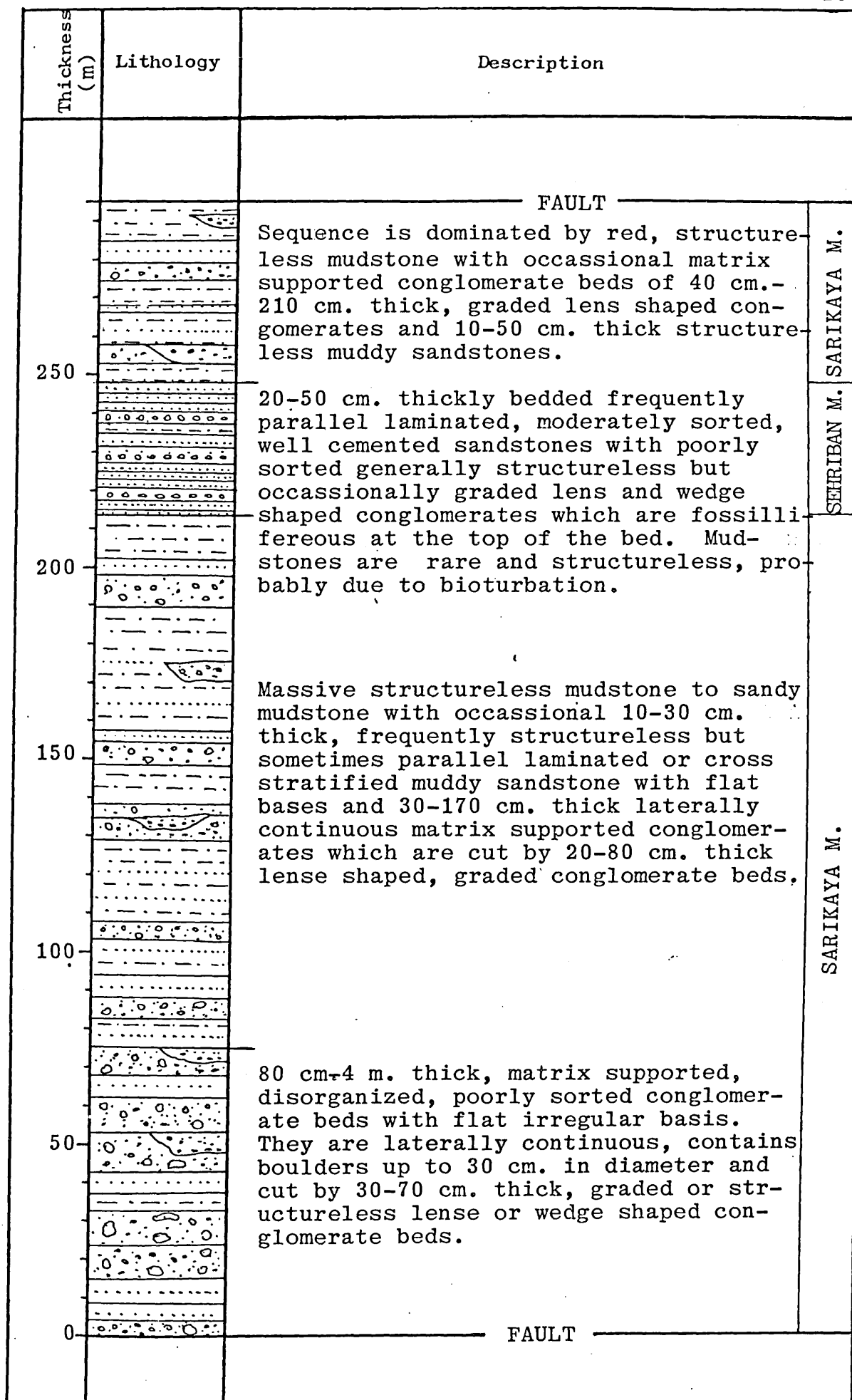


Fig 6.1 - Halaclikisla section.

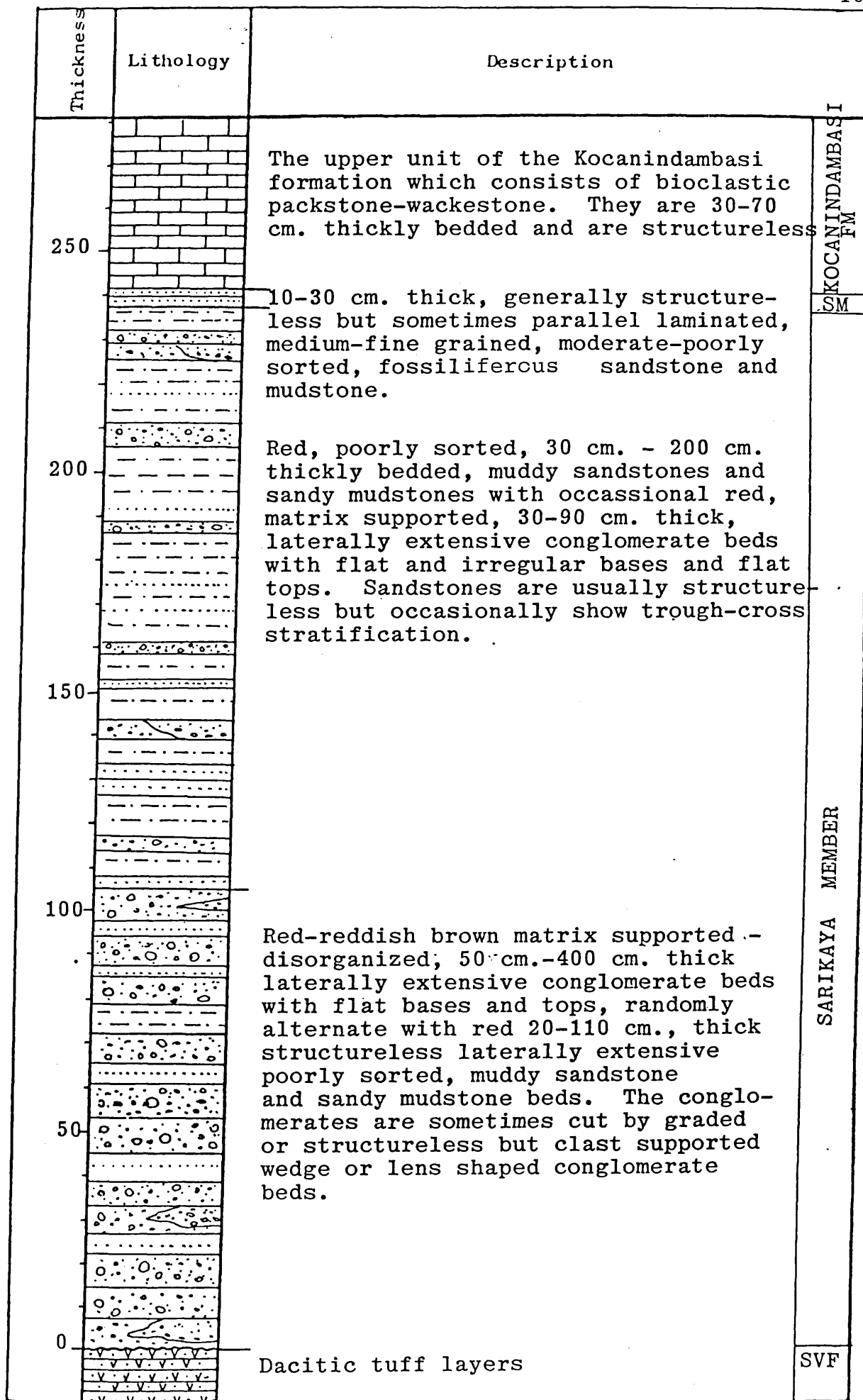


Fig 6.2 - Saridere II section. (SM: Sehriban member, SVF: Saridere volcanic formation)

massive beds up to 2 m. thick with occasional trough-cross beds. The beds are coarse-fine grained sandstones with mudstones and some lens-shaped conglomerate beds. The Sarikaya member, at the top of this sequence, passes up to the Sehriban member, which is 4 m thick and composed of medium to fine grained fossiliferous, sometimes parallel laminated, sandstone and mudstone alternations. The topmost 40 m of the section is represented by 30-150 cm. thick bioclastic limestone of the Kocanindambasi formation.

The lower unit of the Sarikaya member is recorded in the Cesmederesi section (Fig 6.3) where it starts with red-reddish brown, up to 2 m thick, poorly sorted, laterally extensive, generally structureless muddy sandstone, pebbly sandstone and mudstone beds. This succession continues for 70 m from the base of the section and then gradually passes up to 80 m. of red-reddish brown, moderate to poorly sorted lens and wedge shaped, 50-300 cm. thick and sometimes cross-bedded and graded conglomerate beds alternating with structureless sandstone and mudstone beds succession. The following 26 m. of the section consists of the Sehriban members light to brownish grey fossiliferous conglomerate and sandstone beds. The conglomerates and sandstones form poorly developed 50-150 cm thick beds and are generally structureless, apart from some parallel laminations in the sandstone beds. Towards the boundary with the lower unit of the Kocanindambasi formation, their grain size decreases to fine sand and silt and the member gradually passes up to the latter.

6.2.2 Distribution, thickness and field relations

The Sarikaya member shows considerable changes in thickness, boundary relations and distribution along the NE-SW trending exposure (see Fig 6.4). The stratigraphical setting and distribution at different localities is discussed below.

The lower and upper units of the member outcrop between

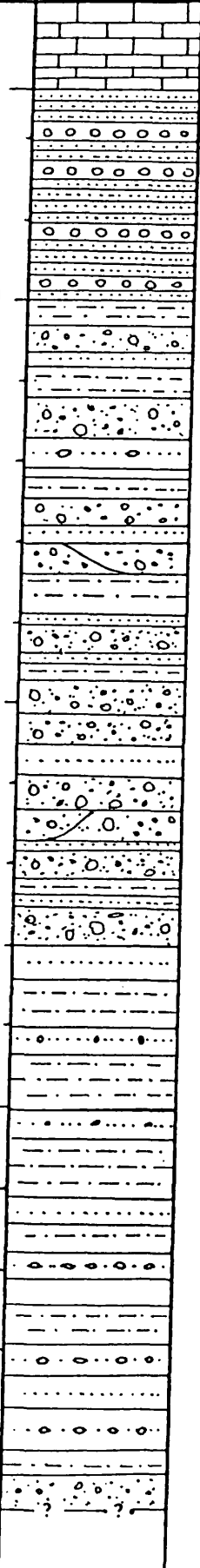
Thickness	Lithology	Description	
		<p>Lower unit of the Kocanindambasi formation consists of subfacies I.</p> <p>Light brownish grey, 70-130 cm. thickly bedded, moderate-poorly sorted sometimes graded but generally structureless fossiliferous conglomerates and 50-150 cm. thickly bedded, sometimes parallel laminated but generally structureless fossiliferous sandstones.</p> <p>Red-reddish brown, 50-300 cm. thickly bedded, disorganized to matrix supported poorly sorted and laterally extensive conglomerates with red, structureless, 25-175 cm. thickly bedded poorly sorted muddy sandstone-sandy mudstone. Conglomerates are sometimes cut by graded, moderate-poorly sorted, lens shaped conglomerate beds which sometimes show cross-stratification towards the top.</p> <p>Red, poorly sorted, 30 cm-200 cm. thickly bedded structureless muddy sandstone, sandy mudstone and pebbly sandstones. Beds are laterally extensive and have flat bases and tops.</p>	<p>KD</p> <p>SEHRIBAN M.</p> <p>SARIKAYA MEMBER</p>
150			
100			
50			
0			

Fig 6.3 - Cesmederesi section.

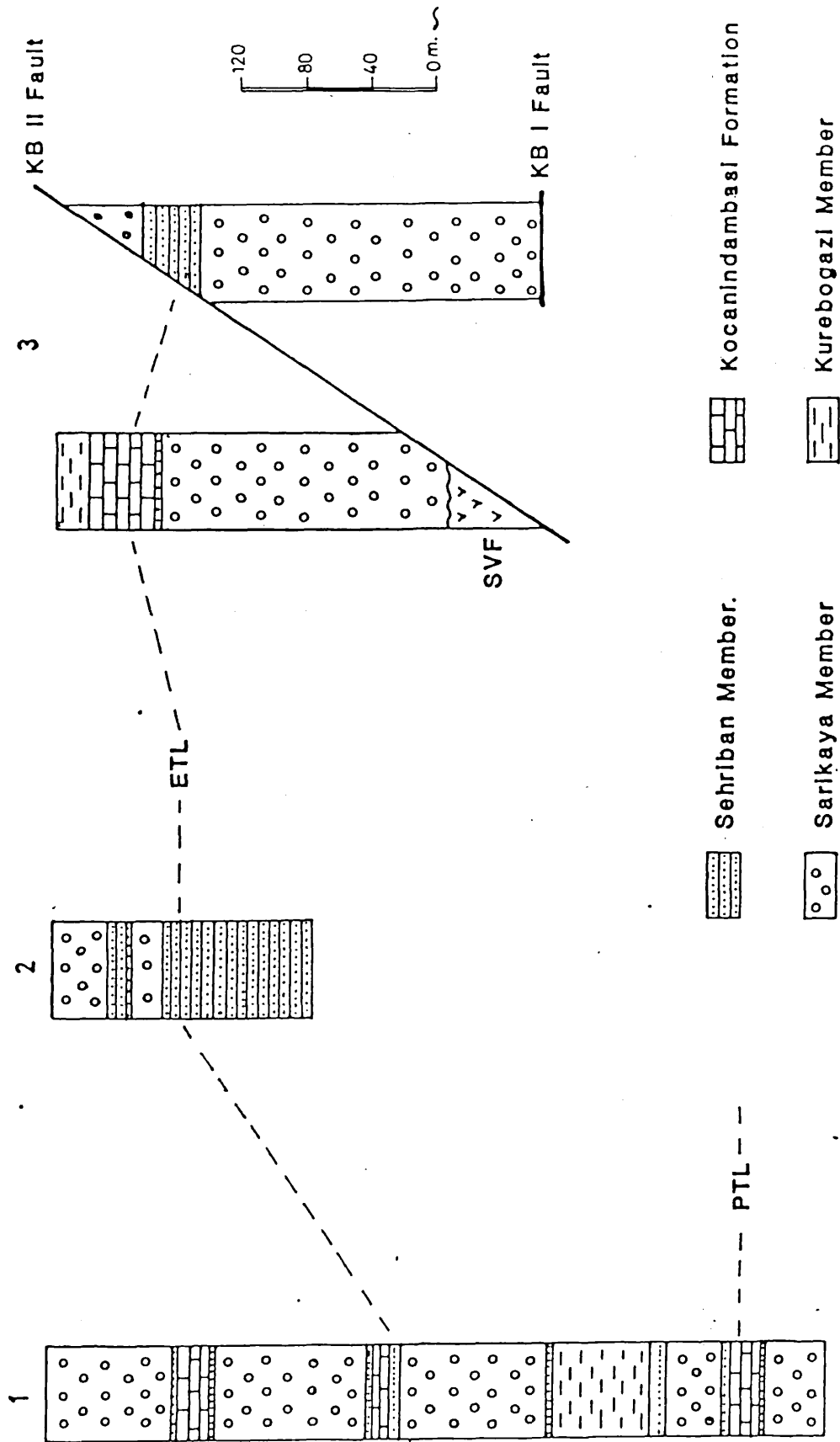


Fig 6.4 - Correlation of the stratigraphical columns of the Ucem formation.

1: around Ucem, 2: around Sehirban, 3: around Sarikaya, KB: Kurebogazi

SVF: Sarikaya volcanic formation, PTL: Palaeocene time line, ETL: Eocene time line.

Ucem (I26) and Kocanindambasi hill (J21). The lower unit has a wedge shaped geometry. It is thicker in the NE and thins towards the SW along the strike. (See cross sections and fig 6.4). The conglomerates of this unit are found to be predominant in the areas SE of Kocanindambasi hill and along the Cesmederesi valley and they become thinner and relatively finer grained towards the SW and NE along the strike in both localities. The base of the unit is not exposed, but at its upper boundary the lower unit of the member underlies and interfingers with the lower unit of the Sehriban member which in turn underlies and interfingers with the lower unit of the Kocanindambasi formation. The actual thickness of the lower unit is not known, but it is 150 m. thick in the Cesmederesi section (Fig 6.3).

In this area the upper unit consists of mudstone and parallel laminated to structureless sandstones with rare lens shaped conglomerate beds and passes up and vertically and laterally interfingers with the upper unit of the Sehriban member which interfingers with the upper unit of the Kocanindambasi formation (Chp 7) after interfingering with the Kurebogazi member of the Bayat formation. (Chp 8). Here the Kocanindambasi formation consists of wackestone and packstone and shows local thickness changes from 10-30 m. The Sarikaya member, here has a wedge shaped geometry as it thins towards the SW.

In the area between Catalcesme (L23) and Kurebogazi (V8) the upper unit of the member is exposed. The unit show different stratigraphical settings on the basin and landward sides of the NE-SW trending Kurebogazi II fault (see map II and Chp 11). In the former, the upper unit, which is conglomerate and sandstone dominated in the lower part and becomes mudstone and sandstone predominated in the upper part, is observed. Here the unit disconformably overlies the Saridere volcanic formation and is in turn overlain by the upper unit

of the Sehriban member.(Fig 6.2.) The Sehriban member shows considerable thickness changes along its strike, is generally represented by sandstones and interstratified with the upper unit of the Kocanindambasi formation. On the landward side of the fault, where the base of the unit is not observed due to faulting, the upper unit, which again consists of conglomerates and sandstones at the base and mudstones and sandstones with occasional conglomerates at the top, gradually passes up and interfingers with the upper unit of the Sehriban member. This member is, in turn, overlain by the Sarikaya member's red mudstone, sandstone and conglomerates; it is generally conglomeratic in nature and shows much lateral and vertical interfingering with the Sarikaya member. In the latter, the size of the clasts and frequency of the conglomerate beds, although showing local variations, appears to decrease towards the SW along the strike.

The Ucem formation is always overlain by the Kizildag formation with a distinct to poorly developed angular disconformity (Plate 6.1 and 2).

6.2.3 Conglomerates

6.2.3.1 General description

Conglomerates make up a considerable proportion of this member and are characteristically red (5 R 3/4) to moderate reddish brown (10 R 4/6). They fall into two main types in terms of internal structure, texture, degree of sorting and bedding types. The first type of conglomerates are generally confined to the lower parts of the units with 70 cm. to 4 m. beds. Beds are well defined, flat based, showing fairly good lateral continuity and, apart from rare very vague inverse and/or normal grading, do not show any sedimentary structures (Plate 6.3). Clasts within the conglomerates are usually angular to subangular and with sizes ranging from granules to boulders. The conglomerates are generally matrix supported



Plate 6.1 - Shows an obvious angular disconformity between the Ucem and Kizildag formations around Sehriban (M21). Note the occurrence of folding in the former.



Plate 6.2 - An angular disconformity between Ucem and Kizildag formations at S of Salaginbeltepe (N18-19)



Plate 6.3 - Matrix supported, structureless conglomerate bed. Note the upward projecting of some clasts and non-erosional base of the bed. Hammer is 30 cm. in length. Locality (R12)

and are poor to extremely poorly sorted. Clast orientations which are rare and inconsistent, occur as an arrangement of long axes of clasts either parallel or vertical to the bedding plane. In this type of conglomerate some lens shaped, poorly sorted and sometimes graded 30-80 cm. thick conglomerate beds are also observed as cut-and-fill type deposits. The second type of conglomerate which occurs as 50 cm to 2 m. thick lens-shaped beds, is observed throughout the member. They are found as isolated lenses within the sandstones and mudstones and occur either as graded, cross-stratified beds with erosional bases or structureless beds with flat bases and interbedded with sandstones (Plate 6.4). Clasts of this type are generally gravel size, and although the degree of rounding ranges from angular to subrounded, in general they are subangular and relatively better rounded than those of the first type. Clasts of the graded conglomerates display orientation parallel to the bedding surface but no clast imbrication has been observed in these apparently structureless conglomerates. Sorting is generally poor and the conglomerates are clast supported.

6.2.3.2 Lithology of the conglomerate clasts

Volcanic Rock Clasts: (VRC): are found more abundantly in the lower unit of the member and consist of dacitic tuff and possibly andesitic rock clasts. The former contains strongly altered feldspar and mica phenocrysts set in a chert-like groundmass which, on some occasions is recrystallized to medium crystalline, equant quartz. Dacitic tuff clasts are widespread within the conglomerates and can be found in both units of the member in varying proportions. Andesite clasts occur as medium-fine plagioclase phenocrysts within a dark groundmass and are more abundant in the lower unit than the upper. Although on most occasions it is almost impossible to identify them as andesites due to strong alteration in some relatively well preserved cases (which show exactly the same texture of the altered ones), andesine and labrodarite-type plagioclases



Plate 6.4 - Lens shaped conglomerate beds within sandstone-Mudstone sequence. They show erosional bases and grading. Locality (Q13)

are identified. On the basis of these identifications and textural and mineralogical similarities between these clasts and the andesite exposed in the Bala area (Chp. 2) it can be safely assumed that these clasts are possibly andesite in origin.

Cherts are the most abundant clasts found in the conglomerates of this member. They usually are of microcrystalline quartz with no relict depositional features. However some chert clasts with megacrystalline quartz fabric and with what appears to be a ghost-shard structure and spherulitic texture are also observed. In the latter two cases it is obvious that cherts are volcanic in origin. However, considering the observations made on the dacitic tuffs of the Saridere volcanics, it is quite possible to have a groundmass of dacitic tuff devitrified to a chert-like groundmass without any trace of original glassy texture. It must be reasonable to assume that at least some, if not all, of the microcrystalline cherts are volcanic in origin.

Sedimentary Rock Clasts (SRC); are mainly quartzite, radiolarite with a few micritic limestone and can be found in the upper unit of the member.

Granite clasts which usually occur as composite quartz clasts sometimes with orthoclase and biotite. Quartz crystals within these clasts are euhedral crystals and show large variation in crystal size with straight slightly undulose extinction. They are only present in the upper unit of the member.

Quartz is usually confined to the granule size clasts and occurs as composite quartz of igneous or metamorphic origin.

Feldspars which are generally present in the upper unit as large orthoclase crystals, are remarkably fresh and angular.

Serpentinite and intraformational mud pellets are seen as accessory clasts.

6.2.3.3 Matrix of the conglomerates is compositionally similar to the sandstones of this formation and is poorly sorted.

6.2.4 Sandstones

6.2.4.1 General description

Sandstones of the Sarikaya member are moderate red (5 R 4/6) to light brown (5 YR 5/6) and may become volumetrically important in some localities. They occur as two types. The first type is generally associated with conglomerates, poorly sorted and form 50 cm. to 2 m. thick; generally structureless, sheet-like beds (Plate 6.5). They show irregular to flat bases and tops and textural variations ranging from pebbly sandstone, which contain scattered pebbles, to sandy mudstone. The second type of sandstones is less common and their bed thickness ranges from 5 cm.-30 cm. They are moderately sorted, laterally extensive, often parallel laminated and sometimes cross-laminated.

6.2.4.2 Texture

The grain size of the sandstones changes with bed thickness and textural type. For example sandstones with a marked muddy matrix and with scattered pebbles do not show any consistent size ranges, while clast supported and laminated sandstones are generally medium grained. Roundness of the sand grains usually increases with increasing size and sorting. Grain contacts are commonly tangential and long; packing proximity ranges from 20%-50%. Sorting of the sandstones is poor to moderate and they are texturally immature. The sandstones of the formation can be classified as volcanic arenites (Folk 1974) (Plate 6.6).

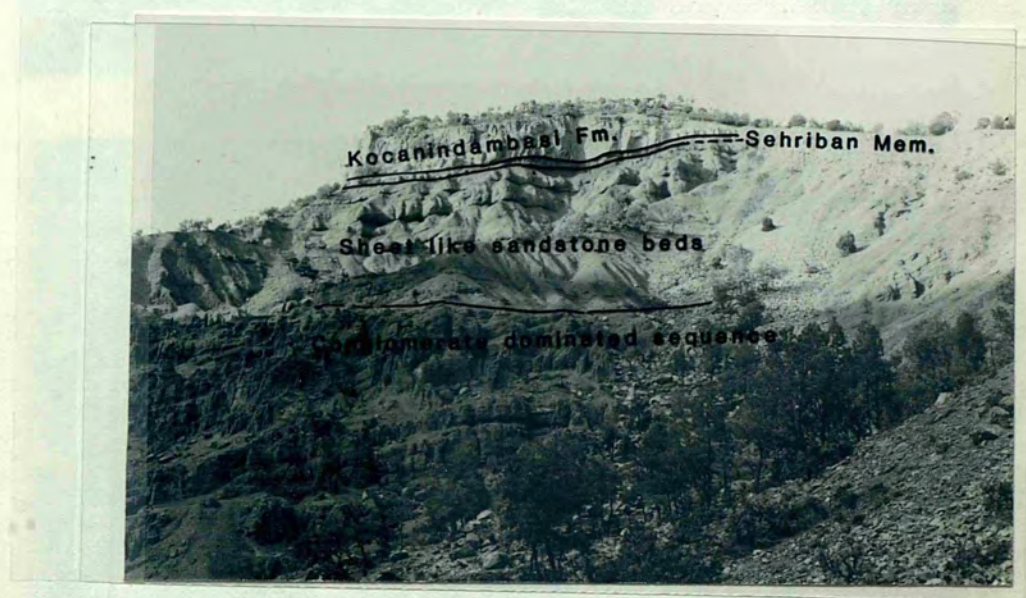
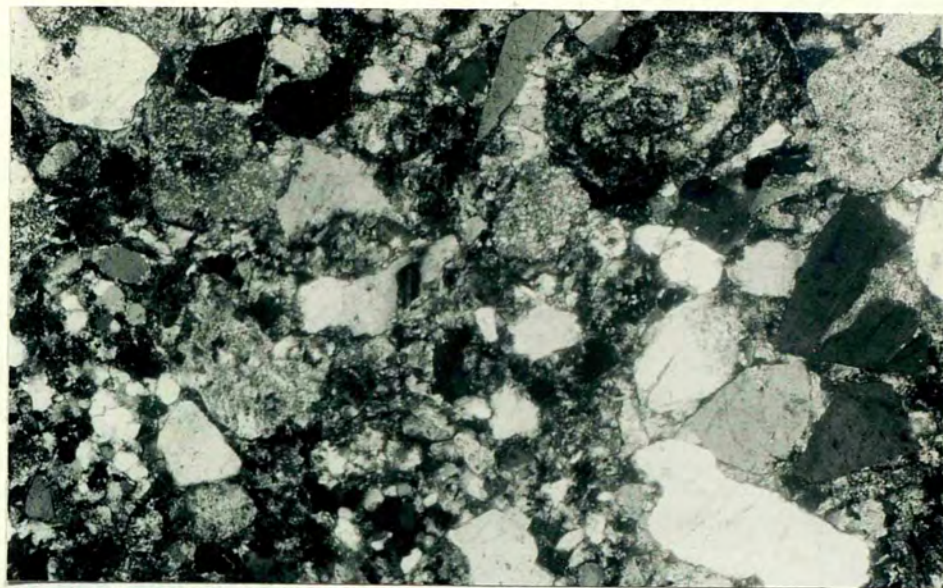
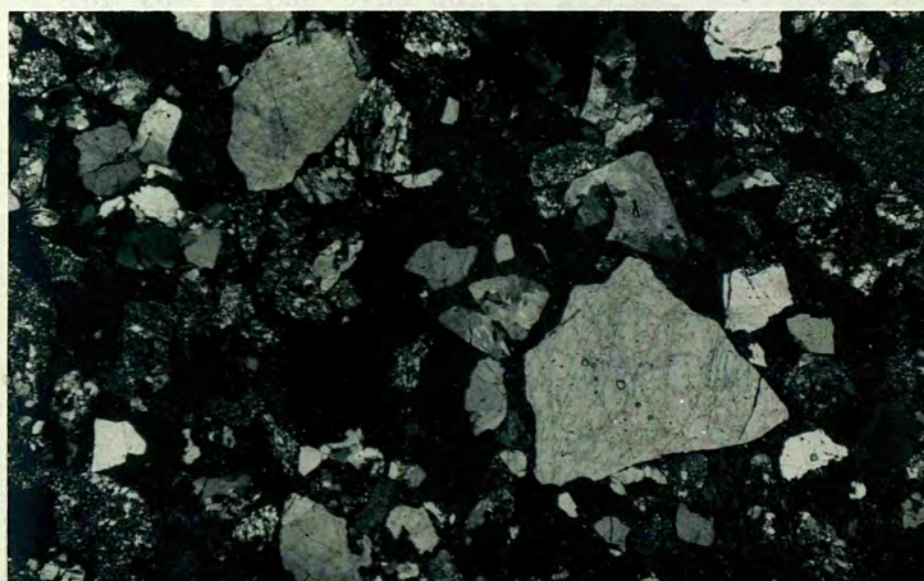


Plate 6.5 - Showing the upper part of the Saridere II section; the lower conglomerate dominated part succeeded with sheet-like sandstone and mudstone succession. The prominent feature of top of the hill is Kocanindambasi formations limestone. Here the Sehriban member is only 4 m. thick and forms the base of the prominent feature.



A



B

Plate 6.6 - Photomicrographs of sandstone.

- A. Volcanic arenite from the lower unit. It consists of volcanic rock fragments, quartz feldspar and matrix. Sample 18, 35x, XN.
- B. Volcanic arenite from the upper unit. It is composed of volcanic rock fragments (mainly dacitic), quartz feldspar and matrix. Sample S3, 35x, XN.

6.2.4.3 Framework grains

Quartz is commonly observed within the sandstones and usually angular to very angular. It occurs in two types. The first type is present as single quartz grains of volcanic origin and shows straight to slightly undulose extinction with few inclusions some of which are "Negative" crystals. The second type occurs as single or composite quartz with straight to strongly undulose extinction and some inclusions. Since it is difficult to designate this type of quartz to one specific origin (due to the fact that above mentioned features can be found in the quartz of igneous and metamorphic rocks) a name common quartz is adapted for the second type quartz grains, following Folk's (1974) classification.

Feldspars are angular to subangular and show distributional changes such that while plagioclases are almost completely absent in the upper unit, they are found in the lower one along with the generally dominant K- feldspars. Feldspars can be fresh, partially altered or completely altered to Kaolinite sericite or vacuoles.

Chert fragments are angular to subrounded and generally microcrystalline (see 6.3.2 for the origin of cherts).

Volcanic Rock Fragments (VRF) consists of andesites, dacites, rhyolites and basalts. They are subangular to subrounded and show alteration. Their proportion fall with reducing grain size and VRF show distributional changes. (see 6.25)

Quartzite, radiolarite, limestone fragments and intraformational sandstone and mudstone fragments occur in varying proportion and they are generally subrounded.

Plant fragments, biotite flakes, granite fragments and some unidentified heavy minerals are also present as necessary components.

6.2.4.4 Matrix and cement

Matrix is the main binding agent in the sandstones and is generally poorly sorted. Although the matrix is predominantly composed of iron oxide (in the form of hematite and less commonly as limonite) stained silt and clay size material, some sand size quartz and feldspar grains also occur. Micrite matrix is also present but confined to the sandstones where this member interfingers with the Sehriban member. Cement is rather rare and usually occurs as sparry calcite.

6.2.5 Compositional variations in the clastic rocks

The conglomerates and sandstones of the Sarikaya member show compositional variations from the lower unit up to the upper unit and along the strike in the upper unit. This lateral variation could not be observed in the lower unit due mainly to limited exposures. In the lower unit, the conglomerates and sandstones are composed predominantly of andesitic, dacitic and rhyolitic fragments and clasts with a few radiolarite clasts confined to the conglomerates outcropping near Ucem. In the northeastern, near Kurebogazi, most exposures are of the upper unit; conglomerates are monomict and composed of dacitic tuff and ignimbrite clasts. In the same unit along the Saridere valley, this lithology, although being predominated by dacitic rock clasts (71%), also contains radiolarite, basaltic and quartzite clasts. In the southwestern exposures in between Salaginbel hill and Catalcesme, the proportion of the quartzite clasts increases significantly. (Table 6.1)

6.2.6 Mudstones

6.2.6.1 General description

Mudstones are found interbedded with sandstones and evaporites and are almost always red except at the boundaries

Parameters Sample No	Quartz	Feldspar	VRF	SRF	Cement	Matrix	Accessory Components	Others	Total %	Total Count
(1)S-3(U)	21.4	11.8	31.8	5.8	5.2	20.2	3.8	-	100.0	500
(1)S-8(U)	13.2	7.4	46.4	11.8	1.4	18.0	2.8	-	100.0	500
(1)234(U)	12.4	9.6	29.6	17.2	10.8	17.2	3.2	-	100.0	500
(1)S27(U)	16.9	3.3	4.8	18.1	1.7	54.0	1.2	-	100.0	480
(1)18 (L)	24.4	1.7	18.4	32.4	10.2	11.9	1.0	-	100.0	512
(2)3-15(U)	4.2	0.4	4.2	89.8	1.4	49.6	0.4	-	100.0	500
(2)S-7(U)	26.7	1.0	21.3	6.4	4.8	36.6	3.2	-	100.0	502
(2)S-17(U)	8.3	3.6	32.0	5.8	0.8	46.5	3.0	-	99.9	503
(2)214(U)	8.3	12.0	28.4	11.6	2.4	34.3	3.0	-	100.0	507
(2)234A(U)	3.4	0.2	25.8	11.4	-	58.2	0.8	-	100.0	500
(2)IVB.24(L)	26.2	1.8	2.0	13.2	1.2	53.8	1.8	-	100.0	500

Table 6.1 - Modal composition of the Ucem formation's sandstones

(1): Sarikaya member, (2) Seheriban member, (U) Upper unit (L) Lower unit.
 Sedimentary Rock Fragments (SRF) includes, radiolarite, quartzite, limestone
 and intraformational sandstone and mudstone fragments and skeletal grains
 which includes fossils in (2). cherts are included to Volcanic Rock Fragments(VRF)

with the Sehriban member. There, greyish green isolated lens-shaped reduction spots are observed. Mudstones are generally 10-20 cm. thick and laminated or massive. Their lower boundaries are usually transitional with the underlying sandstones. The grain-size of the mudstones ranges from silt to clay with small amounts of scattered angular fine grained sand. Mudstones are poorly sorted and cemented. Although most of the grains are too small to be identified by optical means, X-ray diffraction analysis of these rocks revealed that the main components are quartz, calcite, hematite and clay minerals of illite, and kaolinite.

6.2.7 Sedimentary structures

The rocks of the Sarikaya member generally lack well developed sedimentary structures apart from some graded bedding and occasional cross bedding in the lens-shaped conglomerates and poor to well developed parallel lamination and rare cross-laminations in the sandstones. Inverse-to-normal grading are also observed in the poorly sorted conglomerates

Current directions, obtained from the cross-bedding, although showing wide variations, are from S, SE and NE.

6.2.8 Weathering and alteration

Mudstones and sandstones of the member are deeply weathered and eroded due to their poor cementation and the soft nature of the former leaving relatively more indurated conglomerate beds as bold massive units standing out in the mudstone and sandstone successions.

The most significant alteration product is hematite which causes the red colouration of these rocks (see detail discussion on the origin of red beds in section 9.7).

6.2.9 Age of the Sarikaya member

The rocks of the member do not contain any fossils. The age of the member, therefore, is determined on the basis of its stratigraphical relations with the under and overlying formations. The lower unit of the formation is conformably overlain or interfingers with the lower unit of the Kocanindambasi formation of the Middle-Late Palaeocene. Thus for the lower unit an Early-Middle Palaeocene age is proposed. The upper unit of the member underlies and interfingers with the Early-Middle Eocene Sehriban member (see 6.3). Therefore an Early to Middle Eocene age is suggested for this unit.

6.2.10 Source area and environment of deposition

The source area from which the sediments of this member were derived, in spite of local changes, was in the broad sense, the Ankara Melange and the Saridere volcanic formation. This is indicated by the presence of dacitic, andesitic rock clasts (which are well presented in the latter) and radiolarite, quartzite and basaltic rock clasts (which are dominant lithologies in the Ankara Melange) within the rocks of the member. The presence of andesitic rock clasts and fragments in the conglomerates and sandstones of the lower unit and their rarity in the rocks of the upper unit of the member suggests that andesites which occur beneath the dacitic tuffs in the stratigraphical column (see section 2.1), had limited outcrop in areas where the dacitic tuff was thinner. In addition the presence of quartzite and granitic rock fragments and clasts in the sediments of the member suggest limited contribution of detrital material from:

- a) the Kirsehir Massif in which abundant quartzites and metaquartzites are present (see section 1.6)
- b) the Karaca Ali granitic pluton which must have been unroofed prior to the deposition of the upper part of the upper unit.

The coarseness of conglomerates and their angularity

suggest that the source area was near, as the duration of transport was short. The occurrence of mud pellets in the conglomerates indicates a flow which was capable of scouring.

On the basis of the above interpretations, together with the occurrence of local compositional variations and the mode of transportation and deposition of the conglomerates, sandstones and mudstones of the member (see below) it can be concluded that the sediments of this member were derived from local source areas in which particular rock types were dominant in particular localities.

The environment of deposition of the Sarikaya member can be interpreted on the basis of their sedimentological and lithological characteristics. The absence of marine fossils in all lithologies, irrespective of stratigraphical level, while the presence of channeling and red colouration suggest an alluvial origin for these sediments. Two distinct but interrelated subfacies model can be suggested within the framework of alluvial model.

The occurrence of poorly sorted, matrix supported, generally structureless, thick conglomerate beds without erosional bases indicate that these were deposited by sub-aerial debris flows (Bull 1972). This conclusion is supported by the presence of occasional inverse to normal grading in conglomerates (Gloppen & Steel 1981) and upward projecting of the clasts within this lithology. Sheet-like pebbly mudstones and muddy sandstone beds without any sedimentary structures, which are found commonly associated with the conglomerates, most probably resulted from subaerial mud flows. The occurrence of lens-shaped, poorly sorted conglomerate beds with poor to well developed grading, cutting the underlying debris flow deposits, is believed to be deposited by stream channels. It can therefore be suggested that these sediments were deposited as an alluvial fan (Bull 1972).

The occurrence of local source areas and predominantly red colour of these rocks also supports this conclusion.

The sheet like, parallel laminated and/or cross-laminated mudstone and sandstone beds with lens-shaped graded, sometimes cross-bedded, conglomerate beds were most probably deposited in the lower reaches of an alluvial fan by sheetfloods (Bull 1972, Collinson 1980).

6.3 SEHRIBAN MEMBER

6.3.1 General introduction

The Sehriban member occurs closely related to the Sarikaya member and consists of fossiliferous sandstones, conglomerates, mudstones and marls. It shows considerable differences in its basin and landward exposures. Therefore a number of stratigraphical sections were measured from its basinward exposures (Kocanindambasi section, Fig 7.1, Saridere II section see section 6.2.1 and Fig 6.2, Kurebogazi section see section 8.2.1 and Fig 8.1) and landward exposures (Cesmederesi section and Halaclikisla section see section 6.2.1 and Figs 6.3 and 6.1 and Sehriban section which is described below).

In the Sehriban section (Fig 6.5) the member continues to 91 m. from the base of the section as randomly alternating conglomerate and sandstone, mudstone, marl dominated sequences. The conglomerates form 30-460 cm. thick beds, are generally poorly sorted and sometimes show grading. Sandstones are usually 30-50 cm. thickly bedded, sometimes parallel laminated and moderated to poorly sorted. They contain varying proportions of mega- and microfossil fragments and are occasionally intensely bioturbated. Marls and mudstones are parallel laminated, 10-30 cm. thickly bedded and in some cases show bioturbation. In between 91 m. and 109 m. from the base of the section red muddy sandstones and mudstones of the Sarikaya member occur. These lithologies do not show any sedimentary structures and up to 50 cm. thick beds. The following 16 m. of the section is composed of the conglomerates of the Sehriban member showing similar sedimentary properties to the previously described ones. The upper most 31 m. is represented by the structureless, extremely poorly to poorly sorted, up to 2 m. thickly bedded conglomerates of the Sarikaya member, interbedded with red mudstones.

THICKNESS(m)	LITHOLOGY	SAMPLE NUMBER	BED THICKNESS and SHAPE			TEXTURE					SEDIMENTARY STRUCTURES					COLOUR	REMARKS	FORMATION
			CONGLOMERATE	SANDSTONE	MUDSTONE	BOULDERS GRAVELS	SAND			LIMESTONE	GRADING	INVERSE GRADING	LAMINATION	X-STRATIFICATION	PLANT FRAGMENTS			
							Coarse	Medium	Fine									
150 <																		

Fig 6.5 - Sarikaya section

6.3.2 Distribution, thickness and field relations

The Sehriban member outcrops as an elongated unit, parallel to the general NE-SW trend of the Bala basin, in between the Sarikaya member and the Kocanindambasi formation. Its aerial distribution is already described in section 6.2.1, but one important fact about the distribution of rock types is worth mentioning. The conglomerates of the member are confined to its landward exposures where this member interfingers with the Sarikaya member while in the basinward exposures, where it interfingers with the Kocanindambasi formation and grades up to the Kurebogazi member of Bayat formation, the member is represented by sandstones, mudstones and marls. The thickness of the member shows significant changes along the strike from 4 m. (Sarikaya II section Fig 6.2) to 107 m. (Sehriban section Fig 6.5). The member appears to be thicker in the areas where conglomerates are dominant and thins in both directions along the strike from these localities.

6.3.3 Conglomerates

6 3 3 1 General description

The conglomerates of the Sehriban members are light brown (5 YR 6/4) to dark yellowish orange (10 YR 6/6) and are volumetrically less important than the sandstones. Although up to 5 m. thick beds occur, they are generally 50 cm. to 2 m. thick. The beds usually show erosional bases and are generally structureless except for rare inverse or normal grading and show remarkable similarities to the conglomerates of the Sarikaya member with respect to sedimentary structures and composition (Plate 6.7). However they contain abundant fragments and whole tests of megafossils and microfossils and grade into the fossiliferous sandstones. The conglomerates are generally poorly to extremely poorly sorted. In the former case they are matrix supported and less indurated than the clast-supported conglomerates. The clasts

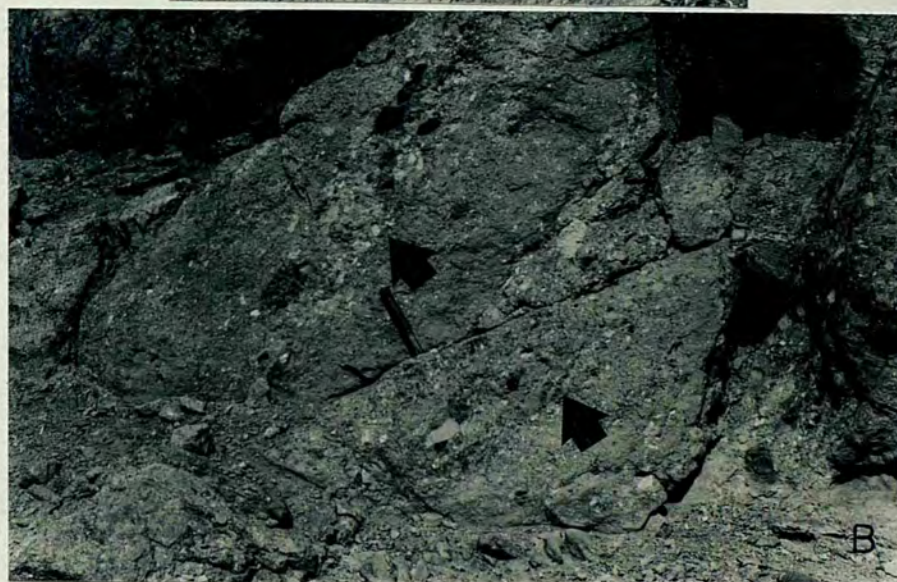


Plate 6.7 - Occurrences of conglomerates

- A. At the base of the Sehriban section. Note the matrix supported nature and grading of the conglomerates to fine grained sandstone and mudstone at the top. Bioturbation of mudstone is especially evident at the right of the photograph.
- B. Two clast supported conglomerate beds within fossiliferous sandstone layers. Locality (S13)

in this lithology range , in size, from boulders to granules, but they are generally gravel size and are subangular to subrounded. The conglomerates show compositional changes in the lower and upper units of the member as well as laterally in the upper unit. In the lower unit they are composed predominantly of andesite, dacitic tuff and ignimbrite and rhyolite clasts with fragments of molluscs, brachiopods, Algae, echinoids and foraminifers (mainly rotaliids, miliolids and Textularia and sometimes as whole tests) within the sandstone matrix but, on some occasions, whole shells of megafossils 5-15 cm. in length occur as clasts. In the upper unit, a compositional change occurs with a pattern which is related to the local predominance of particular rock types in the source areas. In the northeastern-most outcrops (near Kurebogazi) of the upper unit, conglomerates are mainly composed of dacitic tuff and ignimbrite clasts set in a sandy shell matrix containing whole and broken gastropod, echinoid and foraminiferal (discocycline, miliolids, Nummulites sp. Operculina sp. and Assillina sp.) tests. Granite clasts occur towards the top of the member. This composition gradually changes towards the SW along the strike by the reduction of dacitic rock clasts and the introduction and increase of clasts of radiolarite, quartzite, basalt, micritic limestone. Bivalve shells in addition to other skeletal fragments are also observed. In this area clasts seem to be more rounded than the former one. All the conglomerates contain some quartz, red mud pellets, intraformational pebbles and plan fragments irrespective of any particular locality.

The matrix of the conglomerates are poorly sorted and consists of angular to subangular sand and silt size material set in either micrite or clay groundmass which is, in the former case, sometimes recrystallized to sparry calcite. The matrix is compositionally similar to the sandstones of the formation.

6.3.4 Sandstones

6.3.4.1 General description

Sandstones of this member are light brown (5 YR 6/4) to moderate yellowish brown (10 YR 5/4) and especially predominant in the areas where this member interfingers with the Kocanindambasi formation (Chp 7) and grades into the Kurebogazi member (8.2). They consist of quartz, chert, broken and whole large and small benthonic foraminifer tests, a few globigerinids which are completely absent in the landward exposures of sandstone beds, fragments of coralline algae and gastropod, brachiopod and bryozoans with some volcanic rock fragments and K-feldspars in the lower unit (Plate 6.8) and chert, quartz, quartzite, radiolarite, volcanic rock fragments feldspars, granitic rock fragments and fragments of skeletal grains in the upper unit (Plate 6.9). Beds of the sandstones range from 30 cm to up to 1 m. in the landward exposure where they are generally structureless, contain scattered small pebbles throughout the beds and in basinward exposures, they are 10-50 cm. thick, show parallel laminations and bioturbations and are interbedded with mudstones and marls. In these sandstones vertical and U-shaped burrows (*Skolithos* facies of Seilacher, 1967) are observed (Plate 6.10). Sandstone beds have sharp upper and lower contacts with the under-and overlying beds (Plate 6.11). The sandstones also show compositional differences in the upper unit of the member, as did the conglomerates (Table 6.1).

6.3.4.2 Texture

Grain size ranges from fine to coarse but sandstones are generally medium to fine grained in the basinward exposures and coarse to medium grained in the landward exposures. Skeletal fragments show more apparent variations in grain size than the lithoclastics and display various grain shapes. The skeletal grains are more angular than the lithoclastic grains which are generally subangular to subrounded. Longitudinal and tangential grain contacts are commonly observed in the sandstones which show a packing proximity of 30%-70%.

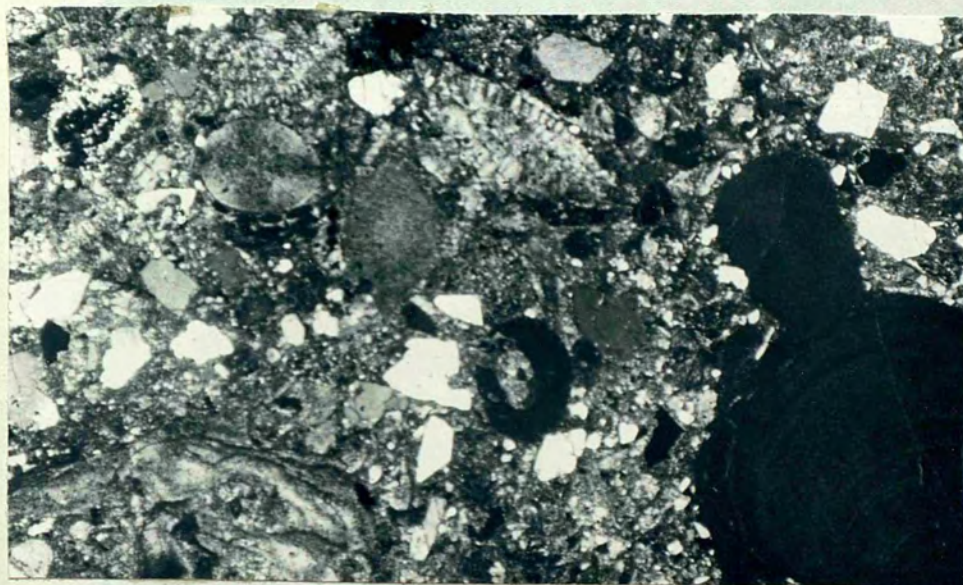
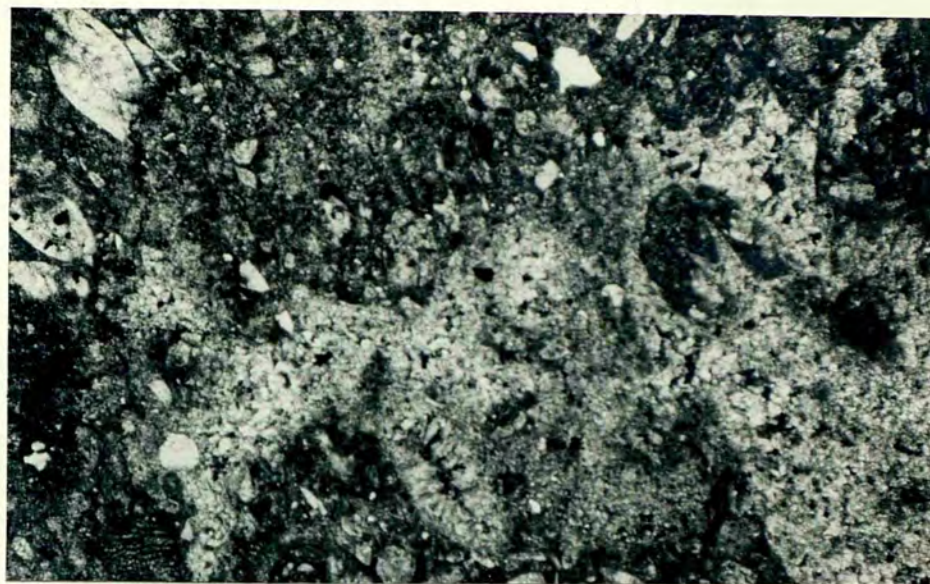
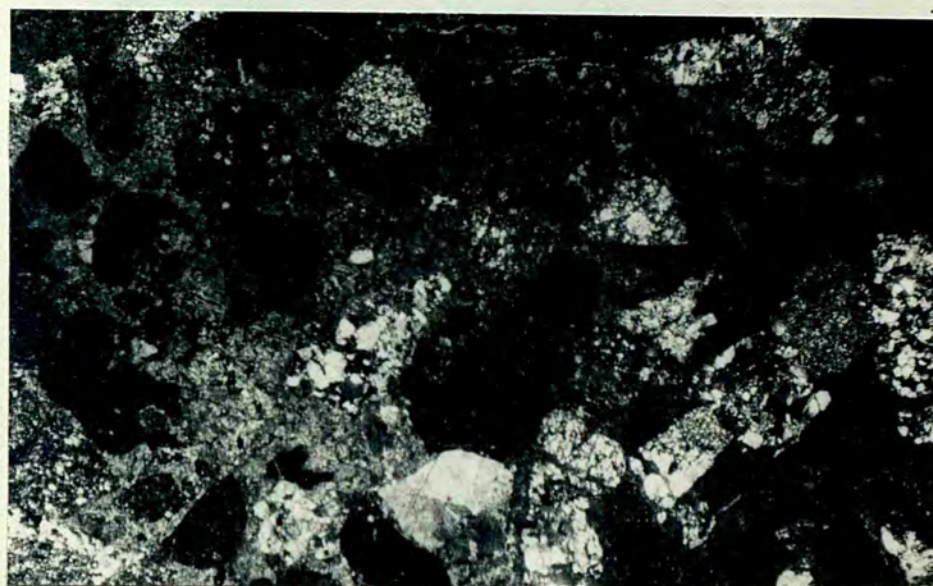


Plate 6.8 - Photomicrograph of fossiliferous lithic arenite from the lower unit of the Sehriban member. The rock consists of various fossil fragments, quartz, volcanic rock fragment, feldspar and matrix. Sample IVA24, 15x.



A



B

Plate 6.9 - Photomicrographs of sandstones from the upper unit of the Sehriban member.

- A. Fossiliferous matrix supported lithic arenite consists of fossil fragments and whole tests, quartz volcanic rock fragment, feldspar and matrix which is partly recrystallized to neomorphic sparry calcite. Sample 1467, 15x, XN.
- B. Lithic arenite is composed of volcanic rock fragments, radiolarite, quartz quartzite feldspar and matrix. Sample 234A, 15x, XN.



Plate 6.10 - Shows vertical (A) and U-shaped burrows (B). Localities A (H27) B (H26).



Plate 6.11 - Shows intercalation of sandstones and mudstones of the Sehriban member. (Hammer is 30 cm. in length) Locality (U7).

Sorting of sandstones is moderate to poor and they are texturally immature.

6.3.4.3 Framework grains

Quartz is the most common type found in these rocks and occurs either as inclusion-free single quartz which shows straight extinction, are euhedral (sometimes with perfectly straight sides) and are angular to subrounded (volcanic quartz) or as composite quartzes with undulose extinction and various inclusions (common quartz see 6.2). The latter quartz grains are commonly found in the upper unit of the member. In the lower unit they are less significant than the former type.

Chert: occurs as microcrystalline aggregates, sometimes with a megacrystalline quartz fabric. It varies in size from coarse sand to silt dimensions (see 6.2.3.2 for the origin of cherts).

Feldspars are almost entirely K-feldspars, usually subrounded to subangular and occasionally showing carlsbald twinning. Plagioclases are labrodorite-andesine in composition and may become proportionally important in some sandstones of the lower unit.

Volcanic rock fragments generally occur as subrounded, coarse to medium sand size grains. They are mainly andesitic and dacitic in origin in the lower unit of the member and dacitic, basaltic and andesitic, in decreasing order of abundance, in the upper part.

Radiolarites, quartzites and limestone fragments also occur in varying proportions in different localities of the upper unit of the member. Radiolarites are also found in the upper part of the lower unit as an accessory component.

Foraminifers, as expected, due to the time-transgressive

nature of the member, show differences in taxa and dominant fossil types. While rotaliids are the main genera together with miliolids and alveolinids in the lower unit, discocyclines, nummulites and assilinas the dominant foraminiferal types, along with the small benthonic foraminifers, in the upper unit of the member.

Fragments of coralline algae (mainly articulated type), echinoids, molluscs and brachiopods are found in varying sizes and shapes. The amount of coralline algae is substantially reduced in the upper unit while mollusc fragments become more important. Initial shell microstructures are usually preserved in the shells which originally had a calcite composition, e.g. brachiopods and bivalves, while those of aragonite, e.g. gastropods, are replaced by sparry calcite.

Plant fragments, biotite flakes and some unidentified heavy minerals also occur as accessory components.

6.3.4.4 Matrix and cement

The matrix is moderate to poorly sorted and composed of micrite, microspar, limonite and clay minerals with some scattered silt to fine sand size detrital grains. It is often replaced by fine to coarsely crystalline sparry calcite.

The first phase cement is almost absent in the sandstones of this member, except in a few samples, and is exclusively sparry calcite.

6.3.5 Mudstones and marls

6.3.5.1 General description

These lithologies are light brown to brownish grey and usually found interbedded with sandstones. They occur as either parallel laminated (laminae are 1 mm. to 1 cm. thick)

or bioturbated (Plate 6.12) 10 to 30 cm. thick beds. The bioturbated beds do not show any sedimentary structures and have sharp bases and tops, while parallel laminated beds sometimes show gradual upper boundary with the bioturbated mudstones and marls. Mudstones consist of silt to clay size material and are well cemented. Compositionally they contain chert, quartz, a few VRF and feldspar within a micrite matrix. Molluscan shells, burrows and plant fragments are commonly observed in these lithologies and they sometimes contain scattered pebbles of up to 10 cm. in diameter. While mudstones are relatively more friable, marls are well cemented and consist predominantly of micrite and microspar.

6.3.6 Age of the Sehriban member

This member contains abundant age diagnostic foraminifers in its upper and lower units. In the lower unit the following benthonic foraminifers are identified and a Middle-Late Palaeocene age is given (C.G. Adams and S. Tekler pers. comm. 1982)

Rotaliids,

Miliolids,

Algae including Distichoplax biserialis

In the upper unit

Assilina sp.

Discocyclina sp.

Nummulites sp.

Sphaerogypsina globula

Operculina sp.

are found and an Early-Mid Eocene age is designated for this unit.

6.3.7 Source area and environment of deposition

The source area for the sediments of the Sehriban member was exactly the same as for the Sarikaya member. This is indicated by the compositional similarities between the sediments



Plate 6.12 - Shows an intensely bioturbated marl. Scale
is 0.8 cm. in diameter. Locality (S13)

of these two member (see section 6.2).

The interfingering of this member with the continental red beds of the Sarikaya member and the presence of abundant diverse and relatively well preserved marine fossils suggest a shallow marine environment of deposition. Although the coarseness of the conglomerates and the broken nature of megafossils may indicate a high-energy environment of deposition, following lines of evidence suggest the opposite:

- a) the moderate rounding and high sphericity of the conglomerate clasts implying a river origin for these clasts, rather than beach one (ibid section 5.9) indicates that the clasts were not subjected to a significant amount of marine reworking;
- b) the poor sorting and high matrix content of the conglomerate and sandstones;
- c) the sedimentary structural similarities of this lithology (inverse and normal grading occurs) with the conglomerates of the Sarikaya member;
- d) the presence of grading from conglomerates, which contain scattered megafossil fragments and shells with a few benthonic foraminifers, to moderately sorted parallel laminated or structureless sandstones with abundant whole tests of benthonic foraminifers, indicate that the conglomerates are only reworked at the top;
- e) the lens shape of conglomerates as opposed to the sheet like geometry of the beach gravel deposits;
- f) the lateral and vertical interfingering of conglomerates with the sandstone and mudstones (see below). The most likely depositional mechanism for these conglomerates is that they were deposited as a result of occasional floods which most probably deposited these coarse clastics into the sea but not before they had incorporated the local marine fauna by erosion. The conglomerates retain their essentially alluvial nature. This conclusion is also supported by the presence

of local compositional variations in the conglomerates. The presence of whole and broken shells of megafossils in close proximity to each other within the same bed suggesting that although there was a post-mortem transportation, the distance was not great and broken fragments were most probably fractured due to biological activity.

The occurrence of parallel lamination, unabraded large megafossil shells, bioturbation and abundant plant fragments together with moderate to poor sorting suggest that the sandstones and mudstones of this member were deposited within a low energy environment. The bioturbated sandstones most likely represent a period of low clastic input into the basin. The gradual decrease, in grain size of the sandstones in the basinward exposures of the member, where it interfingers with the Kocanindambasi formation and grades up to the Kurebogazi member, together with the occurrence of globigerins suggest relatively deeper water conditions for these lithologies.

From all above interpretations, it can be concluded that the Sehriban member was deposited in a shallow marine environment, of predominantly low energy. The lithoclastic material was transported by streams of local generation (see 6.2.10 Sarikaya member) and mixed with the bioclastic material either living in-situ or most likely transported from nearby sites of carbonate accumulation (Kocanindambasi formation, Chp 7). Most of the skeletal fragments found in the sediments of this member are abundantly present in the limestones of the Kocanindambasi formation. Occasional flood-generated conglomerates (as indicated by their size and the occurrence of red mud pellets in these sediments implies high initial discharge with occasional scouring by flows) invaded this shallow marine environment and was deposited in the near-shore areas.

Interbedding of conglomerate and coarse grained sandstone sequences with laminated and bioturbated sand and mud-

stone dominated sequences suggests a fluctuating sea level: something which is also evident in the Kocanindambasi formation. The gradual passing of this member to the Kurebogazi member of the Bayat formation (See 8.2) indicates a marine transgression from the NW.

The depth in which the sediments of the Sarikaya member were deposited, can be estimated on the basis of their fossil content. The occurrence of rotaliids and miliolids (which are found in relative abundance in depth ranging from 10 m.-55 m. and 10 m. to 30 m. respectively (Phleger 1965)) in the lower unit of the member indicates a depth range of 10-55 m. The presence of *Discocyclina*, *Operculina* sp. and miliolids in the upper unit of the formation suggest a similar depth of deposition (0-40 m.) and tropical to temperate climate (Phleger 1965, Murray 1973). This estimation is consistent with the occurrence of vertical and U-shaped burrows which are believed to be characteristic of sublittoral environments (Seilacher 1967).

C H A P T E R 7

KOCANINDAMBASI FORMATION

7.1 General Introduction

The Kocanindambasi formation, a time-transgressive unit, developed from the Middle Palaeocene to Early Eocene, consists of very light grey (N8) to light olive-grey (5 Y 6/1) to yellowish-grey (5.Y 7/2) bioclastic limestone and is divided, because of its time-transgressive nature, into lower (Middle-Late Palaeocene) and Upper Early Eocene Units.

The limestone is composed of bioclastic material, including coralline algae (articulated and encrusting types), foraminifers, corals (occurring as small coral heads or fragments) and fragments of brachiopods, bryozoans, molluscs and echinoids. The influx of terrigenous sediment is apparent in places and is mainly of quartz and chert. Although occasionally some unbedded and poorly bedded sequences occur, it is generally well bedded and the thickness of the beds ranges from 20 cm. to 150 cm. with 50-60 cm. thick beds predominating.

Type sections of the formation are taken from the southern flank of Kocanindambasi hill (J21) for the lower unit (Fig 7.1) and along the Saridere valley (Q12) for the upper unit (Fig 6.3).

Four subfacies are differentiated in the formation on the basis of depositional texture and faunal content, but they are not mapped due to their limited exposure and thin form. These subfacies are

Subfacies I: a mixed fauna of large and small benthonic foraminifers and fragments of other organisms with a terrigenous influx

Subfacies II: a patchy algal-coral boundstone and packstone

Subfacies III: a Rotaliid-algal packstone

200

THICKNESS(m)	SUBFACIES	LITHOLOGY	SAMPLE NUMBER	BED THICKNESS	ROCK TYPE					GRAIN SIZE			FAUNA & FLORA							REMARKS	FORMATION				
					SANDSTONE	BOUNDSTONE	GRAINSTONE	PACKSTONE	WACKSTONE	MUDSTONE				LARGE BENTH. FORA	SMALL BENTH. FORA	AGGLUTINATED FORA	ALGAE					CORALS	TERRIGENEOUS INFILUX		
											COARSE	MEDIUM	FINE				ARTICULATED	ENCrustING							
			35	50	X					X	X													SM	
			34	30				X		X	X	R		R	P				X						
			33	20-50	X		X			X	X												Plant Fragments	SM	
180	I		32	100			X			X	X	C	P		C			X							
			31	60-70			X			X		R	C	P	P	P									
	III		30	40-60						X	X	C	P	R	C										
	II		29		X	X	X						P				C	C							
			28	70-90			X			X		R	R			C	P								
160	I		26-27	60			X			X	X	C	P		C				X						
			24-25	30-60	X					X	X											Plant Fragments	SM		
																		X							
140	I		22-23	50-80			X			X		R	C	P	P	P		X							
120	IV		21	30-45			X	X		X			C	P		P	P								
	II		20		X		X	X					P	R		P	C	C							
	IV		18-19	30			X			X	X														
	II		16-17	40-60			X			X			C	P		P	P								
100			15		X		X						P			P	C	C							
	IV																								
80			8-14	30-60			X			X	X		C	P		P	P		X						
60	II		7		X	X	X							P	R		P	C	C						
40	I		4-6	60-150			X			X		C	P		C			X			Bedding is Poorly developed.				
			3	40			X	X		X	X					P	P								
	IV		IVB-L2	60			X			X	X														
20			17-17A	40-60			X			X		C	P		P		X								
	III		16-16A	20			X			X	X	R	P	P	P										
			11-15	40-50			X			X	X	C	P		C										
	II		10		X		X	X				R	P			C	C	C							
	I		8.9																						
			5.7																						
			IVA-1-4	20-50			X			X	X	C	R	P		C		X						SM	

Fig. 7.1 - Type section of the lower unit of the Kocanindambasi formation. Lithology is not to scale. R= rare
P= present, C= common, SM= Sehriban member.

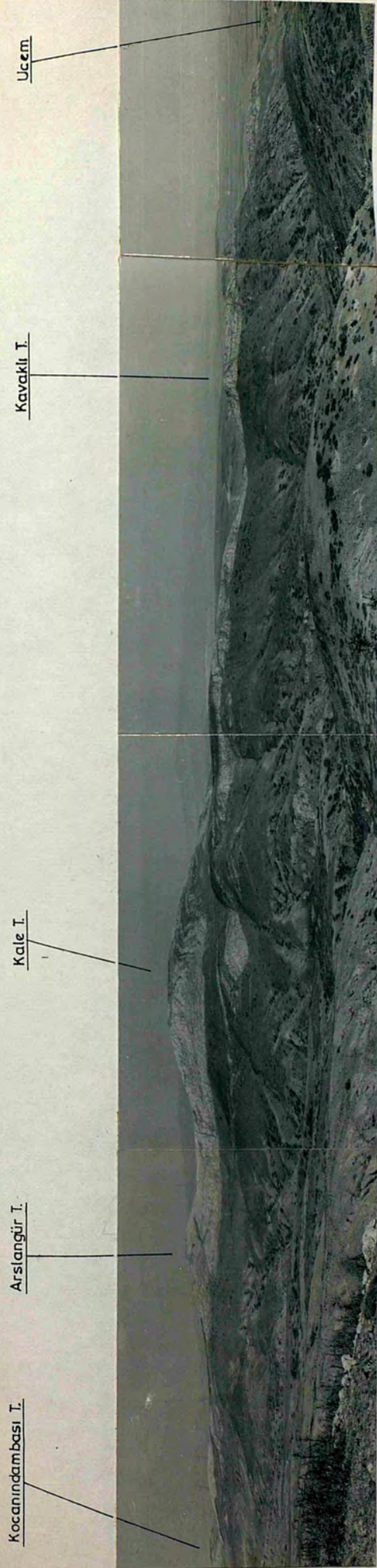


Plate 7:1 - Panoramic view of Kocanindambasi formation between Kocanindambasi hill (J21) and Ucem Village (I26)



A



B

Plate 7.2 - A. Gradual boundary between the underling Ucem formation and the lower unit of the Kocanindambasi formation in Cesmederesi (I26) near Ucem.

B. The upper unit of the Kocanindambasi formation conformably overlying the Ucem formation in Saridere Valley (Q12).

Subfacies IV: dominated by Miliolid-algal packstone with small amount of terrigenous material.

Induration of rocks differs: boundstone-packstones are relatively less well indurated than others, but as a whole the rocks of the Kocanindambasi formation are well indurated compared to adjacent lithologies.

7.2 Distribution, thickness and field relations.

The Kocanindambasi formation outcrops along the southern margin of the Bala basin as an elongated body and lies parallel to the general NE-SW trend (Plate 7.1 & 7.2A). It shows considerable changes in distribution and thickness in both the lower and upper units.

The best development of the formation is observed in the lower unit, in the area between Kocanindambasi hill and Ucem (I 26), where the formation is thicker, well exposed and all four subfacies are represented. Here the formation overlies and interfingers with the Ucem formation and the maximum observable thickness measured is 196 m (Kocanindambasi section Fig 7.1). The upper boundary of the lower unit of this formation with the overlying Sehriban member of the Ucem formation (8.2) is a gradual boundary and is best exposed on the northern flank of the Kocanindambasi hill. The development of the upper unit of the formation is less complete, as indicated by the local absence of subfacies III and IV and it is exposed as an elongated thin carbonate body between Kurebogazi (V8) and SW of Ucem (Plate 7.2B). The upper unit overlies the Sehriban member of the Ucem formation (see Chp.6) and is succeeded by the Sehriban member of the same formation in the area between Kurebogazi and Sarikaya. But in the area between NE of Kekliceck (M16) and SW of Ucem the upper unit shows complex lateral and vertical interfingering with the Ucem formation (see 6.2 for detail description). The thickness of the upper unit ranges from 2 m. to 40 m. in

the Saridere section (Fig 6.2).

7.3 Subfacies I

Widely distributed and volumetrically the most important subfacies of the Kocanindambasi formation, it consists of yellowish-grey (5 Y 7/2) to medium light-grey (N/6), poor to moderately sorted, medium to coarse grained bioclastic packstone which contains an abundant and diverse fauna (Plate 7.3). Small and large benthonic foraminifers, coralline algae, fragments of brachiopods, molluscs and echinoids, globigerinids and a terrigenous component occur within a micrite matrix which is, in places, partly or completely recrystallized to a neomorphic microspar and/or sparry calcite. Limestones of this subfacies are usually found as 60-150 cm. thick massive beds without any sedimentary structures. The thickness of this subfacies ranges from 1 m. to 32 m and it appears to be first limestone unit deposited in the area. It shows a gradual vertical boundary with other subfacies of the formation.

7.3.1 Texture

The size of the bioclastic and lithoclastic grains varies from fine to coarse, but generally they are medium to coarse. Algal fragments and some benthonic foraminifers are relatively larger than others in grain size. Grains occur in various shapes depending on their origin and bioclastic grains are generally angular. The limestones of this subfacies are grain supported and micrite matrix, filling the intragranular and intergranular spaces, is observed.

7.3.2 Framework grains

Miliolids, alveolinids, rotaliids, discocyclines and Nummulites are commonly found. They are usually well preserved although some broken ones occur occasionally. Discocyclines, rotaliids and Nummulites occur as large as 10 mm in length and show a radial fibrous wall structure. (Plate 7.5). Simple forms of Textularia with areneaceous wall structure are also present.

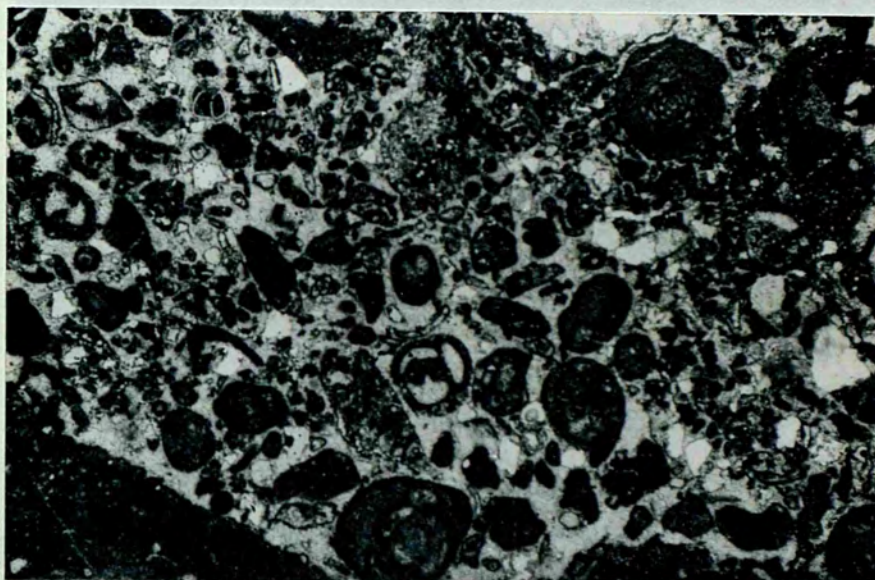
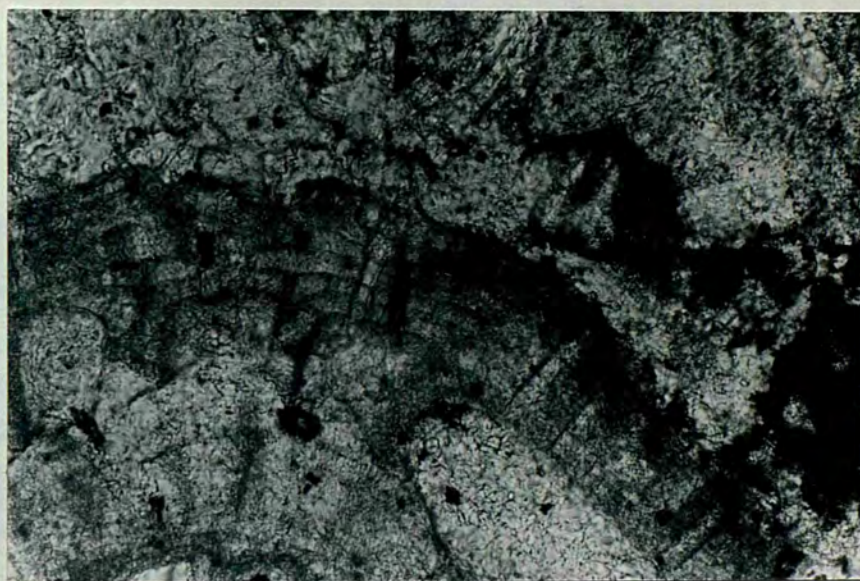


Plate 7.3 - Common texture of the bioclastic packstone of subfacies I. Sample No. IV-B 22 (Kocanindambasi section: KD section) 15X



A



B

Plate 7.4 - A brachiopod shell with parallel fibrous wall structure. Sample No. IV13 (KD section) 35x, XN

Plate 7.5 - Radial fibrous pattern in a rotaliid wall, chambers are filled by neomorphic sparry calcite and microspar. Sample No. IVA8 (KD section) 150X.

Globigerinids are observed in varying abundance and characteristically show a perforated wall structure. In most cases the chambers of foraminifers are filled with sparry calcite, although some micrite filling occurs occasionally.

Coralline algae are found as fragments of encrusting and articulated forms, in sizes ranging from 0.1 mm to 4 mm.

Terrigenous components are mainly quartz and chert.

Less commonly, some volcanic rock fragments, which are usually better rounded than the other grains, are observed. The amount of terrigenous component, which is generally finer than the bioclastics in grain size, ranges from 5% to 20%.

Angular to subangular, from 1 mm to 1 cm fragments of brachiopods (Plate 7.4), molluscs and echinoids are commonly seen.

7.3.3 Binding agent

Micrite is the main binding agent found in the intergranular spaces of the framework and, sometimes, in the chambers of Foraminifera. Sparry calcite and microspar occur either as neomorphic crystals or first phase cement (see Diagenesis 7.9 for further detail). Sorting of the matrix is poor to moderate and some fine rod-like bioclastic fragments, scattered within the micrite, are observed.

7.3.4 Variation in the Composition and Texture

As might be expected, a considerable variation in taxa and relative proportion of particular fossil type occurs between the lower and upper units of the formation: while rotaliids are the main large benthonic foraminifers in the former, discocyclines and Nummulites are the most common type in the latter. The relative proportion of coralline algae also differs and their obvious abundance in the lower unit is signifi-

cantly reduced in the upper unit.

7.4 Subfacies II

This subfacies consists of stromatolite, boundstone, grainstone, wackestone and packstone, all of which may be found in varying proportion within lens shaped, poorly defined beds which show vertical and horizontal transitional contact with the subfacies II, III and IV. Colours of the rocks range from pale yellowish-brown (10 YR 6/2) to greyish-white depending on the composition. Although the rocks of this subfacies show considerable variation in depositional texture, ranging from mudstone, which occurs in the protected spaces of the growth framework, to stromatolite, boundstones and packstones are found to be dominant. The thickness of this subfacies ranges from 2 m to 10 m. It occurs patchily and is better developed in the lower unit.

Stromatolites are found on rare occasions as small pockets of units which are 5-20 cm thick stratiform-stromatolites without any columnar growth overlying boundstones and packstone patches. Beds consist of fenestral limestone at the base and fine to medium size "anti-gravity" laminae towards the top (Plate 7.6). Laminae are well defined and generally gently convex to subconical in macroscopic scale and wavy and wrinkled in finer scale. Two different lamination fabrics are observed: laminoid fenestral and laminated (Monty 1976). Laminoid fenestral fabric resulted from the alignment of elongate fenestral cavities which are enclosed by calcite crystals, along a line. In laminated fabrics lamination is due to differences in crystal size in alternating laminae. This and criteria given below evidently defines this laminated rock as stromatolitic:

- 1) Presence of fenestral fabric and high porosity
(Bathurst 1976)

- 2) Presence of relicts of benthonic foraminifers and intracrysts in the fenestral limestone.

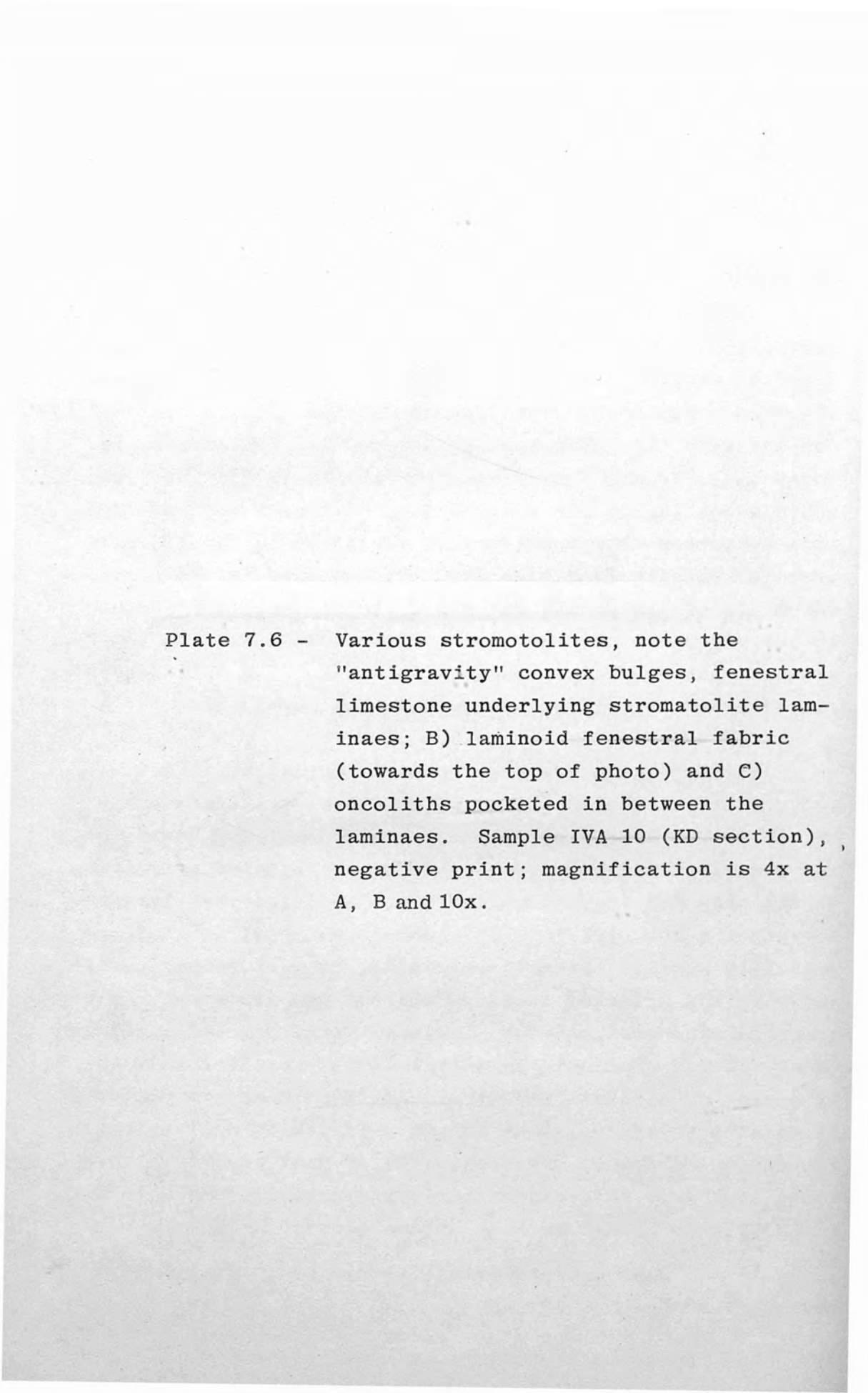
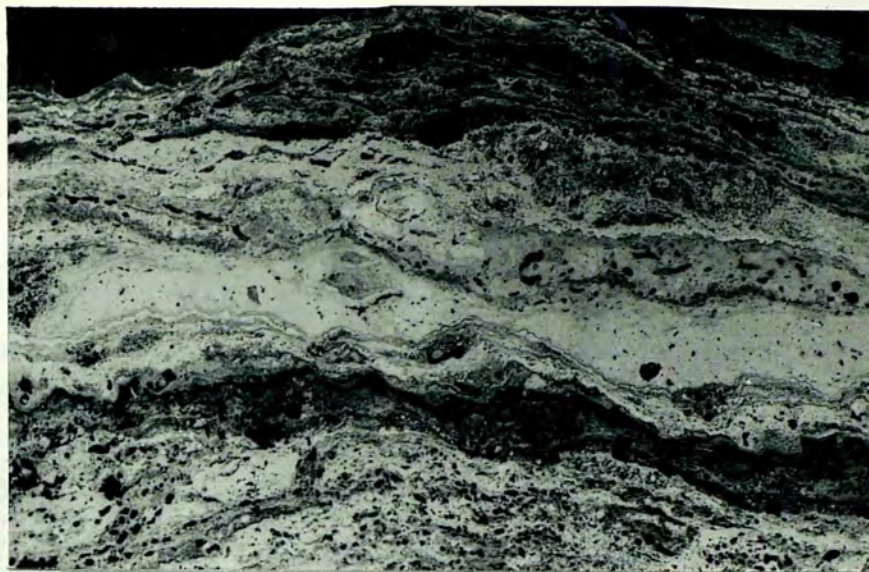
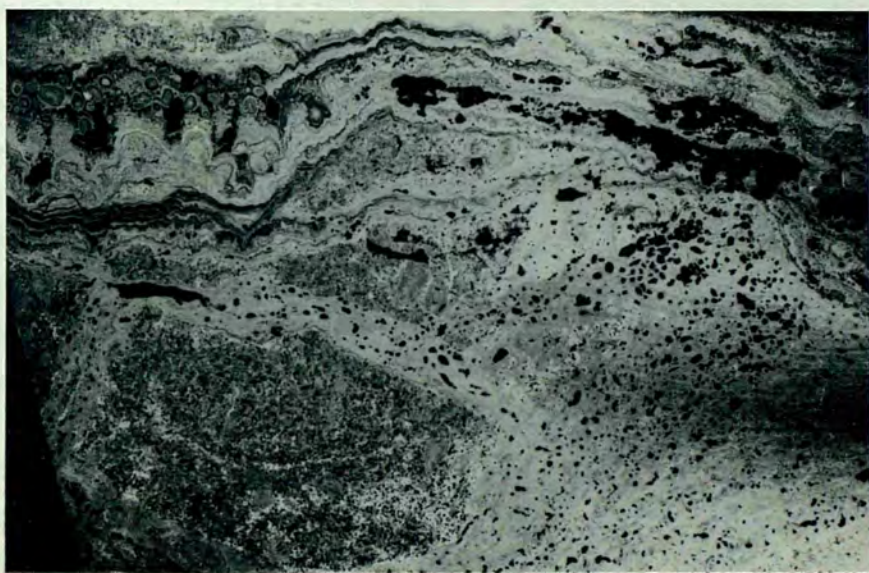


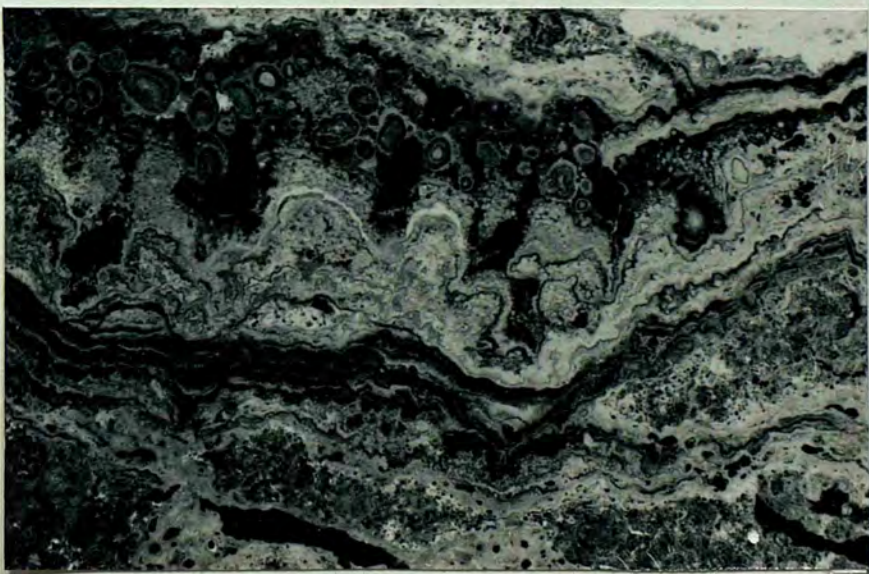
Plate 7.6 - Various stromatolites, note the "antigravity" convex bulges, fenestral limestone underlying stromatolite laminaes; B) laminoid fenestral fabric (towards the top of photo) and C) oncoliths pocketed in between the laminaes. Sample IVA 10 (KD section), negative print; magnification is 4x at A, B and 10x.



A



B



C

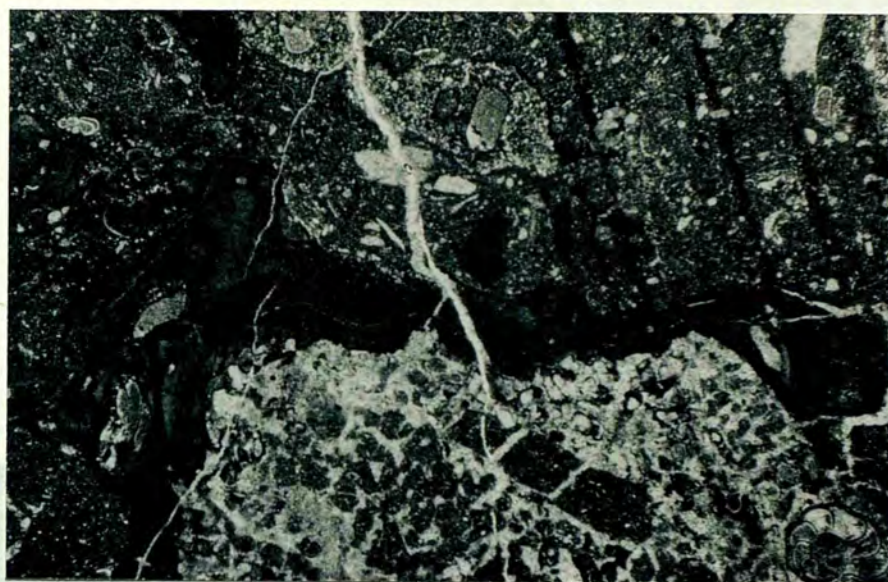
3) Association of these rocks with typical shallow marine carbonate rocks.

4) Presence of upward increasing of the convex bulges.

5) Presence of pockets of oncolites which are differentiated from the calcrete pisoliths by the absence of internal brecciation (Read 1976), association of these with uncoated intraclasts and foraminifers (Dunham 1969) and the similarity of lamination structure of stromatolite and oncolites (Gebelin 1976). The details of the microstructure of laminae have been obliterated by recrystallisation.

Boundstones show a growth structure which is dominated by corals and coralline algae. Foraminifers and fragments of bryozoans, brachiopods, molluscs and echinoids are also found in these rocks bound together by encrusting coralline algae (Plate 7.7). Corals are sclerectinian type and they are most probably hermatypic (Wells 1956) as indicated by their association with shallow marine fauna, although they could not be identified even at genus level due to recrystallization of their aragonitic wall structure to sparry calcite. They were found as small solitary coral heads (Plate 7.8) and colonial corals (Plate 7.9). Encrusting coralline algae which are mainly Lithophyllum (Elliot pers. comm.) play a binding role in this lithology. The thickness of coralline algae layers encrusting corals range from a few layers to many alternating layers (Plate 7.7).

Rocks which are found closely associated with boundstone and filling the spaces in between the corals show significant textural changes, so that they may be called either mudstone where there are only a few skeletal grains scattered within a finely crystalline micrite matrix or wackestone and packstone depending on the amount of grains present. Packstones are the most dominant type and are poor to moderately sorted, containing medium to fine grained diverse skeletal grains which are mainly articulated coralline algae, fragments of



A



B

Plate 7.7 - General texture of the coral-algal boundstone-packstone.

- A. Showing an encrusting coralline algae binding coral and other skeletal grains. Sample no. IVB 7 (KD section) 15X.
- B. Sclerectorian coral, some terrigenous (quartz) and skeletal grains encrusted by coralline algae. At the lower left of the photograph mudstone filling with a small benthonic foraminiferid. Sample 18 (J23). 15X



Plate 7.8 - A Sclerectarian coral head. Wall structure is recrystallized to calcite probably from aragonite and lost its internal structure. At the top left of the photograph radiating septa can be seen. Space in between the fossils is filled by wackestone (KD. section) 3.2X.



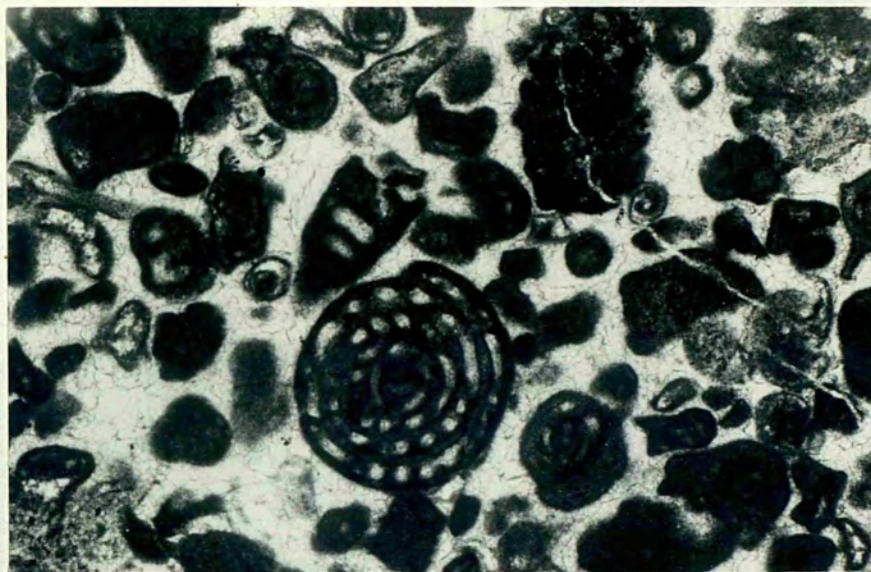
Plate 7.9 - A coral head found in the upper unit of the Kocanindambasi formation. Coin is 2.5 cm. in diameter. (Q14).

encrusting coralline algae and other organisms with foraminifers within a matrix of micrite, microspar and/or neomorphic sparry calcite cement. Coralline algae fragments always occur in bigger grain sizes than other grains and usually retain their original internal structure. In contrast to packstones, mudstones and wackestones are poorly sorted, medium to fine grained and are made up of more restricted fauna of small benthonic foraminifers and coralline algae. The matrix of packstones and mudstones is comprised of micrite, neomorphic microspar and some fine grained skeletal debris

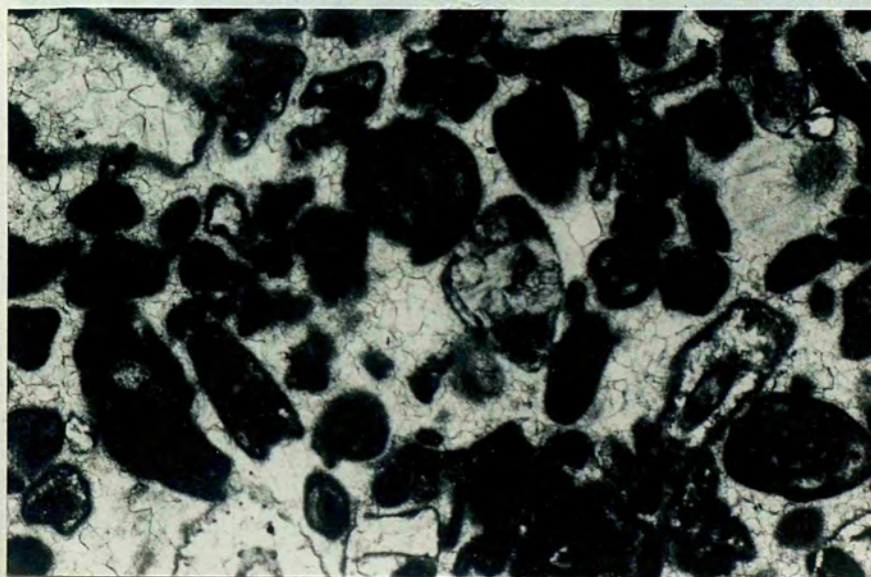
Grainstones occur patchily and are volumetrically less important than the other rock types of this subfacies. They are closely associated with boundstone and packstones and are composed of whole or broken small benthonic foraminifers, fragments of coralline algae and other organisms with small amounts of broken large benthonic foraminifers (Plate 7.10). Although some neomorphic sparry calcite is present filling the intra- and interparticle spaces of grain framework, the main binding agent is first phase sparry calcite cement. Grainstones are well to moderately sorted and contain grains which are generally subrounded to rounded and strongly micritized (Plate 7.10), see Diagenesis), ranging from coarse to fine but they are usually medium grained.

7.5 Subfacies III (Rotaliid-algal packstone)

This subfacies is found in the lower unit of the formation and consists of light grey (N 7) poorly sorted, coarse to medium grained, well bedded and well indurated bioclastic packstone which displays considerable vertical and lateral depositional and compositional texture variations throughout the formation. Packstones contain benthonic and planktonic foraminifers, fragments of coralline algae, broken fragments of corals, molluscs, echinoderms and brachiopods with a few agglutinating foraminifers in places (Plate 7.11). Thickness



A



B

Plate 7.10 - Bioclastic grainstone. Note the
micritization of skeletal grains.
Sample 2B (I26) 35X

of the beds ranges from 40 cm to 50 cm and they do not show any sedimentary structures. A vertical and horizontal bedding boundary between this subunit and other subunits of the Kocanindambasi Formation are observed (Fig. 7.11).

7.5.1 Texture

The texture of these rocks varies with the degree of grain support, in this way they are subdivided into three types:

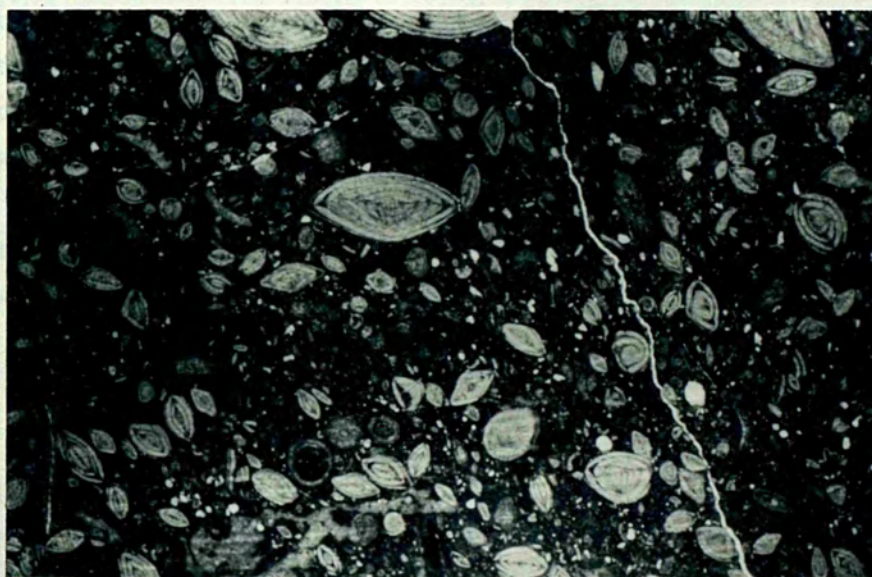


Plate 7.11 - General texture of the large benthonic foraminiferal packstone-grainstone.

Sample No. OSKIVA16 15X (KD Section)

of the beds ranges from 40 cm to 50 cm and they do not show any sedimentary structures. A vertical and horizontal gradational boundary between this subfacies and other subfacies of the Kocanindambasi formation are observed (Fig 7.1).

7.5.1 Texture

The texture of these rocks varies with the degree of grain support, in this way they may sometimes be a grainstone and sometimes a wackestone. Sorting thus ranges from well sorted to extremely poorly sorted, the latter mostly observed in wackestones. Vertical and horizontal compositional changes are marked by the increase of the amount of terrigenous material towards the subfacies I boundary and by an increase in the amount of miliolids where this subfacies passes into subfacies IV (Miliolid-algal packstone).

7.5.2 Framework grains

Benthonic foraminifers, represented by discocyclines and rotaliids, dominate the skeletal grains and may be up to 8 mm in length. They are usually well preserved; the wall crystal fabric consists of radially arranged calcite fibres forming a radial fibrous structure and the infilling of chambers by micrite, microspar and sparry calcite are observed.

Coralline algae fragments are not as abundant as they are in the Miliolid-algal packstone subfacies, but in places may become important proportionally. They are usually broken and may be found in a variety of shapes. Grain size ranges from a fraction of a mm to 8 mm and the internal cell structure is usually visible.

Agglutinated foraminifers may be observed in some parts of this subfacies. They are mainly Textularia ranging from 0.5 mm to 5 mm in length. Walls are composed largely of dark micrite in which angular to subrounded, unorientated, fine

quartz grains are embedded. The size of the quartz grains correlates positively with the size of the fossil.

Planktonic foraminifers, globigerinids, are occasionally found and show perforated wall structure. Chambers are filled by sparry calcite.

Brachiopods occur either as broken or whole shells which usually show foliated shell microstructure (Majewske 1965) or spines. Molluscs are found as large broken shells and always have lost their initial shell microstructure through the inversion of aragonite to calcite. Echinoid spines and plates are fairly common and show characteristic radiating pore patterns in the plates and lacy patterns (Scholle 1978) in the spines (Plate 7.12).

7.5.3. Binding agents

The matrix in this subfacies is poorly sorted, and generally replaced by neomorphic microspar in which relicts of dark micrite are observed. The occurrence of sparry calcite resembles that described in 7.6.4.

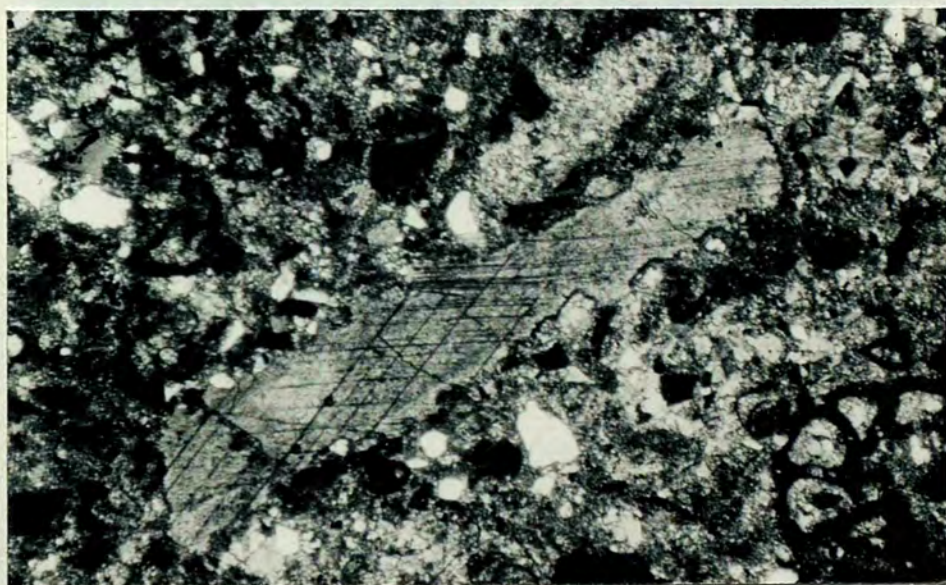
7.6 Subfacies IV (miliolid-algal packstone)

This subfacies is widespread in the lower unit of the formation and consists of very light-light grey (N7-8), generally medium to fine grained and moderate to poorly sorted packstone with minor amounts of wackestone. Packstones are usually dominated by a framework of small benthonic Foraminifera and fragments of coralline algae with subordinate amounts of agglutinating foraminifers and fragments of bryozoans, brachiopods, echinoids and molluscs (Plate 7.13). A proportion of terrigenous material, usually quartz and quartzite may be present at places. Usually well bedded and well indurated, the beds range from 30-60 cm in thickness. This subfacies has a lateral and vertical transitional boundary

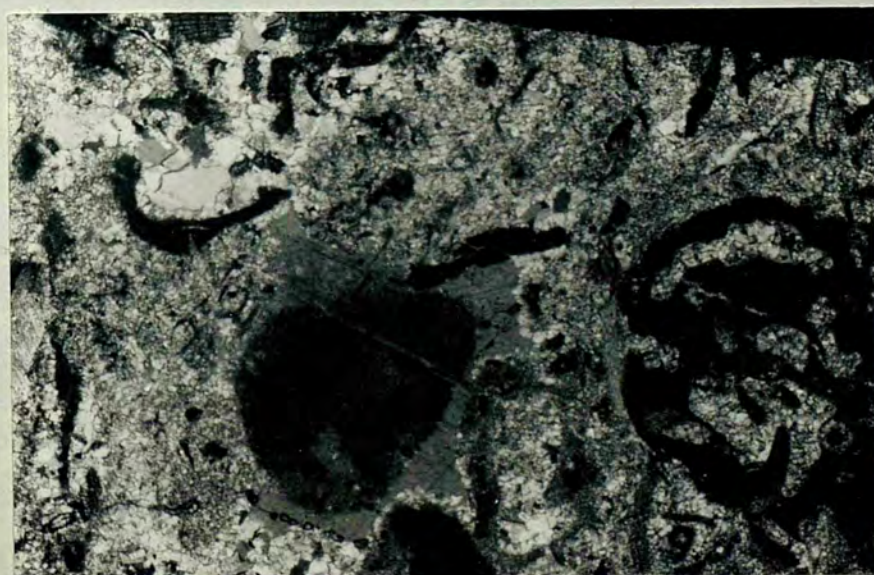
- 392
- Plate 7.12 -
- A) Cross-section of an echinoid spine showing single crystal structure and very characteristic lacy pattern OSK IVB-1 (Crinoid is 0.85 mm in diameter. (KD Section)
 - B) An echinoid fragment with single crystal structure. Note that there is no overgrowth occurred. 15X OSK IVB-1 (KD Section)
 - C) An echinoid fragment showing a syntaxial rim cement which first grew into the voids but later arrival of internally produced micrite prevented the overgrowth Sample IVA 13 (KD Section) 35X



A



B



C

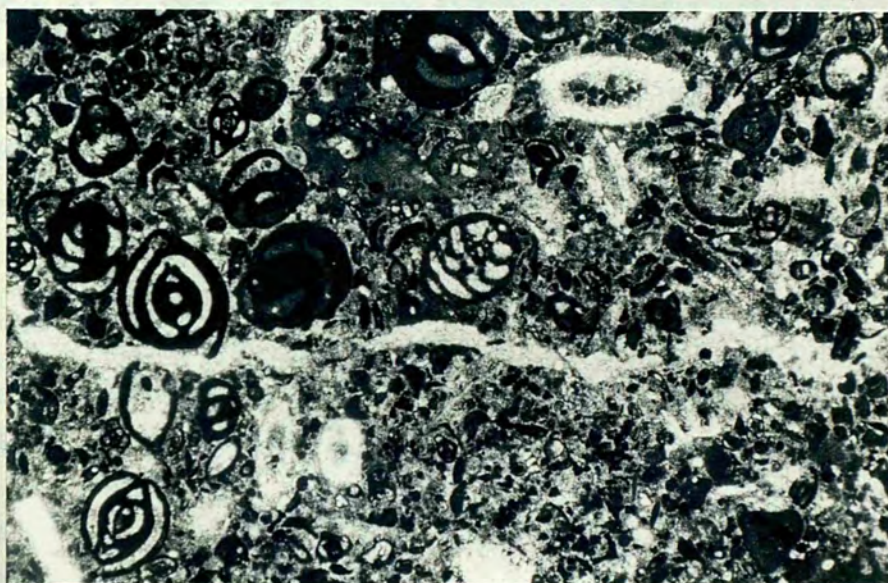


Plate 7.13 - General texture of the small benthonic foraminiferal packstone transverse, oblique and longitudinal sections of miliolids, dark fine grained appearance is typical of porcellaneous shell microstructure.
Sample No. IVA16 (KD section) 15X

with the subfacies III as the amount of large benthonic foraminifers increases and with the subfacies II. It also shows a sharp vertical boundary with the subfacies I.

7.6.1 Texture

Rocks of this subfacies are generally grain supported and contain a substantial amount of mud matrix but this general packstone appearance changes in places to wackestone in which the skeletal grains are supported by mud matrix. Grains are unorientated and show great diversity in grain size and composition. The compositional texture also varies to the extent that in places it can be called an algal packstone.

7.6.2 Framework grains

Small benthonic Foraminifera, mainly miliolids and some alveolinids, occur in varying proportions and sizes. Usually well preserved but some broken tests occur occasionally. Sizes range from 0.1 mm to 0.5 mm in length and chambers are filled with micrite, neomorphic microspar and sparry calcite.

Coralline Algae occur either as articulated forms or fragments of encrusting types, with sizes ranging from 0.1 mm to 4 mm. Although the initial cell structures are commonly preserved, heavily micritized lumps identifiable only by the remains of a few cell structures also occur.

Agglutinating (Arenaceous) foraminifers, Textularia, are more common in this subfacies than in other subfacies. Walls are made up of angular fine quartz grains within a calcareous matrix and chambers are filled by micrite, neomorphic microspar and/or sparry calcite (Plate 7.14).

Fragments of brachiopods, molluscs (sometimes as whole shells), echinoids, (usually as crinoid plates and spines



Plate 7.14 - A large agglutinating Textularia. Walls are made up of quartz and calcite grains and micrite as binding agent. Sample IVA 9 15X (KD Section)

with limited syntaxial overgrowths) and bryozoans (plate 7.15) (sometimes encrusting types) were recognized in a range of sizes.

7.6.3 Binding agents

The main agent in these rocks is the micrite matrix which is usually recrystallized to neomorphic microspar and/or sparry calcite, with some fine skeletal fragments. Generally poorly sorted, it occupies most of the intergranular pore spaces. The formation of sparry calcite appears to have resulted from three different mechanisms:

- a) by precipitation of sparry calcite which occurs either as a first phase cement filling the spaces which were protected by the umbrella effect of large skeletal fragments and as overgrowth from echinoderm fragments (Plate 7.12), or as a second phase cement filling the cavities and veins (Plate 7.19)
- b) by inversion of aragonite to sparry calcite in the grains which originally were aragonitic shells (Plate 7.20)
- c) by recrystallization from micrite or neomorphic microspar to neomorphic sparry calcite (Plate 7.23)

7.7 Fossils and age of the Kocanindambasi formation

Fossils (identified by C.G. Adams, pers. comm. 1982) found in the SW exposures of the formation indicate a Middle to Late Palaeocene age.

Fasciolites (Glomalveolina) spp. including F.G. Primaeva

Fasciolites (Glomalveolina) cf. primaeva Reichel

Caskinolina sp. or Lituonella sp. (rare)

Dictyoconus sp

Miliolids

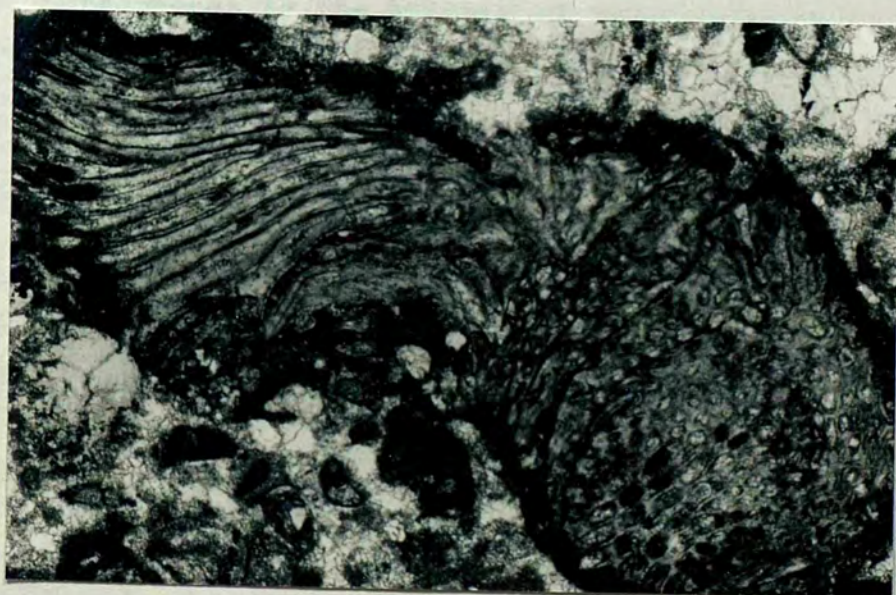
rotaliids and calcareous algae

Distichaplex biserialis

- Plate 7.15 - A) An encrusting bryozoan shell showing small vesicular tissue between zooecia. Vesicles are filled by radially arranged sparry calcite and zooecia filled by micrite 40X. Sample No. IVB 8 (KD Section)
- B) Transverse and longitudinal section of a bryozoan shell, illustrating an algal micritization (dark micrite rims) around the skeleton. Sample No. IVB 1 40X (KD Section)



A



B

Specimens collected from the NE part of the formation were dated as Early Eocene by C.G. Adams and S. Tekler:

Discocyclus sp

Ranikothalia sp.

Fasciolites sp

Nummulites sp.

Triloculina and calcareous algae

Distichoplax biserialis

7.8 Environment of deposition

Rocks of the Kocanindambasi formation were deposited on an open shelf; this is indicated by their exclusively shallow marine fauna. It would be reasonable to assume that the clastic input to the basin was low and physical and chemical conditions (i.e. temperature, salinity) helped organisms to flourish during the time of deposition. Although the environment of deposition of this limestone in a broad sense was uniform, differences in the balance of rate of subsidence and rate of carbonate accumulation and the amount of terrigenous material influx during the Middle-Late Palaeocene and the Early Eocene were the main reasons for the better development of this formation during the Palaeocene.

The deposition of the Kocanindambasi formation started with the accumulation of subfacies I. The diverse fauna and relatively high terrigenous content indicates that this subfacies was deposited as a bioclastic shelf carbonate (Henson 1975) in a slightly agitated, shallow water environment which was most probably below the wave base. This is indicated by the absence of any wave produced sedimentary structures; the presence of mud; abundance of unbroken fossils, and when they are broken, absence of mechanical abrasion; poor to moderate sorting of clastic grains and matrix; mixing of terrigenous material with bioclastic grains (sometimes up to 20%). The occurrence of miliolids and alveolinids which were generally accepted as being characteristic fossils of shallow quiet

water environments together with rotaliids, coralline algae, fragments of echinoids, brachiopods, molluscs and globigerinids which are thought to be an open marine fauna (Boessma 1976, Brady 1965, Watson 1965, Phelanger 1965) suggest that during the deposition of this subfacies no barrier or mounds existed.

Subfacies II was deposited as the core of the patchy carbonate mounds (Wilson 1975) on top of the localized sediment piles which resulted from the mechanical accumulation of subfacies I by wave and current activity. The presence of hermotypic sclerecterian corals which were found in their growth position and encrusting coralline algae which encrusted and bound the sessile corals and other organisms indicate that they were deposited as an in situ, rigid welded growth structure which was stabilized by the surface encrustation of coralline algae so that the normal process of marine erosion could not remove them. However, occurrences of packstones and wackestones which contain fragments of these frame building organisms as well as other skeletal grains, closely associated with this growth structure indicates that it was subjected to some wave agitation and was fragmented as it grew. Accumulation of fine grained sediment in this lithology can be explained by the trapping and baffling of lime mud (internally produced micrite, see diagenesis) and detrital mud. The baffle system which was operated by coralline algae, is known to trap and stabilize sediments (Wray 1977). Stromatolites which are more common in shallow intertidal environments, can form in various environments and depths on a hard substrate, providing:

- a) invertebrate grazers and burrowers are either absent or greatly reduced
- b) it has the potential of rapid cementation (Gebelin 1976).

Occurrence of stromatolites on top of ancient and recent reefs and carbonate banks and mounds as organic veneers or fissure fillings have been reported from all over the

world (Playford et al. 1976, Wilson 1975). Stromatolites found in this subfacies were obviously deposited in shallow water, as indicated by the presence of distinct and well developed laminations, their association with shallow water sediments and being growing on the fenestral limestone (Hoffman 1974, Playford et al. 1976). (Also see Table 7.1 for comparison of shallow water, deep water and stromatolites of this subfacies). The presence of a limited number of convex upward laminae and the absence of columnar growth forms in this lithology further indicate that the depth of water during deposition was very shallow (may be less than 15 cm) (Gebelin 1976). Consequently the effective wave action was absent, deposition on top of the mound slow and there was not an extensive growth of frame-producing organisms during the deposition of stromatolites. However, the occurrence of oncoliths in between the laminae of the stromatolites suggest that during the formation of oncoliths the depth of water increased since it is necessary to have enough agitation to overturn the stromatolite laminae (Eggleson & Dean 1976). The hard substrate for the development of stromatolites was provided by the underlying framework rocks which is usually considered to have the potential of large scale cementation when little or no carbonate precipitation occurs in the surrounding sediment (Alexandersson 1977). The presence of grainstone deposited in a relatively high energy environment, also suggests that the depth of water was changing through time.

The temperature of the sea water during the deposition of this subfacies may be inferred from such organisms as coralline algae and corals. Coralline algae, although they are most abundant in tropical seas, have been found living in all waters ranging from tropical to arctic (Adey & Macintyre 1973). Lithophyllum (encrusting and articulated types) which is the dominant coralline algal genus in the Kocanindambasi limestones is usually found living in tropical to sub-tropical shallow marine areas, although their occurrence in temperate regions

with a decreased growth rate has been recorded (Wray 1977, Milliman 1977). Together with sclerectarian corals which are limited to temperatures of 25° - 27° C (Wells 1956), they suggest the climate during the deposition of the subfacies was subtropical to tropical.

The salinity of the sea water, which appears to control the relative abundance of organisms (Heckel 1972), was normal. This is indicated by the presence of coralline algae, corals and echinoids. Sclerectarian corals which have little or no tolerance for other than normal marine salinity of 27-40 ppt (Wells 1956) together with coralline algae which tolerate much lower salinities (18 ppt) put the range of salinity of the sea water between 18-40 ppt, but most probably considerably narrower.

The depth in which the core of these carbonate mounds were deposited can be estimated again on the basis of its faunal content. The presence of hermatypic sclerectarian corals which are found living between surface to 30 m in present seas, but they obtain their best growth in less than 20 m (Wells 1956), and coralline algae which range in depth from surface to 200 m, but most encrusting algae grow in depths less than 40 m. Milliman (1977) suggests a water depth of 20-40 m. However, the presence of stromatolites, which are believed to form in a considerably shallower depth (see above), and relation of this subfacies with subfacies IV (see below) indicate that depth of the water during the deposition of this subfacies may be less than 20 or even 10 m.

Subfacies III which was differentiated from subfacies I on the basis of either the absence or significant reduction of small benthonic foraminifers and terrigenous material, was deposited as seaward flank beds (Wilson 1975) of the carbonate mounds in a quiet water environment. This is indicated by faunal and lithological characteristics. Large benthonic foraminifers, represented by rotaliids, are

characteristic of this subfacies. Rotaliids are found in relative abundance at depths ranging from 10 m to 55 m, although their presence in waters as deep as 100 m have been recorded (Phleger 1965). Though rotaliids are not good environmental indicators, since they may be found in both back-reef and fore-reef shoals (Henson 1975), their abundance, which suggests in situ fossilisation, large size (up to 6 mm in length) together with their association with globigerinids strongly suggests that this subfacies was deposited on the seaward flank of the carbonate mounds. The relative decrease in the amount of terrigenous material in the subfacies compared to the subfacies I and IV suggests that contamination of these rocks by lithoclastic material was prevented by a barrier between this subfacies and the shore. This inference and the presence of fragments of organisms which were found in the core of the mound further support the above conclusion. Poor to moderate sorting, a mud matrix and absence of any wave and current produced sedimentary structures together with the fauna already described suggest that this subfacies was deposited below breaker-level in a relatively quiet water environment. Some broken tests of foraminifers found in these rocks may have resulted from breaking during transportation from lesser depths and/or the activities of sediment ingesting organisms which caused fragmentation of the tests.

The occurrence of abundant and well preserved miliolids and alveolinids which indicates in situ fossilisation of these organisms in the sub-facies IV, together with the absence of wave produced sedimentological structures, the presence of fragments of algae, poor to moderate sorting, terrigenous material, bioturbation and mud matrix suggest this subfacies was deposited on the landward flank of the carbonate mound, in moderately agitated water, without the development of an extensive lagoon. Miliolids and alveolinids are usually found in protected areas of shallow marine environments and are considered to be the diagnostic

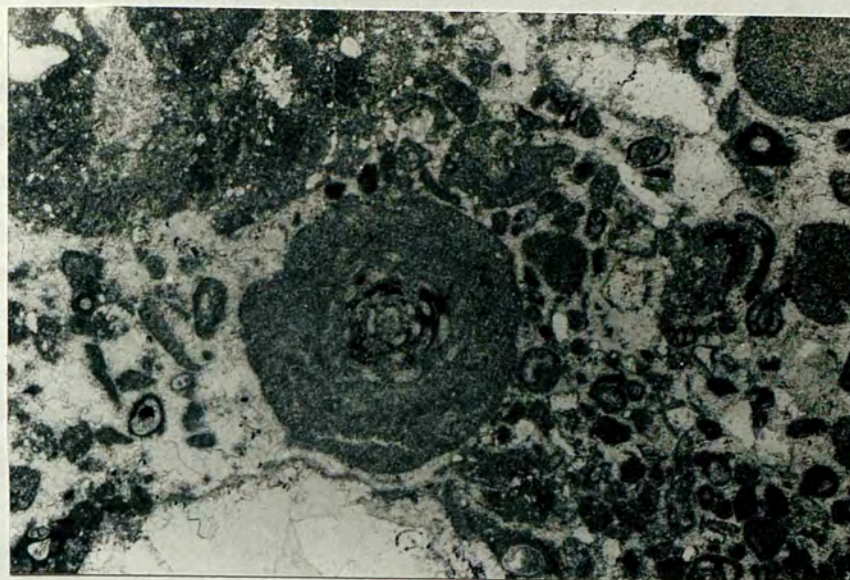
organisms for back-reef and reef environments (Brady 1965, Phleger 1965, Henson 1975, Boessma 1976 and Heckel 1977). The water depth was very shallow as indicated by miliolids (Recent species are found in depths ranging from 10 m to 30 m (Phleger 1965)). The occurrence of agglutinating foraminifers (simple forms) which are abundant and are characteristic of inner-shelf regions (Bandy 1964), together with the presence of intense algal boring, which takes place at less than 40 m and probably less than 15-18 m (Bathurst 1976), are other indicators of a shallow water origin. The most likely explanation for the occurrence of broken coral-line algae in this lithology is fragmentation in the high energy zone of the carbonate mounds and during transport to the depositional site.

7.9 Diagenesis and Post-diagenetic changes

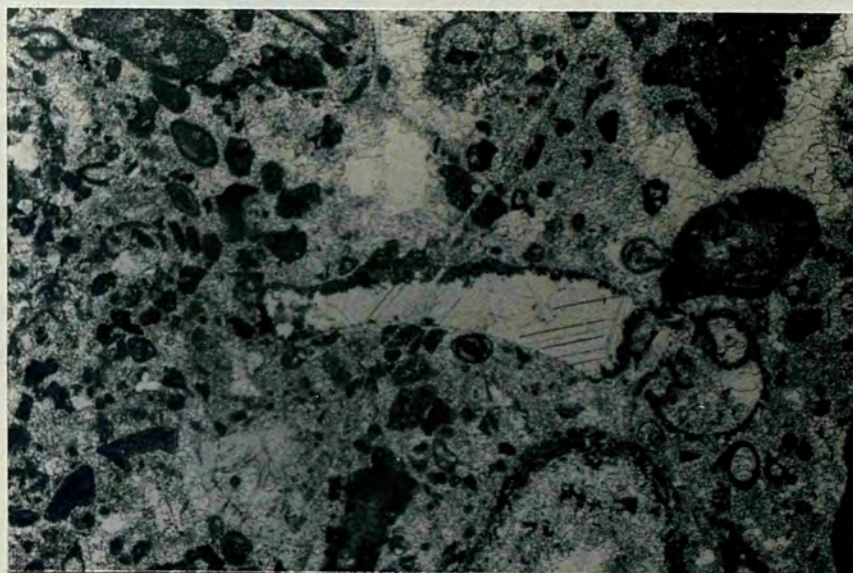
It is generally recognised that the physical, chemical and organic processes begin acting on carbonate grains, which are generally locally produced skeletal fragments, immediately after deposition and lead to lithification. The diagenetic history of the limestones of the Kocanindambasi formation may be put in a chronological order to achieve a better understanding.

STAGE I The boring of unconsolidated grains composed of broken and whole tests of skeletal organisms, by algae and possibly by fungi*, resulted in partial or complete centripetal micritization of these grains (Bathurst 1976). The alteration although found throughout the rocks of the Kocanindambasi formation, is more common in miliolids of the subfacies IV and extend from the outer rim of the grains inward forming a micrite envelope (Plate 7.16) which unlike the accretionary micrite envelopes, has an irregular contact with the host grain and is not uniform in thickness,

* No attempt has been made by the author to distinguish algal and fungal borings.



A



B

Plate 7.16 - A) Micritization of foraminiferid. At the centre the central part of the test is intact and the outer part is completely micritized due to algal boring. At the top right a completely micritized foraminiferid which now as a lump of micrite. IVB 19 (KD Section) 35X

B) Micritization of an echionid fragment. Note the irregular contact of micrite envelope and the host grain. IVB 10 35X (KD Section)

on a residual core of the unaltered skeletal grain. In the more advanced stage of this alteration which results from repeated boring and the filling of bores by micrite, a skeletal grain is turned into a micrite lump (Bathurst 1976) (Plate 7.16). Bathurst (1976) also stated that another important result of algal boring is that the grains affected appear to be more liable to abrasion and easy to breakdown by waves and currents. Although they have been observed, burrowings are less common and occur locally. Breaking and fracturing of some skeletal grains during the compaction is also observed in this stage (Plate 7.17).

STAGE II This stage marks the beginning of CaCO_3 precipitation as a first phase cement in the inter-particle pores as fibrous, bladed, blocky and syntaxial rim cement. Fibrous cement occurs as elongate, tightly packed calcite crystals growing into the intra-and inter-particle pore spaces. The crystals grow with their long axis perpendicular to the host grain and they show undulatory extinction under polarized light (Plate 7.18). Bladed cement, like fibrous cement, usually occurs on foraminifers and algal fragments. The crystals in this cement fabric are also orientated with their long axis perpendicular to the void (or host grain) but the length/width ratio of crystals is between 1.5: 1 and 6:1. Blocky cement ("equant crust" of Folk 1965) is found filling the chambers of the foraminifers inter-particle voids and spaces which were protected by the umbrella effect of the larger grains. This cement fabric has crystals with length/width ratio less than 1.5:1 and size of the crystals increases towards the centre of the void. Syntaxial rim cement is an overgrowth in optical continuity from a single calcite crystal such as an echinoid plate. In the rocks of the Kocanindambasi formation growth of this cement was either completely prevented or restricted by the arrival of internally produced micrite (see below).

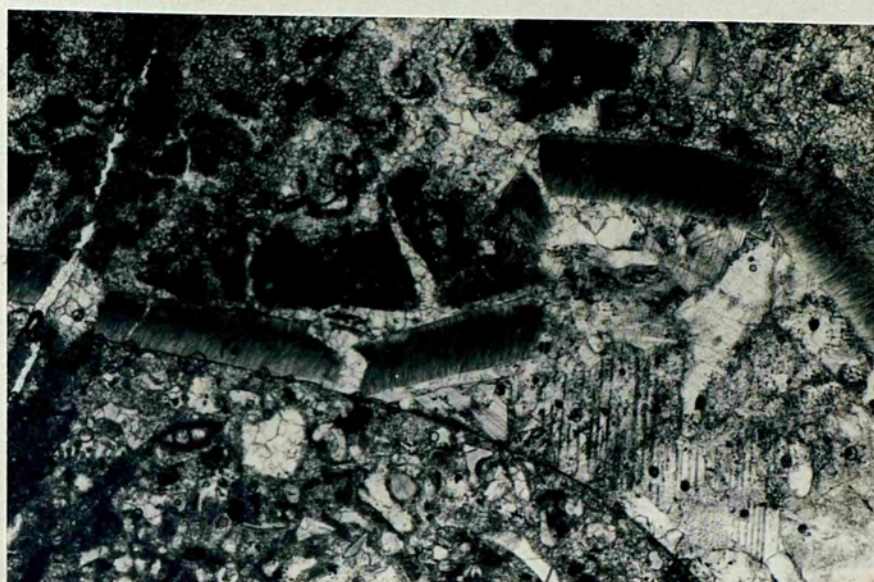


Plate 7.17 - Probably a brachiopod shell which is broken during the compaction. Sample no. IVA5 (KD Section) 35X. XN.

- Plate 7.18
- A. Fibrous cement growing on a foraminifer test the chambers of which are filled with micrite; surrounding microspar and sparry calcite are neomorphic in origin as indicated by the irregular distribution of crystal size and the scarcity of plane intercrystalline boundaries. Sample No. IVB 3 (KD section) 150X
- B. Photomicrograph shows bladed cement growing on a completely micritized skeletal fragment. Sample No. IVA 16 (KD Section) 150X



A



B

STAGE III Micrite, which is quite separate from the primarily deposited matrix, is first introduced to the sediments in this stage. Cloudy in appearance, it is found overlying the first phase fibrous cement and the syntaxial rim cement. Abundant in subfacies IV, it also occurs in the other subfacies of the Kocanindambasi formation. Its relation with the syntaxial rim cement clearly indicates that the latter was formed as void filling cement in spaces where no primary matrix was present and subsequently internally produced micrite was introduced as a late arrival. Thus the overgrowth from the echinoid fragments was inhibited. Occurrence of micrite resting on the first phase fibrous cement also supports this conclusion.

STAGE IV a) Solution cavity filling; is observed in the fragments of molluscs, as a calcite cast which is surrounded by a dark micrite envelope. This is a well known dissolution-precipitation process, proceeding through dissolution of an original aragonitic shell, forming a mould which was supported by the micrite envelope; later, calcite was precipitated in this mould as bladed and blocky cement without any trace of the original shell structure (Plate 7.19).

b) Inversion: a good example of inversion of aragonite to calcite was observed in the subfacies II; Plate 7.20 shows a molluscan shell which is a calcite cast with a strong pseudopleochroism. It is known that the presence of organic matter in the calcite imparts a strong pseudopleochroism to the crystals. This implies that the replacement of the aragonite by calcite did not proceed via a void stage as in solution cavity filling. Rather it is likely that the replacement was achieved by a migrating front along which dissolution of aragonite was accompanied by concomitant in situ precipitation of calcite. Thus the ghost of the primary layers in the original aragonite shell were preserved (dark, vague concentric layers in the photomicrograph) (Bathurst 1976, Shearman pers. comm.

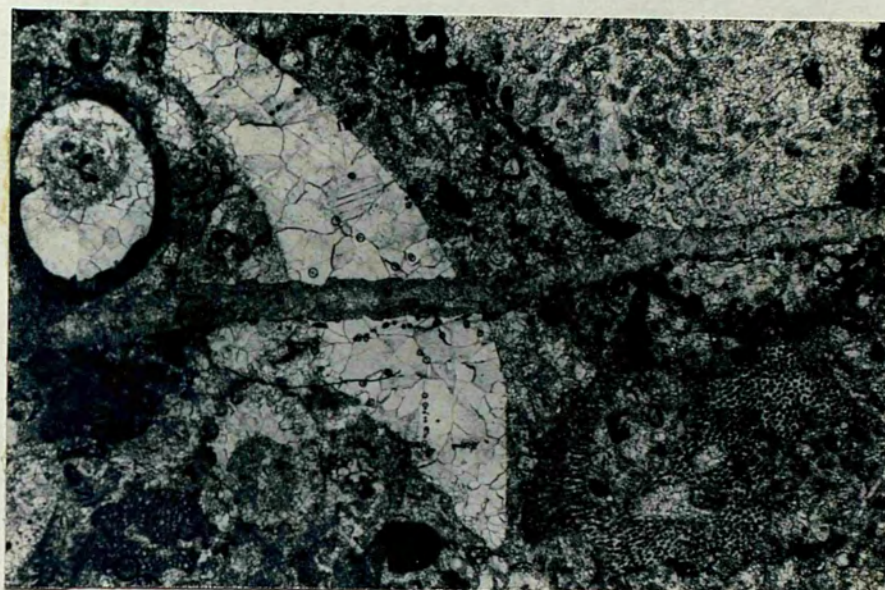
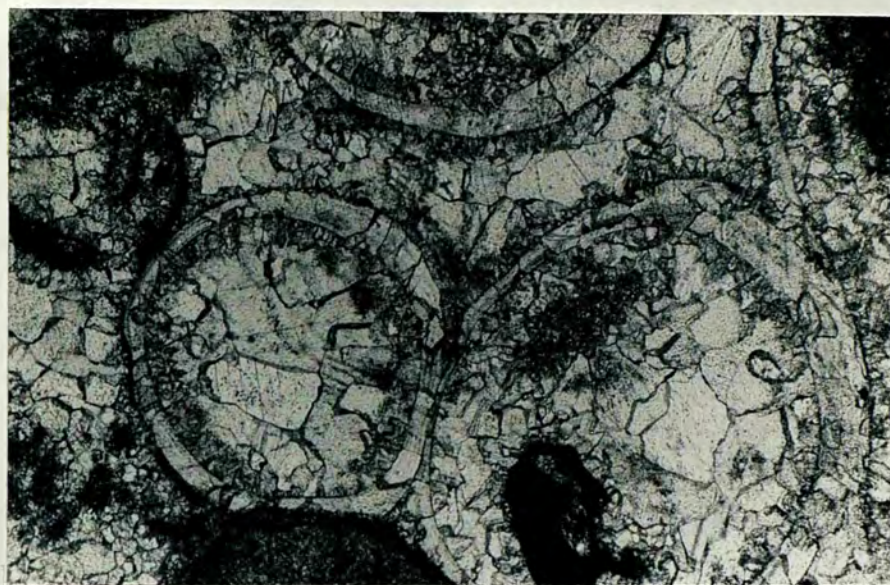
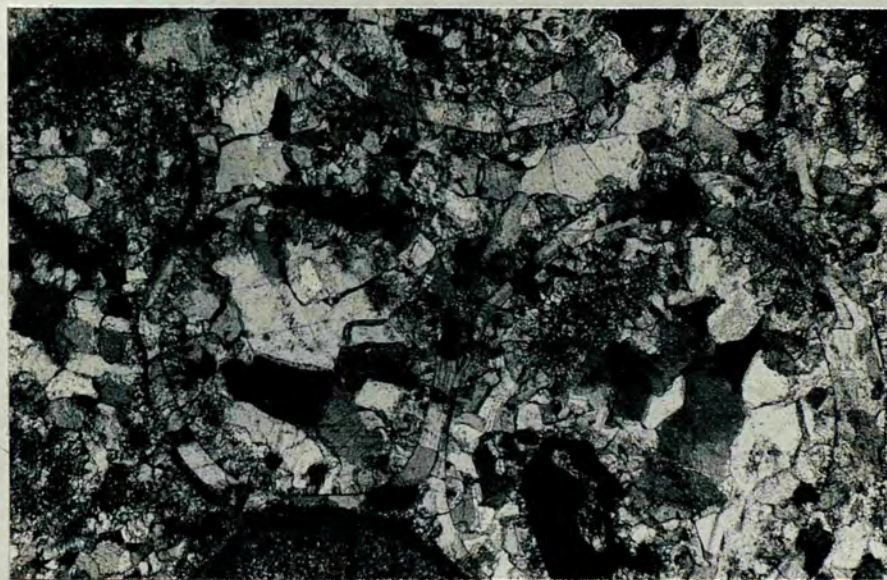


Plate 7.19 - A) Solution cavity fill in molluscan shells at top right corner and centre. A vertical boring running from left to right, filled by micrite. Sample No. IVA 5 (KD Section) 15X

Plate 7.20 - Showing inversion of aragonite to calcite in what is probably a molluscan shell. Note the concentric dark layers in the shell formed by original organic material at A and difference in the crystal fabric of shell and sparry calcite cement indicate that crystallization of those two occurred in different times, at B. Sample No. IVA 5 (KD Section) 35X, B, with XN



A



B

1982). This sort of fabric is believed to be formed in fresh-water diagenetic environments (Shearman pers. comm. 1982).

c) Neomorphic recrystallization of micrite to microspar and sparry calcite is a very common feature in the rocks of the Kocanindambasi formation and resulted from the aggrading neomorphism (see Bathurst 1976). In the inter-particle and intra-particle spaces of these rocks microspar and/or sparry calcite crystals with relict patches of micrite are observed. Neomorphic sparry calcite crystals in contrast to the sparry calcite cement, show an irregular distribution in crystal sizes and scarce plane intercrystalline boundaries. In some cases when there is micrite, microspar and sparry calcite present, a multiple generation of recrystallization can be proposed, thus the original micrite was first neomorphosed to microspar which was composed of equidimensional calcite crystals; later microspar was partially recrystallized to coarse neomorphic sparry calcite (see 1.4.8 for definition of micrite, microspar and sparry calcite). At the most destructive stages of this process walls of foraminifers were replaced by neomorphic sparry calcite (Plate 7.21).

STAGE V In this stage multiple fractures, intercrossing at different angles were developed. They are long well developed and cut across the matrix and the skeletal grains. Sparry calcite cement is found filling these fractures. Styolites and pressure-solution contacts are practically absent in the rocks of this formation.

Apart from the part of subfacies II which at one time most probably had a fresh-water diagenetic environment, the diagenetic changes which affected these limestones took place in a shallow marine environment, and is mainly indicated by the presence of early diagenetic cement, internally produced micrite and possibly an allochthonous source for the CaCO_3

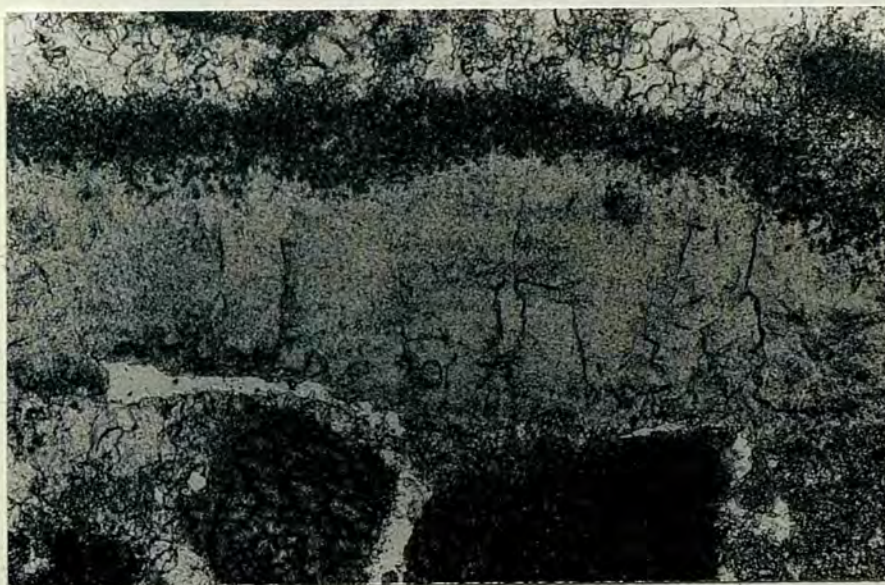
Plate 7.21 - Walls of Foraminifers replaced
by neomorphic sparry calcite.
Sample No. IVB 10 (KD Section)
35X

Plate 7.22 - Algal boring; cavities caused
by boring of algae, later filled
by micrite. Sample No. IVB 3
(KD Section) 150 X

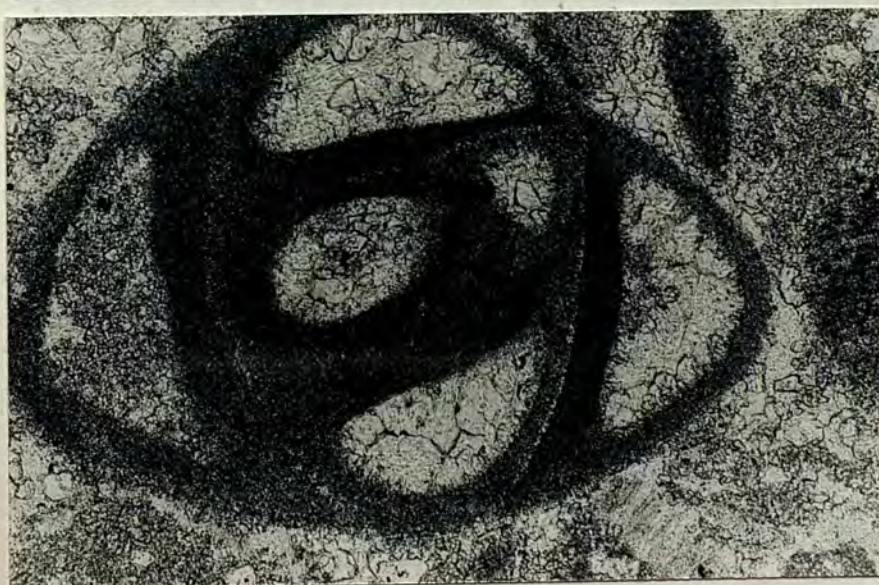
Plate 7.23 - A miliolid shell, walls are micrit-
ized, chambers are filled by bladed
and blocky sparry calcite cement.
Surrounding sparry calcite is neo-
morphic in origin. Sample No. IVB 3
(KD Section) 150X



A



B



C

since there is no sign of grain dissolution which is so characteristic of the meteoric environment.

C H A P T E R 8

BAYAT FORMATION

8.1 Introduction

This formation is Middle Palaeocene - Middle Eocene in age and outcrops extensively in the area studied parallel to the NE-SW trend of the Bala basin. It consists of three interrelated facies, which are given different member names. Although each member could have been given formational status they are collected under one formational name because of their close genetic relationships (see 8.2.2, 3.2.8, & 4.2) and similar rock composition. The first member, the Kurebogazi (U8) consists of shale, marl, fine grained sandstone and calcarenite with occasional conglomerate and coarse grained sandstone lenses with limestone olistoliths. The polymict conglomerate, sandstone, calcarenite and shale dominated second member is named after Ardiclipinar hill (N12). This member also contains widespread limestone olistoliths. The third is named after Buyukdere Valley (K11) where the type section was measured and consists of sandstone calcarenite, shale and marl intercalations. The depositional history of the each member is believed to be interrelated and much complex interfingering occurs between the members. Therefore the definition of the boundaries is difficult.

8.2 KUREBOGAZI MEMBER

8.2.1 Description

The Kurebogazi member consists of light olive grey (5Y 5/2) - pale olive (10Y 6/2) muddy sandstones, medium light grey (N6) calcarenites dark greenish grey (5G 4/1) shales light grey (N7) marls and occasional brownish grey (5YR 4/4) polymict muddy conglomerate and calcirudites with scattered limestone olistoliths. It is believed to represent slope deposits which are separated into upper slope and lower slope facies.

8.2.1.1 Upper slope facies association

This is one of the most widely distributed association of the Kurebogazi member and four different sequences are distinguished.

a. Shales with medium to thin bedded, medium to fine grained sandstone and calcarenites: (see App XII, Fig 8.1&2 and 3.). This is the most common sequence within the upper slope lithologies and is predominantly shaly. Where the shales are well exposed, 1 cm. to 5 cm. thick beds with sharp surfaces and parallel lamination can be observed. In other cases bedding is absent, destroyed by bioturbation. They are very fine grained and contain planktonic and a few benthonic foraminifers. Occasional sandstones and calcarenites (all called sandstones from hereon) interrupt the shales and are 3-40 cm. thick.

They are generally medium to fine grained although some coarse grained sandstones forming up to 40 cm. thick beds can be observed. They occur in two types: turbiditic sandstones and sandstones occurring as couplets. Turbiditic sandstones rarely display complete Bouma sequences (Tabcde) but Tabe and Tbce type sandstones are common. Sandstones with basal division "a", which are generally reduced, (Plate 8.1) are usually coarse-fine grained and show well developed flute casts and groove casts. In some beds load casts of a few cm. deep occur. They have sharp upper boundaries and although in general they are laterally extensive, wedging out of some beds also occurs. Beds without Ta division (base cut out) are usually medium to fine grained and most commonly occur as Tbce type with subordinate amount of Tbcde type. They show sharp upper and lower boundaries and apart from some prod marks, and poorly developed groove casts, they do not display any directional sole structures. The trace fossil Granularia sp. also occurs. These sandstone beds are usually thinner (3-20cm.) than those with Ta division and appear to be laterally more extensive. Sandstones occurring as couplets are rare and only

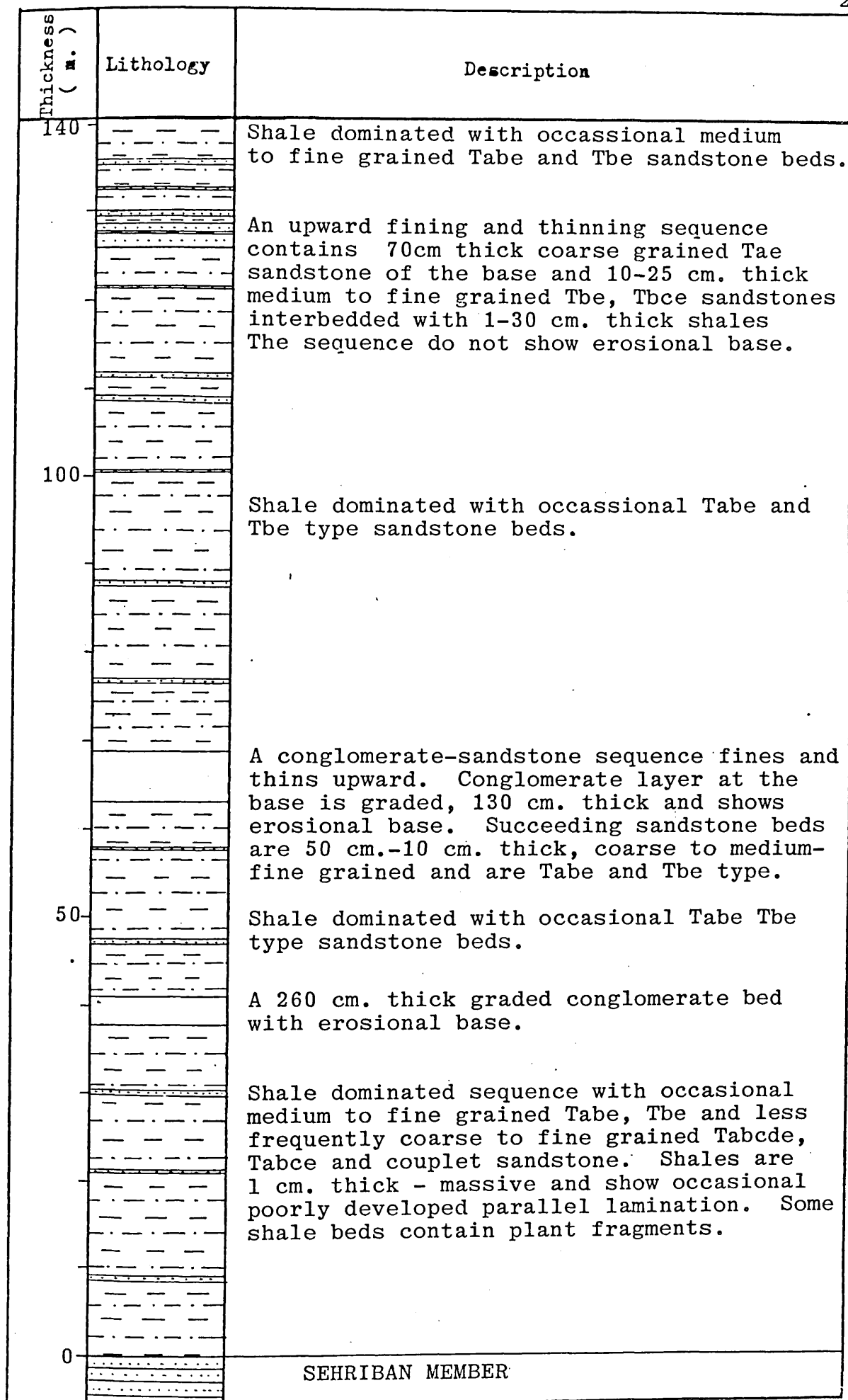


Fig 8.1 - Kurebogazi section.

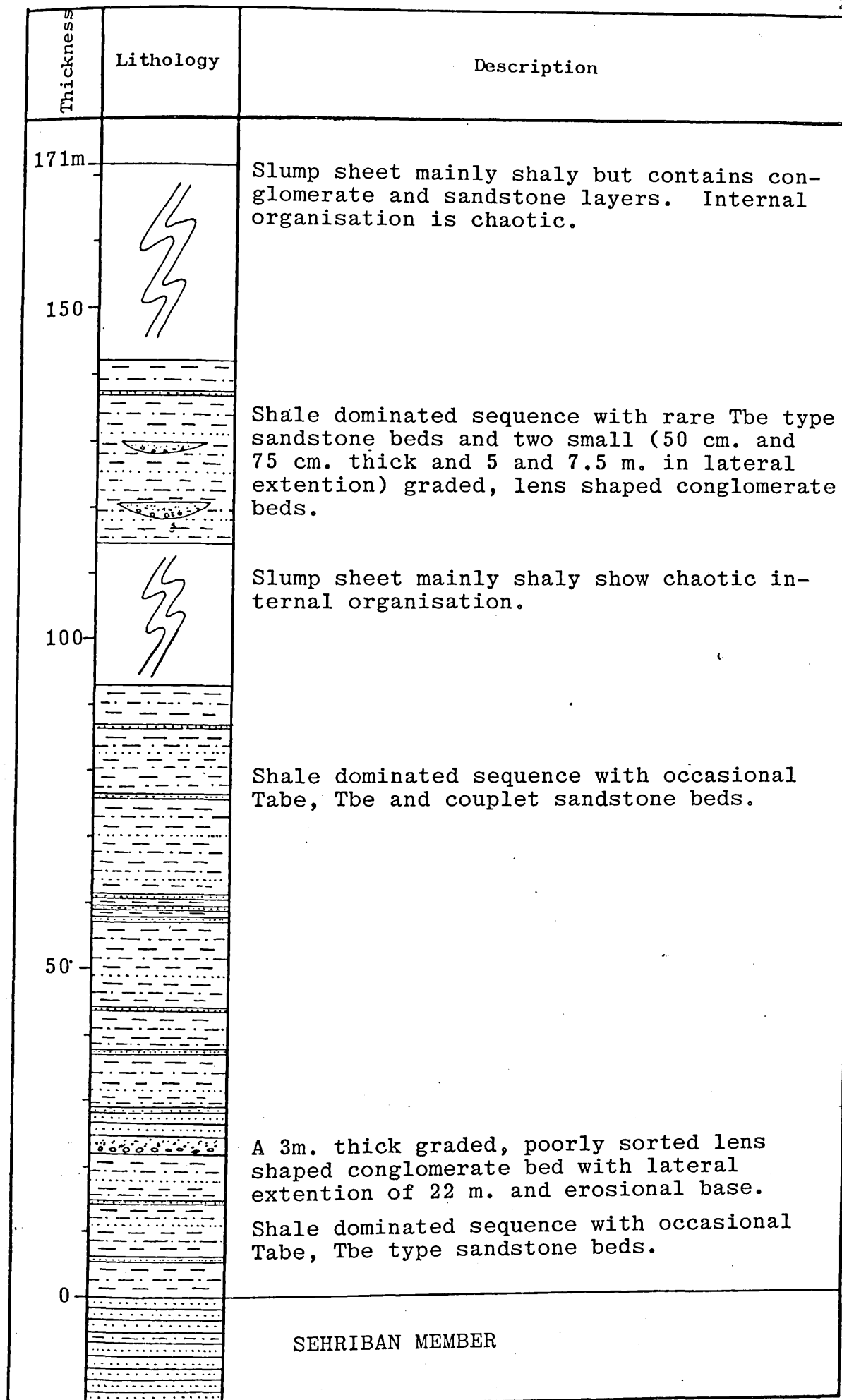


Fig 8.2 - Sarlalikdere section.

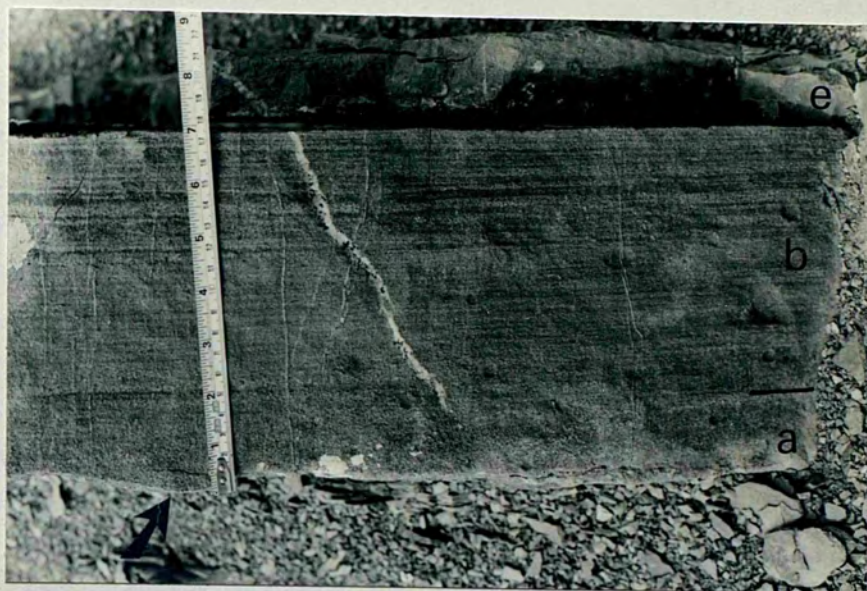


Plate 8.1 - A Tab type sandstone bed:
 Note the reduced Ta division and a
 small load cast on the left of the
 photograph. Locality (014)

found in the lower parts of the Kurebogazi (Fig 8.1) and Sarlalikdere (Fig 8.2) sections. In these the lower graded part of the beds are separated from the parallel laminated upper part by a distinct break (Plate 8.2).

b. Upward fining and thinning sandstone sequences:

These sequences occur as isolated lens shaped bodies and they are best observed in the Kurebogazi section (Fig 8.1) and Buyukdere section (Fig 8.3). In the former it is 4.2 m. thick and comprised of 30-50 cm. Tab_e, coarse grained sandstones at the base and 5-20 cm. thick Tb_e and Tbce medium to fine grained sandstone beds towards the top in an upward fining and thinning sequence without any obvious channeling. Current directions obtained from flute and groove casts indicate flow from the ENE. In the Buyukdere section two of these sequences are recorded. The first, which occurs at 1004 m. from the base of the section and is 9.7 m. thick, although not showing distinct upward fining and thinning, is included into this group because of its single appearance and stratigraphic position. In this sequence, beds are Tb_e and Tbce type, 5-20 cm. thick, medium to fine grained and have sharp upper and lower boundaries. The second is observed at 1165 m., 4.9 m. thick, 65 m. wide and is formed by group of 13 beds ranging in thickness from 70 cm. at the base to 5-15 cm. toward the top of an upward, fining and thinning sequence. (Plate 8.3) The bed at the base is a Tab_e, coarse to medium grained sandstone with a few granule size clasts and shows well developed flute casts which indicate a current direction from SW. The beds in the upper part of the section are Tb_e or Tbce types, medium to fine grained and 10-15 cm. thick.

c. Channeled conglomerate and conglomerate to sandstone sequences.

Widespread in the upper slope facies association they generally occur as single or up to three conglomerate beds



Plate 8.2 - Showing a sandstone bed forming a couplet at the base sandstone is graded.
Locality (Q12)



Plate 8.3 - Showing the second upward fining and thinning sandstone sequence in the Buyukdere section. Note the predominantly shaly nature of the enclosing sediment. This sequence is 4.9 m. thick. Locality (K12)

or conglomerate sandstone sequences (Plate 8.4) which sometimes show upward fining and thinning within broad (5m-325m wide) and shallow (1m-15m. deep) channels. There are two exceptions (see below). In some localities these channels occur as repetitive cycles with a slight shifting of channel axis (Plate 8.5). The conglomerate sequences, which are formed by a single bed or up to three beds (see Kurebogazi (Fig 8.1)), Cataltepe (Fig 5.1) and Sarlalikdere (Fig 8.2) Section) consists of boulder to granule size clasts and often contain intraformational pebbles, mud clasts and plant fragments. They form 25 cm to over 3m. thick, lens shaped beds with lateral dimension of a few metres to tens of metres and can be clast or matrix supported. Although rare disorganized examples (Plate 8.6A) occur, the clast supported conglomerates are generally graded and stratified with obvious erosional bases and flat tops (Plate 8.6B). The sole structures, which are mainly flute casts, are poorly developed and, though showing various flow directions (Fig 12.9&10, in general they are perpendicular or oblique (from SW SE) to the basinal axis. The matrix supported conglomerates (Plate 8.7) do not show any sedimentary structures apart from occasional very indistinctive grading and are extremely poorly sorted as clasts ranging from 85cm in diameter boulders to granules are randomly distributed in the muddy sandstone matrix. They form 80 cm - 2m. thick beds with lateral dimension of 4m-10m. These conglomerate beds can have flat or erosional bases and flat or hummocky convex-up tops.

The conglomerate-sandstone sequences are relatively less common than the conglomerates and show upward fining and thinning as 50cm-4.5m. thick disorganized to graded conglomerates at the base of the sequence gradually pass up to massive or Ta or Tabe type 10 cm-80 cm. thick sandstone beds intercalating with thin (1-15 cm.) shales beds towards the top of the sequences (Plate 8.4A).

The first of the two exceptions mentioned above is observed on the southwestern flank of the Kocaarkac hill (G24).



Plate 8.4 - Conglomerate-sandstone (A) and conglomerate (B) sequences. Note the upward fining and thinning in (A). Hammer is 30 cm. in length..(Localities A(H21 B(G27))

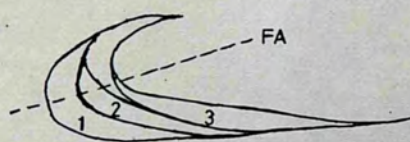


Plate 8.5 - Showing 3 channels build in succession and filled by conglomerate and sandstones. Later they are slumped and occur as recumbent fold. (FA=fold axis)..Locality (Q11)



Plate 8.6 - Clast supported conglomerates. (A) is a disorganised conglomerate bed in which some clasts show upward projection. In (B) a graded conglomerate at base is overlaid by a graded stratified conglomerate bed with erosional base and flat top. Hammer is 30 cm. in length

Localities A(011) B(L15)





Plate 8.7 - Occurrences of matrix supported conglomerates. In (A) the conglomerate beds have irregular base and flat top. In (B) a lens shaped 2 m. thick, conglomerate bed show irregular base and hummocky top. Note the sub parallel arrangement of bed in respect to the enclosing sediment. Locality (R11).

In here a V-shaped 8.5 m. deep and 16m. wide channel with wall slopes of 60° (left side) and 38° (right side) cutting the underlying shaly sequence is recorded (Plate 8.8). The channel is filled entirely by disorganized conglomerates except in the uppermost 1.6 m. where 50 cm.-20 cm. thick Tae and Tab sandstones with thin (1-5 cm. thick) shale beds occur.

The other exception occurs to the NW of Kurebogazi (U8), where a channel 1275m. wide and 81m. deep (at the axis of the channel) is observed. It is a broad channel with wall slopes of 10° - 15° and cut into the shale dominant sequence identical to one which is shown in Fig 8.1. The channel is filled by conglomerates and sandstones. The conglomerates, which make up 75% of the channel fill deposits, form 1-6 m. thick beds with well developed erosional bases and flat tops. They are mainly clast supported, although some matrix supported ones occur, generally disorganized or indistinctively graded and sometimes show crude parallel stratification (Plate 8.9a). The conglomerates consist of chert, quartzite, volcanic rock, radiolarite, limestone and serpentinite clasts in decreasing order of abundance and are poor to extremely poorly sorted. The sandstone are generally massive and commonly amalgamated. Beds are 20 cm-1m. thick and often show dish structures and fluid escape pipes. Turbiditic sandstones are rare and occur only as Tae type beds.

d. Slumped sequences*

These sequences are commonly observed within the upper slope deposits and occur as either slump folds or slump sheets in which internal organization is chaotic (Plate 8.11): These slump sequences involve all the sequences described above (see Salideresi sketch section App.X and Plates 8.5, 10 & 11)

*Sliding and slumping are not differentiated because in most of the cases basal shear planes are not observed. Instead, following Rupke (1980) they are called slumps.

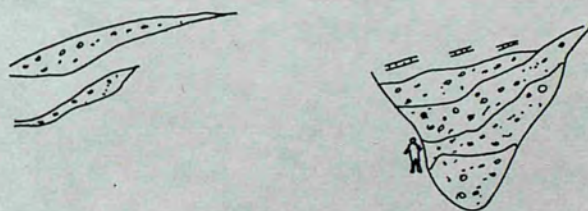


Plate 8.8 - A V-shaped channel filled by disorganized conglomerates. Note the occurrence of two broad shallow channel as graded conglomerates on the left of the photograph. Locality (G24)

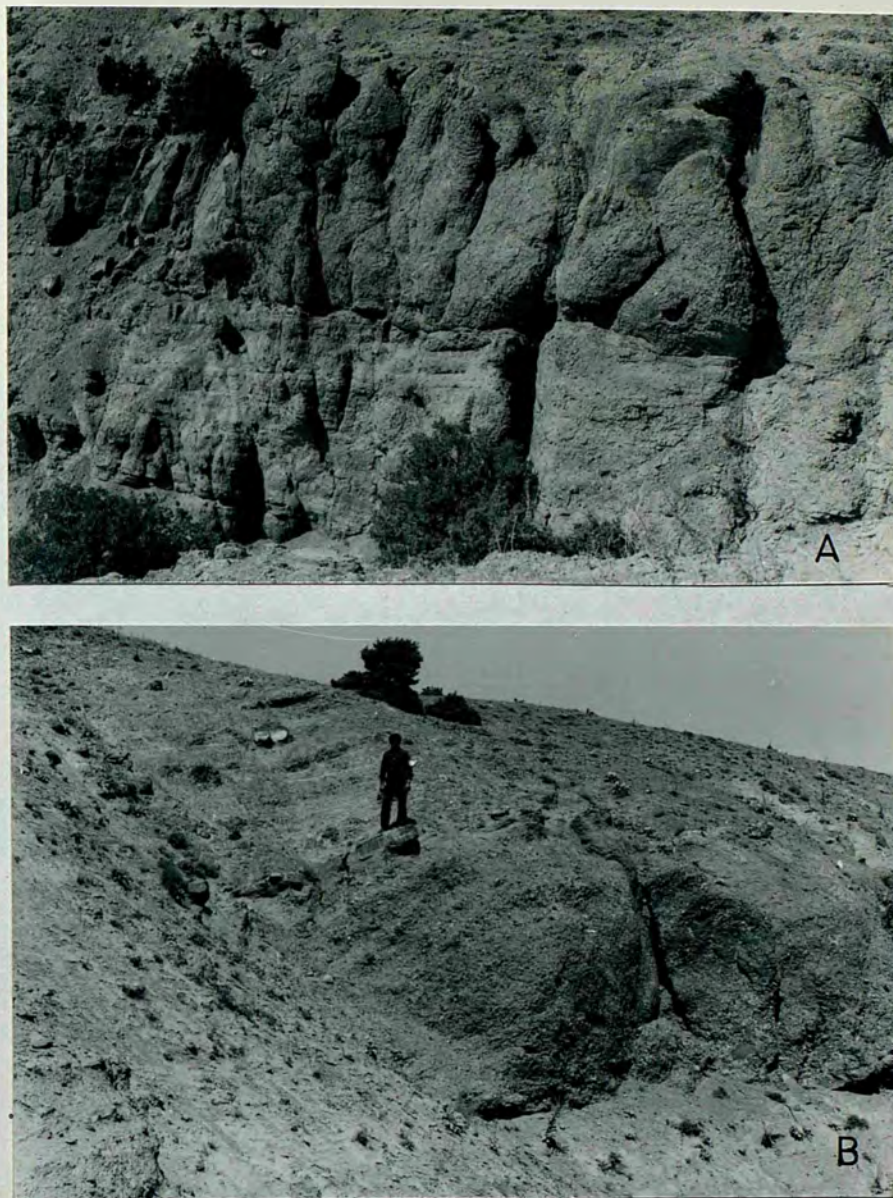


Plate 8.9 - Showing conglomerate and sandstone beds in the channel (see text) in (A) the upper bed is 5 m. thick; Note the occurrence of erosional surface on the base of the upper bed and crude parallel stratification in the lower bed. In (B) a 6 m. thick poorly graded conglomerate bed passes up to the massive sandstone and thin conglomerate beds. Locality (U6 & 7)



Plate 8.10 - Shows two slump sequences in the Salideresi sketch section. Note the erosion of the fold anticlines in the lower slump sequence.

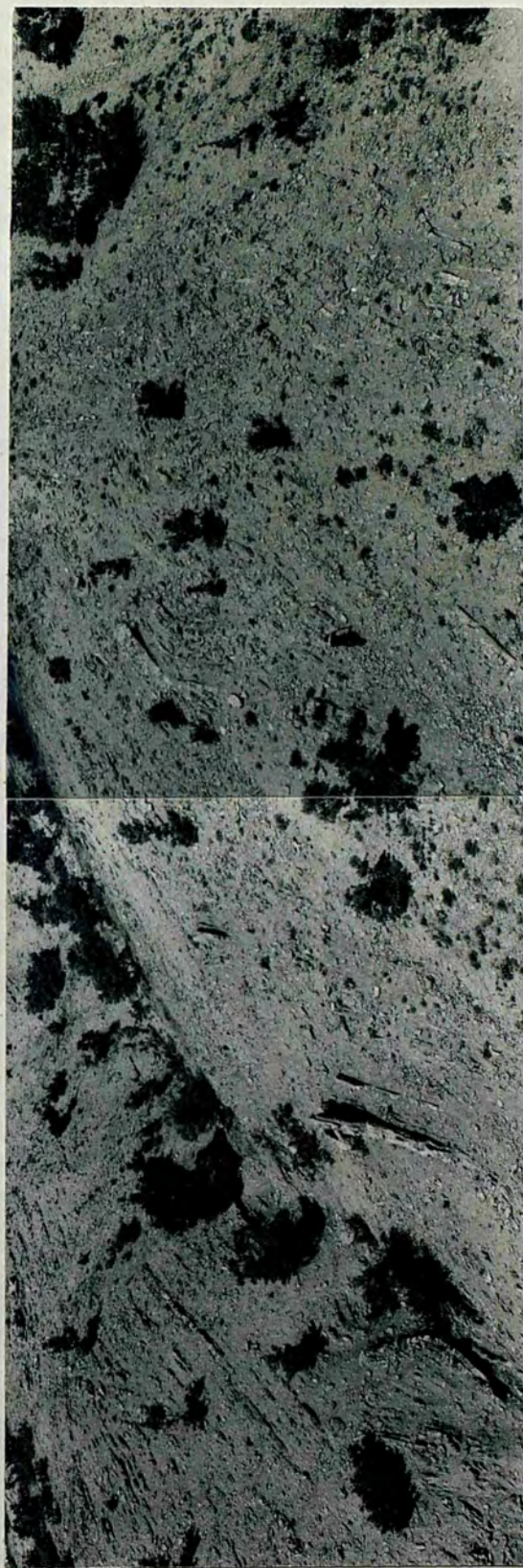


Plate 8.11A- Shows the chaotic internal organisation of a slump sheet. The upper part of the Salideresi sketch section.



Plate 8.11B- The occurrence of slump folds and sheet (left of the photograph) in the upper and lower slope transition, around the llimandere (J13) Note the limestone olistoliths in the slump sheet.

and can occur as either a single sequence isolated within relatively undisturbed beds or as a number of slump sequences preceeding each other (Plate 8.10 & 11 and App. X).. The slump sequences range, in thickness, from 15 m. to over 100m. and their lateral extent could be hundreds of metres. The folds indicate a slump direction towards the centre of the basin compatible with the current directions in other sequences (see Fig 12.9 & 10). The folds can be open to tight, isoclinal, recumbent, monoclinal or bench. In some cases erosion of the fold anticline by overlying slump sequences (Plate 8.10) or depositional fit between the irregularities of the folds' upper surface and overlying beds can be observed. The basal shear plane of the folds are generally difficult to observe since most of the slumps occur in shale dominated sequences. However in rare occasions concave-up inferred bases can be seen. Sometimes the occurrence of tensional faults at the toe (see App. X) and compressional faults at the head of the slumps can be seen. The degree of disruption of beds in the slump sequences depends on the sedimentary sequences involved; generally in slumps involving shale dominated sequences with occasional thin bedded sandstone and calcarenites, the internal organization of the slump is chaotic apart from some small unrelated flop and cascade folds. (Plate 8.11 and App. X). In slump-involving sequences, in which the sandstone/shale ratio is relatively higher than those described above, slump folds of various kinds can be observed.

e. Limestone olistoliths and blocks

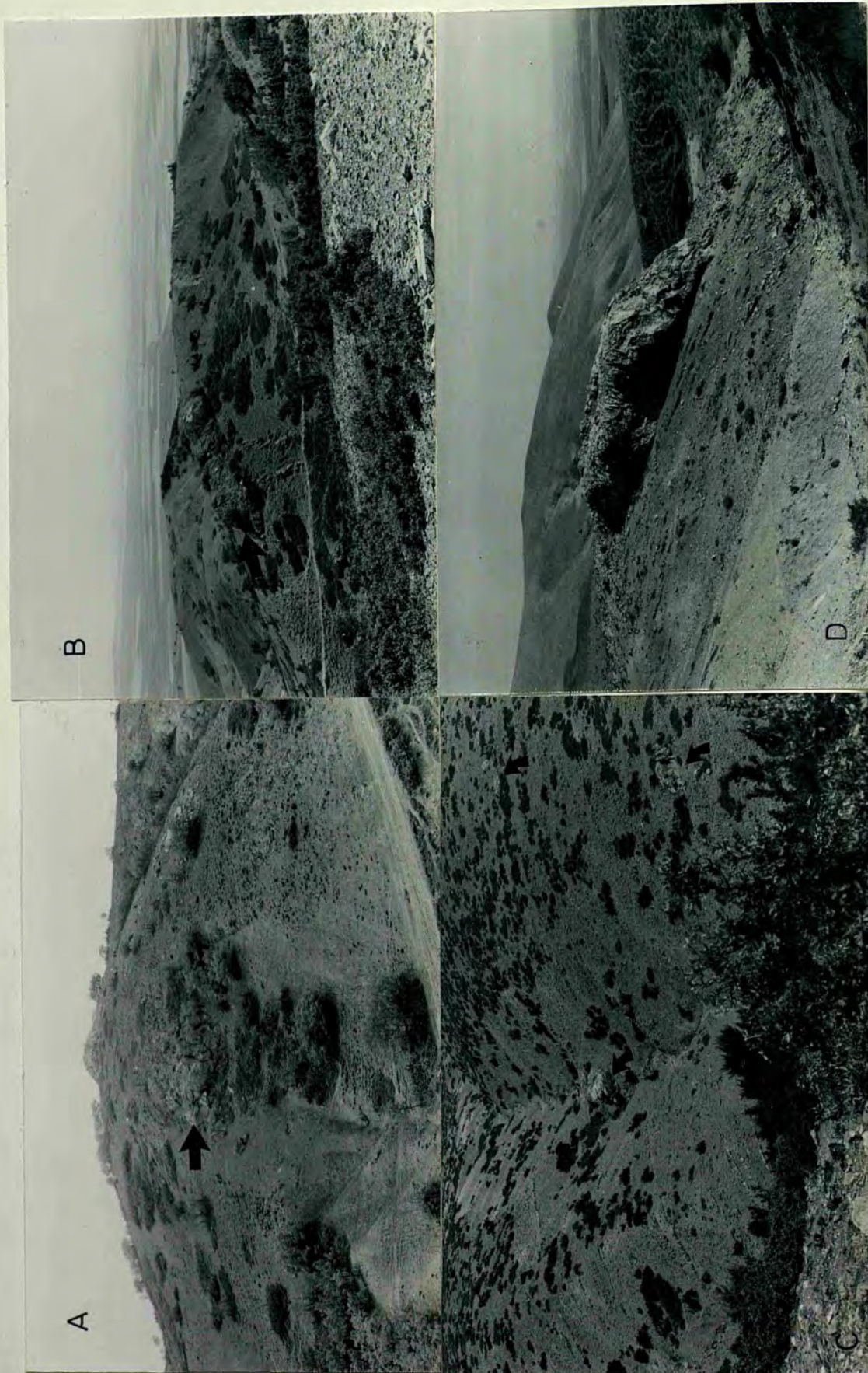
Although these do not form sequences, because of their widespread occurrence it becomes necessary to describe them under a different heading. Limestone olistoliths and blocks (will be referred as limestone olistoliths from hereon) range from 1m. diameter blocks to 135m. wide and 22 m. thick olistoliths. They are similar to the Kocanindambasi formation, in respect of composition, texture, faunal content and age and sometimes can be found as armoured balls. The limestone

olistoliths show various shapes and in large ones initial bedding properties are preserved. They show distributional preference: large olistoliths tend to occur closer to the source than the small ones. All are found in different levels of the stratigraphical column and within different sequences. In the shale dominated sequences they are invariably less than 5 m. in diameter, spheroidal in shape and are concentrated in certain localities. Beds below the olistoliths are deformed (Plate 8.12C). In the slump sequences (Plate 8.11) olistoliths are 1-6 m. in diameter and observed in slump sheets. The biggest in the SE of the area around Ucem (I26), and here they always succeed large slump sequences, the upper part of which is eroded by the olistoliths (Plate 8.12B).

8.2.1.2 Lower slope facies association

This association consists predominantly of shale dominant sequences with some conglomerate layers, small scale slump and pebbly mudstone sequences. The shale dominated sequences occur similar to the sequence a of the upper slope deposits. However here sandstones are thinner, less frequent and both sandstones and shales are finer grained than the corresponding upper slope deposits. The sandstones form Tbce, Tcde or Tb type 1cm-10cm. thick beds with flat bases and tops, laterally extensive and only show a few groove casts and well developed trace fossils (Granularia sp.) Couplet sandstones are absent and beds with Ta division are rare and occur as Tabcde or Tabce type with reduced Ta divisions.

In the lower slope conglomerates and calcirudites form lens shaped, 15cm.-2m. thick beds with lateral extensions of 10m. to over 60m. They are graded or graded/stratified beds and have erosional bases and flat tops (Plate 8.13C & 14). They are sometimes overlaid by massive sandstones and occur as conglomeratic sandstones in which the upper part of the bed is laminated (Plate 8.14). Although their composition is similar to those occurring in the upper slope deposits,



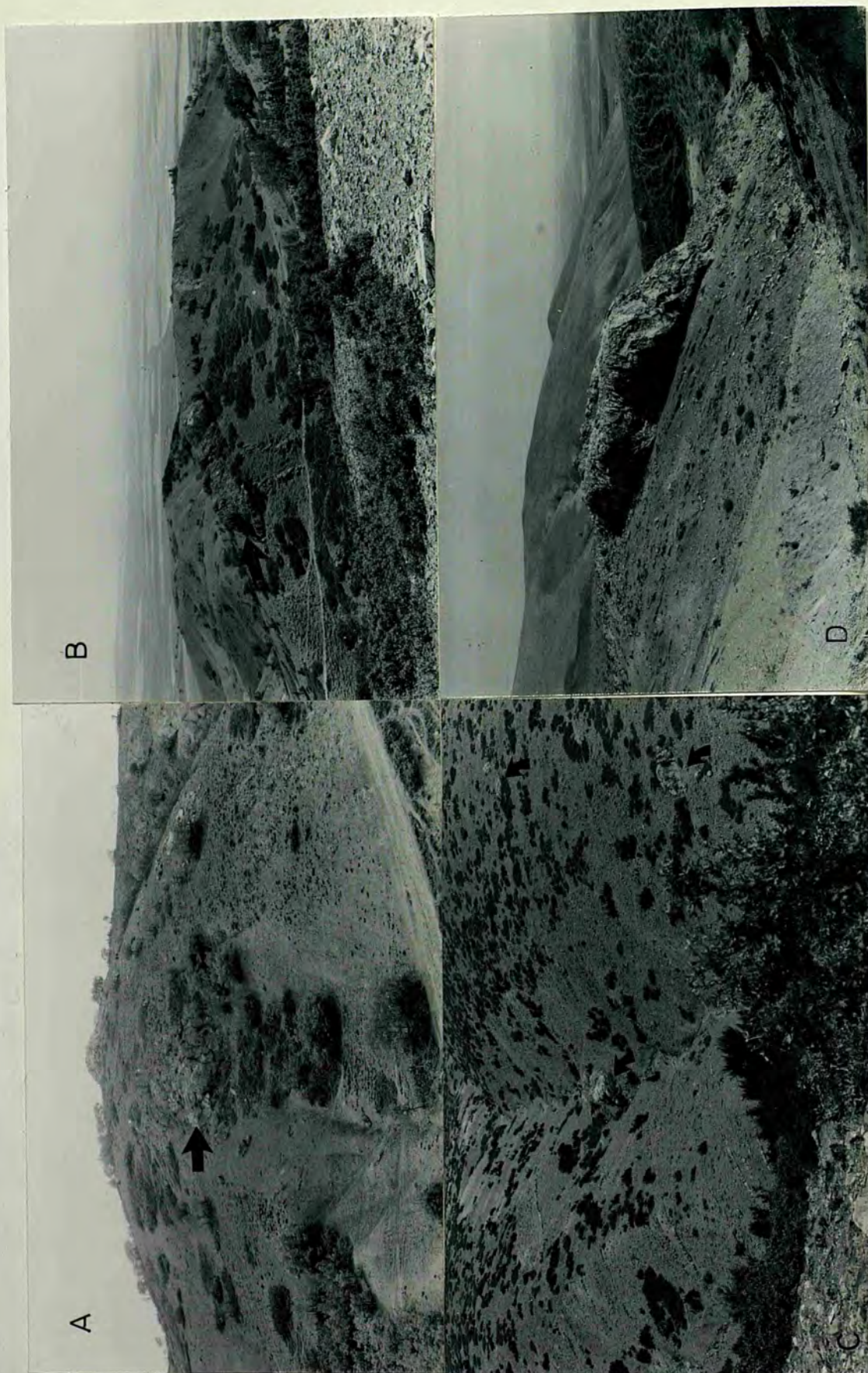


Plate 8.12 - The various occurrences
of limestone olistoliths
(A) within a slump sheet
the olistolith is 6.5 m.
in length. Locality (J26)
(B) the limestone olistoliths
succeeds and erodes the upper part of
a slump sequence.
Locality (H27)
(C) and (D) Olistoliths
within shale dominated
sequences. Note the
curving of beds underneath the olistoliths
particularly apparent
in (D) Localities (J18&G25)

Plate 8.13 - Graded (A) and graded stratified (B) conglomerates in the lower slope. (C) shows a graded conglomerate bed, which is overlaid by a massive sandstone, with erosional base and flat top. Note the parallel and subparallel orientation of the clasts to the bedding plane in (A) and (B). Pencil in (B) is 15 cm. long and hammer in (C) is 30 cm. in length
Localities(H20,G14,M9)





Plate 8.14 - A conglomeratic sandstone bed showing slightly wavy lamination at the upper part which is overlaid by a massive sandstone bed. Notice the load cast at the base and thinning of the conglomeratic zone in the lower part of the bed towards the left of the photograph. Locality (N8)



A



B

Plate 8.15 - Slump sequences in the lower slope. In (A) a 3.5 m. thick slump sequence occur in between relatively undisturbed beds. (Ilimandere (J13)). (b) shows a contorted mudstone sequence. Hammer is 30 cm. in length.

their clast sizes are, relatively, smaller. They show well developed flute casts indicating current directions towards the centre of the basin (see Chap. 12).

The slump sequences are less common and are 40cm.-5m. thick. They usually occur as slump sheets probably due to the involvement of shale dominated sequences. In sequences involving only shales, they occur as a ball-shaped mass contorted beds (Plate 8.15B). Here, in the toe of the slump, beds are parallel to enclosing beds probably indicating that the slump had not moved far.

Pebbly mudstone sequences are quite common in some localities (see Ardıcılipınar section App.XI). They are 30cm-4.5m. thick and consists of scattered volcanic rock, limestone, chert, quartzite and radiolarite gravels in fine grained mudstones. There are no sedimentary structures and the base and top of the sequences appear to be smooth.

8.2.2 Interpretation.

The stratigraphic position of the Kurebogazi member in between the shelf deposits of the Sarıkaya member and Kocanıdambası formation and submarine fan deposits of the Ardıcılipınar and Büyükdere members (see 8.3 and 8.4), together with

- a. the predominantly shaly nature of the sediments with occasional sandstones,
- b. the occurrence of channels incised into these shaly deposits and filled by conglomerate and sandstones,
- c. the presence of abundant slump sequences, limestone olistoliths and other sediment gravity flow deposits and
- d. the occurrence of couplet sandstone beds which are most probably storm deposited (see Chp 10.) (Fig 8.2) suggest that the sediments of this member was deposited on the basin-slope. A further division of slope deposits as upper and lower slope is made on the basis of criteria suggested

by Cook (1979). Thus the upper slope contains thick slump sequences and channels, couplet sandstones and are relatively coarser grained than the lower slope where slump sequences and channels are less common and thinner. (Plate 8.1)

Although turbidity currents were the main depositional mechanism, other sediment gravity processes were also involved in the deposition of these sediments. The common occurrence of the base-cut-out turbiditic sandstones suggest downslope-flow of low density turbidity currents throughout the deposition of these sediments. The alternation of these with sandstones with Ta divisions which require higher density turbidity currents most probably resulted from grain size differences in the source rather than proximity to source or sea level changes. The non-channelled upward fining and thinning sequences were most probably deposited by turbidity currents in a submarine gully. A similar occurrence is reported in the Upper Cretaceous turbidites of San Diego (Nilsen et al 1981). The matrix supported and disorganized conglomerates and pebbly mudstones suggest deposition from debris flows while the graded and graded-stratified examples were deposited from high density and high velocity turbidity currents (Walker 1978). Slump sequences are believed to be formed by sliding or slumping of the semi-consolidated sediments on not necessarily steep slopes (Nardin et al 1979, Rupke 1980). The presence of thick rock fall deposits, however, in the form of large limestone olistoliths, indicates steep slopes at least during the deposition of these rocks, (Nardin et al 1979).

8.3 ARDICLIPINAR MEMBER

8.3.1 Description

This member conformably succeeds the underlying Degirmendere formation with a transitional zone and consists of moderate yellowish brown (10YR 5/4) to pale yellowish brown (10YR 6/2) Polymict conglomerate, medium light grey (N6) to

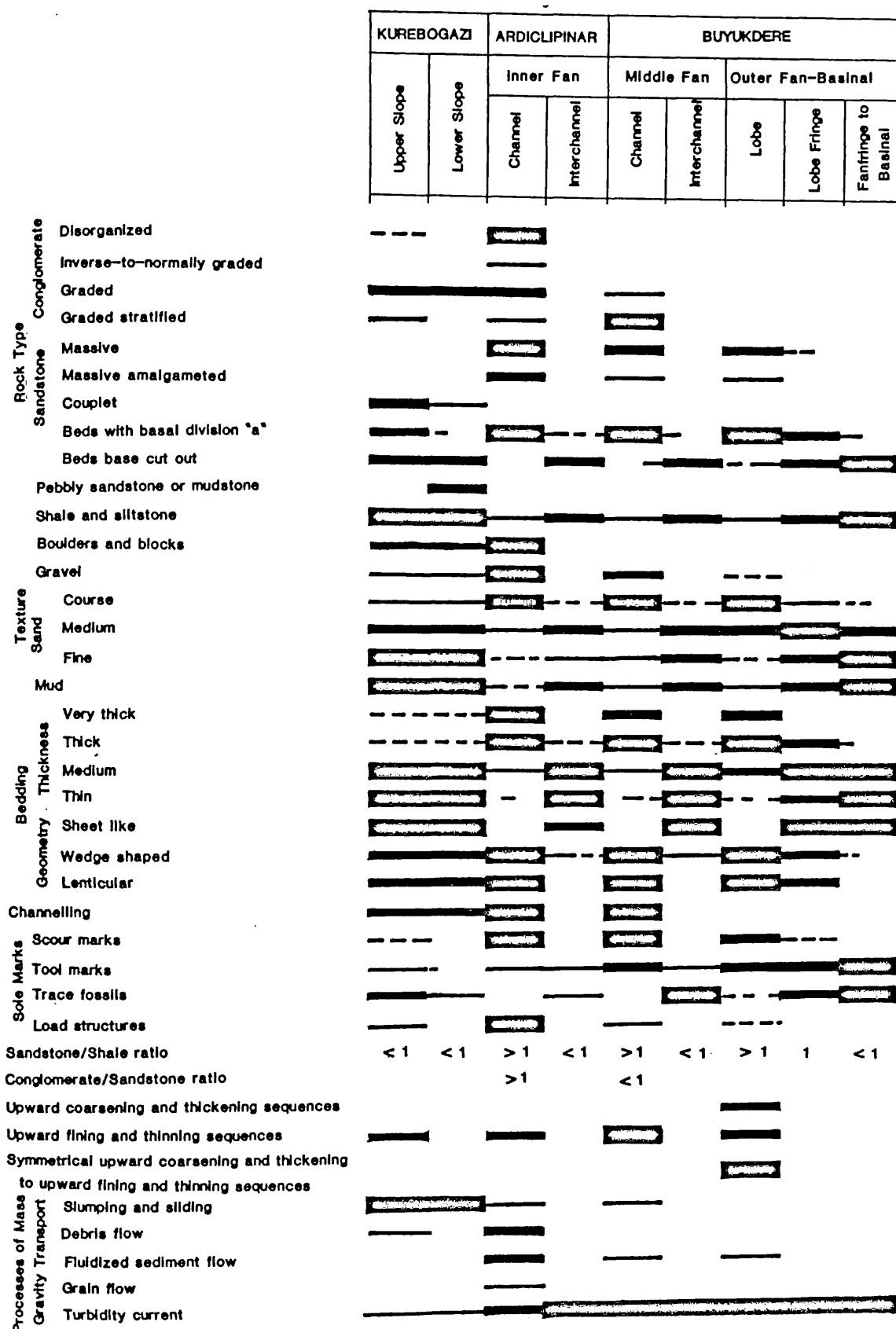


Plate 8.1 - Summary of facies characteristics of the Bayat formation, showing distribution and relative prominence of diagnostic features.

light brownish grey (5YR 6/1) sandstone and calcarenites, dark greenish grey (5G 4/1) to light brownish grey (5YR 6/1) shales and marls with widespread limestone olistoliths within the conglomerates. It is comprised of an inner fan facies association and seen in two different localities; along Savancikol dere (H24) and on the Ardıcılıpinar hill. The most characteristic feature of this member, in both localities, is the sudden occurrence of conglomerate and massive sandstones within multiple channel complexes, cutting the underlying shale and thin bedded fine grained sandstones.

In the Ardıcılıpinar locality, the member is 103 m. thick (Ardıcılıpinar section App. XI) and consists of a number of small and large channel fills (1 m.-32 m. thick), (the lateral extent of which are not determinable due to poor exposure, but not less than 150 m.), levee and interchannel deposits. Channel fill deposits are conglomerates, massive or pebbly sandstones and Tae type sandstones with insignificant amounts of shales and occur as upward fining and thinning sequences or upward fining cycles* with sandstone/shale ratio of 1-100 and conglomerate/sandstone ratio of 0-5. The conglomerates are usually found in the lower part of the sequences and form 50 cm.-7 m. thick lenticular beds with erosional (Plate 8.16) or flat bases (Plate 8.17). They are generally clast supported disorganized or graded conglomerates, are poorly sorted and their clasts, which are subrounded to rounded volcanic, limestone, chert, quartzite, radiolarite and serpentinite clasts in decreasing order of abundance with some intraformational mud and sandstone clasts and large plant fragments, range from up to 6 m. in diameter limestone olistoliths (Plate 8.16) to granules. Sole structures are poorly developed: flute casts indicate a general flow from SW to NE (see App. XI and 12.9&10). The pebbly and massive sandstones are medium to coarse grained, sometimes occurring at the base of the

*Sequences containing two or less beds are considered as upward fining cycles since upward thinning of beds cannot be determined.

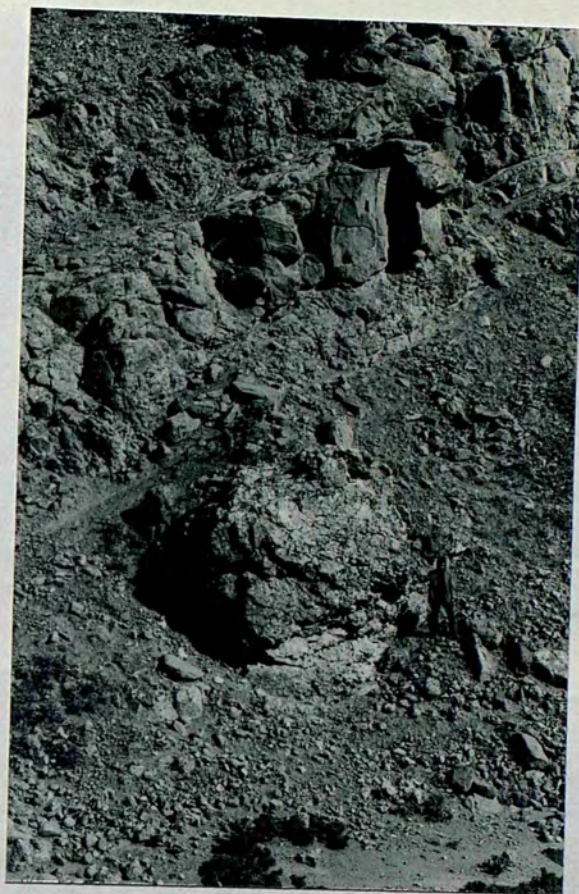


Plate 8.16 - Showing inner fan conglomerates and sandstones around the Ardiclipinar locality. The limestone olistolith in the centre of the photograph is 6 m. in diameter and preserves some of its initial bedding.

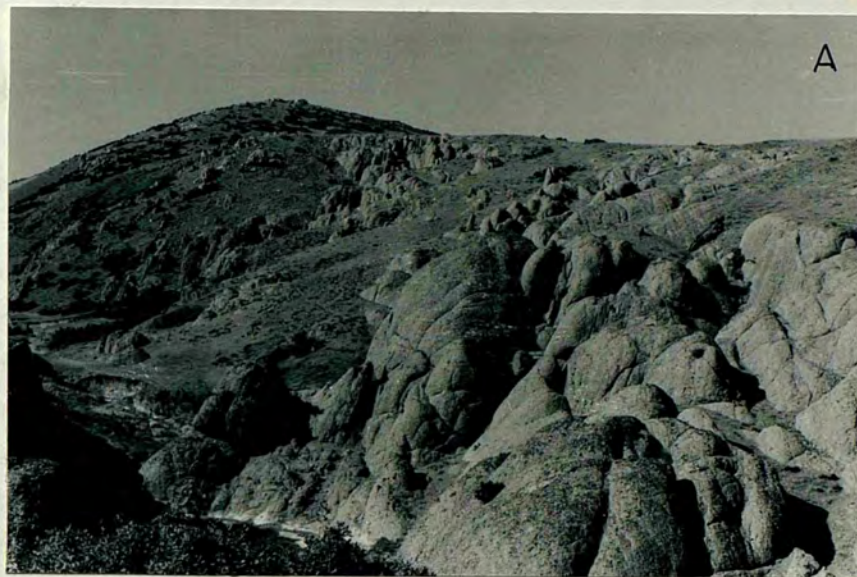


Plate 8.17 - The appearance of inner fan deposits along the Sovancikol (A) shows conglomerates up to 6 m. thick and curving of the beds. (B) Large limestone olistoliths.

sequences but generally succeeding the conglomerates. Their beds are again lenticular, 30 cm.-5m. thick and lack any sedimentary and sole structures apart from some fluid escape pipes, dish structures and load structures. Therefore they usually have flat bases and tops and frequently occur as amalgamated beds. Clasts, in the pebbly sandstones, are mainly chert, volcanic rock and radiolarite and are sub-rounded to rounded. The massive sandstones occasionally contain scattered pebble size mud clasts and plant fragments which are particularly concentrated towards the top of the beds. Turbiditic sandstones are found in the upper part of the sequences, intercalating with 1-15 cm. thick structureless or parallel laminated shales. They are generally Tae type with subordinate amount of Tabe sandstones and coarse to fine grained. They form 10-70 cm. thick lenticular beds with sharp bases and tops and display well developed sole structure as flute cast and groove casts. The current directions obtained from these structures despite being locally variable are, in general, oblique and perpendicular to the basinal axis.

A levee deposit is only observed in the Ardiclipinar section. It occurs as 1.2m. thick sequence at 50.5m. from the base of the section and comprises of 10-15 cm. thickly bedded Tabe, Tbe type medium-fine grained sandstone alternating with 1-10 cm. thick shales, with sandstone/shale ratio of 1 to 5. The sandstone beds have sharp bases and tops and lack directional sole structures. They generally appear to be laterally continuous, (though this cannot be stated with certainty as the beds can only be traced for 30 m.) but some wedge out in as short distance as 12 m.

The interchannel deposits consist of medium and fine grained sandstones intercalating with thick (30-70 cm.) structureless or parallel laminated shales with a sandstone/shale ratio of 0.1. Sandstones form 5-15 cm. thick Tbe, Tbce or less frequently Tabe type beds with sharp bases and tops and sometimes containing abundant plant fragments, parallel to the

bedding planes. The sandstone beds appear to be laterally continuous and some of them show trace fossils of Granularia sp.

The Ardiclipinar member, along the Savancikal valley, (Plate 8.17) is again made up of conglomerates, sandstones and subordinate amounts of shales within a multiple channel complex. The channels are cut into the interchannel deposits are from tens to hundreds of m. wide and 10 to 60 m. deep. Although the internal structures of the conglomerates and sandstones are similar to those occurring in the Ardiclipinar locality, the number of thick conglomerate beds, (and consequently the conglomerate/sandstone ratio), and size of the clasts in them show a significant increase. Also an increase in the size of the limestone olistoliths (up to 20 m. in diameter) is observed. Directional sole structures, which are generally either poorly developed or lacking, are mainly flute casts, (except for some groove casts on the base of the Tae or Taba type sandstones), which indicate a flow from the SW.

8.3.2 Interpretation

On the basis of this member's relationship with the Kurebogazi and Buyukdere members and the occurrence of obvious multiple channels which are filled by rudaceous and coarse-grained, sand size, material passing laterally into interchannel deposits (thin bedded sandstone and shale intercalations), and current directions generally oblique and perpendicular to the basinal axis together with the lack of stratigraphical correlation between adjacent areas, suggests that the sediments of this member was deposited in the inner fan region despite the fact that no obvious fan morphology (i.e. a radiating fan-valley system) is observed. The presence of poorly to extremely poorly sorted, thick disorganized conglomerates containing large blocks and massive and pebbly sandstones and the predominance of Tae and Taba type sandstone beds with very high sandstone/shale and high conglomerate/sandstone ratio in the channels (Fig 8.17), altogether indicate close proximity of these sediments to the source and the abrupt lateral

and vertical distribution of channel and interchannel deposits further support the above conclusion. The sequences with thin, medium-fine grained, predominantly Tbe and Tbce type sandstones intercalated with thick shales, (thus with low sandstone/shale ratios) and showing a close relationship with channel deposits are interpreted as interchannel deposits. The levee deposits differ from the interchannel deposits because of their relatively higher sandstone/shale ratio and their stratigraphic position.

The depth in which these sediments were deposited is estimated on the basis of

- a. the absence of carbonate dissolution suggesting deposition above Carbonate Compensation Depth
- b. the presence of ichnogenera Granularia sp. which is believed to be a facies crossing genera (see 4.9) and interpreted to be in between lower slope and upper bathyal zone.

8.4 BUYUKDERE MEMBER

8.4.1 Description

The Buyukdere member is comprised of middle fan and outer fan facies associations. An attempt to separate these two as different lithological units is not made because of their complex relationship and poor aerial exposure: instead they are collected under a member name but described separately below.

8.4.1.1 Middle fan facies association

This consists of a channel fill and interchannel deposits which forms a distinct and repetitive upward fining and thinning sequence. (Fig 8.3&4)(Plate 8.18)

The middle fan channel fill deposits are made up of coarse to medium grained massive (sometimes amalgamated) and Tae or Tabc sandstones and calcarenites and thin shale and marls with occasional conglomerates or calcirudites and pebbly sand-



Plate 8.18 - Showing two successive upward fining and thinning sequences (indicated by arrows) in the middle fan facies association. Locality (I15)

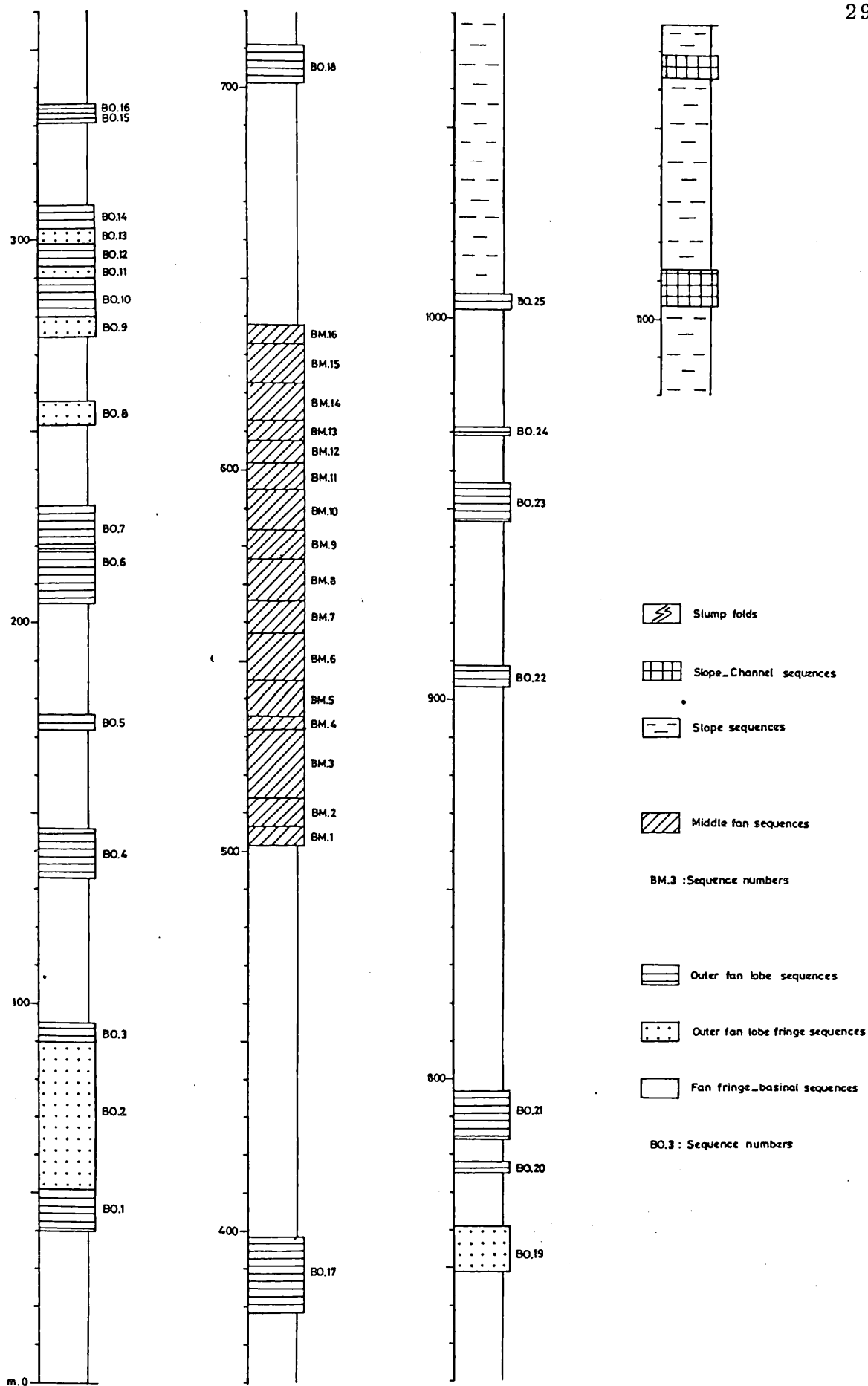


Fig 8.3 - Simplified version of the Buyukdere section
(see App. XII for details)

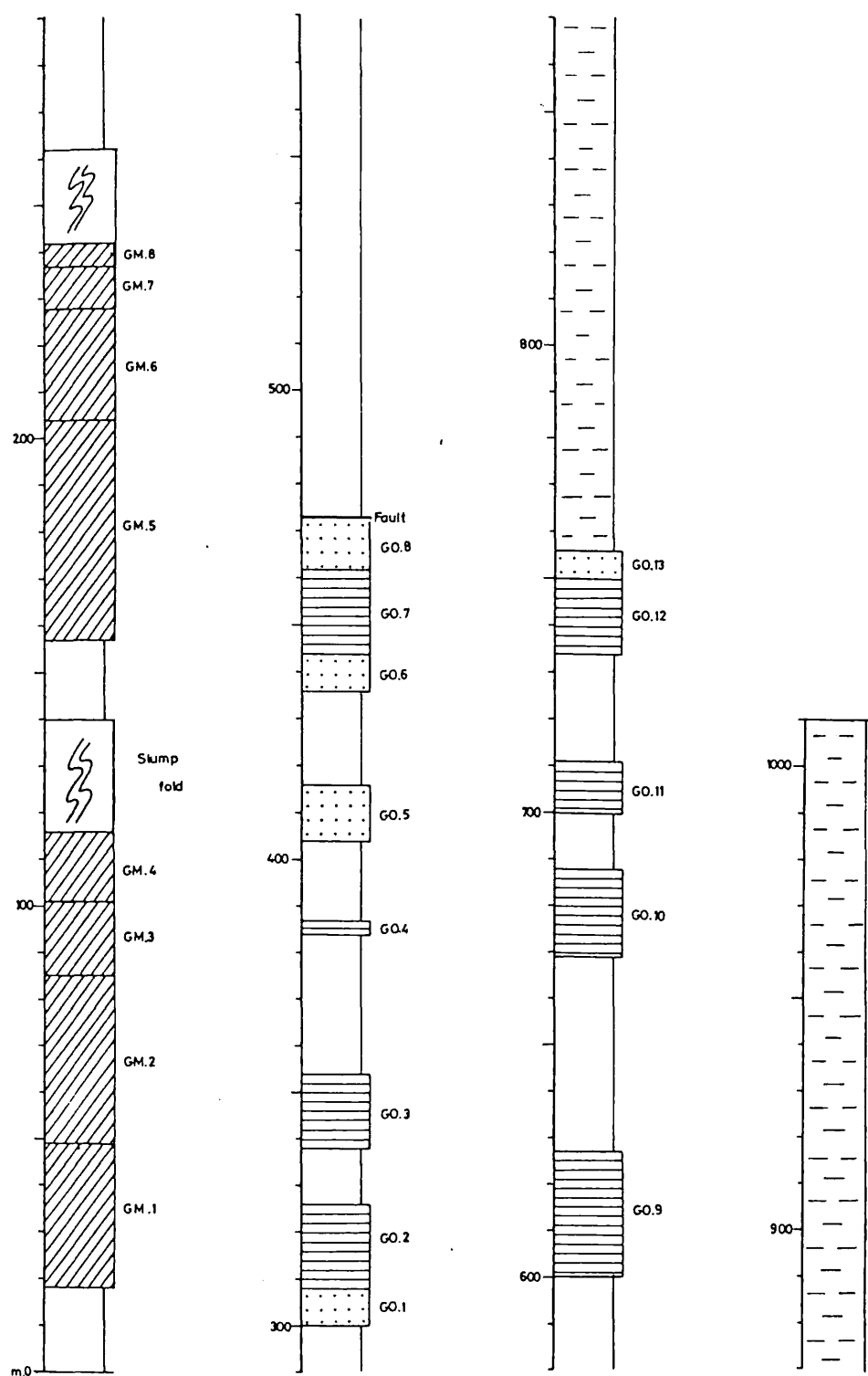


Fig 8.4 - Simplified version of the Geyikardici section.
For explanations see Fig 8.3 and for details
see App. XIII

stones. These lithologies fill broad, flat-based and shallow channels with a varying but always high sandstone/shale ratio. The channels show rapid migration as indicated by the occurrence of interchannel deposits on the upper part of the upward fining and thinning sequences. The interchannel deposits, which always have a less than 1 to 1 sandstone/shale ratio, consists of thin sandstone beds of Tbce or Tbe type and thick shales which are sometimes parallel laminated.

The middle fan sequences are best observed along the Buyukdere and Geyikardıcı valleys from where sections shown in App.XII & XIII are measured

In the Buyukdere section the middle fan sequences occur between 502 m. and 632 m. from the base of the section. In this section 16 upward fining and thinning sequences (BM-1-BM-16 in Fig 8.3), ranging in thickness from 3.2 m. in BM-4 to 18.7 m. in BM-3 are observed (Fig. 8.3 and see App.XII for details). At the base of each sequence a broad shallow channel (depth and lateral extent of channels could not be determined due to poor exposure and translational boundaries between the upper channel-fill deposits and interchannel deposits) filled by 50 cm.-2.4 m. (at BM-15) massive or pebbly sandstones or calcarenites, graded or graded stratified conglomerates and calcirudites (Plate 8.19B) or less frequently Tae and Tabce (Plate 8.19A) sandstones with thin 1-10 cm. or absent shale partings in the lower part and 20 cm. thick Tbe, Tbce, Tbcde or occasional Tabce sandstone and calcarenites alternating with up to 30 cm. thick shale beds in the upper part. Conglomerates and calcirudites have erosional bases and smooth tops and although their clasts are rounded to subrounded except for angular limestones and range from 15 cm. in diameter boulders to granules, they are generally of small gravel-granule sizes. They are compositionally similar to those occurring in the Ardıçlipınar member and sometimes contain plant fragments, intraformational sand and mud clasts as well as partially to well preserved benthonic foraminifers and fragments of shallow

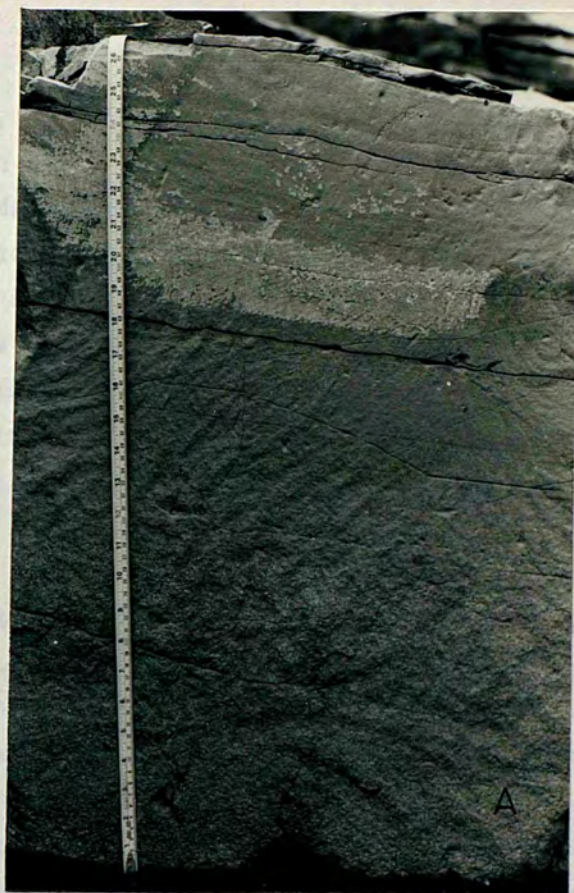
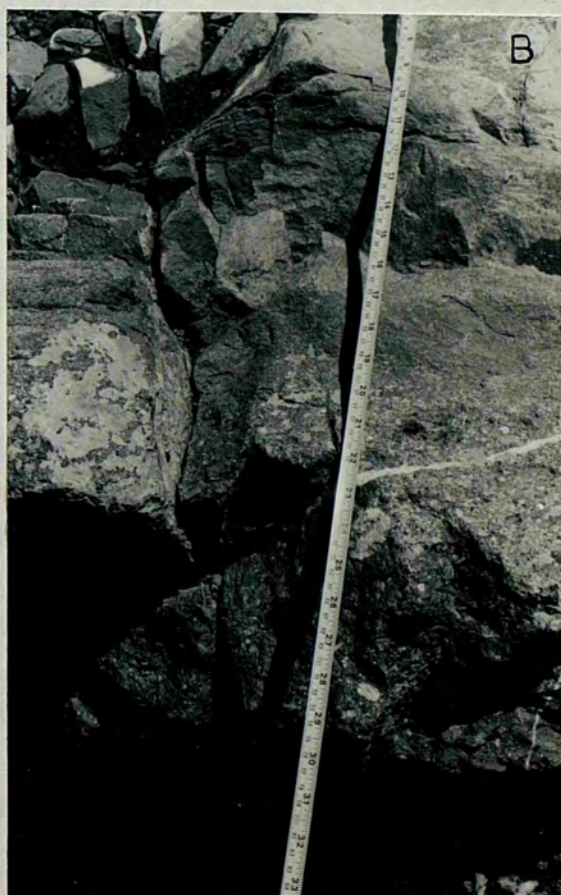


Plate 8.17 - shows Tabce sandstone (A) and graded stratified conglomerate bed at the base of the BM-3 (B).



marine megafauna (molluscs, echionoids, algae) which are comparatively more abundant in these rocks than those occurring in the Ardiclipinar member. Massive and pebbly sandstones are coarse to medium grained and frequently show dish structures and fluid escape pipes and sometimes occur as amalgamated beds. The Tae and Tabe sandstones are coarse to fine grained and on some rare occasions occur as conglomeratic sandstones in which grading from gravel size clasts to fine sand can be observed. (Plate 8.19B) They show well developed flute casts, groove casts and, sometimes, load structures.

The interchannel deposits consist of structureless or parallel laminated shale and Tbce, Tbcde, Tbc and less frequently Tabcde or Tabce, medium to fine grained sandstone and calcarenite interbedded with sandstone/shale ratio of less than 1 to 1. The sandstone and calcarenite beds are 3 cm-30 cm. thick, usually have flat bases and tops and although some wedging out of beds can be observed, they are, in general, laterally extensive. In the Tabcde and Tabce type beds the basal Ta division is reduced (Plate 8.1) the Tc division generally shows well developed convolute or wavy lamination. Sole structures are dominantly groove casts and trace fossils with subordinate amount of flute casts. Trace fossils are believed to be formed by Scolicia sp., Granularia sp. and Taphrhelmintopsis sp.

In the Geyikardici section the middle fan facies association form eight upward fining and thinning sequences, showing similar sedimentary structures and stratigraphical settings to those described in the Buyukdere section (Fig 8.4). However here GM-4 and GM-8 are overlain by 18 m. and 19.5 m. thick slump sequences. They involve interchannel deposits and occur in the form of bench and isoclinal folds indicating slumping from N86°E and S5°W successively. The first fold is preceeded by 20 m. thick interchannel sequence which consists of 30-70 cm. thick shale beds intercalating with 10-25 cm. thick Tabce to

The sandstone and calcarenites, with sandstone/shale ratio of 0.25. The upward fining and thinning sequences are relatively thicker (up to 49 m. in GM-5) and coarser grained than those occurring in the Buyukdere section. Another important difference occurs in composition. In this section the limestone clasts and grains are predominantly of Upper Cretaceous age and radiolarite, quartzite and serpentinite fragments are relatively more abundant than those in the Buyukdere section where Palaeocene limestone clasts and grains are abundant.

8.4.1.2 Outer fan facies association

This is volumetrically more important than the middle fan and is where depositional sandstone lobes, lobe fringe and fan fringe - basinal sequences are recognized.

The lobe sequences, which differ from the middle fan sequences by their broadly lenticular geometry, their isolated occurrence (sometimes flanked by the lobe fringe sequences) in between the fan fringe-basinal sequences and by the absence of channeling, have a high sandstone/shale ratio and display well developed symmetrical upward coarsening and thickening to upward fining and thinning (Plate 8.20); upward coarsening and thickening (Plate 8.21); or upward fining and thinning sequences in decreasing order of abundance. They consist of thick, coarse to fine grained massive beds, which are sometimes amalgamated, Tabe, Tabce, Tabcde and Tbce sandstones and calcarenites with occasional graded and graded stratified thickly bedded conglomerates, interbedded with thin shale beds. On the basis of upward fining or coarsening and thinning/thickening trend, maximum grain size and their basal contact relation, the lobe sequences can be separated into two groups. The first group contains those sequences where only symmetrical upward coarsening and thickening to upward fining and thinning or upward coarsening and thickening can be observed. In these the maximum grain size is generally coarse sand or exceptionally rare gravels and mud clasts and the lower boundary of the sequence with the lobe fringe, or in the absence of lobe fringe with fan



Plate 8.20 - An 8.5 m. thick outer fan lobe. Note the wedging out of the lobe towards the left of the photograph and symmetrical upward coarsening and thickening to upward fining and thinning. Locality (S6)

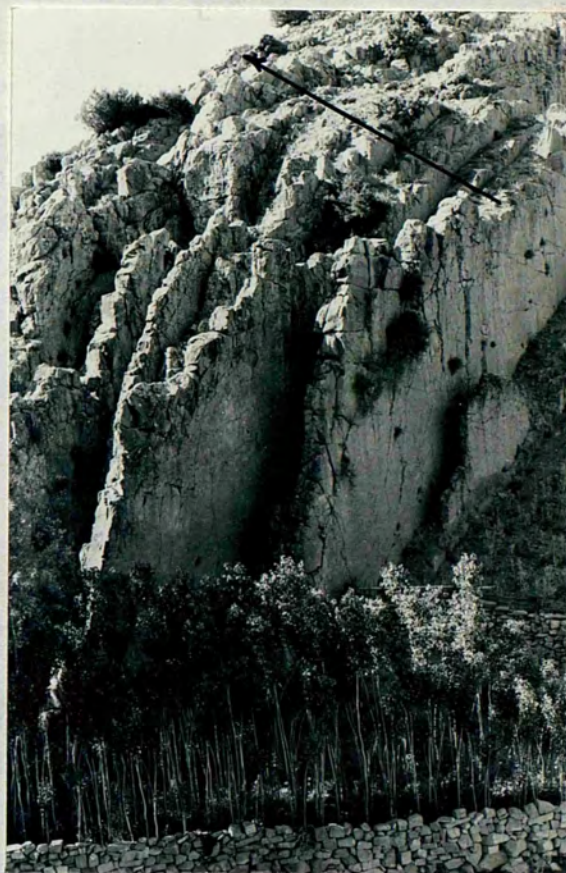


Plate 8.21 - An outer fan lobe showing upward thickening
Locality (R6)

fringe deposits, is gradual. In the second group the sequences show upward fining and thinning, sometimes contain abundant gravels and although no obvious channeling could be observed, they occur abruptly on the fan fringe-basinal deposits with a clear erosional base in the basal bed of the sequence.

The lobe fringe sequences occur either isolated or above and/or below lobe sequences and consist of medium-fine grained, medium-thin bedded Tbce, Tbe Tbcde and occasional Tabce sandstones or calcarenites intercalated with medium to thin bedded structureless or parallel laminated shales or marls with sandstone/shale ratio of around 1 to 1.

The fan fringe-basinal sequences makes up a large proportion of the Buyukdere member and consists of monotonously interbedded sandstones or calcarenites and shales or marls with sandstone/shale ratio of less than 1 (Plate 8.22). The sandstones and calcarenites are medium-fine grained, 1 cm.-20 cm. thickly bedded Tbce, Tbcde Tcde (Plate 8.23) type beds with smooth bases and tops and good lateral continuity. Sole structures in some beds are well developed with groove casts, prod marks and trace fossils. Trace fossils sometimes occur on both sides of the beds, and are generally shallow, freely winding (Taphrhelminthopsis sp.) or straight (Granularia sp., see 4.9 for identification and references) feeding trails of organisms (i.e. the Nereites facies of Seilacher 1967) (Plate 8.24). There are also traces which are believed to be formed by solid fecal strings of Helminthoida sp. (identified and named by comparison with Plate IID of Seilacher 1967) (Plate 8.24C). Differing from these thin bedded and fine grained beds by their thickness, grain size and internal sedimentary structures, occasional and isolated sandstone and calcarenite beds are also observed in the fan fringe-basinal sequences (see Buyukdere section App.XII). These beds are 40 cm.-80 cm. thick, coarse to fine grained sometimes with a few gravels and are of Tabcde to Tbe type. The beds show well developed flute casts and in some



Plate 8.22 - Typical occurrence of fan fringe -
basinal sequences. (Hammer is 30 cm.
in length)..Locality (I15)

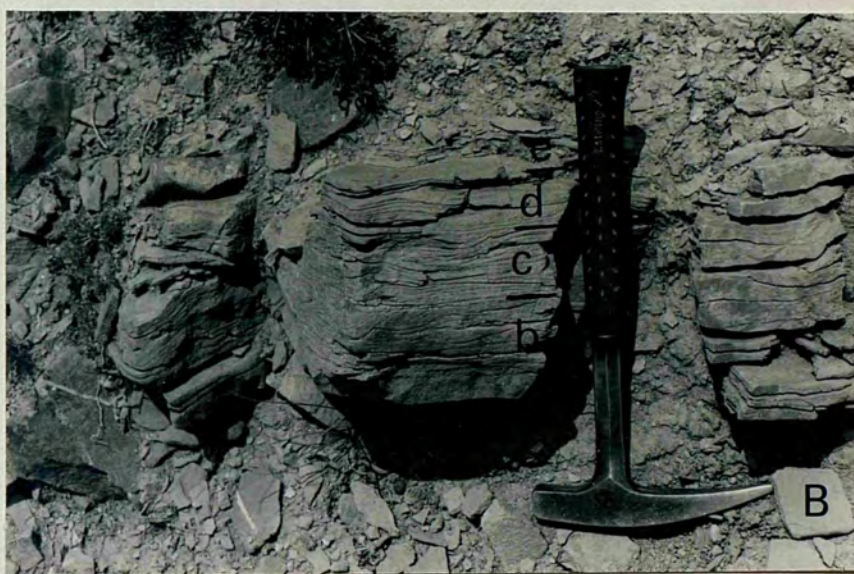
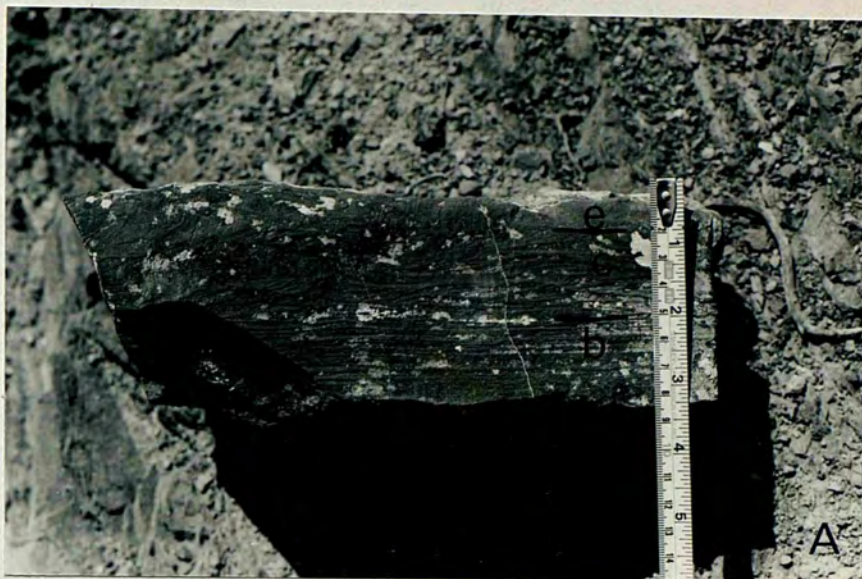
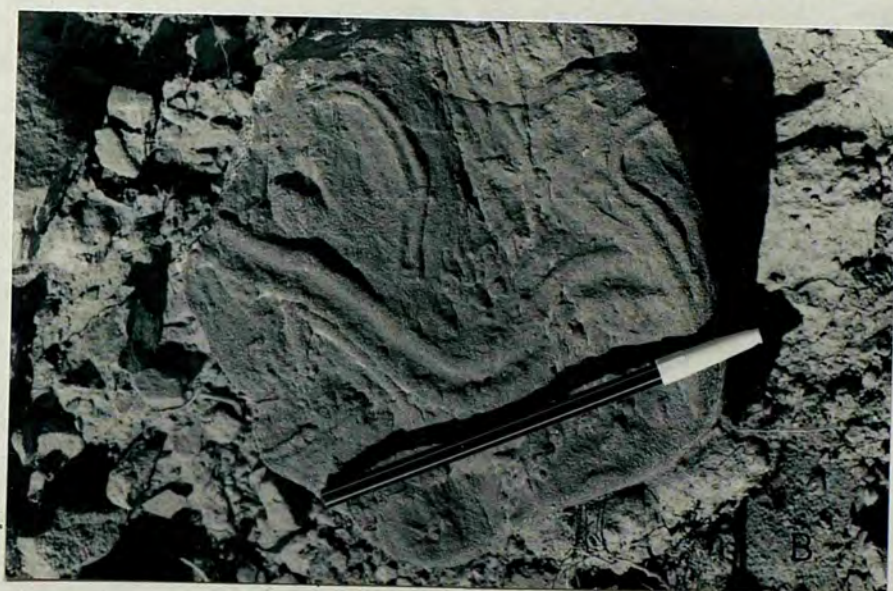
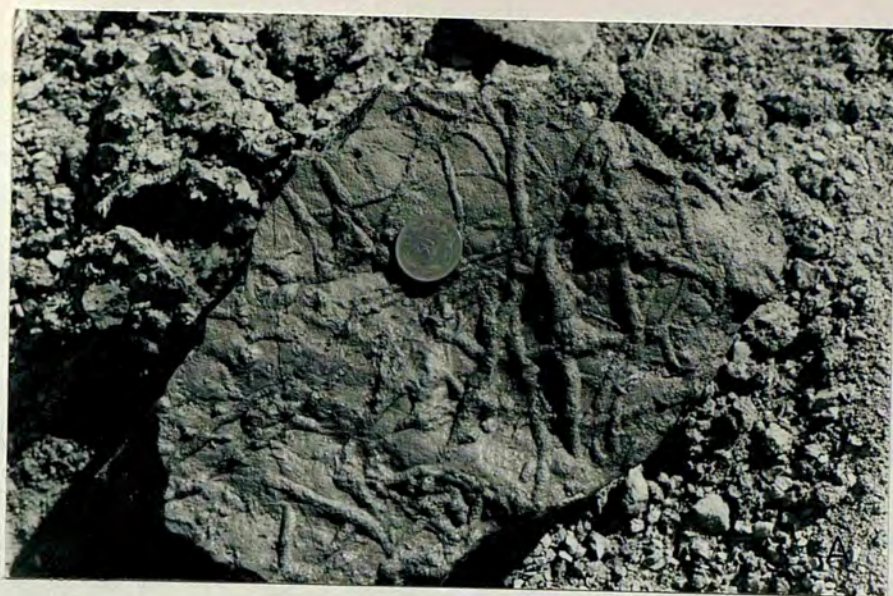


Plate 8.23 - Showing Tbce (A) and Tbcde (B) type sandstone beds. Locality (G15) (Hammer is 30 cm. in length).

Plate 8.24 - Various trace fossils
found in the Buyukdere
member

- a. Granularia sp.
(Coin is 2.5 cm.
in diameter)
- b. Taphrhelminthopsis
sp.
(Pen is 17 cm. in
length).
- c. Fecal strings of
the Helminthoida sp.
(Penknife is 10 cm.
in length).



cases wedging out of these beds is observed.

The outer fan sequences are again best observed in the Buyukdere and Geyikardici sections. In the former 19 lobe and 6 lobe fringe sequences making up 28% of the section are recorded (Fig 8.3). Four of the lobe sequence (BO-16,20,21,24) belong the Group II lobes and range, in thickness, from 2 m. (in BO-16) - 11.5 m. (BO-21) and in sandstone/shale ratio from 2.8 to 9.0. In these lobes bed thicknesses are 50 cm. - 3.2 m. at the base and 10 cm.-40 cm. toward the top of the sequences and apart from BO-24 the remaining three contains gravels at the base. The Group I lobes are 2.8 m. (in BO-15) - 20 m. (in BO-17) thick and bed thickness range from 20 cm. - 2.2 m. (in BO-6). In these lobes sandstone/shale ratio ranges from 2.0 to 8.0. The lobe fringe sequences are 3 m. (in BO-11) to 29 m. (in BO-2) thick and contain beds 1 cm.-20 cm. thick with sandstone/shale ratio of 0.8-1.2. In this section current directions, in general, indicate flows from ENE.

In the Geyikardici section 41% of the outer fan lithologies are made up of 8 lobe and 5 lobe fringe sequences (Fig 8.4). Three of the lobe sequences (GO-4, 11 and 12) are of group II and 2.2 m., 12 m. and 16 m. thick. They all contain conglomerate or conglomeratic sandstone at their bases with sandstone/shale ratio of 4-13, except GO-15 which is unique amongst the Group I sequences for the abundance of conglomerates which are 70 cm-130 cm. thick (graded or graded stratified and contain abundant intraformational sandstone and mudstone clasts) and by the occurrence of fan fringe deposits preceeding this lobe. The Group I lobe sequences range, in thickness, from 16 m. (in GO-3) to 28 m. (in GO-9) and in sandstone/shale ratio from 3 to 8. Except GO-4 and GO-8 in which the basal layer of the sequences contain some granule - small pebble size clasts, they consist of coarse-fine grained sandstones. The lobe fringe and fan fringe basinal sequences of this section are similar to those described in the Buyukdere section. The

current directions in this section are variable and shown in App..XII & XIII

8.4.2 Interpretation

The presence of marine fauna, absence of sedimentary structures suggestive of shallow marine origin and this member's basinward occurrence relative to the Ardıcılıpinar member together with the trace fossils suggest that the sediments of this member were deposited in a deep marine environment (see below for estimate of depth).

The presence of

1. broad shallow channels
 2. repetitive upward fining and thinning sequences
 3. rapid migration of channels
 4. sandstone/shale ratio high in the channel-fill and low in the interchannel deposits
 5. current direction generally perpendicular or oblique to the basinal axis
 6. the transitional boundary between this facies association and outer fan deposits,
- indicate a middle fan environment of deposition for these sediments. The main transportation and depositional mechanism was turbidity currents of varying density except in the massive sandstones in which upward flow of the trapped fluid must have been played significant role as indicated by the presence of fluid escape pipes and dish structures. The occurrence of intraformational mud and sandstone clasts in some beds indicates the erosive power of the depositing current. The obvious differences between the middle fan deposits of the Büyükdere and Geyikardıcı sections in respect to the thickness of sequences, grain size and composition may indicate that either a) the middle fan deposits of the Geyikardıcı section, which have relatively thicker sequences and coarser grain size, were deposited

more proximal to the source or their rate of sediment supply was greater than their counterparts in the Geyikardici section or b) these two originated from two different fan system. The occurrence of slumped interchannel deposits in the Geyikardici section is a further indication of rapid deposition in this area. The occurrence of slump folds in the middle fan deposits are reported from by Nomark (1976) and Nilsen et al (1981).

In these deposits

- a. the absence of channels
 - b. the occurrence of broad lenticular sandstone bodies which show distinct upward coarsening and thickening and symmetrical upward coarsening and thickening to upward fining and thinning and are enclosed by shale and thin bedded fine grained sandstones,
 - c. the gradual transition of these finer grained deposits to sandstone bodies,
 - d. the presence of trace fossils indicating a deeper marine environment than the inner fan and slope deposits (see below)
- suggest that they are deposited in the outer fan environment (Table 8.1) for these criteria are characteristic of the outer fan environment of deposition (Walker & Mutti 1973, Mutti & Ricci Lucchi 1976).

The presence of high sandstone/shale ratio, coarse grained and thick beds together with their lenticular geometry suggest that sandstone bodies were deposited by turbidity currents flowing past the middle fan. However differences in the upward thinning or thickening trend of the Group I and II lobes and the confinement of Group II lobes to the stratigraphically upper levels of the member (see 8.6) may require a special explanation: The upward coarsening and thickening and symmetrical upward coarsening and thickening to upward fining and thinning trends of the Group I lobes can be interpreted as abrupt

abandonment of lobes, probably due to the migration of middle fan channels, lobe progradation and to lobe abandonment. The upward fining and thinning of Group II lobes can be due to

a. a sudden surge of very high density turbidity current causing an overflow in the middle fan channels thus opening a new channel which funnels sediment to the outer fan and deposits those lobes. However this explanation is less likely since there is no evidence in the middle fan deposits for such turbidity currents.

b. or these lobes were formed by sediments funnelled to the basin by channels on the slope. The occurrence of isolated thick coarse grained layers in the fan fringe-basinal deposits which are most probably deposited by the same mechanism but on a smaller scale, appears to support the above conclusion.

The lobe fringe deposits are differentiated from the fan fringe-basinal deposits by their relatively higher sandstone/shale ratio (0.8-1.4), their occurrence above and below the lobes and by the absence of recognizable upward thinning or thickening trends. The isolated lobe fringe deposits are identified due to their similarity to those associated with lobes.

The deposits occurring between lobe and/or lobe fringe deposits are interpreted as fan fringe-basinal deposits on the basis of their low sandstone/shale ratio, abundance of base cut out, laterally extensive fine grained and thin beds.

The presence of carbonate fragments in the rudaceous and arenaceous rocks and marls indicates that the deposition of this member took place above the carbonate compensation depth (3500-5000 m. see 4.9). This together with the trace fossils present (see discussion in 4.9 for their significance as depth indicators) suggests deposition in the bathyal zone for this member.

8.5 Petrography

8.5.1 Definition

The rocks of the Bayat formation show great compositional variety which ranges from a rock that is entirely made up of terrigenous components to one which contains more than 90% allochemical constituents. They are classified by adopting Folk's (1974) classification of sedimentary rocks. Thus conglomerate, sandstones and shales contain 50% or less allochemical constituents while calcirudites, calcarenites and marls have 50% or more allochems. Instead of limestone the names calcirudite, calcarenite and marl are preferred for the purpose of differentiating the Kocanindambasi limestone from these carbonate turbidites.

8.5.2 Limestone olistoliths.

They are found in the Kurebogazi and Ardiclipinar members being especially important in the latter. They are usually angular and show wide variations in size ranging from 4 m. to 100 m. The big blocks generally preserve their initial bedding. The majority of the limestone olistoliths closely resemble the Kocanindambasi limestone's composition, faunal content, texture and a Palaeocene - Early Eocene age while a few of them are Upper Cretaceous carbonate mudstones which contain Globotruncana sp. and some unidentifiable broken shell fragments, and a packstone which consists of fragments of shells, algae and foraminifers within a micrite matrix.

8.5.3 Rudaceous rocks.

Conglomerates of the Bayat formation are compositionally polymictic and found in three types : disorganized, graded and graded stratified. They consist of limestone, volcanic rock and chert boulders and gravels with the interstices being infilled by a sandstone matrix. The disorganized conglomerates show great diversity in grain size so that it is not unusual to find big boulders (75-300 cm. in extreme cases but

usually 30-40 cm. in diameter) mixed with granule size clasts within the same bed while the grain size of the graded and graded-stratified conglomerates is generally confined to gravel size clasts. Thus sorting of the conglomerates ranges from extremely poorly sorted in the disorganized types to poorly sorted in the graded types. Clast shapes varies from oblate to spheroidal and change according to the composition (see below). The conglomerates of the Bayat formation are texturally immature and can be classified as diamictites (Pettijohn 1975)..

Limestone clasts generally occur in larger sizes than other clasts and are angular to subrounded. They show compositional variations according to their grain size, shape and roundness; large boulders and gravels, which are generally angular and oblate, are usually packstone-wackstone-boundstones of Palaeocene to Early Eocene age, in contrast to Upper Cretaceous mudstone and packstones occurring in small pebble to granule sizes which are angular to subrounded. In one case an armoured ball occurrence of the former limestone type was observed.

Volcanic rock clasts are well rounded and spheroidal in shape and they show some of the compositional and textural characteristics of those occurring in the Degirmendere formation (see 5.3.2). However, their abundance and sizes when compared to that formation are significantly reduced. Serpentine clasts are identified by their green colour and are rare. They are usually rounded and occur in pebble or smaller sizes.

Skeletal clasts are molluscs, brachiopods and echionoids in decreasing order of abundance. Also a whole rudist was found and identified as Sabina sp. and a Maastrichtian age is given (M.T.A. pers. com 1980). The skeletal clasts are angular and maximum sizes occur as pebble sizes.

Cherts are found in sizes ranging from cobbles to granules and occur as microcrystalline quartz aggregates.

Quartzite and radiolarite clasts are rare and are generally subrounded.

Matrix is composed of sand, silt and clay grade material and shows a similar composition to the sandstones of the formation. It is poorly sorted.

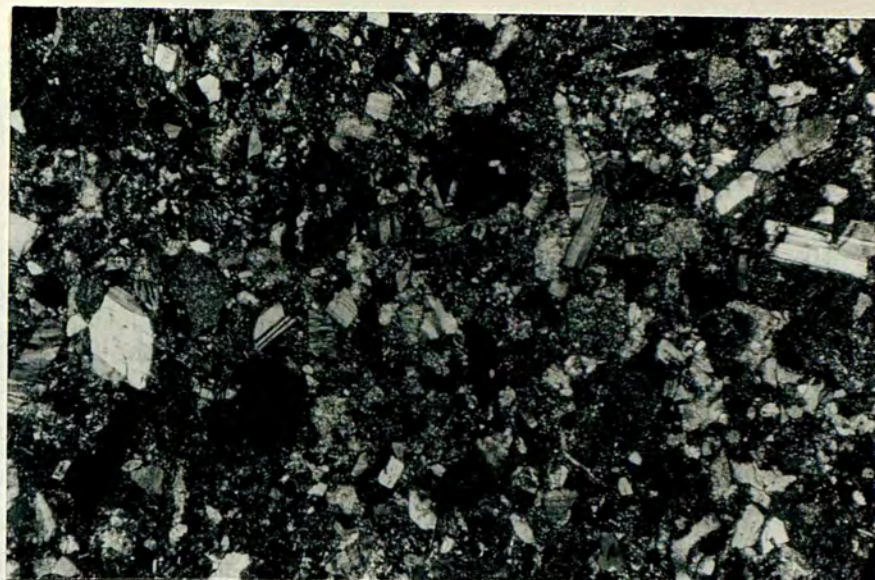
Calcirudites are subordinate to the conglomerates and always occur as graded or graded-stratified beds. The size of clasts in the calcirudites is always confined to small pebble to granule range. Framework grains are similar to those described in the conglomerates except for an increase in the allochemical constituents. Calcirudites are usually well cemented by neomorphic sparry calcite

8.5.4 Arenaceous rocks

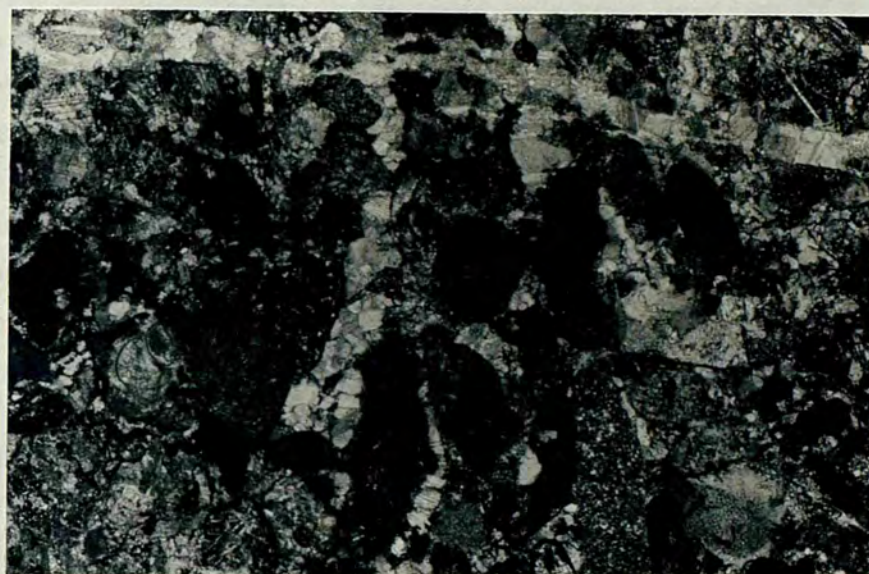
Arenaceous rocks of the Bayat formation occur in four distinct types: pebbly sandstone, massive sandstone, sandstones and calcarenites which can be described by Bouma sequences or as couplets.

Sandstones of the formation are fine to coarse grained and the roundness of grains ranges from very angular to rounded with subangular and subrounded grains being most common. Contact between grains are dominantly long and tangential although some concave-convex and suture contacts occur. Packing proximity ranges from 40% to 70% and the sorting of sandstones increases from poorly sorted in the massive and pebbly sandstones to poor-moderately sorted in the classical turbidites. The sandstones are texturally immature and can be classified as lithicarenite (Plate 8.25).

Quartz, feldspar, sedimentary rock, volcanic rock



A



B

Plate 8.25 - Photomicrographs of sandstones.

A. Volcanic arenite is composed of quartz, feldspar, volcanic and sedimentary rock fragments within a micrite matrix. Sample D-73, 35x, XN.

B. Lithic arenite is composed of volcanic rock, radiolarite, quartzite, limestone and fossil fragments within a micrite matrix. Sample 458, 35x, XN.

and skeletal fragments are the main components of the sandstones and their proportion varies in different samples (see Table 8.2)

Quartz is angular to subrounded and occurs in two types: volcanic quartz which is inclusion free and shows idiomorphic crystal shape with embayments and rounded corner and straight extinction, and common quartz which is generally polycrystalline and has inclusions (mainly vacuoles) and undulose extinction.

Feldspars are andesine, labradorite and K-feldspar and show degrees of alteration. They are angular to subrounded and in some cases are replaced by sparry calcite or microspar. Although it varies in individual samples, K-feldspar/Plagioclase ratio is higher than in the Degirmendere formation.

Sedimentary rock fragments consist of quartzite, radiolarite and limestone particles. Quartzites are generally subangular-subrounded and are formed by tightly locked quartz crystals which show slight to strong undulose extinction. Some of the quartzites contain muscovite crystals and are most probably of metamorphic origin. Radiolarites are usually subrounded. Radiolarias often have lost their initial internal structure and in some cases are replaced by neomorphic sparry calcite. Limestone and skeletal fragments occur as described below. . .

Volcanic rock fragments (VRF) in most cases are unidentifiable due to alteration of mafic minerals. However in some plagioclase crystals of acicular habit with or without clinopyroxene and feldspar phenocrysts, set in a cryptocrystalline groundmass are observed and thus are most probably of andesitic origin. VRF with variolitic and intersertal texture, although less common, are observed and thought to be basaltic. Dacitic rock fragments have a microcrystalline silicate groundmass with some quartz and feldspar phenocrysts. Serpentinites

Parameters Sample No	Quartz	Feldspar	VRF	SRF	Cement	Matrix	Accessory Components	Others	Total %	Total Count
D-14	8.8	1.4	21.2	33.4	1.4	30.6	3.2	-	100.0	500
D-39	7.4	5.6	16.6	33.0	8.4	26.4	2.6	-	100.0	500
D-49	16.6	3.8	8.0	30.2	4.2	83.0	5.2	-	100.0	500
D-73	24.0	10.8	20.8	6.2	14.6	8.2	2.2	13.2a	100.0	500
DD-44	1.4	0.2	21.2	43.0	8.4	23.6	2.2	-	100.0	500
GA-4	3.0	1.2	17.5	59.7	6.3	11.9	0.4	-	100.0	504
GA-19	33.4	6.8	29.2	6.8	8.6	14.6	0.6	-	100.0	500
II-11	7.8	7.2	40.6	9.6	5.0	27.6	2.2	-	100.0	500
II-19	4.0	5.6	44.6	16.6	6.4	20.6	2.2	-	100.0	500
III-15	6.8	6.8	34.6	6.4	5.6	36.6	3.2	-	100.0	500
45	19.6	8.4	32.0	7.2	9.2	21.0	2.8	-	100.0	500
51	12.8	3.0	51.2	-	4.3	27.3	1.4	-	100.0	500
147	14.2	4.2	38.4	15.6	2.8	24.0	0.8	-	100.0	500
424	3.0	2.2	16.2	50.8	6.0	20.2	1.6	-	100.0	500
442	1.6	3.2	12.6	46.8	7.2	25.2	3.4	-	100.0	500
458	1.2	1.4	22.2	39.8	12.2	17.2	6.0	-	100.0	500
490	2.8	14.2	20.8	20.4	16.4	22.6	1.0	-	100.0	500
617	13.6	6.6	31.6	15.4	11.2	17.2	4.4	-	100.0	500
645	8.2	5.6	19.0	31.8	13.4	19.0	2.8	-	100.0	500
660	3.7	4.1	31.2	19.9	0.8	39.6	0.6	-	99.9	509
918	2.6	3.0	17.4	36.6	16.2	20.6	3.6	-	100.0	500

Table 8.2 - Modal composition of the Bayat formation's arenaceous rocks

a: cholorite, Chert fragments are included to Volcanic Rock Fragments (VRF).

are rarely observed and are generally rounded.

Plant fragments and biotite, which are relatively more common in the fine grained sandstones, together with chalcedony, hematite and chlorite occur as accessory components.

The matrix is fine grained and consists of micrite, clay minerals, quartz, feldspar, chlorite and hematite. It is poorly-moderately sorted and is frequently replaced by neomorphic microspar and/or sparry calcite. Apart from rare fibrous or bladed calcite cement there is very little first phase cement present in the sandstones of this formation. Most of the sparry calcites, which in some cases corrode the detrital grains as indicated by an irregular and embayed contact between calcite crystals and grains, are most probably the result of aggrading neomorphism.

Calcarenites are fine to coarse grained, poor to moderately sorted and texturally immature. Their grain contact types are generally long and tangential and packing proximity ranges from 30-70% (Plate 8.26).

Framework grains mainly consist of whole and broken fragments of skeletal organisms and limestone fragments with terrigenous material (quartz, feldspar, chert, radiolarite and VRF) the proportion of which varies from 10%-50%.

Skeletal grains are fragments of coralline algae molluscs, brachiopods, bryozoans and echinoids with broken or whole tests of foraminifers. Coralline algae are usually broken, knobbly and rod-like in shape and their original cell microstructure is well preserved. Their sizes are extremely variable, ranging from a few microns to up to 2 cm. and they are usually subangular. Fragments of molluscs, brachiopods, bryozoans and echinoids are found in various shapes and degree of

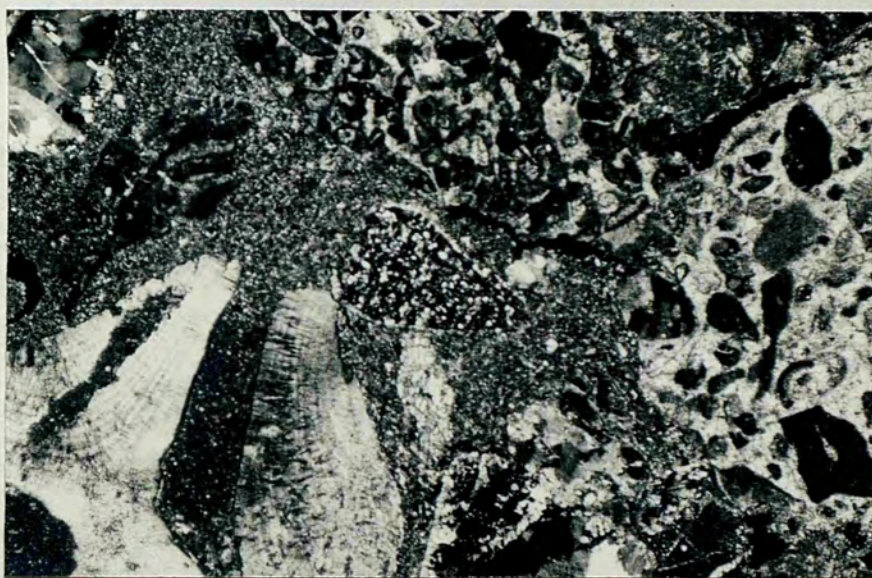


Plate 8.26 - Photomicrograph of calcirudite.

It consists mainly of limestone skeletal,
volcanic rock fragment and micrite matrix.
Sample D.39, 15x, XN.

rounding. Their size ranges from 0.2 mm. to 2 cm. Echinoid fragments show limited overgrowths. Gastropod shells have lost their initial structure through solution of the original aragonite and subsequent precipitation of a cavity filling mosaic of sparry calcite.

Foraminifers are textularids (agglutinating type), miliolids, rotalids, Discocyclines, globigerinids and Globotolias and occur either as a whole or broken tests. Sizes vary from 0.1 mm. to 1 cm. and when broken they are angular to sub-angular. Their chambers are filled either with micrite or neomorphic or first phase calcite cement which are generally similar to the matrix surrounding the tests.

Limestone fragments occur in two types: those which show compositional, textural and faunal similarities to the Kocanindambasi formation are packstones, wackestone and boundstones; other types of limestone fragments are micrite, packstones or recrystallized limestones and are Upper Cretaceous or older in age.

Plant fragments, hematite, chlorite and mica flakes occur as accessory components.

The matrix is fine grained, usually moderate to poorly sorted and made up of micrite, microspar and occasional fine grained quartz and feldspar grains. It is frequently replaced by neomorphic microspar and/or sparry calcite. First-phase sparry calcite cement is very limited in occurrence.

8.5.5 Argillaceous rocks

These fine grained rocks occur either as shales or marls and consist of silt to clay grade material with a few scattered sand grains. They are poorly to moderately sorted and composed of clay mineral, micrite, plant fragments, very fine grained skeletal fragments, biotite flakes and planktonic

foraminifers. Sand size grains are quartz, feldspar, biotite flakes and skeletal fragments. Chlorite, mica and kaolinite are the most common clay minerals observed. Some marl layers which differ from others by their lighter colour (greyish white), relatively finer grain size, absence of sedimentary structures and sand size grains and abundance of planktonic foraminifers, may be interpreted as hemipelagic layers.

8.5.6 Source area of the Bayat formation.

The decrease in the relative abundance of volcanic rock clasts and fragments together with the presence of limestone, serpentinite, quartzite and radiolarite clasts and fragments in the rocks of the formation suggest that the volcanic terrain which was intensely eroded and had supplied sediments to the Degirmender formation, lost its importance and the exposure of the Ankara Melange rocks which were beneath the volcanic rocks became important. The relatively higher K-feldspar/plagioclase ratio of this formation compared to the Degirmendere can be explained;

- a. either by a relatively longer duration of transport, since K-feldspars are more stable than plagioclases, thus probably suggesting a remoter source for the feldspars of this formation than for the Degirmendere
- or b. the source area was particularly rich in K-feldspars.

Basinal sources have provided the skeletal grains and limestone olistoliths.

8.6 Thickness, distribution and field relations of the Bayat Formation.

The formation outcrops extensively in the area studied, lying parallel to the general NE-SW trend. The members of it show complex interfingering with each other and varying stratigraphical relationships with the other formations of the

Bala basin. Therefore the thickness, distribution and field relations of them are described separately below for different parts of the area studied.

In the area between Kurebogazi (U8) and Keklice (M16) the Kurebogazi member is observed, overlying the Sehriban member of the Ucem formation with a gradual boundary. The members upper boundary could not be seen because of the overthrusting of the Degirmendere formation. Therefore the accurate thickness of the member could not be measured. However in the Kurebogazi section it is 141 m. and in the Sarlalikdere section 171 m. thick. Here the member consists mainly of shale dominated sequences with a number of channel-fill conglomerate and conglomerate-sandstone sequences, a largest one of which is observed in the NW of Kurebogazi. (see p. 267) Slump sequences are especially predominant in the SW of this area. Limestone olistoliths which are up to 40 m. in maximum dimension, are only observed in the area between Sarikaya (Q14) and Keklice.

The Ardiclipinar and Kurebogazi members are exposed in the areas between Camli T. (T6) and E of Canavaryurdunun T. (Q10), Karabucakdere (R6) and Aliclicukur T (14) and along the Savanakaldere valley, overlying the Degirmendere formation with a conformable boundary. In these areas Kurebogazi member interfingers and overlies the Ardiclipinar member which, is 103 m. thick at Ardiclipinar locality. The upper boundaries of the former, which contain widespread slump sequences and limestone olistoliths and show great thickness changes along the strike (see Map I and Cross sections), could not be observed due to faulting.

In the areas between Karaustu T (R6) and Geyikdere (G17) and Samanyolu (K17) and NW of Andizli T (F27) the Buyukdere and Kurebogazi members are exposed. In the first area the members have a 15 km. along outcrop lying parallel to the

NE-SW trend and is cut by N-S striking K Bayat strike-slip fault. Here the Buyukdere member conformably overlies the Degirmendere formation and interfingers with and is overlaid by the Kurebogazi member. The latter shows thickness changes from approximately 1000 m. in the Salideresi valley (see App X) to 180 m. in the Buyukdere section (Fig 8.3) and 245 m. in the Geyikardici section (Fig 8.4) and is predominated by slump sequences in the NE while in the SW it consists of shaly sequences with conglomerate and conglomerate-sandstone sequences. The Buyukdere members accurate thickness could not be measured because of faulting which also prevents the observation of the members relationship with the Davdanli formation. However it is 1005 m. thick in the Buyukdere section (Fig 8.3) and 755 m. thick in the Geyikardici section. In the second area the Buyukdere member conformably overlies the Degirmendere formation and is overlaid by the Kurebogazi member.

The Kurebogazi member also outcrops in the area between Ucem (I26) and Inkayaderesi (I25) showing a wedge shaped geometry as it thins from SW to NE. Although the members lower boundary around Ucem could not be observed due to a reverse fault, along the Inkayaderesi a conformable upper and lower boundary with the Sehiban member of the Ucem formation is seen.

8.7 Fossils and age of the Bayat Formation.

Shales of the formation contain abundant planktonic foraminifers which are identified by C.G. Adams and S. Tekler (pers. comn.) as being

Globorotalia sp.

Globoconusa sp.

Subbatina sp.

and a Palaeocene-Eocene age is given. Additionally in the sandstones and calcarenites of the formation abundant shallow

marine benthonic foraminifers, such as; Miliolids, Textularia, Rotaliids, Discocyline, and Assilina of Palaeocene-Middle Eocene, are found. (G.G. Adams and S. Tekler pers. comm.) Although benthonic foraminifers are usually not age diagnostic in turbidites, on the basis of their freshness and their association with the planktonic foraminifers of same age, indicates that they can be considered as in situ fauna.

This fossil assemblage and the formations relation with the Kocanindambasi, Degirmendere and Kizildag formation suggest a Middle Palaeocene-Middle Eocene age for the Bayat formation.

C H A P T E R 9

KIZILDAG FORMATION

9.1 General Introduction

The Kizildag formation of Middle Eocene age is exposed resting unconformably on the older sediments around the entire area studied except in the NE. It consists of red to reddish brown conglomerates, sandstones and mudstone with evaporites. Because of the marked special variation of this formation no type section is given. However the Kizildag section on the eastern flank of Kizildag hill (D28) is believed to be a representative of this formation.

In this section (Fig 9.1) the formation is 63 m. thick starting with a 12 m. sandstone and mudstone dominated sequence which also includes two 60 cm. and a 1.5 m. thick sandstone lenses each with a few gravel size particles at their base. The poorly exposed sandstones are 1-15 cm. thick and parallel laminated. The following 17 m. is composed of cyclic upward fining conglomerate and sandstone lenses separated by mudstone and parallel laminated sandstone intervals. The lenses are 1.2 m. thick and 4-7 m. wide and show erosional bases and sometimes large scale channel-fill cross bedding at the base. The sandstones above the conglomerates are either parallel laminated or show small scale cross bedding. The next 28 m. is dominated by fine grained sandstones and mudstones with a single 70 cm. thick conglomerate lens. Some crudely developed parallel laminations are observed in the sandstones. The uppermost 6 m. of the section is a transitional zone between this formation and the Keklikpinari formation and is made up of interbedded fine grained, sometimes graded greenish-grey sandstones, mudstones and red very thinly laminated (0.5 cm. to 2 mm) mudstones.

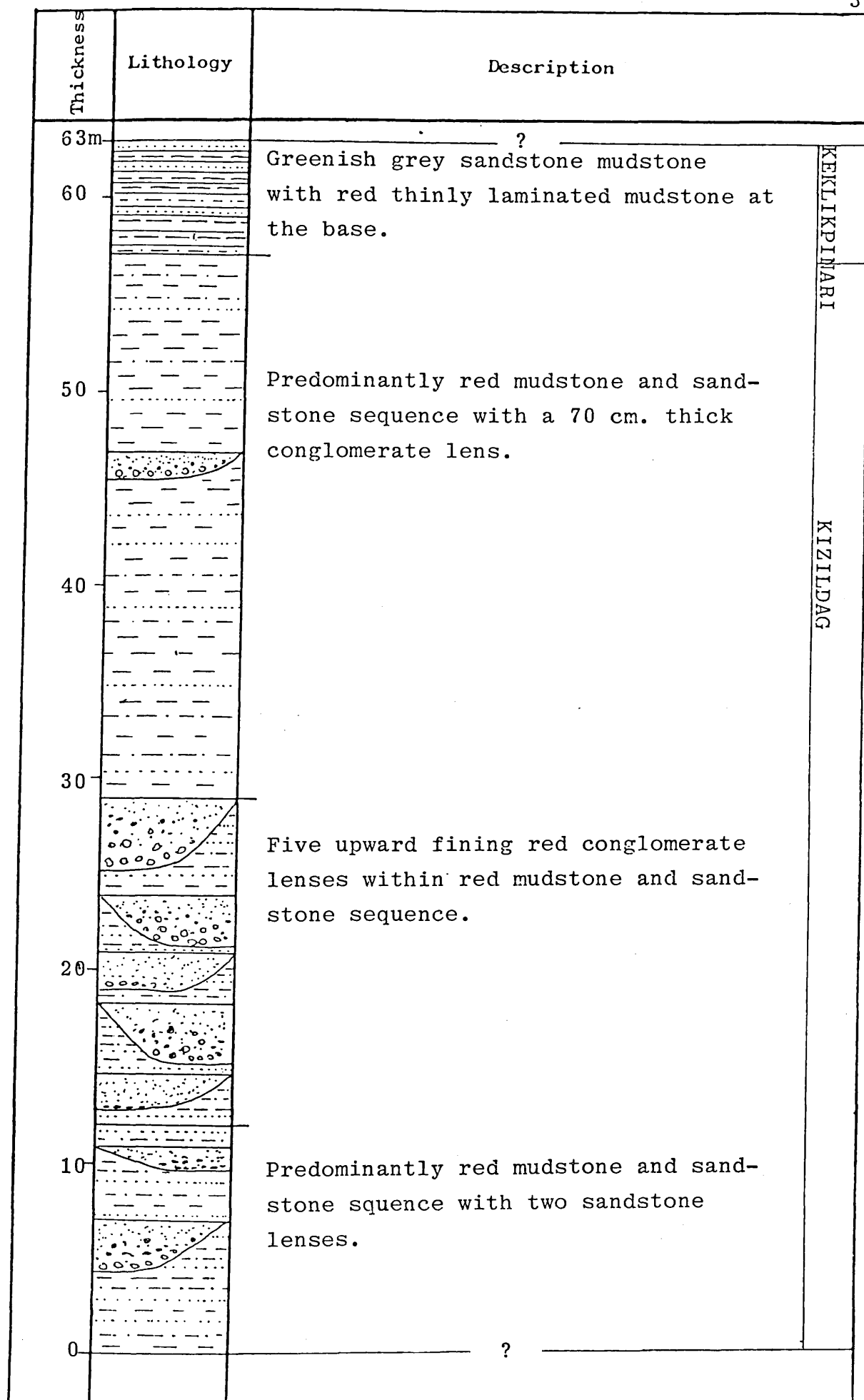


Fig 9.1 - Kizildag section.

9.2 Distribution, thickness and field relations:

The Kizildag formation is exposed in three principal areas and it overlies different formations with an angular unconformity. It shows differing thicknesses and stratigraphical relationships with the overlying Keklikpinari formation (see Fig 9.2 and 9.3).

In the southeastern margin of the Bala basin, the Kizildag formation is poorly developed and rather thin except E of Kurebogazi (V8), where it is thicker and mainly conglomeratic in nature (Fig 9.2A). This contrasts with its generally sandy and muddy occurrence in the SW along the strike. It overlies the Ucem formation with an angular disconformity and interfingers with and passes into the Keklikpinari formation at its upper boundary (see Plate 6.1 and 6.2). Here the latter consists of micritic limestone at the base gradually passing up to laminated and/or massive mudstone and fine grained sandstones with rare fossiliferous 50 cm-1 m. thick conglomerates and lens shaped, 2-7 m. thick, evaporites towards the top of the formation (Fig 9.2B).

In the S, W and NW of the area studied the outcrop of the formation trends approximately N-S direction curving towards the NE around Cataltepe (E29) and overlies the Bayat formation with an angular disconformity (Plate 9.1). In the southern-most part of the area studied, around Cataltepe, the Kizildag formation is predominantly composed of 15-20 cm. thickly bedded, parallel laminated sandstones and mudstones, sometimes interbedded with 50 cm. thick fine grained conglomerates and occasional lens-shaped up to 3 m. thickly bedded conglomerates. The Keklikpinari formation conformably succeeds this formation and is made up of yellowish brown fossiliferous sandstone at the base, grading into mudstone and a fine grained sandstone succession which contains bedded evaporite lenses towards the top. These are overlain by alternations of mudstone and Tabe and Tae-type turbidite sandstone beds

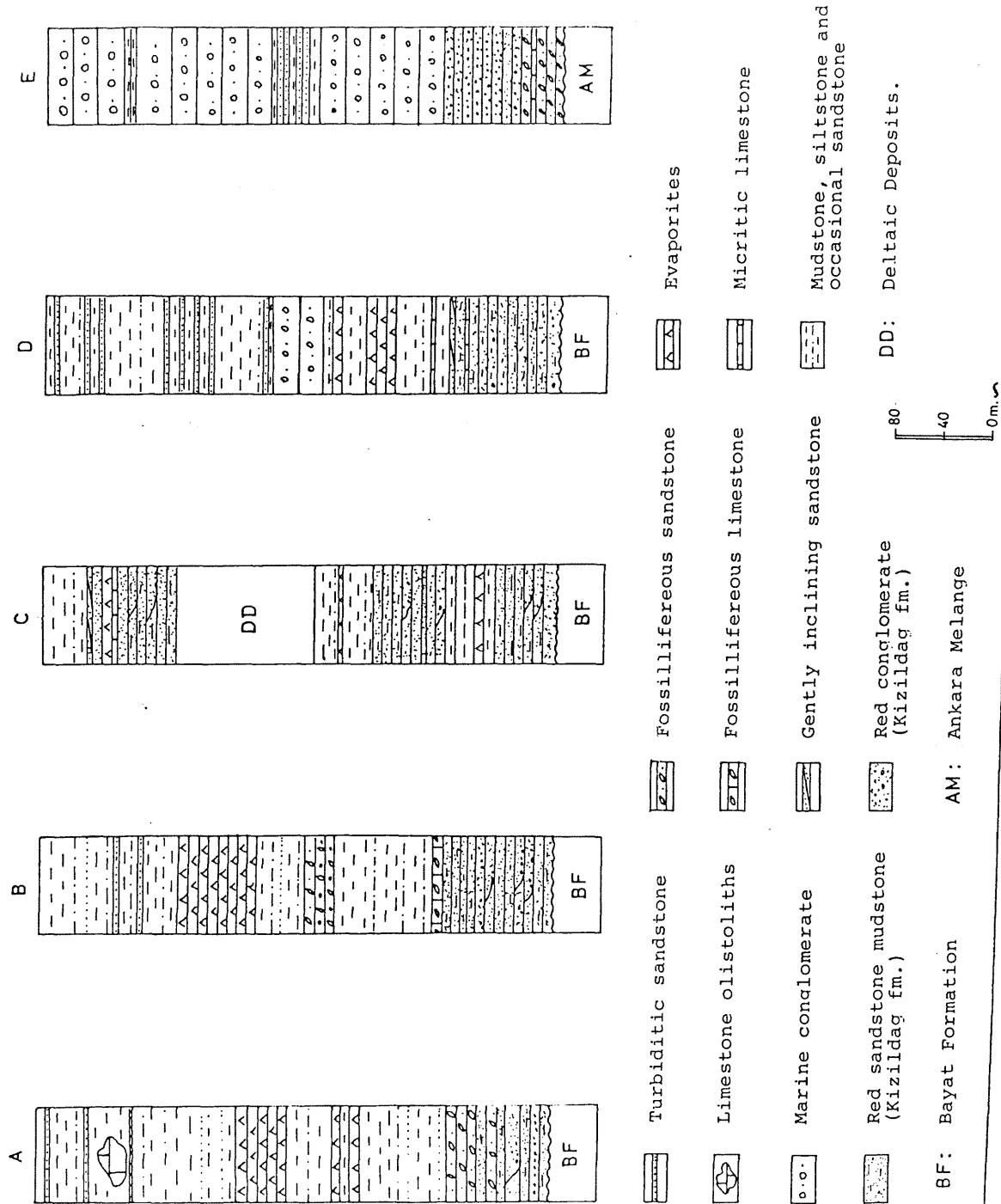


Fig 9.3 - Correlation of the stratigraphic columns of the Kizildag and Keklikpinari formations in the S, W and NNE of the area studied.



KIZILDAG Fm.

KÜREBOGAZI Mem.

Plate 9.1 - Shows the angular disconformity between the Kizildag and Bayat formations.
Note a submarine slump fold in the Kurebogazi member of the Bayat formation.

which sometimes contain up to 2 m. diameter Palaeocene or Early Eocene limestone blocks. This stratigraphical setting changes westwards, between Kizildag (D28) and Ikiz tepe (A30), where the Kizildag formation occurs as described in the Kizildag section and is overlain by a 3.5m thick limestone lens which contains abundant large benthonic foraminifers. This, in turn, is overlain by a shaly sequence which in its upper part passes into yellowish brown fossiliferous conglomerates and sandstones. They underlie a sequence which is predominantly shaly with occasional fine grained, 5-15 cm. thick parallel laminated sandstone beds and which gradually passes up to 50-70 cm. thick parallel laminated bedded evaporites. This deposit sometimes contains lens shaped red patches. The evaporite beds are interbedded with silt to clay size dark grey mudstones and have gradational boundary with these lithologies.

In the area between Aydoğan (E21) and Göktepe (B20), the Kizildag formation is dominated by lens-shape matrix supported conglomerates in the lower part and sandstone and mudstones intertonguing with the Keklikpinari formation N of Aydoğan along strike (Plate 9.2) before grading into the latter with a laminated evaporite and mudstone passage zone. This is overlain by laminated to structureless mudstones and fine grained 1 to 25 cm. thick, generally parallel laminated, sandstone intercalations. This sequence underlies 173 m. thick deltaic deposits which passes upwards into the red beds of the Kizildag formation. Here the latter is dominantly sandy and shaly with occasional lens shaped conglomerates showing well developed cross stratification. W of Göktepe, the Kizildag formation interfingers with and eventually passes up into the Keklikpinari formation which is sandy and muddy at the base and contains conglomerates towards the top (Fig 9.3C)

The Kizildag formation is relatively thinner and

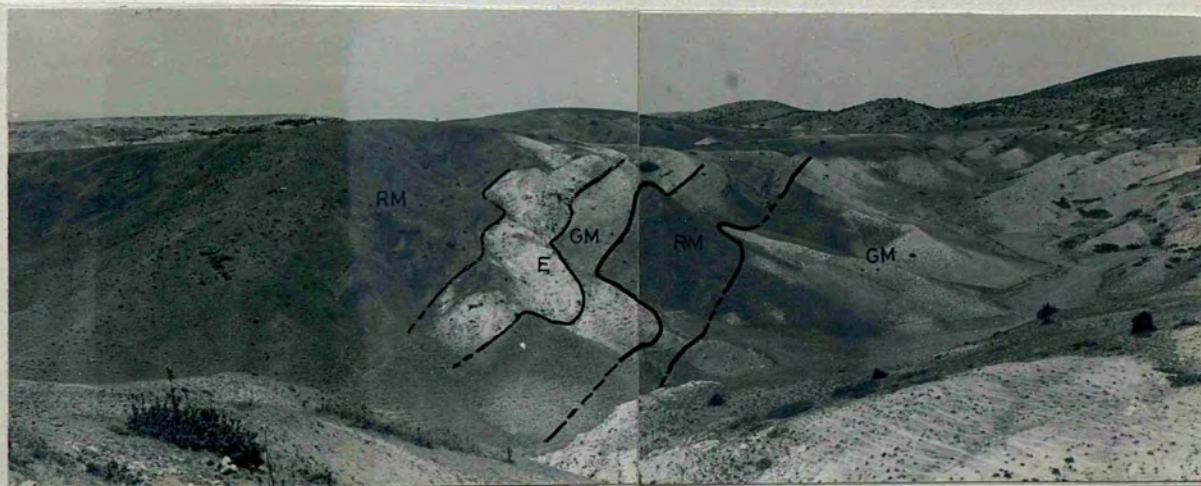


Plate 9.2 - Shows boundary relationships of Kizildag and Keklikpinari formations at W of Sehit T. (E20)
 RM= Red mudstone sandstone of the Kizildag formation, E= Evaporites, GM= grey-green mudstone sandstone of the Keklikpinari formation.

consists mainly of sandstones and mudstones, around Igneliar-kaç tepe (D15). It interfingers with and is overlain by the Keklikpinari formation which consists of isolated micritic limestone lenses within a shaly sequence which also contain a lens-shaped thick evaporite succession before it grades up to the turbiditic sandstone and conglomerates in the upper part of the formation (Fig 9.3D).

The third principal exposure of the Kizildag formation occurs in the N of the area where it overlies the yellowish brown fossiliferous sandstones and micritic limestones of the Keklikpinari formation which rests with an angular disconformity on the underlying Ankara Melange rocks. The Kizildag formation contains sheet-like, matrix-supported conglomerates and sandstones and passes up into the predominantly conglomeratic Keklikpinari formation (Fig 9.3E).

9.3 Conglomerates

9.3.1 General description

Conglomerates, which are subordinate to sandstones and mudstones, are coloured moderate red (5 R 4/6) to moderate reddish brown (10 R 4/6) and occur as lens-shaped units, sometimes as two or three isolated lenses separated by fine grained clastics within the same stratigraphical horizon and less commonly, and always at the base of the formation, as matrix-supported laterally continuous, 1 to 6 m. thick, structureless beds (Plate 9.3). The thickness of the conglomerate lenses ranges from 50 cm. to 2.5 m. and they almost always have erosional bases. Graded bedding, large and small scale cross bedding and crude parallel bedding are observed within the conglomerate lenses (Plate 9.4). The conglomerates are poor to moderately sorted and although they contain clasts ranging from granule to up to 40 cm. diameter blocks, the average size of the clasts are pebbles to small cobbles. Orientation of clasts parallel to the bedding plane



Plate 9.3 - Occurrence of isolated, conglomerate and sandstone filled channels within mudstone to fine grained sandstone sequence. Locality (E21)



Plate 9.4 - A. A conglomerate lens with crude parallel bedding and grading. Locality (B20)
 B. Wedge shaped conglomerate bed within medium to fine grained sandstone. Locality (E25)
 (Hammers are 30 cm. in length.)

is commonly observed. Roundness of the clasts varies with the size: larger clasts are subangular to subrounded; smaller clasts are angular to subangular. Conglomerates of the formation may be classified as diamictites (Pettijohn 1975).

Volcanic rocks, quartzite, metaquartzite, radiolarite, chert, serpentinite, limestone and granite are the lithologies found within the conglomerates as clasts and their proportion varies in different localities. Granitic clasts are only found in the conglomerates near the SE margin of the basin and comprise the largest portion of clasts E of Kurebogazi; limestone, radiolarite, serpentinite and basaltic rock clasts are the sole components of the conglomerates in the N of the area studied (SW of Kocakbaba tepe (I5)). Occasionally some well-rounded intraformational sand/mudstone pebbles are also observed. Volcanic rock clasts are andesites basalts and spilites which are rather difficult to distinguish from each other in hand specimens. They are usually subrounded and show weathered surfaces. Quartzites occur as slightly metamorphosed to very strongly metamorphosed and probably sheared metaquartzite and are generally angular to subangular. They dominate the granule size clasts. Well developed cleavage planes are readily observed in the sheared metaquartzites. Radiolarites are common and red in colour. They are generally subangular and although in most cases they are chert-like in appearance, in some samples recrystallized spherical radiolaria are visible. Cherts are grey and usually angular to subangular while characteristically green and subrounded to rounded serpentinites are rather less common. Some serpentinite clasts show slaty cleavage suggesting a metamorphic origin for these clasts. Limestone clasts are white to grey, generally subrounded to rounded and occur in two types. The first is a micritic limestone, containing a few badly preserved thus unidentifiable planktonic foraminifers. It is relatively less common than the second type which is entirely composed of medium to large calcite crystals. This type most

probably resulted from the recrystallization of a limestone within a metamorphic environment. Granitic clasts are grey, brownish grey and consist of a granular mixture of quartz and K-feldspars with a few plagioclase and biotite clasts. Intraformational pebbles are easily identified in the outcrop by their good rounding and characteristically red colour. Mud pebbles are generally weathered out due to their relatively soft nature.

The matrix of the conglomerates varies in amount in different beds and is compositionally similar to the sandstones of the formation. It is poorly to moderately sorted and generally weakly cemented.

9.4 Sandstones

9.4.1 General description

Sandstones, dusky red (5 R 3/4) to dark reddish brown (10 R 3/4), are volumetrically important. They are observed in two settings in which their textural and sedimentary structural characteristics differ. In one they occur as 70 cm. to 2 m. thick and 1 m. to 12 m. wide upward fining lenses. Within these lenses they show large scale trough cross-bedding at the base, each co-set shows an upward fining sequence, sometimes from gravel (probably as channel-lag gravels) to medium grained sand, and small scale trough cross bedding and parallel lamination towards the top (Plate 9.5). Sandstone lenses show erosional bases and occur as isolated bodies within the mudstone and sandstone succession. In the second setting sandstones are interbedded with mudstones and occur laterally and vertically in between conglomerate and sandstone lenses. They form 1 cm. to 30 cm. thick layers some of which show grading. Parallel laminations and some rare small scale cross bedding are the other observable sedimentary structures (Plate 9.6). These sandstones are generally poorly cemented and are thus prone to intense weathering, consequently the bedding properties of these sandstones are not seen. In better

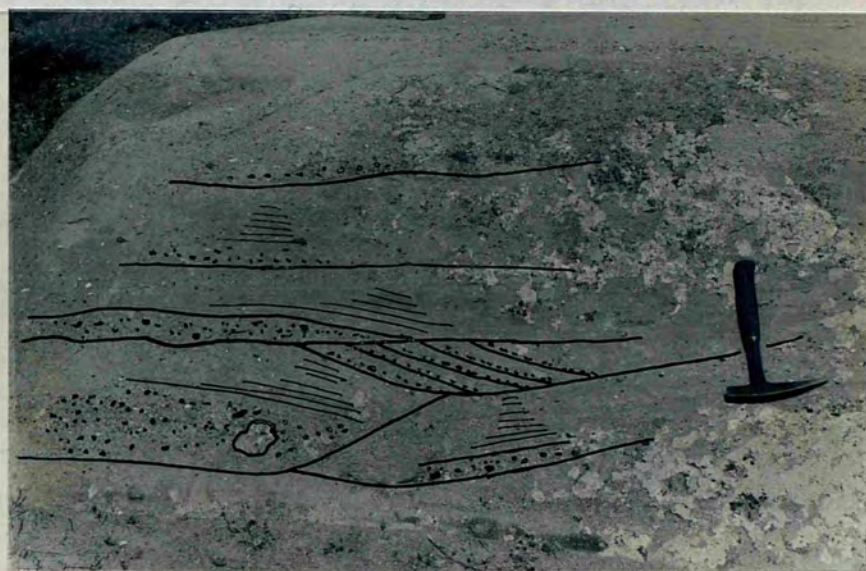
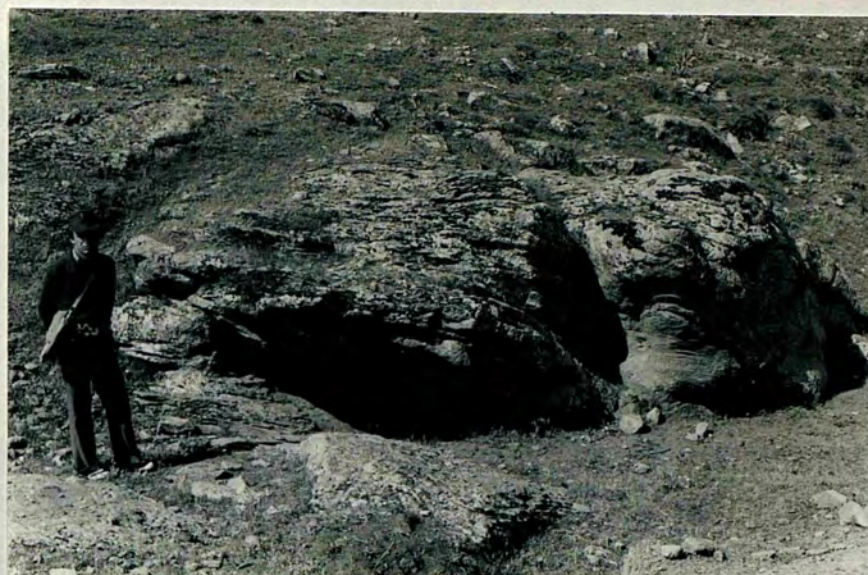


Plate 9.5 - Large and small scale trough-cross stratifications developed in the sandstone lenses. (Hammer is 30 cm. in length) Locality (B21)



Plate 9.6 - Parallel bedded, medium to fine sandstone and mudstone intercalations show tubular cross-stratification at the bottom of the photograph and thin conglomeratic lense at the top.
Locality (B20) Hammer is 30 cm. in length.

exposures, however, the sandstone appear to be laterally extensive and do not show any change in structural and textural properties.

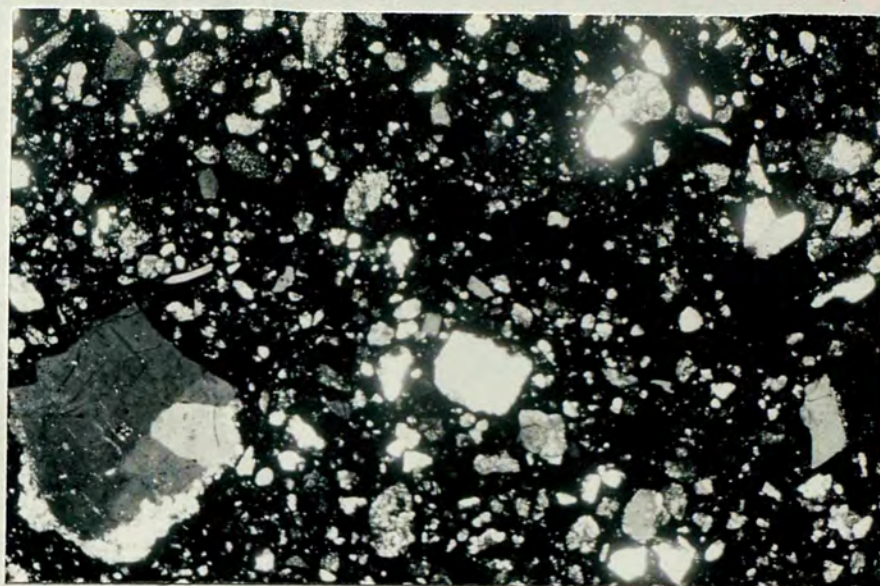
9.4.2 Texture

The grain size is generally coarse to medium in the sandstone lenses and becomes medium to fine grained in the evenly bedded occurrences; the latter are also relatively more poorly sorted than the generally moderately sorted former. Although some matrix supported sandstones are observed, sandstones are usually grain supported with considerable amounts of matrix filling the pore spaces in between the grains. Tangential and long grain contacts appear to be dominant. The packing proximity of sandstones, which are texturally immature, ranges from 30% to 65%.

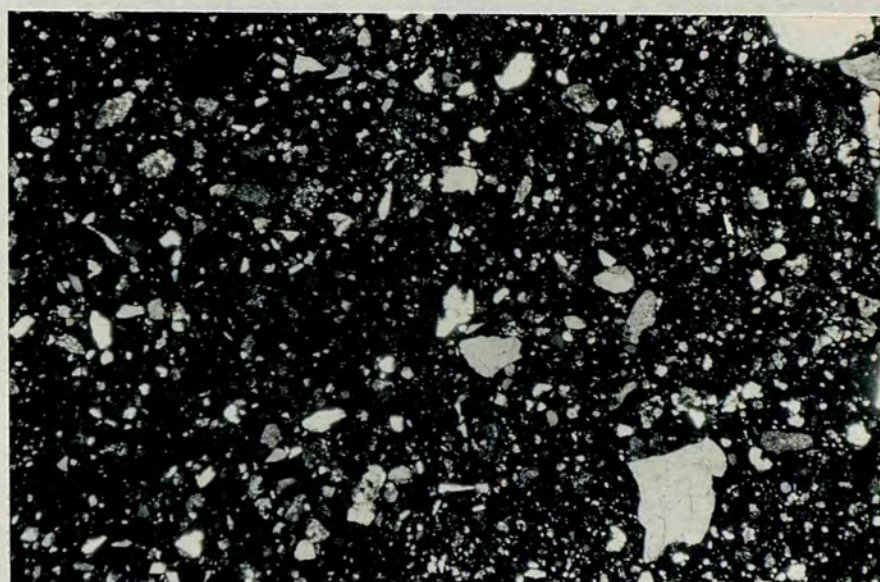
9.4.3 Framework grains

Quartz, metaquartzite, chert, radiolarite, volcanic rock fragments (VRF), granite, serpentinite and limestone fragments are the main constituents of the sandstones of this formation (Plate 9.7). Their presence and relative abundance changes in a pattern like that of the conglomerates (see 9.3.1). and Table 8.1.

Quartz grains are the most common detrital fragments observed in these sandstones. They are angular and occur in three types: common, volcanic and metamorphic. The first two are subordinate to the last and in some thin sections may not appear at all. The common quartz show slightly undulose extinction (full extinction occurs in between 1° - 7°), some inclusions and are equidimensional. The volcanic quartz show crystal outlines, corrosion embayments, straight extinction and a few inclusions. Lastly the metamorphic quartz occurs either as single crystals with very strong undulose extinction and some inclusion or composite quartz which is commonly formed



A



B

Plate 9.7 - Photomicrographs of sandstones.

- A. Lithic arenite is composed of sedimentary rock fragments, volcanic rock fragments, quartz, feldspar and hematite matrix. Sample 1084, 35x, XN.
- B. Lithic arenite consists of quartz, feldspar, volcanic and sedimentary rock fragments with hematite matrix. Note the matrix supported nature of the rock. Sample 610, 35x, XN.

Parameters Sample No	Quartz	Feldspar	VRF	SRF	Cement	Matrix	Accessory Components	Others	Total %	Total Count
80A	25.2	6.8	14.8	19.8	3.4	25.2	4.8	-	100.0	500
153	1.2	0.2	38.7	7.1	1.2	48.5	3.1	-	100.0	420
240A	14.3	11.6	20.2	28.5	2.3	18.1	5.0	-	100.0	481
928	5.5	5.1	29.3	9.3	5.9	43.3	1.5	-	99.9	526
1084	17.8	8.2	19.4	23.1	0.8	28.7	2.0	-	100.0	501
1087	27.6	21.8	9.9	18.2	5.2	15.9	1.4	-	100.0	504

Table 9.1 - Modal composition of the Kizildag formation's sandstones.

by more than 10 semicomposite quartz crystals with undulose extinction. Composite quartz grains are differentiated from the metaquartzite fragments on the basis of the presence of authogenic muscovite in the latter. Some of the single metamorphic quartz grains show well developed Bohemn lamellae which occur as warped, subparallel lines of very small bubbles which are believed to have resulted from intense strain deformation. Needle-like sillimanite crystals are quite commonly observed within single metamorphic quartz grains.

Metaquartzites are angular and show various degrees of metamorphism in different grains, ranging from the slightly metamorphized, composed of medium size interlocked quartz crystals with straight boundaries and authogenic muscovite, to strongly sheared metaquartzites. The latter consist of numerous elongate crenulate quartz crystals welded together.

Cherts are generally microcrystalline quartz although some, show a combination of microquartz and megaquartz. They are angular and generally do not show any relict textures.

Feldspars occur as plagioclases and may be fresh or altered. The fresh plagioclases are generally angular, show albite and albite and carlsbad combined twinnings and are labradorite, bytownite and andesine in composition. The altered plagioclases are subangular and show partial to complete alteration. The most common alteration products are sericite and/or illite and vacuoles which give a cloudy brownish appearance to the plagioclases. In some grains, replacement of plagioclases by sparry calcite is also observed.

VRF are subangular to subrounded and their proportion is reduced in sandstones compared to conglomerates. VRF are dacitic and/or rhyolitic, andesitic and basaltic. Rhyolitic and andesitic fragments are common in the sandstones exposed in the southeastern margin of the basin, their

proportion is substantially reduced in the S, W and NW part of the area while they are completely absent in the northern exposures of the formation. These fragments show similar textural and compositional features to those occurring in the other lithological units of the Bala area. Serpentinite fragments are very rare, subrounded to rounded and show mesh-structure and first order interference colours.

Radiolarite fragments are generally subangular and contain recrystallized radiolarias. Limestone grains occur either as micrite or as large calcite crystals of detrital origin. They are generally subangular to subrounded.

Fragments of bivalve, gastropod and broken foraminifers, although rare, are also observed. In one sample a whole benthonic foraminifer with abraded edges is seen.

Muscovite flakes; some isotropic minerals with a steel blue black colour in reflected light may be magnetite; dark red patchy grains which result from the breakdown of iron bearing minerals - possibly hematite - are also observed as accessory components.

9.4.4 Matrix and cement

Matrix material is the principal binding agent and is generally poorly sorted. It consists of hematite, small quartz crystals, chlorite, micrite, sericite and/or illite which are identified by their high relief and bright white to reddish yellow interference colours. The distinction between replacement and detrital origins could not be achieved due to the complex composition and texture of the matrix. Cement is rare and only occurs as patchy sparry calcite, possibly of neomorphic origin

9.5 Mudstones

9.5.1 General description

The mudstones of this formation are generally dusky red (5 R 3/4) and sometimes show lens shaped grey-green areas at the boundaries with the Keklikpinari formations rocks. They do not show any sedimentary structures apart from parallel lamination. Bed thickness ranges from mm thick laminae to 10 to 15 cm. thick beds. The mudstone beds generally have sharp, sometimes erosional, upper boundaries with the overlying sandstone beds but a transitional contact is usually observed between them and underlying sandstone beds. Locally well developed 2-15 cm. thick carbonate layers and nodules are found within the very fine grained mudstone layers. The grain size of the mudstone varies from silt to clay size and each of these may become important in different localities. In the evaporite - mudstone intercalations, the mudstones are made up of almost all clay grade material. They sometimes contain scattered fine grained quartz grains and are moderate to poorly sorted. Silt size grains which are the only optically observable fragments, are usually angular to very angular. The composition of the mudstones is fairly constant with hematite, calcite, quartz and clay minerals kaolinite and illite) the dominant constituent throughout the mudstones of the formation. However glauconite and goethite are also observed within the green mudstones.

9.6 Evaporites

9.6.1 General description

Evaporites are exposed at the boundary with the Keklikpinari formation. They occur either as interlaminated with reddish and greenish mudstones where the laminae are structureless and 1-2 cm. thick, (Plate 9.8) or 50 cm. to 5 m. thick lens shaped bodies of varying lateral continuity (Plate 9.3), Within these lenses, evaporites form centimetre



Plate 9.8 - Laminated evaporites intercalating with red and greenish grey mudstones. (Hammer is 30 cm. in length) Locality (D21)

thick laminae to 20-25 cm. thick beds, interbedded with 2-10 cm. thick, red to yellowish brown, sometimes laminated but generally structureless mudstone and/or fine grained sandstone layers. The mudstone layer are commonly clay grade material dominant and show transitional upper boundaries with the evaporites. Microscopically, the evaporites consist of very fine grained gypsum crystals forming a mosaic fabric with randomly scattered large gypsum crystals. In some gypsum laminae which are separated by micro crystalline calcite, a reverse grading of crystals from mosaic to coarse crystals are observed. There are also some fine crystals, which cannot be accurately identified by optical means, clustered in certain parts of the thin section. Although they, in the first instance, appear to be relict of anhydrite crystals, they are stained dark red to purple by Alizarin-red and are thus calcite.

9.7 Red colouration

The most characteristic feature of this formation, as with the Sarikaya member (6.2), is the distinctly red to reddish brown colour.

Red beds are widespread geological features and have been identified throughout the stratigraphical column starting late in the Precambrian and being present as recent deposits e.g. in the Sonora desert of northeastern Baja California. They have been assumed, by various authors, to be related to different environments of deposition. These range from deltaic, fluvial, estuarine, lagoonal to near-shore all with various climatic conditions ranging from hot humid tropical to hot arid deserts (Glennie 1970). Iron-oxide, mostly in the form of hematite, staining the particles of clay and coating the sand and silt size fragments within an oxidizing environment (i.e. subaerial deposition or immediate post depositional exposure) is generally thought to be the cause of the red colour. However there has been a considerable controversy concerning the origin and formation of

haematite and various theories have been put forward ranging from predepositional staining and coating of sediments in hot arid deserts to transportation of haematite, formation of which partly resulted from the activities of iron-bacteria, by water which percolated down to the newly deposited sediments (Chukhrov 1973) or intrastratal alteration of iron-bearing minerals after deposition (Walker 1967). (See Glennie 1970 for detailed chronological presentation of theories.)

The red beds of the Bala area indicate that the red colouration was most probably due to intrastratal alteration of iron-bearing minerals after deposition in an arid climate, the latter being suggested by the evaporites associated with red beds. The lines of evidence in support of above conclusion as follows:

- a. the presence of strongly altered iron-bearing minerals, (biotite, volcanic rock fragments and magnetite - the last only observed in the Kizildag formation) with haloes of haematite surrounding the altered grains. (Plate 9.9);
- b. the presence of haematite coating free contacts between grains, suggesting that the haematite coating was post-depositional. (Plate 9.10);
- c. existence of greenish grey spots within the red coloured sediments without any compositional changes in these sediments.

Similar features have been described from the recent sediments of northeastern Baja California (Walker 1967) and it has been demonstrated that the formation of haematite was due to intrastratal alteration of iron-bearing minerals.

The greenish grey reduction spots which are occasionally seen at the boundary between the red beds and marine sediments were believed to be the result of localized high organic carbon content in these spots. These green areas are haematite

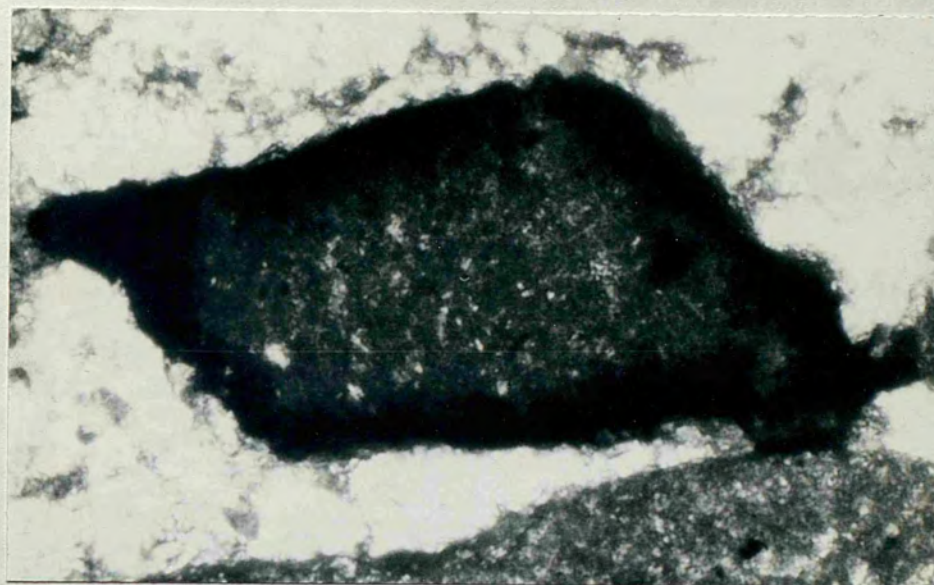


Plate 9.9 - Photomicrograph shows a hematite halo
around a volcanic rock clast: Sample 198,
320x, XN.

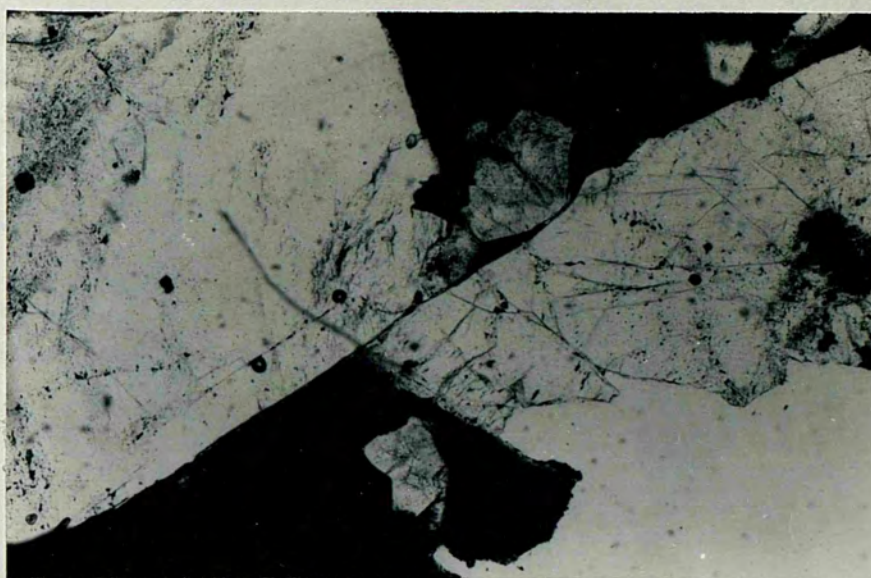


Plate 9.10 - Photomicrograph shows hematite free contact
between two K-feldspar grains. Sample S7, 150x.

free and instead contain glauconite and goethite.

9.8 Sedimentary structures and current directions

The commonly observed large scale cross bedding, which resemble trough-cross bedding within the conglomerates and sandstone lenses, probably resulted from scour and fill action by streams, by the repetition of a process that a trough-shaped scoured-out channel was filled up by graded sandstones and gravels conforming to the shape of the trough-shaped floor. Small scale cross bedding (which, although less frequent, are also observed in the above mentioned lenses) are believed to be formed due to migrating of small current ripples. Parallel lamination is very common and widespread. Some rare occurrences of crude lenticular bedding within the gravel dominated conglomerate lenses are also seen.

Current directions, obtained from the measurement of cross-bedding, are unimodal at any one place but show different flow directions in different parts of the formation. (see Fig 12.11)

9.9 Age of the Kizildag formation

The rocks of the formation do not contain any fossils apart from some plant fragments. Therefore the age of the formation can only be made on the basis of its stratigraphical setting. As was noted earlier (9.1 and 9.2) this formation overlies the Palaeocene to Early-Middle Eocene Ucem and Bayat formations with an angular disconformity and inter-fingers with and underlies the Middle Eocene Keklikpinari formation. Thus a Middle Eocene age is proposed for the Kizildag formation.

9.10 Source area and environment of deposition

Due to its areal extent and depositional nature

(see below) the Kizildag formation had different source areas in different localities. The presence of granite serpentinite, radiolarite, limestone, quartzite, chert and volcanic rock clast and fragments in the sediments of this formation found in the southeastern margin of the basin together with current direction mainly from the SE and N suggest that in this part Kirsehir Massif, Ankara Melange, Karaca Ali Granitic Pluton and Saridere volcanic formation (to a lesser extent) were providing detrital material to the formation. In the S, W and NW part of the formation, the source area was the Bayat formation. Although the absence of any sandstone and calcarenite clasts or fragments, which are the main lithological types of this formation may argue against this suggestion, the presence of bivalve, gastropod and broken and abraded foraminifer fragments within the sediments of the Kizildag formation, compositional similarities of these two formations together with the generally NE and E current directions suggest that the Bayat formation was the most likely source area. This conclusion is also supported by the already mentioned fact that the source of the Kizildag formations sediments was local and proximal indicated by their depositional nature (see below) and the implication that the overlying Keklikpinari formation suggests relatively deeper water conditions towards the S, W and NW. However the absence of the fragments of the Bayat formations lithologies must be explained. The simplest possible explanation is that these lithologies were not completely lithified when they were exposed and eroded. In the northern part of the formation the presence of serpentinite, radiolarite limestone and basaltic rock clasts and fragments which are the main lithological types of the Ankara Melange presently exposed in the N and NE of the formation together with the absence of the clasts of granite and andesite indicate that the latter was the source area during the deposition of this part of the formation.

The occurrence of channels and the absence of fossils (except reworked ones, see above) within the sediments of the Kizildag formation together with their red colour suggest that they were deposited in an alluvial environment. The presence of carbonate layers and nodules in the red mudstones most probably indicate a palaeosoil formation, also supports the above conclusion.

The matrix supported conglomerates of this formation resemble those occurring in the Sarikaya formation and are believed to be deposited by subaerial debris flows (ibid p186). The variation in the sedimentological properties of channel-fill deposits, (the conglomerate and sandstone lenses, i.e. that they are sometimes coarse-medium grained sand and show upward fining sequences and various current formed sedimentary structures (10.8) or they are gravel-boulder dominated, poorly sorted and show either large cross-stratification or crude parallel bedding) indicate two different flow patterns with varying discharge rates. The presence of large scale cross bedding at the bottom of the erosionally based channel, sometimes with channel-lag gravels, overlaid by small scale cross bedding and parallel lamination suggest that these sediments were deposited by meandering streams (Allen 1965, Reineck & Singh 1978). In contrast the occurrence of crude parallel bedded, large scale cross bedded or indistinctly graded channel deposits which are more abundant throughout the formation as well as within the same stratigraphical horizon as isolated lenses, and their coarse grain size indicate that these channels are formed and filled-in by braided streams. These streams had higher discharge rates than the meandering ones as their coarser grain size and the occurrence of intraformational pebbles within these rocks imply. The interbedded sheet like, laminated mudstone and medium to fine grained sandstone beds indicate a low-energy environment. Their association with channel deposits suggest that they were most probably

deposited in the flood plain area, rather than as flood basin sediments which would have channels with well developed levees and contain relatively finer, silt and clay grade, sediments (Reineck & Singh 1978) or as sheet flood deposits which are generally associated with debris flows (Bull 1967)

Considering the occurrence of debris flow deposits generally at the base of the formation, the overall dominance of flood plain sediments over channel-fill deposits and the small sizes and diversity of the latter sediments in the upper part of the formation, it can be further concluded that the Kizildag formation was deposited within an alluvial fan setting in which, through debris flow sediments were deposited on the proximal areas of the fan, small channel and flood plain sediment were laid down in the distal part. In the latter area a number of generally short-lived braided streams were formed by intermittent flash floods. These streams either cut new channels on the flood plain area or caused rapid migration of existing ones depending on the discharge rates. A few of these streams for some reason developed more regular flow patterns as meandering streams and probably flowed for longer periods than the braided streams before they dried out .

Evaporites were probably precipitated in a number of small marginal depressions in the transitional area between this formation and the Keklikpinari formation. This is suggested by the laminated and bedded occurrence of evaporites and their intercalation with the red and greenish grey mudstones. The most probable source for these deposits was the sea water which has higher salinity (see Keklikpinari formation Chp. 10) and was supplied to these pools by high seas during the intermittent storms or even by seepage. Friedman (1978) has described similar formation of evaporites in the Red Sea. There the evaporation takes place

during the summer months with increase salinity of the sea water. Gypsum is the main precipitate. During the winter months the lost sea water is balanced by the influx of water from the Red Sea.

On the basis of the red colouration, the presence of evaporites and rarity of plant fragments, it can be suggested that the climatic regime during the deposition of the Kizildag formation was hot and arid with occasional torrential rains.

C H A P T E R 10

KEKLIKPINARI FORMATION

10.1 General Introduction

The Keklikpinari formation is Middle Eocene to probably Oligocene in age and consists of greyish-green sandstones, shales, conglomerates and greyish white to white limestones and evaporites as lens shaped bodies. A small deltaic deposit mapped and described separately, is also included to this formation (see 10.8). Spacially, the formation shows considerable stratigraphic variations consequently a type section cannot be given. However six composite stratigraphical columns for six different parts of this variable formation are given in Fig 9.1 and 9.2. Additionally, two detailed stratigraphical sections measured near Keklikpinari and from the eastern flank of Asartepé are described.

Near Keklikpinari the first 26 m. of the base of the formation is not seen and the section (Fig 10.1) consists of dark grey to dark green medium to fine grained parallel laminated and thick graded 5-15 cm. sandstones interbedded with up to 190 cm. thick structureless shales. Thick (30-55 cm.) sandstone beds are especially dominant between 6 m. and 13 m. from the base of the section, these are graded and sometimes contain abundant mud pellets at their base. The next 7 m. is represented by an incursion of the Kizildag formation which is muddy and silty at the base and becomes conglomeratic towards the top. The following 11 m. is made up of shales of the Keklikpinari formation with rare 5-20 cm. thick parallel laminated fine grained sandstone beds in the lower part and higher interbedded 4-10 cm. thick, fine grained sandstone and siltstone and 5-15 cm. thick shales. Both lithologies show well developed parallel laminations. The uppermost 3 m. of the section is again Kizildag formation in the same stratigraphical setting. This lithology passes westwards into fossiliferous conglomerates.

Thickness	Lithology	Sample number	Bed thickness and shape			Texture				Sedimentary structures				Colour	Remarks	Formation	
			Conglomerate	Sandstone	Shale	Boulder	Sand			Grading	Paral: Lamina	X-strata	Ball & Pillow				Plant frags
							Gravel	Coarse	Medium								
40		VU-8	60-70 L											r, rb	Poorly sorted, cyclic sedimenta.	Kizildag	
	VU-7		3-5 W, L	3-5 W, L										r, rb			
	VU-6		10-30 L, SL	90-110 L, SL										dg, gr			
	VU-5															Keklikpinari	
	VU-4		4-10 SL	5-15 SL										dg, gr			
	VU-3																
	VU-2																
	VU-1		5-20 SL	70-140 SL										dgr, g			
	30	V-19	150 L											r, rb	Poorly sorted	Kizildag	
		V-18		15 W, SL	100-300 SL									r, rb			
V-16, 17			5-10 SL	10-15 SL									dg, gr				
20															Keklikpinari		
	V-15		7-30 SL	7-120 SL									dgr, g				
	V-14		3-10 SL	10-75 SL									dg, gr				
	V-13																
10	V-12														Keklikpinari		
	V-11																
	V-10																
	V-9		15-55 SL	10-100 SL									dgr	sandstones are relatively poorly sorted			
	V-8													Abundant mud pellets in sandstone			
	V-7																
	V-6		15-30	10-30									dg				
	V-5			190									dgr				
	V-3																
	V-4		10-20	30-50									dg				
V-2																	
V-1			100									dgr					

Fig 10.1 - Keklikpinari section. (Lithology is to scale)

SL: Sheet like, L: Lenticular, W: Wedge shaped.

In colour column; r: red, b: brown, g: grey, gr: green, d: dark.

In the Asartepé section (Fig 10.2) the formation starts with a 22 m. conglomerate dominated zone in which light brown to grey, 60 cm. to 7.5 m. thick conglomerate beds intercalate with parallel or wave-ripple cross laminated siltstone and shales at 4 and 13 m. from the base of the section. These fine grained zones are 20 cm. and 310 cm. in thickness respectively. The conglomerates are structureless, chaotic and matrix-supported (Plate 10.1) except one 150 cm. thick bed, at the top of this part, which shows grading. The remaining 15 m. of the section is composed of structureless dark grey-green shale interbedded with occasional fine grained structureless sandstone and siltstones. About 100 m. W of the section locality, red sandstones and conglomerates outcrop as a 4 m. in length erosional inlier and although no obvious bedding can be determined they appear to conform with the general NW-SW strike and SW dip of the above described lithologies.

10.2 Distribution, thickness and field relations

The distribution and the lower boundary relation of the Keklikpinari formation has been described in section 9.2 of the previous chapter and is not discussed here. At its upper boundary the formation is unconformably overlain by the horizontal Mid-Pliocene Mezgrit formation (see 1.6.4)

The thickness of the formation changes substantially within an obvious pattern in which it is relatively thinner in the area between Ergin (D17) and SW of Bala (A27) and thickens towards the NW and S of the area studied. In the NW the formation is reported to be dominated by extremely poorly sorted, thickly bedded (up to 10 m.) conglomerates which intertongue with basaltic volcanic rocks (Tibetan type post-collision related volcanism: Sengor & Yilmaz 1981) in the uppermost part of the formation near Ankara and over 1000 m. thickness has been estimated for the conglomerates alone (Arikan 1975). In the S the information is scarce due to the extensive cover of the Mid-Pliocene Mezgit formation but the formation is believed to be

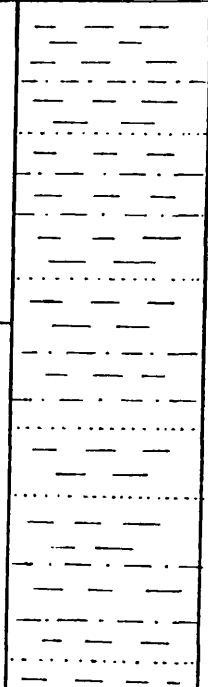


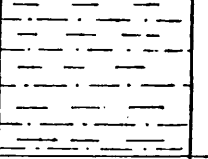


Thickness	Lithology	Description
30		Generally massive and structureless but occasionally parallel laminated dark grey green shale with rare 5-15 cm. thick, sometimes parallel laminated siltstone and fine grained sandstone beds.
20		Indistinctively graded conglomerate.
10		Matrix supported conglomerates
0		Dark grey green, 5-15 cm. thickly bedded, parallel laminated or wave ripple cross laminated siltstone and shale intercalation.
0		Light brown-grey 50 cm.-7.5 m. thickly bedded, matrix supported conglomerates. They have flat irregular bases and flat tops. Clasts of the conglomerates are up to 35 cm. in diameter.
0		Shale-siltstone intercalation. Matrix supported conglomerates.

Fig 10.2 - Asartepe section (Lithology is to scale)



Plate. 10.1 - Matrix-supported, chaotically mixed conglomerate in the Asartepe section. (see text) The entire conglomerate bed is 750 cm. thick. Hammer is 30 cm in length.

mainly turbiditic sandstone and conglomerate and has considerable thickness (V. Yuksel pers. com. 1980)

10.3 Sandstones

10.3.1 Sandstone and conglomeratic sandstone beds with upward fining.

These lithologies are found within shale and siltstone dominated sequences and form 50 cm. to 1.10 m. thick, upward fining layers which on one place (along Acicesme deresi (C26)) is traced for about 700 m. with marked variation in thickness. The layers generally have a conglomeratic sandstone or conglomerate at the base which abruptly grades up into medium-fine grained sandstone with parallel lamination, hummocky cross stratification (Plate 10.2) and/or small scale wave ripples (Plate 10.3). This in turn passes up into the shale and siltstones of the upper part of the sequence. The lower coarse grained part generally shows well developed erosional bases and can be structureless, graded or parallel stratified (Plate 10.2). They sometimes show poorly developed sole structures. They are usually poor to moderately sorted and contain subangular to subrounded gravel and sand size grains in contrast to overlying medium to fine grained moderately sorted sandstones. In the overlying siltstone and shales vertical and horizontal (possibly shallow water) burrowings are observed.

Wave ripples and wave ripple cross laminations are differentiated on the basis of their Ripple Index (RI) and Ripple Symmetry Index (RSI) (Reineck & Singh 1976) and the occurrence of chevron structures (Elliot 1980). On the basis of four measurements on an asymmetrical ripple (see Table 10.1), although the profile of the ripple crests occurring in this formation are not very regular, their less than 4 RI and less than 2 RSI values together with the presence of chevron structures suggest that these are wave ripples. Plate 10.3.



Plate 10.2 - A hummocky cross-stratification in the medium to fine grained sandstone beds. Note the overlying conglomeratic sandstone and its sharp upper and lower boundary. Pen is 15 cm in length. Locality (C27).

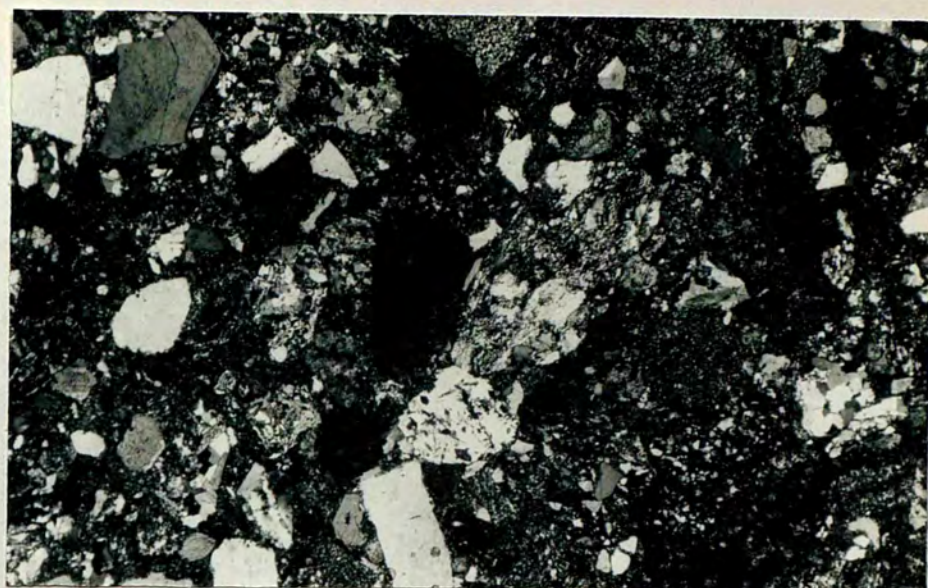


Plate 10.3 - An asymmetric wave ripple in the fine grain-
ed sandstones of the shoestring
type. Note the irregularity of
laminae in the vertical section
at the left of the rock chip.
Penknife is 10 cm. long.
Locality (B26)

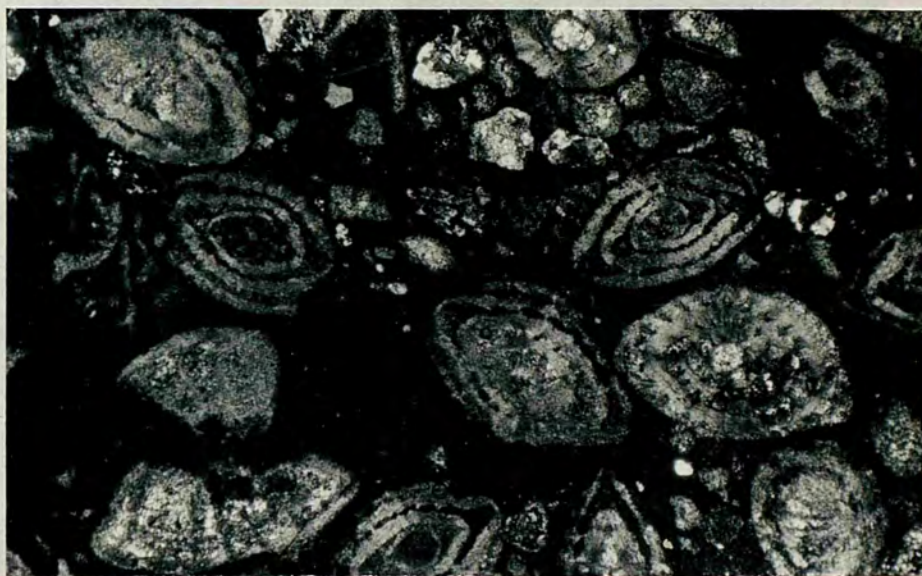
	Measurement	1	2	3	4
A	Ripple length	*1.2	1	1.2	1.4
B	Ripple height	0.5	0.4	0.6	0.4
C	Length of horizontal projection of stoss side	0.5	0.4	0.3	0.6
D	Length of horizontal projection of lee side	0.7	0.6	0.9	0.8
	RI (= A/B)=	2.4	2.5	2	3.5
	RSI (= C/D)=	2.7	0.6	0.3	0.7

Table 10.1 - RI and RSI values of asymmetrical wave ripples
 * Figures are in cm.

These sandstones are composed of quartz, quartzite metaquartzite, radiolarite, limestone, chert, sandstone fragments amygdaloidal basaltic fragments broken and/or whole foraminiferal tests and fragments of mollusc and echinoids within a chlorite, micrite and iron-oxide matrix (Plate 10.4). Granitic rock fragments also occur but are confined to the sandstones in the southeastern margin of the basin. Quartz occurs either as single crystals with slight to strong undulose extinction and with abundant sillimanite inclusions or as composite quartz which again shows strong undulose extinction and sillimanite inclusions. These types of quartz are believed to be metamorphic in origin as indicated by the abundance of sillimanite inclusions (Scholle 1979). Volcanic quartz is very rare and may be absent in some thin sections. Limestone clasts are subangular to subrounded and of two different types. The first is a wackestone with an abundant micritic matrix, a few algal fragments and, unidentifiable due to recrystallization, broken shell fragments. The second type is completely recrystallized calcite and found in smaller grain sizes. Sandstone fragments are composed of quartz, chert and a few skeletal fragments within a micritic matrix.



A



B

Plate 10.4 - Photomicrographs of sandstones.

- A. Volcanic arenite consists of volcanic rock, quartz, feldspar, sedimentary rock fragments and matrix. Sample 740, 35x, XN.
- B. Fossiliferous sandstone contains abundant foraminifers, quartz, feldspar and volcanic and sedimentary rock fragments. Sample 245C. 35x, XN.

Parameters Sample No	Quartz	Feldspar	VRF	SRF	Cement	Matrix	Accessory Components	Others	Total %	Total Count
106	13.0	3.9	48.0	10.7	11.9	10.1	2.4	- -	100.0	506
177	25.2	25.6	6.5	- -	6.5	32.3	3.7	- -	99.8	535
365	8.8	6.0	23.1	23.9	6.2	28.6	3.3	- -	100.0	419
376	10.8	5.3	16.7	45.8	2.5	18.6	0.4	- -	100.1	528
509	17.6	8.2	44.0	6.2	6.4	11.6	6.0	- -	100.0	500
510	14.6	6.6	27.4	23.0	12.8	8.6	2.0	5.0a	100.0	500
539	6.0	12.0	28.4	24.0	7.2	12.4	4.4	5.6b	100.0	500
740	15.8	10.6	21.4	22.6	1.6	25.6	2.4	- -	100.0	500
744	4.0	6.6	49.6	9.0	3.2	26.2	1.4	- -	100.0	500
979A	8.2	13.8	36.8	17.6	8.8	11.8	1.4	1.6b	100.0	500
V.6	8.0	7.6	12.5	26.0	4.3	12.7	5.1	23.8a	100.0	512
1477	19.8	18.6	15.6	18.0	7.8	16.2	1.6	2.4b	100.0	500

Table 10.2 - Modal composition of the Keklikpinari formations sandstones. a: cholarite
b: radiolarite.

The matrices of these sandstones are fine grained, poorly sorted and occasionally are found to be chert which probably resulted from recrystallization.

10.3.2 Sheet-like sandstones

This lithology is found within siltstone and shale sequences (Plate 10.5) and forms beds ranging, in thickness, from 5 cm. to 55 cm., though mainly 10 cm. to 30 cm. beds are generally parallel laminated, but sometimes graded at the base and parallel laminated in the upper parts, and show sharp, sometimes erosional, bases and gradational upper contacts with the overlying shales. Fragments in these sandstones are generally angular to subangular and composed of volcanic quartz, basalt or andesite, limestone, plagioclase (bytownite to andesine), completely recrystallized skeletal fragments (probably gastropod) broken and/or whole benthonic foraminifers (ranging from 2 mm. to 0.2 mm. in length) and chert. Biotites are seen as accessory components and are altered to chlorite. The matrix is chlorite and micrite with subordinate amounts of sparry calcite cement. These sandstones are texturally immature and show compositional variations in different parts of the formation similar to the sandstones in upward fining sequences.

10.3.3. Gently dipping parallel laminated sandstones

This sandstones are found as parallel laminated sets gently dipping towards the W. (Plate 10.6 and 10.7). They form laterally extensive, 2 m.-30m. thick sequences which inter-tongue with red mudstone and siltstones. On one occasion a large trough cross bedded, 4m. thick, sandstone lens cutting these deposits is observed around Goktepe (B20). The thickness of the sets ranges from 50 cm. to 1m and there also exist sets with high angle inclination to the E. These sandstones consist of quartz, quartzite, chert, radiolarite, limestone and broken shell fragments with a few basaltic and/or andesitic rock fragments. They are moderately sorted and texturally submature.

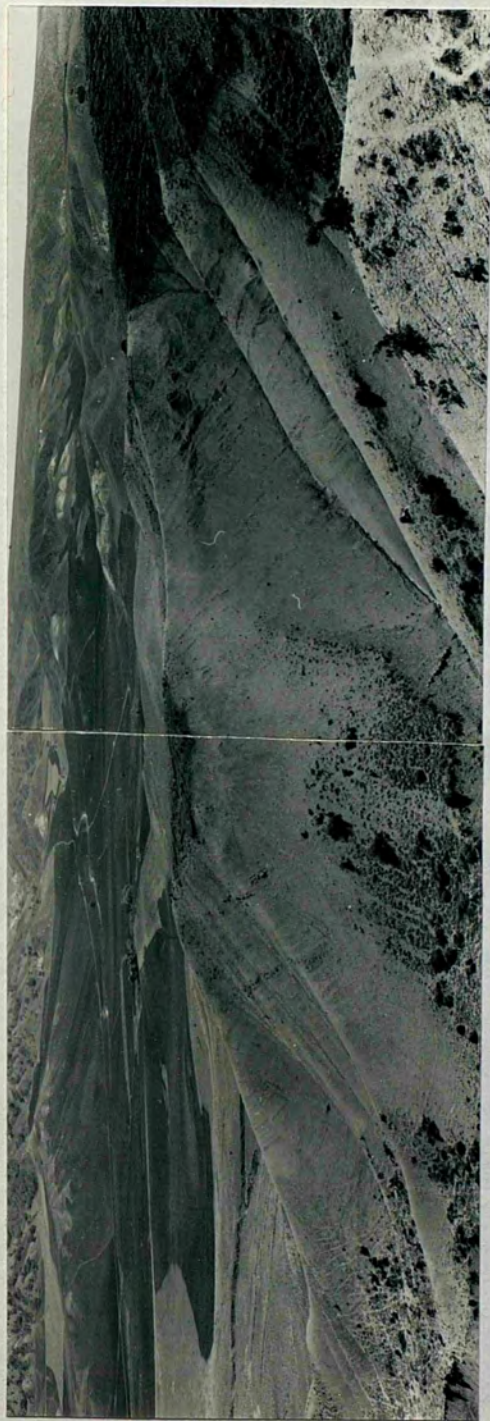


Plate 10.5 - A shale and siltstone dominated sequence on the northeastern flank of Soraktepe (D22). Note the occurrence of occasional thick medium to fine grained sheet like sandstone beds.

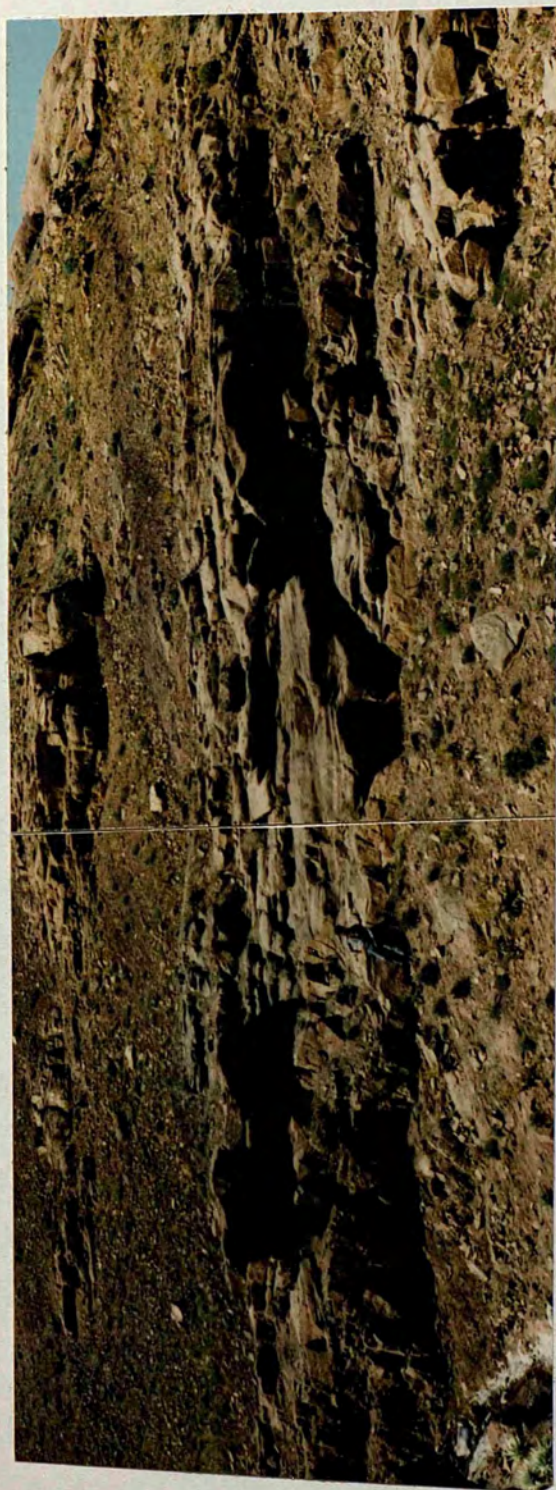


Plate 10.6 - Showing sets of parallel laminated sandstones gently inclined towards the W, intertongued with red mudstones. NE of Ergin (D17)



Plate 10.7 - Gently inclined parallel laminated sandstone beds cut by a lens shaped red trough cross stratified sandstone bed of the upper part of the photograph. Locality (B20)

10.3.4 Turbidite sandstones: beds are found within shaly sequences and will be described in the deltaic deposit (see 10.8)

10.4 Shales and siltstones

Shales and siltstones are the dominant lithological types of the Keklikpinari formation and are characteristically greyish green (5G 5/2) to greyish olive green (5G 3/2). They are often found interbedded and contain scattered large benthonic foraminifers and oysters. (The largest oyster is 20 cm. in length 10.7 cm. in height and all have a low ligamental area, very shallow unbonal cavity in the left valve and show orbicular adductor muscle scars which have an elevation in the ventral portion and located near to the hinge; on these basis they are identified as belonging to family Gryphaeidae (identification is made by using criteria suggested by Stenzel 1971)) Foraminifers are Nummulites sp, Discocyclina sp, Orbitolites sp, Asterocyclina sp, Assilina sp. and Fasciolites sp. But this diversity together with the oysters is only present at the base of the formation and disappears towards the top, where only Nummulites, Assillinas and Discocyclinas are found. Shales and siltstones are generally structureless most probably due to bioturbation, but sometimes parallel laminated or micro cross laminated beds can be found. Bed thickness ranges from millimetre thick laminae to massive 3 m. thick intervals. Quartz and quartzite together with chlorite predominant detrital fragments within these sediments.

10.5 Limestones

10.5.1 Foraminiferal packstones

This lithology is observed in two localities W of Kizildag and SE of Aydogan. It occurs as 40 cm. to 80 cm. thick lens shaped beds with lengths of 5 m. and 11 m. within generally structureless, dark green grey shale sequences. Beds show sharp irregular lower boundaries indistinct grading and

transitional upper boundaries with the overlying parallel laminated marls. The foramineral packstone is composed of generally whole, but less frequently broken tests of large benthonic foraminifers (Assilina sp, Fasciolites sp, Orbitolites sp, Asterocyclina sp, Discocyclina sp, and Nummulites sp all of which are found in the under and overlying shales) and fragments of coralline algae and molluscs with a few intraformational sandstone and lithoclastic fragments, mainly quartz, metaquartzite, radiolarite and chert occurring in varying proportions, within a micritic matrix which is sometimes replaced by neomorphic sparry calcite. They are poorly to moderately sorted and orientation of elongated foraminiferal tests parallel to the bedding plane are clearly observed (Plate 10.8). Foraminifers are 2 cm. to 0.2 cm. in length and are generally well preserved. Occasional vertical and horizontal burrows are also seen in this lithology

10.5.2 Micritic limestone

These limestones are light grey (N8) to pinkish grey (5 YR 8/1) and found as isolated lenses up to 2m thick, of limited areal extent (at the most 21 m., around Igneliarkactepe (E15)). The bedding properties of the limestones within these lenses, which are under and overlain by red or green structureless shales and which occasionally contain thin evaporite layers at the top, are not observable due to intense weathering (Plate 10.9). They are, with the exception of two cases (see below), composed of micrite microspar and sparry calcite crystals with scattered dolomite rhombs in some thin sections (Plate 10.10). Although some ghost structures which may be a skeletal fragment or vertical and horizontal burrows, are observed, their origin could not be ascertained due to recrystallization. The microspar and sparry calcite crystals are most probably neomorphic in origin resulting from the aggrading neomorphism of the micrite. These limestones also show high porosity, the nature of which can not be determined because of the recrystallization. Two limestones which show textural and compositional differences from the micritic limestones are also observed within these lenses.

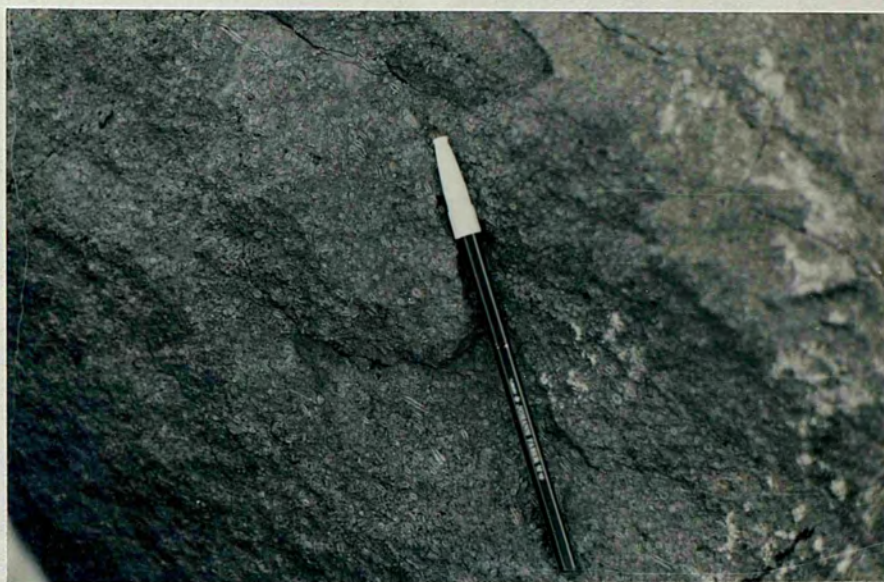


Plate 10.8 - Foraminiferal limestone in the Acicesmederesi valley (C27). Note the orientation of elongated foraminifers parallel to the bedding. Pen is 15 cm. in length.



Plate 10.9 - Micritic limestone lens, S of Igneliarkac-tepe (F15). Note the absence of well developed bedding.

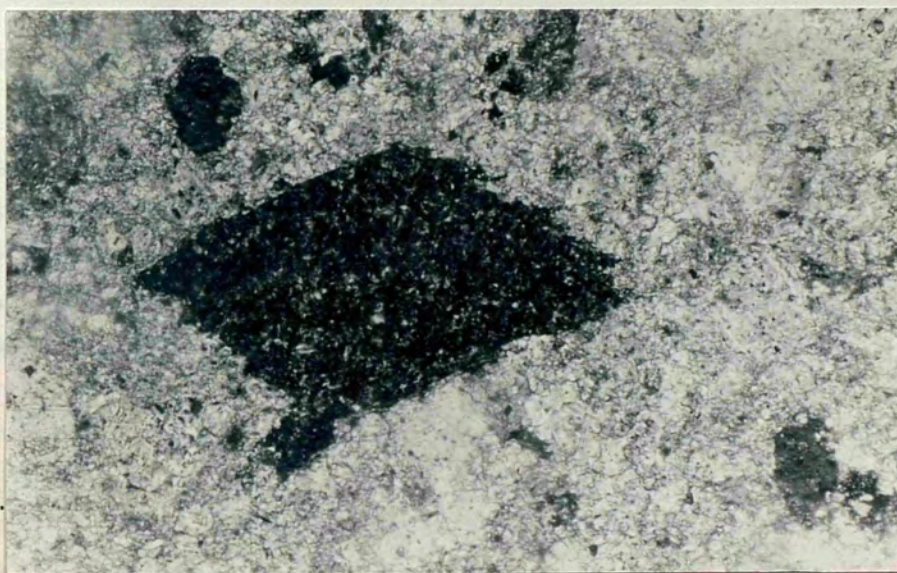


Plate 10.10 - Photomicrograph of micritic limestone, shows
a dolomite rhomb within a micrite matrix.

Sample 1307, 150x XN.

Because of their thin nature and association with micritic limestone, they are included into this group. The first is found within a limestone lens SW of Kocakbabatepe (I5), and is composed of fecal pellets within a neomorphic sparry calcite and micrite matrix (Plate 10.11). Fecal pellets are identified by their uniformity in size and roundness (Scholle 1978, Bathurst 1976) and occur as either spherical or elongated micrite lumps of varying sizes. The second exception occurs around Sehriban (L21) where an interlaminated calcite and what appears to be organic matter - rich layers are observed. Calcite occurs as euhedral, up to 1 cm. long, crystals grown on the dark brown organic-matter-rich layers with their long axis orientated perpendicular to these layers (Plate 10.12).

10.6 Evaporites

Evaporites are exclusively composed of gypsum and found as 20-70 cm. thick beds within lens shaped bodies of varying sizes (Plate 10.13). They are interbedded with thin mudstone beds, some of which, underlying evaporites, show subaqueous shrinkage cracks (Plate 10.14). These are distinct from the subaerial mud cracks with their narrow and poorly developed cracks and the absence of well developed V-shaped cracks (Reineck & Singh 1976). Beds of evaporites are made up of 0.1 mm. to 2 cm. long gypsum crystals with some impurities such as clay (probably illite and/or smectite), silt and sand size grains, (mainly quartz).

10.7 Conglomerates

Conglomerates are found in the NNE parts of the area studied and are yellowish brown to grey. They form structureless to graded and parallel stratified, up to 10 m. thick, beds (Plate 10.15). They show textural differences ranging from matrix-supported conglomerates (Plate 10.1) to conglomeratic sandstones. Clasts are subangular to subrounded and composed of serpentinite, radiolarite, quartzite, chert, basalt and limestones. The conglomerates are poor to extremely poorly sorted and may be classified as diamictites (Pettijohn 1975).

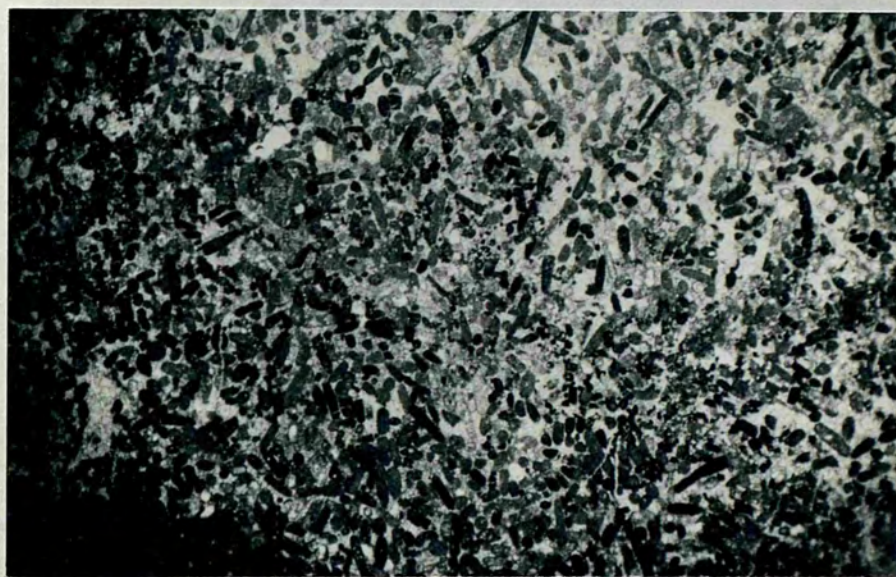


Plate 10.11 - Photomicrograph of Pelloidal limestone consists of feecal pellets within a micrite matrix which is in parts recrystallized to neomorphic sparry calcite. Sample 1305 15x.

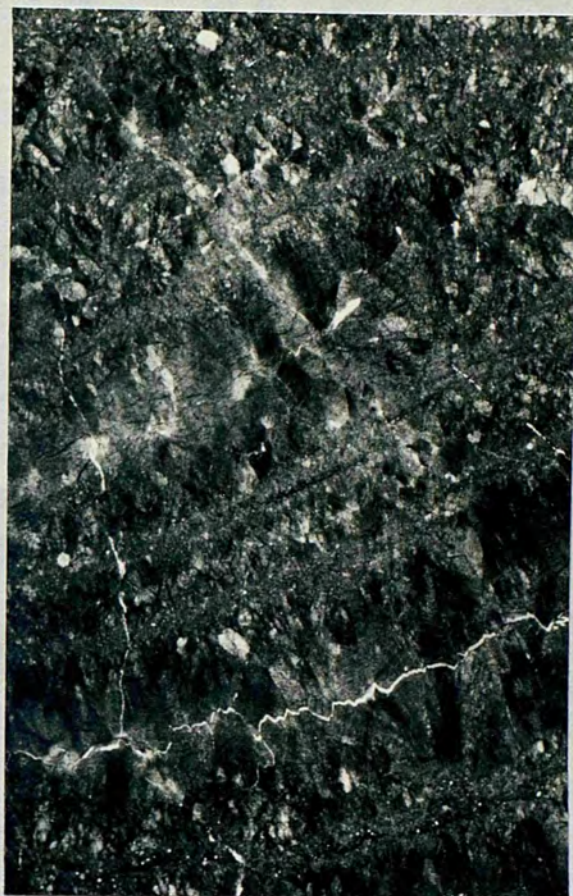


Plate 10.12 - Limestone with large calcite crystals and
organic matter rich laminae at the top.
(fine grained layer) Sample no. 147/A
15x XN

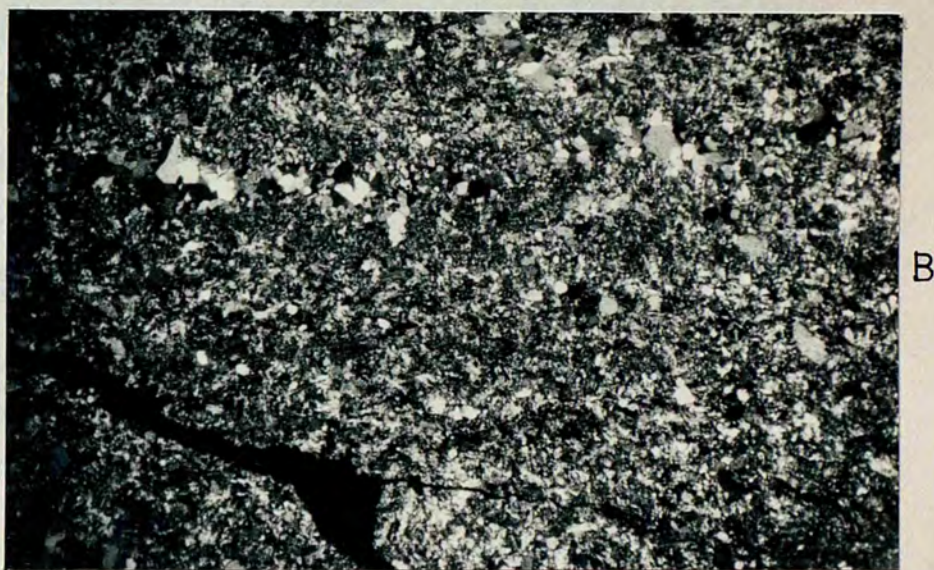


Plate 10.13 - A. A general view of evaporite lense to the SW of Cataltepe (E29)

B. Photomicrograph of evaporite. Gypsum shows reverse grading. Sample 109, 35x, XN.



Plate 10.14 - Subaqueous shrinkage cracks in the shale bed underlying an evaporite deposits. Note their narrow poor development. Hammer is 30 cm in length. Locality (C26)



Plate 10.15 - Thick conglomerate beds showing poor to well developed grading, at Karabâyırtepe (D6).

10.8 Deltaic deposit

10.8.1 General Introduction

A small deltaic deposit is observed around Korattepe (C21). It has a fan-like geometry (see map III) and consists of light brown-grey conglomerates, sandstones and green-grey shales. In the type section which is taken from the south-eastern flank of the Korattepe, a 173 m. thickness is measured. The first 74 m. of the section is made up of generally structureless but sometimes parallel laminated shale and siltstone with occasional parallel laminated sometimes graded, medium-fine grained 5-30 cm. thick sandstone beds (Plate 10.16A). Shales contain scattered benthonic foraminifers (mainly Nummulites sp, Assilina sp and Discocyclina sp). The succession grades up into a predominantly shaly sequence, in which Tabe and Ta type turbiditic sandstone beds intercalating with shales and occasional lens shaped matrix-supported conglomerate beds (Plate 10.16B) in the succeeding 33 m. of the section. In this sequence slump folds of various sizes and shapes are observed. The next 12 m., consists of an upward coarsening sequence. This sequence starts with interbedded siltstone and shales with occasional fine grained sandstones and becomes a medium to coarse grained sandstone, sometimes granule conglomerates towards the top (Plate 10.17). These upward coarsening cycles are occasionally cut by coarse to medium grained structureless sandstone beds with obvious erosional bases. Above, the interbedded shales, siltstones and medium to fine grained sandstone beds with parallel laminations, microcross lamination and parallel stratifications, with a number of conglomerate and medium to coarse grained sandstone lenses (Plate 10.18) represent the next 32 m. of the section. These lenses show erosional bases, are 80 cm. to 2.5 m. thick with up to 36 m. in lateral extension and either massive at the base and parallel laminated at the top (Plate 10.19) or trough cross-bedded. (Plate 10.20). The remaining 22 m. of the section consists of Kizildag formation-type red mudstone and sandstone with occasional channel-fill conglomerates and sandstones of meandering stream origin (see Chp. 9). In their



- Plate 10.16 - A) Interbedded shale and Tabe and Tae type turbiditic sandstone beds with lens shaped matrix-supported conglomerate. The distorted sandstone bed at the lower right of the photograph is due to slumping.
- B) Close-up view of the matrix-supported conglomerate lense in the middle of A. Note the chaotic nature of conglomerate which grades up into the massive sandstone and upward projecting of clasts. Type section (see text)



Plate 10.17 - An upward coarsening cycle in the type section. Note the parallel laminated shale and silt stone at the base and conglomeratic sandstone towards the top.



Plate 10.18 - Laminated and wave-ripple cross laminated (at the right of the photograph) siltstone and shale, eroded in their upper boundary of a channel fill conglomeratic sandstone. Locality (D 21).



Plate 10.19 - Showing distributary channel-fill deposits. Note the size of the boulders at the base of the conglomerate lens which is 2.4 m. thick in A and parallel bedding in B. Localities (C20&21)

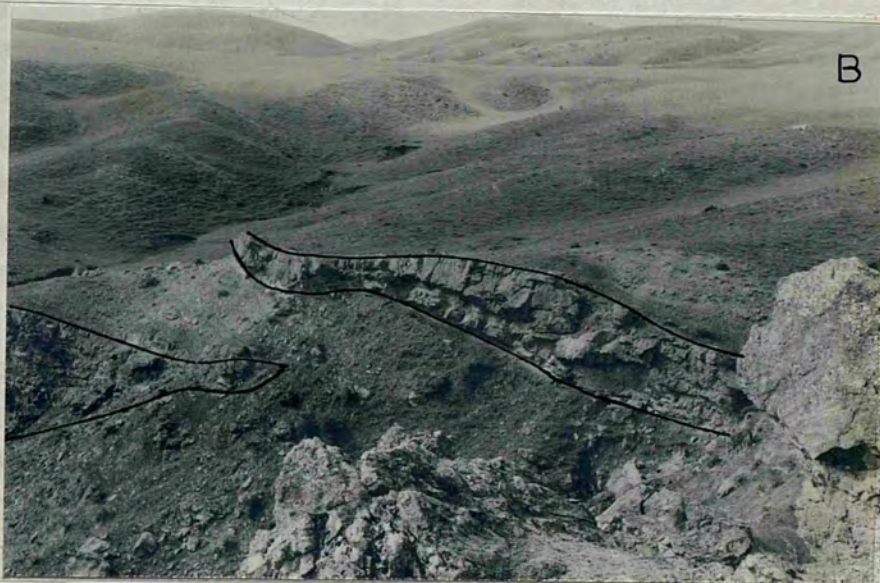


Plate 10.20 - Two trough-cross bedded distributary channel-fill deposits. Note the grading of each set from conglomerates to sandstone in A (bed is approximately 1.8 m. thick), and two channel-fill sandstone beds separated by interdisturbance sandstone, siltstone and shale beds in B (the upper bed is 1.5 m. thick in its thicker part) Localities. A (D20) B (C21)

lateral extension, 1-3 m. thick lens shaped evaporites are also observed.

10.8.2 Lithologies of the deltaic deposit

10.8.2.1 Conglomerates

They occur in two different types. The matrix supported conglomerates which occur as 50 cm. to 2 m. thick lens shaped beds with irregular lower and sharp upper contacts, sometimes graded up into massive sandstone beds are composed of gravel and boulder size, subrounded to rounded, limestone, quartzite, serpentinite, radiolarite and volcanic rock clasts within a coarse to fine grained sand and silt size poorly sorted matrix. The matrix contains abundant benthonic foraminifers and is compositionally similar to the sandstones. These beds, on the basis their matrix supported, chaotic nature and the presence of upward projecting clasts and marine fossils, are interpreted to be deposited by subaqueous debris flows (Middleton & Hampton 1976). The clast supported conglomerates again occur as lens shaped beds with thicknesses of 50 cm. to 3 m. but show well developed sedimentary structures. The most common one is trough cross stratification, in which each set shows grading at the conglomeratic base and parallel lamination towards the sandy upper part. Less commonly they are structureless at the base and show parallel bedding and lamination towards the top with a decrease in grain size. The size of the clasts and composition of the conglomerates are generally similar to those of matrix-supported conglomerates, except the occurrence of foraminifers which are only present in a few conglomerate beds of this type.

10.8.2.2 Sandstones

Tabe and Tae-type turbiditic sandstones are 10 cm. to 50 cm. thickly bedded, show grading and parallel lamination with poorly developed flute casts and other sole marks, the former indicates radiating current directions generally from W, NW and N. Grain sizes in these sandstones range from coarse

to fine, which positively correlates with bed thickness, and they are poor to moderately sorted and consist of subangular to subrounded quartz, quartzite, metaquartzite, radiolarite, basalt, chert, limestone and feldspar fragments together with broken shell and large benthonic foraminifers. Quartz occur as common, volcanic and metamorphic quartz and is generally more angular than the other grains. Feldspars are predominantly labrodorite plagioclases and usually subangular. The matrix is made up of chlorite, micrite and less commonly iron-oxide and is poorly sorted. Cement is rarely found and is exclusively calcite. Neomorphic sparry calcite is also observed, sometimes corroding the detrital fragments.

Other types of sandstones (parallel bedded, upward coarsening, parallel laminated and trough-cross bedded) show similar textural and compositional properties to those described above and parallel laminated sandstones (with the exception of those found in the sandstone and conglomerate lenses) sometimes show micro cross-lamination, generally medium to fine grained and are relatively better sorted.

10.8.2.3 Siltstones and shales

Siltstones are dusky yellow green (5 GY 5/2) to greyish green (5 G 5/2), 1 mm. to 2 cm. thickly laminated to 10 cm. thickly bedded and show sharp upper and lower contacts. Parallel lamination and less commonly wave-ripple lamination is observable but generally they are structureless. Quartz grains with abundant chlorite are the only positively identifiable fragments in thin sections.

Shales are greyish olive green (5 GY 3/2) to greyish green and occur as millimetre thick laminae to 2 m. thick beds. They are structureless, poorly laminated or finely laminated and in XRD analysis show calcite, quartz, chlorite and mica minerals as main constituents.

10.8.3 Interpretation

The presence of large benthonic foraminifers and their good preservation imply an in-situ fossilization of these organisms which together with the gradual passing up of these sediments to the continental deposits of the Kizildag formation suggests that they were deposited within a shallow marine environment. As can be seen from the type section, an overall increase in grain size, indicating increasing energy conditions and a change from marine to continental conditions together with their fan-like geometry, (Plate 10.21), suggest that these sediments were deposited by a prograding delta (Reineck & Singh 1975, Selley 1976, Elliot 1980). This conclusion is further supported by detailed facies analysis of these sediments. The occurrence of shale and siltstone succession with marine fauna at the base of the section, indicate a low energy environment and deposition mainly from suspension and is interpreted as prodelta deposits accumulated within quiet marine conditions. Succeeding this sequence, the shale dominated but turbiditic sandstone and debris flow conglomerate containing succession, indicate an increasing energy condition. This together with the presence of slump folds suggest an inclined surface of deposition. Thus the succession is thought to be deposited on the lower part of the delta slope which was most probably steep. The occurrence of turbiditic sandstone beds and debris flow conglomerates imply that sands, gravels and boulders deposited on the edge of the subaqueous delta platform were slumped down to deeper parts causing turbidity currents and debris flows. Although there could be a number of reasons for the slope instability, rapid deposition and earthquake shocks appear to be the two most likely causes of instability as indicated by coarse grain size of conglomerate lenses and the presence of slump folds (Plate 10.22). The upward coarsening succession overlying the above sequence is believed to be characteristic of the upper delta slope facies (Selley 1976). The cross bedded and structureless but parallel bedded erosionally based conglomerate and sandstone lenses with their radiating pattern suggest that they were deposited by a high energy current which was capable of erosion and carrying

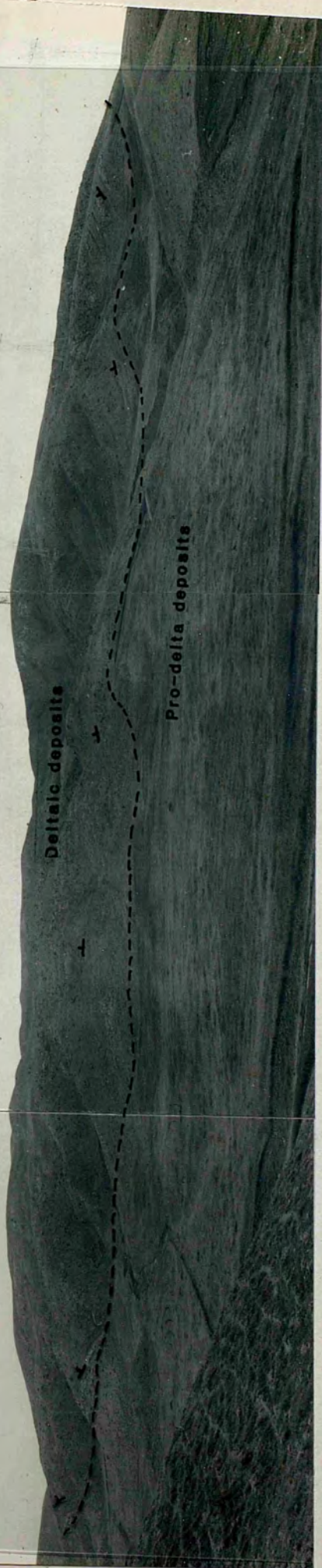


Plate 10.21 - A panoramic view of the deltaic deposits around Karattepe looking from the S. Note the changing of strike NW - SE at the left of the photograph to N-S in the right



Plate 10.22 - Showing slump folds in the eastern flank of the Korattepe looking towards the S. The sense of facing directions of folds are generally to E.

large size boulders to be distributary channel-fill deposits on the delta platform. Wave ripple cross laminated siltstones, parallel laminated sandstone and shale within these channel deposits, indicate that they were deposited on the interdistributary areas of the delta platform. The occurrence of evaporites together with the absence of swamp deposits or coal measures, on top of the deltaic sequence suggest that the climate was arid and hot so that no appreciable vegetation was present during the deposition of these sediments. An additional conclusion can be drawn from the shape of the deltaic deposit and abundance of shale and siltstones in these sediments that delta was built in low-wave energy conditions and fluvial process was dominant during the building of the delta.

10.9 Age of the Keklikpinari formation.

Abundant large benthonic foraminifers are found in the rocks of this formation and they are identified by G.C. Adams (Pers. Comn. 1982) as being.

Assilina sp

Discocyclina sp

Fasciolites sp

Nummulites sp

Nummulites spp (of Middle Eocene type)

Sphaerogypsina globula (Reuss)

Orbitolites sp

Asterocyclina sp

and a Middle Eocene age is proposed. In addition Arikan (1975) reported that the conglomerates of this formation in their upper part (around Ankara) reveal an Oligocene age on the basis of pollen analysis. Thus a Middle Eocene to probably Oligocene age is designated for this formation.

10.10 Source area and environment of deposition

The compositional similarities of the formation to the Kizildag formation, suggest that the source areas for these

sediments were the same as those described in the Kizildag formation (9.10)

The interfingering of this formation with the continental deposits of the Kizildag formation, the occurrence of deltaic deposits associated with these sediments, well preserved marine fauna and a number of sedimentary structures which are believed to be formed in shallow water environments (see below) suggest that they were accumulated in a shallow marine environment of deposition.

Shales and siltstones which are the predominant lithological types of this formation, with their large benthonic foraminifers which indicate 0-40 m. depth in temperal and tropical seas (Murray 1983) and oyster (Gryphea-shaped oysters are characteristically found in low energy muddy environments (Stenzel 1971)) fauna were deposited in a shallow marine low energy environment. This is also suggested by their fine grain size and generally structureless to parallel laminated stratification. This together with the general absence of wave ripples indicate that these sediments were deposited below wave base. The gently dipping laminated sandstones are thought to be deposited on uppershore face-beach environments as indicated by their intertonguing with the continental red siltstone and mudstones and their good lateral continuity, moderate sorting and gentle inclination of parallel laminated sandstone sets towards the west which is believed to be the seaward side. All these features are considered to be characteristic of coastal sand deposits (Heckel 1972, Howard 1972, Reineck & Singh 1975, Elliot 1980). The occurrence of sandstones and conglomeratic sandstones forming upward fining sequences, foraminiferal packstones and sheet-like sandstone beds within shale-siltstone successions were most probably the result of storms. This is suggested by the following lines of evidence:

- a. deposition of these lithologies in waning energy conditions as indicated by the presence of coarse grained sand-

stone and/or conglomeratic sandstone or conglomerates at the base of the upward fining sequences grading up into medium to fine grained parallel laminated, hummocky cross stratified or wave ripple laminated sandstones and grading at the base and parallel laminated in the upper parts of the sheet-like sandstones and foraminiferal packstones,

b. the presence of sharp and erosional bases which most probably resulted from scouring (which is also indicated by the occurrence of intraformational pebbles) during storms or sudden onset of deposition from storm-suspended sediment, and gradational tops of these lithologies,

c. the occurrence of lag deposits which contain the same fauna as found in the under and overlying shales, in the upward fining sequences. (This is one of the main differences between turbidity current deposited beds and storm deposits, since turbidities contain transported fauna which is completely different from the fauna of the interbedded shales),

d. the abrupt gradation from lag deposits to suspension deposits in the upward fining sequences in contrast to continuing gradation of turbidite beds from coarse to fine grained sediments,

e. the presence of thickness changes in the beds along the strike,

f. interbedding of these lithologies with fair weather deposits (siltstones and shales),

g. the occurrence of limestone boulders which also indicates storm activity

The compositional difference between foraminiferal packstones and grain size and thickness differences between the upward fining sequences and sheet like sandstone beds may be best explained by:

a. availability of type of sediment,

b. energy level and direction of storms relative to the shoreline, and

c. depth of water (Johnson 1980).

Recent and ancient sedimentary rocks showing similar stratigraphical settings and sedimentary structures to this formation have been reported and were interpreted to be deposited storm and wave dominated shallow seas (Reineck & Singh 1975, Kumar & Sanders 1976, Johnson 1980, Kresia 1981).

The micritic limestones, on the basis of their close association with evaporites and the presence of dolomite crystals which is believed to indicate increased salinity of the water in the environment of deposition (Blatt et al 1972, Bathurst 1976) together with their fine grain size and the vertical and horizontal burrows, were deposited within a restricted quiet water environment, which most probably were marginal pools.

Thick evaporite deposits occur as laterally extensive but lens shaped bodies. Evaporites are thought to have been deposited in short lived offshore shoal basins at times of lower sea level (Blatt et al 1972). This conclusion is suggested by their association with shallow water shales and siltstones. There is no evidence for emergent barrier islands or bars which would have created long lasting lagoons.

The conglomerates, found in the NNW part of the area and with limited exposure, are difficult to interpret. However considering the absence of fossils, the poor to extremely poor sorting and their sometimes matrix-supported nature, together with the occurrence shale interbeds, suggest that they are deposited in a transitional environment between shallow marine and an alluvial fan environment when continuing uplift of the Ankara Melange in the NNE (see Chp. 12) contributed abundant amounts of coarse clastics to alluvial fans which were most probably very close to the basin. Sediments, probably transported by debris flows, streams and sheet floods, were dumped into the apparently low energy sea which was not capable of reworking them. The most probable cause of the turbidite beds in this part of the area, is the mobilising of the previously deposited sand size material by turbidity currents.

The decrease in the diversity of foraminiferal species and the absence of oysters in the stratigraphically upper part of the formation, may additionally conclude that:

a. increased depth, which appears to be unlikely due to presence of *Discocyclina* and the absence of planktonic foraminifers, or

b. increased salinity, this seems to be more probable as *Gryphiadae* oyster has little tolerance for changes in salinity (Steckel 1971).

CHAPTER 11

STRUCTURAL GEOLOGY

11.1 Introduction

The Bala area being within an extensively tectonized region (Fig 11.1) shows a very complex structural pattern. The existence of abundant gravity-induced folding and related faulting in some formations of the area further adds to this complexity. However once these syn-sedimentary structures are differentiated a relatively less complex structural pattern may be accomplished. Because the detail structural geology of the area is out of the purpose of the present thesis only a general outline of it, established during the mapping, will be given in the following pages.

The present structure of the area studied can be divided into three major structural units.

a. Ankara Melange, extremely complex internal structure of this unit has not been studied. However it is thrust upon to the second unit with series of reverse faults with dip of 50° - 60° . (Norman 1973)

b. Second unit contains Maastrichtian to Middle Eocene sedimentary rocks and is extensively tectonized. In this unit a number of asymmetric and overturned folds and reverse faults which are approximately parallel to the axis of the folds and later developed strike-slip or oblique fault cutting the previous structures are observed. Although the axis of the folds show local variations, they are generally in NE-SW direction..

c. Third unit contains Middle Eocene to probable Oligocene Kizildag and Keklikpinari formations and it is relatively less disturbed although folds and fault of various types striking NE-SW and N-S directions can be observed.

11.2 Syn-sedimentary structures

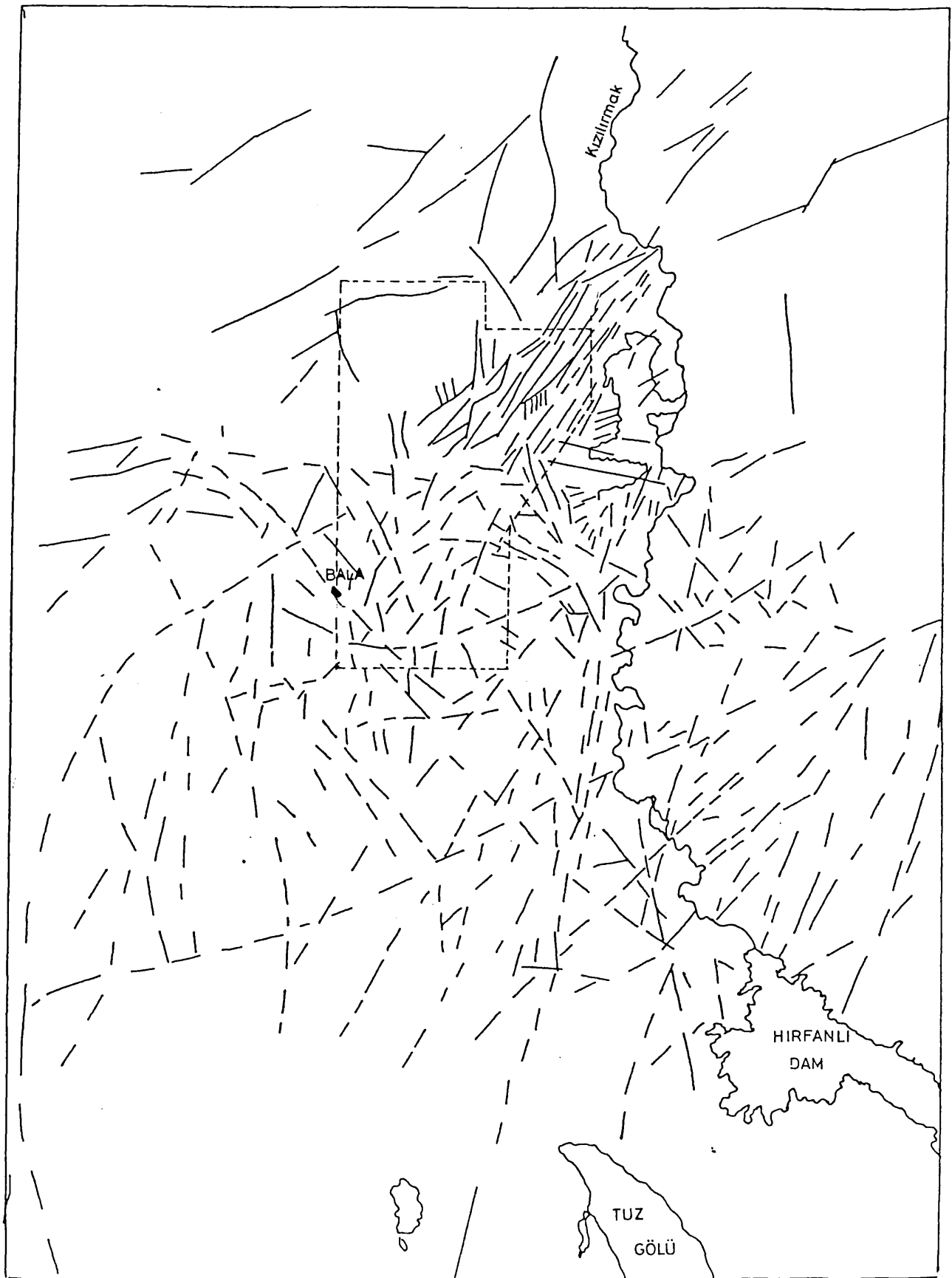


Fig 11.1 - Map shows the tectonic lines drawn from the land-sat aerial photographs. The area studied is also shown.

A. Slump folds

As was mentioned in the foregoing chapters slump folds either in small or large scale are widespread in the deep marine sediments of the Bala area. These folds show variable style, varying wave lengths and are sometimes found between undisturbed beds. Although in the majority of cases preferred orientation of fold axes are parallel or slightly oblique to the general NE-SW tectonic strike (see Map II), on the existence of following features these are identified as slump folds.

- a. the folds occur between undisturbed beds
(This observation is commonly made in folded zones up to 30 m. thick).
- b. Variable and irregular fold style; i.e. an open fold, followed by an isoclinal or recumbent fold (see App. X Salideresi sketch section).
- c. a welded contact between fold and the overlying sediment exists
- d. a shear plane occurs between the folds and the underlying beds.
- e. erosion of the upper part of folds are present (Plate 8.10).
- f. sediment draping is observed
- g. development of cleavage at the hinge of the folds are absent, indicating soft sediment deformation.

B. Pseudo-anticlines and synclines and depositional dip.

The pseudo-anticlines and synclines are commonly observed in the Kizildag formation, as gentle undulatory structures. Their fold axes can be vertical, oblique or parallel to the general tectonic trend and they are believed to have been formed due to the irregularities of the depositional surface. Two of such folds are also observed in the Kocanindambasi formation at the southeastern flank of the Arslangur T (J23). Their fold axes are NW-SE in direction, perpendicular to the general NE-SW tectonic trend.

The abrupt changes of dip and sometimes strikes of the beds in close proximity in the Kizildag formation and the beds of the turbidites overlying the slump sequences were most probably resulted from palaeotopographical irregularities. Thus they are believed to be depositional rather than tectonic in origin.

11.3 Tectonic structures

11.3.1 Folds

As was mentioned earlier, several large and small folds are observed in the Bala area. In the second unit they are mainly of parallel style, asymmetric or overturned folds, inclining to the SE and trend NE-SW direction in the NE of the area studied and gently curve to NNE-SSW direction in the SW. where they are relatively less tightly folded than those in the NE. The folds are continuous for many kilometres with slight undulation of their hinge lines along their course. In some occasions probable small parasitic folds (the nature of these folds are difficult to determine as they are closely resembled to slump folds. However they can be differentiated in good continuous exposures by their consistency in folding style) formed on the northwestern limbs of the anticlines are observed. The folds are unexceptionally plunges to the SSW with angles of 20° - 50° . The most exceptional of them is observed between Kamislibala and Kamislizir where only the overturned southeastern limb of an anticline involving more than 1200 m. thick sediment is observed. It is either a recumbent or an overturned fault (This cannot be ascertained because the northwestern limb of the anticline could not be observed). and is bounded with a reverse fault on the southeastern limb.

Folds in the third unit are symmetrical to asymmetrical and show different directions in the southeastern and western exposures of the third unit. In the former area folds are usually NE-SW direction parallel to the general trend and more tightly folded than those which occur in the

latter area where folds extend in a NNE-SSW direction.

11.3.2 Faults

In the area studied numerous and generally high angle faults are observed. They can be divided into three groups. A- Reverse faults, B- Strike-Slip faults and c- Normal faults.

A. Reverse faults: They are the most common fault type found in the Bala area and are only observed in the second structural unit. The reverse faults generally trend in a NE-SW direction, closely following the trends of the folds and the majority of them extend many kilometres dipping to the NW with an angle of 50° - 75° . Although most of these faults appear to be high angle faults (Plate 11.1), some of them give an impression that they are curving underneath the surface. A good example for these sort of appearances is observed within the Davdanli formation around Davdanli (J10). As it can be seen in (Plate 11.2) beds on the left of the photograph, before the reverse fault which dips towards the NW with an angle of 72° , form a bench fold probably indicating that the faults are parallel to the bedding. This resembles to a ramping structure. The only relatively low angle reverse fault in the area is the Degirmendere fault (see Map II) which is approximately 28 km. long, extending from the north of Goksuderesi (U6) in the N to the southwest of Ucem (G27) in the S and dips towards the NE with an angle of 25° - 45° . Another important reverse fault is the Kurebogazi II fault (see map II), not only because of its great lateral extend but also its implied strike-slip component. (see section 13.4). It is about 40 km. long dipping towards the NE with an angle of 70° - 85° and faithfully marks the lower boundary of the Saridere volcanic formation along the southeastern margin of the basin. The vertical displacement of the fault is difficult to calculate because of poor exposure and probable strike-slip movement. However in the area between Kurebogazi (V8) and Sarikaya (Q14) vertical displacement of at least 116 m. can be suggested on the basis of the Saridere volcanic formation's thickness.

B. Strike-slip faults: These faults are found in

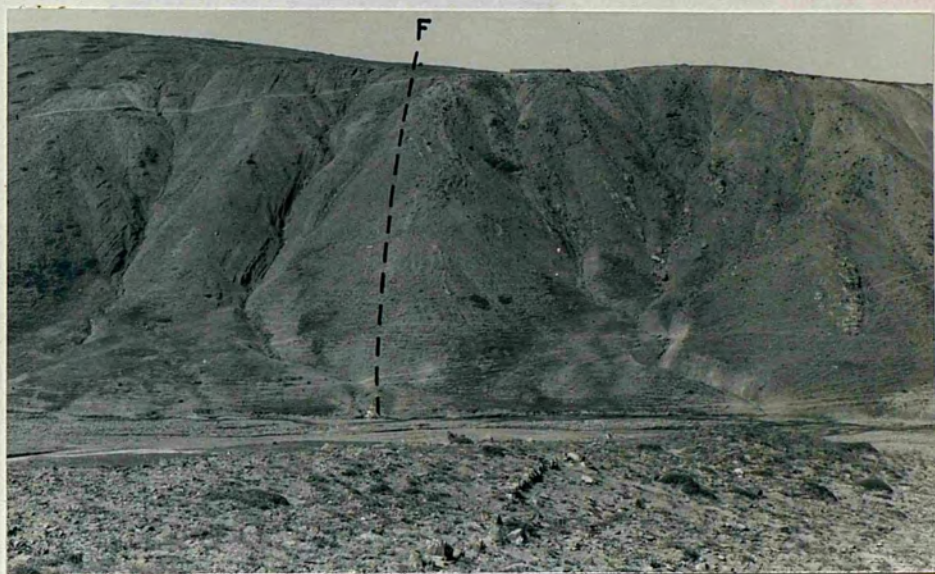


Plate 11.1 - Shows a high angle reverse fault in the boundary between the Kamisli and Davdanli formations. Locality (I10).



Fig 11.2 - Shows a reverse fault around Davdanli (J10). (see the text for explanation.

both (second and third) structural units cutting the reverse faults and/or folds with an angle varying from oblique to right angle. They are especially predominant within the Kamisli and Davdanli formations, in the north of the area studied and along the southeastern margin of the basin. They are found branching off from or cutting each other. The most important strike-slip fault is the sinistral K. Bayat fault which extends from the northeast of Kamislibala (M6) to the east of K. Bayat (L18) and is 14 km. long. It dips to the west with an angle of 75° - 88° and has an offset of approximately 1.5 km.

C. Normal faults: The normal faults are the least common fault types in the Bala area. They generally occur parallel to the general NE-SW tectonic trend and are high angle faults (Plate 11.3). The Kurebogazi I fault is the most important normal fault observed in the area. It occurs parallel to the Kurebogazi II fault and implies a strike-slip movement too. It extends from Kurebogazi to the northeast of Sarikaya (S13) dipping towards the NW with an angle of 75° - 88° and marks the boundary between the Ankara Melange and Sarikaya member.



Plate 11.3 - A normal fault within the Bayat formation.
Locality (G17).

C H A P T E R 1 2

PALAEOGEOGRAPHY and SEDIMENTARY
HISTORY of the BALA BASIN

As was mentioned earlier, the Bala basin is one of the number of small basins, evolving on the northern margin of the Kirsehir Block (see Ch. 13) during Upper Cretaceous-Tertiary times and which periodically were connected to each other (see below, Norman *et al* 1980, Arikian 1975). The area under consideration is believed to have developed after the Late Cretaceous (see 13.2) on the active northern margin of the Kirsehir Block and went through subduction, oblique subduction, transform fault and continent to continent collision stages as the block rotated through 90° anti-clockwise.

The Ankara Melange forms the basement. However because the boundary between this and the Upper Cretaceous-Tertiary rocks is faulted in the area studied and is controversial in other areas, the nature of the relationship between these two is not known. Nevertheless two hypotheses can be proposed.

a. The first is based on Norman's (1972) observations that a transitional boundary exists between the Unit II of Ankara Melange (see 1.6) and the counterpart of the Kamisli formation in the Kirikkale area. In this case it can be suggested that the Unit II of the Ankara Melange is the earliest deposits of the Bala basin which was either a fore-arc basin or a basin which was first formed during the advancement of the Bozkir Ophiolitic Nappe (Unit I of Ankara Melange see 1.6 and Chp. 13) causing a number of depressions in front of the advancing nappes due to difference of crustal loading, and which later became a fore-arc basin as subduction of northern Neo-Tethys beneath the Kirsehir massif started.

and b. based on the supposed existence of a disconformity between the two sequences described above, which most probably indicates that the Bala basin was first formed at the beginning of the Maastrichtian as a fore-arc basin due to above mentioned subduction. At present it is difficult to favour one of these suggestions at the expense of the other.

The depositional history of the Bala basin started during the Maastrichtian with the eruption of the Saridere volcanics on the margin and the deposition of the Kamisli formation within the basin. The Saridere volcanics (andesites, dacite and their pyroclastics associated with alluvial fan deposits) were deposited on the southeastern margin of the basin from subaerial volcanoes. The gradual thinning of tuff from NE to SW may indicate that volcanic centre was towards the NE.

Some general conclusions concerning the nature and origin of the Saridere Volcanic rocks and the volcanic rock clasts of the Kamisli and Degirmendere formations (which are believed to be derived from the Saridere volcanic formation due to their close resemblance in chemical and mineral composition (See 3.10, 5.9 and Table 12.1), may be drawn from their chemical compositions. Because of alteration of the mafic minerals in some of these rocks and in order to achieve simplicity, a chemical compositional classification proposed by Gill (1981) is preferred (in which rocks with SiO_2 values less than 53% are classified as basalts, 53%-63% andesites, 63%-73% dacites and more than 73% as rhyolites) to other classifications, one of which is shown in Fig(12.1). In this $\text{Na}_2\text{O}+\text{K}_2\text{O}$ values are used against SiO_2 values and rocks were found to be trachy-andesite, dacite rhyolite, andesite and trachybasalt in decreasing order of abundance. (Although Na_2O and K_2O are likely to be affected by low temperature alteration, tight clustering of the results in Fig 12.2 suggests that the effect of the alteration is not significant). When these rocks are plotted in an AMF diagram (Fig 12.2) they

Sample No	(1) 267C	(2) 267D	(3) 386	(4) 238	(5) 552-II	(6) 768	(7) 267A	(8) 227	(9) 552-I	(10) 767-II	(11) 769-I	(12) 590
SiO ₂	75.47	74.60	67.67	64.94	63.47	61.42	61.66	58.70	57.80	57.15	56.83	55.78
Al ₂ O ₃	13.24	13.12	15.88	16.92	14.53	19.22	16.60	16.40	17.09	17.04	17.53	15.98
MgO	0.10	0.30	0.60	0.45	1.45	0.39	0.45	0.85	0.56	1.32	1.50	1.12
MnO	0.05	0.05	0.03	0.10	0.11	0.06	0.07	0.05	0.07	0.14	0.07	0.15
Fe*	1.75	1.75	3.76	5.60	6.15	7.82	6.24	6.34	5.51	7.38	6.25	6.45
TiO ₂	0.11	0.11	0.50	0.50	0.58	0.62	0.50	0.53	0.55	0.56	0.56	0.53
CaO	1.48	1.74	2.91	3.05	3.18	3.30	4.65	5.91	7.73	7.36	7.45	7.82
K ₂ O	5.25	4.80	4.78	4.50	3.66	5.70	4.05	5.10	3.90	4.02	4.11	4.63
Na ₂ O	3.14	3.00	2.38	3.60	1.79	0.57	3.16	2.96	3.72	2.90	3.61	4.41
P ₂ O ₅	0.03	0.03	0.16	0.16	0.16	0.18	0.15	0.17	0.18	0.21	0.20	0.20
Total	100.62	99.50	98.67	99.82	95.08	99.28	97.53	97.01	97.11	98.08	98.11	97.07
Total Fe as FeO	1.57	1.57	3.38	5.04	5.53	7.04	5.61	5.70	4.96	6.64	5.62	5.80
K ₂ O + Na ₂ O	8.39	7.80	7.16	8.10	5.45	6.27	7.21	8.06	7.62	6.92	7.72	9.04

Trace elements (ppm)

Th	34	34	18	26	20	27	24	24	29	24	18	19
Nb	19	16	10	13	13	11	14	12	14	11	9	12
Y	14	17	25	13	24	18	19	20	21	15	22	23
Sr	117	115	431	510	316	545	403	366	488	591	563	665
Rb	226	221	127	136	117	158	140	202	129	142	132	89
Zr	136	128	139	125	135	141	134	161	133	138	134	134

Fe* : Total Fe as Fe₂O₃

Table 12.1 - Chemical composition of the Bala Basin Volcanic Rocks (BBVR). 1&2: rhyolite 3-5: dacite, 6-12: andesite 590 from the VRC of the Kamisli formation, 238, 386, 767II, 768 and 769-I are from Saridere Volcanic Formation and 227, 267A, C&D and 552 I&II are from the VRC of the Degirmendere formation.

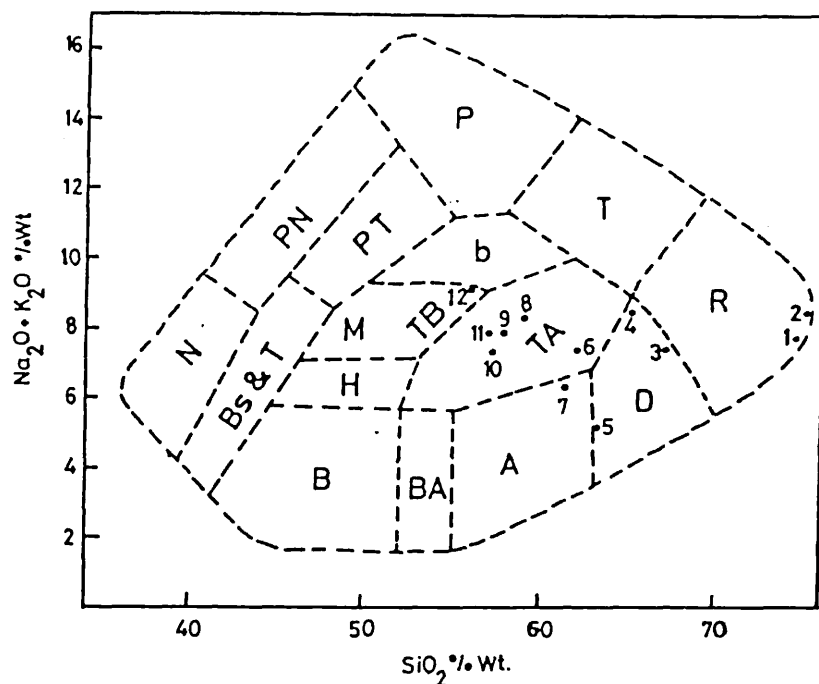


Fig 12.1 - SiO_2 vs $\text{Na}_2\text{O}+\text{K}_2\text{O}$ diagram for the chemical compositional classification of BBVR. N: Nephelinites, PN: Phonolitic Nephelinites, P: Phonolites, BS&T -Basanite and terphrites, PT: Phonolitic tephrites, B: Benmorioites, M: migaerites, TB: Trochy basalts, T: trochytes, TA: Trochyandesites, R: Rhyolites, D: Dacites, A: Andesites, B: Basalts, BA: Basaltic andesites, H: Howaiites (After Cox et al 1979)

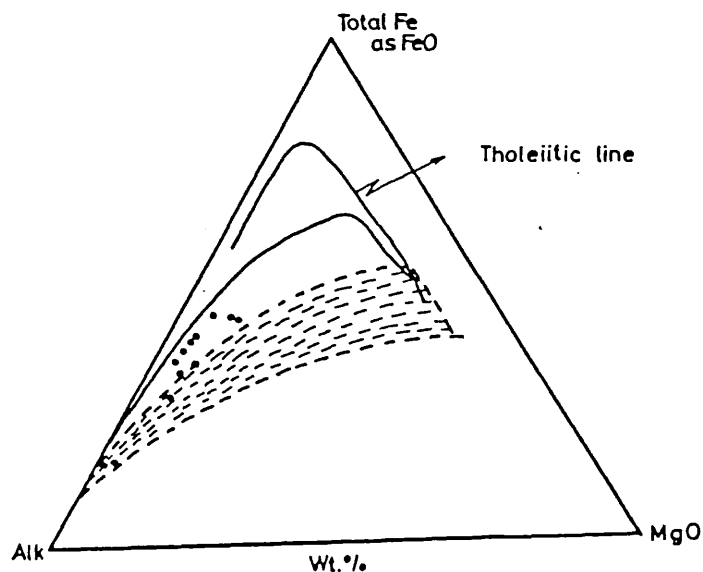


Fig 12.2.- AMF diagram. (See text for explanation)

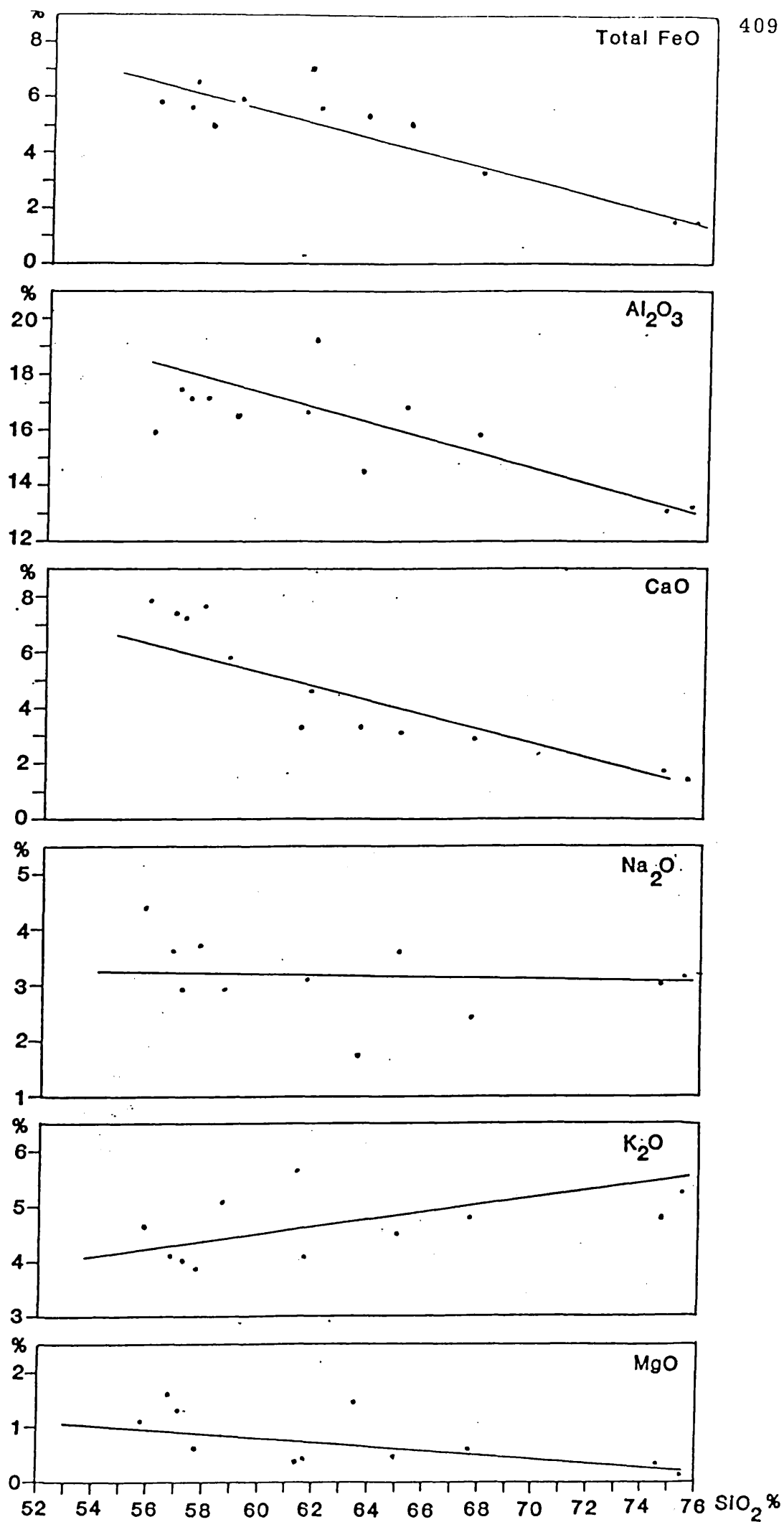
fall along a line intermediate between tholeiitic and calc-alkaline trends due to low MgO which most probably resulted from the alteration of mafic minerals. Nevertheless the presence of an andesite-dacite-rhyolite* suite with the absence of alkali-suite volcanic rock types (alkali olivine basalt, hawaiite, mugearite) leads to a conclusion that they can be considered as high-K, calc-alkaline type volcanic rocks (Hatch et al 1972, Jakes & White 1972). This conclusion is further supported, when the chemical composition of the Saridere volcanics and volcanic rock clasts of the Kamisli and Degirmendere formations (from here on they will be referred as Bala Basin Volcanic Rocks (BBVR)) are compared with those of modern and ancient calc-alkaline suites. As is shown in Table 12.2, although major element values of the BBVR differ from the calc-alkaline rock suites, average major element values within a given SiO_2 range show comparability in total Fe (as FeO), MgO , K_2O , TiO_2 and CaO when these oxides are plotted against SiO_2 . In both the island arc calc-alkalines and the BBVR, while K_2O is increasing with increasing SiO_2 the FeO , MgO , TiO_2 and CaO content shows an inverse correlation with SiO_2 . However Na_2O is almost constant in the BBVR while this oxide correlates positively with SiO_2 in island arc calc-alkaline volcanic rocks (Fig 12.3). The most obvious differences occur in Al_2O_3 which correlates positively with SiO_2 in calc-alkaline suites in contrast to a negative correlation between Al_2O_3 and SiO_2 in the BBVR.

The absolute trace element abundance in the BBVR also favours their calc-alkaline origin. In Table 12.3 the BBVR always show higher trace element values than the island arc tholeiites. In particular, high Rb, K and Sr with relatively low Nb values are typical of calc-alkaline magmas (A. Saunders pers.

*Rhyolites are only found in the VRC of the Degirmendere member and their absence in the Sarikaya volcanic formation is believed to have resulted from their complete removal by erosion during the depositional period of the Bala basin.

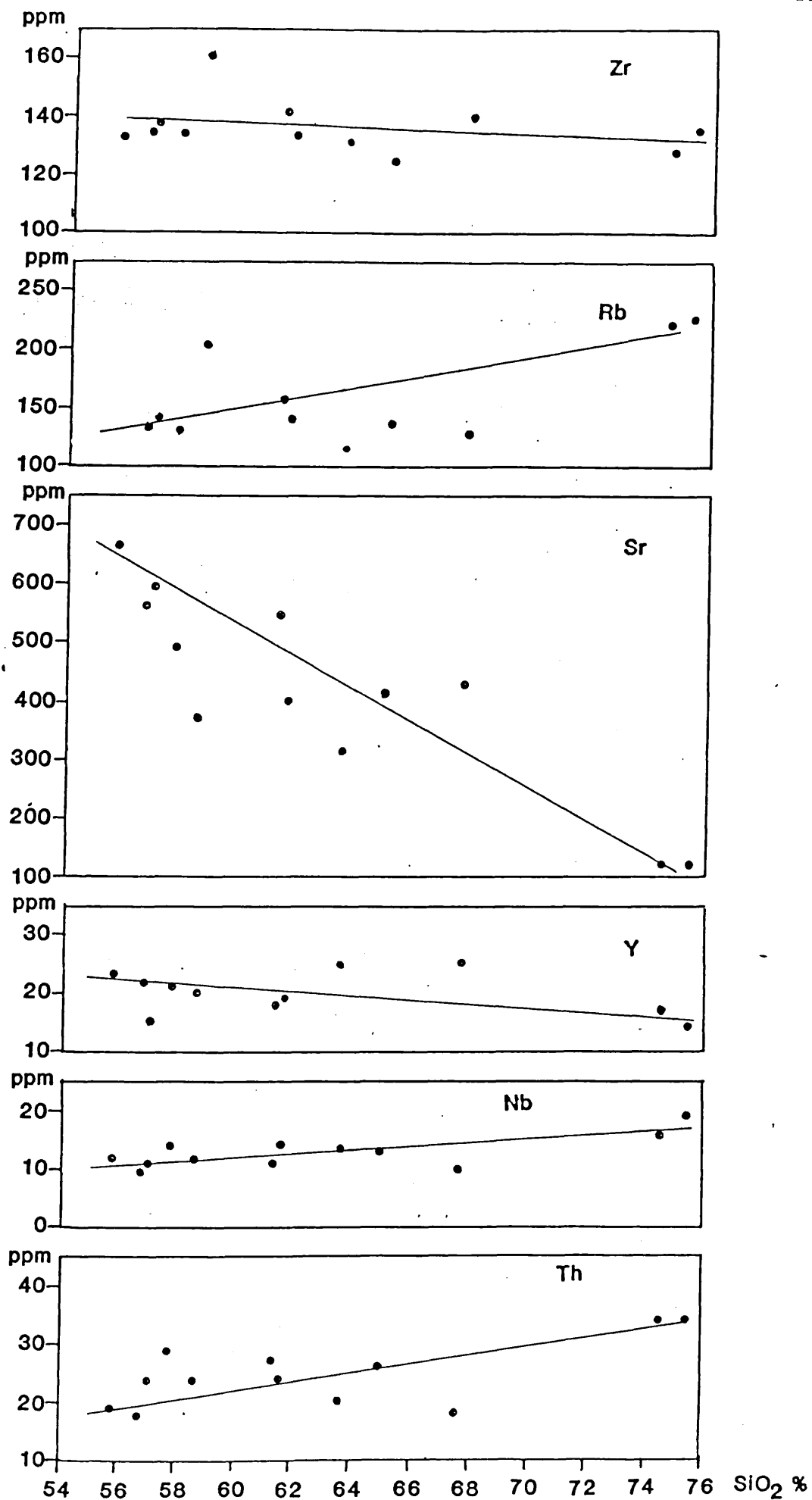
	Island arc tholeiites			Calc-alkaline rocks								
	Basalt	Tholeiitic andesite	Tholeiitic dacite	High-Al basalts	Low-Si andesite	Low-K andesite	Andesite	High-K andesite	Dacite	Trachy-basalt	*Trachy-andesite	+Dacite
SiO ₂	51.57	57.40	79.20	50.59	54.54	59.05	59.64	58.52	66.80	55.78	58.43	66.30
TiO ₂	0.80	1.25	0.23	1.05	1.13	0.69	0.76	0.76	0.23	0.53	0.54	0.50
Al ₂ O ₃	15.91	15.60	11.10	16.29	16.26	17.07	17.38	16.20	18.24	15.98	16.93	16.40
Fe ₂ O ₃	2.74	3.48	0.52	3.66	2.31	3.90	2.54	2.93	1.25	6.45	6.34	4.68
FeO	7.04	5.01	0.90	5.08	5.40	2.57	2.72	3.28	1.02	-	-	-
MnO	0.17	-	-	0.17	0.12	0.15	0.09	0.09	0.06	0.15	0.08	0.06
MgO	6.73	3.38	0.36	8.96	6.97	3.25	3.95	4.14	1.50	1.11	0.64	0.55
CaO	11.74	6.14	2.06	9.50	7.50	7.09	5.92	5.59	3.17	7.82	6.62	2.98
Na ₂ O	2.41	4.20	3.40	2.89	3.64	3.80	4.40	3.64	4.97	4.41	3.27	2.98
K ₂ O	0.44	0.43	1.58	1.07	1.49	1.27	2.04	2.67	1.92	4.63	4.23	4.64
P ₂ O ₅	0.11	0.41	-	0.21	0.23	0.20	0.28	0.25	0.09	0.20	0.18	0.16

Table 12.2 - Major element abundances in volcanic rocks of island arcs (Jakes & White (1972) and BBVR. Trachybasalt, trachyandesite and dacite are classified according to classification shown in Fig 12.1.
*,+: average composition of trachyandesites and dacites of BBVR.

Fig 12.3 - SiO_2 vs Oxides diagrams.

	Island arc tholeiites			Calc-alkaline association			BBVR	
	Basalt	Andesite	Dacite	Basalt	Andesite	Dacite	Andesite	Dacite
SiO ₂	52%	58%	63%	52%	58%	63%	58%	62%
Rb	5	6	15	10	30	45	129	136
Sr	200	220	90	330	385	460	488	510
Y	-	-	23	20	21	20	21	25
Th	0.5	0.31	1.6	1.1	2.2	1.7	29	26
Zr	70	70	125	100	110	100	133	125

Table 12.3 - Trace element abundance in volcanic rocks from island arcs
(Jakes & White 1972) and BBVR.

Fig 12.4 - SiO₂ vs Trace elements diagrams

comn.)

On the basis of major and trace element abundance of the BBVR, a further subdivision within the calc-alkaline family can be made by comparing their chemical composition with those of island arc calc-alkalines and continental margin calc-alkaline volcanic rocks (Andean type). As shown in Table 12.3 the BBVR are more closely comparable with the latter in the SiO_2 range, total Fe (as FeO/MgO ratio), trace element abundance at the same K_2O and SiO_2 levels, and mineralogy. This together with:

a. lower K/Rb in BBVR (190-220) than in island arc calc-alkalines (>400), (as in Andean type this ratio is around 190) (Jakes & White 1972).

b. In island arc calc-alkalines, rocks with $\text{SiO}_2 > 63\%$ are rare (<10%) and rocks with less than 56% SiO_2 are moderately abundant, whereas in continental areas the calc-alkaline association has up to 75% SiO_2 and characterized by the presence of andesite-dacite-rhyolite (suites (Gill 1981, Jakes & White 1972).

c. Close resemblance of trends obtained from the BBVR and Andean type volcanic rock with similar SiO_2 content, when they are plotted on a sample/chondrite vs trace element abundance diagram (Fig 12.5) suggests that the BBVR are Andean type volcanic rocks related to a convergent boundary where TiO_2 is lower ($\text{TiO}_2 < 1\%$) in contrast to intraplate volcanic rocks which always have $\text{TiO}_2 > 1\%$ (Gill 1981).

Thus it can be suggested that during the Maastrichtian the Bala basin was in a fore-arc position in front of a NE-SW trending continental margin volcanic arc which caused the formation of the Saridere volcanic rocks.

While the Saridere volcanics were forming on the southeastern margin of the NE-SW elongated Bala basin, in the

	Island arc tholeiites	Calc-alkaline suite	BBVR
Stage	Early	Late	?
Dominant	Basalt and basaltic andesite	Andesite	Andesite
SiO ₂ -mode	55%	60%	61%
Fractionation	Tholeiitic	Calc-alkaline	?
Cr, Ni, Mg, Ti	Low	High	Low Mg, high Ti
K/Na	Low	High	High
Incompatible elements	10-30 x chondritic	30-100 x chondritic	?

Table 12.4 - Comparision of tholeiitic and calc-alkaline volcanic rocks (Ringwood 1974) with BBVR

	Continental margin	BBVR	Island arcs
Range of SiO ₂	56-75%	54-75%	50-66%
Total FeO/MgO	Higher than 2.0	Higher than 2.0	Lower than 2.0
K ₂ O/Na ₂ O	0.66-1.1	1.0-2.1	Less than 0.8
Trace elements at same K ₂ O, SiO ₂	Higher Rb, Ba, Sr, Th, U, Zr	High Rb, Sr, Zr, Th	Lower Rb, Ba, Sr, Th, Zr
Phenocrysts	Biotite, horn- blende, clino- pyroxene, ortho- pyroxene, rare quartz garnet, cordierite	Biotite, hornblende, rare quartz, clinopyroxene	Clinopyroxene, orthopyroxene, hornblende (rare biotite), no quartz, garnet or cordierite

Table 12.5 - Generalised comparision of calc-alkaline volcanic rocks of island arcs, those of continental margins (Jakes & White 1972) and BBVR.

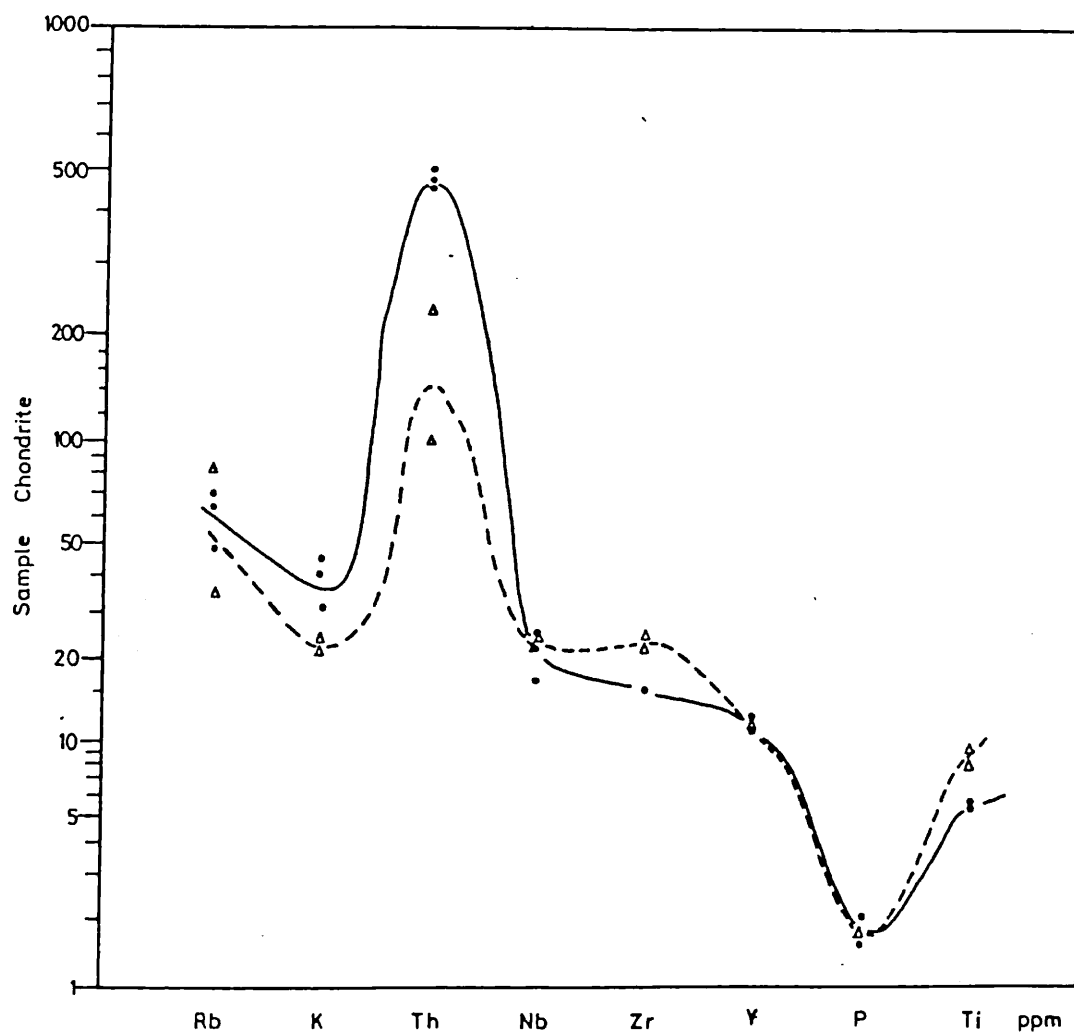


Fig 12.5 - Comparison of sample/chondrite diagrams of BBVR and andean type calcalkaline rocks from Chile. (Saunders et al 1979). Dots represent samples 238, 769-I and 590 from BBVR. Normalising values are from Wood et al 1979.

basin the Kamisli formation was being deposited on the basin floor by turbidity currents flowing from NE, parallel to the basin axis as indicated by the current directions * (Fig 12.6). The entry of the turbidity currents into the basin was from NE outside the area studied. The presence of reworked-tuff layers in a number of levels in the stratigraphical column of the lower part of the formation indicates periods of volcanic activity during which abundant amounts of volcanic ash ejected from the volcanoes was at first settled in the shallower part of the basin and subsequently transported to the deeper parts. The compositional difference of these reworked-tuff layers at different levels of the stratigraphical column (3.6) suggest that the composition of volcanic ejecta was changing from acid, during which K-feldspar dominated beds were deposited, to intermediate composition which caused the deposition of layers with high plagioclase content. The deposition of the Kamisli formation was rather rapid. (Although 123 cm. per 10,000 years depositional rate is calculated on the basis of present measurable thickness, this figure must be considerably higher if the loss due to faulting and thrusting the Ankara Melange are included.) The occurrence of conglomeratic sandstones and an overall increase in grain size of sandstones in the upper part of the formation relative to lower part most probably resulted from increasing proximity to source. The abundant occurrence of slump folds and their close association with coarse grained and thick beds and the presence of disorganized conglomerates of a composition different from sandstones suggest continuous seismic shocks which were created either by eruption of volcanoes or tectonic activity during the deposition of the earlier part and tectonic activity in later times.

*Current directions in this formation as well as other formations of the basin, are expected to give general results as no fold plunge corrections were made because of the complex structural pattern and the presence of slump folds in the area studied

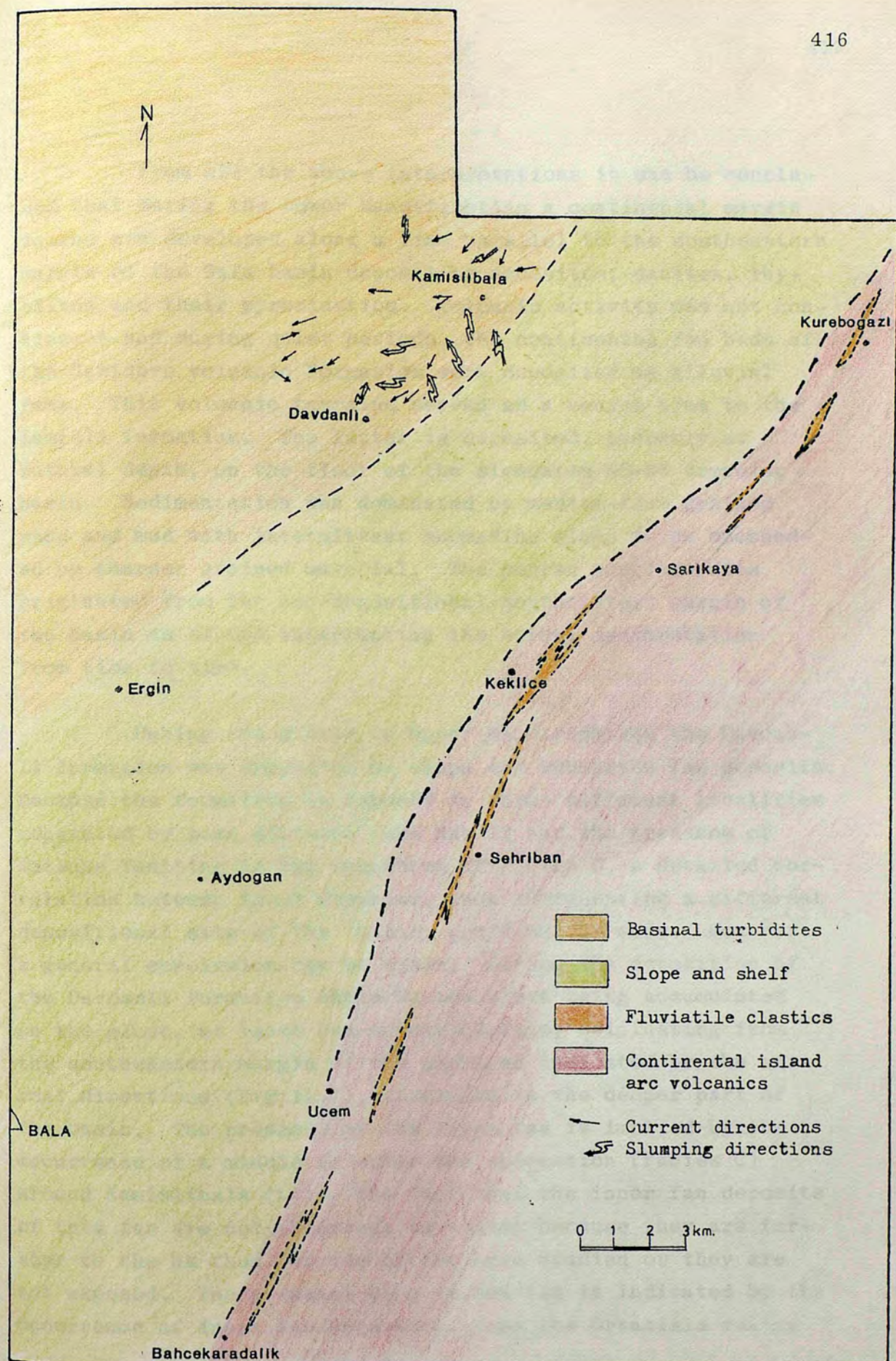


Fig 12.6 - Lower Maastrichtian palaeogeography of the Bala area.
(Non-palinspastic)

From all the above interpretations it can be concluded that during the Lower Maastrichtian a continental margin island arc developed along a line parallel to the southeastern margin of the Bala basin depositing andesites, dacites, rhyolites and their pyroclastics. Volcanic activity was not continuous and during quiet periods, the continental red beds of the Saridere volcanic formation were deposited as alluvial fans. This volcanic terraine served as a source area to the Kamisli formation. The latter is deposited, probably at bathyal depth, on the floor of the elongated NE-SW trending basin. Sedimentation was dominated by medium-fine grained sand and mud with intermittent submarine slump folds succeeded by coarser grained material. The coarse conglomerates originated from the non-depositional southeastern margin of the basin as slumps interrupting the normal sedimentation from time to time.

During the Middle to Upper Maastrichtian the Davdanli formation was deposited as slope and submarine fan deposits. Because the formation is exposed in three different localities separated by some distance (see Map I) and the presence of intense faulting in the exposures of Facies C, a detailed correlation between these deposits, each representing a different depositional site of the basin, could not be made. However a general conclusion can be drawn. During the deposition of the Davdanli formation while Facies B was being accumulated on the slope, at least two submarine fans, originating from the southeastern margin of the basin, as indicated by the current directions (Fig 12.7), developed in the deeper part of the basin. The presence of the first fan is implied by the occurrence of a middle to outer fan succession (Facies C) around Kamislibala (L7). The fact that the inner fan deposits of this fan are not observed, is either because they are further to the NE thus outside of the area studied or they are not exposed. The presence of a second fan is indicated by the occurrence of inner fan sequences along the Ortakisla valley

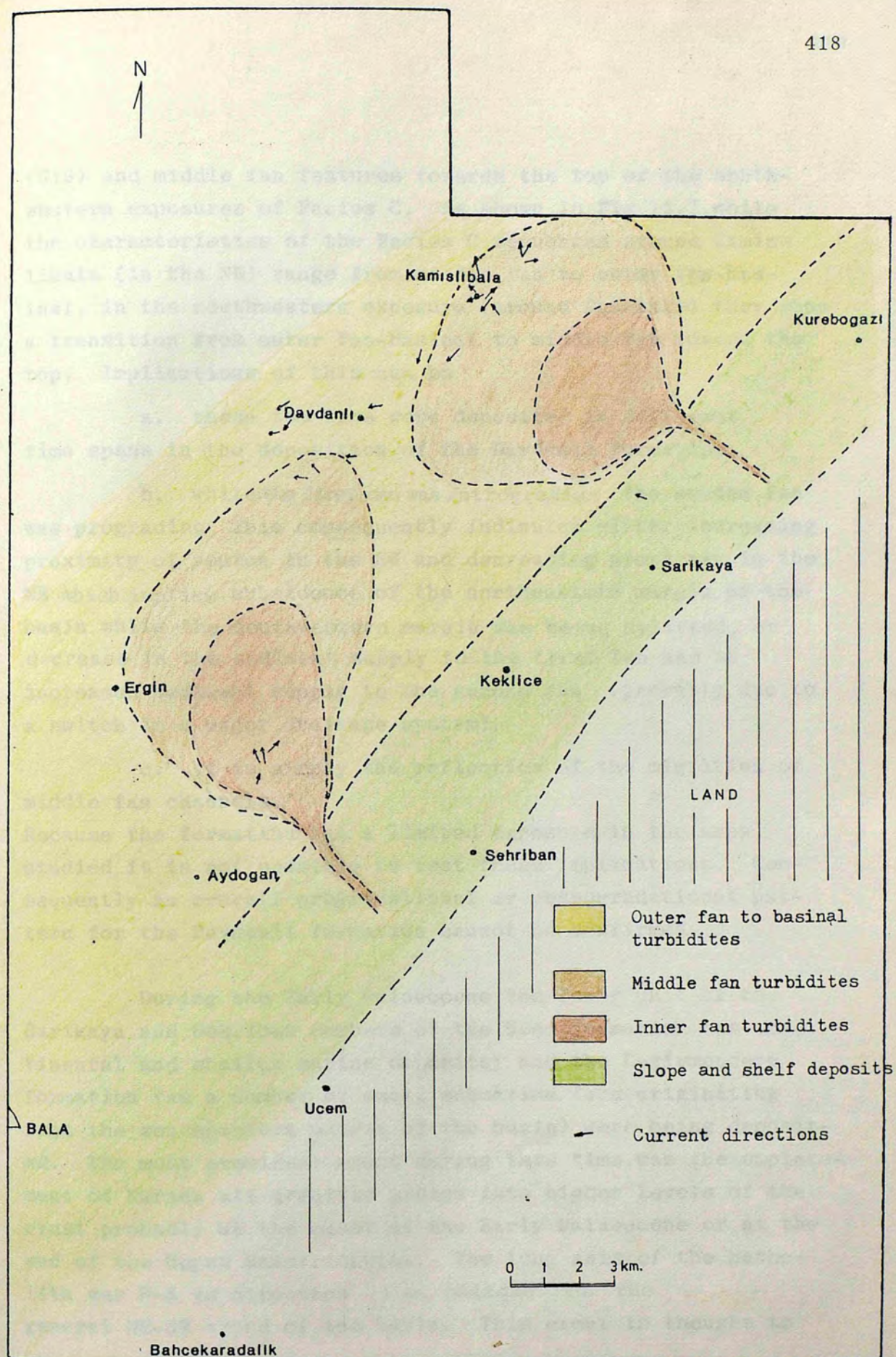


Fig 12.7 - Middle-Upper Maastrichtian palaeogeography of the Bala area (Non-Palinspastic)

(G19) and middle fan features towards the top of the southwestern exposures of Facies C. As shown in Fig 12.7, while the characteristics of the Facies C sequences around Kamislibala (in the NE) range from middle fan to outer fan-basinal, in the southwestern exposure (around Davdanli) they show a transition from outer fan-basinal to middle fan toward the top. Implications of this can be

a. these two fans were deposited in different time spans in the deposition of the Davdanli formation

b. while the first one was retrograding the second fan was prograding This consequently indicates either increasing proximity of source in the SW and decreasing proximity in the NE which implies subsidence of the northeastern margin of the basin while the southwestern margin was being uplifted, or decrease in the sediment supply to the first fan and an increased sediment supply to the second fan (probably due to a switch in a major drainage system).

c. it is simply the reflection of the migration of middle fan channels.

Because the formation has a limited exposure in the area studied it is not possible to test these implications. Consequently an overall progradational or retrogradational pattern for the Davdanli formation cannot be confirmed.

During the Early Palaeocene the lower unit of the Sarikaya and Sehriban members of the Ucem formation (as continental and shallow marine deposits) and the Degirmendere formation (as a number of small submarine fans originating from the southeastern margin of the basin) were being deposited. The most prominent event during this time was the emplacement of Karaca ali granitic pluton into higher levels of the crust probably at the onset of the Early Palaeocene or at the end of the Upper Maastrichtian. The long axis of the batholith was N-S in direction i.e. oblique to the general NE-SW trend of the basin. This event is thought to

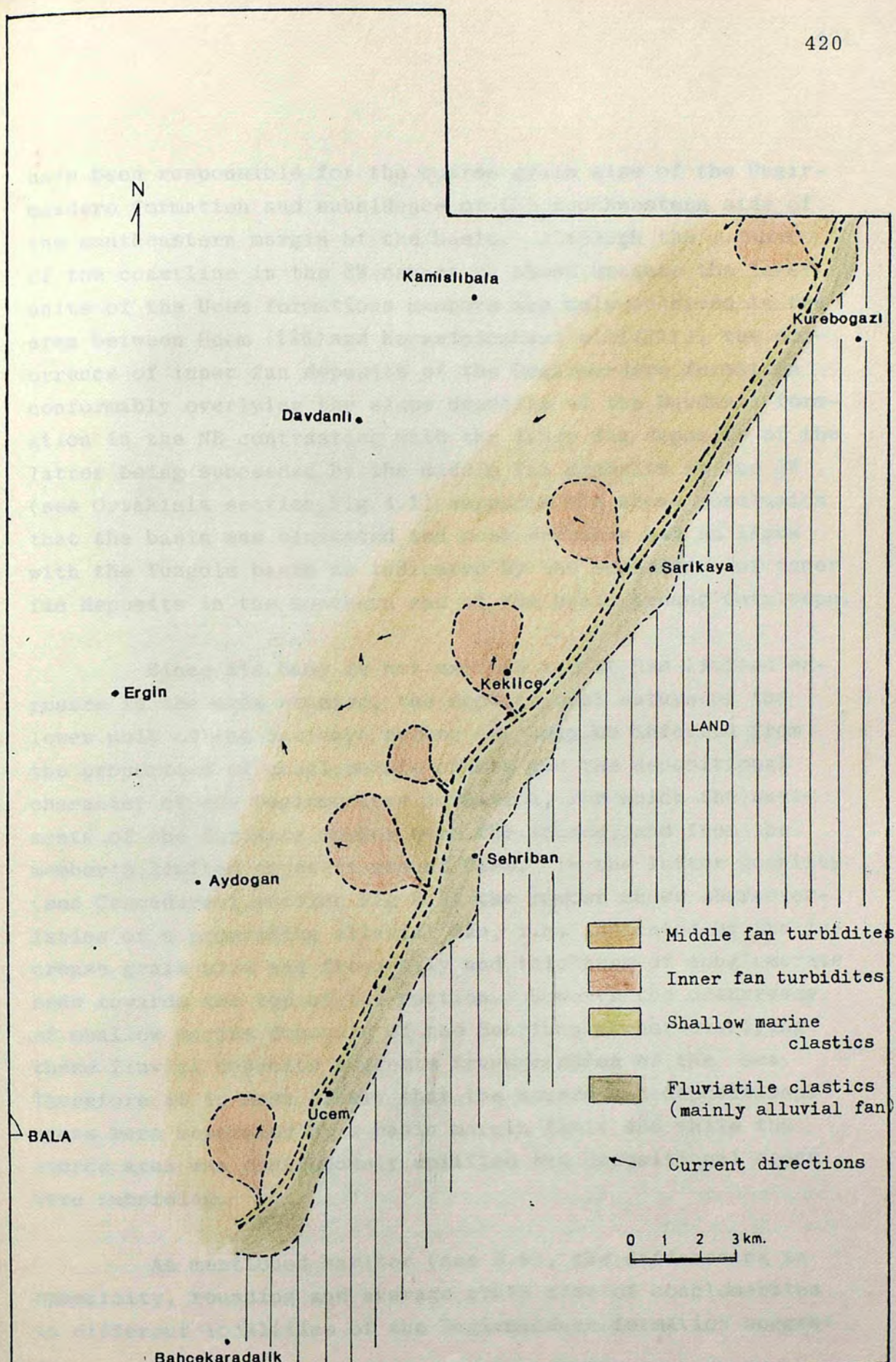


Fig 12.8 - Early Palaeocene palaeogeography of the Bala area (Non-palinspastic).

have been responsible for the coarse grain size of the Degirmendere formation and subsidence of the southwestern side of the southeastern margin of the basin. Although the nature of the coastline in the SW cannot be shown because the lower units of the Ucem formations members are only observed in the area between Ucem (I26) and Kocanindambasi hill (J21), the occurrence of inner fan deposits of the Degirmendere formation conformably overlying the slope deposits of the Davdanli formation in the NE contrasting with the inner fan deposits of the latter being succeeded by the middle fan deposits in the SW (see Ortakisla section, Fig 4.1) supports the above conclusion that the basin was elongated and most probably had no links with the Tuzgolu basin as indicated by the occurrence of inner fan deposits in the southern end of the basin around Cataltepe.

Since its base is not exposed and it has limited exposure in the area studied, the depositional nature of the lower unit of the Sarikaya member can only be inferred from the properties of conglomerate clasts and the depositional character of the Degirmendere formation, for which the sediments of the Sarikaya member were the source, and from the member's limited exposure around Ucem. In the latter locality (see Cesmederesi section Fig 6.3) the member shows characteristics of a prograding alluvial fan, i.e. indicated by the increase grain size and frequently and thickness of conglomerate beds towards the top of the section. However the occurrence of shallow marine deposits of the Sehriban member overlying these fluvial deposits suggests transgression of the sea. Therefore it is most likely that the source and depositional areas were separated by a basin margin fault and while the source area was continuously uplifted the depositional areas were subsiding.

As mentioned earlier (see 5.9), the differences in sphericity, rounding and average grain size of conglomerates in different localities of the Degirmendere formation suggest

that there were a number of submarine fans, sediments of which were supplied locally either by small deltas building up in front of the alluvial fans or by direct underflow of marine waters by high density sediment-laden fluvial waters. The presence of conglomerates in the Sehriban member showing similar sedimentological characteristics to those in the Sarikaya member may be taken as an indication of these flows. The occurrence of

a. abundant conglomeratic material of local origin in the lower units of the Ucem formations members and in the Degirmendere formation,

b. generally poor - extremely poor sorting of sediments

c. the abundance of debris flow deposits especially in the basin margin exposures of the Degirmendere formation, together with the absence of continuity between turbidites of the Degirmendere and shallow marine clastics of the Sehriban member, suggest that slope was non-depositional, steep and unstable; the deltaic plain was narrow and the delta edge was as always unstable. These can only be explained by a second basin margin fault. Although no deltaic deposits are observed in the Sehriban member, probably because the member has a limited and thin exposure in the area studied, the occurrence of some thick inner fan deposits in the Degirmendere formation requires a continuous supply of sediment and this cannot be explained by sporadic sediment-laden fluvial water flow.

On the basis of the above conclusions it can be suggested that during the Early Palaeocene two basin margin faults subparallel to the Upper Cretaceous basinal axis (probably Kurebogazi I and II) were developed in response to either emplacement of Karaca-ali granitic pluton or a change in the relative position of Kirsehir block to the northern branch of Neo-Tethys. These faults separated the volcanic source area from the alluvial and shallow marine depositional area and the

latter from the basinal areas. A number of alluvial fans built up near the coast and stream and sheet flows of these fans transported coarse material to the shallow marine parts of the basin and either to be deposited as deltas or passing the deltas to form submarine fans. Sediments deposited as deltas, due to the instability of slope and/or dumping of more and more sediment to the delta edge, subsequently slumped down from the steep slope to form small submarine fans.

From the Middle Palaeocene to some time in the Middle Eocene, the Sarikaya member of the Ucem formation on the continent, the Sehriban member of the same formation and the Kocanindambasi formation in the shallow marine and the Kurebogazi, Ardiclipinar and Buyukdere members of the Bayat formation on the slope and bathyal depths of the basinal areas of the Bala basin were deposited.

The upper parts of the Sarikaya and Sehriban member's lower units interfinger with the lower units of the Kocanindambasi formation suggesting that their deposition was continuing from the Early Palaeocene. However at first they are mainly sandstones and mudstones with occasional conglomerate lenses. The upper units of the members, which are complexly interfingering with each other, as well as the upper unit of the Kocanindambasi formation, are exposed all along the southeastern margin of the basin. The upper unit of the Sarikaya member was deposited as alluvial fans in the area between Sarikaya (Q14) and Kurebogazi (V8) in the NE, where the interfingering is less complex (Fig 12.9), while in the SW the lower reaches of alluvial fan or flood plain conditions prevailed. The upper unit of the Sehriban member was deposited as coastal to shallow marine clastics of varying thickness. These thickness changes were probably due to local topographical variations.

The Kocanindambasi formation was deposited as a bio-

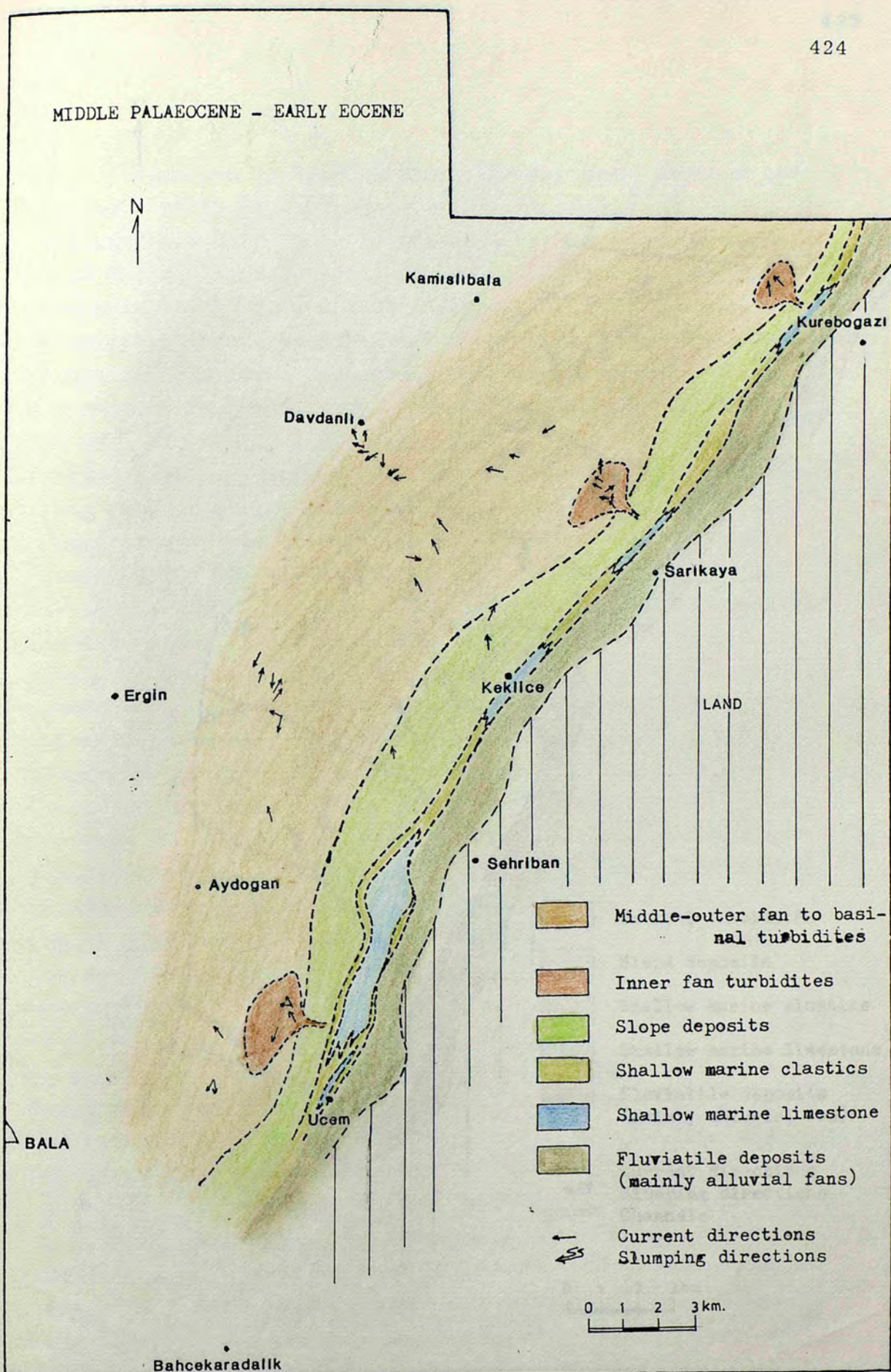


Fig 12.9 - Middle Palaeocene - Middle Eocene palaeogeography of the Bala area (Non-palinspastic).

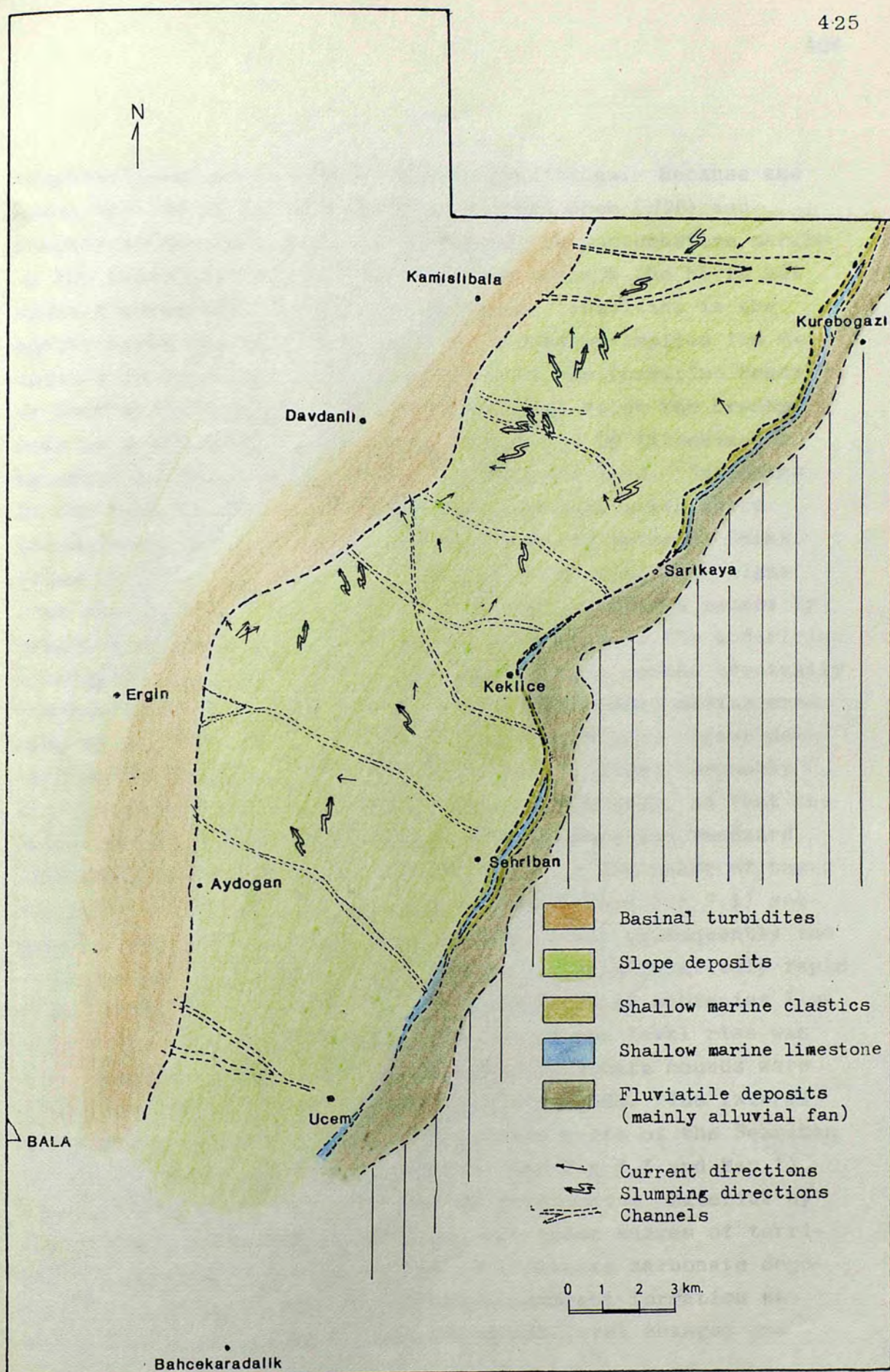


Fig 12.9 continues

clastic limestone in shallow marine conditions. Because the lower unit of it is only observed between Ucem (J26) and Kocanindambasi hill (J21) in the SW of the southeastern margin of the basin, its nature and extent towards the NE is not known, however the presence of limestone olistoliths in the northeastern exposures of the Bayat formation implies its existence in this area. The lower unit of the formation began to form with the deposition of subfacies I below the breaker zone as a bioclastic limestone contaminated by lithoclastic material probably derived from the adjacent land. Subfacies II was deposited on top of the subfacies I in areas where accumulation of the latter created localised sediment banks. Frame building organisms such as corals and coralline algae grew abundantly and formed small, patchy, carbonate mounds by trapping and baffling the carbonate sediments on the underlying bioclastic sediment bank. When these organic mounds eventually reached wave base they were protected from normal marine erosion by surface encrustations of coralline algae. Later developments of organic veneers or fissure fillings, probably by blue green algae, further protected the mounds, so that the subfacies III and IV were deposited as seaward and landward flanking beds respectively. The volumetric dominance of these flanking beds over the core of the mounds (see Fig 7.1) suggests a gradual sea level rise (Wilson 1975), consequently the core was buried by the flanking beds. Later a relatively rapid rise in sea level resulted in the deposition of subfacies I on top of the carbonate mounds. The rate of sea level rise was not constant so that a number of small carbonate mounds were developed during the relatively stable periods. The lateral and vertical interfingering of the lower units of the Sehriban member and Kocanindambasi formation (see Fig 7.1 and Map I) suggest that an occasional input of terrigenous material by flash flood type streams occurred, but these surges of terrigenous material were not enough to terminate carbonate deposition. The upper unit of the Kocanindambasi formation was deposited as subfacies I. The rapid sea level changes pre-

vented the proper development of subfacies II as carbonate mounds, instead only very small patchy coral-coralline algae organic build-ups were formed without development of the flank beds.

The Kurebogazi member was accumulated as slope deposits conformably overlying the inner fan deposits of the Degirmendere formation. Frequent and large scale submarine slumping was the main depositional mechanism with a number of conglomerate and sandstone filled channels incised into these deposits. Its prograding nature is most probably due to the increase in the slope length as large masses of sediment slumped down to the basin, since there is no indication of a large scale progradation of shallow marine sediments (see above).

The inner fan deposits of the Ardiclipinar member observed in two localities in the lower part of the Bayat formation indicate that during the early depositional history of the formation two submarine fans were developed. They originated from southeastern margin of the basin as indicated by the current directions.

The Buyukdere member was deposited as middle and outer fan to basinal sediments. The middle fan deposits again being observed in the lower part of the Bayat formation. Although the occurrence of middle fan deposits in between outer fan-basinal sequences in the Buyukdere section (Fig 8.3) may suggest successive progradation and regradation of a fan, it is believed, on the basis of

- a. the absence of any inner fan deposits in the upper part of the Bayat formation,
- b. prograding nature of slope deposits,
- c. the presence of upward fining and thinning sandstone depositional lobes in the outer fan-basinal deposits

overlying the middle fan sediments, that the proper fan development took place only during the lower part of the Bayat formation. Later sedimentation was mainly through channels crossing the slope and depositing their load in the basinal areas. This conclusion is also supported by the increase in the number and thickness of channel-fill deposits on the slope.

On the basis of the above conclusion, the sedimentary history and palaeogeography of the basin during the Middle Palaeocene - Middle Eocene can be made. The source areas which were partly Saridere volcanic formation and partly Ankara Melange along the southeastern margin of the basin. These changes most probably resulted from the slowing down of rate of uplift and subsidence in the source and depositional areas and a slow transgression of sea towards the SE. This consequently caused a relative reduction of the terrigenous input, which in turn allowed the deposition of the bioclastic limestone as carbonate mound and normal shelf carbonate and deposition of the slope deposits as the slope became less steep than during the deposition of Degirmendere formation. Despite this slowing down the basin margin faults were still active and their vertical and probably strike-slip movements (see 13.3) were causing complex interfingering in the basin margin and initiating large scale slumping in the slope. Their activity was spasmodic and continued throughout the depositional period. In the earlier episodes of sedimentation, continental red beds and shallow marine clastics and carbonates were being deposited on the basin margin, which the slope was mainly accommodating fine grained sand and mudstones and small channels cutting these sediments. During this time two submarine fans were developed, containing newly deposited semiconsolidated limestone olistoliths and coarse terrigenous conglomerates. As sedimentation continued tectonic activity became more significant, large scale submarine slumping, accompanied by large limestone olistoliths sliding down from the upper slope, began to

characterise the slope. This, consequently, increased the length of the slope. These activities were also initiating the mass movement of previously deposited shallow marine sediments which continuously advanced to the slope edge, in spite of the continuing transgression, and down to the slope. These coarse grained sediments were incising channels into the slope and were carrying their load to the deeper parts of the basin, creating sandstone depositional lobes. The rate of slope progradation was not uniform, thus the relatively more rapid progradation of the slope in the NE caused the migration of the basinal axis toward the NW. During this time a connection between Tuzgolü and Bala basins probably existed as indicated by the continuation of these sediments towards the S SW.

This depositional pattern continued to sometime in the Middle Eocene when the whole area was uplifted and for the first time a northeastern margin of the basin emerged. This uplift resulted in NE-SW trending folds and reverse faults and NNW-SSE trending strike slip faults.

While the Bala basin was being uplifted and deformed a new depositional site in the WNW and SSW of the area studied was created, surrounding the newly emergent area (Fig 12.10). This basin received sediment during the Middle Eocene-Oligocene. During this period, the Kizildag formation as continental and the Keklikpinari formation, as marine sediments, were deposited. The frequent and complex interfingering of these formations and their extreme thickness variation indicate sea level fluctuations and variations in local topography. The latter is well demonstrated in the WNW exposures of the Kizildag formation. Here the formation is thin when it overlies an anticline formed by the Middle Eocene uplift, in contrast to its relatively greater thickness when it overlies synclinals (see Map I).

The Kizildag formation was subaerially deposited as

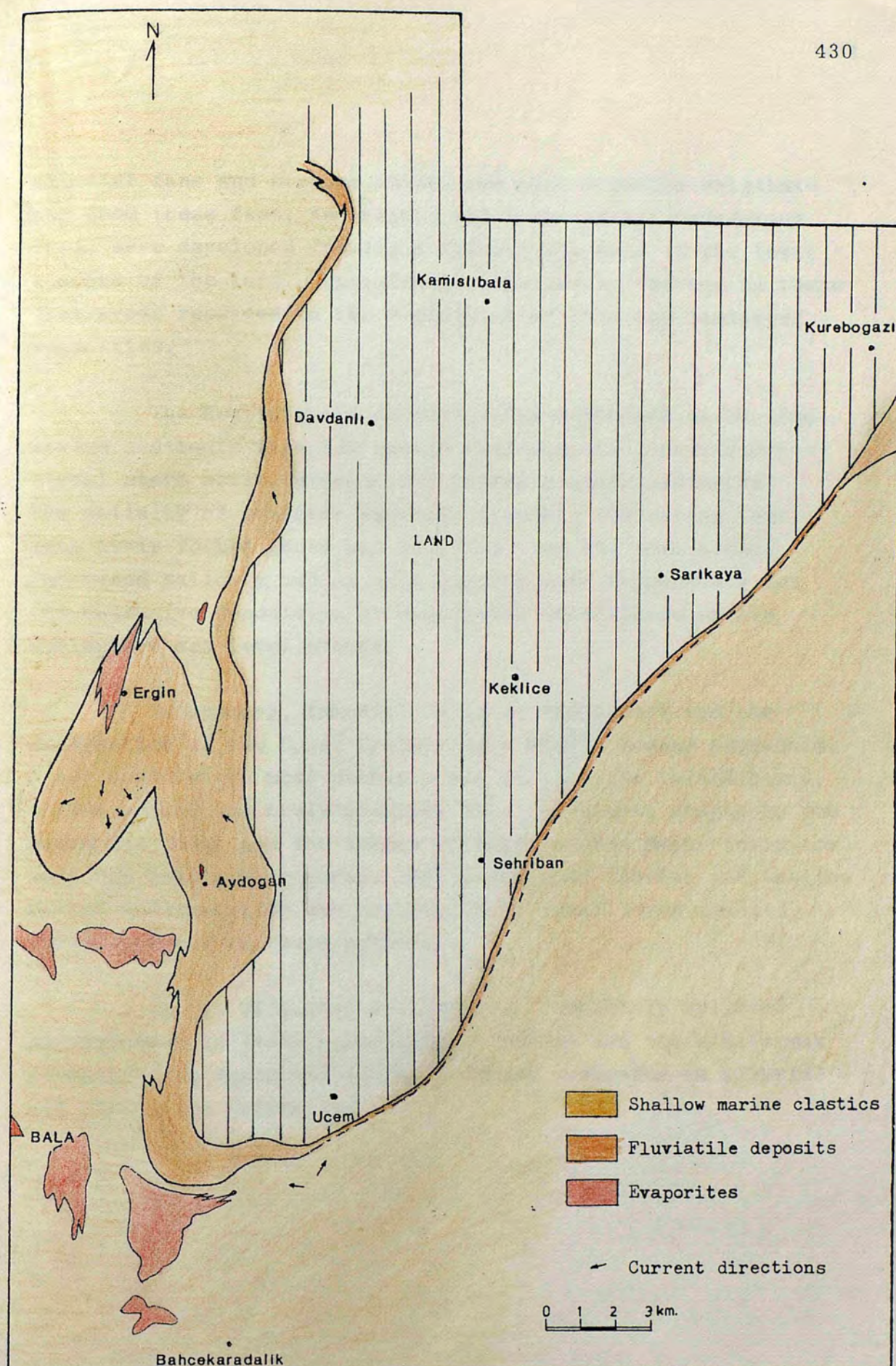


Fig 12.10 - Middle Eocene - Probable Oligocene palaeogeography of the Bala area. (Non-palinspastic).

alluvial fans and streams which were most probably originating from these fans, as braided and occasionally meandering types were developed forming a flood plain area in the lower reaches of the fans. Occasional invasions by the sea in these flat areas resulted in the deposition of thin and laminated evaporites.

The Keklikpinari formation was deposited as shallow marine sediments in a low energy environment. However occasional storm activity deposited coarse grained sediments. The salinity of seawater was high probably indicating that this newly formed basin was isolated from the open ocean. Increased salinity and an arid climate were responsible for the extensive deposition of evaporites in offshore shoals during low sea level stands.

In summary, immediately after the uplift and the deformation of the Upper Cretaceous - Middle Eocene sediments, a new basin which most probably was an isolated inland basin, formed around the newly emergent area. Sediment supply to the basin was local and the Ankara Melange and the Bayat formation were the main source rocks. The pattern of fluvial and shallow marine sedimentation was controlled by local topographical variations and tectonic activity.

In the Oligocene the area was completely uplifted and deformed by NW-SE compressional forces and the Kizilirmak formation was deposited on the deformed sediments as alluvial and playa lake sediments.

C H A P T E R 13

GEOTECTONIC EVOLUTION OF BALA BASIN WITHIN THE FRAMEWORK OF ANATOLIAN MOBILEBELT

13.1 Geotectonic evolution of Analolian Mobile Belt.

13.1.1 General Introduction

In order to explain the geotectonic evolution of Bala basin adequately, the general tectonic setting of Anatolia must be discussed. The geotectonic evolution of Anatolia is not yet fully understood due to the complexity of the geology of the region and the lack of detailed geological studies. Numerous hypotheses, sometimes contradictory, have been proposed (see below).

13.1.2 Historical background

The first attempt to interpret the Anatolian orogen was by Nauman (1896) who divided the Anatolian mountain range into two branches: the "Pontique" in the north and "Tauran" in the south, stating that they were formed by the movement of Gondwaland towards Eurasia. His hypothesis was later developed by Alpine geologists such as Argand (1922), Straub (1924, 1928), Seiditz (1931).

Kober, after his introduction of the concept of intermediate massifs in the evolution of geosynclines in 1931, recognized Pontids, Intermediate massifs and Taurids from the north to the south across Anatolia, comparing them to units in the Alps. The Pontids were linked to Alpids by means of High Balkans and Carpathians while the Taurids were linked to the Hellenids and Dinarids.

Later on a further subdivision was proposed by Arni (1939), who divided Anatolia into more units (Pontids: a) northern branch b) southern branch; Anatolids; Taurids; Iranids; Anatolian-Iranian Border folds a) inner b) outer

and Syrian-Arabian block), comparing Eastern Anatolia with the mountain belts of Western Iran.

Blumental (1946) and Egeran (1947) both accepted Arni's classification in general but Blumental introduced a new unit "Iraqid" and separated the Palaeozoic or Crystalline basement from the Mesozoic-Tertiary cover. Egeran increased the number of tectonic units in Anatolia to ten, on the basis of magmatic activity and metallogenic provinces.

In 1950 Bailey and McCallien recognized the existence of the Steinmann trinity (pillow lava, serpentinite, radiolarite) in Central Anatolia and called it the Ankara Melange. They stated that the Central Anatolian region was a geosynclinal domain and that the present structure of the region formed by the southward thrusting of the Pontids over the Taurids. The crystalline massifs (e.g. Kirsehir), preserved in the synclinal areas but covered by younger sediments in the anticlinal areas between the Pontids and Taurids, were believed to be segments of an enormous thrust sheet with a postulated minimum horizontal displacement of 350 km. from the north to the south.

Pinar and Erdem (1954) proposed another subdivision by dividing the Taurids into intermediate fold belts and intermediate massifs (Fig 13.1B).

Ketin (1959 and 1966) put forward another hypothesis in which he believed that the rocks of Anatolia were deposited within a long-lived geosyncline by continuous sedimentation from Palaeozoic to Upper Cretaceous. He disputed the supposed Pre-cambrian to Palaeozoic age of the metamorphic massifs by pointing out the conformable boundary between the Upper Mesozoic ophiolites and massifs. He suggested that metamorphism of these massifs occurred during the Alpine orogeny which had migrated from the north to south first forming the Pontids as the oldest geotectonic unit in the north and followed by the

southward evolution of Anatolids, Taurids and Border Faults (Fig 13.1A).

Muratov (1964) reviewed the geotectonic evolution of southeastern Europe and Anatolia and recognized two major episodes in the Phanerozoic history of these regions:

1. A Palaeozoic episode which was terminated by the Hercynian orogeny with rocks deposited in the Caledonian and Hercynian geosynclines and now found either as intermediate massifs or within the cores of Alpine folded structures;

2. A Mesozoic-Cenozoic episode which was terminated by the Alpine orogeny. This period is subdivided into

- i. The geosynclinal stage proper

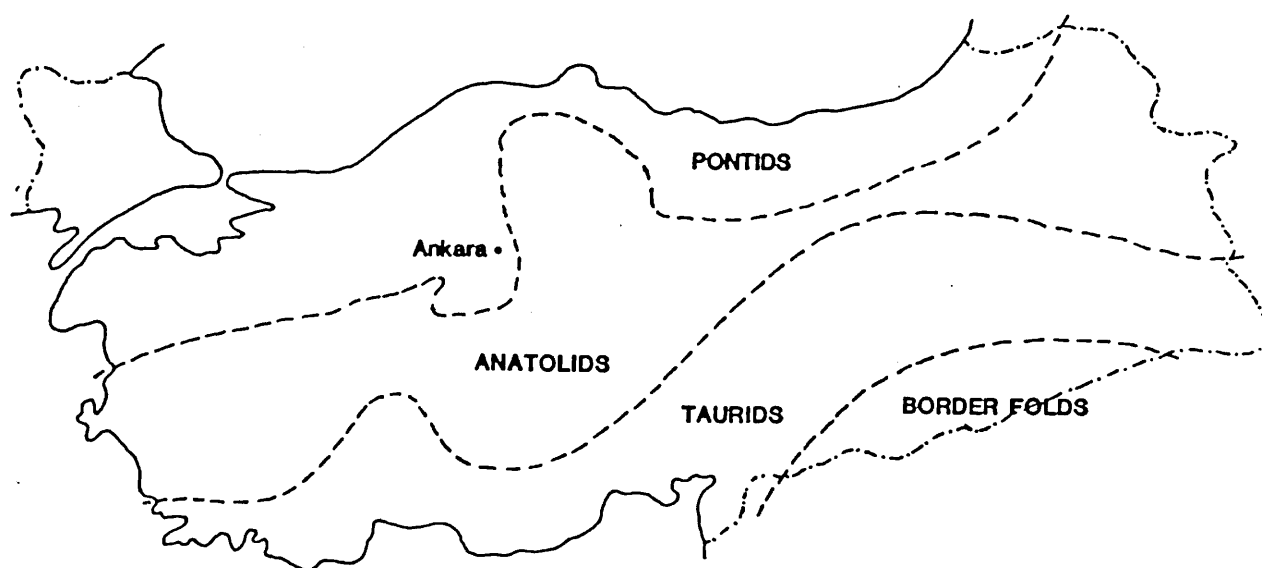
- i.a. Early phase: beginning marked by the formation of a number of new basins which were filled by mainly carbonates (marine and lagoonal) while volcanism played an important role in deep, fault bounded trenches. This phase lasted through Triassic, Lower and Middle Jurassic and in some places Upper Jurassic and Lower Cretaceous without a break.

- i.b. Maximum developments of troughs ("flyschogenic"); started with the development of new geosynclinal troughs which were filled by flysch-type sediments, with volcanic rocks predominating in some of these troughs, along a mainly E-W trending fault systems and continued from the Lower Cretaceous to Middle Eocene. In this phase in Anatolia a number of new troughs formed in areas of former carbonate deposition.

- i.c. Closure of geosynclines; the "flyschogenic" geosynclines were closed during the Upper Eocene and Oligocene or beginning of the Miocene. This resulted in intensive folding and faulting and in the termination of the geosynclines

- ii. The final stage of geosyncline developments and mountain building: The uplifting of the geosynclines formed the basis of the Alpine mountain system and intermontane depressions, which are generally bounded by faults

(A)



(B)

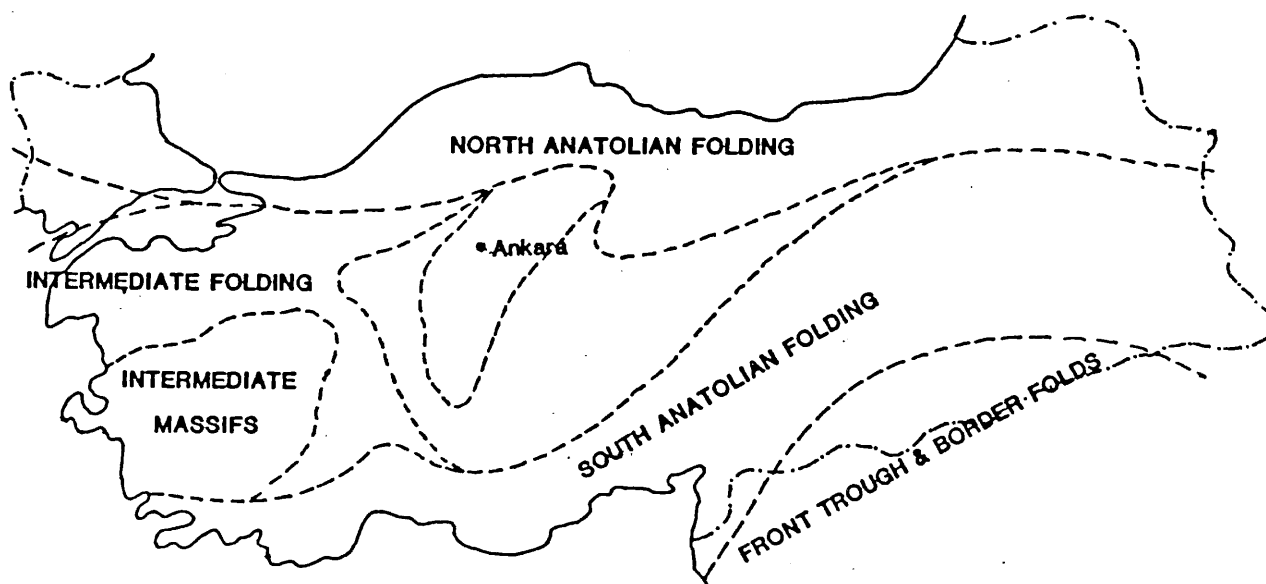


Fig 13.1 - Maps showing the proposed tectonic unites in Anatolia' (A) after Ketin (1959) and (B) after Pinar & Erdem (1954)

imposed on various older structural elements, were also formed in this phase. These depressions were filled by sediments derived from the surrounding mountains.

Application of the plate tectonic theory to the Anatolian mountain range by McKenzie (1970) opened a new phase. He recognized two major and three minor plates in the Eastern Mediterranean region on the basis of fault-plane boundaries. These are the Eurasian, African, Arabian, Turkish and Aegean plates. He also indicated the relative motion of the African, Arabic, Turkish and Aegean plates.

In 1970 Dewey and Bird reviewed the present plate-tectonic arrangement of the Mediterranean and claimed that the African and Arabian plates are moving towards the north and being consumed in the Ionian Trench indicating that the future collision of north east Africa with Greece is inevitable.

Horstink (1971) proposed another plate-tectonic setting. Three major phases are recognised in the Mesozoic and Cenozoic history of central and eastern Turkey:

1. Pre-Senonian, during which three major continental masses Pontia, Anatolia and Arabia were drifting towards each other.
2. Senonian, when the continents collided and oceanic ophiolites were pushed as nappes over parts of Anatolia and Arabia.
3. Post-ophiolitic, Late Cretaceous and Tertiary, characterised by the formation, infilling and deformation of intermontane troughs.

Within the last, tectonism was almost continuously active (the final and strongest of which was in the Lower Pliocene) resulting in strong deformation near the edges of Anatolian platform and gentle folding and upthrusting on the platform itself) and three sedimentary cycles are distinguished.

a) Upper Cretaceous - Middle Eocene: The greater part of Central Anatolia remained high and was surrounded by shallow seas, except in the Sivas region in the north-west, where a deeper intermontane trough existed.

b) Middle Eocene - Oligocene: An east-west elongated line of intermontane basins separated by shallow barriers developed to the north of the uplifted Bitlis - Binboga Massif. The northern and central part of Anatolia remained or became uplifted.

c) Lower Miocene - Pliocene: This cycle started with a widespread transgression covering most of Anatolia. Regression set in during the Middle Miocene and thick continental and lagoonal sedimentary sequences were deposited in areas of strong subsidence.

Later Oktay (1973) put forward another hypotheses to explain the geotectonic evolution of Anatolia with special emphasis on the Bolkardag-Ulukisla-Tuzgolu areas. He suggested that Tethys, which existed in between Eurasia, Anatolian arc and Gondwanaland was closed by the collision of these plates in the Late Palaeozoic. Re-opening of Tethys in the Early Mesozoic was established approximately on the same geo-suture (Tethyan and Anatolian Trenches) due to rifting. The Anatolian arc was dislocated by Jurassic rifting and in addition to two major plates, two smaller plates (mid-Anatolian Continent in the W and Malatya-Bitlis Block in the E) were created. An extensive ocean floor spreading in between these four plates resulted in the formation of large oceanic troughs. Re-closure of Tethys, by the relative movements of these plates towards each other, started during the Upper Cretaceous period creating three new trenches (Bolkardag - Ulukisla - Tuzgolu trough, Hatay-Cyprus Trough, East Pontid Trough) in addition to three previous ones (Izmir - Anakara - Sivas Trough, Western Taurus - Pindus Trough and South Eastern Taurus - Zagros Trough) in between two major and three

smaller plates. Middle-Upper Eocene and Middle Upper Miocene movements caused the further closure of Tethys and finally, the collision of the Eurasian and Afro-Arabian plates welded the small continental blocks of previously generated sub-plates.

Dewey et al (1973) presented a complex plate tectonic model for the Mediterranean region. The complexity is due to the presence of various microplates between the two major continents Eurasia and Africa and these mega and micro continents had different motions during different geological ages. Nevertheless they proposed an evolutionary model for this region based on geologic facies, structural fabrics and palaeomagnetic criteria. They concluded that Turkey is a grouping squeezed as in a vice between Africa and Europe since the Early Mesozoic.

In 1976 Biju-Duval et al produced another plate tectonic model and a series of palaeogeographic maps starting from the Early Triassic to Recent based on geologic structure, adjacent folded belts and associated basins and on the evolution of the North Atlantic Ocean according to the magnetic anomaly information. They concluded that the evolution from Tethys to the present Mediterranean occurred in two main stages:

1. From Triassic to Uppermost Cretaceous:

In this period the main motion was the left lateral movement of Africa relative to Eurasia. In the Early Triassic a wide Tethys Ocean existed between Eurasia and Africa and three intermediate plates Iberia, Apulia and Anatolia (from W to E) existed. During the Triassic and Jurassic a period of extension created the Mesogea (Palaeo-Mediterranean) ocean separating the Apulia and Anatolia plates from the Africa in the S and Iberia in the W. In the Upper Jurassic, Apulia was cut into three sections by intracontinental faults and Anatolia collided with the Eurasian plate. During the Cretaceous collision of these plates resulted in complete closure of Tethys, initiated the opening of Black Sea and fracturing of Anatolia and Apulia.

2. From Uppermost Cretaceous to Recent, left lateral movement of Africa ceased and it started right lateral motion until the Ypresian. North-South compression of the Eastern Mediterranean caused by the rotation of Africa. During the Lutetian, Anatolia is fully accreted to Arabia but a new active margin to the south of the Caucasus was initiated. In the Tortonian the opening of the Red Sea initiated the North Anatolian Fault (Fig 13.2).

Hsu (1977) argued that the eastern Mediterranean is a relict of the Mesozoic Tethys and originated from Jurassic and Cretaceous sea-floor spreading. Genesis of this and other Tethyan geosynclinal basins was related to sea-floor spreading in the Atlantic which displaced Africa eastward relative to Europe. Late Cretaceous and Cenozoic shrinkage of the eastern Mediterranean and the elevation of the Mediterranean Ridge were caused by movements which brought Africa and Europe together again. He also concluded that the Aegean Basin is a back-arc basin underlain by sialic basement and it started to subside in the Middle or Late Miocene.

Recently Sengor & Yilmaz (1981) reviewed the plate tectonic setting of Anatolia by using a number of geological geophysical and structural data available. In spite of the number of discrepancies, their account is the most comprehensive so far and forms the basis of the following section (13.2.2) in which terms proposed by authors are adopted.

13.2.2 A review of the geotectonic evolution of Anatolia within the concept of Plate Tectonic Theory.

The Palaeozoic palaeogeography and plate tectonic setting of Anatolia cannot be determined for, although Palaeozoic rocks are recorded, they are much deformed and covered by thick Mesozoic-Cenozoic sediments and volcanics. A few models for the Palaeozoic plate tectonic evolution of the Turkey have been proposed. Although it is generally accepted that, during the Palaeozoic, a major sea-way existed

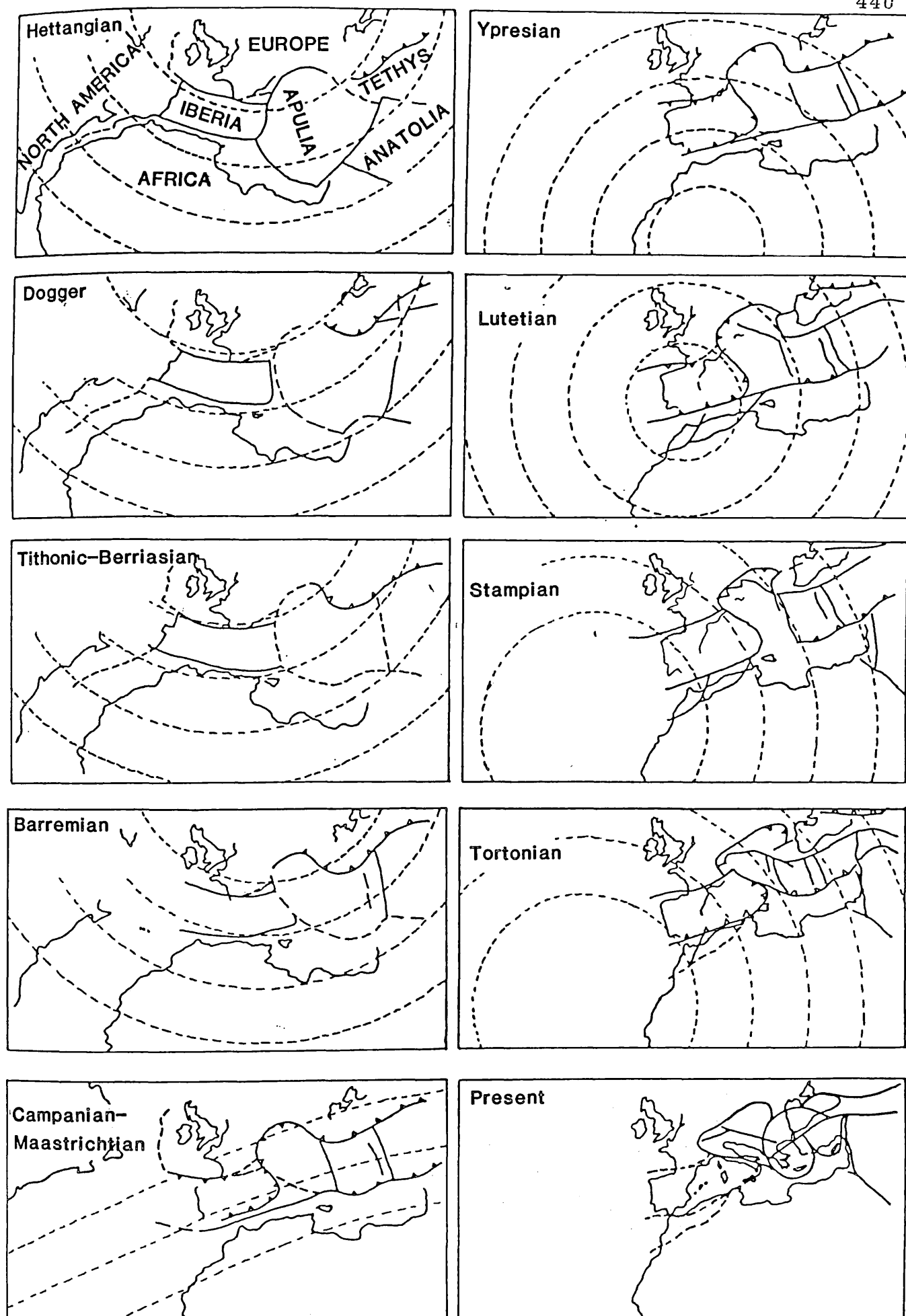


Fig 13.2 - Proposed plate tectonic evolution of Mediterranean from Jurassic to Present (After Biju-Duval et al 1976)

between Eurasia and Gondwanaland, Oktay (1973) argued the presence of an island arc (Anatolian island arc) between the North Anatolian Welt (Eurasia) and Afro-Arabian plate (Gondwanaland) which were believed to be colliding during the Late Palaeozoic and re-opened from the same geo-suture at the beginning of Early Mesozoic, in contrast to the view taken by Dewey et al (1973) Bijou-Duval et al (1977) and Sengor & Yilmaz (1981) who rejected the occurrence of an island arc and any collision event. Sengor & Yilmaz (1981) differed from Bijou-Duval et al (1977) with respect to the position of Pontids and Anatolids. The former authors pointed out the existence of Permian andesitic volcanism, which they believed resulted from the south-dipping subduction of palaeo-Tethys, in the eastern part of the eastern Pontids and that during the Permian the entire area of the present Turkey was part of the northern margin of Gondwanaland (see also Sengor et al 1979) contesting the previously taken view of Bijou-Duval et al (1977) in which the Pontids were part of Laurasia and the Anatolids were part of Gondwanaland. The present data indicates that the former conclusion is more acceptable. During the Permian most of Turkey was the site of neritic carbonate deposition with quiet platform conditions except near the coastal regions of the Black-Sea, where continental red bed deposition was taking place and south of Marmara Sea and southern Turkey where shallow marine clastics were being deposited.

At the beginning of the Triassic (Fig 13.3) a rifting process ruptured the central northern part of the platform along a line extending from the Biga Peninsula, north of Bursa, through Bilecik and Ankara to the Tokat Massif (Bingol 1976) which led to the opening of Karakaya marginal sea. The basin was filled mainly by distal turbidites associated with radiolarties, spilitic basalts, pillow lavas and ultramafics in the early phases of its development, mainly by olistostromes in the later stages and closed before the beginning of the early Jurassic, The absence of a well

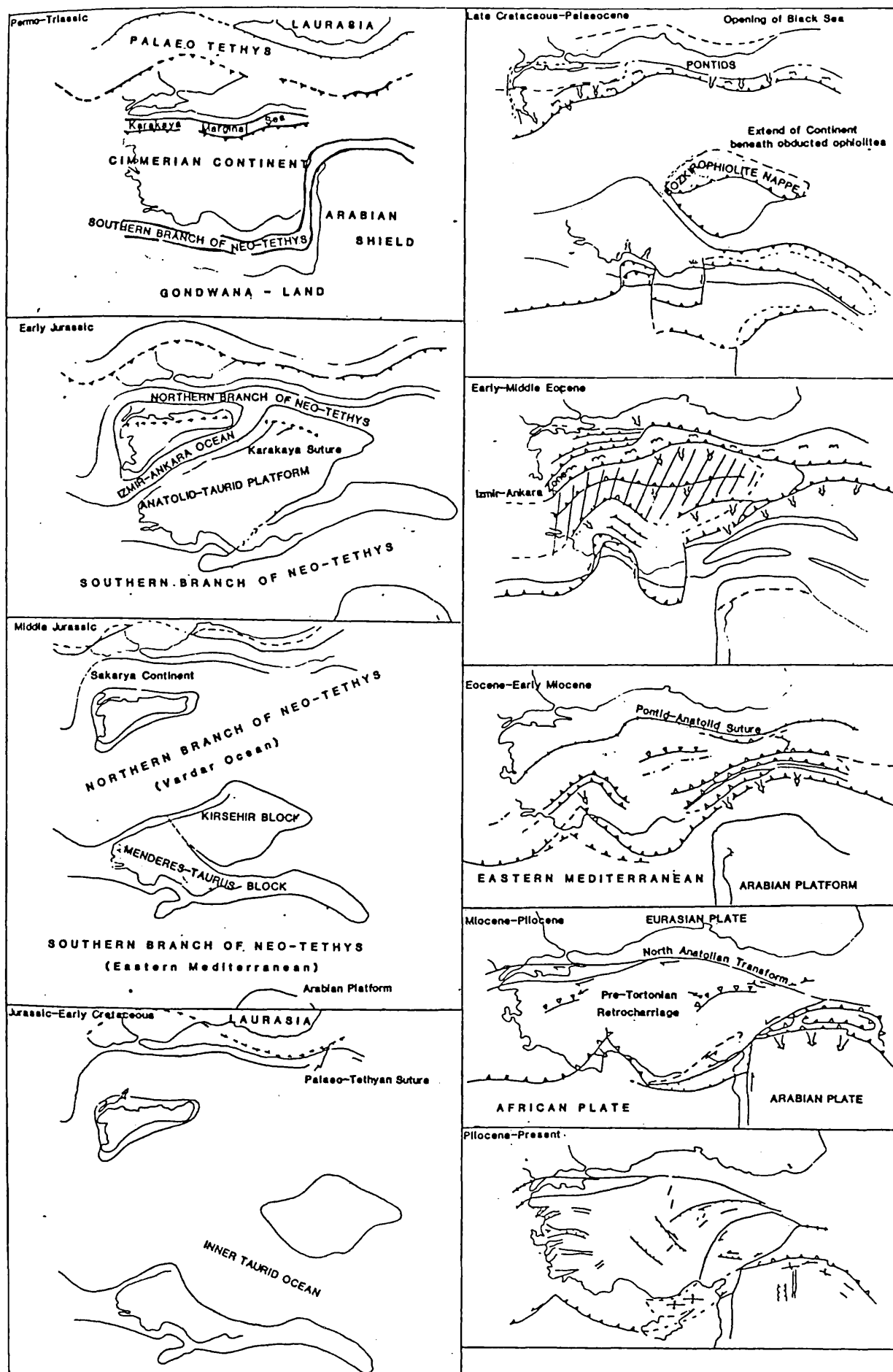


Fig 13.3 - Plate tectonic evolution of Anatolia. (Modified after Sengor & Yilmaz 1981 and Sengor *et al* 1982)

volcanism in the north and, to the south a melange wedge developed ophiolitic suite within these basins led Bingol (1976) to assume that this rifting, never produced a real oceanic crust and Sengor & Yilmaz (1981) interpreted this basin as a marginal sea due to its short life span and its location behind the Palaeo-Tethyan trench and arc, resembling the present Black-Sea (for more detailed discussion of this basin see 13.3). Later, in the Ladinian-Norian another rifting event occurred to the south of Karaya marginal sea, leading the separation of the Cimmerian Continent from Gondwanaland and the formation of the southern branch of the neo-Tethys. During this time the Alanya Massif was also rifted away from the Anatolid-Taurid Platform (see below) and the consumption of palaeo-Tethys continued.

During the Early Jurassic a number of rifting processes disintegrated the Cimmerian continent and caused separation of the Palaeo-Tethys volcanic arc (P-TVA), Sakarya Continent (SC), Anatolid-Taurid Platform (A-TP). Although A-TP was considered as a single unit, later works of Sengor (1981, 1982) showed that the Menderes Massive which forms the western end of the A-TP and Kirsehir Massive had separate structural evolutions. Thus Sengor *et al* (1982) continued the inner Taurid ocean around Tuzgolu to join the Izmir-Ankara ocean separating the A-TP into the Kirsehir Block (KB) and Menderes-Taurus Block (M-TB), (returning to the model suggested by Oktay (1973)). The opening of the northern branch of neo-Tethys, in between P-TVA and SC in the W and KB in the E, occurred near the volcanic axis of the P-TVA due to the subduction of progressively the older oceanic lithosphere of the palaeo-Tethys ocean. This rifting resulted in a faunal differentiation between the P-TVA (which became dominated by Laurasian fauna indicating that the size of the palaeo-Tethys was reduced to permit the Laurasian fauna to reach P-TVA) and the rest of Turkey. The Izmir-Ankara ocean also started to open during this time separating SC from the M-TB and KB. A rifting event which

separated M-TB and KB leading to the formation of the Inner-Taurid Ocean occurred by splitting the Poturge and Malatya-Keban massifs and Bol kardag mountains away from the KB and by rotating the Bitlis massif after it began rifting from the eastern Pontids.

In the Middle Jurassic the most important event was the terminal closure of Palaeo-Tethys which resulted in the collision of P-TVA and Lourasia. This collision caused intense deformation in the Pontids while the rest of Turkey was the site of quiet platform-shelf carbonate deposition.

During the Late Jurassic - Early Cretaceous period the eastern part of the eastern Pontids was subject to crustal thickening and Tibetan-type volcanism (due to continued convergence) in the Late Jurassic and later (Albian-Aptian) extensive tholeiitic basaltic sills production. The Rhodope-Pontid fragment between western Thrace and Zonguldak was emergent while the rest of the eastern Pontids was the site of extensive carbonate shelf deposition together with turbidites in the deeper parts. The SC was also dominated by neritic carbonate deposition during the Late Jurassic. During the Early Cretaceous, however, deep water cherty limestone deposition indicates a sudden foundering of the SC. The M-TB and KB, at this time, was also the site of neritic carbonate deposition, interrupted by pelagic carbonate-filled elongated troughs.

The Late Cretaceous - Palaeocene was the time of an extensive convergent regime which caused a number of melanges and nappe formations all over the Turkey. A north-dipping subduction beneath the Pontids produced the Pontid volcanic arc, which closely follows the present coasts of the Black sea (which had also started opening during the late Cretaceous) a number of fore-arc basins which are filled by thick volcanogenic flysch deposits and a melange wedge in front of this basins. The Sakarya continent was dominated by Calc-alkaline

volcanism in the north and, to the south a melange wedge developed during the Turonian-Campanian and later was overlain by Maastrichtian-Palaeocene shallow marine sediments. The intra-Pontid ocean which was between SC and R-TVA was closed during the Palaeocene-Lutetian. The obduction of ophiolites on to the KB, eastern extension of M-TB (on to the Bitlis-Poturge Massif) and the northern portion of the Arabian Platform was also started during the Late Cretaceous. The obduction of the Bozkir ophiolitic nappe on the northern margin of the KB caused active subsidence in the continental shelf of KB and led to the deposition of flysch and ophiolitic olistostromes. A south-dipping subduction immediately after the obduction of nappes onto the Bitlis-Poturge Massif led to the formation of Yuksekova volcanic arc and its western continuation into the Ulukisla volcanic arc. During the late Cretaceous the Pamphylian basin between the M-TB and Alanya Massif was closed by the overriding of the latter.

During the latest Palaeocene to Middle Eocene KB, M-TB (which are to be called as Anatolid-Taurid platform (APT)) and Pontids collided starting internal imbrication and the initial burial metamorphism of the blocks with extensive retrocharriage development in the Pontids. While arc magmatism was active during the Early-Middle Eocene in the Pontids, the deformed Anatolid-Pontid suture zone was filled by shallow water and terrestrial deposits. The Cungus and Maden basins of SE Turkey reached their maximum development resting on an accretionary prism and filled by deep marine sediments associated with mafic pillow lavas. A north dipping subduction of the floor of the inner-Taurid ocean beneath the eastern part of M-TB was also started during the Early Eocene, after the cessation of activity in the Yuksekova volcanic arc during the Early Palaeocene and initiated by the anti-clockwise rotation of the Bitlis-Poturge massif.

During the Late Eocene-Early Miocene, continuing north-

south convergence resulted in the further advancement of Bozkir nappes towards the interior of A-TP and more continental material was being fed beneath the crystalline massifs resulting in the uplift of crystalline massifs and deep crystal melting under the over-thickened sectors thus in turn, causing widespread silicic volcanism throughout western Anatolia. In the south, the inner-Taurid ocean and Maden basin were closed. Following this closure, the Africa-Eurasia convergence began to be taken-up along a sinuous, uniformly north-dipping subduction zone beneath Turkey.

In the Early to Middle Miocene the initial collision of Arabia and Eurasia started and formed the north and east Anatolian transforms and Anatolian plate.

From Pliocene to Recent continued convergence and thickening of the Turkish-Iranian high plateau resulted in widespread Plio-Quaternary Tibetan-type volcanism on the plateau and border folds are formed on the Arabian platform. The Aegean extensional regime continued its activity.

13.3 Geotectonic evolution of Bala area.

The Bala basin, is one of the series of Upper Cretaceous-Early Tertiary basins developed on the northern margin of the Anatolid-Taurid platform (A-TP). These basins (Çankiri-Corum, Bala, Tuzgolu, and Haymana from E to W) are fault bounded, elongated in shape (generally E-W except the Tuzgolu basin which has a N-S trend) and sometimes in their history were connected to each other (see Chp. 12, Norman *et al* 1980, Arıkan 1975). They have similar basements and depositional characteristics. Thus, the geotectonic evolution of the Bala basin is inseparable from the geotectonic evolution of the region and must be considered within this framework.

During the Permian, the Ankara-Tuzgolu region (which

covers the area shown in Fig 13.4) was situated on the central-northern part of the Cimmerian continent and on the south of the Palaeo-Tethys ocean. During this time much of present Turkey was the site of extensive platform carbonate deposition. However, the existence of Permian detritic blocks within the Karakaya formation (see 1.6) suggest that deposition of terrigenous clastics was taking place, although they are not exposed in the region.

At the commencement of the Lower Triassic a rifting process along a line approximately parallel to the northern margin of the Cimmerian continent started the development of the Karakaya marginal sea (Fig 13.3) (Sengor & Yilmaz 1981). Extension occurred from the Biga peninsula in the W to Tokat in the E and distal turbidites, associated with radiolarite, spilitic basalts, pillow lavas, diabase dykes and ultramafics, were deposited within this depression. The occurrence of peridotite and diabase dykes in the Ankara-Tuzgolu region (Akyurek 1982) but the absence of these lithologies in the Biga Peninsula (Bingol 1976) suggest that rifting was more extensive olistostromes, which are mainly made up of Permo-Carboniferous limestone and clastic rock olistoliths were deposited, most probably indicating the cessation of rifting and uplift of the basin margins. Termination of olistostrome deposition was progressive from the Middle Triassic in the Biga peninsula where these deposits are overlain by the Middle-Upper Triassic turbidite deposits with an angular unconformity, to Early Jurassic in the Ankara-Tuzgolu region. In the northern exposures (Sabanozu area, Location 1 in Fig 13.4 and section 1 in Fig 13.5) of the latter area, the Middle-Upper Triassic shelf limestones overlie the Lower Triassic olistostrome deposits with an angular unconformity but its interfingering with same deposits in the Elmadag-Kalecik-Ankara area (Location 3 in Fig 13.4 and section 3 in Fig 13.5) suggests syndeposi-

* Present geographic setting is used throughout this section.

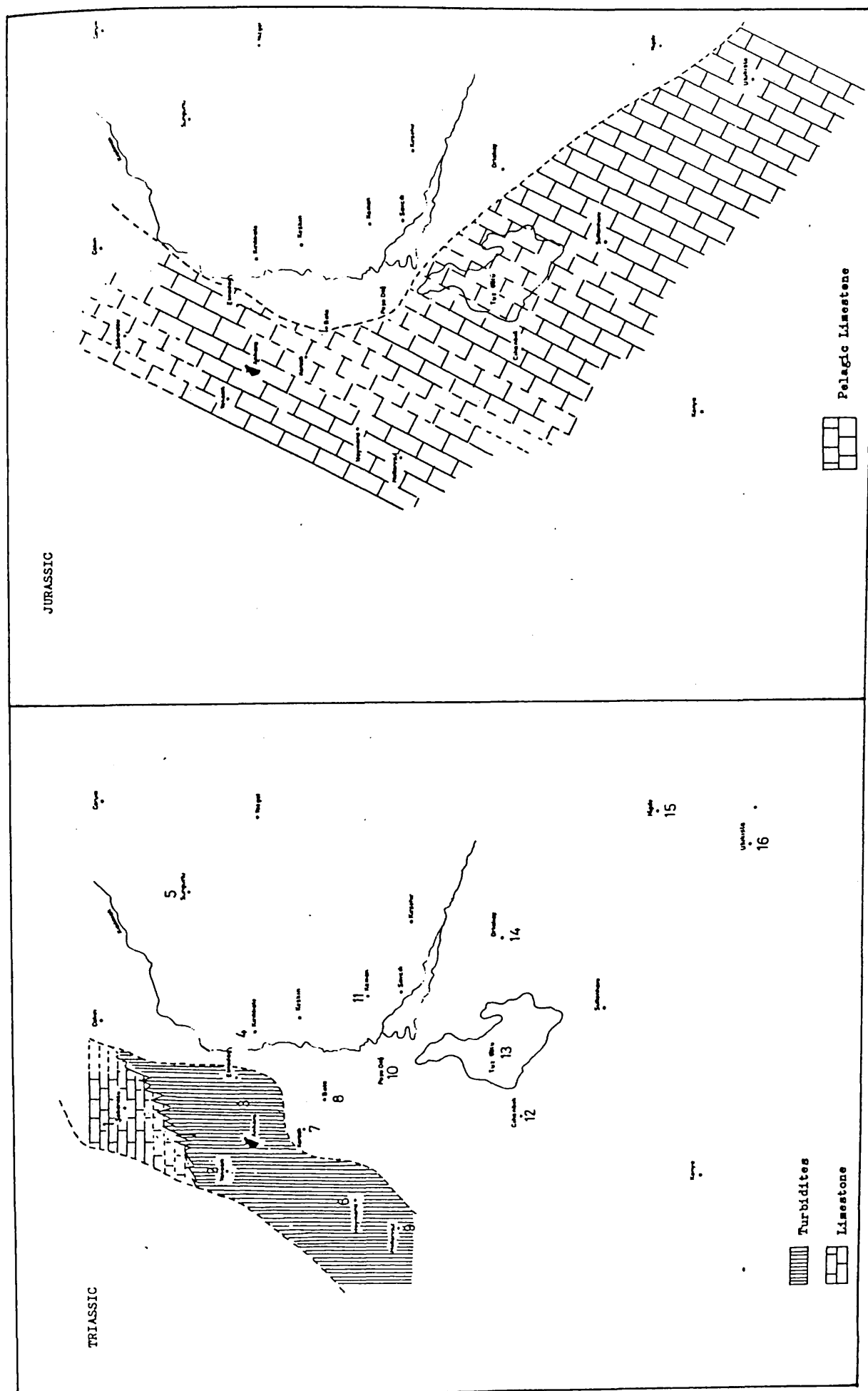


Fig 13.4 - Non-Palinspastic palaeogeographical maps of the Ankara Tuzgolu region.

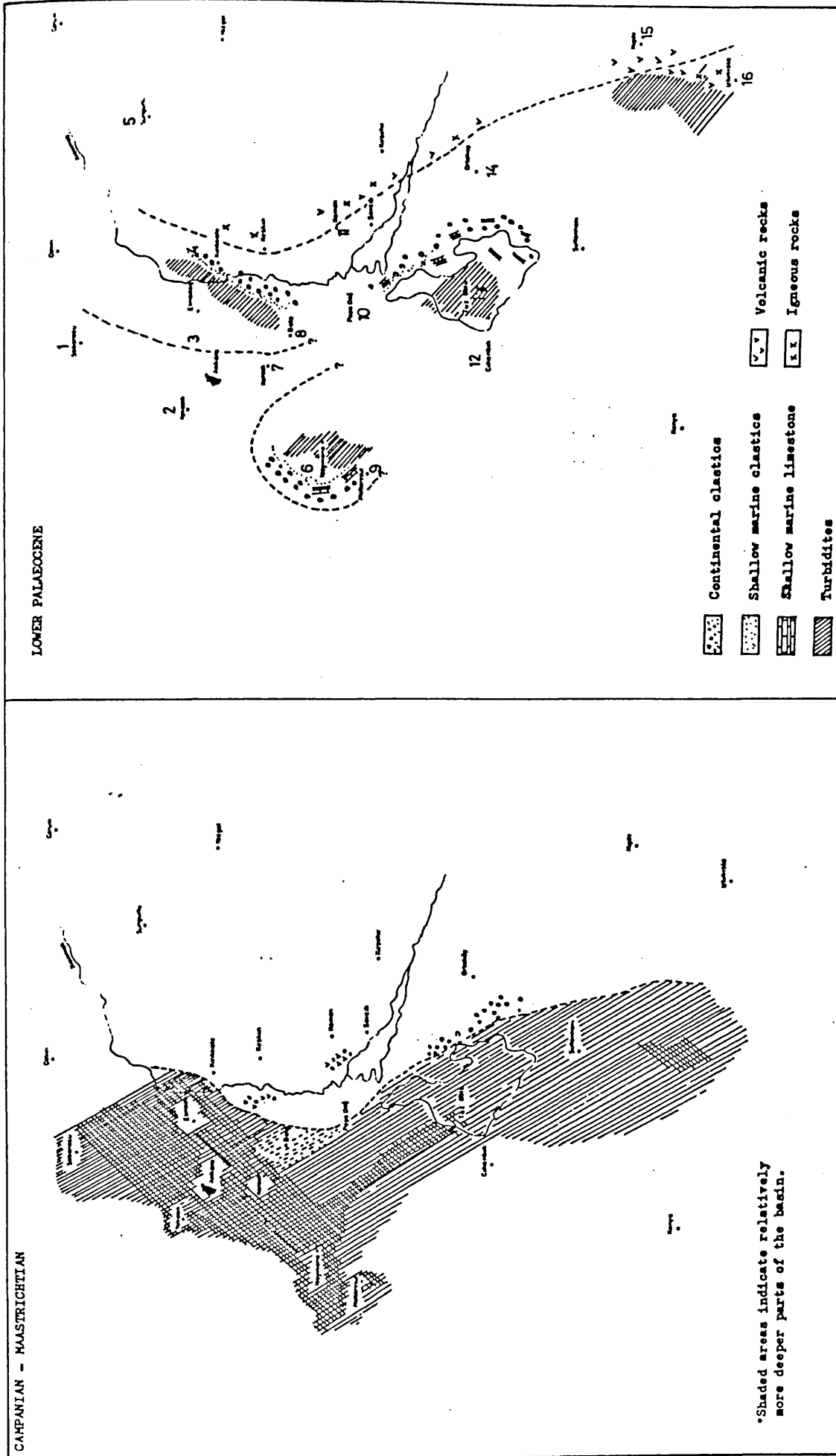
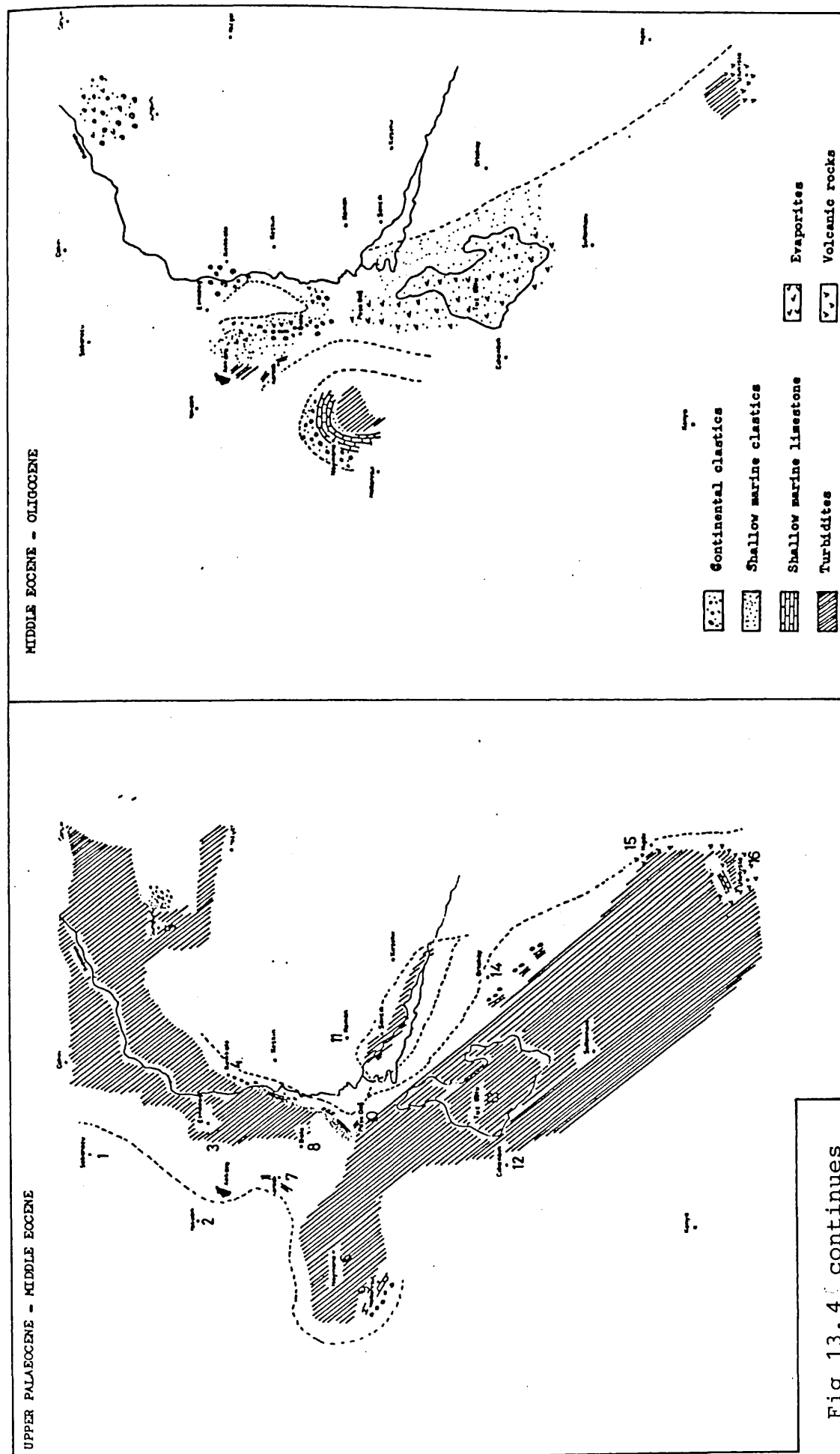


Fig 13.4 continues



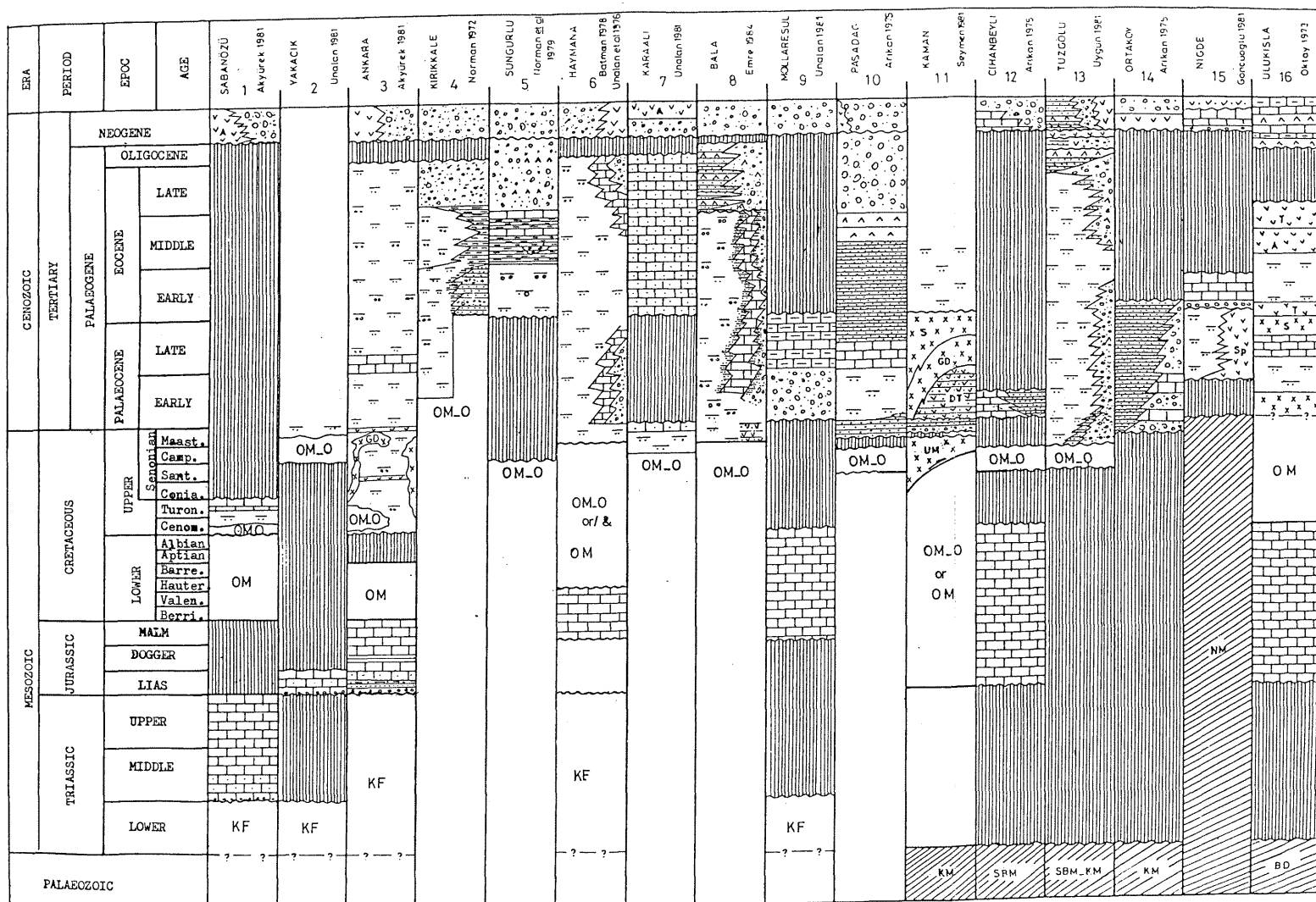



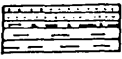
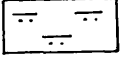
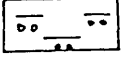
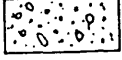

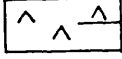
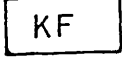
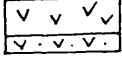
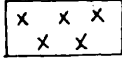
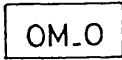

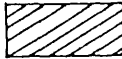
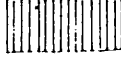


Fig 13.5 - Stratigraphic correlation table for the Ankara-Tuzgözü region. Shaded areas represent non-deposition or erosion.

	Limestone
	Sandy limestone
	Muddy limestone
	Shallow marine sandstone, siltstone mudstone
	Distal turbidites
	Proximal turbidites
	Red continental clastics
	Basal conglomerate
	Evaporites (Massive or bedded)
	Karakaya formation
	Volcanic and their pyroclastics Sp: Spilite, A: Andesit
	Igneous rocks
	Ophiolitic melange-olistroamel
	Ophiolitic melange
	Massifs KM: Kirsehir Massif NM: Nigde massif SBM: Sivrihisar Bozdağ massif BM: Bolcardağ massif.
	Non-deposition or erosion.

tional tectonism in the basin which was most probably caused by the vertical movement of the basin margin faults. A similar occurrence in the Middle-Upper Triassic turbidite deposits of the Karakaya formation is also recorded in the Biga peninsula (Bingol 1976). Additionally the absence of any Middle to Upper Triassic sediments in the Mollaresul area (Location 9 in Fig 13.4 and section 9 in Fig 13.5) (Unalan 1982) together with the presence of Middle to Upper Triassic olistostrome deposits in the area north of Haymana (Location 6 in Fig 13.4 and section 6 in Fig 13.5) suggest that the deepest part of the Karakaya basin, which here had a NE-SW alignment, was between the Elmadag-Kalecik-Ankara area and Haymana area. The southern margin of the basin was uplifted and probably being eroded during this time. The final closure of the Karakaya marginal sea was at the beginning of the Jurassic as shown by the deposition of extensive Early Jurassic neritic limestone on the deformed stratas of the Karakaya basin (Fig 13.5).

The Early Jurassic-late Lower Cretaceous was a time of extensive rifting and initiation and expansion of the various branches of Neo-Tethys throughout the eastern Mediterranean (Sengor & Yilmaz 1981, Biju-Duval 1979, Dewey 1973). During this time the northern branch of Neo-Tethys, Izmir-Ankara ocean and Inner-Taurid ocean were opened, separating the Rhodope-Pontid Fragment, Sakarya Continent, Menderes-Taurus Block and the Kirsehir Block, on the northern and western margin of which the Ankara-Tuzgolu region was situated. (Sengor et al 1982, Sengor & Yilmaz 1981 Oktay 1973). While the evidence for the Jurassic rifting of the Kirsehir Block from the Rhodope-Pontid Fragment along the Izmir-Ankara and Erzincan sutures is abundant (Izmir-Ankara and Ilgaz-Erzincan ophiolite belts), a widespread proof for the continuation of the Inner-Taurid ocean towards the north is lacking, probably due to the extensive cover of the Neogene sediments. However based on the existence of some patchy ophiolite outcrops west of the Tuzgolu basin and

the fact that the Kirsehir massif had a different structural history from those of Menderes and Bolcardag massifs (Seymen 1981), it is thought that the Inner Taurid ocean was continuous towards the north and joins the Izmir-Ankara ocean around Eskisehir. (Sengor et al 1982, Oktay 1973). Throughout the Jurassic to late Lower Cretaceous times the Ankara-Tuzgolu region was the site of platform carbonate deposition indicating tectonic stability as extensional regime continued.

The occurrence of ophiolitic nappes (Ankara Melange Unit I of the present author see 1.6) which are thought to represent oceanic crust and emplaced during the Aptian-Albian period, overlying the Jurassic carbonates with a tectonic boundary (Akyurek 1981) suggests that the initial obduction of the ophiolitic nappes onto the Kirsehir block started during the late Lower Cretaceous; a view contrary to the common belief that the compressional regime in Anatolia started in the Late Cretaceous. The obduction of the ophiolitic nappes (Bozkir ophiolitic nappes of Ozgul 1978) was from the north (present geographical position) resulted in depressions in front of the advancing nappes due to the differential crustal loading (Sengor & Yilmaz 1981). In these depressions, the Ankara Melange Unit II (of the present author) was emplaced as large scale olistostromes associated with other mass flow deposits. The sediments were derived from the ophiolitic nappes and sedimentation continued until the Campanian. The nature of the sedimentary melange of Unit II has been well documented by Norman (1975) who suggested that most of the linear features which were previously interpreted as faults were, in fact, flow lines or pathways of olistostromes.

The occurrence of continental island arc type volcanism (Saridere volcanic formation Chp.2) in the NNW and the Baranadag plutonic complex (mainly calc-alkaline granites) in the WSW margin of the Kirsehir block, at the beginning of the Maastrichtian (Fig 13.6), suggest a south dipping subduction of the floor of the northern branch of Neo-Tethys beneath the Kirsehir block which, on the bases of Sanver & Ponat's (1981)

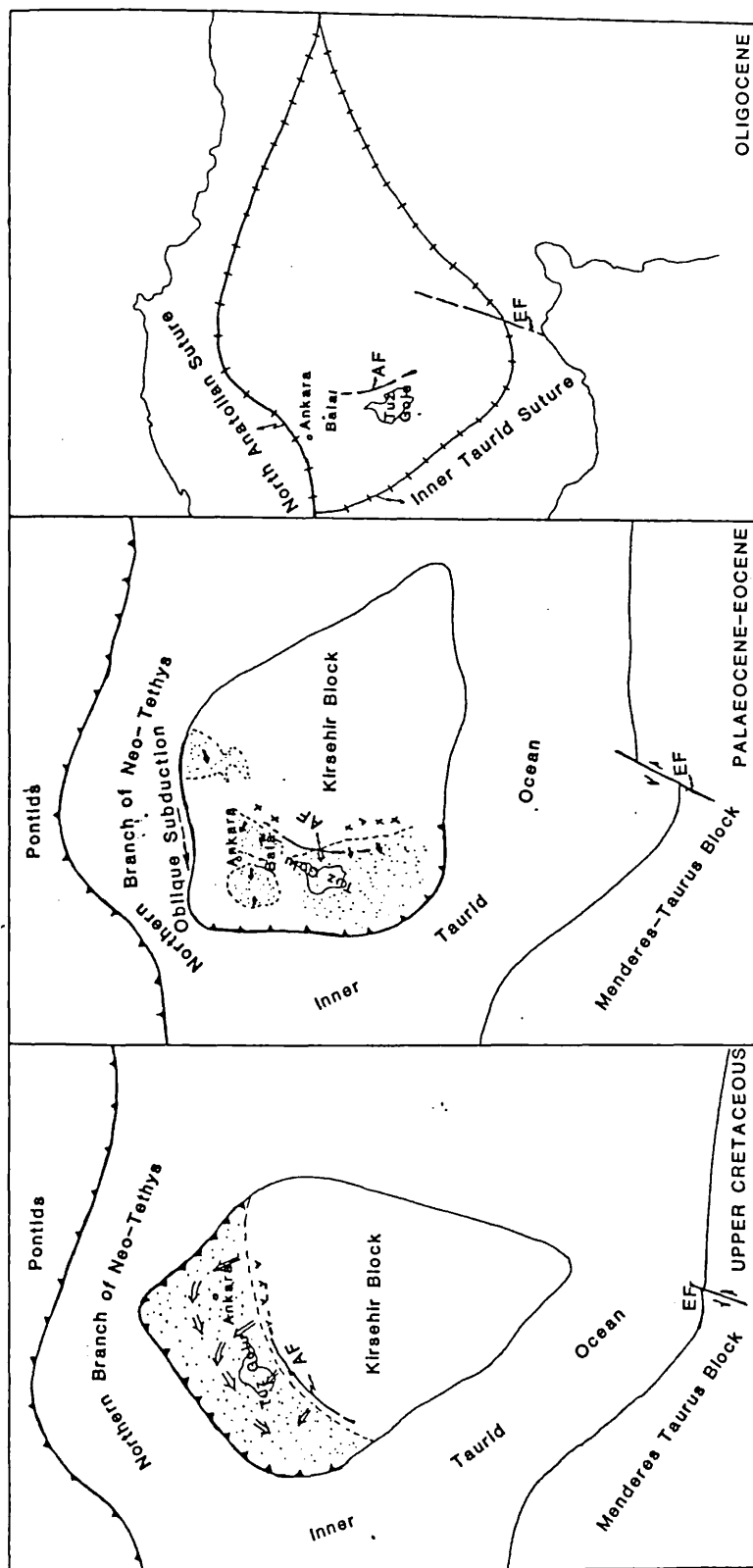


Fig 13.6 - Palaeotectonic maps showing the plate tectonic evolution of central Anatolia from the upper Cretaceous to Oligocene. Stippled areas: turbidite depocenters arrows indicate current directions, V: Continental island arc volcanic, X: continental island arc igneous rocks, EF: Ecebus Fault, AF: Aksary fault.

palaeomagnetic data. was 90° (clockwise) from its present orientation. Considering that there should be at the least a 10 my gap between the initiation of subduction and volcanic activity (Gill 1981), it can be suggested that the starting of the subduction occurred in the Santonian. Because of this north facing continental island arc probably two forearc basins were formed, either as continuation of the depression caused by the obduction of ophiolitic nappes or as a response to the subduction (see Chp. 12 for discussion). The first extended from Cankiri in the NE to Haymana in the SW and the second was the Tuzgolu basin which extended from Haymana in the N to Ulukisla in the S. In the first, during the Lower Maastrichtian, the Kamisli and Davdanli formations (see Chp. 3,4) and their counterparts in Cankiri-Corum, Kirikkale and Haymana areas were deposited as interbedded volcanoclastic and pyroclastic, fine grained turbidites which reached a thickness of up to 1800 m in the Haymana area. (Norman et al 1980, 1979, Unalan et al 1976). The sediments are lithologically and compositionally similar in all areas except for the Haymana area where mixing of some ophiolitic debris with the volcanoclastics and pyroclastic were observed. The sediment transport in all these areas generally paralleled the NE-SW basinal axis, and mainly originated from the ESE margin. In the Tuzgolu basin while red clastics associated with evaporites were being deposited on the continental areas towards the E (in the basinal areas) fine grained turbidites were accumulating. (Uygun 1981, Gorur 1981). Although the depositional pattern in the Tuzgolu basin was similar to the basin extending from Cankiri to Haymana, it differs in the composition of its sediments which was mainly ophiolitic. This together with the occurrence of ophiolitic debris with volcanoclastics and pyroclastics in the Haymana area and the absence of any palaeocurrent or compositional evidence suggesting sediment transport from the Western margin of the basin suggest that:

A. at this time the Baranadag plutonic complex had

not yet emerged thus sediments were mainly derived from the obducted ophiolitic nappes,

B. volcanic activity was confined to the north and northwestern part of the continental island arc.

C. the basin was a terraced forearc basin similar to those of the Shimanto belt of Japan (Taira *et al* 1982) Another feature in this forearc setting was the Aksaray fault situated trenchward of the arc axis and extending from Aksaray in the S to Kirikkale in the N. This fault probably was an upper slope discontinuity separating the arc, which was being uplifted, from the subsiding forearc basins.

From such interpretations it is concluded that during the Santonian the floor of the Inner-Taurid ocean started to subduct under the Kirsehir block. The mid-ocean ridge junction of the Inner-Taurid ocean either with Izmir-Ankara Ocean or with the northern branch of Neo-Tethys was probably to the NE of the Cankiri-Corum area. As a result of this subduction a continental island arc paralleling the NNW and WSW margin of the Kirsehir block, formed during the Early Maastrichtian creating probably two forearc basins which are separated from the arc by a major upper slope discontinuity. The existence of two basins is implied by the compositional difference in the sediments of the Tuzgolu and the basin extending from Conkiri to Haymana separated, probably, by a submerged ridge. However it is possible that there was only one forearc basin extending from Conkiri in the N to Ulukisla in the S and the compositional difference referred to above was a product of changes in source areas. Unfortunately because the link between the Haymana and Bala area and Tuzgolu basin cannot be seen it is not possible, at present, to decide which of these models is the true one. In the basin(s) sediments, always transported from the eastern margin of the basin(s), were deposited mainly as fine grained turbidites predominantly from longitudinal transport. Thus any basin was a terrace forearc basin and around 2 km of

sediment was deposited during the Maastrichtian. Volcanic activity was restricted to the NNW part of the arc and most probably ceased at the beginning of the Middle Maastrichtian. Because of volcanic activity and active tectonism, a number of slump folds and slump sheets occurred within the succession.

The great extent of the basin(s), generally fine grain- ed nature of the sediment, sediment transport directions pre- dominantly parallel to the basinal axis and lithological and compositional continuity of the sediments, in terms of tens of kilometres, are features in excellent agreement with the sedimentation pattern proposed for a forearc basin, suggested by Howell et al (1980), for the Late Mesozoic forearc basins of California and Baja California.

At the beginning of the Palaeocene (Fig 13.6B) a change in the plate tectonic setting of the basins due to the anti-clockwise rotation of the Kirsehir block resulted in oblique subduction or transform faulting in the area between Conkiri and Haymana. The Tuzgolu basin retains its forearc basin characteristics. The reflection of this change in basin configuration and sedimentation pattern was obvious as the Bala basin was separated from the Tuzgolu, Haymana and Conkiri- Corum basins. The structural and sedimentological evidence for changing the tectonic regime from a subduction related forearc setting to strike-slip fault dominated basin setting, from the Bala area, is given below by taking the points suggested by Reading (1975, 1980a, 1980b, and 1982) and Howell et al (1980) for the recognition of the strike-slip fault related basins.

a. The basins are small (in terms of a few tens of kilometres) fault bounded and deep.

b. The later continent-continent collision of the Kirsehir Block with the Pontids (including the Sakarya continent) and the Menderes-Taurus Block, resulted in extensive

thrusting of the Ankara Melange to the Upper Cretaceous-Tertiary sediments during the pre-Miocene. Thus the major faults involved in the Palaeocene strike-slip movements were either obliterated or became unrecognizable and the lateral matching of the displaced palaeogeographies became impossible

c. Vertical and lateral movements of the faults:

Although there is evidence, in the Bala area, vertical movement of the southeastern margin of the basin (i.e. abundance of conglomerates, indicating proximity of the source area to the basin, rapid lateral facies variation, thick and rapid sedimentation showing abrupt thickness changes, the occurrence of regressive and transgressive cycles succeeding each other and the presence of abundant submarine slumping (see Chp. 12) only the lateral movement of the faults can only be observed in some degree of certainty. Along the Saridere, alluvial fan deposits of the Sarikaya member of the Ucem formation (Chp. 6) on the southeastern and northwestern side of the Kurebogazi-II fault show compositional and textural differences which are interpreted as related to lateral movements on the fault. (see Chp. 11). However, the amount of the offset of the fault cannot be estimated due to poor exposure and the effect of later tectonism. Another important criterion implying of lateral movements again comes from the alluvial deposits which, in spite of having granite gravels, indicating a local source, borders the Ankara Melange along the Kurebogazi I fault.

d. The presence of extreme lateral and vertical facies variation is especially evident in the basin margin deposits. (see Chps. 6, 7 and 12)

e. The availability of frequent conglomerates in the turbidites indicating a high gradient and narrow deltaic plain (i.e. a narrow shelf) together with the general absence of extensive shelf deposits, suggests slope instability due to basin margin faults (Van de Kamp et al 1974)

f. The occurrence of extensive slope sedimentation (see Chp. 8) which is considered to be one of the most important depositional processes in the strike-slip fault controlled basins (Nardin et al 1979 b)

g. The existence of localized uplift and erosion as indicated by the occurrence of an angular unconformity in the Bala area between the Middle Eocene probably Oligocene deposits of the Kizildag and Keklikpinari formations with the underlying Upper Cretaceous-Middle Eocene sediments which contrasts with their uninterrupted sedimentation around Kirikkale (Norman 1972)

h. The occurrence of compressional and tensional areas in the same tectonic belt (as shown in the (Figs 13.4 & 5)) is likely. Although evidence for the separation of the Bala basin from the Cankiri-Corum basin is sparse, the separation of the Haymana, Bala and Tuzgolü basins is evident in the SE. As shown in the Fig 13.5, during the Palaeocene-Middle Eocene period, while sedimentation was continuing in the basins, the area extending from Karaali (Location 6) to SE of Mollaresul (Location 9) was uplifted and eroded. In addition the area around Pasadag (Location 10) most probably was uplifted at least during the lower Palaeocene as during this time the Bala and Tuzgolü basins appears to have been separated (see Chp. 12)

g. So far as structural style concerned, later tectonism makes it difficult to unravel the structural features. However the occurrence of thrust faults slightly oblique to the Kurebogazi I fault which was most probably one of the major strike-slip faults and the occurrence of normal and strike slip faults with varying but always oblique to perpendicular angles to the thrust faults give a picture similar to that indicated by Reading (1980) for the structural style of strike-slip fault related basins.

h. The absence of metamorphism.

i. The absence of magmatic activity apart from the emplacement of the Karaca ali granitic pluton at the beginning of the Palaeocene. This event is thought to be a continuation of subduction related events since it is accepted that igneous activity may continue after the cessation of the subduction for up to 5 my (Gill 1981).

Although all these criteria, can be individually interpreted differently, their combination clearly suggests a basin which was, during the Palaeocene-Eocene period, controlled by strike-slip fault movements. Consequently it is suggested that, due to the rotation of the Kirsehir block (confirmed by the palaeomagnetic data of Sonver & Ponat (1981) which suggested a 90° anti-clockwise rotation in the upper Cretaceous-Eocene), the area between Cankiri and Haymana changed from a forearc setting to a strike-slip fault related setting while Tuzgolu basin, throughout its life span remained as a forearc basin.

Although the absence of any sediment derivation from the northwestern margin of the Bala basin is somewhat unusual for a strike-slip related basin, it is probably because either the northwestern part of the basin is underneath the overthrust Ankara Melange thus unobservable or the Bala basin during the Palaeocene-Middle Eocene period remained as a terrace forearc basin controlled by strike-slip fault movements.

The collision of the Kirsehir block with the Menderes-Taurus block along the Inner-Taurid suture and with the Pontids along the Ankara-Erzincan suture probably commenced during the Late Eocene or Early Oligocene and continued until the end of the Oligocene. This event resulted in the welding of these continents (Fig 13.6) and overthrusting of the Ankara Melange onto the Upper Cretaceous-Tertiary sediments.

CHAPTER 14

SUMMARY and CONCLUSION

The rocks exposed in the area studied which is situated on the northern extension of the Tuzgolu basin, central Anatolia, Turkey, range from Upper Cretaceous to Tertiary and include the stratigraphically upper part of the Ankara Melange which forms the basement. The successions in the Bala area, are composed of volcanic, clastic and carbonate rocks with evaporites. A total of nine formations is distinguished and in ascending order the formations are;

a. Saridere Volcanic Formation: This is inferred to be Maastrichtian in age and consists of andesites, dacitic, tuff and ignimbrites together with some red conglomerates, volcanic lithic arenites and mudstones of alluvial fan origin, deposited during an inactive period of volcanism. The volcanics, on the basis of their chemical composition, are Andean type calc-alkaline rocks.

b. Kamisli Formation: It is Lower Maastrichtian and consists of interbedded volcanic lithic arenites, reworked tuffs, which are particularly dominant in the lower part of the formation, and shales. The formation also contains a number of small and large scale submarine slump sequences which are believed to be an indication of the seismicity of the area rather than a particular environment of deposition in the basin. The Kamisli formation is interpreted as being deposited on the basin floor by longitudinal transport.

c. Davdanli Formation: This is Middle-Upper Maastrichtian, overlies the Kamisli formation conformably and consists of polymict conglomerates, lithic arenites, shales and marls, which are believed to have been accumulated as slope and inner, middle, and outer fan deposits.

d. Degirmendere Formation: This is Lower Palaeocene and comprised of monomict volcanic conglomerates, volcanic arenites and shales. It is interpreted as having been deposited by a number of small submarine fans.

e. Ucem Formation: Middle Palaeocene - Early Eocene in age, it has two members; Sarikaya and Sehriban. The former consists of red polymict conglomerates, lithic arenites and mudstones, and the latter has fossiliferous lithic arenites, mudstones, and some polymict conglomerates. They are interpreted as fluviatile (mainly alluvial fan) and shallow marine deposits respectively.

f. Kocanindambasi Formation: This formation is Middle Palaeocene - Early Eocene in age, interfingers with the Ucem formation and is a bioclastic limestone which was deposited as carbonate mounds. Four subfacies are recognised;

1. packstone and wackestone containing a mixed fauna of large and small benthonic foraminifers and fragments of other skeletal organisms together with some planktonic foraminifers

2. a patchy coral-algal boundstone and packstone

3. a Rotaliid-algal packstone

4. Miliolid-algal packstone and wackestone. They are interpreted to have been deposited as normal shelf carbonates, carbonate mounds, seaward flanking and landward flanking beds respectively. The diagenetic environment was mainly marine apart from episodes of brackish water diagenesis.

g. Bayat Formation: The Middle Palaeocene-Early Eocene Bayat formation conformably overlies the Degirmendere formation and interfingers with the Ucem and Kocanindambasi formations. It consists of polymict conglomerates, calcirudites, lithic arenites, calcarenites, shales, marls and

Middle Palaeocene-Early Eocene limestone olistoliths, and has three members. The Kurebogazi member contains upper and lower slope sediments, the Ardiclipinar member represents inner fan deposits and the Buyukdere member is comprised of middle and outer fan to basinal deposits. The outer fan-basinal deposits are separated into sandstone depositional lobes, lobe fringe and fan fringe to basinal sequences.

h. Kizildag Formation: It is Middle Eocene in age and overlies the previous formations with an angular discontinuity. The formation is comprised of red polymict conglomerates, lithic arenites and mudstones with laminated evaporites and thought to have been a fluvial deposit with evaporites in local depressions.

i. Keklikpinari Formation: This conformably overlies and interfingers with the Kizildag formation and is Middle Eocene to probably Oligocene in age. It consists of lithic arenites, mudstones, polymict conglomerates, limestones (as foraminiferal packstone and mudstone), and bedded evaporites forming lens shaped bodies. A small deltaic deposit is also included into this formation. These sediments show characteristics of shallow marine environment of deposition.

The sedimentary history of the Bala basin started during the Lower Maastrichtian with the deposition of Sari-dere volcanic formations rocks on a continental margin island arc, at the southeastern margin of the basin while the turbidites of the Kamisli formation were being deposited in the basinal areas mainly by longitudinal transport. The effect of volcanic activity and active tectonism caused extensive submarine slumping. During the Middle-Upper Maastrichtian, the Davdanli formation succeeded the Kamisli formation as submarine fans and slope deposits. In the Early Palaeocene, the Degirmendere formation accumulated as number of small

submarine fans of local origin. The higher emplacement of Karacaali granitic pluton and/or change in the tectonic setting of the basin (see below) was responsible for this formation's extremely coarse grained nature. During the Middle Palaeocene-Middle Eocene period, on the southeastern margin of the basin the Sarikaya member was deposited as alluvial fans, the Sehriban member as shallow marine clastics and the Kocanindambasi formation as shallow marine carbonates interfingering with each other. These show a number of regressive and transgressive episodes. In the basinal areas the Kurebogazi member accumulated on the upper and lower slope, the Ardiclipinar member on the inner fan and the Buyukdere member on the middle to outer fan to basinal areas. About the Middle Eocene, the basin was uplifted and deformed and the Kizildag formation was deposited as continental red clastics with evaporites while the Keklilpinari formation was accumulated as shallow marine clastics, carbonates and evaporites, both resting on the deformed strata of the previous formations.

The present structure of the area is the result of active tectonism during late Alpine movements. The movements controlled the conditions of sediment accumulation.

The Bala basin evolved on the northern continental margin of the Kirsehir block. A brief period of south dipping subduction, which created a continental island arc, was followed by oblique subduction, transform fault and continent to continent collision stages. These determined the shape and depositional characteristic of the basin. This is supported by independent magnetic evidence suggesting a 90° anti-clock wise rotation of the Kirsehir block during the Upper Cretaceous-Eocene period.

REFERENCES

- ABBATE, E., BORTOLOTTI, V. & PASSERINI, P., 1970. Olistrostromes and Olistoliths. Sediment. Geol., 4, 521-557
- ADEY, W.H. & MACINTYRE I.E., 1973. Crustose coralline algae: a re-evaluation in the geological science. Bull. Geol. Soc. Am., 84, 883-904
- AKYUREK, B., 1981. Ankara Melanji'nin Kuzey bolumunun temel jeoloji ozellikleri. Ic Anadolunun jeolojisi simpozyumu. T.J.K. 35. Teknikve Bilimsel Kurultayi Mart 1981. Ankara 41-45
- AKYUREK, B., BILLGINER, E., CATAL, E., DAGERZ., SOYSAL, Y. SUNU, O., 1979. Eldivan-Sabanozu (Gankiri) dolayinda ofiyolit yerlesmesine iliskin bulgular. J.M.D. VAYIN ORGANI, SAYI 9 Ankara
- ALEXANDERSSON, T., 1977. Carbonate cementation in recent Coralline Algal construction. In: FLUGEL, E. (Ed) Fossil Algae, 261-269 Springer-Verlag
- ALLEN, J.R.L., 1965. A review of the origin and characteristics of recent alluvial sediments. Sedimentology, 5, 89-191
- ALLEN, J.R.L. 1982. Sedimentary Structures: Their character and physical basis. Developments in Sedimentology 30 A,B. Elsevier.
- ALLMAN, M & LAWRENCE, D.F. 1972. Geological Laboratory Techniques. London Blandford Press. 328 pp.
- ALTINER, D., 1974. Geology of Kamislibala-Keklicecek area, Bala-Ankara. M.E.T.U. MS thesis (unpublished).
- ARGAND, E., 1922. La Tectonique de l'Asie. Congress Geol. Intern. XIII Sess. Belgique, Foscl
- ARIKAN, Y., 1975. Tuz golu havzasinin jeolojisi ve petrol imkanlari. M.T.A. Bull., No: 85 Ankara 17-37.
- ARNI, P., 1939. Tektonische Grundzuge Ostanatoliens und benachbarter Gebiete. Veroff. Inst. Largerstattenforsch, Turkei, Ser. B. 4: 90 pp.
- BAILEY, F.R.S. & MCCALLIEN, W.J., 1950. The Ankara Melange and Anatolian Thrust. Nature, 166, 938-940
- BAILEY, F.R.S. & MCCALLIEN W.J., 1953. Serpentine lavas, the Ankara Melange and the Anatolian thrust. Trans. Roy Soc. Edinb., LXII, Part II. 11, 403-442.
- BANDY, O.L., 1964. General correlation of foraminiferal structure with environment. In: IMBRIE, J. & NEWELL, N.D. (Ed's), Approaches to Paleoecology. JOHN WILEY - New York. 75-90
- BATHURST, R.G.C., 1976. Carbonate Sediments and Their Diagenesis. Development in Sedimentology 12. ELSEVIER 658 pp.

- BATMAN, B., 1978 (a). Geologic evolution of Northern part of Haymana Region and study of Melange in the area I, Yerbilimleri, Vol. 4, 95-124.
- , 1978 (b). Geologic evolution of Northern part of Haymana Region and study of Melange in the area II, Yerbilimleri, Vol. 4, 125-134.
- BAYKAL, F., 1943. Kirikkale-Kalecik ve Keskin-Bala mintik-
alarindaki jeolojik etudler. M.T.A. Derleme Ra-
poru, no. 1448.
- BIJU-DUVAL, B., DERCOURT, J., PICHON, X.Ie., 1976. From the
Tethys ocean to the Mediterranean seas: a plate
tectonic model of the evolution of the western
Alpine system. In: BIJU-DUVAL B. & MONTADERT,
L. (Ed's) Structural History of the Mediterranean
Basins: Symposium Intern. Split-Yugoslavia.
- BINGOL, E., 1976. Evolution geotectonique de l'Anatolie de
l'Ouest. Bull. Soc. Geol. Fr. Ser. 7, 18: 235-254.
- BLATT, H., MIDDLETON, G., & MURRAY R., 1972. Origin of Sed-
imentary Rocks. PRENTICE - Hall, Inc. New
Jersey 634 pp.
- BLUMENTHAL, M., 1946. Die neue geologische Karteder Turkai
und einige ihrer stratigraphisch-tektonischen
Grundzuge. Eclogae. Geol. Helv., 39, No. 2
- BONATTI, E., 1968. Mechanism of deep sea volcanism in the
South Pacific. In: ABELSON, P.H. (Ed); Research-
es in Geochemistry. New York, WILEY, 453-491.
- BOESSAMA, A., 1978. Foraminifera. In: HAQ, B.U. & BOESSAMA
A (Eds) Introduction to Marine Micropalaentology.
Elsevier.
- BRINKMANN, R., 1976. Geology of Turkey. FERDINAND ENKE VERLAG
Stuttgart 153 pp.
- BULL, W.B., 1972. Recognition of alluvial fan deposits in
the stratigraphic record. In: RIGBY, J.K. &
HAMBLIN, W.K. (Ed's) Recognition of Ancient Sed-
imentary Environments. Soc. Econ Paleont Mineral.
Special Publ. 16. 63-83
- CHUKHROV, F.V. 1973. On minerological and geochemical cri-
teria in the genesis of red beds. Chemical Ge-
ology, 12, 67-75.
- CLAY MINERALS: A guide to their X-ray identification. Geol.
Soc. Am. Spec. Paper. 126
- COLLINSON, J.D., 1980. Alluvial sediments. In: READING H.G.
(Ed). Sedimentary Environment and Facies. Black-
well Scientific Publ. 15-60
- COOK, H.E., 1979. Ancient continental slope sequences and
their value in understanding modern slope devel-
opement. In: DOYLE, L.J. & PILKEY, O.H. (Ed's).
Geology of Continental Slopes. Soc. Econ. Paleont.
Mineral. Special Publ., 27, 287-305

- COX, K.G., BELL, J.D. & PANKHURST R.J., 1979. The Interpretation of Igneous Rocks. GEORGE ALLEN & UNWIN LTD. London. 450 pp.
- CRIMES, T.P., 1977. Trace fossils of an Eocene deep-sea sand fan, northern Spain. In: CRIMES, T.P. & HARPER, J.C. (Ed's) Trace Fossils 2, Steel House Press, Liverpool. 71-90.
- DEWEY, J.F. & BIRD, J.M., 1970. Mountain belts and the new global tectonics. Journ. Geophys. Research., 75, 2625-2647.
- DEWEY, J.F., PITMAN, W.C., III, RYAN, W.B.F. & BONNIN, J., 1973. Plate tectonics and the evolution of the Alpine System. Geol. Soc. Am. Bull. 84, 3137-3180.
- DUNHAM, R.J., 1962. Classification of carbonate rocks according to depositional texture. In: HAM, W.E. (Ed), Classification of Carbonate Rocks. Am. Ass. Petrol. Geol. Mem. 1. 108-121
- DUNHAM, R.J., 1969. Vadose pisolite in the capitan reef (permian), New Mexico and Texas. In: FRIEDMAN, G.M. (Ed) Depositional Environments in Carbonate Rocks. Soc. Econ. Paleon. Mineral. Spec. Publ. 14 182-191
- DZULYNSKI & WALTON, 1965. Sedimentary Features of Flysch and Graywacke, Developments in Sedimentology, 7, Elsevier
- EGERAN, E.N., 1947. Tectonique de la Turquie, et relations entre les unites tectonique et les gites metalliferes. These Nancy.
- EGGLESTON, J.R. & DEAN, W.E., 1976. Freshwater stromatolitic bioherms in Green lake, New York. In: WALTER, M.R., Stromatolites. Developments in Sedimentology, 20, 479-488
- ELLIOT, T. 1980. Deltas and clastic shorelines. In: READING H.G. (Ed). Sedimentary Environments and Facies. Blackwell Scientific Publ. 97-177.
- ERK, S., 1980. Ankara Flisi. TBTAK VII. Bilim Kongresi Tebligleri Ozeti. P.16
- ERKAN, Y., 1981. Orta Anadolu masifinin metamorfizmasi uzerinde yapilmis calismalarda varilan sonuclar. Ic Anadolunun Jeoloji si Simpozyumu, T.J.K. 35
- EROL, D., 1956. Ankara guneydogusundaki Elma Dagive cevresinin jeolojisi ve jeomorfolojisi uzerinde bir arastirma. MTA Yay. D.9. Ankara
- FAIRBRIDGE, R.W., & BOURGEOIS, J., 1978. The Encyclopedia of Sedimentology. DOWDEN, HUTCHINSON & ROSS INC. Stroudsburg. 901 pp.

- FISHER, R.V., 1961. Proposed classification of volcanoclastic sediments and rocks. Bull. geol. Soc. Am., 72, 1409-1414.
- FISHER, R.V., 1966. Rocks composed of volcanic fragments and their classification. Earth Sci. Rev., 1, 287-298.
- FISKE, R.S. & MATSUDA, T., 1964. Submarine equivalents of ash flows in Takiwa Formation, Japan. Amer. Jour. Sci., 262, 76-106
- FOLK, R.L., 1965. Some aspects of recrystallization in ancient limestones. In: PRAY L.C., & MURRAY R.C. (Ed's). Dolomitization and Limestone Diagenesis: a Symposium. Soc. Econ. Paleont. Mineral. Spec. Publ., 13, 14-48.
- FOLK, R.L., (1974). Petrology of Sedimentary Rocks. Hemphill Publishing Company, Austin, Texas. 182 pp.
- FRIEDMAN, G.M., 1978. Depositional environments of evaporite deposits. In: DEAN W.E. & SCHREIBER, B.C. (Ed's). Marine Evaporites. Soc. Econ. Paleont. Mineral. Short Course, 4, 177-184
- GANNSEER, A., 1959. Ausseralpine Ophiolitprobleme. Eclog. Geol. Helv. 52, 659-680
- GEBELEIN, C.D., 1976. Open marine subtidal and intertidal stromatolites (Florida, the Bahamas and Bermuda). In: WALTER, M.R. (Ed.) Stromatolites, Developments in Sedimentology, 20, 381-388.
- GILL, J., 1981. Oragenic Andesites and Plate Tectonics. Springer-Verlag, New York, 387 pp.
- GLENNIE, K.W., 1970. Desert sedimentary environments. Developments in Sedimentology, 14, 222 pp. Elsevier
- GLOPPEN, T.G. & STEEL, R.J., 1981. The deposit, internal structure and geometry in six alluvial fan-fan delta bodies (Devonian-Norway). In: ETHRIDGE, F.G., & FLORES, R.M. (Ed's), Recent and Ancient Non marine Depositional Environments. Soc. Econ. Paleont. Mineral. Spec. Publ. 31, 49-70.
- GOKCEN, S.L., 1976. Haymana guneyinin sedimentolojik incelemesi 1. stratigrafik birimler ve tektonik. Yer-bilimleri 2. 161-201.
- GONCUOGLU, M.C., 1981. Nigde masifinin jeolojisi. Ic Anadolunun jeolojisi simpozyumu. T.J.K. 35. Bilimsel ve Teknik Kurultayi. Mart 1981, Ankara 16-19

- GORUR, N., 1981. Tuzgolu ve Haymana havzasinin strati-grafik analizi. Ic Anadolunun jeolojisi simpozyumu. T.J.K. 35. Teknik ve Bilimsel Kurultayi. Mart 1981. Ankara 60-65
- HATCH, F.H., WELLS, A.K. & WELLS, M.K., 1972. Petrology of Igneous Rocks. THOMAS MURBY & CO. London 551 pp.
- HECKEL, P.H., 1972. Recognition of ancient shallow marine environments. In: RIGBY, J.K. & HAMBLIN WM.K. (Ed's), Recognition of Ancient Sedimentary Environments. Soc. Econ. Paleon. Mineral. Spec. Publ., 16, 226-286
- HENSON F.R.S., 1975. Cretaceous and Tertiary reef formations and associated sediments in Middle East. In: Carbonate Rock III; Organic Reefs. Am. Assoc. Petrol. Geol. Reprint series 15.
- HESSE, R. & BRUTT, A., 1976. Palaeobathymetry of Cretaceous turbidite basins of the east Alps relative to the Calcite Compensation Level. J. Geol., 84 505-553
- HEWARD, A.P. & READING, H.G., 1980. Deposits associated with a Hercynian to late Hercynian continental strike-slip system. Contabrian Mountains, Northern Spain. In: BALLANCE, P.F. & READING H.G., Sedimentation in oblique Strike-Slip Mobile Zones. Spec. Publ. Int. Ass. Sediment. 4, 105-125
- HOFFMAN, P., 1976. Stromatolite morphogenesis in Shark Bay, Australia. In: WALTER, M.R. (Ed) Stromatolites, Developments in Sedimentology, 20, 261-272
- HORSTINK, J., 1971. The late Cretaceous and Tertiary evolution of eastern Turkey. In: KESKIN, C. & DEMIRMEN, F. (Ed's) Proceedings of First Petroleum Congress of Turkey. 25-41
- HOWELL, D.G., CROUCH, J.K., GREENE, H.G., MCCULLOCH, D.S. & WEDDER, J.G. Basin development along the late Mesozoic and Cainozoic California margin: a plate tectonic margin of subduction, oblique subduction and transform tectonics. In: BALLANCE, P.F. & READING, H.G. (Ed's) Sedimentation in oblique strike-slip Mobile Zone. Spec. Pub. int. Ass. Sediment., 4, 43-62
- HSU, K.J., 1971. Franciscan Melanges as a model for eugeo-synclinal sedimentation and underthrusting tectonics. J. Geophys. R., 76 1162-1170
- HSU, K.J. 1977. Tectonic evolution of the Mediterranean basin. In: NAIRN, A.E.M., KANES, W.H. & STEHLI, F.G., (Ed's). The Ocean Basins and Margins 4A The Eastern Mediterranean 29-76

- JAKES, P. & WHITE, A.J.R., 1972. Major and trace element abundances in volcanic rocks of orogenic areas. Bull. geol. Soc. Am., 83, 29-40
- JOHNSON, H.D., 1980. Shallow siliciclastic seas. In: READING, H.G. (Ed) Sedimentary Environments and Facies. Blackwell Scientific Publ. 207-258
- KERR, P.F., 1959. Optical Mineralogy. McGraw-Hill, New York. 441 pp.
- KETIN, I. 1959. The orogenic evolution of Turkey. Bull. Miner. Rec. Explor. Inst. Turkey, 53, 82-88
- KETIN, I., 1963. Explanatory Text of the Geological Map of Turkey, Kayseri sheet, 1/500000 scale, MTA publication, ANKARA/Turkey
- KETIN, I. 1966. Tectonic Units of Anatolia. Bull. Miner Res. Expl. Inst. Turkey, 66, 23-35
- KEUNEN PH.H., 1958. Problems concerning source and transport of flysch sediments. Geol. Mijnbouw., 20, 329-339
- KOBER, L., 1931. Das Alpine Europa. Berlin.
- KRESIA, R.D., 1981. Storm-generated sedimentary structures in subtidal marine facies with examples from the Middle and Upper Ordovician of southwestern Virginia. J. Sediment. Petrol. 51. 823-848
- KSIAZKIEWICZ, M. 1970. Observations on the ichnofauna of the Polish Carpatian. In: CRIMES, T.P. & HARPER, J.C., Trace Fossils. Steel House Press, Liverpool. 283-322.
- KUMAR, N. & SANDERS, J.E., 1976. Characteristics of shore-face storm deposits: modern and ancient examples. J. Sediment Petrol. 46 145-162.
- MCKENZIE, D.P., 1970. Plate tectonics of Mediterranean region. Nature, 226, 239-243
- MAJEWSKE, O.P., 1969. Recognition of Invertebrate Fossil Fragments in Rocks and Thin Sections. Leiden 101 pp.
- MIDDLETON, G.V. & HAMPTON, M.A., 1976. Subaqueous sediment transport and deposition of sediment gravity flow. In: STANLEY D.J. & SWIFT, D.J.P. (Ed's), Marine Sediment Transport and Environmental Management. John Wiley New York, 197-218
- MILLIMAN, J.D., 1977. Role of calcereous algae in Atlantic continental margin sedimentation. In: FLUGEL, E., (Ed) Fossil Algae, Springer-Verlag, 232-247.
- MONTY, C.L.V., 1976. The origin of development of cryptalgal fabric. In: WALTER, M.R. (Ed). Stramatolites. Developments in Sedimentology 20. 193-249. Elsevier

- MURATOV, M.V., 1964. History of the tectonic development of Alpine folded region of southeastern Europe and Asia Minor-New data on the tectonic structure and history of development of the Alpine zone of Europe. In: Int. Geol. Review, 6, 99-118.
- MURRAY, J.W., 1973. Distribution and Ecology of Living Benthonic Foraminiferids. Crane, Russak and Co, New York. 274 pp.
- MUTTI, E., 1974. Examples of ancient deep-sea fan deposits from circum-Mediterranean geocynclines. In: DOTT, R.H. Jr. & SHAVER, R.H. (Ed's), Modern and Ancient Geosyncline Sedimentation. Soc. Econ. Paleont. Mineral. Spec. Publ., 19, 92-105
- MUTTI, E. & RICCI LUCCI, F., 1975. Turbidite facies and facies associations. In: Examples of Turbidite Facies and Facies Associations from selected Formations of the Northern Apennines. Field Trip Guide book A-11, IX. Intr. Sediment Congr. Nice. 21-36
- NARDIN, T.R., HEIN, F.J., GORSLINE, D.S. & EDWARDS, B.D., 1979. A review of mass movement process, sediment and acoustic characteristics, and contrasts in slope and base-of-slope versus canyon-fan-basin floor systems. In: DOYLE, L.J., & PILKEY D.H. (Ed's). Geology of Continental Slopes. Soc. Econ. Paleont. Mineral. Special Publ., 27, 61-74
- NARDIN, T.R., EDWARDS, B.D. & GORSLINE, P.S., 1979. Santa Cruz basin, California borderland: Dominance of slope process in basin sedimentation. In: DOYLE, L.J. & PILKEY, D.H. (Ed's). Geology of Continental Slopes. Soc. Econ. Paleont. Mineral. Special Publ. 27, 209-227
- NAUMAN, E., 1896. Die Grundlini Anatoliens und Zentralasian. Geogr. Zs. 2.
- NELSON, C.H. & KULM, L.D., 1973. Submarine fans and deep sea channels. In: Turbidite and Deep-Water Sedimentation. Soc. Econ. Paleont. Mineral. Short Course Mainheim 39-78
- NELSON, C.H. & NILSEN, T.H., 1974. Depositional trends of modern and ancient deep-sea fans. In: DOTT, R.H. Jr. & SHAVER, R.H. (Ed's), Modern and Ancient Geocyncline Sedimentation. Soc. Econ. Paleont. Mineral. Spec. Publ., 19, 69-91
- NELSON, H., MUTTI, E., LUCCI, F., 1977. Upper Cretaceous resedimented conglomerates at Wheeler Gorge, California: Description and field guide. Journal of Sed. Petrol. 47, 926-934

- NEMEC, W., POREBSKI, S.J., STEEL, R.J., 1980. Texture and structure of resedimented conglomerates: examples from Ksiaz Formation (Fomennian-Tournaisian), Southwestern Poland. Sedimentology 27, 519-538
- NILSEN, T.H. & ABBOTT, P.L., 1981. Palaeogeography and sedimentology of Upper Cretaceous turbidites, San Diego, California. Bull Am. Assoc. Petrol. Geol. 65, 1256-1284
- NORMAN, T.N., 1972. Ankara-Yahsihan bolgesindeki U. Kre-tase-A. Tersiyer ıstrfinin stratigrafisi. T.J.K. Bulteni. Cilt 15 Sayı 2, 180-276
- NORMAN, T.N., 1973. Ankara-Yahsihan bolgesindeki U. Kre-tase-A. Tersiyer sedimentasyonu. T.J.K. Bulteni Cilt 16 Sayı 1, 41-66
- NORMAN, T.N., 1975. Flow features of Ankara Melange. IXne Congres International de Sedimentologie, Nice 1975. Theme 4, 261-269
- NORMAN, T.N., GOKCEN, S.L. & SENALP, M., 1979. Late Cretaceous-Early Tertiary sedimentation in the Central Anatolian basin (Turkey). Cretaceous-Tertiary Boundary Events Symp. Proc., 207-213
- NORMAN, T.N., GOKCEN, S.L. & S.L. & SENALP, M. 1980. Sedimentation pattern in Central Anatolia at the Cretaceous Tertiary boundary. Cretaceous Res., 1, 61-84
- NORMARK, W.R., 1970. Growth patterns of deep-sea fans. Bull Am. Ass. Petrol. Geol. 54, 2170-2195
- NORMARK, W.R., 1974. Submarine canyons and fan valleys: factors affecting growth patterns of deep-sea fans. In: DOTT, R.H. Jr. & SHAVER, R.H. (Ed's), Modern and Ancient Geosyncline Sedimentation. Soc. Econ. Paleont. Mineral. Spec. Publ., 19, 56-68
- OKTAY, F.Y., 1973. Sedimentary and tectonic history of the Ulukisla area, southern Turkey. Unpubl. Univ. College. London Ph. D. Thesis 414 pp.
- PETTIJOHN, E.J., 1975. Sedimentary Rocks. Harper & Row. 628 pp.
- PETTIJOHN, F.J., POTTER, P.E. & SIEVER, R., 1972. Sand and Sandstones. Springer-Verlag, New York 618 pp.
- PHLEGER, F.B., 1965. Ecology and Distribution of Recent Foraminifera. The John Hopkings Press; Baltimore 297 pp.
- PINAR, N. & ILHAN, E., 1954. Nouvelles considerations sur la tectonique de l'Anatolie, Turquie, Asie Mineure. Bull. Soc. Geol. France., 6, 11-34

- PLAYFORD, P.E., COCKBAIN, A.E., DRUCE, E.C. & WRAY, J.L. 1976. Devonian stromatolites from the Canning Basin, Western Australia. In: WALTER, M.R. (Ed) Stromatolites. Developments in Sedimentology 20., 543-565
- POTTER, P.E. & PETTIJOHN, F.S., 1963. Palaeocurrents and Basin Analysis. Springer-Verlag Berlin 296 pp.
- POWERS M.C., 1953. A new roundness scale for sedimentary particles. Jour. Sed. Petrology, 23, 117-119
- READ, J.F., 1976. Calcretes and their distinction from stromatolites. In: WALTER, M.R. (Ed) Stromatolites. Developments in Sedimentology 20 55-72. Elsevier
- READING, H.G., 1975. Strike-slip fault systems; an ancient example from the Cantabrians. IX. Intr. Congr. Sedimentologie, Nice 1975. Theme 4(2), 289-292
- READING, H.G. 1980(a). Characteristics and recognition of strike-slip fault systems. In: BALLANCE, P.F. & READING, H.G. (Ed's) Sedimentation in Oblique Strike-Slip Mobile Zones. Spec. Publ. Int. Ass. Sediment., 4, 7-26
- READING, H.G. 1980 (b). Sedimentation and tectonics. In: READING, H.G., Sedimentary Environments and Facies. Blackwell Scientific Publ., 439-478
- READING, H.G. 1982. Sedimentary basins and global tectonics. Proc. Geol. Assoc. London., 93, 321-350
- REINECK, H.E. & SINGH, I.B., 1972. Genesis of laminated sand and graded rhythmites in storm-sand layers of shelf mud. Sedimentology, 18, 123-128
- REINECK, H.E. & SINGH, I.B., 1975. Depositional Sedimentary Environments. Springer-Verlag Berlin 439 pp.
- RIGO de RIGI, M. & CORTESINI, A., 1959. Regional studies central Anatolian basin, progress report 1. Turkish Gulf Oil Com.: Pet. Is. Gen. Md. Ankara (Unpublished).
- RUPKE, N.A., 1976. Sedimentology of very thick calcarenite. marlstone beds in a flysch succession, south-western Pyrenees. Sedimentology 23, 43-65
- RUPKE, N.A., 1980. Deep clastic seas. In: READING, H.G., Sedimentary Environments and Facies. Blackwell Scientific Publ., 372-415.
- SANVER, M. & PONAT, E., 1981. Kirsehir ve dolaylarina iliskin paleomanyetik bulgular. Kirsehir Masifinin rotasyonu. Istanbul Yerbilimleri 2 231-238.
- SAUNDERS, A.D., TARNEY, J., STERN, C.R. & DALZIEL, I.W.D., 1979. Geochemistry of Mesozoic marginal basin floor igneous rocks from southern Chile. Bull. geol. Soc. Am., 90, 237-258
- SCHEIBNEROVA, V. 1974. Cretaceous foraminifera of the Great Australian Basin. Sydney, Geol. Survey of New South Wales. Mem. 17, 110 pp.

- SCHMIDT, C.G., 1960. Geological evolution of the licences 360-363 and 365-367 District II. Petrol. Dairesi, Ankara, Turkey. Unpublished.
- SCHREIBER, B.C., 1978. Environments of subaqueous gypsum deposition. In: DEAN, W.E. & SCHREIBER, B.C. (Eds) Marine Evaporites Soc. Econ. Paleont. Mineral. Short Course, 4, 43-73.
- SCHOLLE, P.A., 1978. A Colour Illustrated Guide to Carbonate Rock Constituents, Texture, Cement and Porosity. Am. Assoc. Petrol. Geol. Memoir 27.
- SCHOLLE, P.A., 1979. A colour illustrated guide to constituents, texture, cement and porosities of sandstones and associated rocks. Am. Assoc. Petrol. Geol. Memoir 28.
- SEIDITZ, W., 1931. Discordanzen und Orogenese der Gebirge am Mittelmeer. Berlin.
- SEILACHER, A., 1967. Bathymetry of trace fossils. Marine Geology, 5, 413-428
- SELLEY, R.C., 1976. Ancient Sedimentary Environments. Chapman and Hall, London 237 pp.
- SENGOR, A.M.C. & YILMAZ, Y., 1981. Tethyan evolution of Turkey: A plate tectonic approach. Tectonophysics 75. 181-241
- SENGOR, A.M.C., YILMAZ, Y. & KETIN, I., 1982. Remnants of a pre-Late Jurassic ocean in northern Turkey. Fragments of Permian-Triassic Palaeo-Tethys.? Bull. geol. Soc. Am. 93, 932-936
- SEYMEN, I., 1981. Kaman (Kirsehir) dolayinda Kirsehir masifinin metamorfizmasi. Ic Anadolunun jeolojisi simpozyumu. T.J.K. 35. Bilimsel ve Teknik Kurultayi Mart 1981. Ankara 12-15
- SEYMEN, I., 1982. Kaman dolaylarinda Kirsehir Masifinin jeolojisi. ITU Maden Fak. Docentlik Tezi. 164 pp.
- STANLEY, D.J. & UNRUG, R., 1972. Submarine channel deposits, fluxoturbidites and other indicators of slope and base-of-slope environments in modern and ancient marine basins. In: RIGBY, J.K., & HAMBLIN, K. Wm. (Ed's), Recognition of Ancient Sedimentary Environments. Soc. Econ. Paleont. Mineral. Spec. Publ., 16, 287-340.
- STANLEY, D.J., PALMER H.D., & DILL, R.F., 1978. Coarse sediment transport by mass flow and turbidity current processes and downslope transportation in Annat Sandstone canyon-fan valley system. In: STANLEY, D.J. & KELLING, G. (Ed's), Sedimentation in Submarine Canyons, Fans, and Trenches. Stroudsburg, Dowden, Hutchinsonson and Ross Inc., 85-126

- STENZIEL, H.B., 1971. Oysters. In: MOORE, R.C. (Ed), Treatise of Invertebrate Palaeontology, N. Bivalva 3. N 953-1224, Univ. of Kansas Press.
- STRAUB, R., 1924 & 1928. Der Bau de Alpen. Bern.
- TAIRA, A., OKADA, H., WHITAKER, J.H., McD. & SMITH, A.J. The Shimanto Belt of Japan: Cretaceous-Lower Miocene active margin sedimentation. In: LEGGET, J.K. (Ed), Trench-Forearc Geology. Geol. Soc. London. Spec. Publ. 10., 5-26
- UYGUN, A., 1981. Tuzgolu havzasinin jeolojisi, evaporit olusumlari ve hidrokarbon olanaklari. Ic Anadolunun Jeolojisi Simpozyumu. T.J.K. 35. Teknik ve Bilimsel Kurultayi Mart 1981. Ankara 66-71
- UNALAN, G., 1981. Ankara guneybatisindaki "Ankara Melanjinin" stratigrafisi. Ic Anadolunun Jeolojisi Simpozyumu. T.J.K. 35. Teknik ve Bilimsel Kurultayi. Mart 1981 Ankara 46-52
- UNALAN, G., YUKSEL, V., TUNA, T., GONENC, O., SEYIRT, Z. & HUSEYIN, S., 1976. Haymana-Polatli yoresinin (guneybati Ankara) Ust Kretase-Alt Tersiyer stratigrafisine paleocografik evrimi. Bull. of Geol. Soc. of Turkey, 19, 159-176
- VAN DE KAMP, J.D., HARPER, J.D., CONNIFF, J.J., & MORRIS, D.A., 1974. Facies relations in the Eocene-Oligocene in the Santa Ynez Mountains, California. J. geol. Soc. London., 130, 545-565.
- WALKER, R.G., 1978. Deep-Water sandstone facies and ancient submarine fans: Models for exploration of stratigraphical traps. Bull. Am. Assoc. Petrol. Geol., 62, 932-966
- WALKER, R.G. & MUTTI, E., 1973. Turbidite facies and facies associations. In: Turbidite and Deep-Water Sedimentation, Soc. Econ. Paleon. Mineral Pacific Section Short Course Mainheim, 119-157.
- WALKER, T.R., 1967. Formation of red beds in modern and ancient deserts. Bull. geol. Soc. Am., 78 353-368.
- WALTON, W.R., 1955. Ecology of living benthonic Foraminifera, Todos Santos Bay, Baja California. J. Paleont., 29, 952-1018.
- WELLS, J.W., 1956. Sclerecterian Corals. In: Treatise on Invertebrate Palaeontology. Part F Coelenterata. Geol. Soc. of. Am.
- WENTWORTH, C.K., 1922. A scale of grade and class terms for clastic sediments. J. Geol., 30, 377-392

- WILSON, J.L., 1975. Carbonate Facies in Geological History. Springer-Verlag. 470 pp.
- WINN, Jr. R.D. & DOTT, Jr. R.H., 1979. Deep-water fan-channel conglomerates of Late Cretaceous age, southern Chile. Sedimentology, 26, 203-228.
- WRAY, J.L., 1977. Calcareous Algae. Developments in Palaeontology and stratigraphy, 4.
- ZINGG, T.H., 1935. Beitrag zur Schotter-analyse. Schweiz. Min. U. Pet. Mitt, Bd. 15 39-140

A P P E N D I X I

METHOD USED IN PETROGRAPHIC STUDIES.

For the petrographic examination of sedimentary rocks the method outlined below is used. It was developed by combining various schemes suggested by Folk (1974) for detailed studies of properties of sedimentary rocks.

i Megascope properties

Colour, induration, sedimentary structures (e.g. grading, lamination), observable framework grains and fossils.

ii Microscopic description

A. Texture

A1. Grain size: determined according to the Wentworth scale and percentage of gravel, sand and mud fractions are estimated by the aid of a visual percentage chart proposed by Terry & Chilingar (1955). Comparison between grain size and composition noted in the cases where it is established and a textural name is given to the rocks according to the classification by Folk (1974) e.g. muddy sandstone.

A2. Roundness

A3. Sorting; determined by using comparison chart for sorting and sorting classes proposed by Pettijohn, Potter & Siever (1972)

A4. Fabric

i General homogeneity of rock; e.g. whether it is a single rock type or interlaying occur

ii Grain contact types and packing proximity

iii Grain orientation

A5. Textural maturity

Defined on the basis of Folk's (1974) textural maturity flow diagram.

Immature — >5% — Clay matrix content

<5%

Submature — >0.5 ϕ — sorting

<0.5 ϕ

Mature — subangular — roundness
(<3.0p)

Supermature — rounded —————
(>3.0p)

B. Framework grains

B1. Terrigenous minerals

Quartz; type of extinction, presence or absence of inclusions and mode of occurrence, e.g. whether single quartz type or a composite quartz grain

Feldspar; type of plagioclases are determined by Michelle-Levy method on unaltered plagioclase crystals showing albite twinning.

Chert

Mica

Rock Fragments (sedimentary, plutonic, volcanic and metamorphic)

B2. Bioclastic grains, all broken or whole tests of organisms are considered as bioclastic.

C. Bonding agent; matrix and cement

D. Weathering and alterations

E. Petrographic name; is given after selected samples are point counted and results are plotted on the triangular diagram of Folk (1974)

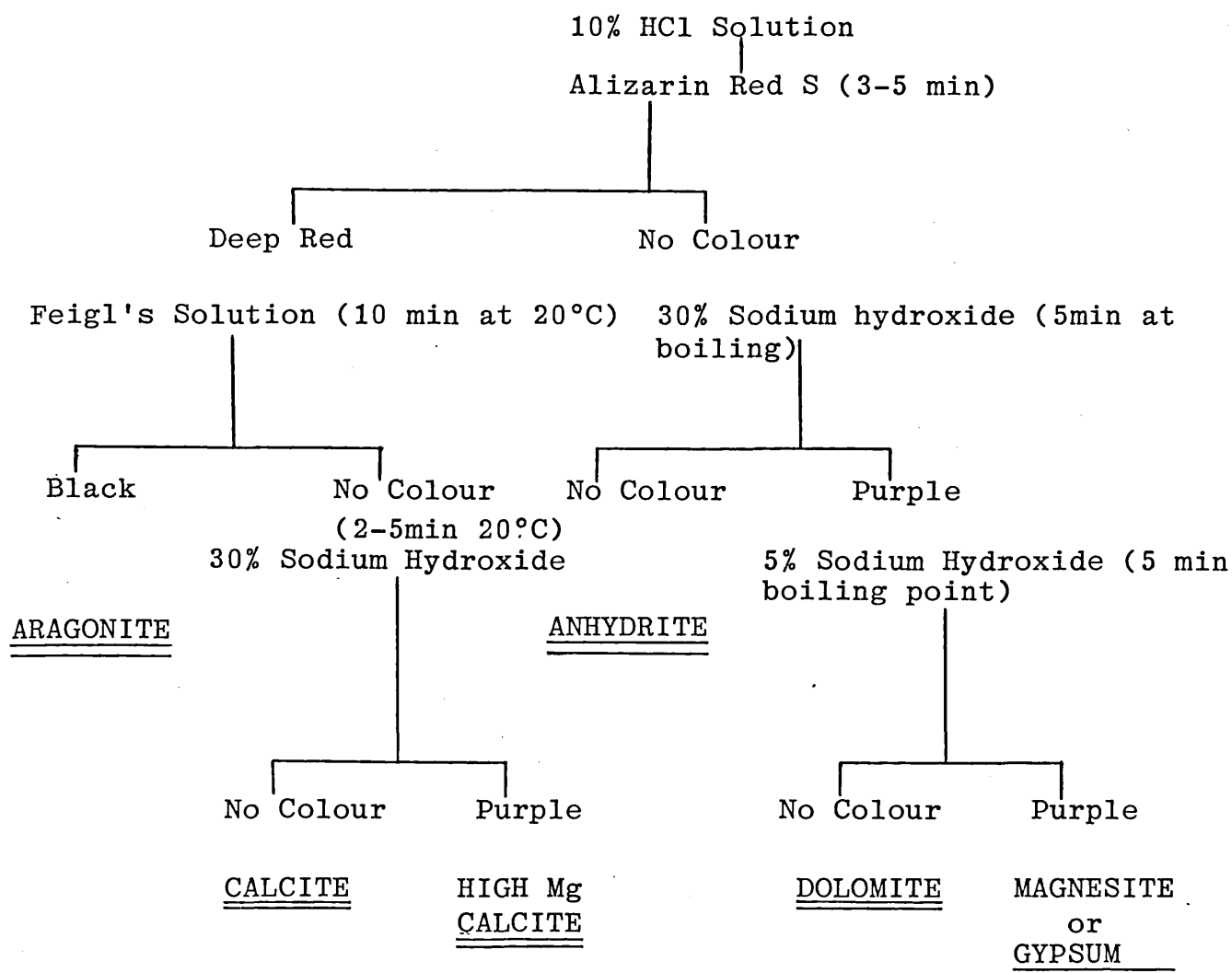
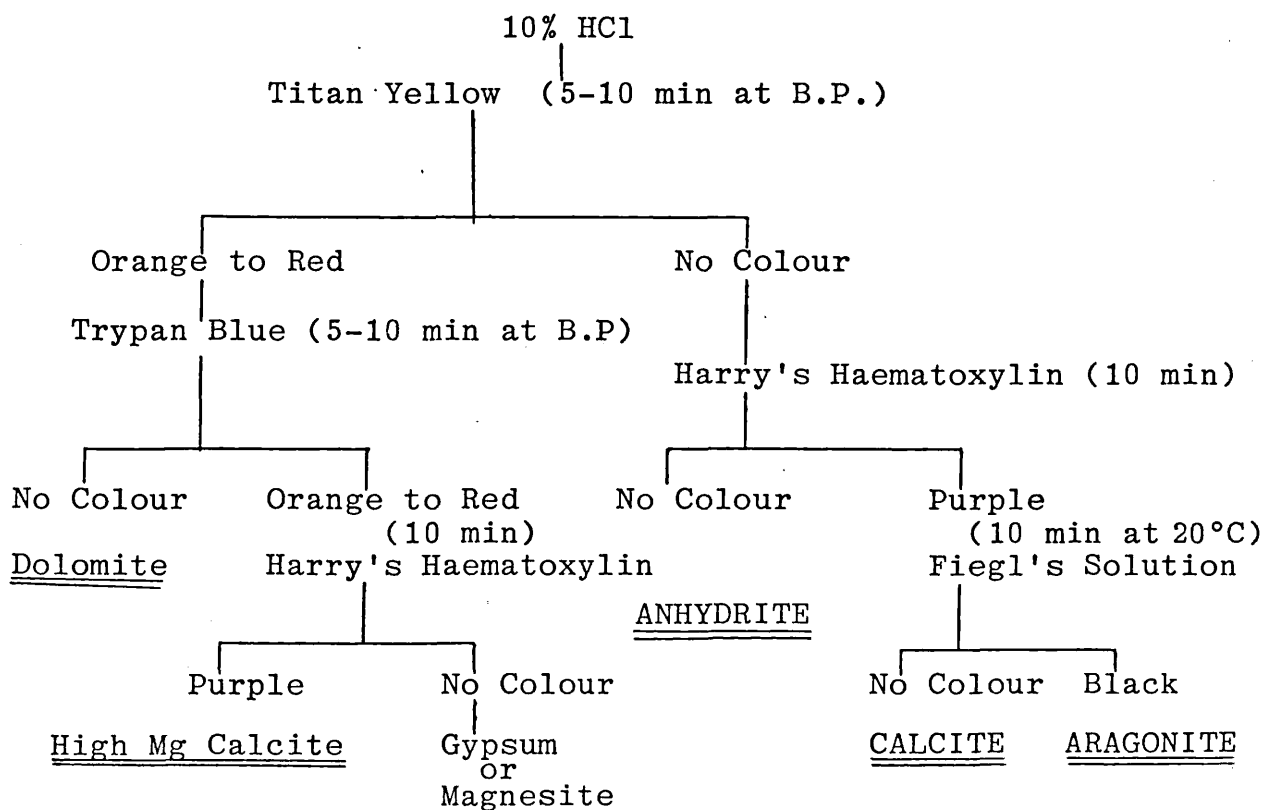
A P P E N D I X I I

STAINING TECHNIQUES FOR CARBONATE MINERALS

In the staining of carbonate chips for the identification of different carbonate minerals Friedmans schemes I and II is used (Allman & Lawrence 1972)

1. Sample preparation: Hand specimens were first cut by a general purpose rock cutter to obtain a flat surface which was progressively smoothed by 320, 600 and 800 (Aloxite) grade carborandum. Then the polished surface was immersed into 10% HCL solution for 1-2 minutes and the solution is constantly agitated. After washing the sample under running tap water (the processed surface facing down in order to avoid any erosion by running water), it is allowed to drain and dry in the room temperature.

2. Staining procedure: was carried out on the same sample following the flow chart presented below. Stained surface of the samples are grounded clean with 600 grade carborundum after each step.

FRIEDMAN'S SCHEME IFRIEDMAN'S SCHEME II

A P P E N D I X I I I

X-RAY DIFFRACTION

An X-ray diffraction technique was used to identify clay mineral types present in the shale and mudstones of the area studied. At least 5 samples are analysed from each formation or member by using Philips PW1210 generator at Geology Department, Bedford College

III. 1 Sample preparation

The following procedure is carried out for the preparation of each sample.

a. Sample (whether semi-consolidated or unconsolidated) is crushed to pea size lumps by a hammer.

b. The bulk of the sample is separated in a riffle sampler and 50 gr. representative sample is taken.

c. This sample is then placed into a 300 cc. glass bottle and 150 ml of 2% Calgan (Sodium hexametaphosphate) solution is added. The Calgan solution is prepared by adding 2 gr. dried calgan to 1000 ml distilled water and used in order to avoid flocculation of clay size material. Then a cap is screwed on the bottle and it is shaken vigorously for 2 minutes. The suspension is left to stand for 3-7 days, shaking the bottle at least 3 times a day, to achieve complete dispersion of sediment.

d. At the end of this period the suspension is wet-sieved through a 63 micron nylon sieve by using 1000 ml or less Calgan solution during the process. The suspension which went through the sieve is collected in a large dish and then poured into a 1000 ml. volumetric cylinder

e. The volumetric cylinder is filled up to exactly 1000 ml. with distilled water and is then taken to a constant temperature room which was preset to 20°C and the suspension

is stirred vigorously by a specially made stirring rod.

f. As soon as the stirring rod emerged from the suspension for the last time, a stop watch is started and after 2 hours and 3 minutes a pipette is inserted to a depth of 10 cm. and 25 ml. of suspension, which by then only contains fragments less than 2 micron, is withdrawn and poured into a small glass bottle.

g. The sample is then poured onto a clean glass slide at the bottom of an aluminium centrifuge tube. The tube is centrifuged for 15 minutes at 1000 rpm then 15 minutes at 1500 rpm to orientate the clay minerals. At the end of this time the tube is removed and excess water is poured away slowly and carefully not to disturb the settled clay size material on the glass slide. Then the slide is removed and left to dry at room temperature.

III. 2 Analysis procedure

The prepared sample is placed into the X-ray diffractometer which is set to $2\theta=3^\circ$ and CuK α radiation with $\lambda=1.5418\text{\AA}$ is used. 2θ values obtained from the resultant diffractogram converted to d spacings in Angstrom units by using JCPDS Search Manual. Then the sample is placed into a small desiccator containing ethylene glycol. The desiccator is placed in an oven at 60°C for two hours. It is then removed and left to cool at room temperature. The glycolated samples are run on the diffractometer in order to differentiate Montmorillonite Group minerals. After this the sample is placed into a furnace with the temperature of 560°C and left there for an hour. After heating and cooling in a desiccator a third diffractogram is made. By comparing these three diffractograms, the common clay minerals present are identified.

A P P E N D I X IV

X-RAY FLUORESCENCE SPECTROMETRY

Major and trace element analyses on volcanic rocks were obtained using a Philips PW 1400 automatic X-ray spectrometer.

IV. 1 Sample preparation

Any superficially weathered material from the samples, is removed by using a diamond lap and samples are washed with water and acetone to remove dust and marking ink then dried. The bulk of samples are crushed in a laboratory jaw crusher until the largest dimension is less than 0.5 cm. These fragments are split in a riffle sampler and approximately 200 gr. is taken for crushing again. Each 200 gr representative sample is placed in an agate Tema barrelled swing mill for about 60-90 seconds until all grains passed through a 200 mesh B.S. nylon sieve. Any particle not passing through after gentle brushing, is hand-ground down using an agate mortar and pestle. The powdered representative sample is then placed into a glass bottle and stored.

IV. 2 Major element analysis

For the major element analysis, a fusion method is used for specimen preparation, by using lithium tetraborate (Johnson-Matthey spectroflux 104) flux. Fusion techniques have the advantage of eliminating the mineralogical, chemical and particle size effect inherent in the use of pressed powder pellets, and the low proportion of rock in the fusion reduces inter-element absorption effects. Two fusion beads per sample are made, because of the weighing errors involved. A single fusion disc was made up from the following procedures:

Before weighing, in order to drive off interstitial moisture spectroflux and rock powder were dried in an oven

at 105°C and then placed in a desiccator to cool down to room temperature before use. 0.4 gr. rock powder and 2.4 gr. spectroflux are weighed (to 4 decimal places) into a clean 25 cc. 95% pt-5% Au crucible. The mixture is immediately fused in a furnace at 900°C-1000°C for 20 minutes. The crucible is then removed from the furnace and the molten mixture is swirled while holding the crucible over a Meaker burner (to prevent the melt from cooling) to eliminate gas bubbles at the bottom of the melt and to ensure homogeneity. At this point, the molten mixture was quickly poured onto a 30 mm. diameter aluminium disc which is preheated to a constant temperature of 240°C and a plunger is lowered on top, pressing out a glass disc. To ensure complete annealing the disc is wrapped in a clean paper towel and left to cool on an asbestos plate to room temperature. After cooling, any surplus glass around the rim of the disc is trimmed off. Then it is labelled on the curved (reverse) side and stored in a dessicator within a sealed polythene bag. A silver target X-ray tube was used to analyse for the major element Si, Ti, Al, Fe, Mn, Mg, Ca, K, Na and P. The duplicated discs, a standard rock and an artificial machine drift standard were counted twice for each element peak. The output data are used to calculate oxide percentages using a computer. This program computed the drift corrected average of the two sets of counts and applied mass absorbtion corrections

IV. 3 Trace element analysis

A pressed powder pellet was prepared, using a standard piston press assemblage from 6.00g of rock powder ground down to 200 mesh and 1.00g of powdered bakelite PF resin (Grade R 0214/₁). 1.00g of bakelite PF resin was weighed into a 25cc plastic phial and 6.00g of rock powder added with 4 glass beads (Hopkin & Williams 3.5-4mm in diameter) to facilitate mixing. The mixture was well mixed and homogenised by an automatic shaker for 20 minutes. The glass beads were removed and the mixture poured into a 30mm diameter collecting ring on a base

disc to ensure even distribution of the powder. The piston was then lowered by pumping with a pressure of 15 tonnes. The pellet so formed was baked in an oven at 110°C for about 25 minutes to harden the resin to form a durable pellet. Three standard samples and an artificial machine drift standard were counted twice for each element peak. A silver target tube was used to analyse for Nb, Rb, Sr, Y, Zr and Th and mass absorption corrections were calculated from the backscattered silver radiation for these elements. The mass absorption corrections for Cr, Ni and V were calculated from the major element analyses.

A P P E N D I X V

SAMPLE PREPARATION FOR SCANNING ELECTRON
MICROSCOPY FOR NANNO-FOSSILS

Eight marl samples from the Kamisli formation are selected for examination. The samples are first placed in a laboratory paper towel and crushed by a hammer on a firm surface to obtain as small particles as possible. Then a small amount from each sample is placed into a 300 cc. glass bottle and %2 Calgan solution is added. After shaking the bottles vigorously they are left to stand for 24 hours. At the end of this period the bottles are shaken well and after a minute the solution from each sample is poured into a centrifuge tube, leaving the non-dispersed particles in the bottle. Then the samples are centrifuged first for 15 seconds at 350 rpm and then 850 rpm for 3 one minute periods. The tubes are removed and solutions are poured into small containers without disturbing settled clay and silt size material at the bottom of the tubes. A drop from each sample is placed onto a round glass slide which is the same size as a SEM stub. The samples are then left to dry at room temperature and when they are completely dried, the glass slides are glued on top of the stubs which are later coated in the SEM unit.

A P P E N D I X VI

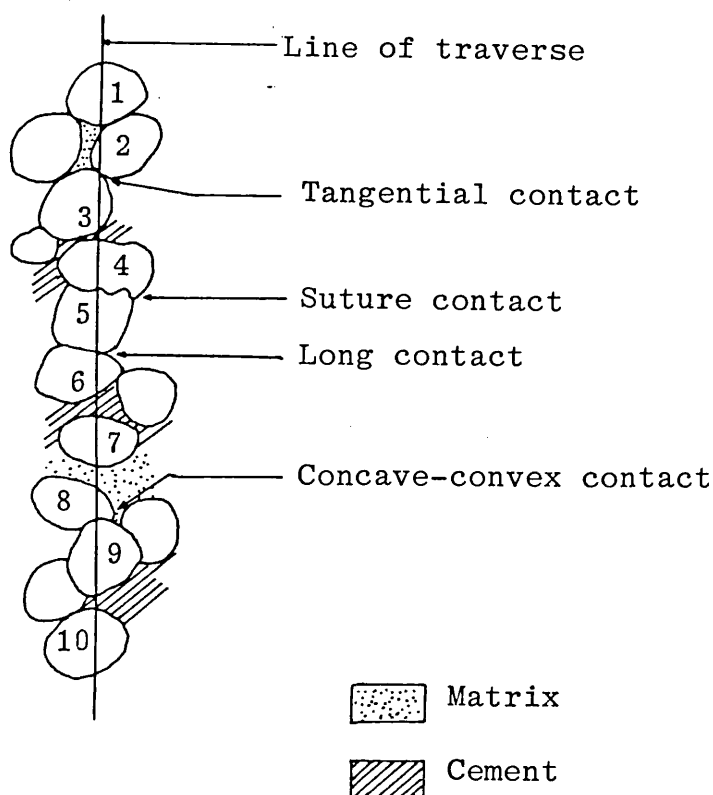
GRAIN CONTACT TYPES AND PACKING PROXIMITY

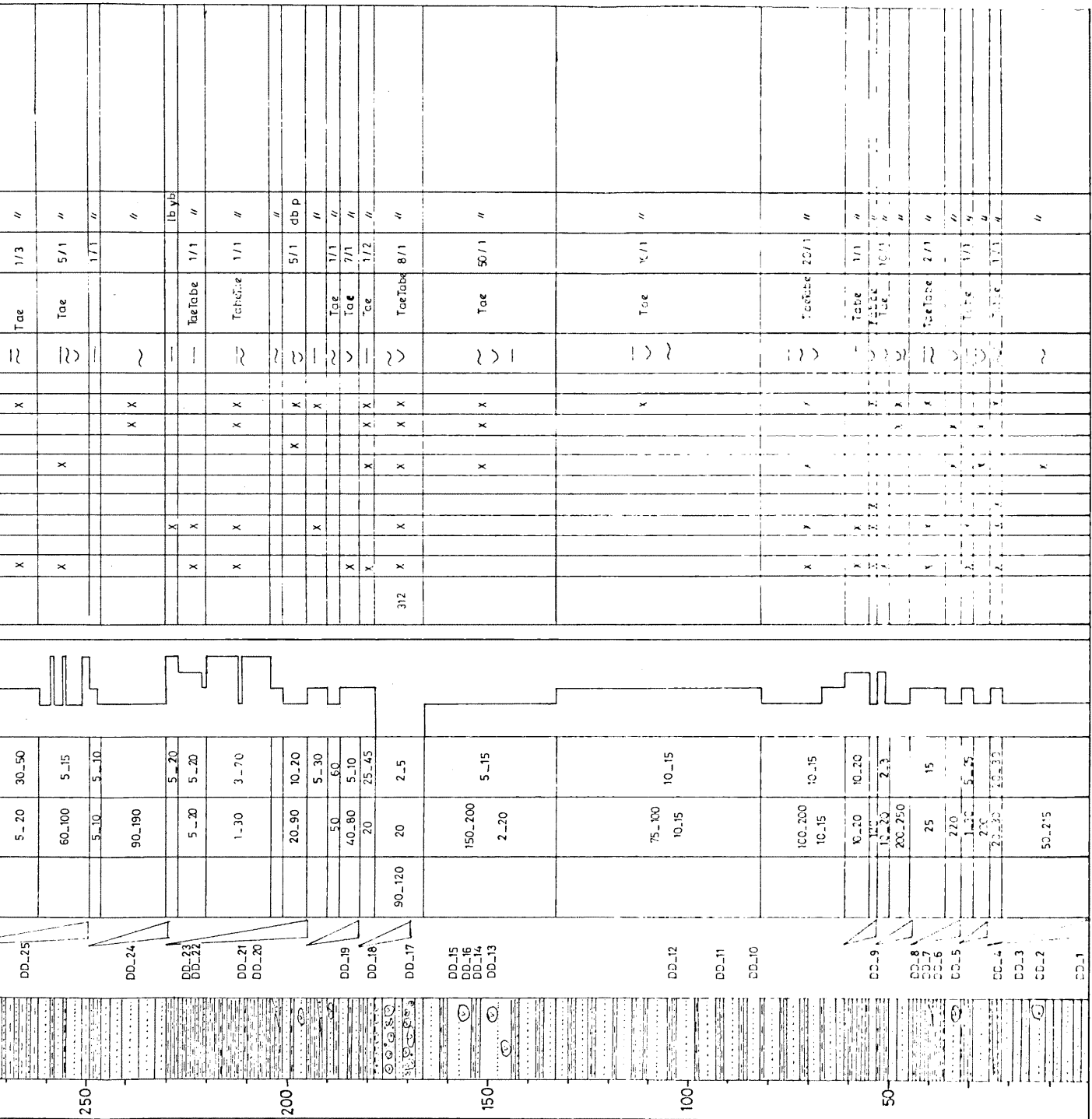
Fig Vl.1 Showing grain contact types (After Blatt et al 1976)

The definition of grain contact types and packing proximity of Blatt et al (1976) is followed. Contact types are defined as being tangential where grains touch each other in one point; long where contact is straight line; suture where contact is crenulated and concave-convex where one of the grains pushes against the other. Packing proximity is calculated by counting the number of grains and grain contacts irrespective of their types, on a line of a traverse and dividing the number of contacts by the number of grains counted e.g. in Fig Vl.1

Number of contacts counted :	4
Number of grain counted :	10
Packing proximity :	40%

For abbreviations and legend see App. VII.

[illegible]

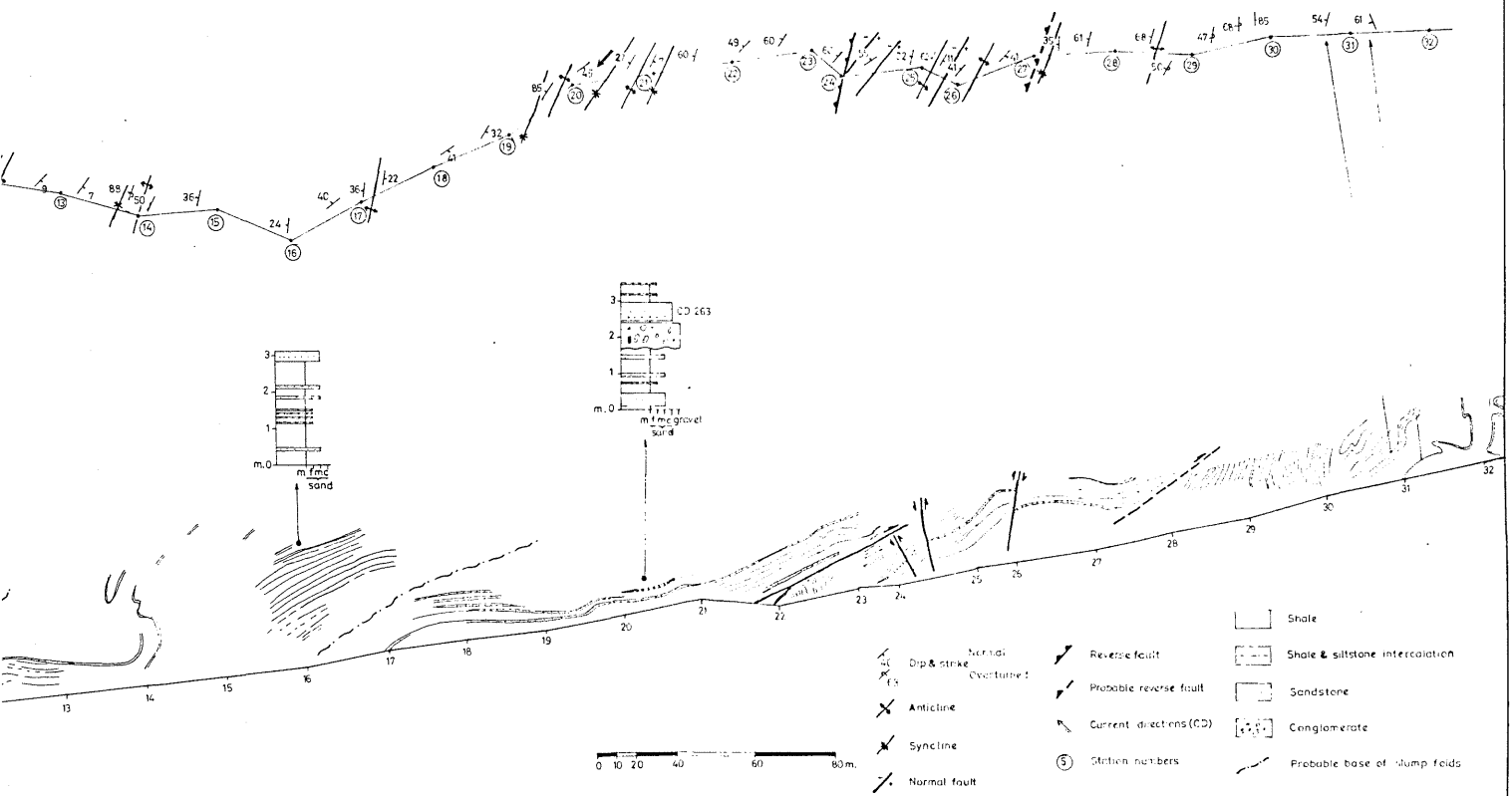


APPENDIX IX - Type section of the Degirmente formation.

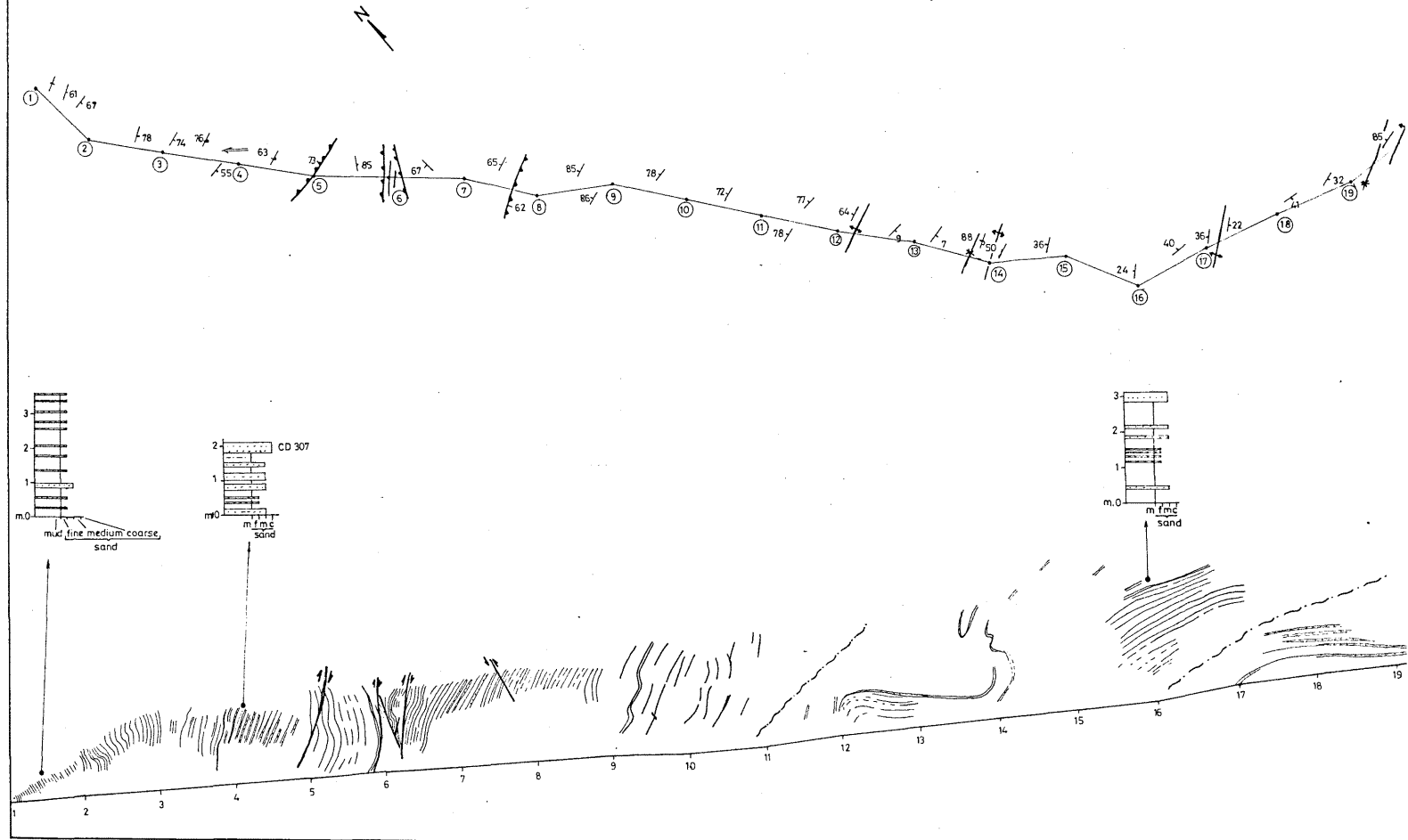
*Lithology is not to scale.

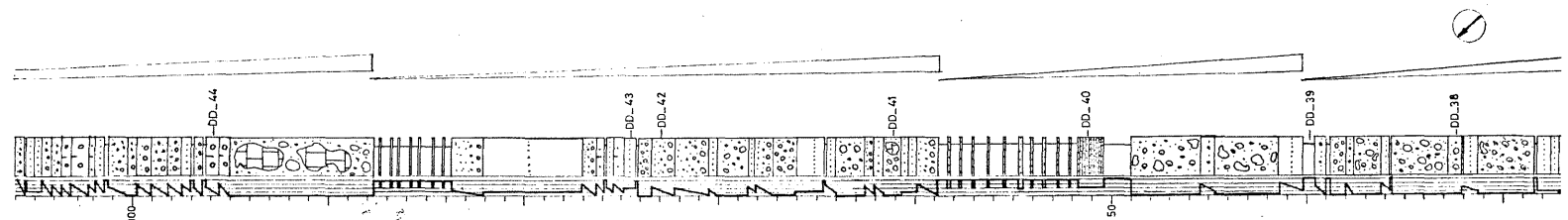
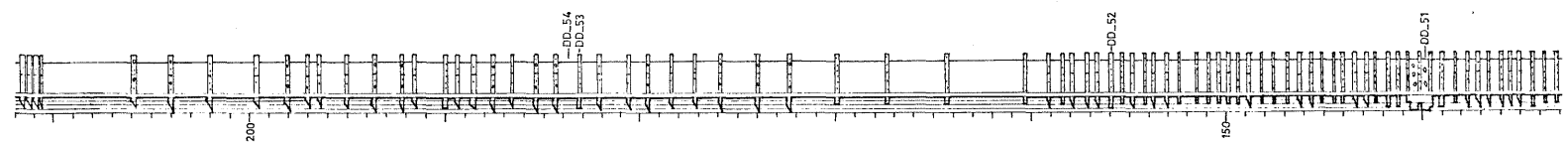
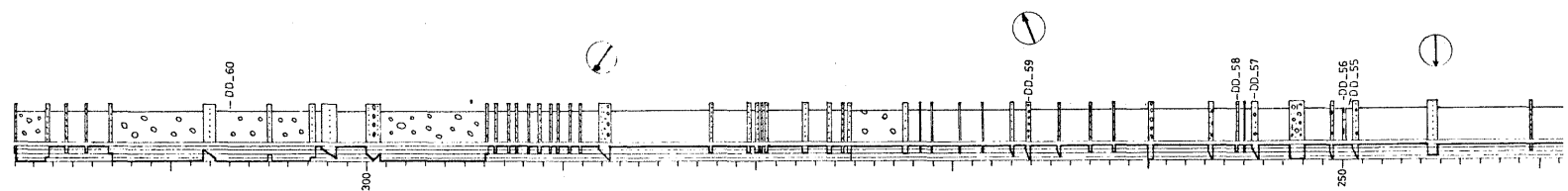
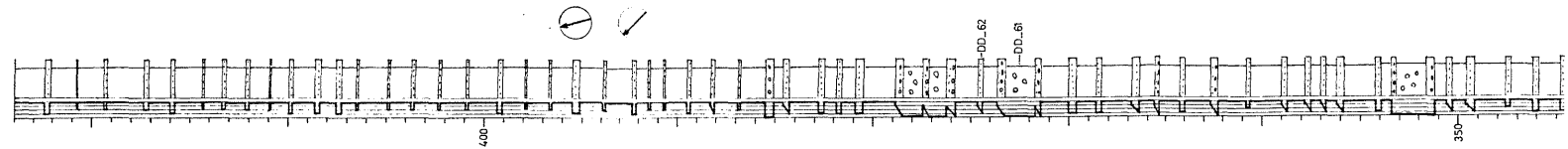
**For abbreviations and legend see App. VII.

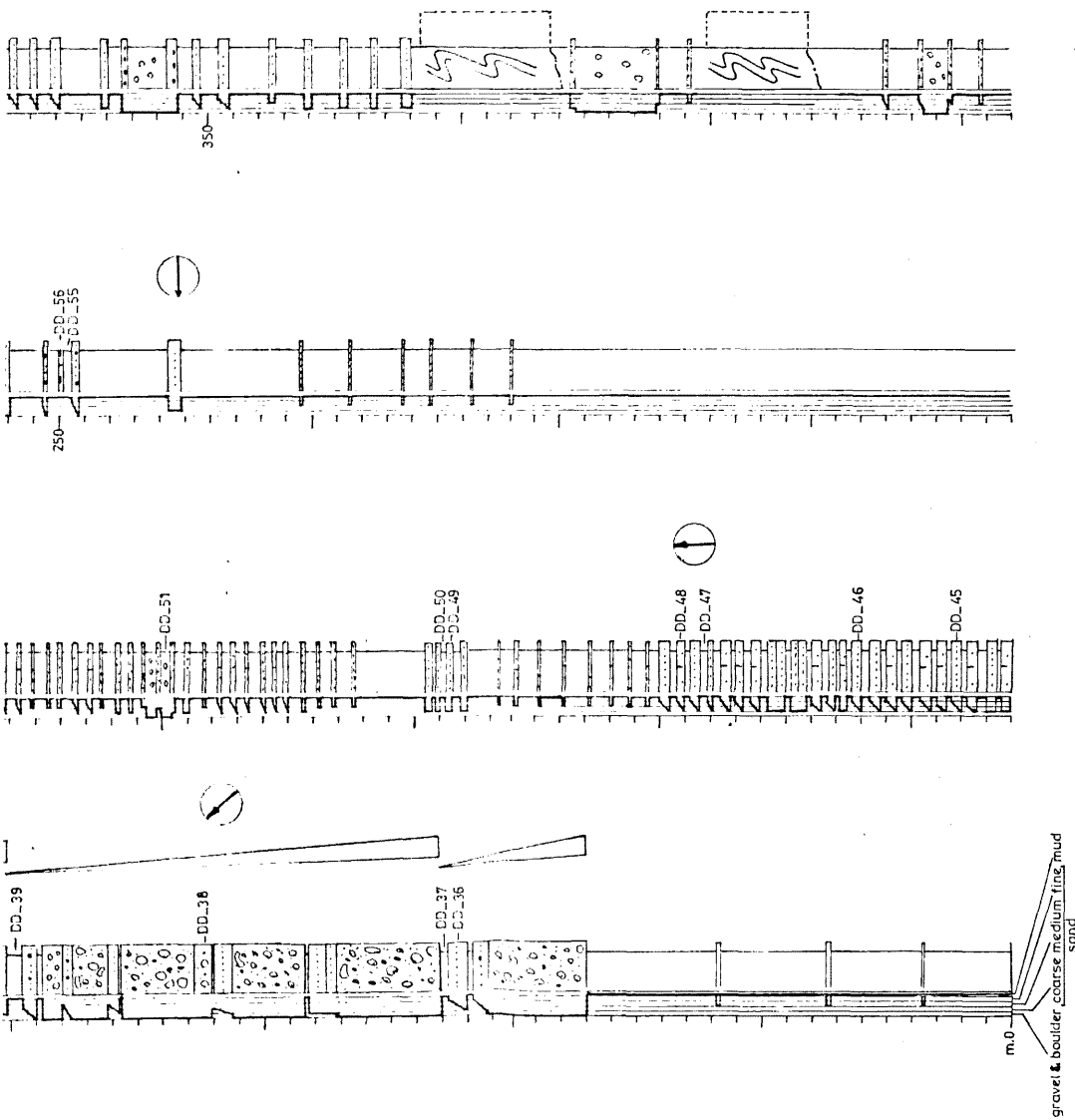
tch Map and Section



Salideresi Sketch Map and Section

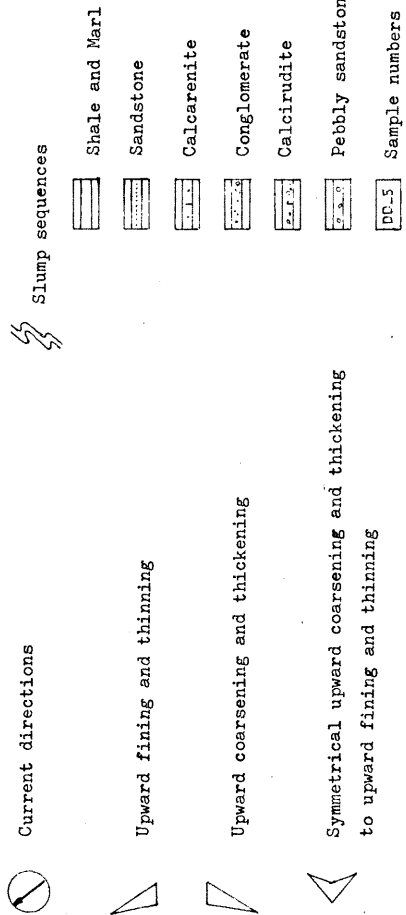


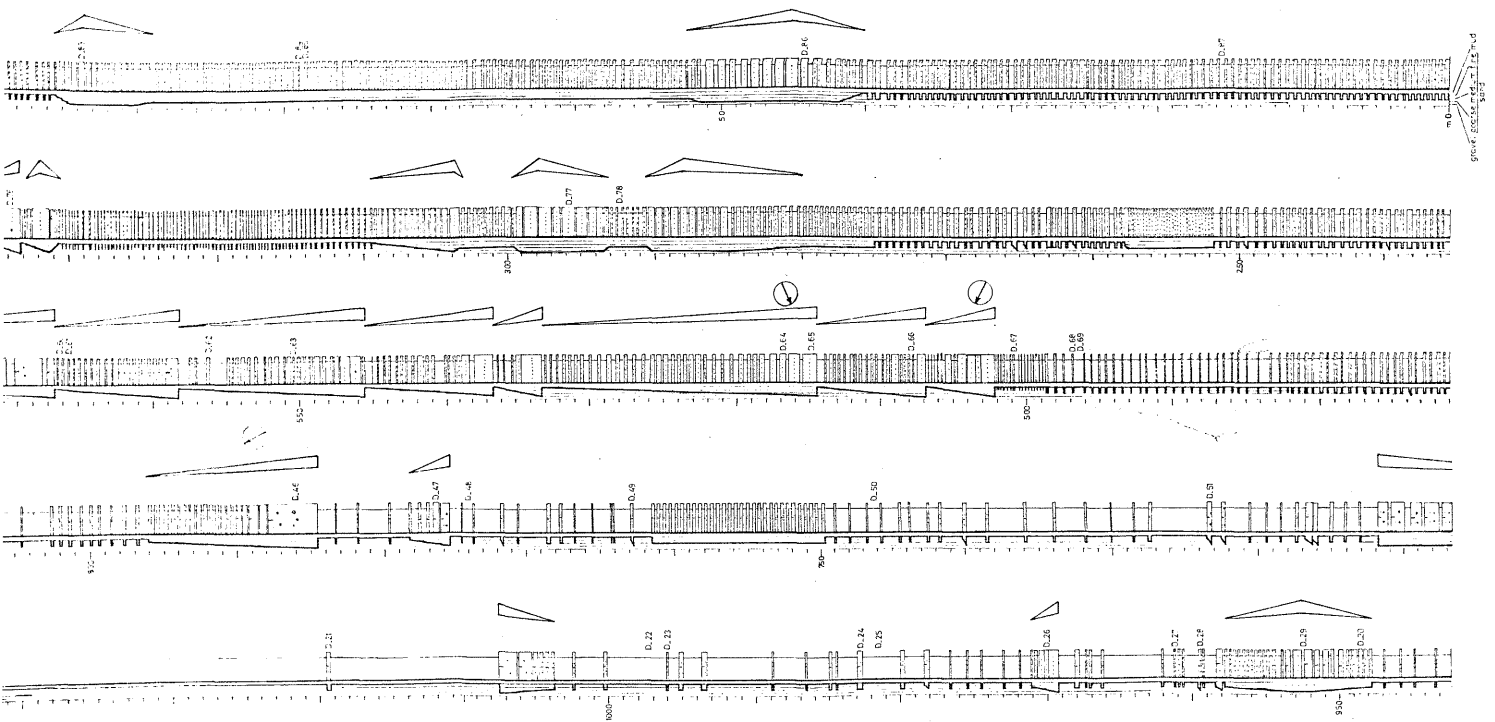




APPENDIX XI- Type section of the Ardicipinar member.

*Lithology is to scale.

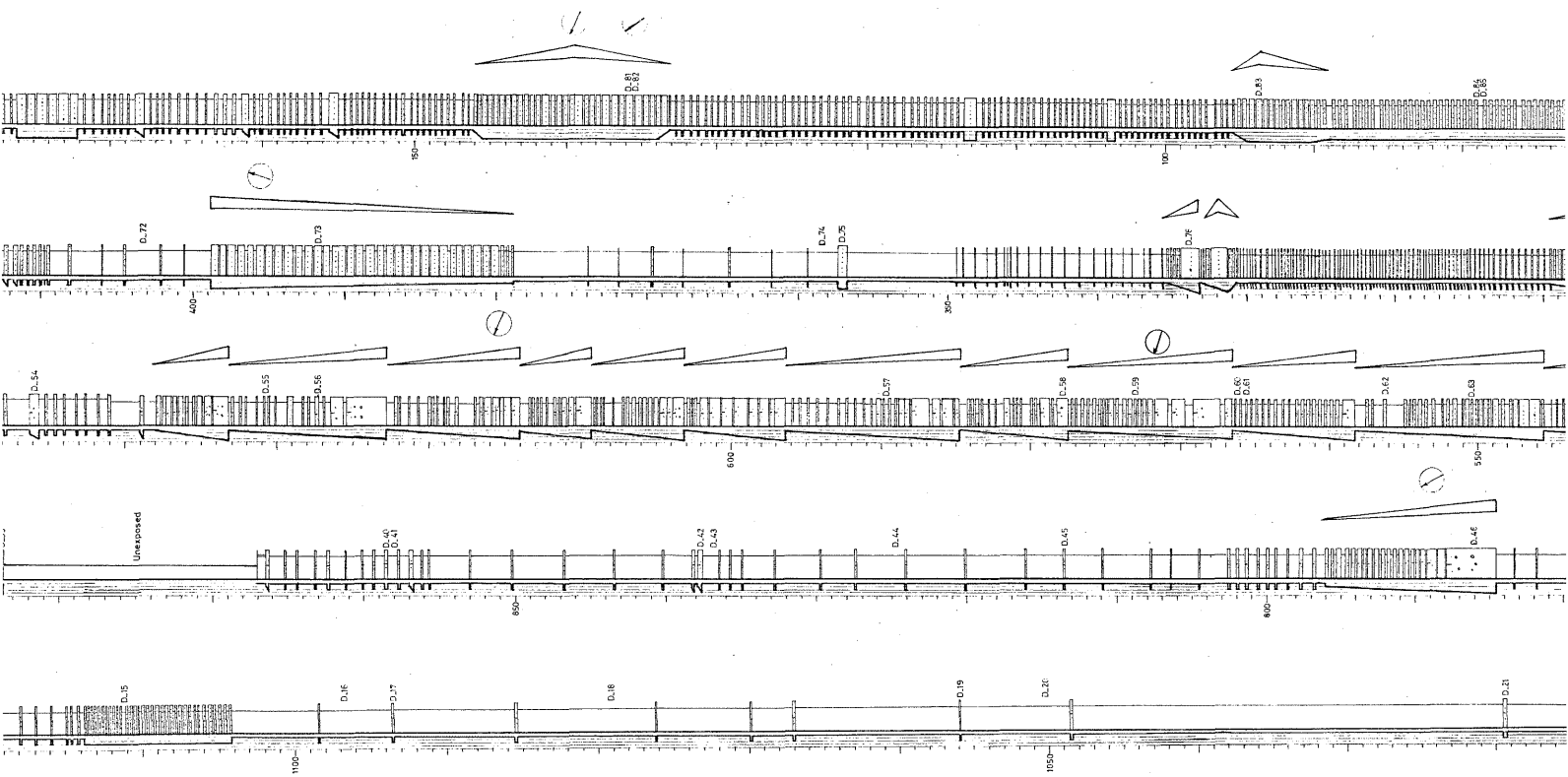


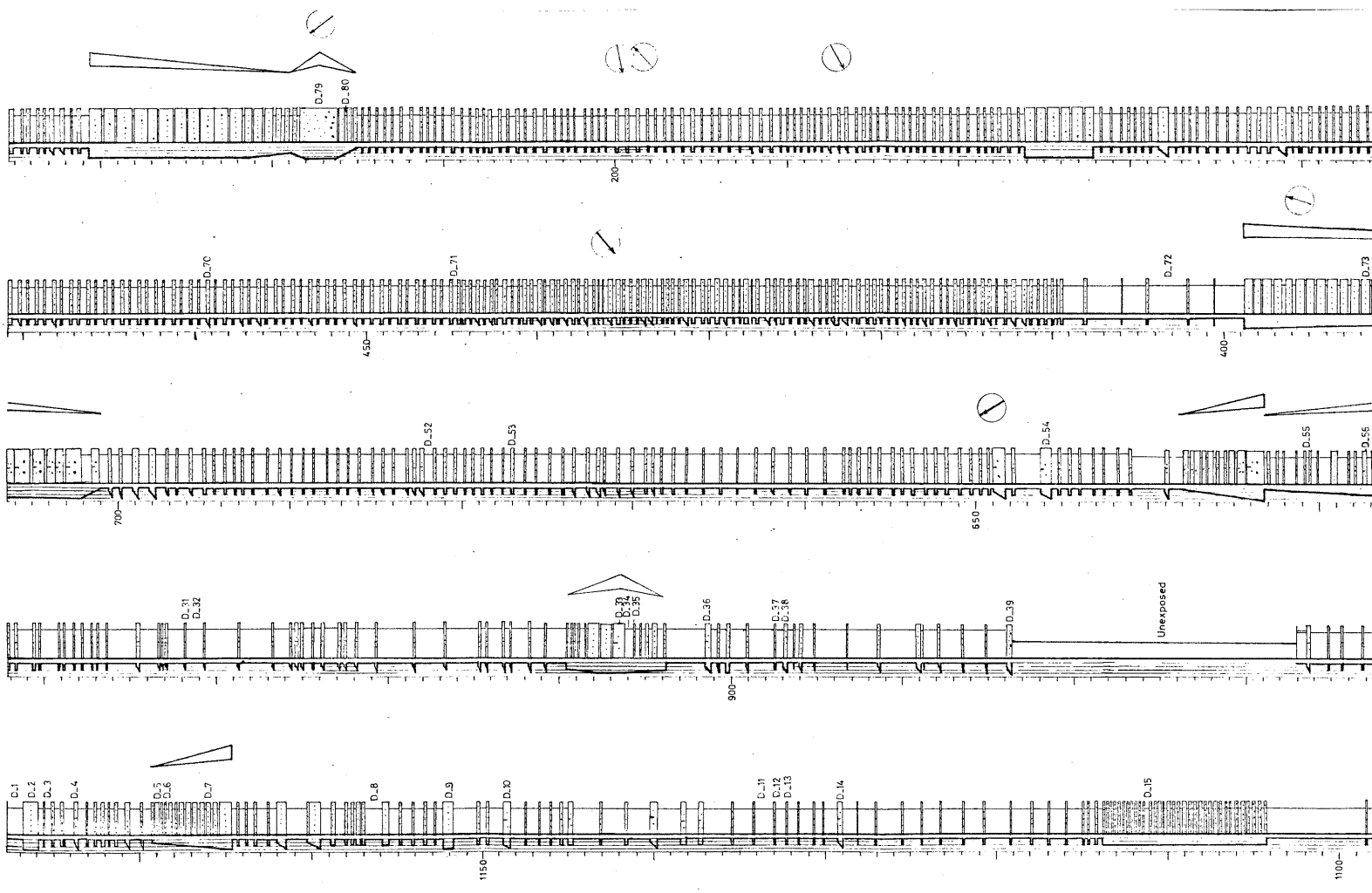


APPENDIX XII- Type section of the Bupkare member.

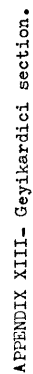
*Lithology is to scale.

**For abbreviations and legend see App.V





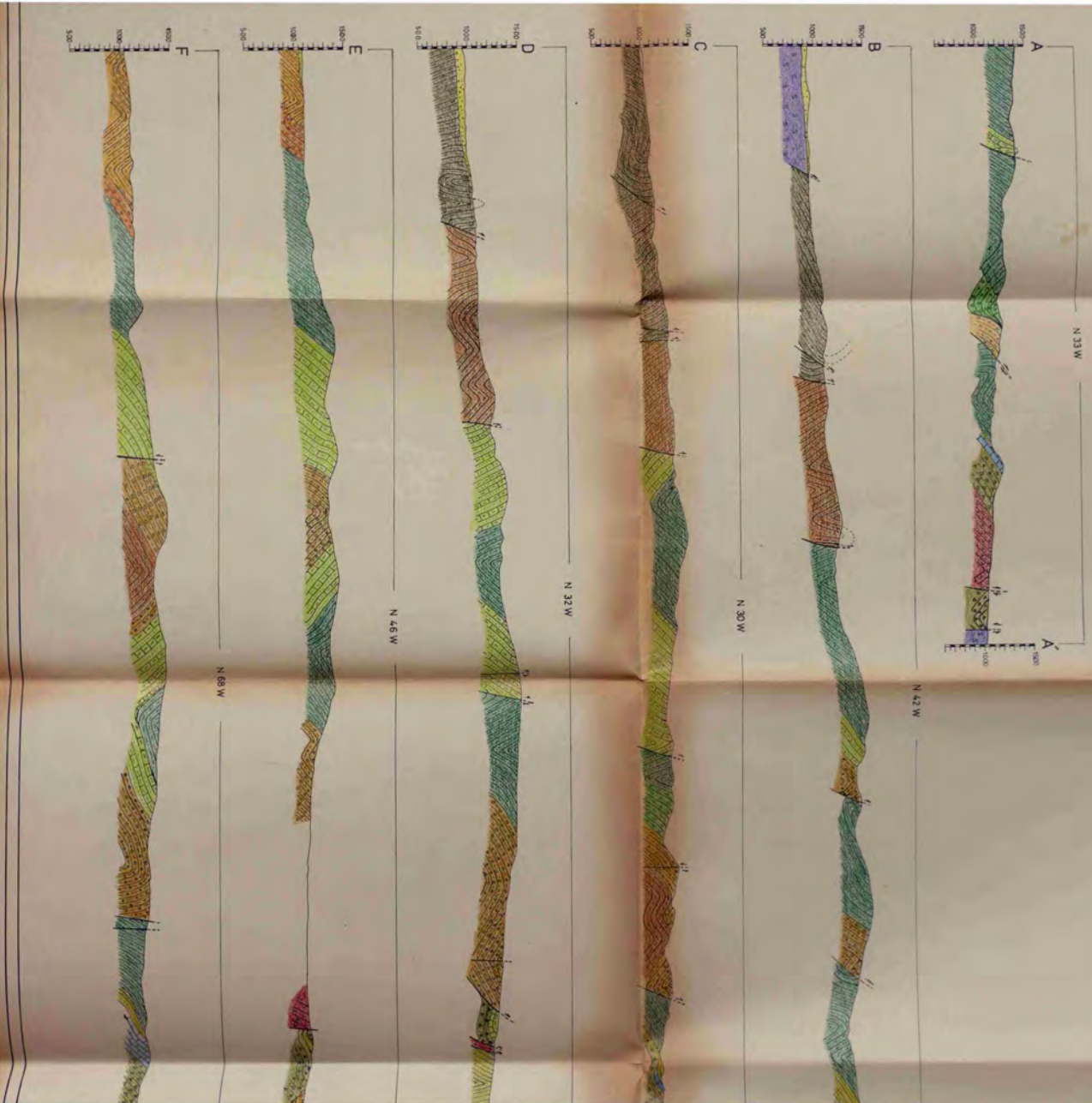
[illegible]



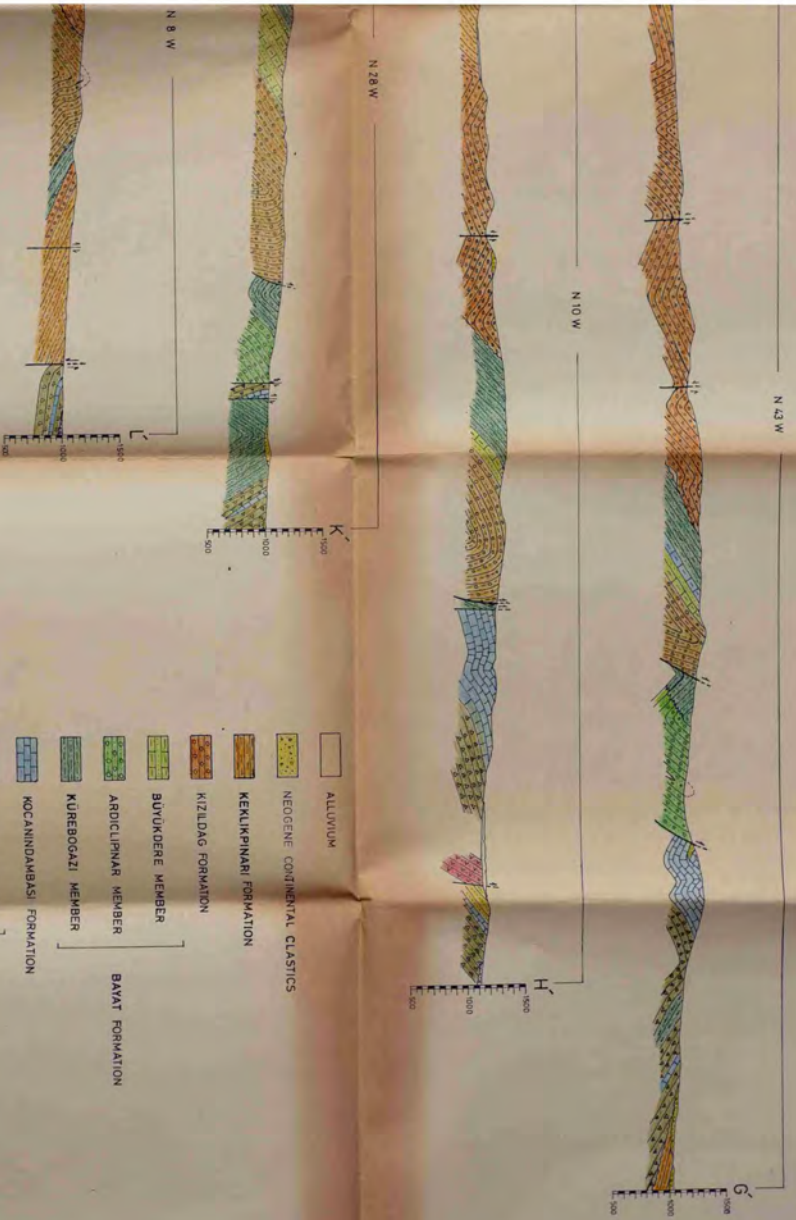
*Lithology is not to scale.

***For abbreviations and legend see App. VII.

GEOLOGIC



URKEY

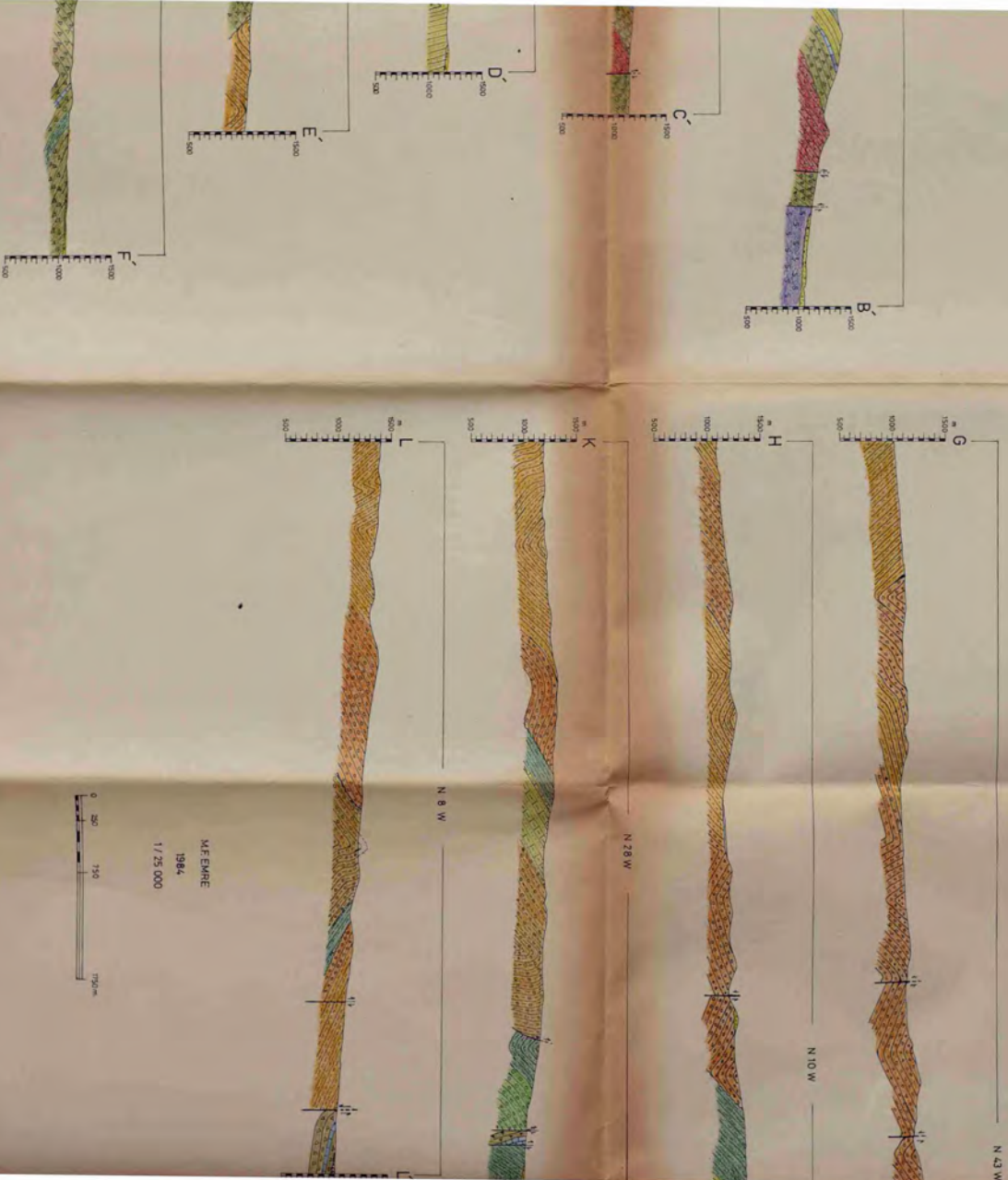


- ALLUVIUM
- NEOGENE CONTINENTAL CLASTICS
- KELEKPINARI FORMATION
- KIZILDAĞ FORMATION
- BUYUKDERE MEMBER
- ARDICILINAR MEMBER
- KUREBOGAZI MEMBER
- KOCANINDAMBASI FORMATION
- SEHRIBAN MEMBER
- SARIKAYA MEMBER
- DEGIRMENDERE FORMATION
- DAVDANLI FORMATION
- KAMISLI FORMATION
- SARDERE VOLCANIC FORMATION
- ANKARA MELANGE

MEEMRE
1984
1/25 000



CAL CROSS SECTIONS OF BALA AREA, TURKEY





GEOLOGICAL MAP
OF KORAT
TEPE AREA

M.F. EMRE

1985

1 / 5 000

0 25 50 100 200 m.

GÖK T.

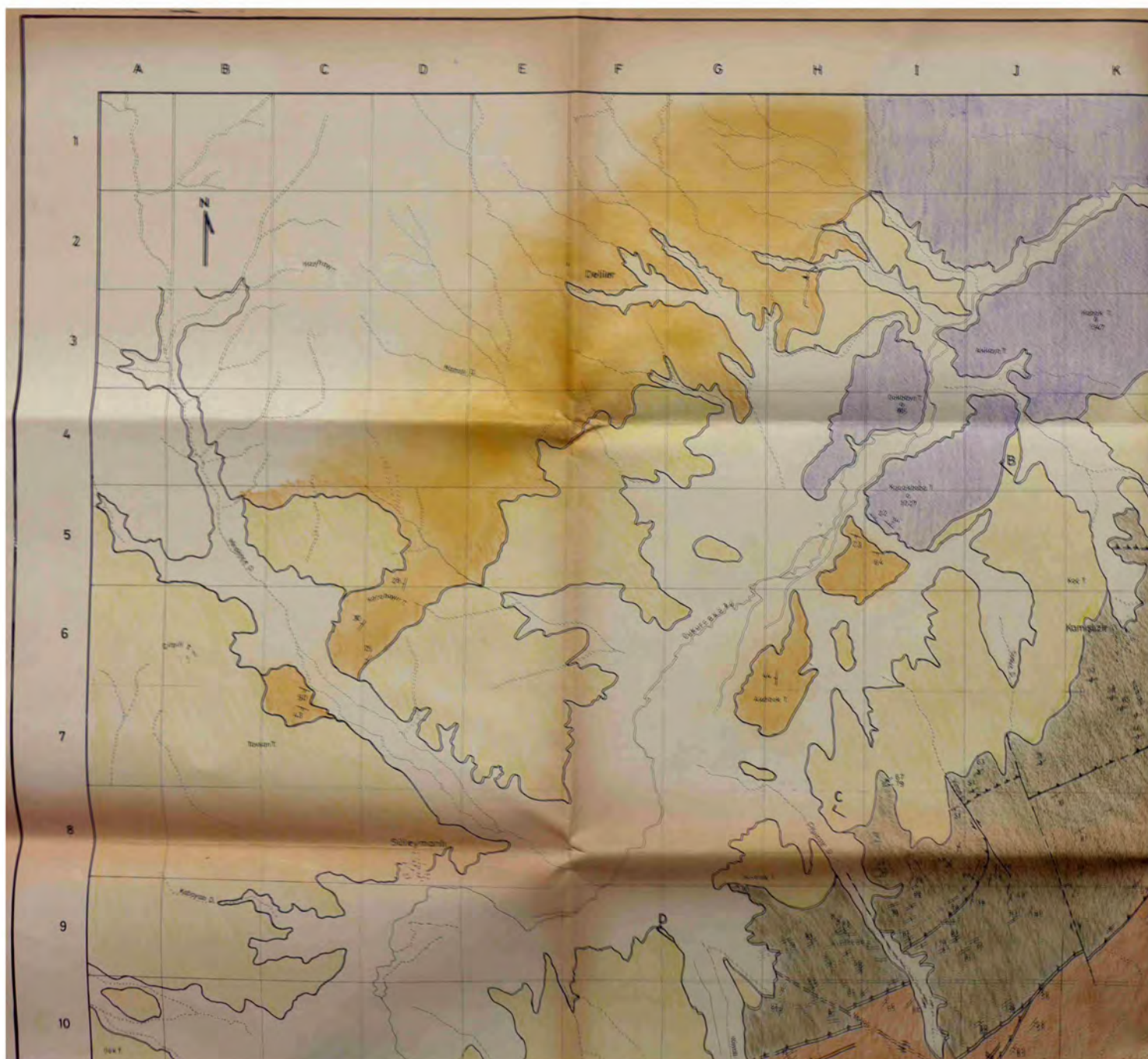


LEGEND

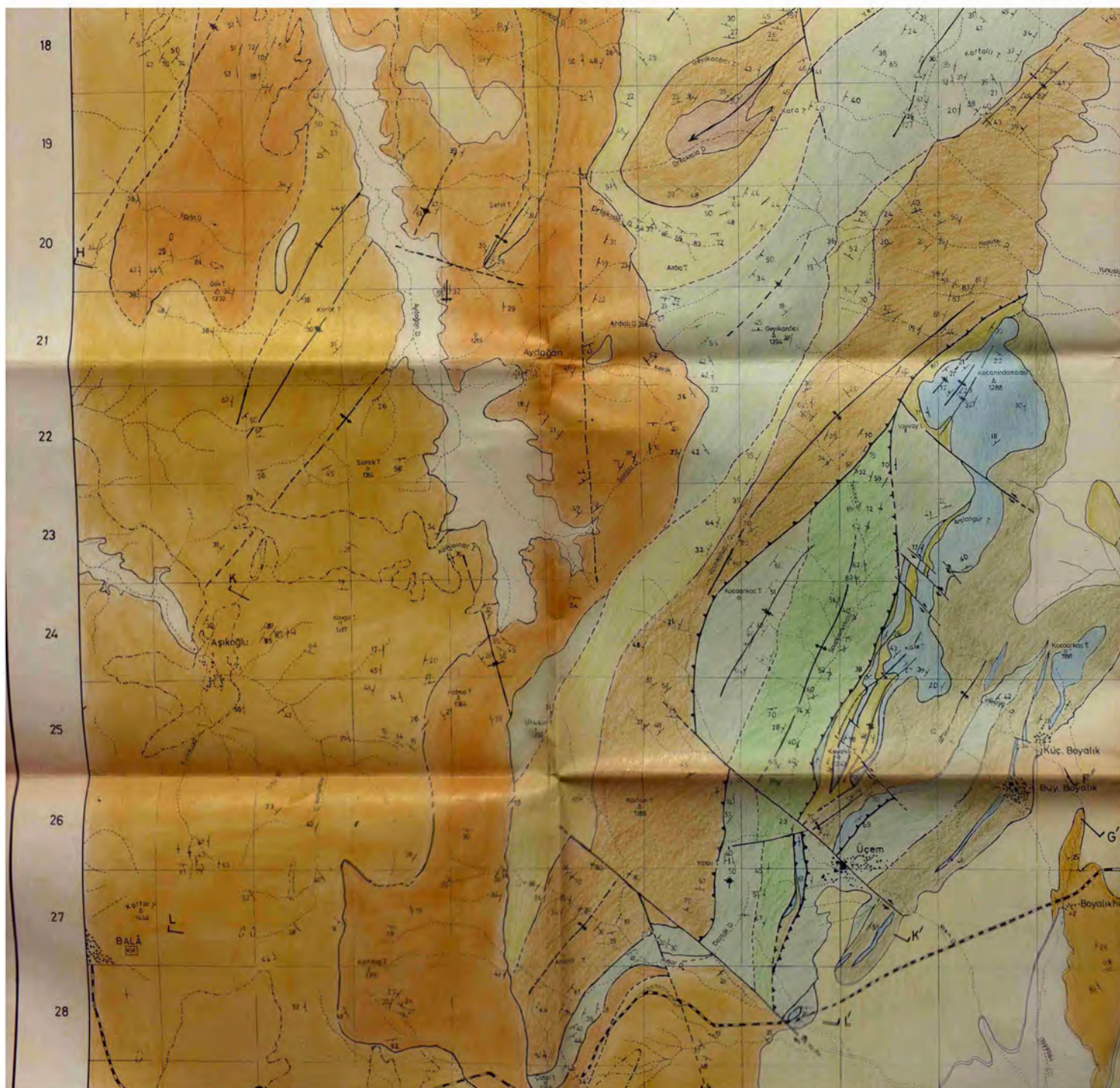
- ALLUVIUM
- NEOGENE CONTINENTAL CLASTICS
- KIZILDAG FORMATION
- EVAPORITE LENSES
- DELTA SAND & SILTSTONE
- CONGLOMERATE & SANDSTONE LENSES
- PRODELTA SHALE & SILTSTONE

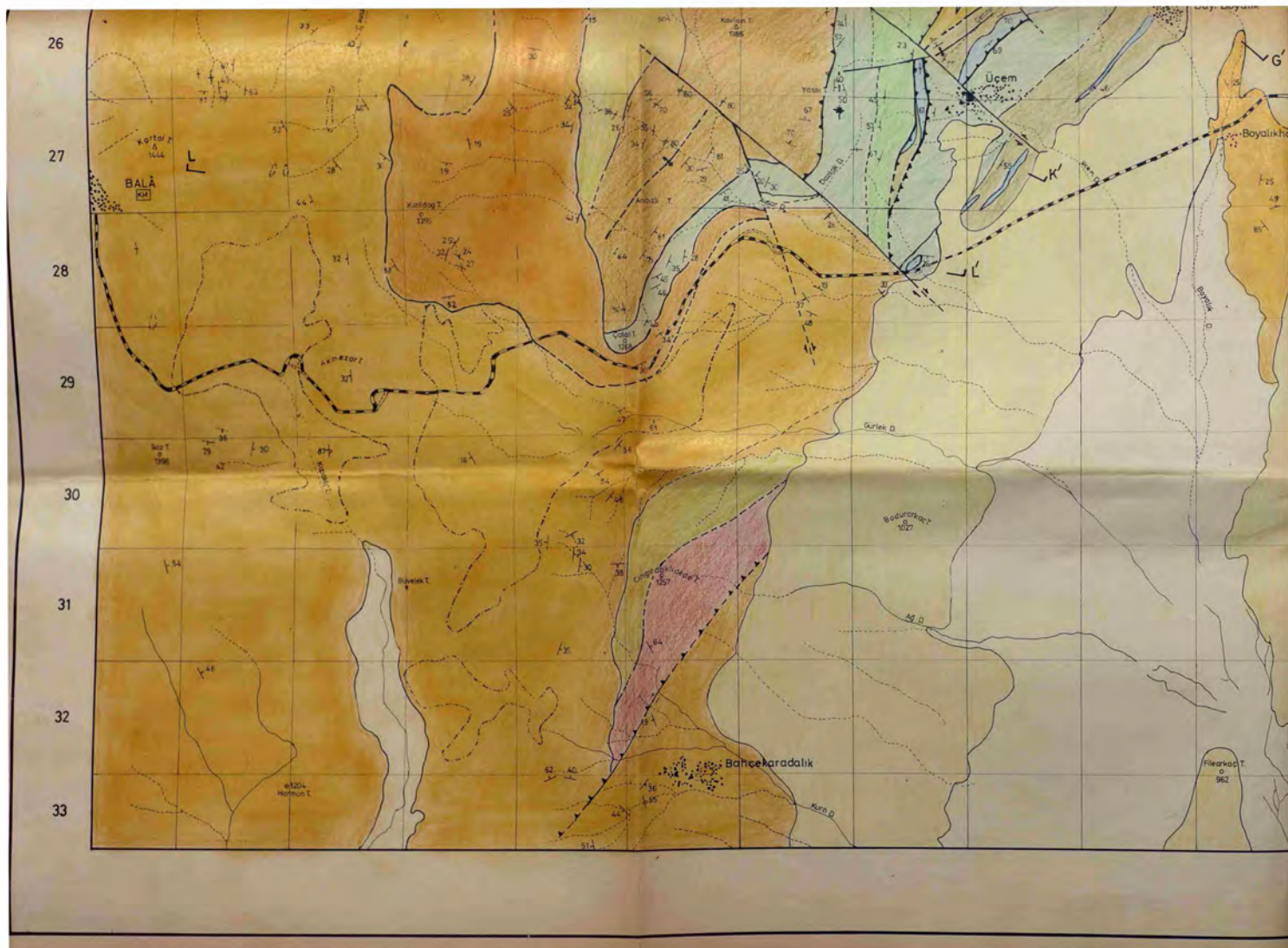
- Boundary
- Dip & Strike
- Anticline
- Syncline
- Slump Folds

K O R A T









GEOLOGICAL MAP OF BALA AREA, TURKEY

M.F. EMRE

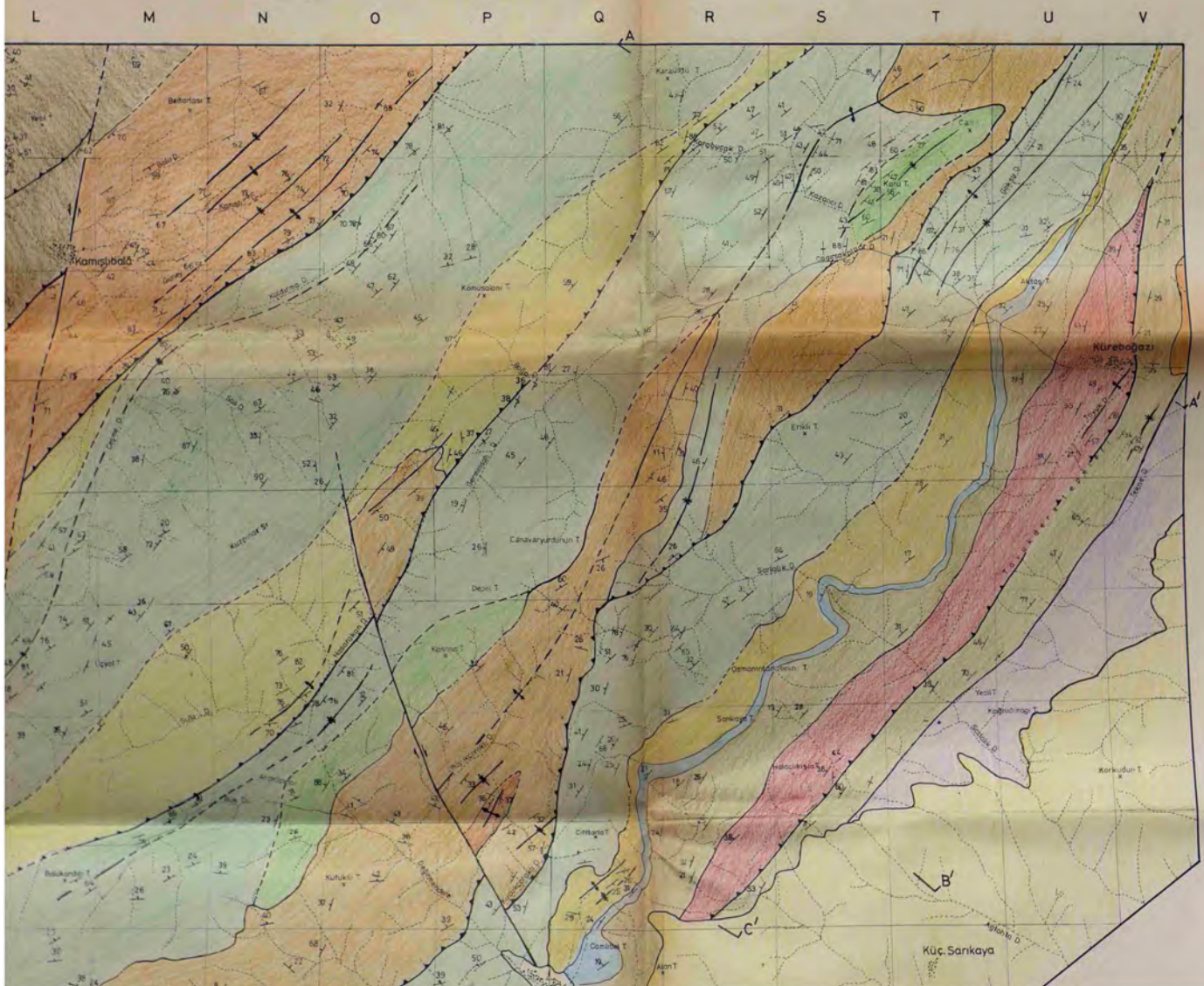
1984

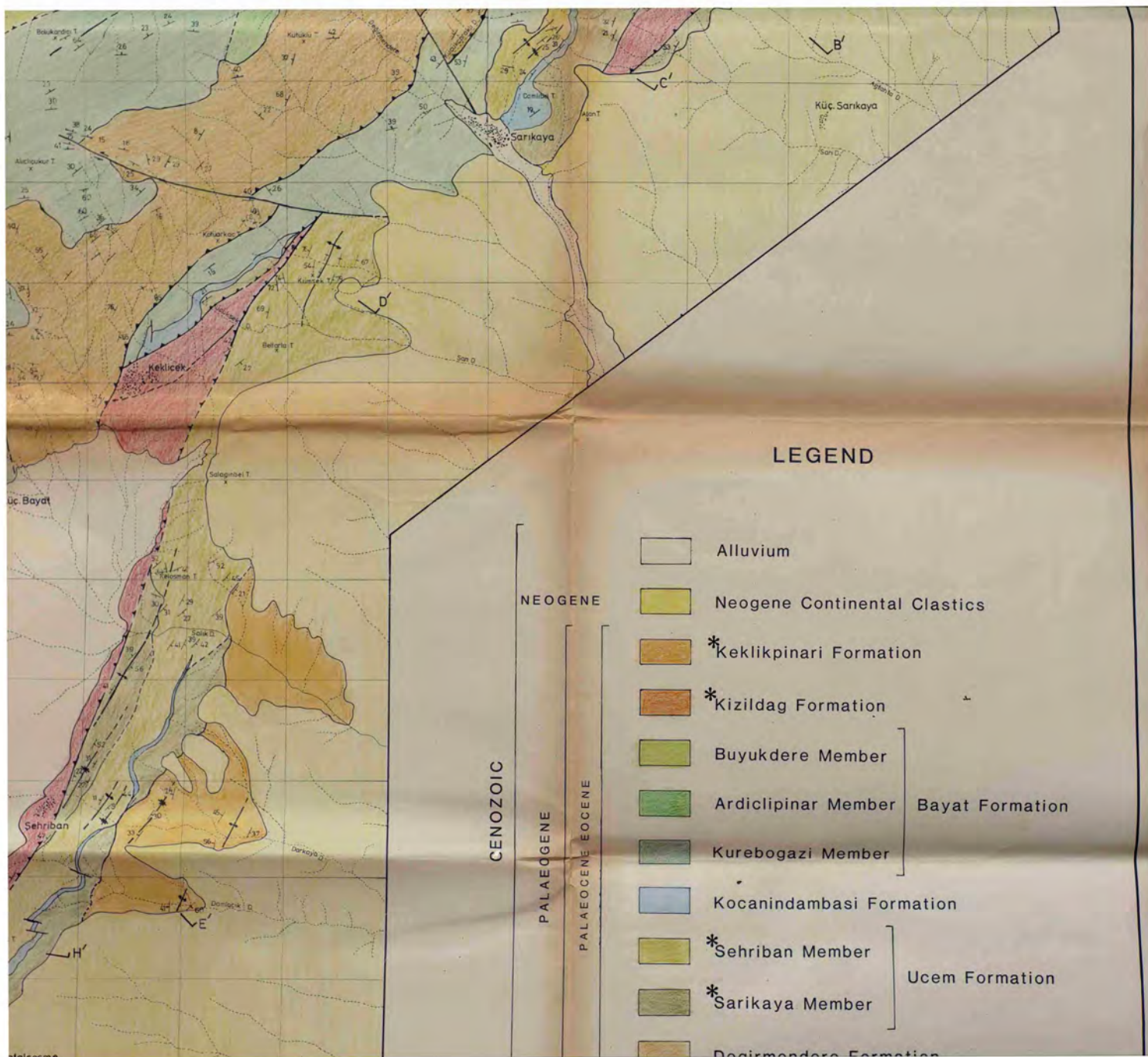
1/25 000

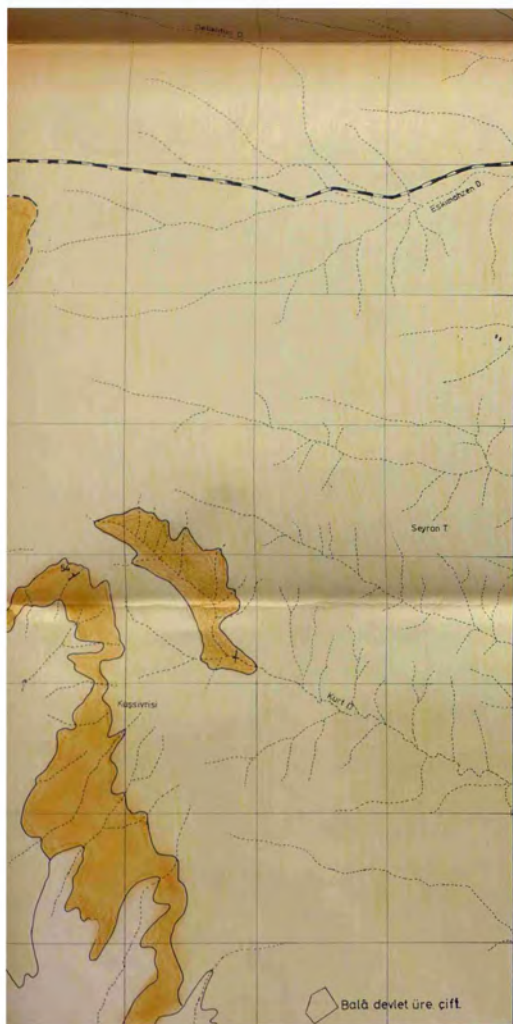




1/25 000







Batı deviet üre çift.

Ankara-Kirsehir Highway
 Üçentuz
 Settlements
 Stream

Boundary
 Probable Boundary
 Reverse
 Normal
 Strike-Slip
 Probable Reverse
 Probable Normal
 Probable Strike-Slip

Faults

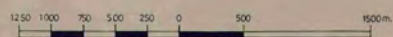
Anticline
 Syncline

Normal
 Overturned

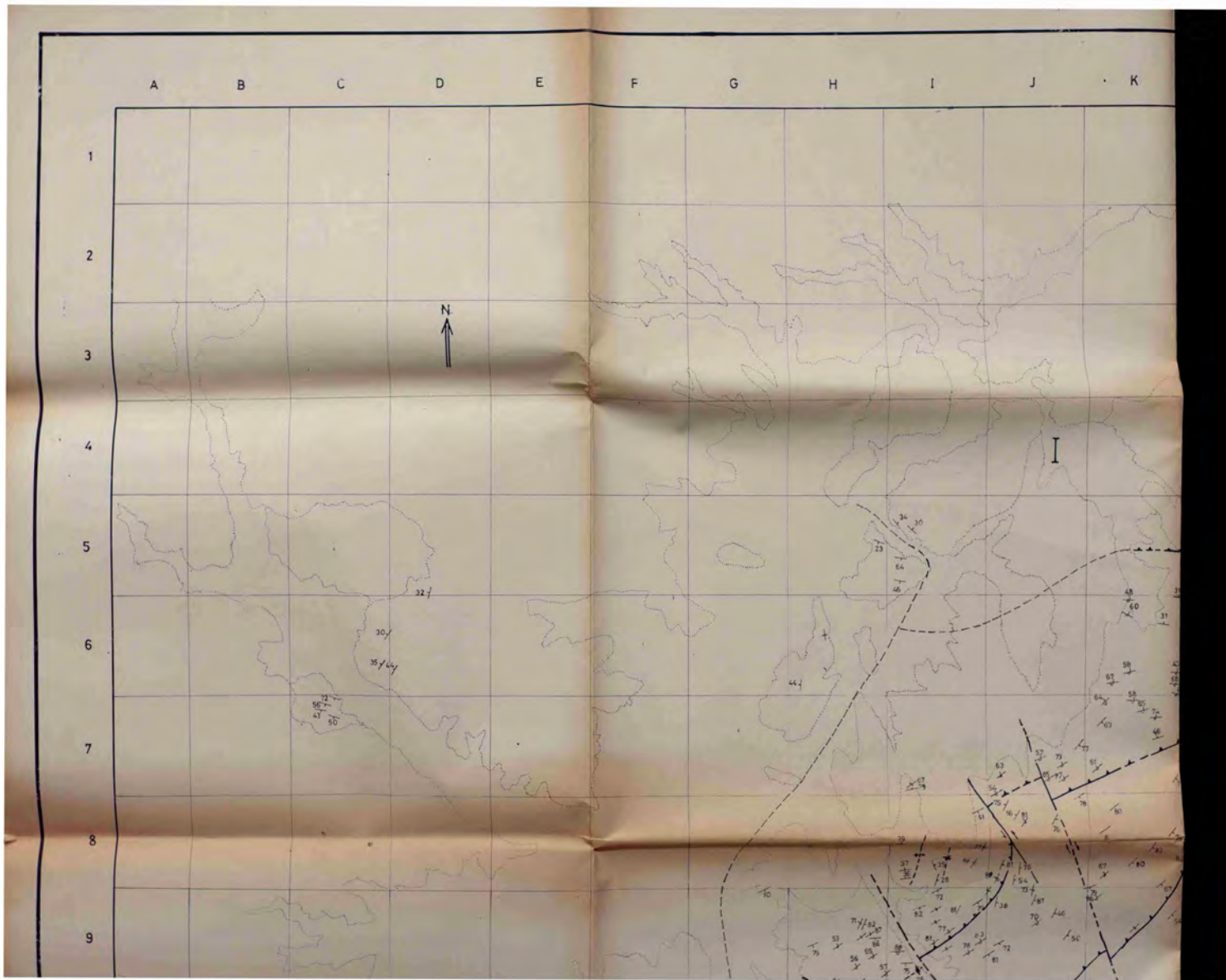
Dip & Strike

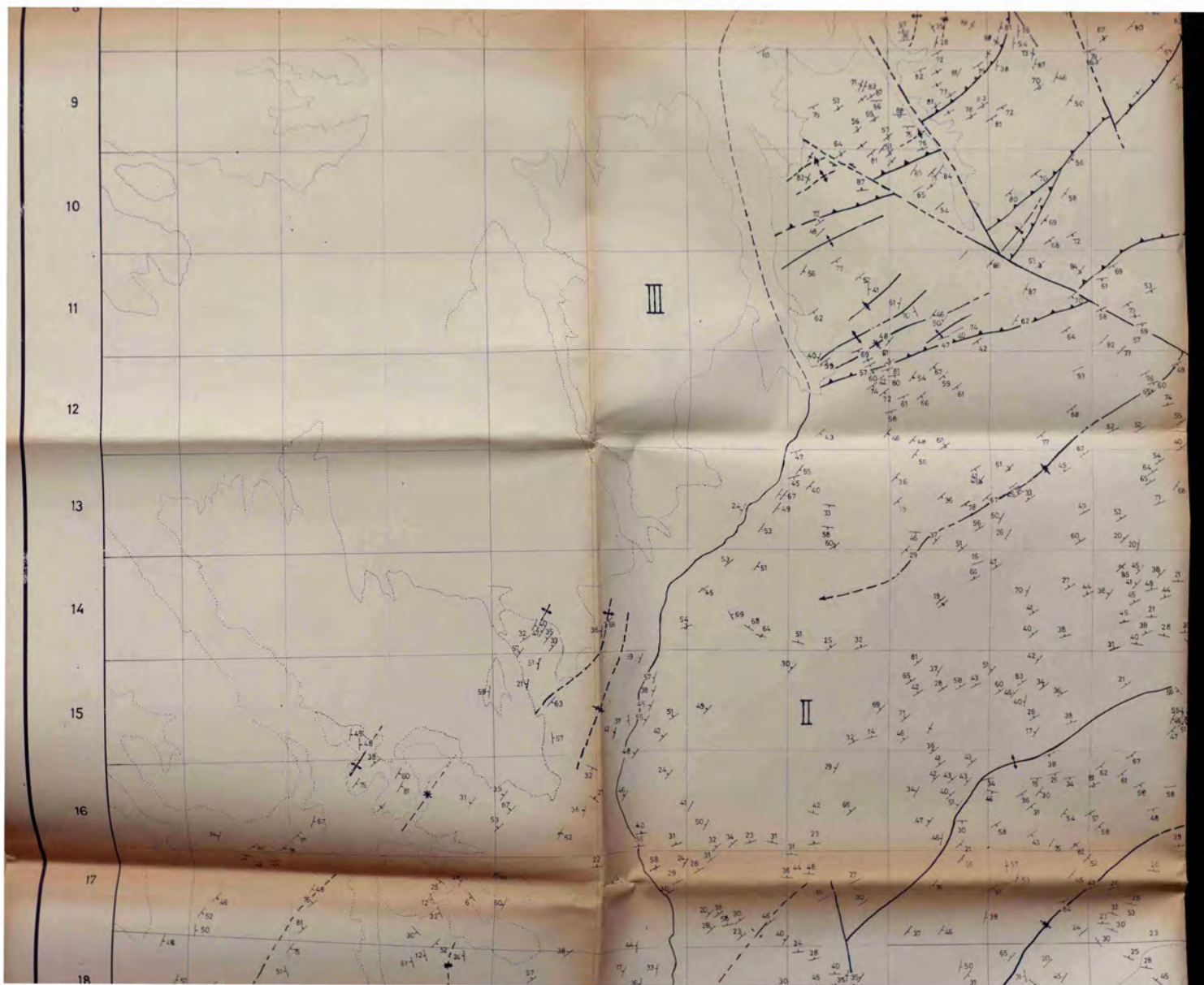
Outlines of Evaporites

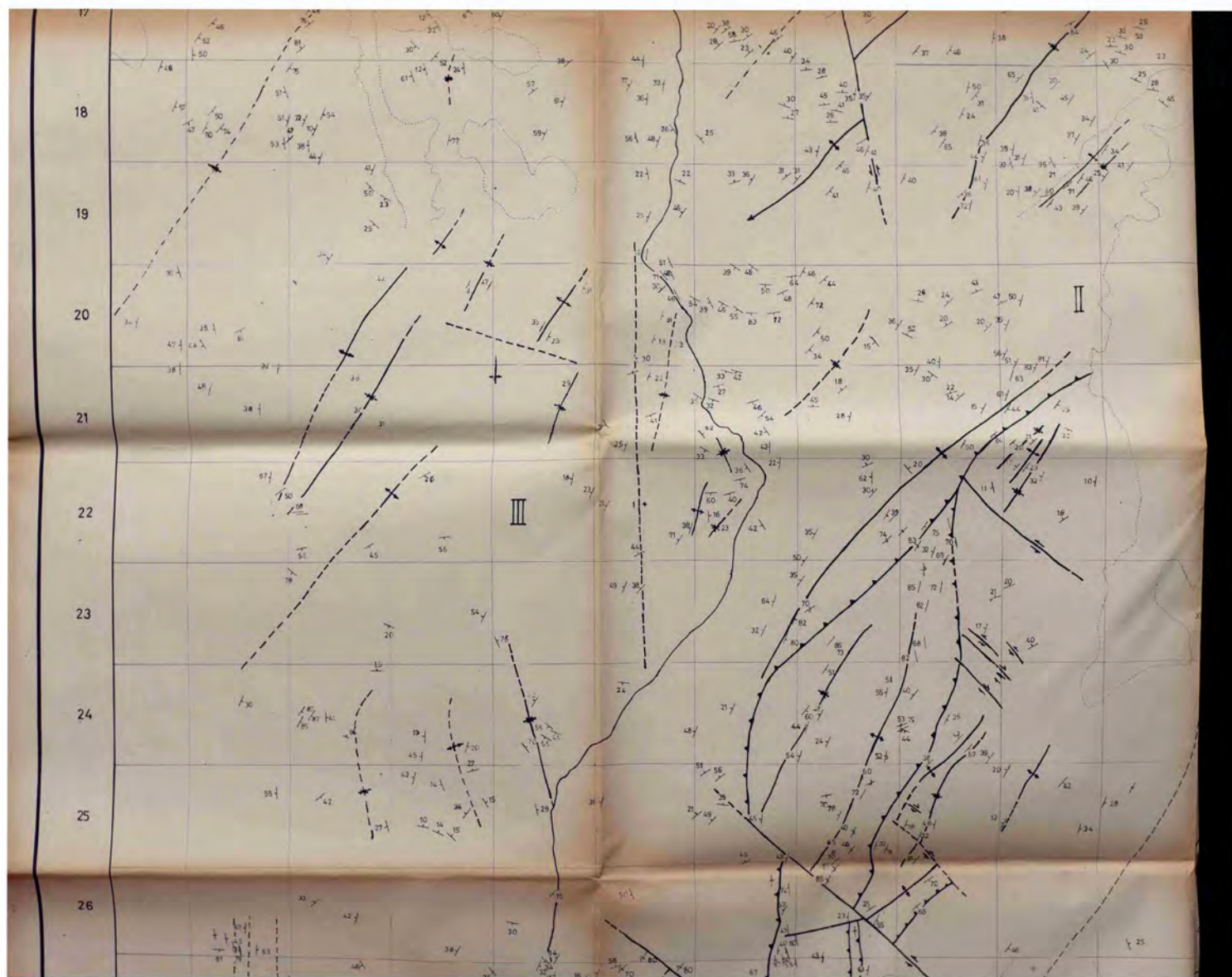
Cross Section

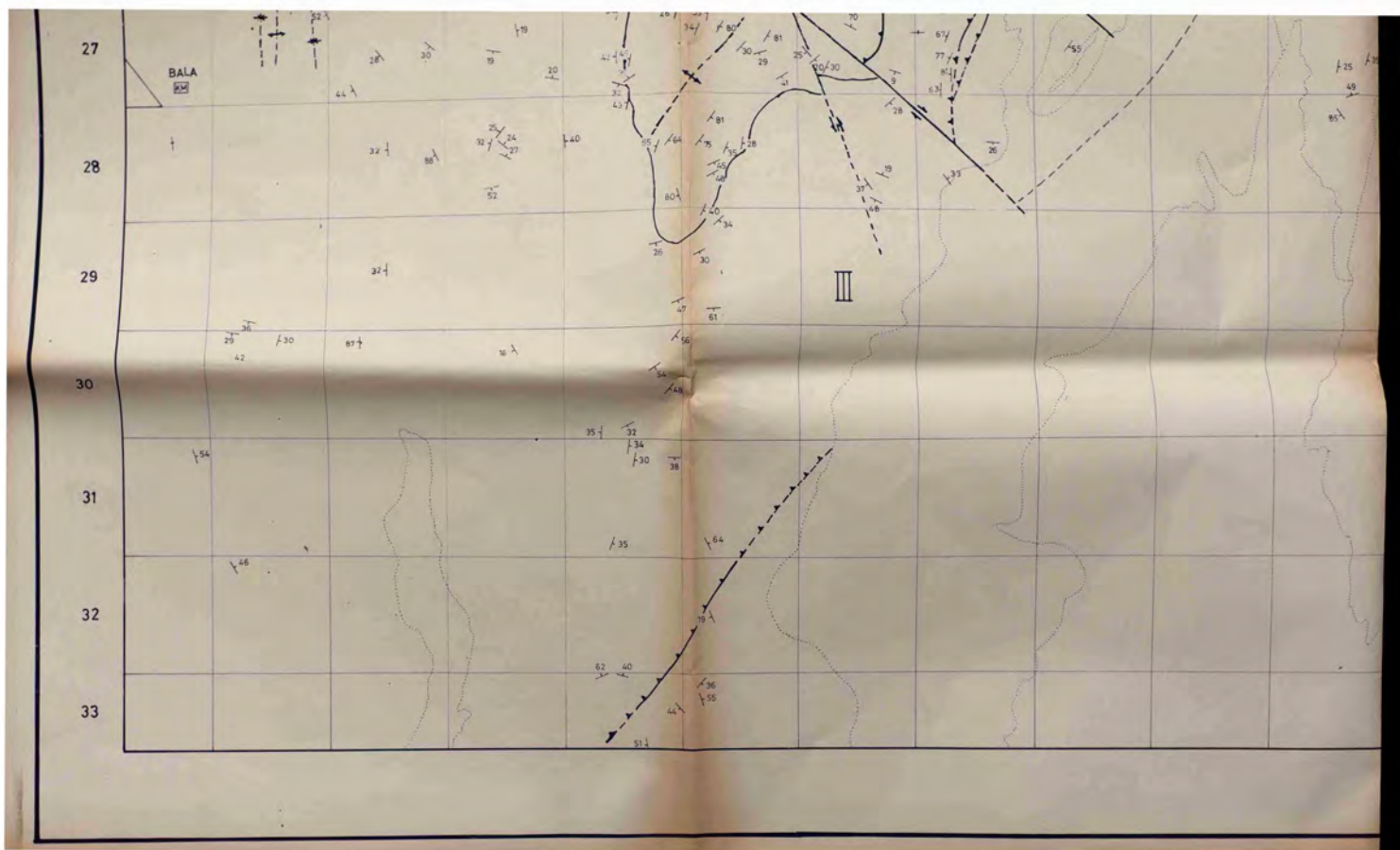


*The precise nature of the boundary relationships is dealt with in the text of the thesis.









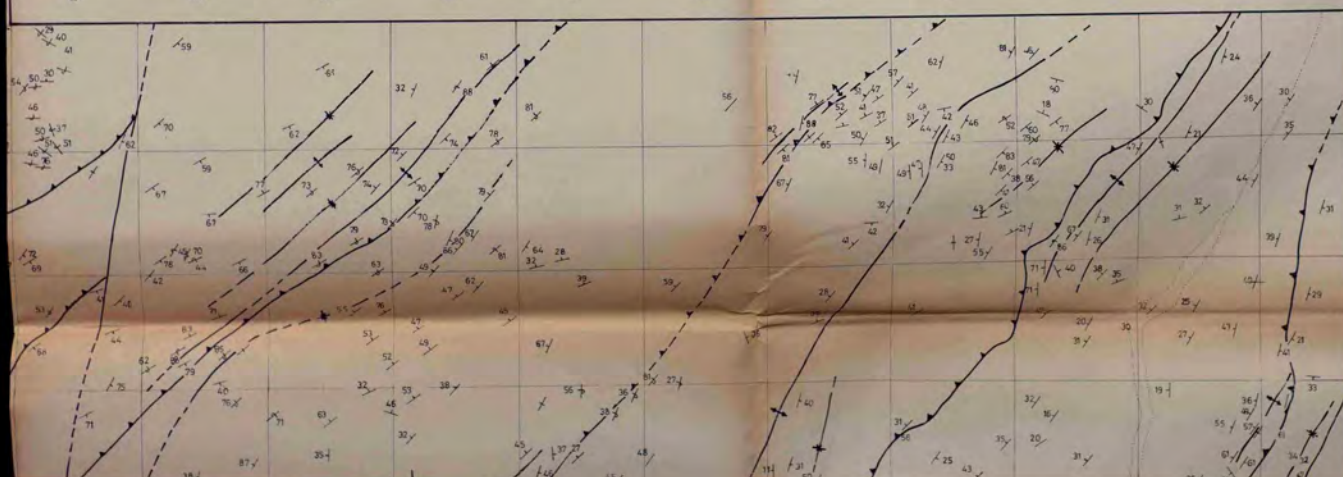
STRUCTURAL MAP OF BALA AREA ,TURKEY

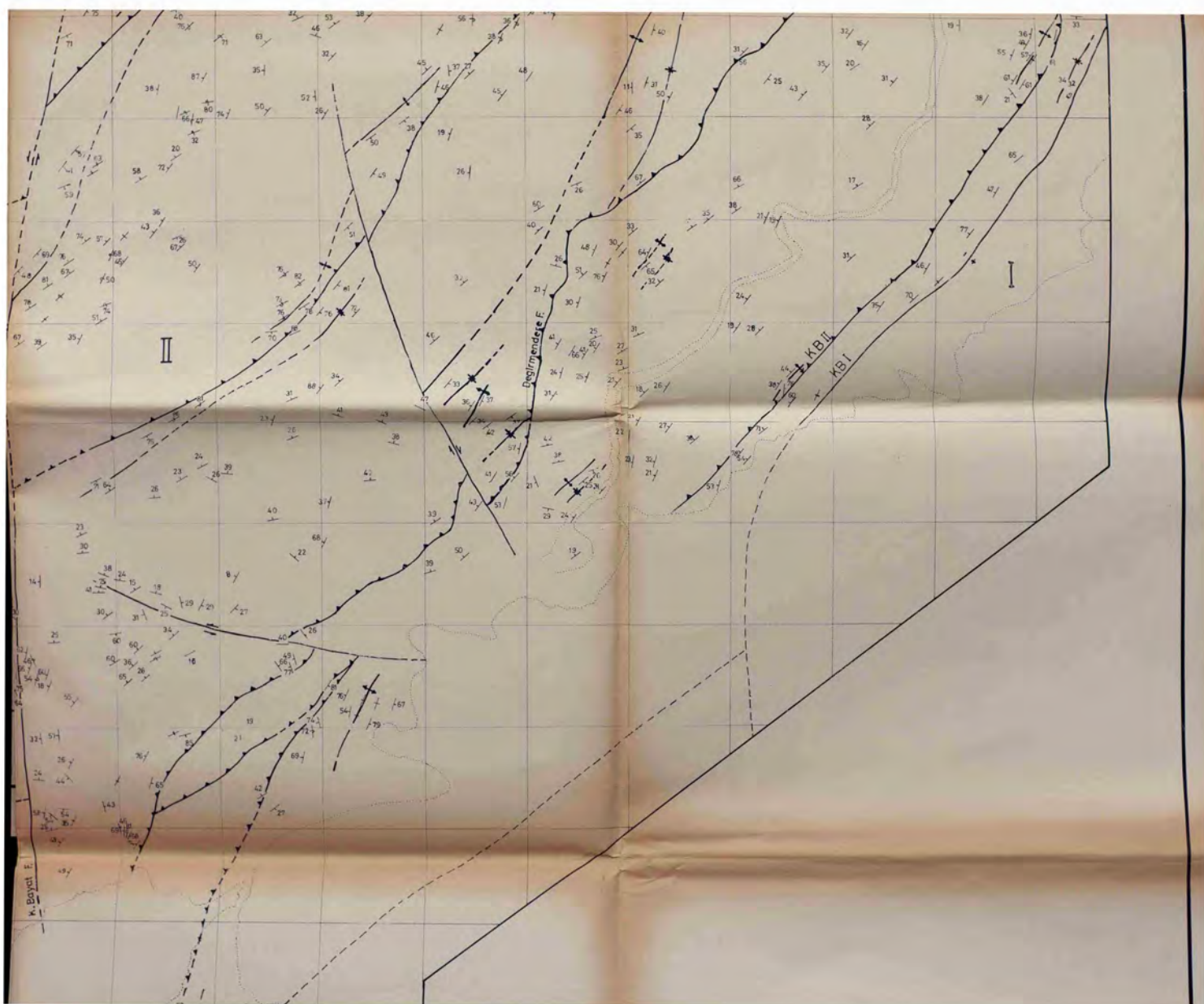
M.F. EMRE

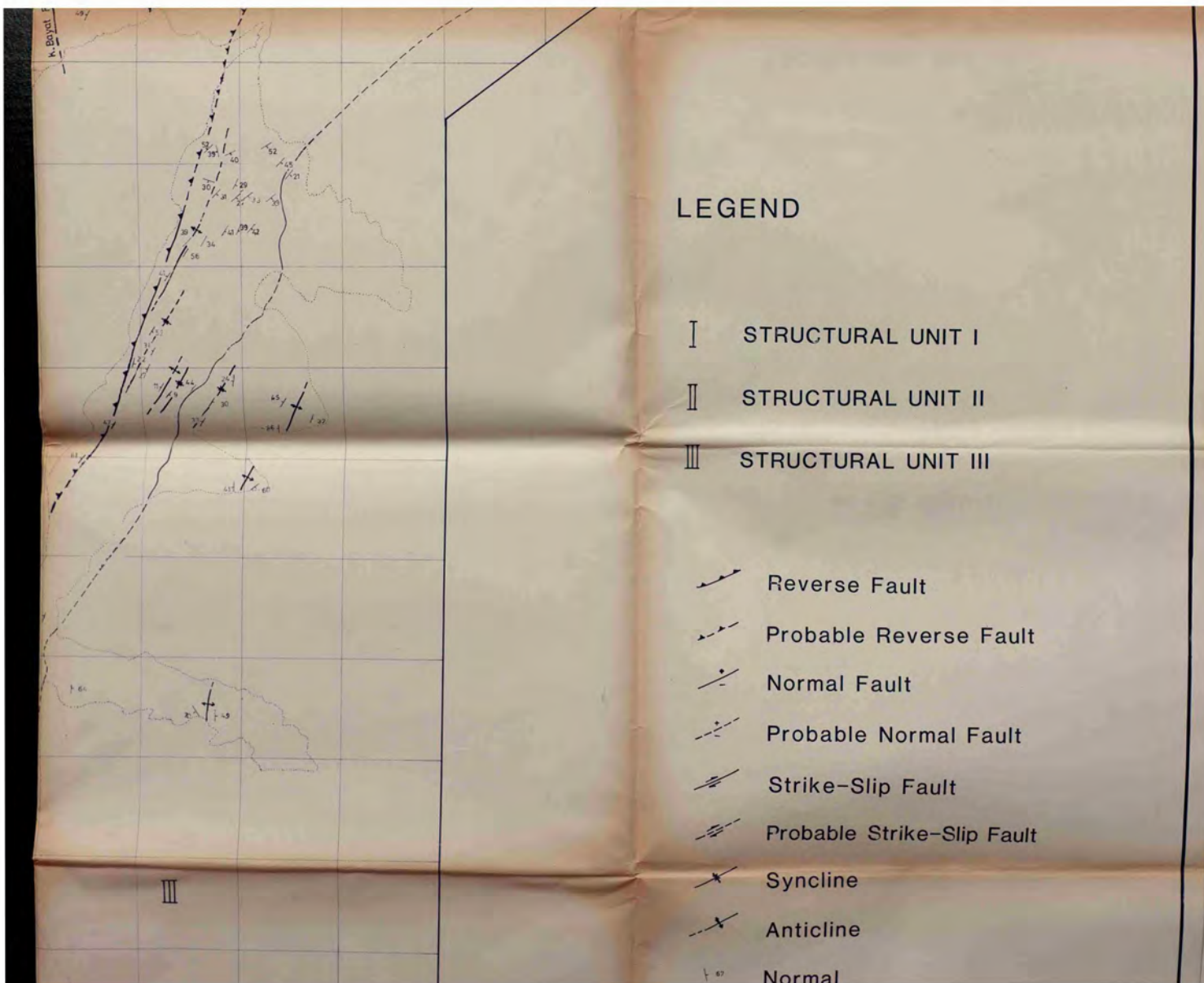
1984

1/25 000

L M N O P Q R S T U V







III

Strike Slip Fault

Probable Strike-Slip Fault

Syncline

Anticline

Normal

Overtained

Dip & Strike

1000 500 0 250 500 1000 m.